

Springer Tracts in Civil Engineering

Rajandrea Sethi
Antonio Di Molfetta

Groundwater Engineering

A Technical Approach to Hydrogeology,
Contaminant Transport and
Groundwater Remediation

 Springer

Springer Tracts in Civil Engineering

Series Editors

Giovanni Solari, Wind Engineering and Structural Dynamics Research Group,
University of Genoa, Genova, Italy

Sheng-Hong Chen, School of Water Resources and Hydropower Engineering,
Wuhan University, Wuhan, China

Marco di Prisco, Politecnico di Milano, Milano, Italy

Ioannis Vayas, Institute of Steel Structures, National Technical University of
Athens, Athens, Greece

Springer Tracts in Civil Engineering (STCE) publishes the latest developments in Civil Engineering - quickly, informally and in top quality. The series scope includes monographs, professional books, graduate textbooks and edited volumes, as well as outstanding PhD theses. Its goal is to cover all the main branches of civil engineering, both theoretical and applied, including:

- Construction and Structural Mechanics
- Building Materials
- Concrete, Steel and Timber Structures
- Geotechnical Engineering
- Earthquake Engineering
- Coastal Engineering
- Hydraulics, Hydrology and Water Resources Engineering
- Environmental Engineering and Sustainability
- Structural Health and Monitoring
- Surveying and Geographical Information Systems
- Heating, Ventilation and Air Conditioning (HVAC)
- Transportation and Traffic
- Risk Analysis
- Safety and Security

Indexed by Scopus

To submit a proposal or request further information, please contact: Pierpaolo Riva at Pierpaolo.Riva@springer.com, or Li Shen at Li.Shen@springer.com

More information about this series at <http://www.springer.com/series/15088>

Rajandrea Sethi · Antonio Di Molfetta

Groundwater Engineering

A Technical Approach to Hydrogeology,
Contaminant Transport and Groundwater
Remediation

Translation by Elena Dalla Vecchia

Rajandrea Sethi
Groundwater Engineering Group, DIATI
Politecnico di Torino
Turin, Italy

Antonio Di Molfetta
Bortolami - Di Molfetta s.r.l.
Turin, Italy

ISSN 2366-259X ISSN 2366-2603 (electronic)
Springer Tracts in Civil Engineering
ISBN 978-3-030-20514-0 ISBN 978-3-030-20516-4 (eBook)
<https://doi.org/10.1007/978-3-030-20516-4>

© Springer Nature Switzerland AG 2019

This work is subject to copyright. All rights are reserved by the Publisher, whether the whole or part of the material is concerned, specifically the rights of translation, reprinting, reuse of illustrations, recitation, broadcasting, reproduction on microfilms or in any other physical way, and transmission or information storage and retrieval, electronic adaptation, computer software, or by similar or dissimilar methodology now known or hereafter developed.

The use of general descriptive names, registered names, trademarks, service marks, etc. in this publication does not imply, even in the absence of a specific statement, that such names are exempt from the relevant protective laws and regulations and therefore free for general use.

The publisher, the authors and the editors are safe to assume that the advice and information in this book are believed to be true and accurate at the date of publication. Neither the publisher nor the authors or the editors give a warranty, expressed or implied, with respect to the material contained herein or for any errors or omissions that may have been made. The publisher remains neutral with regard to jurisdictional claims in published maps and institutional affiliations.

This Springer imprint is published by the registered company Springer Nature Switzerland AG
The registered company address is: Gewerbestrasse 11, 6330 Cham, Switzerland

To Laura, Luca and Nicola

Antonio Di Molfetta

To Michela and Anna

Rajandrea Sethi

Preface

Almost 95% of the available freshwater present on our planet is contained in aquifer systems. Groundwater resources are, however, extremely vulnerable to natural and anthropogenic pressures. On the one hand, overexploitation of aquifers may lead to source depletion; on the other, direct contamination arising from industrial waste discharge, landfill leachate, accidental spills of toxic liquids, and agricultural activities can impair the quality of groundwater. This poses a tangible threat for human health and the environment at large, since polluted groundwater can be transported in the subsurface toward drinking water wells or other receptors including surface water bodies.

Despite these facts, regulations and directives specifically aimed at protecting groundwater resources have only recently been issued. The earliest standards for drinking water abstractions were defined both in the USA and in Europe in the mid-70s, but these mainly referred to surface waters and put small emphasis on the protection of the source. It was not until the early 2000s, following the second amendment to the Safe Drinking Water Act in the USA and the definition of the Water Framework Directive in the EU that groundwaters began to receive specific legislative attention and protection. In particular, in 2006 the Ground Water Rule was implemented in the USA and the Groundwater Directive was issued by the European Parliament and Council. These regulations define quality and quantity standards that should be respected for the protection of groundwater resources from contamination and overexploitation. However, their implementation strongly relies on a thorough understanding of groundwater flow and transport of chemicals within geological formations.

This book employs a technical and quantitative approach to subsurface hydrology and hydrogeology in order to offer a transversal overview of groundwater-related topics. Its main aim is to instruct readers on the characterization of subsurface flow of pristine and polluted water, and to provide them with the tools for the design of engineering interventions. Targeted applications range from groundwater exploitation as a drinking water supply to the remediation of contaminated aquifers (i.e., the system composed of groundwater within its host geological formation), from the definition and safeguard of drinking water sources'

protection areas to the assessment of the human health risk deriving from a groundwater contamination event. Rather than extensively addressing subsurface flow and transport from a theoretical standpoint, this text aims at providing readily applicable tools for the design of water supply systems, of groundwater contamination sampling campaigns, and of remediation interventions. Key criteria in its writing have been practicality, nomenclature consistency, and clarity.

The book opens with an introduction to the main properties of aquifer systems and to Darcy's law (Chap. 1). An illustration of the theoretical foundations of the groundwater flow equations in a polar coordinate system (Chap. 2) and its analytical solutions in steady and transient conditions for confined, leaky, and unconfined aquifers follows (Chap. 3). These solutions lay the foundations for the interpretation of pumping, recovery, and slug aquifer tests, and thus for the description of the hydraulic behavior of an aquifer and the determination of its main hydrodynamic features (i.e., storativity and transmissivity; Chap. 4). Having established the main aquifer characterization approaches, the aspects that need to be kept into account for the optimization of a water supply system are described, i.e., well efficiency (Chap. 5) and productive capacity of such a system (Chap. 6). The main methods for assessing an aquifer's vulnerability (Chap. 7) and the protection of drinking water supply sources (Chap. 8) are then presented, with the goal of providing the tools necessary for a sustainable exploitation of groundwater resources.

The second part of the book deals with groundwater contamination and remediation. The most common aquifer contaminants are characterized from a chemical, physical, and toxicological point of view, and the international (i.e., European, American, and WHO) guidelines regarding groundwater and/or drinking water contamination are presented (Chap. 9). In Chap. 10, the transport mechanisms of chemical compounds in porous media are illustrated qualitatively for both conservative and reactive substances. Contaminant propagation mechanisms include hydrological (i.e., advection, diffusion, and dispersion) as well as chemical, physicochemical, and biological phenomena, which contribute to compound degradation. Chapters 11–13 are dedicated to a quantitative description of conservative and reactive solute propagation in an aquifer by presenting the differential equation of mass transport and its solutions derived for various geometries and types of input. The transport of immiscible substances, instead, is presented in Chap. 14.

The transport models described in Chaps. 11–14 provide essential information for the understanding of a contamination event; from a practical point of view, however, a sampling campaign is necessary for the characterization of the contaminant distribution. The main strategies for the sampling design, and the main methods and devices available for sampling the different subsurface phases (groundwater, soil gas, and soil) in both the saturated and unsaturated media are illustrated in Chap. 15. Based on the characterization of the aquifer and of the contamination, it is possible to conduct a human health risk assessment, with the goal of establishing the necessity for a remedial action (Chap. 16). The final part of this book reviews the different containment and remediation strategies that can be

implemented in a contaminated aquifer and provides valuable information to support the choice of the most suitable approach (Chap. 17).

The primary expected readership are environmental and civil engineering and geological sciences upper undergraduate or early graduate students; however, the book may also appeal to practitioners and decision-makers in the fields of water resource management, exploitation, and safeguard, who are interested in, or required to approach, the field of groundwater engineering.

The book is the adaptation and translation of the Italian textbook *Ingegneria degli Acquiferi* published by Springer in 2012 and is the result of more than 40 years of teaching, research, and professional experience of the authors.

Any book stems from evolving ideas and concepts, and their systematization owes a great deal to the inspiration drawn from often unaware colleagues, collaborators, and students. It would be impossible to mention each of them individually, but we would, nevertheless, like to acknowledge present and past members of the Groundwater Engineering Group (www.polito.it/groundwater) at Politecnico: Massimo Rolle, Tiziana Tosco, and Valerio Zolla for their specific contributions. We would also like to thank Gianna Sanna and Lucia Re for thoroughly proofreading, respectively, the original Italian and the English manuscripts, and Dario Forneris, who created the illustrations. Finally, we would like to thank Elena Dalla Vecchia, for translating the original text to English and offering critical editorial input.

Turin, Italy
June 2019

Rajandrea Sethi
Antonio Di Molfetta

Contents

1	Basic Concepts	1
1.1	Water and its Properties	2
1.2	Groundwater	5
1.2.1	Gravitational Water	5
1.2.2	Pendular Water	5
1.3	Aquifer Types and Classification Criteria	8
1.4	Hydraulic Head	9
1.4.1	Field Measurements of the Hydraulic Head	11
1.5	Storage and Release Capacity	12
1.5.1	Storage in Unconfined Aquifers: Specific Yield and Retention	14
1.5.2	Storage in Confined Aquifers	16
1.6	Flow Capacity	17
1.6.1	Darcy's Law	17
1.6.2	Hydraulic Conductivity and Permability	18
1.6.3	Transmissivity	21
1.7	Leakage Between Different Aquifers	22
1.8	Field Applications of Darcy's Law	22
1.8.1	Potentiometric Surface and Flow Field Mapping	22
	References	25
2	The Groundwater Flow Equation	27
2.1	Derivation of the Equation of Continuity	27
2.2	The Groundwater Flow Equation	30
	References	32
3	Analytical Solutions of the Groundwater Flow Equation	33
3.1	Confined Aquifers	34
3.1.1	Unsteady (or Transient) State	34
3.1.2	Steady State Flow	37

3.2	Leaky Aquifers	38
3.2.1	Unsteady or Transient State	39
3.2.2	Steady State Flow	42
3.3	Unconfined Aquifers	42
3.3.1	Unsteady or Transient State	44
3.3.2	Steady State Flow	50
3.4	Radius of Investigation and Radius of Influence	51
	References	52
4	Aquifer Characterization	55
4.1	Aquifer Test Classification and Planning	56
4.2	Aquifer Tests	61
4.2.1	Hydraulic Behavior Identification	61
4.2.2	Interpretation Procedure	64
4.3	Recovery Tests	81
4.4	Slug Test	83
4.4.1	Interpretation Models	84
4.4.2	Bouwer and Rice's Method	85
4.4.3	Cooper, Bredehoeft and Papadopoulos' Method	90
4.4.4	The KGS Method	93
4.5	Other Methods for the Determination of Parameters Characterizing an Aquifer	96
4.5.1	Determination of Hydraulic Conductivity or Transmissivity	96
4.5.2	Determination of the Storativity	106
4.5.3	Determination of the Specific Yield	107
4.5.4	Determination of the Effective Porosity	108
	References	111
5	Well Testing	113
5.1	Operating Conditions of a Well Test	114
5.2	Theoretical Foundations and Interpretation of Step-Drawdown Tests	114
5.3	Well Productivity and Efficiency	117
5.4	Estimation of the Coefficients B_2 and B_3	120
5.4.1	Estimation of the Coefficient B_2	120
5.4.2	Estimation of the Coefficient B_3	122
5.4.3	Calculation of B_2 and B_3	123
5.4.4	Correlation Between Specific Capacity and Transmissivity	124
5.5	Recent Developments in the Interpretation of Step-Drawdown Tests	124
	References	125

- 6 Optimization of a Water Supply System 127
 - 6.1 Water Supply System Description 128
 - 6.2 Assessment of Head Losses in the System 129
 - 6.3 Head Losses in the Well-Aquifer Sub-system 129
 - 6.4 Head Losses in the Pipe Network 129
 - 6.4.1 Distributed Head Losses 129
 - 6.4.2 Local Head Losses 130
 - 6.5 Optimization of the Productive Capacity of the System 134
 - 6.6 Changes Over Time 134
 - References 136

- 7 Aquifer Vulnerability and Contamination Risk 137
 - 7.1 Vulnerability Assessment Methods 138
 - 7.1.1 Overlay Methods 139
 - 7.1.2 Index Methods 141
 - 7.2 Comparison of Different Vulnerability Assessment Methods 151
 - 7.3 Contamination Risk 151
 - 7.4 An Example of Contamination Risk Reduction 153
 - 7.4.1 Reduction of the Probability of Occurrence of the Event 153
 - 7.4.2 Reducing the Intensity of the Event 154
 - 7.4.3 Reducing Potential Damage 156
 - References 158

- 8 Well Head Protection Areas 161
 - 8.1 Approaches for the Definition of Protection Areas 162
 - 8.1.1 Analytical Definition of the Protection Area of a Single Well in a Confined Aquifer 162
 - 8.1.2 General Application of the Time of Travel Criterion 163
 - 8.2 Dynamic Protection 166
 - References 168

- 9 Groundwater Contaminants 169
 - 9.1 Chemical Classification 171
 - 9.1.1 Inorganic Contaminants 171
 - 9.1.2 Organic Contaminants 171
 - 9.2 Physical Characteristics 182
 - 9.2.1 Physical State 182
 - 9.2.2 Miscibility 182
 - 9.2.3 Density 183
 - 9.2.4 Solubility 183
 - 9.2.5 Octanol-Water Partition Coefficient 184

9.2.6	Vapor Pressure	184
9.2.7	Henry's Constant	185
9.3	Contaminant Toxicity and Regulatory Framework	187
9.3.1	Toxicological Classification	187
9.3.2	Regulation of Contaminants in Groundwater	190
	References	191
10	Mechanisms of Contaminant Transport in Aquifers	193
10.1	Hydrological Phenomena	194
10.1.1	Advection	194
10.1.2	Molecular Diffusion	195
10.1.3	Mechanical Dispersion	197
10.1.4	Hydrodynamic Dispersion	199
10.2	Chemical Phenomena	203
10.2.1	Reaction Models	203
10.2.2	Chemical Reactions	205
10.3	Biological Processes: Biodegradation	208
10.4	Physico-Chemical Processes: Sorption	210
10.5	Concomitant Processes	215
	References	216
11	The Mass Transport Equations	219
11.1	Contaminant Mass Balance	219
11.2	Conservative Solutes	220
11.3	Reactive Solutes	222
11.4	Initial and Boundary Conditions	223
12	Analytical Solutions to the Differential Equation of Mass Transport for Conservative Solutes	225
12.1	One-Dimensional Geometry	226
12.1.1	Continuous Input	226
12.1.2	Pulse (or Instantaneous) Input	229
12.2	Two-Dimensional Geometry	230
12.2.1	Vertical Line Source, Pulse Input	231
12.2.2	Vertical Line Source, Continuous Input	231
12.3	Three-Dimensional Geometry	233
12.3.1	Point Source, Pulse Input	233
12.3.2	Plane Source, Continuous Input	234
	References	236
13	Analytical Solutions of the Differential Equation of Mass Transport for Reactive Solutes	239
13.1	One-Dimensional Geometry	239
13.1.1	Continuous Input	240
13.1.2	Pulse Input	242

- 13.2 Two-Dimensional Geometry 244
 - 13.2.1 Line Source, Pulse Input 244
 - 13.2.2 Line Source, Continuous Input 244
- 13.3 Three-Dimensional Geometry 245
 - 13.3.1 Point Source, Pulse Input 246
 - 13.3.2 Plane Source, Continuous Input 246
- References 247
- 14 Transport of Immiscible Fluids 249
 - 14.1 Properties of a Solid–Liquid Multiphase System 249
 - 14.1.1 Wettability 250
 - 14.1.2 Interfacial Tension and Capillary Pressure 251
 - 14.1.3 Effective and Relative Permeability 251
 - 14.1.4 Imbibition and Draining 253
 - 14.2 Qualitative Models of NAPL Behavior in the Ground 255
 - 14.2.1 Behavior of LNAPLs 255
 - 14.2.2 Behavior of DNAPLs 256
 - 14.3 Secondary Contamination Due to NAPLs 257
 - 14.4 Quantitative Approach 258
 - 14.4.1 Geometrical and Temporal Characterization 259
 - 14.4.2 NAPL Mass Distribution 259
 - 14.5 Concluding Remarks 261
 - References 262
- 15 Characterization of a Contamination Event 263
 - 15.1 Sampling Design 264
 - 15.2 Sampling the Unsaturated Medium 268
 - 15.2.1 Minimum Number of Sampling Points 268
 - 15.2.2 Soil Sampling 268
 - 15.2.3 Rotary Techniques 269
 - 15.2.4 Direct Push or Drive Drilling Methods 269
 - 15.2.5 Soil Sampling for Volatile Compound Analysis 270
 - 15.2.6 Soil Gas Sampling 271
 - 15.2.7 Pore Water Sampling 273
 - 15.3 Sampling the Saturated Medium 277
 - 15.3.1 Vertical Sampling 278
 - 15.3.2 Multilevel Monitoring Wells 278
 - 15.3.3 Direct Push Techniques 279
 - 15.4 Purgings 280
 - 15.4.1 Well Volume Based Criterion 281
 - 15.4.2 Criterion Based on Physico-Chemical Parameters
Stabilization 281
 - 15.4.3 Well Storage and Hydrodynamic Parameters
Based Criterion 281

- 15.4.4 Low-Flow Purging and Physico-Chemical Parameters Stabilization 282
- 15.5 Sampling 283
 - 15.5.1 Sampling Rate 283
 - 15.5.2 Sample Collection 284
- 15.6 Sampling and Purging Mechanisms 285
 - 15.6.1 Bailers 286
 - 15.6.2 Submersible Centrifugal Pumps 287
 - 15.6.3 Bladder Pumps 289
 - 15.6.4 Peristaltic Pumps 290
 - 15.6.5 Inertial Lift Pumps 291
- 15.7 On Site Measurement of Water Quality Parameters 292
- 15.8 Sample Filtration 293
- 15.9 Quality Control 294
- 15.10 Equipment Cleaning and Decontamination 295
- 15.11 Sample Storage 296
- 15.12 Blanks and Replicates 297
- 15.13 Materials 298
- References 298
- 16 Human Health Risk Assessment 301
 - 16.1 Definition of Human Health Risk 302
 - 16.2 Features of Risk Assessment 303
 - 16.2.1 Phases 303
 - 16.2.2 Risk Assessment Tiers 305
 - 16.3 Risk Assessment Development 307
 - 16.3.1 Characterization Plan 307
 - 16.3.2 Calculation of the Concentration at the Point of Exposure 308
 - 16.4 Toxicological Models and Parameters 319
 - 16.5 Risk Assessment 320
 - 16.5.1 Determination of the Concentration at the Point of Exposure 320
 - 16.5.2 Rate of Exposure 321
 - 16.5.3 Risk Calculation 322
 - 16.5.4 Acceptability Criteria 325
 - 16.6 Risk Management 326
 - 16.7 Concluding Remarks 327
 - References 328
- 17 Remediation of Contaminated Groundwater 331
 - 17.1 Free Product Recovery 332
 - 17.1.1 Free Product Removal with Skimming Systems 333
 - 17.1.2 Free Product Recovery with Water Table Depression 333

17.1.3	Vacuum Enhanced Extraction	336
17.2	Subsurface Containment	336
17.3	Pump and Treat	338
17.3.1	Design of a P&T System	338
17.3.2	Flushing Water Volume	348
17.3.3	Performance of a P&T System	351
17.3.4	Potential P&T Limitations	353
17.3.5	Extracted Water Treatment Technology	354
17.4	Air Sparging and Biosparging	355
17.4.1	Design and Aim	356
17.4.2	Applicability	357
17.4.3	Dynamics of the Process	359
17.4.4	Air Sparging System Design	360
17.5	Permeable Reactive Barriers	361
17.5.1	Laboratory Tests	365
17.5.2	Design of a PRB	368
17.5.3	Technical Solutions for Constructing a Permeable Reactive Barrier	371
17.5.4	Monitoring Network	376
17.5.5	Iron Microparticles and Nanoparticles	377
17.5.6	A Case Study: The Permeable Reactive Barrier in Avigliana	379
17.6	In Situ Flushing	385
17.7	In Situ Oxidation	388
17.8	In Situ Bioremediation	391
17.8.1	Factors Contributing to Biodegradation	392
17.8.2	Biodegradation of Organic Contaminants	397
17.8.3	Biodegradation of Petroleum Products	397
17.8.4	Biodegradation of Chlorinated Organic Compounds	398
17.8.5	Enhanced in Situ Bioremediation	402
	References	405
	Appendix A: Exponential Integral or Well Function	411
	Appendix B: Hantush and Jacob Function	415
	Appendix C: Function K_0	421
	Appendix D: Dimensionless Neuman's Function $s_D(t_s, b)$ Valid for Short Times	423
	Appendix E: Dimensionless Neuman's Function $s_D(t_s, b)$ Valid for Extended Periods of Times	427
	Index	433

Symbols, Acronyms, and Abbreviations

This list describes the notation used consistently across the text (unless otherwise specified) of most relevant, and recurring, symbols.

A	Surface area (L^2)
B	Leakage factor (L)
b	Saturated thickness (L)
b'	Thickness of the aquitard (L)
B ₁	Linear aquifer-loss constant (TL^{-2})
B ₂	Partial penetration and completion head-loss constant (TL^{-2})
B ₃	Skin effect head-loss constant (TL^{-2})
C	Concentration (ML^{-3})
C	Well-loss constant (in Chap. 5) ($T^nL^{-(3n-1)}$)
c	Leakage coefficient of the aquitard (T^{-1})
C ₀	Concentration at time 0 (ML^{-3})
C _a	Molar concentration of a compound in the gas phase (L^{-3})
c _f	Compressibility of the formation (LT^2M^{-1})
C _{oct}	Concentration of a compound in octanol (ML^3)
C _w	Concentration of a compound in water (ML^3)
c _w	Compressibility of water (LT^2M^{-1})
D ₀	Molecular diffusion coefficient (including tortuosity) (L^2T^{-1})
d ₁₀	Size of the sieve through which only 10% in weight of the sediment grains pass (L)
D _{C:L}	Longitudinal mechanical dispersion coefficient (L^2T^{-1})
D _{C:T}	Transverse mechanical dispersion coefficient (L^2T^{-1})
D _d	Molecular diffusion coefficient (L^2T^{-1})
E	Young's modulus ($ML^{-1}T^{-2}$)
E	Well efficiency (in Chap. 5) (-)
e	Void ratio (-)
ED	Exposure duration (T)
f _{oc}	Fraction of organic carbon (-)

g	Gravitational acceleration (LT^{-2})
h	Hydraulic head (L)
h_0	Static hydraulic head (L)
h_p	Pressure head (L)
i	Hydraulic gradient (-)
I_{eff}	Effective infiltration
J_0	Bessel function of the first kind and order 0
J_1	Bessel function of the first kind and order 1
j_A	Advective mass flux ($MT^{-1}L^{-2}$)
j_C	Kinematic dispersive mass flux ($MT^{-1}L^{-2}$)
j_i	Hydrodynamic dispersion mass flux (L^2T^{-1})
j_M	Diffusive mass flux ($MT^{-1}L^{-2}$)
K	Hydraulic conductivity tensor (LT^{-1})
K	Hydraulic conductivity (LT^{-1})
K_d	Solid-liquid partition coefficient (L^3M^{-1})
K_{oc}	Partition coefficient between organic carbon and water (L^3M^{-1})
K_{ow}	Octanol-water partition coefficient (-)
K_r	Radial hydraulic conductivity (LT^{-1})
K_{sw}	Soil-leachate partition coefficient (L^3M^{-1})
K_z	Hydraulic conductivity along the z-axis (LT^{-1})
l	Depth of pumping well (L)
M_f	Final mass in the REV, after dt (M)
M_i	Initial mass in the REV (M)
M_{in}	Mass entering the REV during dt (M)
M_{out}	Mass exiting the REV during dt (M)
n	Porosity (-)
NAF	Natural attenuation factor (-)
n_e	Effective porosity (-)
NOAEL	No-observed-adverse-effect level (T^{-1})
p	Pressure ($ML^{-1}T^{-2}$)
p_a	Partial pressure of a compound in the gas phase (MLT^{-2})
P_{vp}	Vapor pressure ($ML^{-1}T^{-2}$)
Q	Water discharge (L^3T^{-1})
q	Darcy velocity, apparent velocity, or specific discharge (LT^{-1})
R	Radius of influence (in Chaps. 3 and 4) (L)
R	Retardation factor (-)
r	Radial distance from the well (L)
r_c	Radius of the unslotted casing (L)
r_d	Distance beyond which the aquifer is undisturbed (L)
R_e	Distance beyond which the head variation is dissipated (L)
REV	Representative elementary volume
r_r	Distance from the real well (L)
r_w	Well radius (L)
S	Storativity or storage coefficient (-)
s	Drawdown (L)

s'	Residual drawdown (L)
S_b	Pseudo-skin factor (-)
s_D	Dimensionless function, solution of the diffusion equation
s_e	Effective solubility (ML^3)
S_k	Skin coefficient (-)
s_m	Measured stabilized drawdown (L)
S_r	Specific retention (-)
S_s	Specific storage (L^{-1})
S'_s	Specific storage of the aquitard (L^{-1})
S_w	Saturation (-)
S_y	Specific yield (-)
T	Temperature (H)
T	Transmissivity (L^2T^{-1})
t	Time (T)
t_s	Dimensionless parameter in Neuman's solution ($t_s = \frac{Tt}{S_r b^2}$) (-)
t_y	Dimensionless parameter in Neuman's solution ($t_y = \frac{Tt}{S_y r^2}$) (-)
UF	Uncertainty factor (-)
v	Seepage velocity or average linear velocity (LT^{-1})
v_c	Contaminant seepage velocity (LT^{-1})
V_s	Solid volume (L^3)
V_t	Total sample volume (L^3)
V_v	Pore volume (L^3)
V_w	Water volume (L^3)
V_{wg}	Volume of gravitational water (L^3)
V_{wr}	Volume of pendular (or residual) water (L^3)
$W(u; r=B)$	Hantush and Jacob's well function for leaky aquifers
$W(u)$	Theis' well function
Y_0	Bessel's function of the second kind and order 0
Y_1	Bessel's function of the second kind and order 1
z	Elevation (L)
z_D	Dimensionless depth in Neuman's solution (-)
a_L	Longitudinal dispersivity (L)
a_T	Transverse dispersivity (L)
b	Dimensionless parameter in Neuman's solution ($b = \frac{K_z}{K_r} \left(\frac{r}{b}\right)^2$) (-)
U	Force potential or potential energy (L^2T^{-2})
γ	Specific weight ($ML^{-2}T^{-2}$)
l	Dynamic viscosity ($ML^{-1}T^{-1}$)
ν	Kinematic viscosity (L^2T^{-1})
q	Density (ML^{-3})
r'	Effective stress ($ML^{-1}T^{-2}$)
r	Dimensionless parameter in Neuman's solution ($r = \frac{S}{S_y}$) (-)

Chapter 1

Basic Concepts



Abstract The largest source of human drinking water is stored and flows in the subsurface. Geological formations saturated in mobile groundwater that can be exploited for human use are called aquifers. This chapter introduces basic notions that set the ground for the understanding and description of subsurface water flow. First, the main properties of water are illustrated, with a particular focus on the forces it establishes with the solid matrix of a porous medium and on how these affect its mobility. Then, broad aquifer classifications are provided, based on their geographical location, their permeability characteristics as a function of the type of porosity (i.e., intergranular, fracture or karst), and their degree of confinement. The latter, which categorizes aquifers as unconfined, leaky or confined, has crucial implications on both their storage capacity and hydrodynamic behavior. The key parameters that characterize an aquifer's storage capacity are porosity and storativity. While the former is indicative of the total amount of water that can be stored within a porous medium, the latter indicates the fraction that can be released. Both these notions apply to any aquifer type although the mechanism of water release is distinct in unconfined and confined aquifers: in the former, water is released under the effect of gravity alone, and storativity is called specific yield; in the latter, water is released as a result of water expansion that follows a pressure drop. Subsurface water transport, instead, is driven by the existence of a hydraulic gradient (i.e., a drop in hydraulic head, or piezometric level). Under specific hypotheses, groundwater flow can be described by Darcy's law, which establishes a proportionality relationship between flow rate and hydraulic gradient, and can be used to map an aquifer's flow field. The relation defined by Darcy's law is measured by an aquifer-specific parameter called hydraulic conductivity. This parameter is crucial not only in the description of the transport capacity of a porous medium, but also in the calculation of its productivity, which is a function of the hydraulic conductivity and the thickness of an aquifer.

Aquifers are geological formations capable of storing water within their pores or fractures and of favoring its flow with a discharge sufficient to allow profitable human

exploitation. The water they store is called *groundwater*. This definition highlights a few key notions.

1. An aquifer is composed of two interacting phases: the permeable formation and water.
2. Three conditions must be simultaneously satisfied for an aquifer to be called as such:
 - storage capacity;
 - flow capacity;
 - potential for use as water supply.
3. In groundwater systems storage and flow capacity are considered in combination; this is in contrast to surface water systems, in which these properties are distinct (for instance, think of a water storage facility, such as a reservoir, and the surface water network that feeds it).

In the following paragraphs, key concepts such as aquifer storage, flow and release capacity, aquifer classification criteria, and leakage between aquifers will be introduced, along with a brief description of the parameters used to quantify them. In particular, the fundamental properties that define the storage and flow capacity of an aquifer are porosity and hydraulic conductivity, respectively.

A thorough understanding of these aquifer characteristics and of the properties of water is essential when dealing with issues that concern groundwater resources.

1.1 Water and its Properties

Water is a small asymmetrical molecule with a diameter of about $3 \cdot 10^{-10}$ m, composed of one oxygen and two hydrogen atoms. Each hydrogen atom forms a strong polar covalent bond with the oxygen atom (see Fig. 1.1). The term *covalent* refers to the electron pairs shared between the atoms that constitute the bond; whereas *polar* indicates that these electrons gravitate preferentially around the oxygen nucleus.

The asymmetrical structure of water (the two hydrogen atoms form an angle of about 105°) causes the barycenter of the positive and negative charges not to coincide and, in turn, the molecule to have a high dipole moment.

Thus, a water molecule behaves like a small dipole. Attraction forces over a thousand-fold stronger than gravity develop when a water molecule is in close proximity to other polarized molecules. These attraction forces may act between water molecules, forming polarized chains or particles, or between water molecules and solid grains constituting rock formations or aquifers, thus determining water-solid interactions.

The remarkable strength of the covalent bond that holds hydrogen and oxygen atoms together and its significant dipole moment are the reason for water's solvent capacity, fundamental to life. Water molecules are attracted to the majority of mineral compounds: in most cases, the attraction force is sufficient to break the bonds

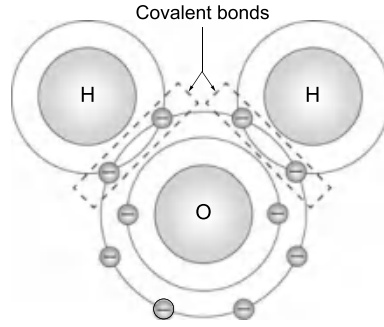


Fig. 1.1 Hydrogen and oxygen atoms configuration in a water molecule

between the atoms constituting other molecules. It is common to say that substances such as sodium chloride dissolve in water; more specifically, the oppositely charged components of these substances are no longer joined together because the attraction force between them is significantly reduced—by about 80 times—in water compared to vacuum, due to water’s high dielectric constant.

Of the known chemical elements, about half can be found dissolved in natural waters. This property is one of the essential factors of life on Earth since it allows and facilitates, for instance, nutrient exchanges in plants, animals and humans: roots would not be able to adsorb nutrients present in the soil (gases, minerals, etc.) if they weren’t dissolved in water.

The main properties of water are summarized in Table 1.1 as a function of temperature; for some of these, relations have been determined.

Perrochet [11], for instance, estimated the coefficients of the sixth order polynomial that most closely approximates the relation between density, ρ , and temperature, T , between 0 and 100 °C (Fig. 1.2):

$$\rho(T) = a + bT + cT^2 + dT^3 + eT^4 + fT^5 + gT^6, \quad (1.1)$$

where:

$$\begin{aligned} a &= 9.998396 \cdot 10^2 & b &= 6.764771 \cdot 10^2 & c &= -8.993699 \cdot 10^3 \\ d &= 9.143518 \cdot 10^5 & e &= -8.907391 \cdot 10^{-7} & f &= 5.291959 \cdot 10^{-9} \\ g &= -1.359813 \cdot 10^{-11}. \end{aligned}$$

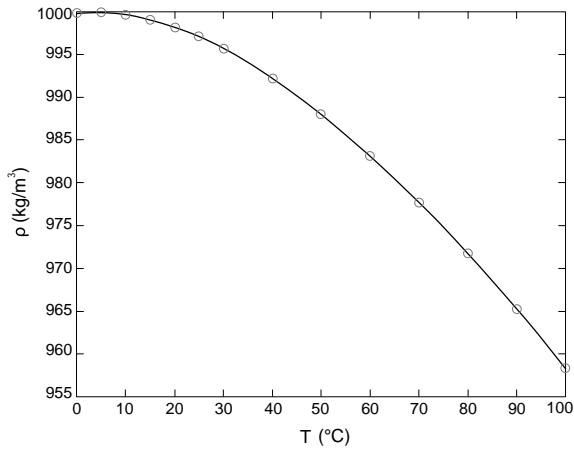
In Eq. (1.1) temperature is expressed in °C and the coefficient a represents the density of water at 0 °C.

From a rheological point of view, water is a Newtonian fluid. It is thus characterized by a linear relationship between shear stress and shear rate, whose slope is the dynamic viscosity. Mercer and Pinder [10], determined an empirical relation expressing dynamic viscosity, μ , of water as a function of temperature (Fig. 1.3):

$$\frac{1}{\mu(T)} = \frac{1 + 0.7063\zeta - 0.04832\zeta^3}{\bar{\mu}_0} \quad \text{where} \quad \zeta = \frac{T - 150}{100}. \quad (1.2)$$

Table 1.1 Values of main water properties at different temperatures

Temperature T (°C)	Density ρ (kg/m ³)	Specific weight γ (kN/m ³)	Dynamic viscosity μ (10 ⁻³ Pa·s)	Kinematic viscosity ν (10 ⁻⁶ m ² /s)	Vapor pressure P_{vp} (kPa)	Compressibility c_w (10 ⁻¹⁰ Pa ⁻¹)	Young's modulus E (10 ⁶ kPa)
0	9.805	999.8	1.781	1.785	0.61	5.098	2.02
5	9.807	1000.0	1.518	1.519	0.87	4.928	2.06
10	9.804	999.7	1.307	1.306	1.23	4.789	2.10
15	9.798	999.1	1.139	1.139	1.70	4.678	2.15
20	9.789	998.2	1.002	1.003	2.34	4.591	2.18
25	9.777	997.0	0.890	0.893	3.17	4.524	2.22
30	9.764	995.7	0.798	0.800	4.24	4.475	2.25
40	9.730	992.2	0.653	0.658	7.38	4.422	2.28
50	9.689	988.0	0.547	0.553	12.33	4.417	2.29
60	9.642	983.2	0.466	0.474	19.92	4.450	2.28
70	9.589	977.8	0.404	0.413	31.16	4.515	2.25
80	9.530	971.8	0.354	0.364	47.34	4.610	2.20
90	9.466	965.3	0.315	0.326	70.10	4.734	2.14
100	9.399	958.4	0.282	0.294	101.33	4.890	2.07

**Fig. 1.2** Water density as a function of temperature

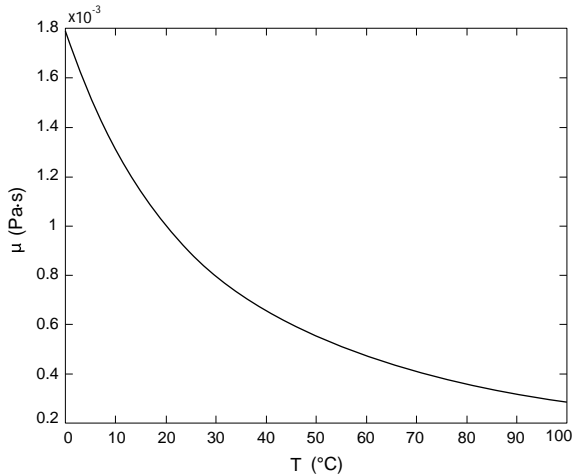


Fig. 1.3 Dynamic viscosity of water as a function of temperature

1.2 Groundwater

Water present in the ground interacts with the solid matrix of the formation and due to this can be mobilized more or less easily. On this basis it can be classified as gravitational (can be drained) or pendular (retained under gravity).

1.2.1 *Gravitational Water*

Gravitational water is the fraction of water present in the ground that can be drained under the sole effect of gravity. This is, therefore, the only portion of water that flows below the surface due to hydraulic gradients, be they natural or induced by the presence of water abstraction systems. All water used by man is gravitational water.

1.2.2 *Pendular Water*

Pendular water is the fraction of groundwater that adheres to the surface of an aquifer's solid matrix by forces more powerful than gravity, and that cannot, therefore, be mobilized in the field but only in the laboratory. Pendular water can be classified into three types: adsorbed (or hygroscopic), pellicular and capillary water.

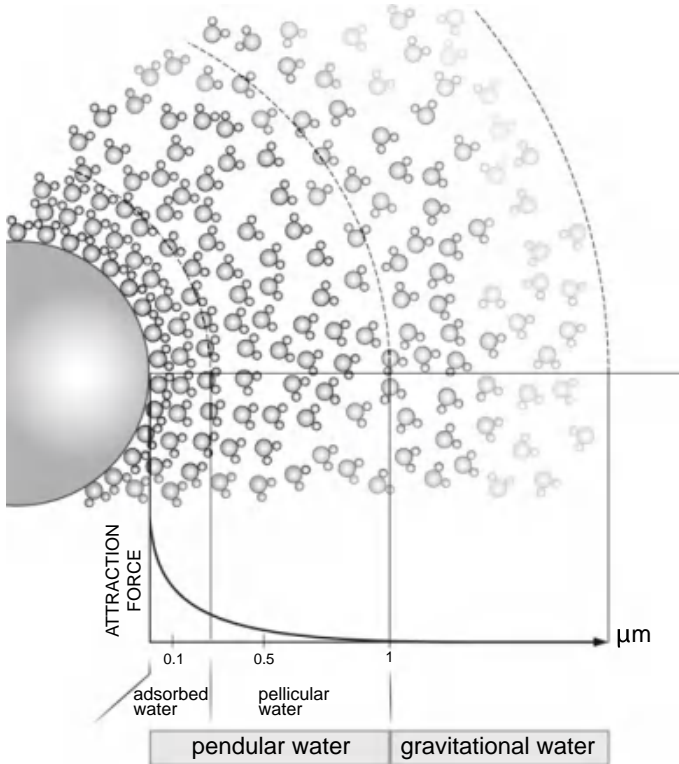


Fig. 1.4 Water-soil physical interaction

Hygroscopic or Adsorbed Water

A very thin layer (of the order of $0.1 \mu\text{m}$) of so-called hygroscopic water is formed around the solid grains due to molecular attraction forces, which can exceed $10^5 \times g$ (see Fig. 1.4). These are determined by the strong dipole moment of water molecules, and are so intense that hygroscopic water can only be released by heating an aquifer matrix sample above 100°C in the laboratory.

Pellicular Water

Molecular attraction forces decrease with distance from the grain surface. A pellicular water layer of about $1 \mu\text{m}$, held by molecular attraction forces of 1 to $10^5 \times g$, envelops the solid grains and the hygroscopic water (see Fig. 1.4). Pellicular water can be extracted from an aquifer sample by centrifugation in the laboratory.

Capillary Water

In addition to hygroscopic and pellicular fractions, also capillary water cannot be removed by gravity and is, therefore, considered a type of pendular water. It can be extracted in the laboratory by centrifugation. Capillary water is fixed in the smaller pores of the unsaturated matrix (the remaining pores are saturated by air) and can be continuous or suspended. The former constitutes the capillary fringe, located at the interface between saturated and unsaturated zones; the latter can be found in the unsaturated zone. Its presence is attributable to the capillary forces that originate at the contact surface between two non-miscible fluids (in this case water and air) and the solid matrix.

Table 1.2 summarizes the different types of water present in the ground, also depicted in Fig. 1.5.

Table 1.2 Types of water in the subsurface: exerted forces, extractability and availability (modified from [2])

Type of water		Acting forces	Available for	
			Extraction	Evapotranspiration
Hygroscopic		Molecular attraction	No (pendular water)	No
Pellicular				Yes
Capillary	Suspended			
	Continuous			
Gravitational		Gravity	Yes	

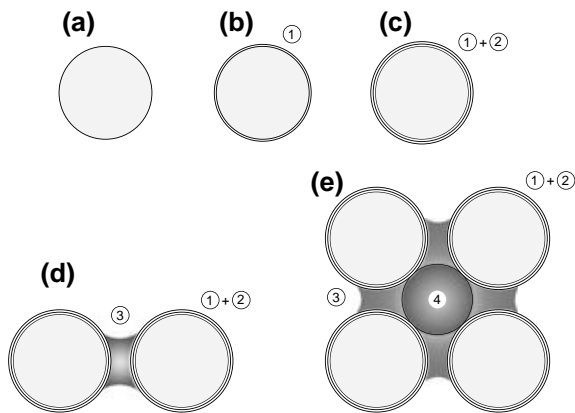


Fig. 1.5 Schematic representation of water in the subsurface: 1—hygroscopic water; 2—pellicular water; 3—capillary water; 4—gravitational water; **a** single solid grain; **b** grain surrounded by hygroscopic water; **c** single grain with hygroscopic and pellicular water; **d** two grains with capillary water generation; **e** porous medium containing gravitational water in the central part of the empty inter-granular space

Table 1.3 Aquifer classification criteria

Classification criteria	Classification	Main feature
Geographical location	Coastal	The aquifer is in contact with seawater
	Inland	There is no contact with seawater, but there could be with rivers, lakes, etc.
Permeability characteristics	Intergranular	Water circulates in the intergranular voids present between the grains of the formation
	Fractured or karst	Water flows mainly in fractures, fissures, joint voids that constitute the induced or secondary porosity system
Level of confinement	Unconfined	In static conditions, the water level in well coincides with the phreatic surface level
	Confined	The water level in well is higher than the aquifer's upper boundary
Hydrodynamic behavior	Unconfined with delayed draining	The aquifer is composed of well-graded permeable material and sits on a poorly permeable layer; atmospheric pressure is exerted on the phreatic surface
	Semi-confined	The aquifer is delimited by a semi-permeable formation
	Confined	The lower and upper boundary layers of the aquifer are impermeable formations

1.3 Aquifer Types and Classification Criteria

Having discussed the properties of groundwater and its microscale interactions with the solid matrix, we now approach it at the macroscale, i.e., at the aquifer level. Aquifers can be described and classified according to various parameters, which include geographical location, permeability characteristics, type and extent of confinement, and hydrodynamic behavior (see Table 1.3). The former two parameters are very intuitive and allow differentiation between coastal and inland, porous and fractured aquifers. Confinement, instead, refers to the upper and lower boundaries that enclose an aquifer, and affects the last criterion, hydrodynamic behavior.

A groundwater basin may contain one or more distinct aquifers separated by impermeable or poorly permeable layers. An *aquiclude* (or *aquifuge*) is a geological formation characterized by such low permeability that, despite being potentially capable of storing water, it does not allow its circulation. Clays are typical examples of aquicludes.

Conversely, an *aquitard* is a saturated formation with low permeability that cannot be used for water supply, but can allow water to flow between two adjacent aquifers

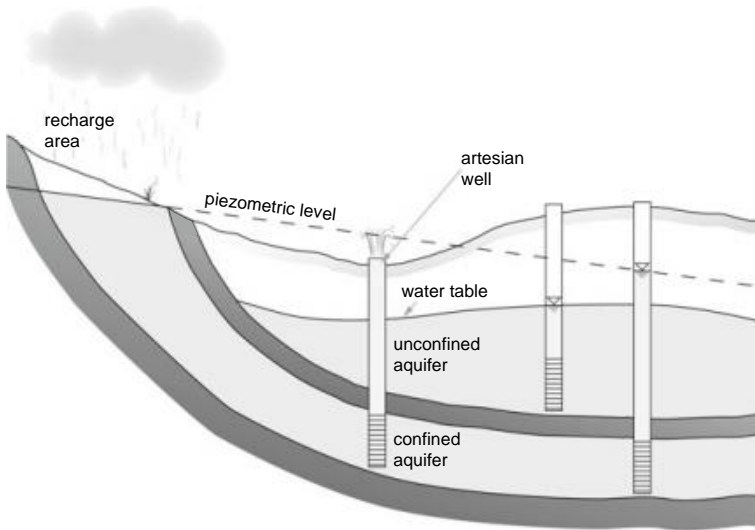


Fig. 1.6 Schematic representation of confined and unconfined aquifers

in response to dynamic hydraulic load variations, thus favoring the vertical recharge of the aquifer with a lower hydraulic load. Silt or silty-sand formations are classic examples of aquitards.

An aquifer is referred to as *confined* if both its upper and lower boundaries are aquicludes, as *leaky* (or *semi-confined*) if it is enclosed between an aquiclude and an aquitard. Confined and semi-confined aquifers are sometimes called *artesian*, since the water they store is under greater than atmospheric pressure (Figs. 1.6 and 1.7).

By contrast, aquifers without an upper boundary are called *unconfined* and are characterized by the fact that the water they contain is under atmospheric pressure. They are also called *water table* or *phreatic* aquifers (Fig. 1.6).

The extent of confinement reflects on the characteristics of groundwater flow, with each aquifer type exhibiting a different hydrodynamic behavior. This is evident from their response to the disturbance induced by pumping, as depicted in Fig. 4.4 in Chap. 4, in which the hydrodynamic behavior of aquifers is explained in detail and the differential equations used to describe flow and their analytical solutions are presented.

1.4 Hydraulic Head

The different pressure exerted on artesian and phreatic aquifers affects the level reached by water inside a well installed within them, called the *piezometric level*. In the case of an unconfined aquifer, the piezometric level coincides with the water table; in artesian aquifers, instead, the pressurized groundwater rises until it reaches

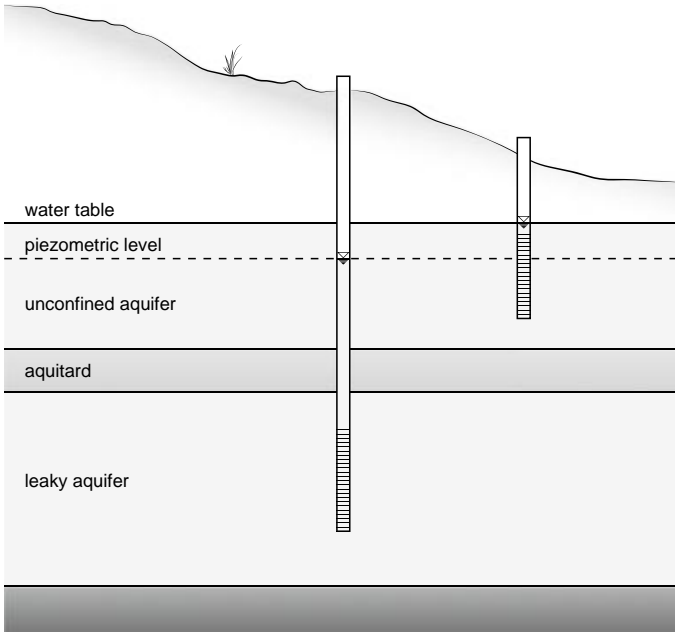


Fig. 1.7 Leaky (semi-confined) aquifer

equilibrium with the atmospheric pressure (see Figs. 1.6 and 1.7). The piezometric level is defined by, and coincides with, the hydraulic head, h , i.e., the total energy per unit weight of a water particle [6]:

$$h = \frac{v^2}{2g} + z + \frac{p}{g\rho}, \quad (1.3)$$

where $\frac{v^2}{2g}$, z , and $\frac{p}{g\rho}$ represent the kinetic, elevation and pressure components, respectively.

Given the slow velocity of groundwater, the kinetic term is negligible and the hydraulic head is reduced to the following:

$$h = z + \frac{p}{g\rho} = z + h_p, \quad (1.4)$$

where z represents the elevation head and h_p the pressure head at the point of measurement, with p being pressure, g gravity, and ρ density (see Fig. 1.8a) [1].

In addition to *hydraulic head*, the terms *potential energy* or *force potential* are often used. The force potential, Φ , is the fluid's energy per unit mass. The relation between potential energy and hydraulic head can be described as follows:

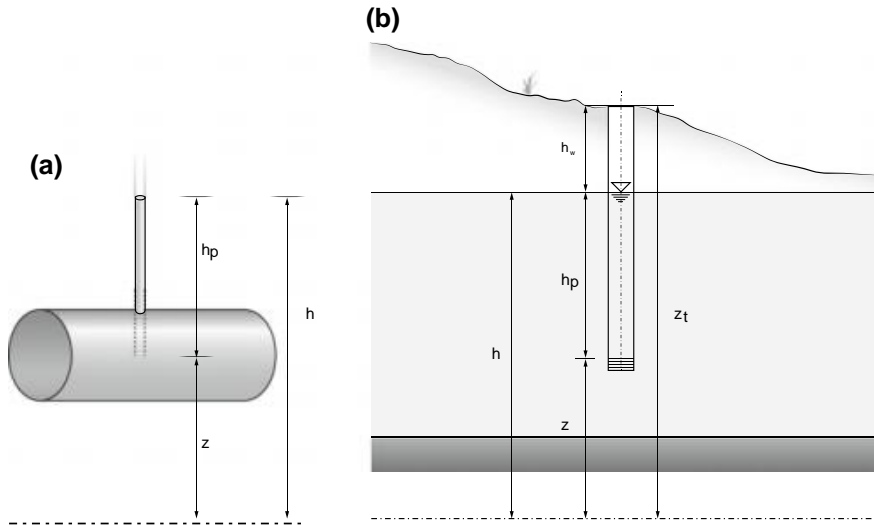


Fig. 1.8 **a** Schematic representation of the components of hydraulic head; **b** hydraulic head measurement

$$\Phi = gh = gz + \frac{p}{\rho}. \tag{1.5}$$

1.4.1 Field Measurements of the Hydraulic Head

Hydraulic head is gaged by measuring the depth to water in a well or in a piezometer (a narrow well installed for qualitative or quantitative monitoring of groundwater resources). Piezometers are open at the top and have a short screened section at the bottom to allow water to enter the pipe. It is essential for the observation well or piezometer to be screened only in the aquifer under investigation, while any aquifer present above it should be cased off [4].

Such measurements are carried out with a water level meter, i.e., a probe that emits a signal when the sensor reaches the water level (see Fig. 1.9).

The value of the hydraulic head is given by the piezometric level, H , calculated as the difference between the elevation at surface, z_t (usually relative to the mean sea level), and the depth to water measured in the piezometer, h_w (see Fig. 1.8).

$$H = z_t - h_w = h = z + h_p. \tag{1.6}$$

As we will see later in this chapter, hydraulic head is one of the main factors influencing groundwater flow (see Sect. 1.6), and its measurement can be used to

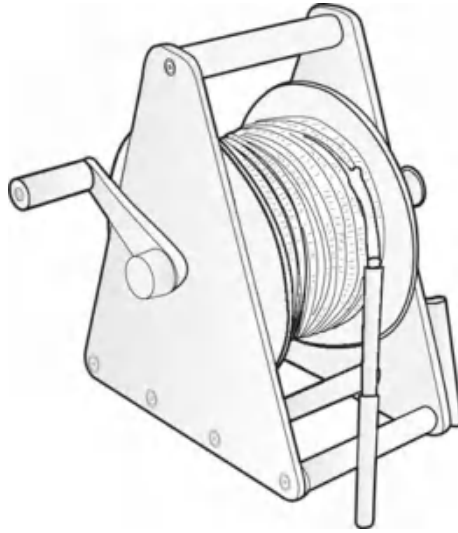


Fig. 1.9 Water level meter or phreatimeter

visually represent the directions and rates of flow (see Sect. 1.8.1). Before describing groundwater flow capacity, however, it is important to introduce the storage properties of an aquifer.

1.5 Storage and Release Capacity

The ability of a geological formation to store water is quantified by its porosity. The *porosity*, n , of an aquifer sample is defined as the ratio between its pore volume, V_v , and the sample's total volume V_t :

$$n = \frac{V_v}{V_t} = \frac{V_v}{V_v + V_s}, \quad (1.7)$$

with V_s being the solid volume of the sample.

In geotechnics an analogous property, the void ratio, e , is used:

$$e = \frac{V_v}{V_s}, \quad (1.8)$$

from which the following relations can be derived:

$$n = \frac{e}{1 + e}, \quad e = \frac{n}{1 - n}.$$

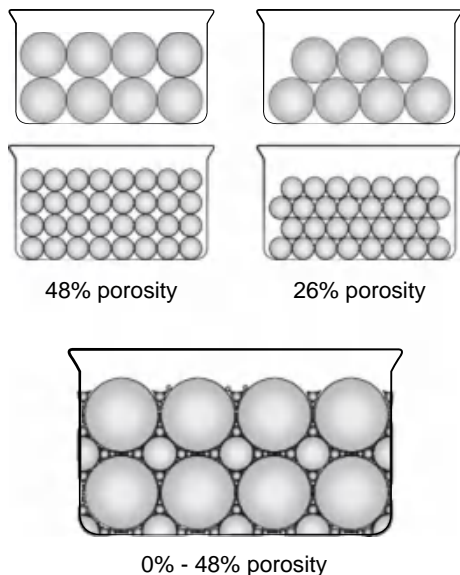


Fig. 1.10 Intergranular porosity: effect of grain arrangement and size heterogeneity

The value of porosity depends on the shape and size of the grains composing the matrix, on their arrangement, on the overburden pressure exerted on them, and on their mineralogical composition (Fig. 1.10). Porosity values range between 0 and 48%.

The concept of porosity is independent of the type of voids: in addition to intergranular (or primary) porosity, deriving from the spaces between solid grains, a formation can also have fracture porosity. Fracture porosity, also called secondary or induced porosity, is associated with fissure, fracture and joint voids induced by tectonic and/or chemical dissolution (karst processes), see Fig. 1.11.

Water tends to fill the space between the solid grains of the formation, and the ratio between the volume of water, V_w , contained in a sample and the corresponding pore volume, V_v , is called *saturation*, S_w :

$$S_w = \frac{V_w}{V_v}. \tag{1.9}$$

Like porosity, saturation can be expressed as a decimal fraction or as a percentage:

$$0 \leq S_w \leq 1 \quad \text{or} \quad 0 \leq S_w \leq 100\%, \text{ respectively.}$$

If we exclude the layer within which the phreatic surface of unconfined aquifers fluctuates, an aquifer is, by definition, a formation whose pores are completely filled

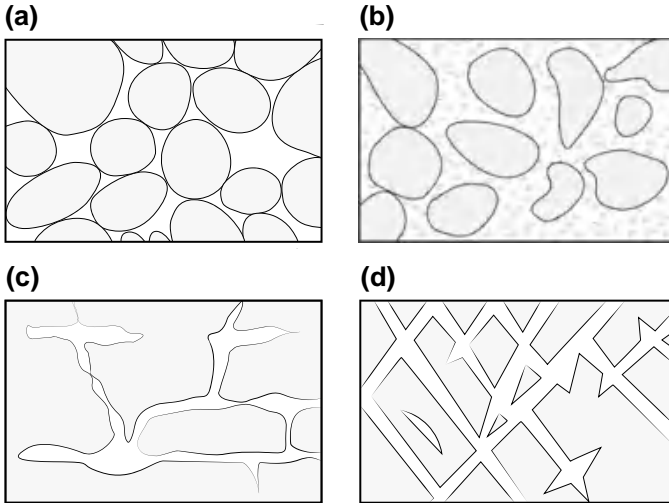


Fig. 1.11 Relation between granulometry and porosity: **a** poorly graded sediments with high porosity; **b** well graded sediments with low porosity; **c** rock with dissolution fractures (karst); **d** fractured rock

with water. Therefore, the saturation of an aquifer formation is equal to one, and for this reason it can also be referred to as a saturated porous medium.

Porosity quantifies the total water volume stored in an aquifer, but only a fraction of it can be exploited by man.

The ability of an aquifer to release water is quantified by its *storativity* (or *storage coefficient*), S , defined as the volume of water released by a portion of aquifer of any thickness per unit cross-sectional area and unit hydraulic head drop. Storativity is, therefore, a dimensionless parameter.

The above definition is independent of the type of aquifer and is, therefore, valid for both confined and unconfined aquifers. However, the water release mechanisms are significantly different, as depicted in Fig. 1.12 and described in the two following sections.

1.5.1 Storage in Unconfined Aquifers: Specific Yield and Retention

In the case of water-table aquifers, where water is only under atmospheric pressure (and hence is released under the sole effect of gravity drainage), storativity is often called *specific yield*, S_y , and the two terms are used interchangeably:

$$S = S_y. \quad (1.10)$$

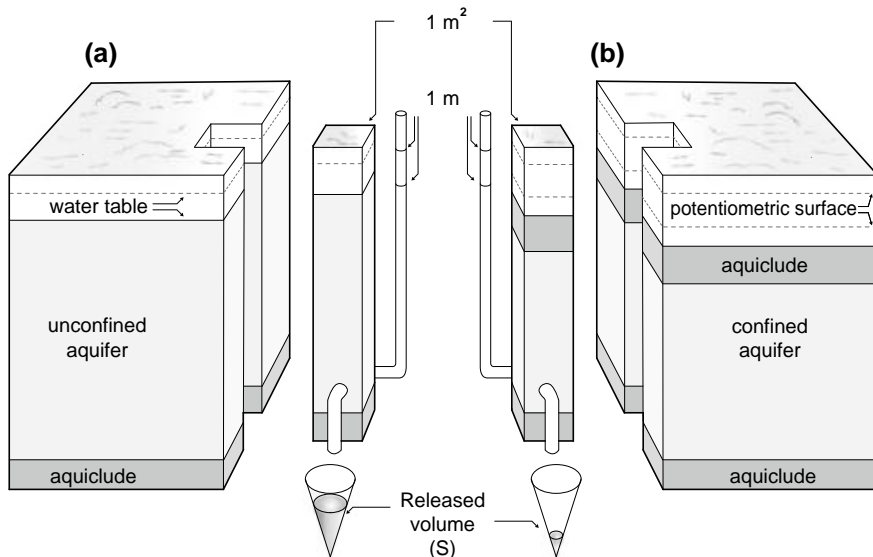


Fig. 1.12 Schematic representation of the concept of storage in **a** unconfined and **b** confined aquifers (modified from [8])

Sometimes, the specific yield is also referred to as *effective porosity*, n_e . Throughout this text, the term specific yield will consistently be used to refer to the storativity of unconfined aquifers, while the effective porosity is a parameter that will be used in the quantification of flow in both confined and unconfined aquifers (see Sect. 1.6). For further details, the reader may refer to more specialized literature such as [1].

The specific yield is defined as the ratio between the volume of water, V_{wg} , released by a saturated aquifer sample under gravity alone and the total sample volume. Its measurement should allow for enough time for the water to be released; a commonly used duration time is 24 h.

A saturated cubic sample with a volume of V_t has a specific yield of:

$$S_y = \frac{V_{wg}}{V_t}. \tag{1.11}$$

If $V_t = 1$, the specific yield coincides with the volume of water released under gravity; hence, the specific yield can be described as the volume of water released under gravity per unit aquifer volume. Table 1.4 shows some average specific yield values for different aquifers, normally in the range $S_y = S = 0.1 - 0.3$.

Only part of the water contained in the pores can be drained under gravity; the remaining amount constitutes the pendular (hygroscopic, pellicular and capillary) fraction of groundwater. The ratio between the volume of pendular (or residual) water, V_{wr} , and the total sample volume, V_t , is called specific retention, S_r :

Table 1.4 Average specific yield values (%) of the main lithologies in unconfined aquifers (modified from [9])

Lithology	Specific yield S_y		
	Maximum	Minimum	Average
Clay	5	0	2
Sandy clay	12	3	7
Silt	19	3	18
Fine sand	28	10	21
Medium sand	32	15	26
Coarse sand	35	20	27
Sand and gravel	35	20	25
Fine gravel	35	21	25
Medium gravel	26	13	23
Coarse gravel	26	12	22

$$S_r = \frac{V_{wr}}{V_t}. \quad (1.12)$$

Like porosity and specific yield, also specific retention can be expressed as a decimal fraction or as a percentage.

The larger the grain size, the smaller the specific retention and the greater the specific yield. In an aquifer, which is, as previously remarked, a saturated medium, the following relation is valid:

$$n = S_y + S_r. \quad (1.13)$$

1.5.2 Storage in Confined Aquifers

In confined aquifers water release that follows a decline in hydraulic head is caused by the expansion of water due to the pressure drop, as well as by the contraction of the solid matrix due to the increase in effective stress. The expansion of water can be expressed as follows:

$$dV_w = c_w n V_t dp = c_w n V_t \rho g dh, \quad (1.14)$$

while the solid matrix compaction can be described as:

$$dV_t = -c_f V_t d\sigma' = c_f V_t \rho g dh, \quad (1.15)$$

Table 1.5 Ranges of specific storage values for different lithologies in confined aquifers

Lithology	Specific storage $S_s(m^{-1})$
Clay	$2.0 \cdot 10^{-2} - 9.2 \cdot 10^{-4}$
Loose sand	$1.0 \cdot 10^{-3} - 4.9 \cdot 10^{-4}$
Compacted sand	$2.0 \cdot 10^{-4} - 1.3 \cdot 10^{-4}$
Sand and gravel	$1.0 \cdot 10^{-4} - 4.9 \cdot 10^{-5}$
Fractured rock	$6.9 \cdot 10^{-5} - 3.3 \cdot 10^{-6}$
Compact rock	$<3.3 \cdot 10^{-6}$

where c_w and c_f are the compressibilities of water (as a function of neutral pressures, see Table 1.1) and of the aquifer formation (as a function of effective stress, σ'), respectively.

If we define specific storage, S_s , as the volume of water released by an aquifer per unit volume and per unit hydraulic head drop:

$$S_s = \frac{\rho g}{V_t} \left(\frac{dV_t}{dh} + \frac{dV_w}{dh} \right) = \rho g(c_f + nc_w), \quad (1.16)$$

Typical values of specific storage in confined aquifers are in the range: $S = 10^{-2} - 10^{-5}$. In Table 1.5 the ranges of the parameter are reported for different aquifer lithologies.

Confined aquifer storativity, S can be described as the product of specific storage and the saturated thickness of the system, b :

$$S = S_s b = \rho g b(c_f + nc_w). \quad (1.17)$$

1.6 Flow Capacity

As mentioned in the introduction to this chapter, not only do aquifers store water, but they also favor its flow. Water flows in presence of an hydraulic gradient (whose magnitude, i , is the ratio of the head drop, Δh , over the length, L), in the direction from higher to lower hydraulic head values. The propensity of an aquifer to allow water circulation is measured by the hydraulic conductivity, K .

1.6.1 Darcy's Law

Darcy's law [1, 3, 6] defines the linear relationship between the water discharge, Q , passing through a porous medium of cross-section, A , and the hydraulic gradient, i , see Fig. 1.13:

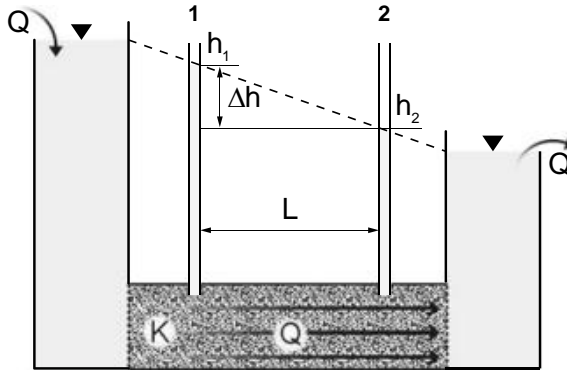


Fig. 1.13 Laboratory device used to verify Darcy's law

$$Q = KA \frac{\Delta h}{L} = K A i, \quad (1.18)$$

Darcy's law is an empirical equation valid in steady state. Its validity relies on the following conditions:

- flow is laminar (i.e., Reynold's number is less than one);
- the system is totally saturated by a single fluid;
- there are no physical or chemical interactions between the fluid and solid phases.

1.6.2 Hydraulic Conductivity and Permeability

Hydraulic conductivity can be defined as the water discharge that flows through a unit cross-sectional area of a porous medium under the effect of a unit hydraulic gradient, at 20 °C. It has the physical dimension of a velocity, so in the SI it is measured in m/s. The hydraulic conductivity of a porous medium varies between 10 and 10^{-9} m/s (see Fig. 1.14), although the most frequent values found in aquifers range between 10^{-1} and 10^{-6} m/s, which still spans five orders of magnitude.

From Darcy's law one can derive the Darcy velocity or specific discharge, q (apparent velocity):

$$q = \frac{Q}{A} = K i. \quad (1.19)$$

Given that part of the cross-sectional area through which flow takes place is partially occupied by the solid matrix, the velocity at which water is actually moving, called seepage velocity, v (also referred to as average linear velocity or interstitial velocity), is [7]:

$$v = \frac{q}{n_e} = \frac{K i}{n_e}, \quad (1.20)$$

K (m/s)		10^1 10^0 10^{-1} 10^{-2} 10^{-3} 10^{-4} 10^{-5} 10^{-6} 10^{-7} 10^{-8} 10^{-9} 10^{-10} 10^{-11}										
GRANULOMETRY	homogeneous	Gravel			Sand		Very fine sand		Silt		Clay	
	varied	Medium and coarse gravel		Gravel and sand		Sand and clay						
PERMEABILITY LEVEL		HIGH				LOW				NONE		
FORMATION TYPE		PERMEABLE				SEMI-PERM.				IMPERM.		

Fig. 1.14 Hydraulic conductivity values for different natural systems as a function of their lithology and granulometry

where n_e is the effective porosity with respect to flow. n_e expresses the fraction of porosity available for groundwater flow, and is always less than the total porosity, n [1]. For unconfined aquifers $n_e \approx S_y$.

Often, in common speech the term *permeability* is used instead of hydraulic conductivity. However, it should be noted that permeability is, even dimensionally, a distinct physical property, although a relation of direct proportionality exists between the two parameters.

The relation between hydraulic conductivity, K , and intrinsic permeability (often simply called permeability), k , is the following:

$$K = \frac{\rho g k}{\mu}, \tag{1.21}$$

where g is gravitational acceleration, ρ is the density of the fluid, and μ is its dynamic viscosity. Physical dimension analysis shows that permeability has the dimensions of a length to the power of two, and is, therefore, measured in m^2 in the SI. However, the values of permeability in nature are much smaller than this measure; therefore, for practical applications a custom unit is used, the *darcy*:

$$1 \text{ darcy} = 0.987 \cdot 10^{-12} \text{ m}^2.$$

By applying Eq. (1.21) the following relation can be derived:

$$k = 1 \text{ darcy} \rightarrow K \sim 10^{-5} \text{ m/s} = 10^{-3} \text{ cm/s}.$$

It is important to note that absolute permeability is an intrinsic property of a porous medium, while hydraulic conductivity depends also on the properties of the fluid under consideration, as it is a function of its density and dynamic viscosity, the latter being also strongly affected by temperature (water is usually considered at 20 °C).

Up to now, we have only referred to unidimensional flow, analogous to the one that can be reproduced in the laboratory with equipment similar to that used to ver-

ify Darcy's law. In order to generalize the concept of flow, and extend it to a three dimensional geometry, one must take account of the fact that due to the nature of deposition processes, hydraulic conductivity can take on different values depending on the direction of measurement: in particular, horizontal is usually greater than vertical hydraulic conductivity. This implies that hydraulic conductivity, unlike porosity, isn't a scalar but a tensor.

Therefore, Darcy's law can be expressed in vectorial terms as follows:

$$\mathbf{q} = -\mathbf{K} \nabla h, \quad (1.22)$$

with

$$\mathbf{K} = \begin{pmatrix} K_{xx} & K_{xy} & K_{xz} \\ K_{yx} & K_{yy} & K_{yz} \\ K_{zx} & K_{zy} & K_{zz} \end{pmatrix}, \quad (1.23)$$

being the hydraulic conductivity tensor, and $K_{xy} = K_{yx}$, $K_{xz} = K_{zx}$, and $K_{yz} = K_{zy}$.

Assuming the Cartesian coordinate system coincides with the direction of the eigenvectors of the \mathbf{K} matrix (basically, assuming that one of the Cartesian axes coincides with the direction of maximum permeability), the hydraulic conductivity tensor is reduced to the three entries of the main diagonal:

$$\mathbf{K} = \begin{pmatrix} K_{xx} & 0 & 0 \\ 0 & K_{yy} & 0 \\ 0 & 0 & K_{zz} \end{pmatrix}, \quad (1.24)$$

and the components of the Darcy velocity are:

$$\begin{aligned} q_x &= -K_{xx} \frac{\partial h}{\partial x}, \\ q_y &= -K_{yy} \frac{\partial h}{\partial y}, \\ q_z &= -K_{zz} \frac{\partial h}{\partial z}. \end{aligned} \quad (1.25)$$

An aquifer with $K_{xx} \neq K_{yy} \neq K_{zz}$ is called anisotropic; if, instead, the values coincide (although this is often an approximation) it is called isotropic.

An aquifer is called heterogeneous if its properties (porosity, hydraulic conductivity, etc.) vary from point to point in the spatial domain; while it is called homogeneous if the values of such properties are constant [1].

Combining the two concepts, it follows that an aquifer can be homogeneous and isotropic, homogeneous and anisotropic, or heterogeneous and anisotropic.

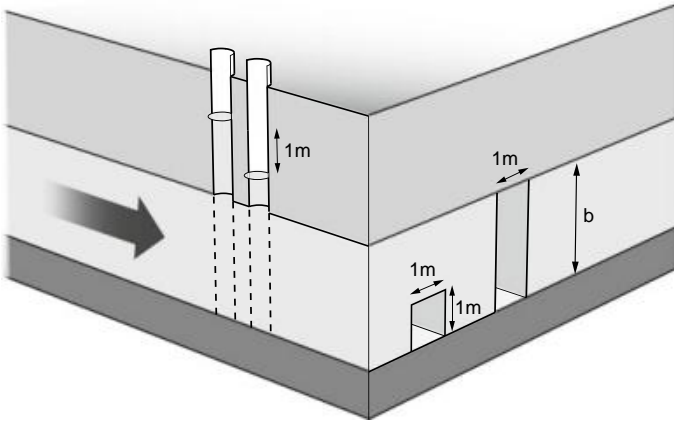


Fig. 1.15 Difference between hydraulic conductivity and transmissivity (modified from [5])

1.6.3 Transmissivity

Although it is an important parameter for defining the flow capacity of a porous medium, hydraulic conductivity alone is not sufficient to define an aquifer's productivity. Clearly, given the same hydraulic conductivity, a 100 m thick aquifer can yield a much greater discharge than one that is 10 m thick. It is, therefore, necessary to introduce a property that takes into account both the hydraulic conductivity and the thickness of an aquifer. This value is the transmissivity, T , defined as the integral of the hydraulic conductivity over the aquifer's thickness, b :

$$T = \int_0^b K dz. \quad (1.26)$$

If the hydraulic conductivity can be considered constant along the entire thickness of an aquifer, of course:

$$T = K \cdot b. \quad (1.27)$$

Hence, transmissivity, which measures the productivity of an aquifer, dimensionally is a length to the power of two divided by a time, and is therefore measured in m^2/s in the SI. The value of an aquifer's transmissivity is normally between 10^{-1} and $10^{-5} \text{ m}^2/\text{s}$.

Figure 1.15 highlights the difference between hydraulic conductivity and transmissivity from a practical standpoint.

1.7 Leakage Between Different Aquifers

As previously mentioned, in dynamic conditions a leaky aquifer can be fed by a vertical flow through the confining aquitard.

The (usually vertical) flow per unit area transferred across a reduced permeability layer is called leakage, which can be quantified as follows:

$$\frac{Q_v}{A} = \frac{K'(h_0 - h)}{b'} = c(h_0 - h), \quad (1.28)$$

with Q_v being the vertical recharge flow rate, A is the area, h_0 the hydraulic head of the feeding aquifer, h the hydraulic head of the semi-confined aquifer, c the leakage coefficient of the aquitard (defined as the ratio between its hydraulic conductivity, K' , and its thickness, b').

For practical purposes, a parameter called leakage factor, B , is often used to quantify the leakage capacity between two neighboring aquifers, defined as the square root of the ratio between the transmissivity of the semi-confined aquifer and the leakage coefficient of the aquitard:

$$B = \sqrt{\frac{T}{c}} = \sqrt{\frac{Kbb'}{K'}}. \quad (1.29)$$

The leakage factor has the dimensions of a length and usually falls between 30 and 3000 m.

Since c is in the denominator of expression (1.29), the leakage factor is inversely proportional to the leakage; the greater the value of B , the greater the degree of confinement of an aquifer.

1.8 Field Applications of Darcy's Law

Understanding water movement in the ground is an essential requirement for any investigation focusing on groundwater resources. A first step to this end is to derive groundwater flow directions and rates, which can be represented graphically in flow field maps.

1.8.1 Potentiometric Surface and Flow Field Mapping

The surface representing the piezometric level (and, thus, the hydraulic head) of groundwater is called potentiometric surface: this term can be applied to both confined and unconfined aquifers. In the case of unconfined aquifers, the potentiometric surface coincides with the water table.

In order to derive the potentiometric surface the piezometric level should be measured in as many points as possible (see Sect. 1.4.1). Ideally, these measurements should be taken at the same time, to avoid inaccuracies related to groundwater level fluctuations.

If a potentiometric surface is approximated to a plane (the simplest type of surface), three data points are the minimum number necessary to define it. With more than three data points, the represented surface is more reliable and is created using a series of triangles or quadrilaterals that cover the entire measurement area. Figure 1.16 illustrates the simple interpolation method used to produce a map of the potentiometric surface.

A contour map of the potentiometric surface is called potentiometric map (see Fig. 1.17) and is created using a great number of data points and projecting *equipotential lines* onto the horizontal plane. Equipotential lines connect points of equal hydraulic head (and hence of equal piezometric level). Potentiometric maps usually also provide information on the direction of groundwater flow, represented by *flow lines*. These are imaginary lines describing the flow paths of water particles that move in an aquifer. The network of flow and equipotential lines of a section of an aquifer is called *flow net*.

In isotropic aquifers, flow lines cross equipotential lines at a right angle; conversely, in anisotropic aquifers, flow and equipotential lines intersect at an angle which depends on the degree of anisotropy (see Fig. 1.18).

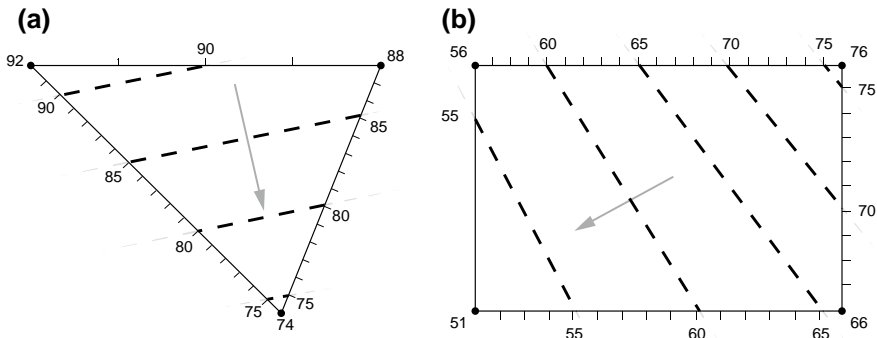


Fig. 1.16 Interpolation method to contour equipotential lines and determine the hydraulic gradient and flow direction when **a** three or **b** four data points available

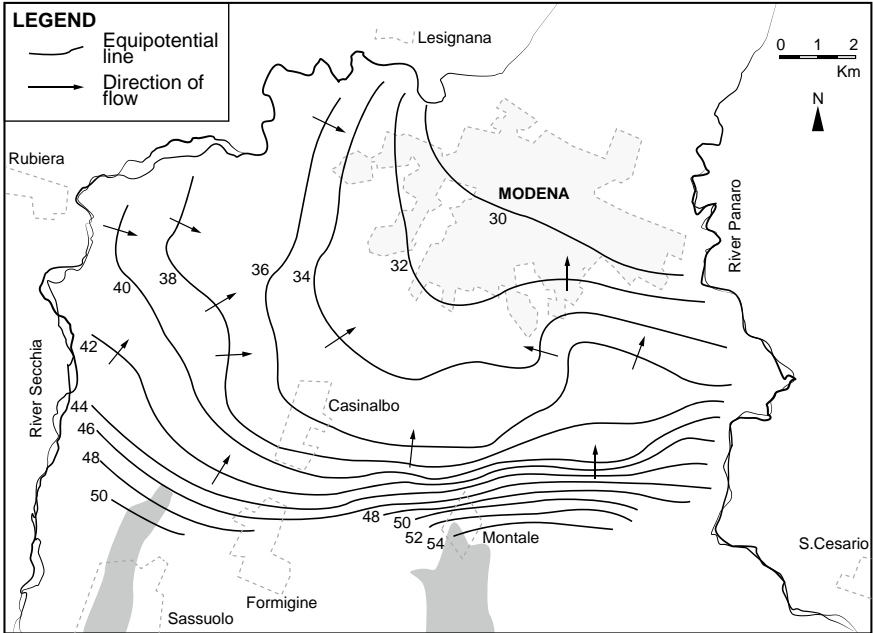


Fig. 1.17 Example of a potentiometric map

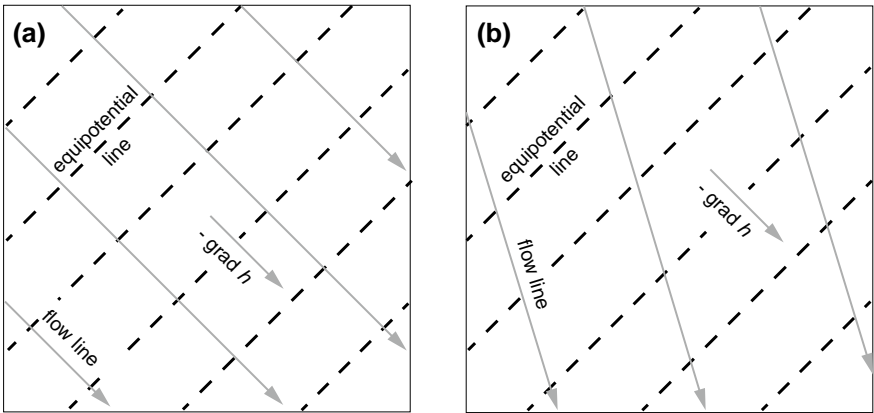


Fig. 1.18 Relation between flow and equipotential lines in a isotropic and b anisotropic aquifers (modified from [7])

The modulus of the hydraulic gradient between two equipotential lines $i = |\nabla h| = \frac{\Delta h}{\Delta l}$ is calculated by dividing the hydraulic head contour interval Δh by the distance Δl measured perpendicularly to the two lines. Groundwater flows from higher to lower hydraulic head; thus, the direction of flow is opposite to that of the hydraulic gradient. By convention, during potentiometric surface map construction, the contour interval is usually set to be constant; therefore, closely spaced equipotential lines indicate a greater hydraulic gradient than farther spaced lines.

References

1. J. Bear, *Dynamics of Fluids in Porous Media* (Courier Corporation, 1972)
2. P. Celico, *Prospezioni idrogeologiche* (Liguori, Napoli, 1986)
3. H. Darcy, *Les fontaines publiques de la ville de Dijon* (Dalmont, 1856)
4. P.A. Domenico, F.W. Schwartz, *Physical and Chemical Hydrogeology* (Wiley, 1998)
5. J. Ferris, D. Knowles, R. Brown, R. Stallman, *Theory of Aquifer Tests*. USGS Numbered Series 1536-E (U.S. Government Print. Office, 1962)
6. C.W. Fetter, *Contaminant Hydrogeology* (Macmillan Publishing Company, 1993)
7. C.W. Fetter, *Applied Hydrogeology (English)*, 4th edn. (Pearson Education, Long Grove, 2014)
8. R.C. Heath, *Basic Ground-Water Hydrology (tech. rep.)*, vol. 2220 (U.S. Geological Survey, 1983)
9. A. Johnson, *Specific Yield: Compilation of Specific Yields for Various Materials*. USGS Numbered Series 1662-D (U.S. Government Printing Office, Washington, DC, 1967)
10. J.W. Mercer, G.F. Pinder, Finite element methods in flow problems, in *Finite Element Analysis of Hydrothermal Systems* (ed. Oden J.T. et al), Proceedings of 1st Symposium (University of Alabama Press, Swansea, 1974), pp. 401–414
11. P. Perrochet, Personal communication, EPFL Lausanne. GEOLEP Laboratoire de géologie, Lausanne (Switzerland), in *Feflow Reference Manual H.-J.G. Diersch* (WASY GmbH, 1996)

Chapter 2

The Groundwater Flow Equation



Abstract In this chapter, the differential groundwater flow equation that governs the distribution of the flow directions and rates in an aquifer is derived. The problem is examined at a macroscopic scale, neglecting an analysis of detailed solid–liquid interface distribution, which would entail excessive analytical and computational complexity, without contributing useful information from an operational standpoint. The equation is thus determined as a combination of the equations that express the law of mass conservation (whose terms are described for a representative elementary volume), Darcy’s law, and the storage variation due to changes in hydraulic head. Unsteady state groundwater flow in each aquifer type is described by a different equation, each defining the Laplacian of the hydraulic head as a function of the aquifer’s storage and transport capacity, and of the hydraulic head’s partial derivative with respect to time. In particular, in the case of confined aquifers, flow is a function of specific yield and transmissivity, as is the case even for leaky aquifers, whose hydrodynamic behavior is, however, also affected by the leakage between aquifers (quantified by the leakage factor). A rigorous description of flow in unconfined aquifers would require a nonlinear and nonhomogeneous differential equation due to the inclination of the water table with flow; however, under simplifying conditions an approximate description, analogous to the confined aquifer equation, can be defined as a function of specific yield and transmissivity.

Solving any flow problem, analytically or numerically, entails understanding the equations that govern the directions and rates of flow; in other words, determining the spatial distribution of hydraulic head and flow velocity in an aquifer.

2.1 Derivation of the Equation of Continuity

Flow through a porous medium could be analyzed at the microscale by solving the Navier–Stokes equations. However, the complexity of the domain would involve

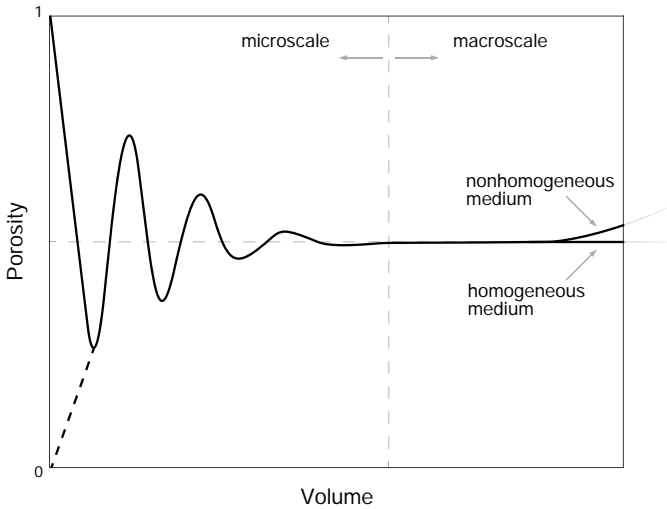


Fig. 2.1 Influence of volume size on average porosity

excessive computational costs and would be, overall, pointless from a practical point of view. It is, therefore, necessary to use a macroscopic approach that neglects the details about the solid–liquid interface distribution. The latter information can be incorporated into upscaled coefficients included in the flow equations, which provide a sufficiently accurate description of the system for practical purposes [1].

The first step in the transition from a discrete microscopic model to a continuous model, is the identification of a representative volume of the porous medium within which its characteristic properties can be averaged, yielding so-called macroscopic properties. The Representative Elementary Volume (REV) should be large enough not to display microscale variations, but small enough to reflect the local variability of macroscopic properties (Figs. 2.1 and 2.2).

The continuity equation can be derived by applying the the law of mass conservation to the REV under consideration:

$$M_{out} - M_{in} = M_i - M_f, \quad (2.1)$$

with M_{in} and M_{out} being, respectively, the mass of water flowing in and out of the REV during the time interval dt ; and $M_i - M_f$ being the change of water mass (initial minus final mass) in the same REV, during the time interval dt . Analytically, these terms can be described as follows:

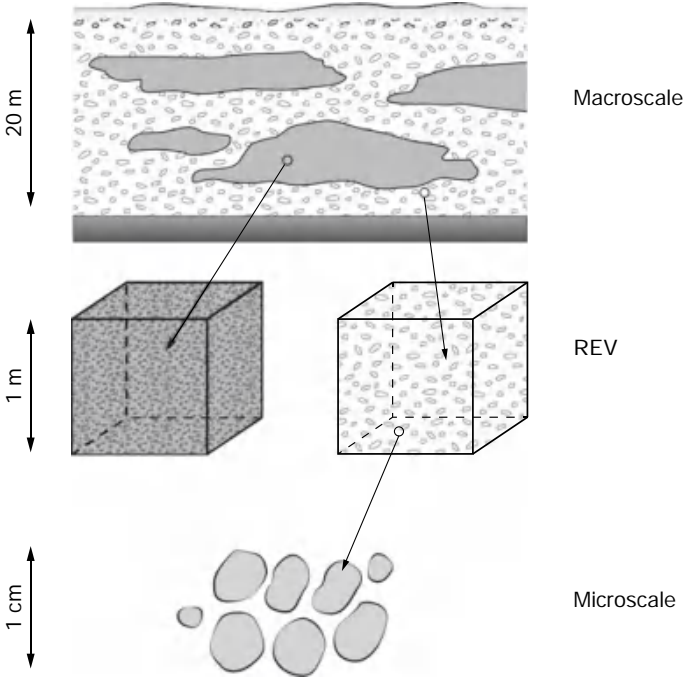


Fig. 2.2 Representative Elementary Volume and heterogeneity range in a porous medium

$$\begin{aligned}
 M_{in} &= (\rho q_x dydz + \rho q_y dx dz + \rho q_z dx dy) dt, \\
 M_{out} &= \left[\rho q_x + \frac{\partial}{\partial x} (\rho q_x) dx \right] dydzdt + \left[\rho q_y + \frac{\partial}{\partial y} (\rho q_y) dy \right] dx dzdt + \\
 &\quad + \left[\rho q_z + \frac{\partial}{\partial z} (\rho q_z) dz \right] dx dy dt, \\
 M_i &= \rho n dx dy dz, \\
 M_f &= \left[\rho n + \frac{\partial}{\partial t} (\rho n) dt \right] dx dy dz,
 \end{aligned}$$

with ρ being water density, n porosity, and q_x , q_y , and q_z the components of flow velocity along the three coordinate axes.

Therefore, by applying the mass balance expressed in Eq. (2.1) to the above expressions, the equation of continuity becomes:

$$\frac{\partial}{\partial x} (\rho q_x) + \frac{\partial}{\partial y} (\rho q_y) + \frac{\partial}{\partial z} (\rho q_z) = -\frac{\partial}{\partial t} (\rho n), \quad (2.2)$$

which can be written in the following, more compact form:

$$\frac{\partial}{\partial t} (\rho n) = -\nabla \cdot (\rho \mathbf{q}), \quad (2.3)$$

or

$$\frac{\partial}{\partial t} (\rho n) = -\mathbf{div} (\rho \mathbf{q}). \quad (2.4)$$

2.2 The Groundwater Flow Equation

The groundwater flow equation governs the distribution of flow directions and rates in an aquifer. It combines the equations that express the law of mass conservation, Darcy's law, and the storage variation due to changes in hydraulic head [2]:

$$\nabla \cdot (\rho \mathbf{q}) = -\frac{\partial}{\partial t} (\rho n), \quad (2.5)$$

$$\mathbf{q} = -\mathbf{K} \nabla h, \quad (2.6)$$

$$\frac{\partial}{\partial t} (\rho n) = \rho S_s \frac{\partial h}{\partial t}, \quad (2.7)$$

with \mathbf{K} being the hydraulic conductivity tensor, S_s the specific storage, ρ the density of water.

In the case of leaky aquifers, which are fed by an external source, an additional term, accounting for leakage (see Eq. 1.28 in Sect. 1.7), must be added to the previous equations:

$$\frac{Q_v}{A} = \frac{K' (h_0 - h)}{b'} = c (h_0 - h),$$

from which the following equation can be derived by dividing both terms by the transmissivity, T :

$$\frac{Q_v}{AT} = \frac{h_0 - h}{B^2}, \quad (2.8)$$

where B represents the leakage factor, with units of length (L).

Combining the above equations and multiplying the terms by the saturated thickness, the groundwater flow equation is derived:

$$\text{for confined aquifers } \nabla^2 h = \frac{S}{T} \cdot \frac{\partial h}{\partial t}, \quad (2.9)$$

$$\text{for leaky aquifers } \nabla^2 h - \frac{(h_0 - h)}{B^2} = \frac{S}{T} \cdot \frac{\partial h}{\partial t}, \quad (2.10)$$

$$\text{for unconfined aquifer, to a first approximation } \nabla^2 h = \frac{S_y}{T} \cdot \frac{\partial h}{\partial t}. \quad (2.11)$$

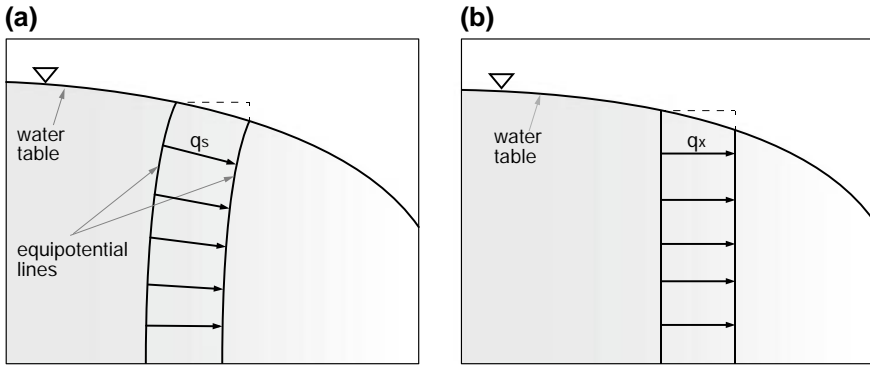


Fig. 2.3 Deformation of equipotential and flow lines in unconfined aquifers: **a** actual situation; **b** approximation made by Eq. (2.11)

In the previous equations, ∇^2 is the Laplace operator (or Laplacian), which can be formally expressed as follows, according to the flow geometry:

- *One-dimensional flow*

$$\nabla^2 = \frac{\partial^2}{\partial x^2};$$

- *Two-dimensional flow*

$$\nabla^2 = \frac{\partial^2}{\partial x^2} + \frac{\partial^2}{\partial y^2} \text{ in the horizontal plane,}$$

$$\nabla^2 = \frac{\partial^2}{\partial x^2} + \frac{\partial^2}{\partial z^2} \text{ in the vertical plane,}$$

$$\nabla^2 = \frac{\partial^2}{\partial r^2} + \frac{1}{r} \cdot \frac{\partial}{\partial r} = \frac{1}{r} \cdot \frac{\partial}{\partial r} \left(r \frac{\partial}{\partial r} \right) \text{ in a polar coordinate system (characterized by radial symmetry);}$$

- *Three-dimensional flow*

$$\nabla^2 = \frac{\partial^2}{\partial x^2} + \frac{\partial^2}{\partial y^2} + \frac{\partial^2}{\partial z^2} \text{ in a generic three-dimensional geometry,}$$

$$\nabla^2 = \frac{\partial^2}{\partial r^2} + \frac{2}{r} \frac{\partial}{\partial r} = \frac{1}{r^2} \cdot \frac{\partial}{\partial r} \left(r^2 \frac{\partial}{\partial r} \right) \text{ in a spherical coordinate system.}$$

Equations (2.9), (2.10) and (2.11) are valid for unsteady—or transient—flow; in a steady state the term $\frac{\partial h}{\partial t}$ can simply be set equal to zero.

A rigorous description of flow in an unconfined aquifer entails the use of a non-linear and nonhomogeneous differential equation; therefore, it is approximated with Eq. (2.11), analogous to the confined aquifer equation (2.9). The complexity of the rigorous differential equation for unconfined aquifers results from the inclination of the water table, which causes equipotential lines not to be straight (see Fig. 2.3). Thus, a vertical component of velocity is induced, and transmissivity ceases to be constant, as a consequence of decreasing saturated thickness with increasing proximity to the well.

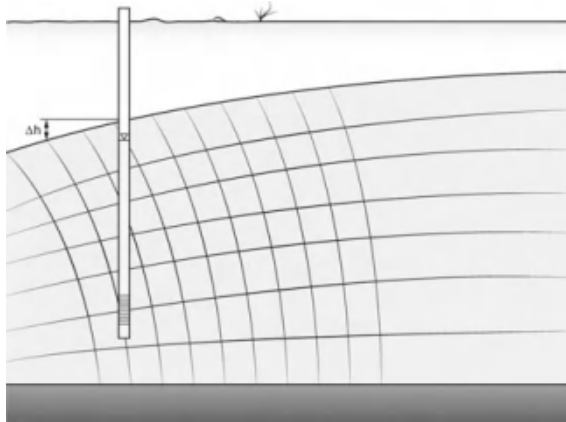


Fig. 2.4 Influence of partial penetration of a monitoring well on the piezometric level reading in an unconfined aquifer. In this specific case, this partially screened well would provide a smaller hydraulic head value than if it were fully penetrating (screened over the entire saturated thickness)

The smaller the water table inclination, the more the approximation is acceptable and the vertical component of velocity negligible. For those cases in which the approximation applied by Eq. (2.11) is not acceptable, and in particular for the solution of flow problems in the proximity of pumping wells, please refer to Sect. 3.3.1.

The inclination of the water table has important implications from a practical perspective: the piezometric level measured in a partially penetrating monitoring well completed in an unconfined aquifer depends on the depth of the screened section (see Fig. 2.4).

References

1. J. Bear, *Dynamics of Fluids in Porous Media* (Courier Corporation, North Chelmsford, 1972)
2. P.A. Domenico, F.W. Schwartz, *Physical and Chemical Hydrogeology* (Wiley, New York, 1998)

Chapter 3

Analytical Solutions of the Groundwater Flow Equation



Abstract The differential groundwater flow equation derived in Chap. 2 can be solved analytically in various geometries, provided that certain hypotheses are satisfied. In this chapter, a polar coordinate system with radial geometry, describing the radial groundwater flow towards a well, is considered. The hypotheses underlying the analytical solutions concern the aquifer's geometry (constant thickness, homogeneity and isotropy, unlimited horizontal extension, initially horizontal potentiometric surface) and the pumping well (fully penetrating, infinitesimal radius, negligible storage, laminar flow and constant pumping rate). Steady state and transient analytical solutions, respectively describing the drawdown as a function of the distance from the well (r), or of r and time, are provided for confined, leaky and unconfined aquifers. Theis' (and Cooper and Jacob's approximation) and Thiem's equations describe, respectively, the transient and steady state solutions of the groundwater flow equation for confined aquifers. Hantush and Jacob, instead, derived the transient analytical solution for leaky aquifers, while De Glee formalized the steady state solution. In the case of unconfined aquifers, the steady state solution formally coincides, except for an adjustment to the drawdown, to Thiem's solution. The transient solution was, instead, derived by Neuman, under specific simplifying hypotheses, given that a fully rigorous description of flow in unconfined aquifers would entail the use of a nonlinear and nonhomogeneous differential equation due to the inclination of the water table with pumping and the generation of a vertical component of flow velocity.

Groundwater flow towards a well can be described as a radial flow problem, and thus can be analyzed in a polar coordinate system with radial symmetry. This is a one-dimensional coordinate system in which flow lines are straight and converge towards the well axis (see Fig. 3.1), the flow configuration is identical in every plane, whatever its elevation.

In order for a radial flow model to offer an appropriate description of the system, the following two conditions must be respected simultaneously [5, 6]:

- (a) aquifer thickness is constant;
- (b) the well is fully penetrating (i.e., screened over the entire saturated thickness of the aquifer).

Regardless of geometry, the groundwater flow equation can only be solved analytically if the following hypotheses can be considered valid for the system under investigation:

- (c) the aquifer is homogeneous and isotropic;
- (d) the aquifer is unlimited in size on the horizontal plane, at least for the duration of the analysis;
- (e) the potentiometric surface is initially horizontal.

As concerns the pumping well, the following hypothesis are assumed to be valid:

- (f) its radius is infinitesimal;
- (g) well storage is negligible;
- (h) the flow is laminar;
- (i) the discharge is constant;

The main analytical solutions of the groundwater flow equation, derived under the assumption that hypothesis (a)–(i) are valid, are presented below for different aquifer types, in both steady and unsteady state.

3.1 Confined Aquifers

Confined aquifers are aquifers under greater than atmospheric pressure, delimited above and below by impermeable formations (aquicludes). Figure 3.1 depicts the resulting well-aquifer system.

3.1.1 Unsteady (or Transient) State

According to the previously illustrated conditions, the differential equation that governs water flow is:

$$\frac{\partial^2 h}{\partial r^2} + \frac{1}{r} \frac{\partial h}{\partial r} = \frac{S}{T} \frac{\partial h}{\partial t}, \quad (3.1)$$

and the initial and boundary conditions are [5]:

$$h(r, 0) = h_0, \quad (3.2)$$

$$h(\infty, t) = h_0, \quad (3.3)$$

$$\lim_{r \rightarrow 0} \left(r \frac{\partial h}{\partial r} \right) = \frac{Q}{2\pi T} \text{ for } t > 0. \quad (3.4)$$

Equation (3.2) represents the initial condition of horizontal, undisturbed, piezometric surface; (3.3) is the boundary condition imposing an infinite horizontal exten-

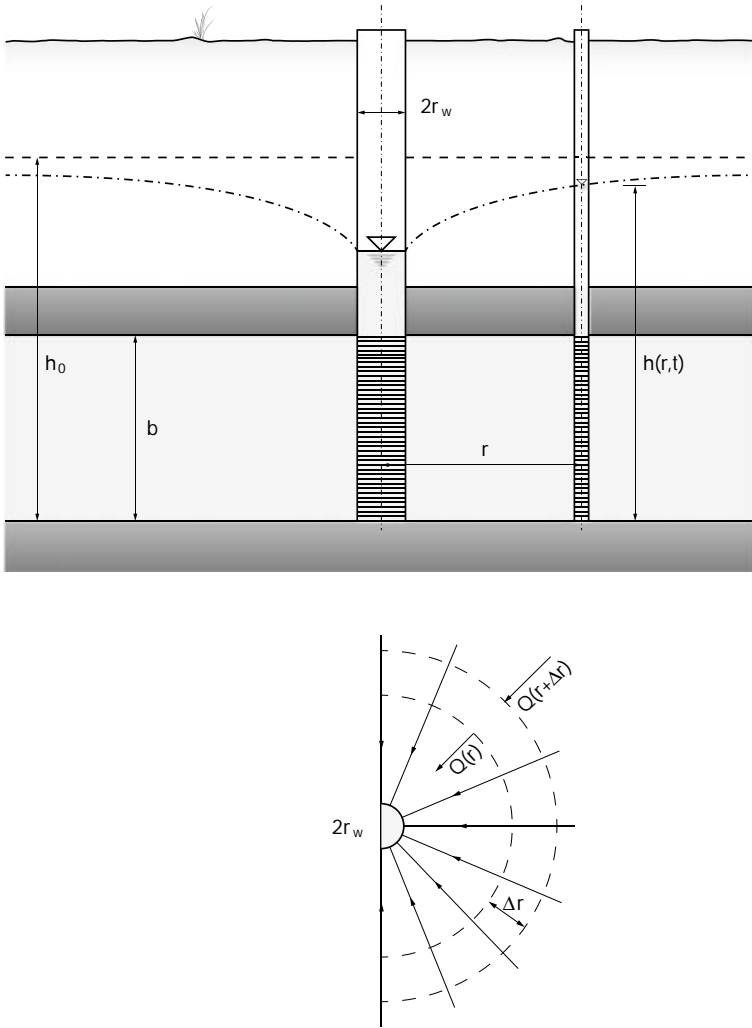


Fig. 3.1 Schematic representation of radial flow in a confined aquifer

sion, undisturbed at all times; and (3.4) expresses mathematically that the pumping rate is constant.

The analytical solution was first derived by Theis [13], who used the analogy between groundwater flow and heat flux in solids to solve the equation. The solution, known as the Theis (or nonequilibrium) equation. The Theis solution reads as follows:

$$s(r, t) = h_0 - h = \frac{Q}{4\pi T} \int_u^\infty \frac{e^{-u}}{u} du, \tag{3.5}$$

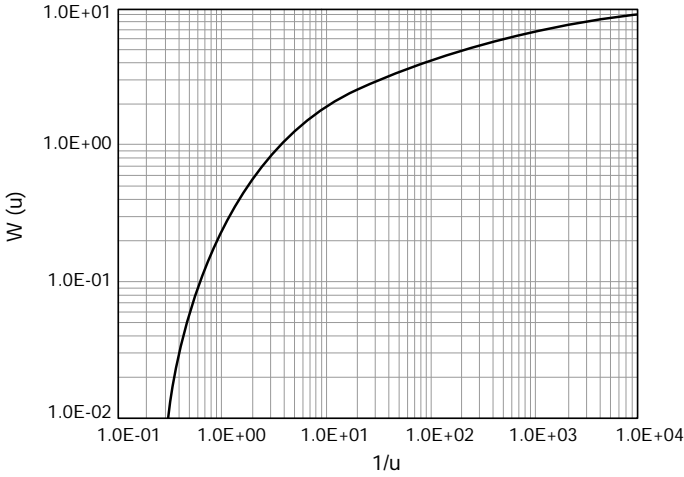


Fig. 3.2 Dimensionless well function

with

$$u = \frac{Sr^2}{4tT} \tag{3.6}$$

The dimensionless function $\int_u^\infty \frac{e^{-u}}{u} du$, whose graph is shown in Fig. 3.2, is known as *exponential integral*, $E_1(-u)$, in the field of applied mathematics; in groundwater engineering, instead, it is usually called *well function*, $W(u)$.

Given that $1/u$ is proportional to time, the shape of the curve in Fig. 3.2 indicates that in a confined aquifer the drawdown induced by a constant discharge at a generic distance from the pumping well continues to increase with time.

Figure 3.3 shows the drawdown induced by a fully penetrating well with infinitesimal radius and pumping a constant discharge, as a function of radial distance and time.

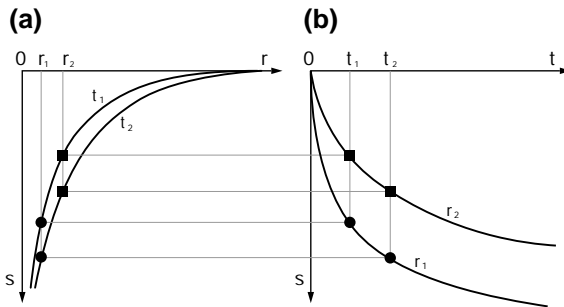


Fig. 3.3 Drawdown as a function (a) of radial distance from the pumping well and (b) of time

Solution (3.5) can be written in a more compact form by including the well function in it:

$$s(r, t) = \frac{Q}{4\pi T} \cdot W(u). \quad (3.7)$$

Well function values are listed in Appendix A; they can also be calculated through the series expansion of the exponential integral:

$$\begin{aligned} \int_u^\infty \frac{e^{-u}}{u} du &= E_i(-u) = W(u) = \\ &= \left[-0.5772 - \ln u + u - \frac{u^2}{2 \cdot 2!} + \frac{u^3}{3 \cdot 3!} - \frac{u^4}{4 \cdot 4!} \dots \right]. \end{aligned} \quad (3.8)$$

For small values of u , such that $u \leq 0.02$, thus $\frac{Sr^2}{4Tt} \leq 0.02$ and consequently $t \geq 12.5 \frac{Sr^2}{T}$, the series expansion of the function $W(u)$ can be truncated at the first two terms:

$$W(u) \approx -0.5772 - \ln u = -\ln(1.781 \cdot u) = \ln \frac{1}{1.781 \cdot u}. \quad (3.9)$$

Therefore, the Theis equation becomes:

$$s(r, t) \approx \frac{Q}{4\pi T} \ln \left(2.25 \frac{T \cdot t}{Sr^2} \right), \quad (3.10)$$

known as the Cooper and Jacob equation [3, 9].

If the common logarithm (to base 10) is used instead of the natural logarithm, and 4π is included in the numeric constant, the equation becomes:

$$s(r, t) \approx 0.183 \frac{Q}{T} \log \left(2.25 \frac{T \cdot t}{Sr^2} \right). \quad (3.11)$$

The Cooper and Jacob equation highlights the logarithmic increase of drawdown with time, after the initial transient phase.

Cooper and Jacob's logarithmic approximation is valid during a time range defined as quasi-steady state (see Table 3.1), because the drawdown at a generic radial distance tends to vary progressively less with time.

3.1.2 Steady State Flow

The steady state solution can be derived from the groundwater flow differential equation (3.1) by setting the derivative with respect to time equal to zero, or directly from Darcy's law, which is valid in steady state conditions.

Table 3.1 Minimum amounts of time necessary for Cooper and Jacob's approximation to be applicable to confined aquifers. Unless otherwise specified, times are expressed in hours

r (m)	$T = 10^{-2} \text{ m}^2/\text{s}$		$T = 10^{-4} \text{ m}^2/\text{s}$	
	$S = 10^{-4}$	$S = 10^{-2}$	$S = 10^{-4}$	$S = 10^{-2}$
10	12 s	0.3	0.3	34.7
50	0.09	8.7	8.7	868.1
100	0.3	34.7	34.7	3472.2
200	1.4	138.9	138.9	13888.9

Referring to the polar coordinate system depicted in Fig. 3.1, Darcy's law can be written in the following form:

$$Q = 2\pi r b K \frac{dh}{dr} = 2\pi T r \frac{dh}{dr}.$$

The variables can then be separated and both terms integrated between the values of a generic radius, r , and the *radius of influence*, R , i.e. the distance at which the hydraulic head has not varied from its initial value h_0 (note that this boundary condition is different from the one used to derive the Theis solution). These operations yield the following:

$$Q \cdot \int_r^R \frac{dr}{r} = 2\pi T \cdot \int_h^{h_0} dh,$$

and thus:

$$s(r) = h_0 - h = \frac{Q}{2\pi T} \cdot \ln \frac{R}{r}. \quad (3.12)$$

If, instead of a generic radius r , the well radius, r_w , is considered, the equation becomes:

$$s_w = h_0 - h_w = \frac{Q}{2\pi T} \cdot \ln \frac{R}{r_w}, \quad (3.13)$$

known as the Thiem equation [14].

3.2 Leaky Aquifers

Leaky aquifers are under pressure and delimited by an aquiclude and an aquitard. The latter is a geological formation characterized by a smaller hydraulic conductivity than the aquifer, but sufficient to allow a vertical flow (leakage). In dynamic conditions, such leakage can feed the aquifer, as illustrated in Fig. 3.4. The water feeding the leaky aquifer comes from an unconfined aquifer, which overlies the aquitard, and not from the aquitard itself.

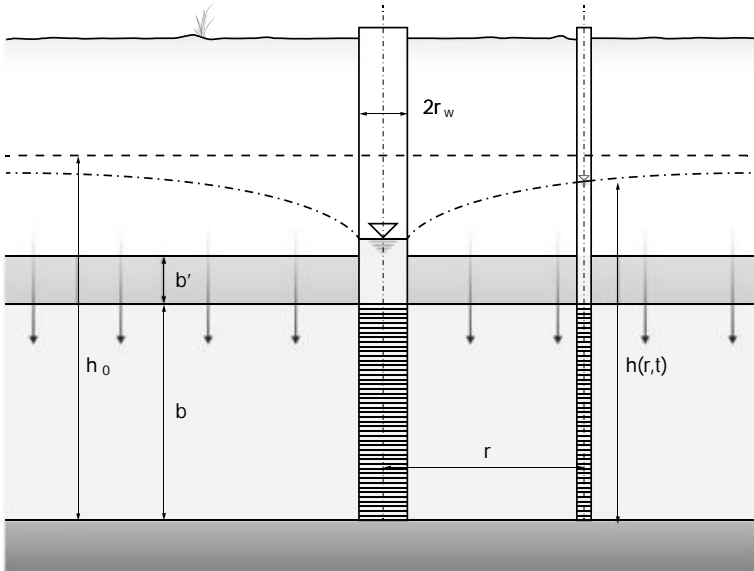


Fig. 3.4 Schematic of a fully penetrating well in a semi-confined aquifer

The analytic solutions presented below are valid under the assumption that conditions (a)–(i), described at the beginning of this chapter, are respected, and that also the following hypotheses are observed:

- (i) the level of the water table of the unconfined aquifer, h_0 , remains constant over time and at $t = 0$ this level coincides with the piezometric level of the leaky aquifer;
- (l) flow through the aquitard is exclusively vertical, whereas in the leaky aquifer it is horizontal;
- (m) the vertical recharge does not occur at the expense of the water stored in the aquitard: this implies that the aquitard, unlike the leaky aquifer, is incompressible [6].

3.2.1 Unsteady or Transient State

The groundwater flow equation is:

$$\frac{\partial^2 h}{\partial r^2} + \frac{1}{r} \frac{\partial h}{\partial r} - \frac{h_0 - h}{B^2} = \frac{S}{T} \cdot \frac{\partial h}{\partial t}, \tag{3.14}$$

and the initial and boundary conditions are:

$$h(r, 0) = h_0, \quad (3.15)$$

$$h(\infty, t) = h_0, \quad (3.16)$$

$$\lim_{r \rightarrow 0} \left(r \frac{\partial h}{\partial r} \right) = \frac{Q}{2\pi T} \text{ per } t > 0, \quad (3.17)$$

$$\frac{Q_v}{A} = \frac{K'}{b'} \cdot (h_0 - h) \text{ per } t > 0, \quad (3.18)$$

where Q_v is the vertical recharge flow rate, A is the area, h_0 the hydraulic head of the feeding aquifer, h the hydraulic head of the leaky aquifer, and B , K' and b' are the leakage factor, hydraulic conductivity and thickness of the aquitard. The analytical solution was derived by Hantush and Jacob [7]:

$$s(r, t) = \frac{Q}{4\pi T} \cdot \int_u^\infty \frac{1}{y} \cdot \exp\left(-y - \frac{r^2}{4B^2y}\right) dy, \quad (3.19)$$

with

$$u = \frac{Sr^2}{4Tt'} \quad (3.20)$$

$$B = \sqrt{\frac{T}{c}} = \sqrt{\frac{K}{K'}bb'}. \quad (3.21)$$

Since the dimensionless integral in Eq. (3.19) is a function of u , r e B , it is usually written in the following compact form:

$$\int_u^\infty \frac{1}{y} \cdot \exp\left(-y - \frac{r^2}{4B^2y}\right) dy = W\left(u, \frac{r}{B}\right), \quad (3.22)$$

so the solution of the flow equation becomes:

$$s(r, t) = \frac{Q}{4\pi T} \cdot W\left(u, \frac{r}{B}\right), \quad (3.23)$$

known as the Hantush and Jacob solution or the Hantush-Jacob formula [7].

The graph of function $W\left(u, \frac{r}{B}\right)$, which can be called the *well function for leaky systems* [8], is shown in Fig. 3.5 and its values are tabulated in Appendix B.

Graphically, the curves $W\left(u, \frac{r}{B}\right)$ vs $\frac{1}{u}$ belong to the family of Walton's type curves [15]. They all display a horizontal asymptote (constant drawdown over time), that indicates the achievement of a steady state due to the veal recharge from the

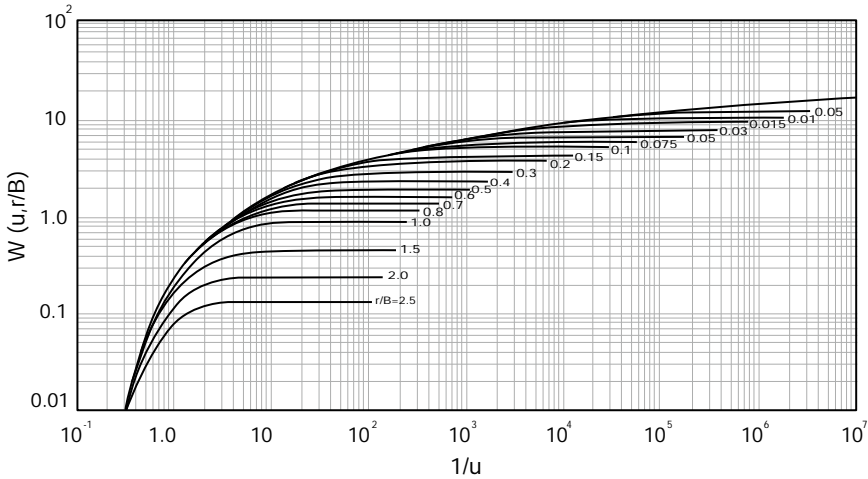


Fig. 3.5 Dimensionless Hantush and Jacob function for leaky aquifers. The curves are also known as Walton's type curves

aquitard. The greater the value of B (and thus the smaller the value of $\frac{r}{B}$), the greater the aquitard's resistance to leakage and, thus, the later the steady state is reached. As B tends to infinity, the leakage tends to zero, and the function $W(u, \frac{r}{B} \rightarrow 0)$ tends to coincide with the well function used for confined aquifers.

At a generic time during the transient phase, if Q is the well pumping rate, Q_s is the fraction deriving from the aquifer's storage, while the remaining Q_l is the fraction leaking through aquitard from the overlying unpumped aquifer:

$$Q_s = Q \cdot \exp\left(-\frac{Tt}{SB^2}\right), \tag{3.24}$$

$$Q_l = Q - Q_s. \tag{3.25}$$

As previously mentioned, the Hantush and Jacob solution is only valid if, amongst other conditions, the aquitard storage is negligible. This, however, leads to a slight overestimation of the drawdown. Neuman and Witherspoon [12] demonstrated that this effect can be neglected if:

$$\frac{r}{4b} \cdot \left(\frac{K'}{K} \cdot \frac{S_s'}{S_s}\right)^{0.5} < 0.01, \tag{3.26}$$

with S_s' and S_s being the specific storage of the aquitard and of the leaky aquifer, respectively.

3.2.2 Steady State Flow

Leaky aquifers are the only type of aquifer that, due to leakage through the aquitard, reaches a steady state. Under such conditions, the groundwater flow equation becomes:

$$\frac{\partial^2 h}{\partial r^2} + \frac{1}{r} \cdot \frac{\partial h}{\partial r} - \frac{h_0 - h}{B^2} = 0, \quad (3.27)$$

the solution of which was derived by De Glee [4]:

$$s(r) = \frac{Q}{2\pi T} \cdot K_0\left(\frac{r}{B}\right), \quad (3.28)$$

in which $K_0\left(\frac{r}{B}\right)$ is the modified Bessel function of the second kind and order 0, whose values are reported in Appendix C. For $r/B \leq 0.10$ (thus, in close proximity to a well):

$$K_0\left(\frac{r}{B}\right) = \ln\left(1.123 \frac{B}{r}\right), \quad (3.29)$$

hence De Glee's equation can be simplified to the form:

$$s(r) = \frac{Q}{2\pi T} \cdot \ln\left(1.123 \frac{B}{r}\right). \quad (3.30)$$

In particular, by setting $r = r_w$ the steady state drawdown is:

$$s(r_w) = \frac{Q}{2\pi T} \cdot \ln\left(1.123 \frac{B}{r_w}\right). \quad (3.31)$$

Equation (3.31) can also be written as a function of the logarithm to the base 10; in this way, if the constant 2π is incorporated in the numerical coefficient, the equation becomes:

$$s(r_w) = 0.366 \frac{Q}{T} \cdot \log\left(1.123 \frac{B}{r_w}\right). \quad (3.32)$$

3.3 Unconfined Aquifers

As mentioned in Sect. 2.2, under certain simplifying hypotheses, the differential equation used for confined aquifers can be applied also to water table aquifers. This is only possible if the initial transient phase is not considered and the observation point is sufficiently far from the pumping well, whereas it is completely inadequate to describe the aquifer's behavior in other cases.

Before approaching the mathematical solutions of the problem, it is worth taking a closer look at the physical phenomenon. Let us consider a well completed in an unconfined aquifer and with well discharge, Q , as depicted in Fig. 3.6.

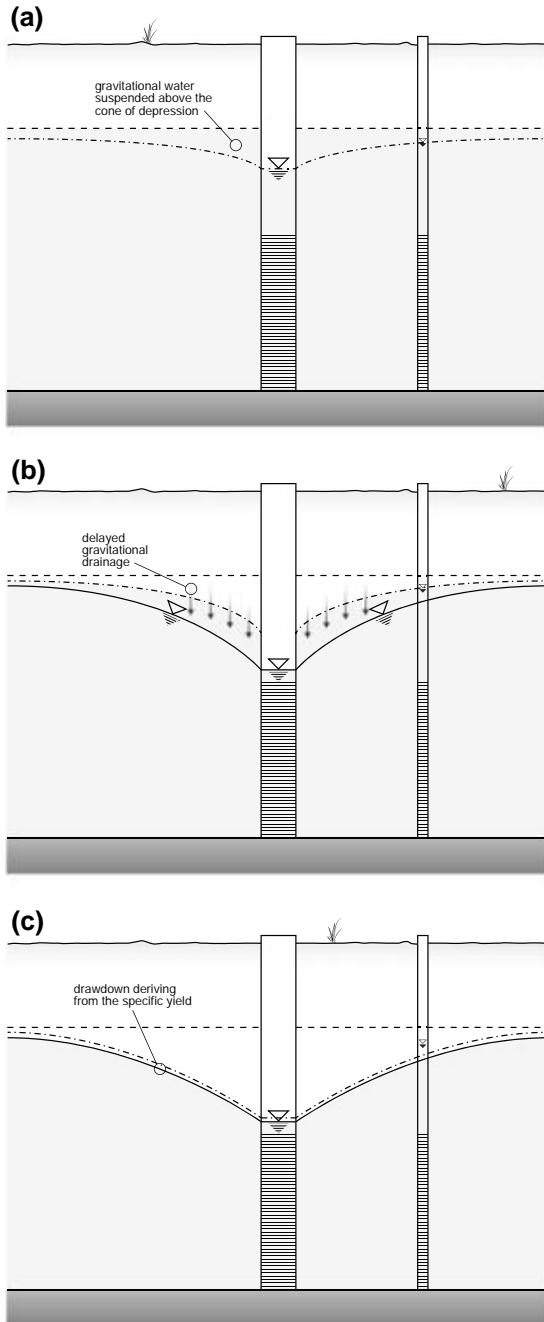


Fig. 3.6 Hydrodynamic behavior of a well in an unconfined aquifer: **a** initial cone of depression; **b** delayed gravitational drainage; **c** after the vertical drainage ends, the transient phase continues depending on the specific yield

In the first phase of the transient regime, the water derives from the elastic storage of the aquifer, with an expansion mechanism analogous to what occurs in confined aquifers. The piezometric level declines rapidly in response to the pumping, but not fast enough for gravity to mobilize the gravitational water contained in the portion of the aquifer overlying the cone of depression. This portion of the aquifer, therefore, remains saturated even though the piezometric level is lower. In this phase, the time-drawdown plot resembles the Theis curve, similarly to a confined aquifer, due to the elastic storativity, S .

Over time, the portion of aquifer above the depression cone begins to contribute to the pumped discharge, due to gravitational drainage. This drainage results in a vertical recharge of the aquifer, and is reflected in the decreased evolution rate of the depression cone. This mechanism, occurring with a lag relative to the beginning of pumping, is called *delayed gravity drainage*.

Since the volume affected by the depression cone increases progressively over time, while the well discharge remains constant, the drawdown increase at a generic radius decreases progressively, and the gravity drainage reaches the depression cone. Starting from this point, the delayed drainage stops, the specific yield S_y becomes the parameter responsible for water production, and the drawdown curve regains the shape of a Theis curve.

To summarize, the hydrodynamic behavior of an unconfined aquifer follows three steps (see Fig. 3.7):

- (a) initially, the water supply derives from the elastic storage, S , of the aquifer, analogously to confined aquifers;
- (b) a phase dominated by delayed gravity drainage follows, during which the time-drawdown curve flattens out somewhat;
- (c) once the effect of gravity drainage ends, the drawdown starts to increase again depending on the value of the specific yield S_y .

The duration of the first two stages is variable and depends on the granulometry of the aquifer, and thus on its permeability and homogeneity; however, all unconfined aquifers follow this behavior. Therefore, if the problem that needs solving does not involve the beginning of the transient phase, stages (a) and (b) can be neglected, and the same equation used for confined aquifers can be used, replacing the storativity S with the specific yield S_y . If, instead, the beginning of the transient phase is important (such as for the interpretation of an aquifer test, see Chap. 4), a differential equation that keeps into account also phases (a) and (b), which characterize the initial pumping stage, must be used. Such an equation will be presented in the following paragraphs.

3.3.1 *Unsteady or Transient State*

An analytical solution for the analysis of unsteady-state flow in unconfined aquifers is provided in this section.

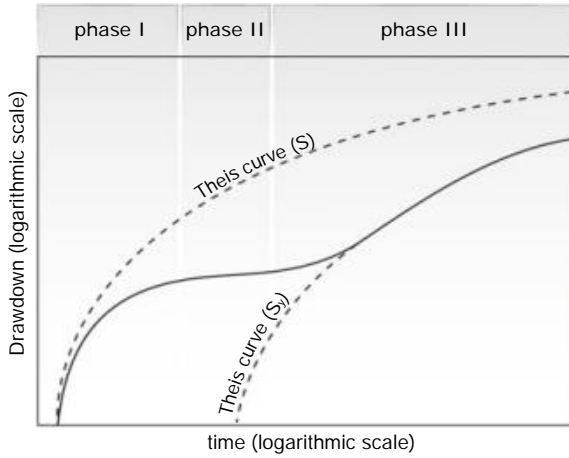


Fig. 3.7 Hydrodynamic behavior of an unconfined aquifer

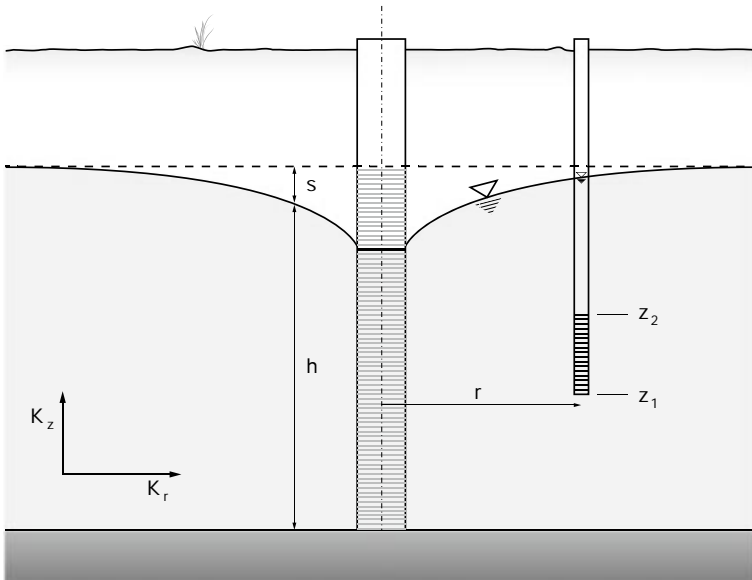


Fig. 3.8 Schematic of a well-piezometer-unconfined aquifer system for the application of Neuman's solution

3.3.1.1 Neuman's Solution

Let us consider the well-aquifer system depicted in Fig. 3.8; taking into consideration the gravity drainage implies analyzing the vertical component of flow; consequently, it is possible to consider the anisotropy of the hydraulic conductivity on the vertical

plane, if any. The Neuman differential equation is, thus [10, 11]:

$$K_r \frac{\partial^2 h}{\partial r^2} + \frac{K_r}{r} \frac{\partial h}{\partial r} + K_z \frac{\partial^2 h}{\partial z^2} = S_s \frac{\partial h}{\partial t}. \quad (3.33)$$

When defining the initial and boundary conditions, one should keep in mind that the position of the water table of an unconfined aquifer moves in space during the transient phase, thus effectively representing a mobile boundary condition (see Fig. 3.8).

In analytical terms, the initial and boundary conditions (referred to the bottom of the aquifer) are:

$$h(r, z, 0) = h_0 = b, \quad (3.34)$$

$$h(\infty, z, t) = h_0 = b, \quad (3.35)$$

at the bottom:

$$\frac{\partial h(r, 0, t)}{\partial z} = 0, \quad (3.36)$$

at the well:

$$\lim_{r \rightarrow 0} \int_0^b r \frac{\partial h}{\partial r} dz = \frac{Q}{2\pi K_r}, \quad (3.37)$$

at the water table

$$\frac{\partial h(r, b, t)}{\partial z} = -\frac{S_y}{K_z} \cdot \frac{\partial h(r, b, t)}{\partial t}. \quad (3.38)$$

The analytical solution obtained by Neuman [11] is:

$$s(r, z, t) = \frac{Q}{4\pi T} \cdot \int_0^\infty 4y J_0(y\beta^{\frac{1}{2}}) \cdot \left[\omega_0(y) + \sum_{n=1}^\infty \omega_n(y) \right] dy, \quad (3.39)$$

where J_0 is the zero order Bessel function of the first kind,

$$\omega_0(y) = \frac{\{1 - \exp[-t_s \beta (y^2 - \gamma_0^2)]\} \cdot \cosh(\gamma_0 z_D)}{\left\{ y^2 + (1 + \sigma) \gamma_0^2 - \left[\frac{(y^2 - \gamma_0^2)^2}{\sigma} \right] \right\} \cdot \cosh(\gamma_0)}, \quad (3.40)$$

$$\omega_n(y) = \frac{\{1 - \exp[-t_s \beta (y^2 + \gamma_n^2)]\} \cdot \cosh(\gamma_n z_D)}{\left\{ y^2 + (1 + \sigma) \gamma_n^2 - \left[\frac{(y^2 + \gamma_n^2)^2}{\sigma} \right] \right\} \cdot \cosh(\gamma_n)}, \quad (3.41)$$

and the terms γ_0 and γ_n the solutions of the equations:

$$\sigma \gamma_0 \cdot \sinh(\gamma_0) - (y^2 - \gamma_0^2) \cdot \cosh(\gamma_0) = 0 \text{ with } \gamma_0^2 < y^2, \quad (3.42)$$

$$\sigma \gamma_n \cdot \sin(\gamma_n) + (y^2 + \gamma_n^2) \cdot \cos(\gamma_n) = 0, \quad (3.43)$$

where

$$(2n - 1) \cdot \frac{\pi}{2} < \gamma_n < n\pi, \quad n \geq 1.$$

Equation (3.39), known as Neuman's solution, can be written in the following compact form:

$$s(r, z, t) = \frac{Q}{4\pi T} \cdot s_D(\sigma, \beta, t_s, z_D), \quad (3.44)$$

with s_D being the dimensionless drawdown and:

$$\sigma = \frac{S}{S_y} = \frac{t_y}{t_s}, \quad (3.45)$$

$$\beta = \frac{K_z}{K_r} \cdot \left(\frac{r}{b}\right)^2, \quad (3.46)$$

$$t_s = \frac{T \cdot t}{Sr^2}, \quad (3.47)$$

$$z_D = \frac{z}{b}. \quad (3.48)$$

Combining Eqs. (3.45) and (3.47) the following is obtained:

$$t_y = \frac{T \cdot t}{S_y r^2}. \quad (3.49)$$

If we refer to the average drawdown measurable in a piezometer located at a distance r from the pumping well, screened between the depths z_1 and z_2 (see Fig. 3.8), and defined as:

$$s_{z_1, z_2} = \frac{1}{z_1 - z_2} \cdot \int_{z_1}^{z_2} s(r, z, t) dz, \quad (3.50)$$

Neuman's solution (3.44) becomes independent from z_D , and can be simplified to the following form, which is the most commonly used in practical applications:

$$s(r, t) = \frac{Q}{4\pi T} \cdot s_D(t_s, t_y, \beta) = \frac{Q}{4\pi T} \cdot s_D. \quad (3.51)$$

Note that in the argument of the function s_D in Eq. (3.51) using σ or t_y is equivalent, since the two parameters are interdependent, as per Eq. (3.45):

$$t_y = \sigma \cdot t_s.$$

Even in its simplest form, Neuman's solution depends on three dimensionless parameters (t_s, t_y, β) and hence is difficult to represent graphically. To overcome this

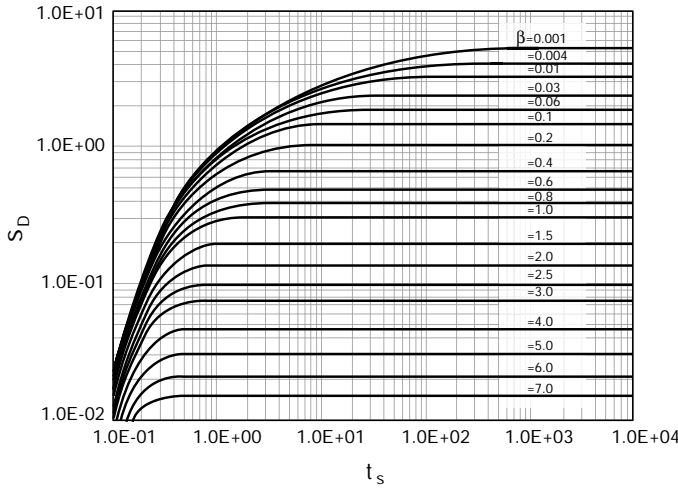


Fig. 3.9 Neuman's dimensionless function $s_D(t_s, \beta)$ valid for short times

issue, Neuman [10] followed Boulton's conceptual framework [1, 2] and, keeping into account that $S \ll S_y$, calculated the function s_D for $\sigma \rightarrow 0$ (basically, $\sigma = 10^{-9}$ was used), and obtained the two following families of curves:

$$s_D = s_D(t_s, \beta) \quad \text{which is valid for short periods of time}$$

$$s_D = s_D(t_y, \beta) \quad \text{valid for longer periods of time and obtained by imposing } t_y = 10^{-9}t_s.$$

The two families of curves are depicted in Figs. 3.9 and 3.10, and their values are reported in Appendices D and E, respectively.

Once the actual value of σ for a specific aquifer is known, the two families of curves can be combined into a single graph (see example in Fig. 3.11, plotted for $\sigma = 10^{-4}$).

3.3.1.2 Long Lasting Transient State

If we consider a pumping time that exceeds the duration of the delayed gravity drainage, the time-drawdown curve follows a Theis curve for which $S = S_y$ [13]:

$$s(r, t) = \frac{Q}{4\pi T} \cdot W(u), \tag{3.52}$$

with

$$u = \frac{S_y r^2}{4T \cdot t}. \tag{3.53}$$

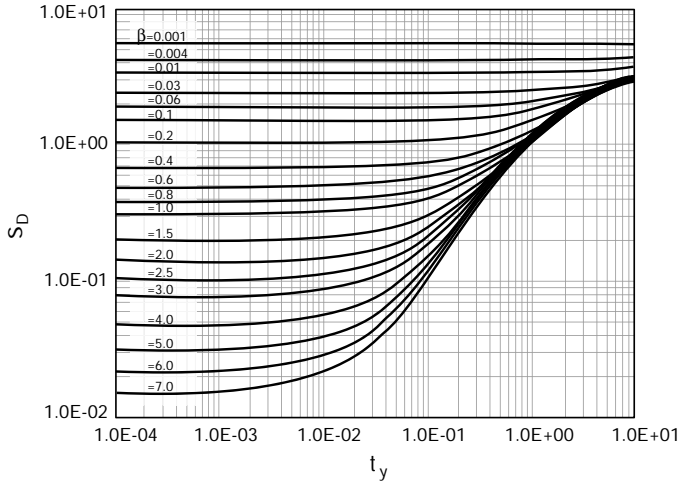


Fig. 3.10 Neuman's dimensionless function $s_D(t_y, \beta)$ valid for extended periods of time

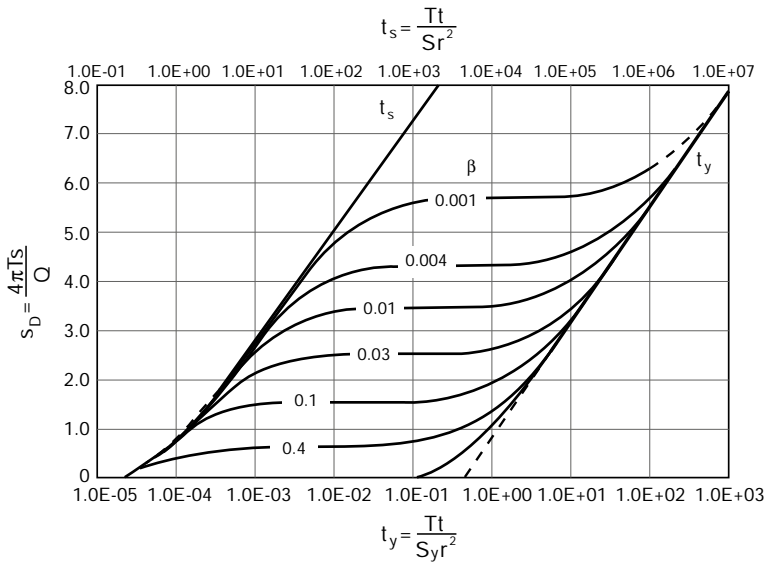


Fig. 3.11 Neuman's dimensionless curves $s_D(t_s, t_y, \beta)$ represented for $\sigma = 10^{-4}$

Table 3.2 Minimum time required for the application of Cooper and Jacob's logarithmic approximation to unconfined aquifers (times are expressed in hours)

r (m)	$T = 10^{-2} \text{ m}^2/\text{s}$		$T = 10^{-4} \text{ m}^2/\text{s}$	
	$S_y = 0.1$	$S_y = 0.3$	$S_y = 0.1$	$S_y = 0.3$
10	3.5	10.4	347.2	1041.2
50	86.8	260.4	8680.6	26041.7

If, in addition, $t \geq 12.5 \frac{S_y r^2}{T}$, the drawdown increases logarithmically, according to Cooper and Jacob's approximation [3]:

$$s(r, t) = \frac{Q}{4\pi T} \cdot \ln \left(2.25 \frac{T \cdot t}{S_y r^2} \right), \quad (3.54)$$

which can also be expressed through logarithms to base ten:

$$s(r, t) = 0.183 \cdot \frac{Q}{T} \cdot \log \left(2.25 \frac{T \cdot t}{S_y r^2} \right). \quad (3.55)$$

Since $S_y \gg S$, the time needed to be able to apply the logarithmic approximation to an unconfined aquifer is much longer than for a confined aquifer, see Table 3.2.

The values reported in Table 3.2 show that the logarithmic approximation is effectively inapplicable at distances greater than 50 m from the pumping well. However, even close to the well the values are very high: neglecting this aspect is the primary cause of error in the interpretation of aquifer tests conducted in unconfined aquifers.

3.3.2 Steady State Flow

The steady state solution of the groundwater flow equation can be obtained directly by integrating Darcy's law and keeping into account that the aquifer's transmissivity is not constant near the pumping well, but decreases with the drawdown:

$$Q = 2\pi r h K \frac{dh}{dr}, \quad (3.56)$$

from which, separating the variables and integrating:

$$\frac{Q}{2\pi K} \cdot \int_r^R \frac{dr}{r} = \int_h^{h_0} h \, dh,$$

the following equation is obtained:

$$h_0^2 - h^2 = \frac{Q}{\pi K} \cdot \ln \frac{R}{r}, \quad (3.57)$$

where R is the radius of influence, i.e. the distance from the well at which drawdown is negligible.

Since:

$$h_0^2 - h^2 = (h_0 - h) \cdot (h_0 + h) = s \cdot (h_0 + h_0 - s) = 2h_0s', \quad (3.58)$$

where s' is Cooper and Jacob's correction:

$$s' = s - \frac{s^2}{2h_0}, \quad (3.59)$$

Equation (3.57) can be re-written as follows:

$$s' (r) = \frac{Q}{2\pi T} \cdot \ln \frac{R}{r}. \quad (3.60)$$

Equation (3.60) is identical to Thiem's solution for confined aquifers except for the replacement of the theoretical drawdown $s(r)$ with the corrected drawdown $s'(r)$. Note that in the previous expression $T = K \cdot h_0$, which is the initial value of transmissivity under undisturbed conditions.

3.4 Radius of Investigation and Radius of Influence

If we exclude leaky aquifers, provided that

$$t \geq 12.5 \frac{SR^2}{T}, \quad (3.61)$$

the transient phase for the other types of aquifer (i.e. confined and unconfined) can be described with Cooper and Jacob's equation:

$$s(r, t) = \frac{Q}{4\pi T} \cdot \ln \left(2.25 \frac{T \cdot t}{SR^2} \right). \quad (3.62)$$

From a theoretical point of view, Eqs. (3.61) and (3.62) are valid for confined as well as unconfined aquifers, although one should keep in mind that in the latter the storativity S coincides with the specific yield, and that the time needed for inequality (3.61) to become true can be very long.

Let us introduce the concept of radius of investigation (also called transient drainage radius), r_{inv} , as the radial distance that satisfies the following identity:

$$\ln \frac{r_{inv}}{r} = \frac{1}{2} \ln \left(2.25 \frac{T \cdot t}{Sr^2} \right). \quad (3.63)$$

If we apply the properties of logarithms, the following can be derived:

$$r_{inv} = 1.5 \sqrt{\frac{T \cdot t}{S}}. \quad (3.64)$$

The radius of investigation represents the maximum distance at which an effect of the pumping well, and the consequent head drop, is detectable. It is a function of the transmissivity and storativity, but also, notably, of time, with the square root of which it has a relation of direct proportionality.

By replacing r in Eq. (3.60) with r_{inv} , as defined in Eq. (3.64), the following is obtained:

$$s(r, t) = \frac{Q}{2\pi T} \cdot \ln \frac{r_{inv}}{r}, \quad (3.65)$$

which, written for the well radius, becomes:

$$s(r_w, t) = \frac{Q}{2\pi T} \cdot \ln \frac{r_{inv}}{r_w}. \quad (3.66)$$

As can be observed, Eq. (3.66) coincides with Thiem's equation for steady state conditions, except for the substitution of the radius of influence, R , with the radius of investigation, r_{inv} . In other words, during unsteady flow, the radius of investigation can be considered an instantaneous radius of influence at a generic time; and, therefore, a transient regime problem can be addressed with a steady state equation referring to the radius of investigation.

The radius of influence R is a parameter used for practical applications because, technically, a steady flow is never reached in confined and unconfined aquifers, and represents the limit approached by the radius of investigation after an extended period of time.

References

1. N.S. Boulton, Unsteady radial flow to a pumped well allowing for delayed yield from storage. *Int. Assoc. Sci. Hydrol.* **37**, 472–477 (1954)
2. N.S. Boulton, Analysis of data from non-equilibrium pumping tests allowing for delayed yield from storage. *Proc. Inst. Civ. Eng.* **26**, 469–482 (1963)
3. H.H. Cooper, C.E. Jacob, A generalized graphical method for evaluating formation constants and summarizing well-field history. *Eos Trans. Am. Geophys. Union* **27**, 526–534 (1946)

4. G. De Glee, Over grondwaterstromingen bij wateronttrekking door middel van putten, Dutch, Ph.D. thesis, Technical University, Delft (The Netherlands), printed by J. Waltman (1930)
5. H.J. Diersch, *FEFLOW finite element subsurface flow and transport simulation system - reference manual*, WASY GmbH (2002)
6. C.W. Fetter, *Applied Hydrogeology*, English, 4th edn. (Pearson Education, Long Grove, Ill, 2014)
7. M.S. Hantush, Analysis of data from pumping tests in leaky aquifers. *Eos Trans. Am. Geophys. Union* **37**, 702–714 (1956)
8. M.S. Hantush, C.E. Jacob, Non-steady radial flow in an infinite leaky aquifer. *Eos Trans. Am. Geophys. Union* **36**, 95–100 (1955)
9. P.M. Meier, J. Carrera, X. Sánchez-Vila, An evaluation of Jacob's method for the interpretation of pumping tests in heterogeneous formations. *Water Resour. Res.* **34**(5), 1011–1025 (1998)
10. S.P. Neuman, Theory of flow in unconfined aquifers considering delayed response of the water table. *Water Resour. Res.* **8**, 1031–1045 (1972)
11. S.P. Neuman, Supplementary comments on theory of flow in unconfined aquifers considering delayed response of the water table, English (US). *Water Resour. Res.* **9**, 1102–1103 (1973)
12. S.P. Neuman, P.A. Witherspoon, Applicability of current theories of flow in leaky aquifers. *Water Resour. Res.* **5**, 817–829 (1969)
13. C.V. Theis, The relation between the lowering of the piezometric surface and the rate and duration of discharge of a well using ground-water storage. *Eos Trans. Am. Geophys. Union* **16**, 519–24 (1935)
14. G. Thiem, *Hydrologische Methoden* (Gebhardt, Leipzig, 1906)
15. W.C. Walton, Selected analytical methods for well and aquifer evaluation, English, Technical report 49 (Illinois State Water Survey, 1962)

Chapter 4

Aquifer Characterization



Abstract Aquifer tests are the most appropriate method to determine the hydraulic behavior of an aquifer and the distribution of the hydrodynamic parameters that govern such behavior. This chapter illustrates the different type of aquifer tests (i.e., pumping, recovery and slug tests) and how to plan, execute and interpret them. Pumping tests consist in measuring the drawdown induced by the extraction of water from a well at a constant discharge rate in one or more observation points. They allow to first identify the hydraulic behavior of the aquifer, and thus to classify it as confined, leaky or unconfined, and then to determine, via a type curve matching method, the aquifer's horizontal hydraulic conductivity, transmissivity and storativity. In the case of leaky aquifers, also the leakage factor can be calculated; and in the case of unconfined aquifers, the effective porosity and the vertical hydraulic conductivity can also be derived. Clearly, this interpretation relies on a number of ideal hypotheses being satisfied; this chapter also illustrates how to interpret pumping tests in the presence of factors that cause a deviation from the ideal behavior (e.g., finite, as opposed to infinitesimal, well radius and volume; partially penetrating well; presence of recharging or impermeable boundaries; inconsistent pumping rate; permeability damage close to the well). During recovery tests, residual drawdown measurements are carried out following the interruption of the pump at the end of a constant discharge pumping test. Their recovery method, based on the superposition principle and normally used for the interpretation of the test, allows to determine the transmissivity of an aquifer. The last type of aquifer test, i.e., the slug test, consists in inducing an instantaneous variation of the static water level in a well or piezometer, and subsequently measuring the recovery over time of the undisturbed level in the same well. This method is used to determine the hydraulic conductivity of the aquifer in proximity of the well. In this chapter, the most common interpretation methods are presented, as well as the strategies to overcome limitations due to the existence of factors that cause a deviation from the ideal behavior. Finally, a suite of correlation-based, laboratory, and field methods available for the determination of an aquifer's hydrodynamic parameters in alternative to aquifer tests are presented, and the applicability to different aquifer types and situations of each method, as well as their reliability is discussed.

The characterization of an aquifer entails the determination of its hydraulic behavior and of the distribution of the hydrodynamic parameters that govern its behavior.

Aquifer tests are the most suitable method to reliably obtain this information. In fact, they represent the only objective approach for the evaluation of an aquifer's hydraulic behavior and of the effect of certain boundary conditions [10, 30].

4.1 Aquifer Test Classification and Planning

During steady flow, storativity and specific yield do not contribute to the water produced by pumping an aquifer. Therefore, in order to investigate these parameters, aquifer tests must be conducted in transient regime, which are also cheaper and last less.

From a practical point of view, there are three main categories of aquifer tests (see Fig. 4.1) [11, 30]:

- *pumping tests*, the aquifer is pumped at a single constant discharge rate, at a varying discharge rate, or at a succession of constant pumping rates, and the drawdown is measured over time;
- *recovery tests*, conducted just after a pumping test by stopping the pump and measuring the residual displacement as a function of time at zero discharge, until the static water level is recovered;
- *slug tests*, consisting in generating a sudden perturbation in the water level in the control well, and measuring the recovery of the initial water level over time.

Aquifer tests can be conducted in a single well or by employing one or multiple data collection points (single or multi-well tests, respectively). In the former case, the water level variation induced by pumping, by its interruption or by a sudden perturbation is measured in the pumped well itself (control or main well); in the latter case, instead, the level variation is measured in one or multiple observation wells (or piezometers), distinct and far from the pumped well. Tests in which perturbation and observation occur in distinct wells can be called *interference test*.

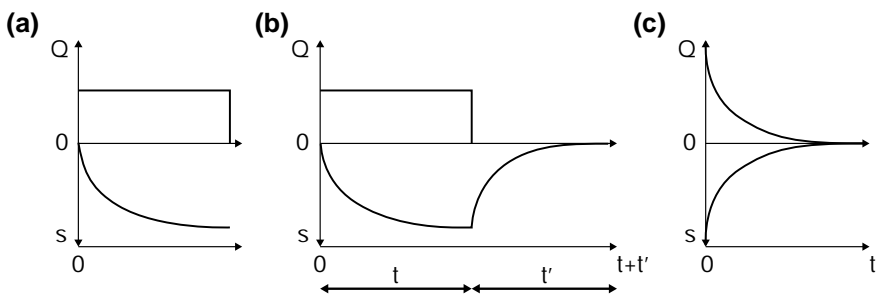


Fig. 4.1 Aquifer testing methods: **a** constant-rate, or decline test; **b** recovery test; **c** slug test

Pumping or recovery tests are, preferentially, multi-well (or interference) tests. They should be performed in a single well exclusively if there is no possibility of using a separate observation well: in this case, some of the hypotheses that underlie the analytical solutions of the groundwater flow equation used to interpret the test are not valid; hence, the interpretation step becomes more complex. Conversely, the greater the number of observation points available for an aquifer test, the greater the interpretation reliability and the amount of derivable information.

Slug tests are, instead, single-well tests. Even though such tests provide less and more localized information compared to multi-well tests, the aquifer's horizontal hydraulic conductivity can be determined.

Performing an aquifer test requires thorough planning and a series of practical decisions need to be made regarding: the choice of the site, the completion characteristics of pumping and observation wells, the duration of the tests, measurement instruments, and measurement frequency and method.

Underestimation of any of these aspects, some of which may appear obvious, can undermine the success of the entire test.

4.1.1. The site for an aquifer test whose objectives have been defined can rarely be chosen freely, since in most cases preexisting wells need to be used; hence, the site is often defined a priori. In certain cases, however, pumping and/or observation wells must be drilled specifically for the test. This commonly occurs, for example, when a contaminated site has to be characterized to plan remediation interventions, and significant economic resources are available. In such cases, a series of aspects—discussed below—need to be kept in mind in order to identify the most suitable site for the test; the same aspects should also be used to assess the suitability of predetermined sites.

The ideal site should be easily accessible, relevant to the area under investigation, far from sources of disturbance that could mask or alter the signals recorded during the test (e.g., proximity of other active production wells, or of sources of vibrations, such as railways or major roads). It should also be far from hydrogeologic boundaries (be they impermeable, draining or recharging), unless one of the goals of the test is their characterization. In addition, the gradient of the piezometric surface should be small. Finally, most importantly, the site should enable the disposal of the pumped water at a distance greater than the radius of influence of the aquifer test to prevent it from penetrating the ground, returning to the aquifer and influencing the cone of depression induced by the pumping test itself [30, 37].

4.1.2. If the pumping well is already existing, it is of fundamental importance for a correct interpretation of the test to know the lithography of the ground and the characteristics of the well (i.e., diameter of the casing; depth; number, type and position of the screens).

If, instead, the well has to be constructed specifically for the test, it should be designed to have a diameter of 300–500 mm, and to be fully penetrating and screened over the entire saturated thickness, in order to fulfill one of the theoretical conditions that facilitate the interpretation of the test [30]. If economic or technical limitations

prevent the construction of a fully penetrating well, its final design should be available and kept into account during data interpretation.

Except in the case of slug tests, the well should be equipped with a submersible pump and power generator (if connection to the electrical grid is unavailable or its power isn't sufficient), capable of sustaining the discharge rate during the entire duration of the test.

4.1.3. With the exception of slug tests, that require a single well, aquifer tests typically exploit multiple wells. The observation wells, located at a distance, r , from the main well, are used to record the water level displacement induced by pumping (or its interruption), and should fulfill specific requirements.

Pre-existing piezometers or wells can be used as monitoring wells, provided that they penetrate the same aquifer as the pumping well, that their design is known and that they are located at a suitable distance from the well. This distance should be sufficient to measure significant drawdowns and allow reliable data interpretation; it depends on the aquifer type and its transmissivity, as well as on the pumping rate and the duration of the test. The transmissivity affects the shape and extension of the cone of depression: higher values will produce a wide and flat cone, while lower values will generate narrow and steep cones [30]. The aquifer type, instead, is of seminal importance because it affects the order of magnitude of the storativity and, thus, the extent of the portion of aquifer affected by the test at a specific time: in the case of unconfined aquifers, significant data will hardly be collected in a piezometer placed more than 100 m from the main well, whereas in the case of confined aquifers, piezometers can be located at greater distances, even beyond 400 m [30].

Of course, if the piezometers have to be drilled especially for the test, it is preferable to locate them well within the above-mentioned limits, specifically between 5 m and $1/3$ of the radius of influence of the test. If preliminary information necessary to estimate this parameter is unavailable, distances of 10–20 m and of 50–70 m are recommended for observation points in unconfined and confined aquifers, respectively; intermediate distances can be used for leaky aquifers.

It is also advisable to install piezometers whose diameter isn't be too big because it would delay the response, nor too small to avoid the probe generating a surging effect. Recommended values are between 5 and 10 cm [37].

As previously mentioned, the greater the number of observation points, the greater the reliability of the data and the amount of derivable information from its interpretation. Therefore, if it is possible to install more than one monitoring well, it is preferable to locate them in different directions with respect to the pumping well, and at distances that increase logarithmically, such that: $\ln \frac{r_{i+1}}{r_i} = a = \text{const}$. For $a = 1.1$, the application of this criterion implies that $r_{i+1} = 3r_i$.

If at least three observation wells positioned in different directions are available in an aquifer test, it is possible to estimate, in addition to the basic parameters, also the anisotropy of the hydraulic conductivity, potentially present in the horizontal flow plane.

4.1.4. The ideal duration of an aquifer test is between 6 and 72 h, depending on the type of test, the flow regime and the characteristics of the aquifer (i.e., type,

hydrodynamic parameters and presence of boundaries). A slug test, instead, lasts significantly less, usually between 1 and 100 min.

4.1.5. All aquifer tests entail the measurement of the piezometric level displacement over time induced by a well pumping a specific discharge (or by its interruption), or by an instantaneous stress imposed on the water level itself in the control well. Therefore, in order to conduct an aquifer test, time, water level and discharge measurement devices must be installed.

For measuring the water level, a choice between a manual system (i.e., a water level meter or phreatimeter) or an automatic data acquisition system capable of compensating for atmospheric pressure (pressure sensor and data logger) will have to be made, although nowadays the former is rarely used. In the case of pumping or recovery tests it is basically a matter of personal choice, depending mainly on the availability of instrumentation; in order to conduct a slug test automatic data acquisition methods are necessary. This is due to the fact that in medium to high permeability aquifers, water level variations are too fast to allow for precise manual measurements.

It is worth discussing in greater detail discharge measurements, an aspect that is often underestimated in the field, despite being a determining parameter in the interpretation of aquifer tests.

The most common methods used during aquifer tests are [11, 30, 37]:

- (a) container method, which consists in measuring the time necessary for the pumped water to fill a container of known capacity (normally 200 to 500 l); it is the simplest method and is suitable for small discharges, since the filling time should be at least 30–60 s, to limit measurement errors (for this method the relative error is between 1 and 2%);
- (b) in line water meters, usually of the Waltmann type, which allow a direct reading of the water volume (with an error of approximately 2%); its diameter should be selected based on the range of pumping discharge and should be installed along a horizontal pipe, which should be aligned up and down of the meter, and at least 20 times the pipe diameter long. A gate valve should be installed downstream of the meter, to ensure the pipe is always filled with water;
- (c) sharp-crested weirs, with which the discharge is measured by correlating the thickness of the nappe (i.e., the overflowing sheet of water) flowing over the notch and the design of the weir itself (this measurement is affected by an approximate error of 1.5–2.5%);
- (d) flumes, which cause an acceleration of water and an increase in the water level by restricting flow within a channel. The head displacement can, thus, be correlated to the discharge;
- (e) orifice weirs, which exploit Bernoulli's principle to estimate the discharge (5% approximate error), by recording the value of the hydraulic head upstream from the orifice. The orifice should be a perfectly round hole mounted at the end of a smooth and horizontal section of pipe which is straight for a length equal to at least 20 times its diameter;

- (f) orifice buckets: the well discharge is directed through an approach pipe into a container with perfectly round holes in the bottom and a piezometer tube on the side; the water level in the piezometer can be used to determine the discharge, depending on the size of the holes and on the diameter of the approach pipe;
- (g) jet-stream method, which consists in measuring the dimensions of the of a stream discharged from an open pipe into the air; the flow can be vertical or horizontal. The flow rate can be roughly calculated by knowing the dimensions, or the trajectory, of the stream of water.

4.1.6. The frequency and method of data acquisition during an aquifer test have to be such that the drawdown resulting from pumping a well is recorded over time in the same well and/or in one or more observation wells. The collected data can either be a set of drawdown values acquired at specific times, or a set of time values corresponding to predefined drawdown values.

In the first case, one must keep in mind that, except for the beginning of the test and its final phases, when the effect of external or internal boundaries may appear, the time-drawdown curve evolves logarithmically; therefore, it is pointless to measure the drawdown at regular time intervals, and it is, instead, preferable to follow a time series such as: $t_{i+1} = e^\alpha \cdot t_i$, with α being a constant.

However, since the deviation from the logarithmic behavior at early and late stages cannot be known a priori, recommendations available in the literature traditionally encourage the use of empirical measurement methods that tend to reduce the acquisition frequency over time. Some examples for confined and unconfined aquifers are given in Table 4.1. This measurement approach is advisable, in particular, when an automatic acquisition system that can be set according to such frequencies is available.

When, instead, a manual procedure is used, greater precision can be achieved, by reading the time at which predetermined drawdown values are reached. By reading time rather than depth, measurement imprecisions associated to the resolution

Table 4.1 Recommended drawdown measurement frequency in the observation wells in confined and unconfined aquifers

Time from test start (min)	Measurement interval (confined aquifers) (min)	Measurement interval (unconfined aquifers) (min)
0–2	0.5	0.25
2–5	1	0.5
5–15	5	1
15–60	5	5
60–120	15	10
120–240	30	30
240–360	60	30
360–720	60	60
720–2880	60	180
>2880	60	480

Table 4.2 Recommended depth measurement intervals in the observation wells as a function of the cumulative drawdown value

Cumulative drawdown (cm)	Depth interval (cm)
0–30	1
30–50	2
50–100	5
> 100	10

of water level meters are eliminated; furthermore, the risk of missing important timepoints—and, thus, significant segments of the time-drawdown curve—because they aren't included in the predetermined acquisition time series can be prevented.

If this acquisition method is used, it is recommended to scan the drawdown according to depth intervals similar to those suggested in Table 4.2: depth intervals increase as the test progresses, since very close drawdown values are difficult to represent in a log-scale, and yield scarce additional information.

As regards slug tests, data acquisition must be automatic due to the short duration of the test, and time intervals of 1–3 s are usually recommended.

4.2 Aquifer Tests

Constant-rate pumping tests are the main kind of aquifer test. They consist in measuring the drawdown induced by the extraction of water from a well at a constant discharge rate in one or more observation points (Fig. 4.1a).

The correct interpretation of pumping tests during which the water level declines requires a rigorous procedure, illustrated in Fig. 4.2.

4.2.1 Hydraulic Behavior Identification

The main objective of an aquifer test with declining water level is the hydraulic characterization of an aquifer, in order to be able to calculate and thus predict the effects of a specific pumping regime. This is possible because the relation between discharge and the time-drawdown behavior is not unique: the equation that governs the groundwater flow directions and rates depends on specific hydraulic boundary conditions. Therefore, since an analytical solution of the groundwater flow equation is necessarily used regardless of the interpretation method (various available options are described in the sections that follow), the choice of the method must be preceded by the identification of aquifer's hydraulic behavior [30].

This can be achieved by using the data acquired during the constant rate aquifer test to plot a diagnostic curve, which is a log-log graph of the time-drawdown data (s versus t) recorded in one of the observation points, as shown in Fig. 4.3.

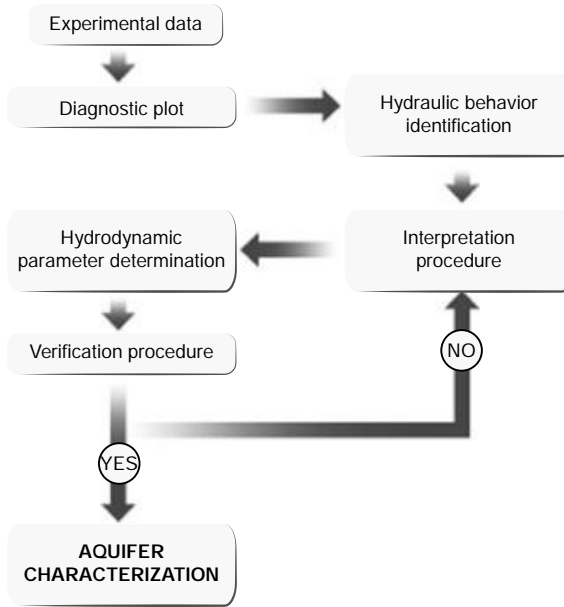


Fig. 4.2 Interpretation procedure of a constant discharge aquifer test for the characterization of an aquifer

The shape of the experimental diagnostic curve facilitates the identification of the aquifer’s hydraulic behavior (see Fig. 4.4), and, thus, of the physical model that best describes the hydrodynamic behavior of the groundwater subjected to the test.

The identification of the physical model and of the corresponding analytical model through the observation of the experimental data is reproducible and objective, and sets the foundations for the interpretation of the pumping test. The choice of the physical model cannot derive only from a lithostratigraphic and hydrogeological characterization of the subsurface: a geological model is useful and applicable to a

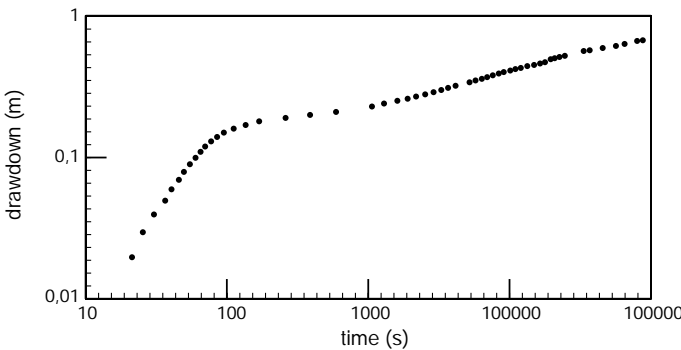
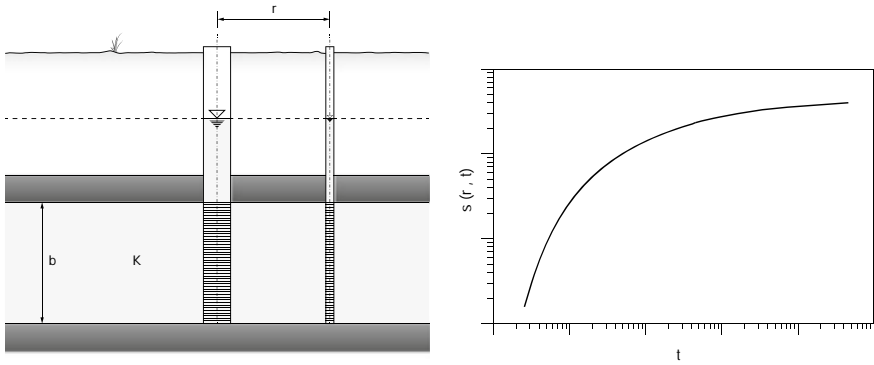
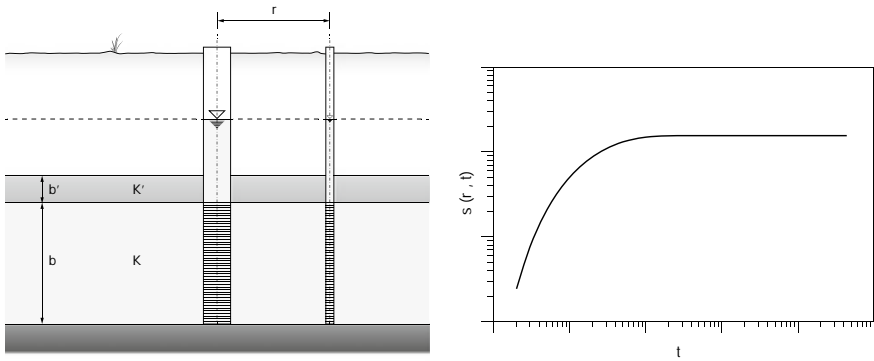


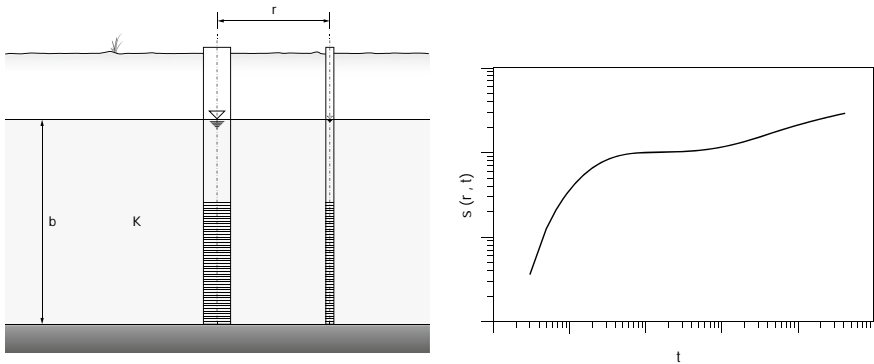
Fig. 4.3 Example of a diagnostic curve



(a) Confined



(b) Leaky



(c) Unconfined

Fig. 4.4 Identification of an aquifer’s hydraulic behavior based on the drawdown curve recorded over time in an observation well located at a distance, r , from the active well, during a constant-rate pumping test: **a** confined aquifer; **b** leaky aquifer; **c** unconfined aquifer

much broader scale than the one investigated by an aquifer test, while the description of the lithological layers crossed by the well, however accurate, provides only local information, which is irrelevant to the hydrodynamic behavior of the aquifer.

An a priori assumption of a physical model, not based on the experimental response of the system to an aquifer test, is one of the most frequent causes of erroneous aquifer characterization.

4.2.2 Interpretation Procedure

Once the aquifer's hydraulic behavior has been identified, one or more methods have to be selected for the interpretation of the test, in order to determine the most likely value of the hydrodynamic parameters, the number of which depends on the chosen physical model.

There are many interpretation methods, but they can be grouped into two general categories depending on the basic hypotheses and the boundary conditions necessary for the solution of the corresponding differential groundwater flow equation.

4.2.2.1 Basic Methods

The most frequently used methods fall into this category, and are based on the fulfillment of the following hypotheses [11, 30]:

- the medium is homogeneous and isotropic, and has constant thickness;
- Darcy's law is valid;
- the fluid's density and viscosity are constant;
- the potentiometric surface is in equilibrium and the initial hydraulic gradient is negligible compared to the effects induced by the pumping well;
- the flow is radial during pumping;
- the aquifer's horizontal extension is unlimited;
- the pumping well has an infinitesimal radius and volume, is open to flow over the entire saturated thickness (fully penetrating well) and is 100% efficient (see Chap. 5 for further details on the efficiency of water supply systems);
- the discharge is constant throughout the entire test;
- the observation wells or piezometers are completed with the same features as the main well.

For leaky aquifers the following additional conditions must be respected as well:

- the leaky aquifer is overlain by an aquitard, which is crossed by a vertical leakage flow;
- the storage in the aquitard can be neglected;
- the potentiometric surface of the aquifer that feeds the leaky aquifer through the aquitard is horizontal and does not vary as a consequence of leakage.

Table 4.3 Basic methods most frequently used for the interpretation of aquifer tests carried out in unsteady regime with constant discharge. The interpretation procedure, the equation describing the solution of the appropriate groundwater flow equation, the parameters that can be determined and the type of graph used to plot the experimental data of the test are reported [11, 15, 30]. In order for the logarithmic approximation used in Cooper and Jacob’s method for unconfined aquifers to be valid, the duration of the test must be very long

Aquifer type	Method	Interpretation procedure	Equation	Derivable parameters	s vs. t graph
Confined	Theis	Type curve matching	$s = \frac{Q}{4\pi T} W(u)$	T, S, K _r	log-log
	Cooper-Jacob	Linearization	$s = \frac{Q}{4\pi T} \ln 2.25 \frac{tT}{Sr^2}$	T, S, K _r	semilog
Leaky	Walton	Type curve matching	$s = \frac{Q}{4\pi T} W\left(u, \frac{r}{B}\right)$	T, S, B, K _r	log-log
Unconfined	Neuman	Type curve matching	$s = \frac{Q}{4\pi T} s_D(t_s, t_y, \beta)$	T, S, n _e , K _r , K _z	log-log
	Cooper-Jacob	Linearization	$s = \frac{Q}{4\pi T} \ln 2.25 \frac{tT}{ne^2r^2}$	T, n _e , K _r	semilog

The main methods used for the interpretation of aquifer tests are summarized in Table 4.3. The table only refers to tests conducted in an unsteady state since, as previously mentioned, steady state tests provide fewer parameters, despite being more expensive.

As evident from Table 4.3, the most commonly used procedure is the type curve matching method (delineated later in this section), which can be used for all aquifer types, provided that the correct family of curves is used [11, 15, 30].

It is a very simple method whose use is justified by the general solution of the groundwater flow equation:

$$s(r, t) = \frac{Q}{4\pi T} s_D(u) \quad \text{with} \tag{4.1}$$

$$u = \frac{Sr^2}{4Tt}, \tag{4.2}$$

and s_D the generic dimensionless function, solution of the diffusion equation, that reproduces the hydrodynamic behavior of the considered aquifer type; for confined aquifers $s_D = W(u)$, for leaky aquifers $s_D = W(u, r/B)$, for unconfined aquifers $s_D = s_D(t_s, t_s, \beta)$.

If a logarithm is applied to both terms of Eqs. (4.1) and (4.2) we obtain:

$$\log s = \log \frac{Q}{4\pi T} + \log s_D. \tag{4.3}$$

$$\log t = \log \frac{S r^2}{4T} + \log \frac{1}{u}. \quad (4.4)$$

Since both terms $\frac{Q}{4\pi T}$ and $\frac{S r^2}{4T}$ represent constants, Eqs. (4.3) and (4.4) indicate that the experimental time-drawdown curve, s versus t , recorded during the aquifer test has the same shape as the dimensionless s_D versus $1/u$ curve, characteristic of the aquifer type that best describes the behavior of the analyzed system, provided that the two curves are plotted on log-log graphs with the same scale (i.e., the logarithmic cycles have the same amplitude).

The implementation of the method is illustrated in all its phases in Fig. 4.5, with reference to a semi-confined aquifer [15, 30]:

- (a) the experimental data are reported in a log-log plot (diagnostic graph), to identify the hydraulic behavior;
- (b) a set of dimensionless theoretical curves corresponding to the identified type are selected, making sure the two plots have the same scale;
- (c) the plots are superimposed: historically this used to be done manually using tracing paper, but nowadays softwares capable of carrying out an automatized non-linear fitting are employed;
- (d) one of the graphs should be shifted over the other, maintaining the axes rigorously parallel, until the best superimposition of the experimental and type curves is obtained, thus identifying the theoretical reference model;
- (e) the values of the hydrodynamic parameters are calculated by applying Eqs. (4.1) and (4.2) to the coordinates of a chosen match point.

Another widely used method, albeit inappropriately, is the linearization of the experimental data in a semilogarithmic plot; this procedure, known as Cooper and Jacob's method, is only applicable to confined and unconfined aquifers (see Table 4.3) and is based on the logarithmic approximation of the well function [15, 30]:

$$s(r, t) = \frac{Q}{4\pi T} \ln 2.25 \frac{tT}{S r^2}, \quad (4.5)$$

$$\text{valid for } t \geq 12.5 \frac{S r^2}{T}. \quad (4.6)$$

If the test lasts long enough to obtain sufficient data points to identify a straight segment in the decline curve, the interpretation of the test also allows for the determination of the transmissivity, by using Δs the drawdown corresponding to a logarithmic time cycle on the straight line, and of the storativity by establishing the value of t_0 as the intersection of the straight line with the x-axis (Fig. 4.6). Once the test interpretation has been carried out by linearizing the experimental data, and the parameters T and S have been determined, it is necessary to verify that the considered points respect inequality (4.6). If (4.6) is not valid, the interpretation procedure must be repeated, eliminating early time data points.

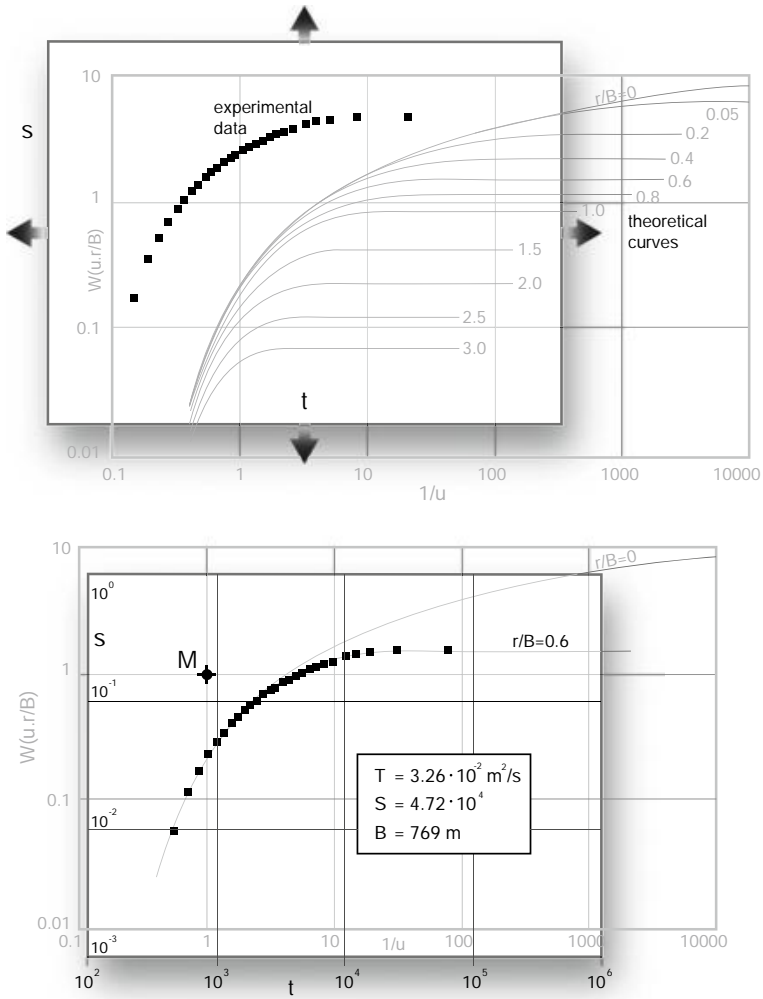


Fig. 4.5 Interpretation procedure of an aquifer test through the type curve matching method, in the case of a semi-confined aquifer

Inequality (4.6) indicates that the lower validity limit of Jacob’s approximation is strongly affected by the distance of the observation points, as well as by the value of the hydrodynamic parameters. However, in the range of distances recommended in Sect. 4.1, whilst no problems incur for confined aquifers, the extension of Cooper and Jacob’s method to water table aquifers requires a very long duration of the test (often greater than 12 h), due to the role played by the specific yield (two to three orders of magnitude greater than confined aquifers’ storativity).

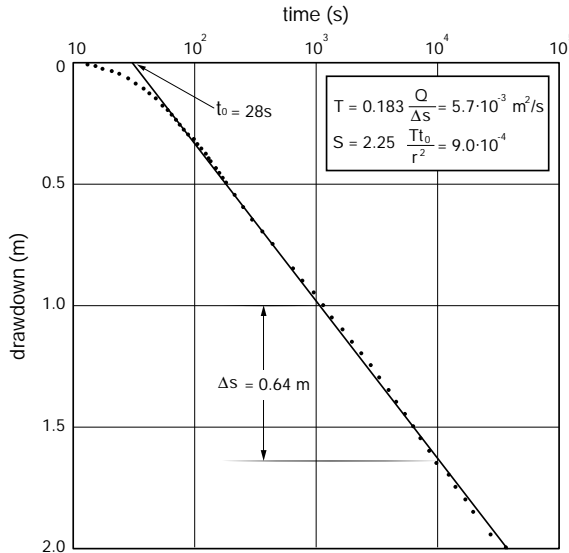


Fig. 4.6 Interpretation of a constant discharge aquifer test in a confined aquifer using Cooper and Jacob's method

4.2.2.2 Deviation from Ideal Behavior

Some of the hypotheses assumed as foundations for validity of the analytical solutions of the groundwater flow equation and, consequently, of aquifer test interpretation methods, cannot be fulfilled in reality (e.g., infinitesimal well radius and volume); others are very rarely satisfied by the actual physical situation (e.g., discharge may be variable, boundaries may be present within the area affected by the test, the well is often only partially penetrating). A particularly relevant cause of deviation from the ideal behavior of most aquifer tests is the so called *skin effect*: the formation damage that can occur in the annulus around the well as a result of the use of perforation fluids during drilling and inappropriate well development.

Hence, from a practical point of view, there are many factors which determine a deviation from the ideal behavior, whose underestimation inevitably leads to an erroneous interpretation.

Table 4.4 summarizes some of the main deviation factors, their influence, and the procedure that should be followed to keep them into account.

Finite Well Radius

Naturally, in order to fulfill its function, any well must have a finite radius, r_w , which is distinct from the infinitesimal value assumed in the solution of the groundwater flow equation; therefore, the dimensionless functions listed in Table 4.3 cannot be used below a certain limit (i.e., for $r < 20 r_w$). This limitation is irrelevant for all practical purposes, since it simply imposes not to construct any boreholes at a distance smaller than $20 r_w$ from the main well (maximum 5–6 m).

Table 4.4 Factors causing a deviation from the ideal behavior of a well, and their influence on the interpretation of an aquifer test

Theoretical assumption	Real situation	No effect for	How to address the deviation
Infinitesimal well radius	Finite radius	$r > 20 r_w$	Observation wells or boreholes at a distance of $r > 20 r_w$
Infinitesimal well volume	Finite volume (storage effect)	$t > \frac{25 C_{well}}{\pi T}$	Neglect data points for the first 60–100 s
Fully penetrating well	Often different	$r > 1.5 b$	For $r < 1.5 b$ interpret the test with specific methods (e.g., Neuman's method for unconfined aquifers, and Hantush and Jacob's method confined aquifers, respectively)
Unlimited aquifer	Sometimes, there are permeability or recharging boundaries	—	Use the image well system: Stallman's method
Constant permeability	Sometimes, permeability is affected in proximity of the well	Observation well	Perform well-borehole tests or, in single-well tests, quantify the damage
Constant discharge	Sometimes it changes	—	Apply the superposition principle
Negligible storage in the aquitard	Sometimes it changes	$\frac{r}{4B} \left(\frac{S'}{S}\right)^{0.5} < 0.01$	Use Hantush and Jacob's method based on the function $H(u, \beta)$

Finite Well Volume

The direct consequence of a well having a finite radius, is that it also has a finite volume, and this has more significant implications, since it causes the so called *wellbore storage effect*. In fact, upon activation from undisturbed conditions, a pump initially extracts the water stored in the wellbore, and groundwater only starts flowing once the water level inside the well has decreased.

The wellbore storage effect is quantified as:

$$C_{well} = -\frac{dV_w}{ds_w} = \pi(r_w^2 - r_p^2), \tag{4.7}$$

with r_p being the radius of the pump's discharge pipe.

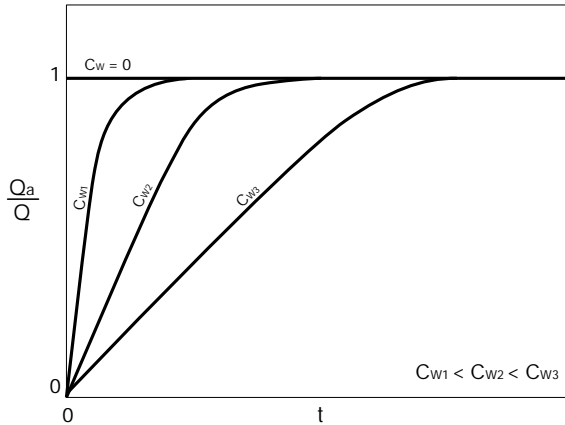


Fig. 4.7 Influence of well storage effect

It determines a shift between time zero, when the test begins, and the time at which the discharge, Q_a , provided by the aquifer is equal to the discharge, Q , supplied by the pump, and the larger the size of the well, the greater the time shift (see Fig. 4.7).

The influence of the wellbore storage effect, identifiable on the diagnostic graph as a segment with slope equal to one, becomes negligible for

$$t > \frac{25}{\pi} \cdot \frac{C_w}{T}. \quad (4.8)$$

Therefore, drawdown values collected earlier than this time should not be included in the interpretation.

Partially Penetrating Well

Another basic hypothesis which is rarely respected in reality is that the screened section of the pumping well fully penetrates the saturated thickness of the aquifer. The effect of partial penetration is a modification of the radial flow geometry towards the well, with an increased concentration of flow lines in correspondence of the screened section and the generation of vertical flow components. This results in increased drawdown; however, this effect is negligible at a distance greater than $1.5 b$, with b being the saturated thickness of the aquifer [15, 19, 30].

Therefore, if the observation points are located at a distance greater than $1.5 b$ from the pumping well, the effect of the partial penetration can be neglected. Conversely, if the distance is smaller, the effect will have to be kept into account by applying specific interpretation methodologies [30], such as Neuman's [34] or Moench's [33] method for unconfined aquifers, or Hantush' method [21] for confined aquifers.

Neuman's Method

A few years after determining the solution for fully penetrating wells in unconfined aquifers with delayed drainage, Neuman [35] offered a solution for partially penetrating wells.

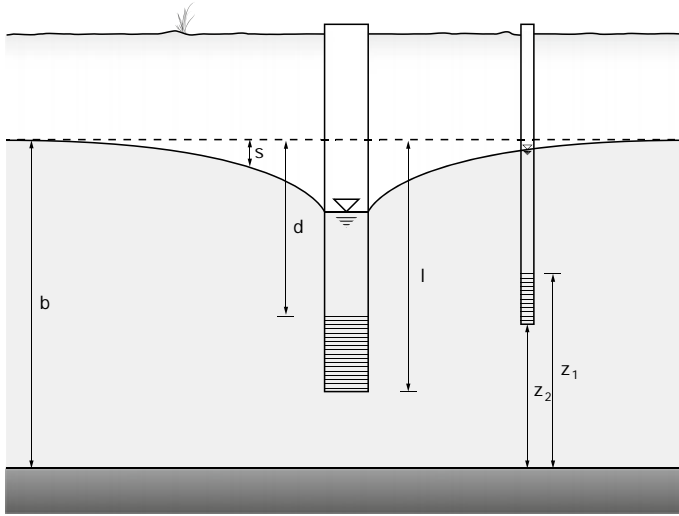


Fig. 4.8 Geometry parameters for the definition of the extent of partial penetration or completion of pumping and observation wells in an unconfined aquifer

If we refer to the geometry in Fig. 4.8, the drawdown at a distance r from the well pumping a constant discharge, Q , can be determined with Neuman's solution:

$$s(r, z, t) = \frac{Q}{4\pi T} \cdot \int_0^\infty 4yJ_0(y\beta^{\frac{1}{2}}) \cdot \left[u_0(y) + \sum_{n=1}^\infty u_n(y) \right] dy, \quad (4.9)$$

where

$$u_0(y) = \frac{\{1 - \exp[-t_s\beta(y^2 - \gamma_0^2)]\} \cdot [\sinh(\gamma_0 z_{2D}) - \sinh(y_0 z_{1D})]}{\{y^2 + (1 + \sigma)\gamma_0^2 - (y^2 - \gamma_0^2)^2 / \sigma\} \cosh(\gamma_0)} \cdot \frac{\sinh[\gamma_0(1 - d_D)] - \sinh[\gamma_0(1 - l_D)]}{(z_{2D} - z_{1D})\gamma_0(l_D - d_D) \sinh(\gamma_0)}$$

$$u_n(y) = \frac{\{1 - \exp[-t_s\beta(y^2 + \gamma_n^2)]\} \cdot [\sin(\gamma_n z_{2D}) - \sin(y_n z_{1D})]}{\{y^2 - (1 + \sigma)\gamma_n^2 - (y^2 + \gamma_n^2)^2 / \sigma\} \cos(\gamma_n)} \cdot \frac{\sin[\gamma_n(1 - d_D)] - \sin[\gamma_n(1 - l_D)]}{(z_{2D} - z_{1D})\gamma_n(l_D - d_D) \sin(\gamma_n)}$$

and the terms γ_0 and γ_n are the solutions of the equations

$$\begin{aligned} \sigma \gamma_0 \cdot \sinh(\gamma_0) - (y^2 - \gamma_0^2) \cdot \cosh(\gamma_0) &= 0 \\ \text{for } \gamma_0^2 &< y^2 \\ \sigma \gamma_n \cdot \sin(\gamma_n) + (y^2 + \gamma_n^2) \cdot \cos(\gamma_n) &= 0 \\ \text{where } (2n - 1) \cdot (\pi/2) &< \gamma_n < n\pi \text{ and } n \geq 1. \end{aligned}$$

Equation (4.9) can be compacted to the form [30]:

$$s(r, z, t) = \frac{Q}{4\pi T} \cdot s_D(l_D, d_D, z_{1D}, z_{2D}, \sigma, \beta, t_D), \quad (4.10)$$

with z_D , d_D , z_{1D} , and z_{2D} being, respectively, the parameters l , d , z_1 , and z_2 made dimensionless by dividing them by the saturated thickness b (e.g., $l_D = l/b$) and, in addition:

$$\begin{aligned} \sigma &= \frac{S}{S_y} = \frac{t_y}{t_s}, \\ \beta &= \frac{K_z}{K_r} \left(\frac{r}{b}\right)^2, \\ t_D = t_s &= \frac{T}{S r^2} \cdot t \text{ for short times,} \\ t_D = t_y &= \frac{T}{S_y r^2} \cdot t \text{ for long times.} \end{aligned}$$

It is worth noting that the definitions of σ , β , t_s , and t_y coincide with those already proposed by Neuman for fully penetrating wells (see Sect. 3.3.1.1).

Equation (4.10) highlights that s_D is a dimensionless function of seven parameters, four of which (i.e., l_D , d_D , z_{1D} and z_{2D}) depend on the geometry of the well, and the other three on the physical characteristics of the aquifer (i.e., σ , β , t_D).

This large number of independent parameters makes it impossible to generate a unique family of type curves to use in the interpretation of the aquifer test. In order for them to be usable, the type curves have to be expressed as a function of no more than two independent parameters. This goal can be achieved in the specific case that:

- (a) the geometry of the well-piezometer system is known;
- (b) the parameter σ is imposed to tend towards zero.

The first condition entails the generation of a new family of curves specific to the examined geometry for each pumping test. The condition of σ tending towards zero means that the storativity, S , is negligible with respect to the specific yield, S_y .

In an unconfined aquifer with delayed drainage, each theoretical curve is characterized by an initial and a final segment, separated by a straight horizontal segment whose length depends on the parameter σ . When σ tends towards zero, this intermediate straight segment becomes of infinite length. Two family of curves derive from this procedure, called *type A* and *type B* curves, that need to be plotted on distinct graphs, the former with respect to t_s and the latter with respect to t_y , see Fig. 4.9.

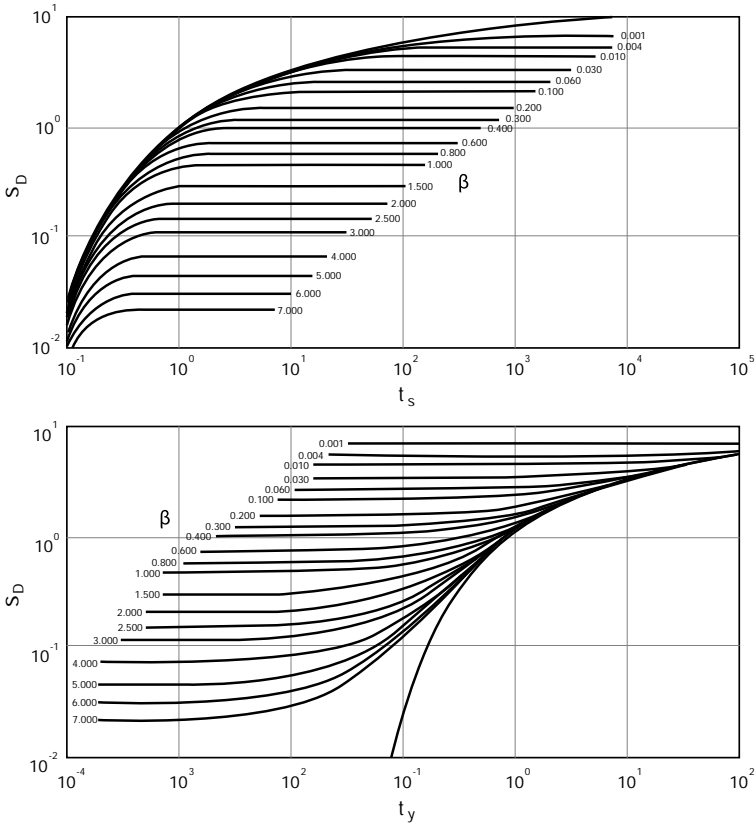


Fig. 4.9 Example of theoretical type A and B Neuman curves for the interpretation of pumping tests in unconfined aquifers with delayed drainage and only partially penetrating main and observation wells. In this specific case $\sigma = 10^{-9}$, $l_D = 0.94$, $d_D = 0.56$, $z_{1D} = 0$, and $z_{2D} = 1$

Type A and B curves represent the initial and final segments, corresponding to the first and third phase in Fig. 3.7, respectively.

Once the geometry parameters l_D , d_D , z_{1D} , and z_{2D} are known for each specific situation, and with σ tending towards zero, it is possible to calculate the dimensionless drawdown, s_D , as a function of t_s (or of t_y) and for different values of β [36].

It is, therefore, possible to generate the two families of type curves A and B for the interpretation of aquifer tests, which is implemented with custom softwares.

Moving on to the actual interpretation, we have that:

$$s_D = \frac{4\pi T}{Q} \cdot s,$$

$$t_D = \frac{T}{Sr^2} \cdot t,$$

where t_D can take on the values of t_s or t_y . By applying base 10 logarithms:

$$\log(s_D) = \log \frac{4\pi T}{Q} + \log(s),$$

$$\log(t_D) = \log \frac{T}{Sr^2} + \log(t).$$

In a log-log scale there is a linear relation between s_D and s , and between t_D and t . Therefore, in log-log plots with the same scale, the theoretical curve, t_D versus s_D , and the experimental one, t versus s , coincide save for a constant, meaning that they are simply translated one with respect to the other. The translation is equal to $T/(Sr^2)$ along the x-axis, and to $4\pi T/Q$ along the y-axis.

Based on the above, the operational procedure for the interpretation of the test is the following:

- (a) match the final part of the experimental data with the type B curves, keeping the axes of the two plots parallel until the best superimposition has been identified;
- (b) take a note of the identified value of β ;
- (c) select an arbitrary match point in the overlapping part of the plots. The coordinates of the match point are s^* , t^* on the experimental plot, and s_D^* , t_y^* on the theoretical plot;
- (d) determine the transmissivity T and the specific yield S_y :

$$T = \frac{Q}{4\pi} \cdot \frac{s_D^*}{s^*},$$

$$S_y = \frac{T}{r^2} \cdot \frac{t^*}{t_y^*};$$

- (e) match the initial part of the experimental curve with the type A curves, maintaining the axes of the two plots parallel to each other until the best superimposition has been identified. The corresponding value of β must coincide with the one determined in point b;
- (f) select a second match point whose coordinates are s^* , t^* on the experimental curve with s_D^* and t_s^* on the theoretical one;
- (g) determine the transmissivity, T , and the elastic storativity, S :

$$T = \frac{Q}{4\pi} \cdot \frac{s_D^*}{s^*},$$

$$S = \frac{T}{r^2} \cdot \frac{t^*}{t_s^*};$$

the value of T thus calculated should be equal, or at least very close, to the value determined in point (d);

(h) determine the hydrodynamic parameters:

horizontal permeability coefficient:	$K_r = T/b;$
degree of anisotropy:	$K_D = \beta b^2/r^2;$
vertical permeability coefficient:	$K_z = K_D \cdot K_r;$
specific storage:	$S_s = S/b.$

Figure 4.10 depicts the type curve matching between the dimensionless curves in Fig. 4.9 and the experimental data of an aquifer test.

Hantush' Method

This method represents a modified version of Cooper and Jacob's, developed to keep into account partial well penetration or completion [21]. If a partially penetrating well and piezometer in a confined aquifer are considered, such as in Fig. 4.11, according to the Hantush method the drawdown induced by a well pumping a constant discharge, Q , at a distance, r , from the well itself is:

$$s(r, z, t) = \frac{Q}{4\pi T} \cdot \left\{ W(u) + f_s \left(\frac{r}{b}, \frac{l}{b}, \frac{d}{b}, \frac{z}{b} \right) \right\}, \quad (4.11)$$

where $z = \frac{l+d}{2}$, $W(u)$ is the well function, while f_s is the dimensionless function that keeps into account the partial penetration or completion and determines an additional drawdown relative to the Theis solution [21]:

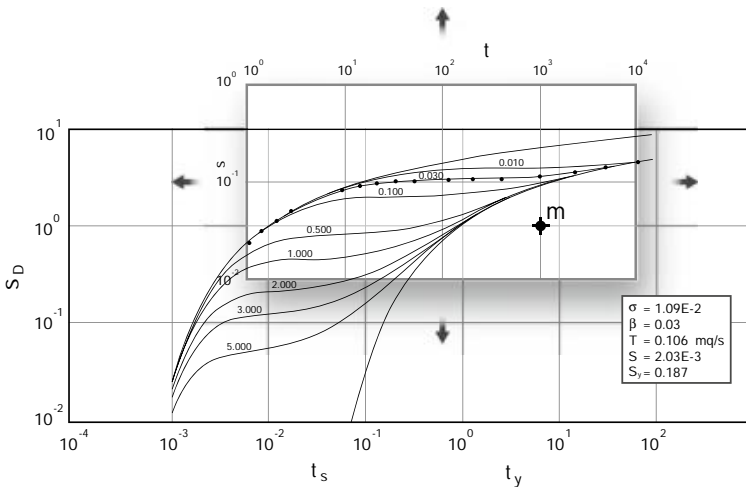


Fig. 4.10 Example of interpretation of a pumping test conducted in a partially penetrating well-borehole system in an unconfined aquifer with delayed drainage. The geometry of the well-borehole system is equal to the values reported in Fig. 4.9

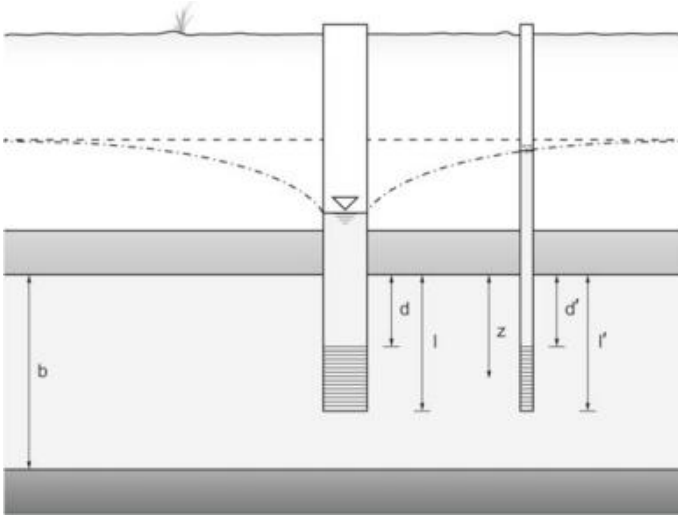


Fig. 4.11 Geometry parameters used to define the degree of partial penetration or completion of the pumping and observation well in a confined aquifer

$$f_s = \frac{4b^2}{\pi^2 t(l-d)(l-d')} \cdot \sum_{n=1}^{\infty} \left\{ \left(\frac{1}{n^2} \right) - K_0 \left(\frac{n\pi r}{b} \right) \cdot \left[\sin \left(\frac{n\pi l}{b} \right) - \sin \left(\frac{n\pi d}{b} \right) \right] \cdot \left[\sin \left(\frac{n\pi l'}{b} \right) - \sin \left(\frac{n\pi d'}{b} \right) \right] \right\}.$$

The function f_s depends exclusively on the geometry of the well-borehole system, and is independent of time. Therefore, once the time limit for the application of the logarithmic approximation has passed, the above equation becomes:

$$s = \frac{Q}{4\pi T} \cdot \left\{ \ln t + \ln \left(2.25 \frac{T}{Sr^2} \right) + f_s \right\}. \quad (4.12)$$

In a semi-logarithmic s versus $\ln t$ plot, (4.12) is the equation of a straight line, see Fig. 4.12.

The transmissivity can, therefore, be calculated based on Δs , the drawdown corresponding to a logarithmic time cycle on the straight line in Fig. 4.12 [30]:

$$T = \frac{Q}{4\pi \Delta s}.$$

If t_0 is defined as the intersection of the interpolating straight line with the x-axis ($s = 0$), then [30]:

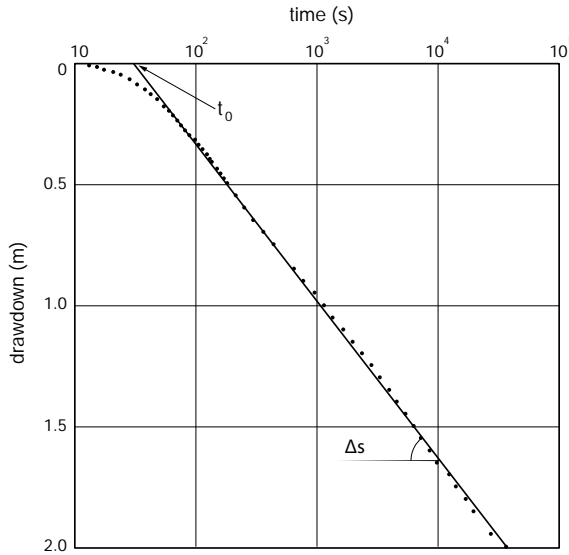


Fig. 4.12 Semi-logarithmic plot of an aquifer test data at constant discharge

$$\ln t_0 + \ln \left(2.25 \frac{T \cdot t_0}{Sr^2} \right) + f_s = 0, \text{ hence,}$$

$$\ln \left(2.25 \frac{T \cdot t_0}{Sr^2} \right) = -f_s, \text{ so the storativity is equal to:}$$

$$S = 2.248 \frac{T \cdot t_0}{r^2} \cdot e^{f_s}. \tag{4.13}$$

Since the partial completion of the well does not influence the slope of the straight line s versus $\ln t$, ignoring the partial geometry shouldn't cause any error in the determination of the transmissivity, whereas it impacts the calculation of the storativity.

Presence of Boundaries

In certain circumstances, the evolution of an aquifer test can be influenced by the existence of one or more boundaries in the area affected by the test. Such boundaries, which can be recharging (e.g., rivers, canals, lakes) or impermeable (barrier or permeability boundaries; e.g., a change in the lithology of the aquifer, presence of impermeable faults), invalidate the hypothesis of unlimited aquifer, which is one of the foundations of the analytical solution of the groundwater flow equation.

The problem can be solved by employing the image well system, which consists in defining the analytical function that reproduces a hydraulic situation equivalent to the existing physical system, as depicted in Fig. 4.13 [14, 30].

As a first simple example, let's consider the existence of a recharging boundary within the area affected by the pumping well. The aquifer behaves as if it were unlimited until the radius of investigation reaches the boundary; from that point on, the recharging effect begins, and the cone of depression develops asymmetrically.

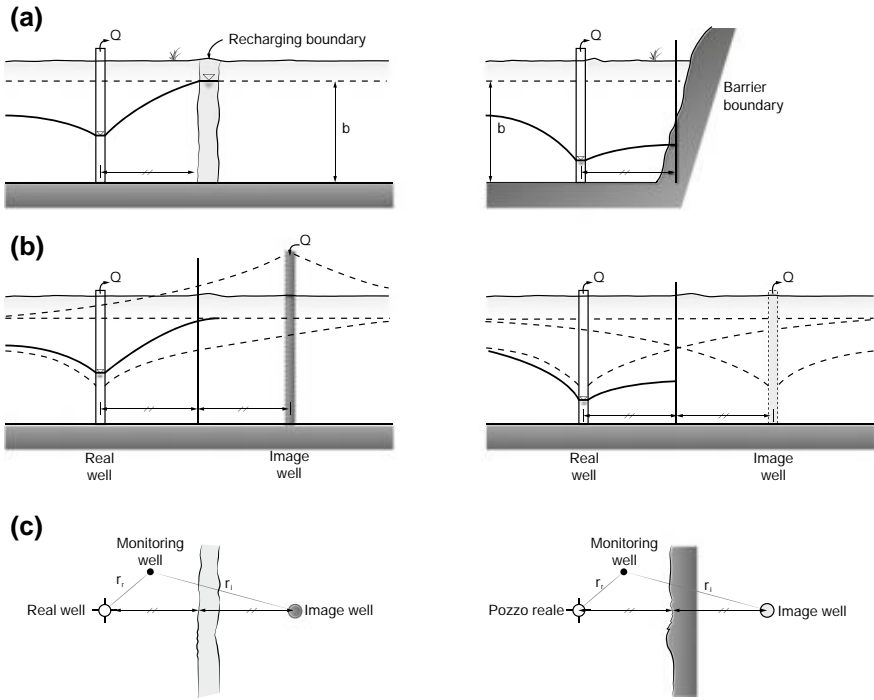


Fig. 4.13 Influence of recharging or barrier boundaries: **a** actual physical situation; **b** equivalent hydraulic model (cross-section); **c** equivalent hydraulic model (plan view) (modified from [30])

Conceptually, the actual physical situation can be replaced by a hydraulically equivalent virtual configuration, i.e., the virtual system causes the same effects on flow directions and rates as the existing boundary. In the considered case, the hydraulically equivalent situation is represented by a virtual well, called *image well*, located symmetrically to the real one and into which a discharge, Q , equal to the discharge pumped by the real well, is injected from time $t = 0$. The resulting cone of depression derives from the superimposition of the cone of depression created by the real well and the cone of recharge created by the virtual well.

Mathematically, the drawdown at a generic distance, r_r , from the real well can be calculated by applying the superposition principle, according to Stallman’s method, as quoted by [14, 30]. In the case of an unconfined aquifer, and if the delayed drainage effect is neglected, this leads to the following solution:

$$s(r_r, t) = \frac{Q}{4\pi T} \cdot [W(u_r) - W(u_i)], \tag{4.14}$$

where $u_r = \frac{Sr_r^2}{4Tt}$ and $u_i = \frac{Sr_i^2}{4Tt}$.

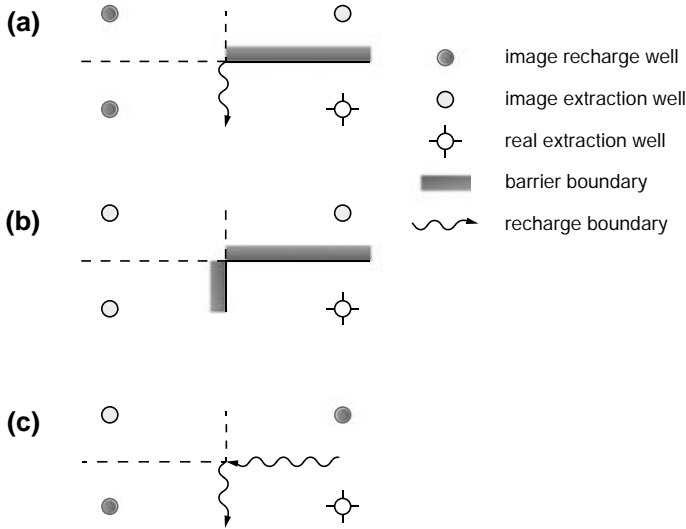


Fig. 4.14 Image well configuration for perpendicular boundaries

If $\beta = \frac{r_i}{r_r}$ represents the ratio between the distances of the observation point from the image and the real well, respectively, Eq. (4.14) can be re-written as follows:

$$s(r_r, t) = \frac{Q}{4\pi T} \cdot [W(u_r) - W(\beta^2 u_r)] = \frac{Q}{4\pi T} \cdot W(u, \beta), \quad (4.15)$$

with $W(u, \beta)$ being the analytical function resulting from the superposition principle.

If there is a barrier boundary, the conceptual approach does not change, except for the fact that the virtual injection well will be replaced by a pumping well abstracting the same discharge Q as the real well. Analytically, therefore, we will have:

$$s(r_r, t) = \frac{Q}{4\pi T} \cdot [W(u_r) + W(\beta^2 u_r)] = \frac{Q}{4\pi T} \cdot W(u, \beta). \quad (4.16)$$

Comparing the cited examples, one can conclude that a barrier boundary produces a well of the same sign as the real well, while a recharging boundary produces one of the opposite sign.

If two boundaries form a right angle, three image wells will have to be used (see Fig. 4.14), while if two parallel boundaries are present, infinite virtual wells are necessary, because infinite images of the images are created (see Fig. 4.15).

Consequently, the drawdown induced by a well pumping a constant discharge Q from a finite aquifer with generic geometry can be expressed as follows [14, 30]:

$$s(r_r, t) = \frac{Q}{4\pi T} \cdot \left[W(u_r) + \sum_{i=1}^n \pm W(\beta_i^2 u_r) \right] = \frac{Q}{4\pi T} \cdot W(u, \beta_{1 \rightarrow n}), \quad (4.17)$$

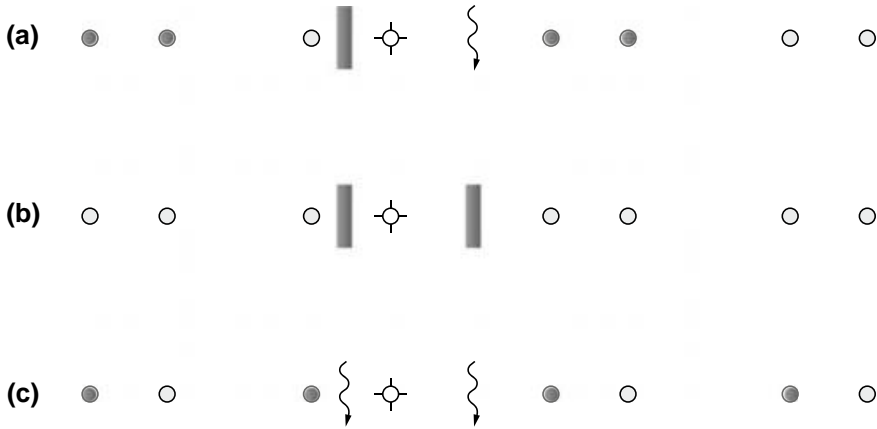


Fig. 4.15 Image well configuration for parallel boundaries

where n is the total number of image wells, and the index i indicates the i th image well.

The main conclusions that can be drawn from Eq. (4.17) are that:

- (a) regardless of the type and geometry of the boundaries present in the area influenced by a generic pumping well, the problem can be solved analytically by identifying a hydraulically equivalent image well system;
- (b) a recharging boundary is always represented by an image well of opposite sign relative to the real well, while a barrier boundary always corresponds to an image well of the same sign;
- (c) the further the image well, the smaller its effect; therefore, even in the presence of parallel boundaries, it isn't necessary to extend the summation present in Eq. (4.17) to infinity, and it is sufficient to interrupt it at a term generically identified as n , which corresponds to the last image well producing a measurable effect on the flow directions and rates;
- (d) once the function $W(u, \beta_{1 \rightarrow n})$ is built for the specific geometry under consideration, the type curve matching method can be applied to it to interpret a constant discharge pumping test (Stallman's method [14, 30]).

Aquifer Heterogeneity

One of the basic hypothesis of any analytical solution is that the formation is homogeneous. Without entering the discussion about the actual validity of this hypothesis in real aquifers, one cannot, however, forget that in close proximity to a well there can be areas with reduced permeability. These can result from the potential damage caused by inappropriate deployment of perforation fluids, not removed by an adequate well development.

Also in this situation, an additional hydraulic head drop can be measured at the pumping well, while, of course, its effect is almost null in the observation points.

This is one of the reasons for which it is preferable to carry out multiple- rather than single-well pumping tests. In the case of a single-well geometry, the effect of damage next to the well must be kept into account (see Sect. 5.4.2).

Varying Discharge

Finally, if operational conditions hinder the achievement of a constant discharge during the test, the superposition principle in time can be applied to interpret the experimental data [14], although an additional degree of complexity is introduced in the identification of potential anomalies.

Aquitard Drainage

Up until here, factors producing a deviation in the ideal behavior that are independent of the aquifer type have been discussed. If we focus our attention on leaky aquifers, however, we find that the hypothesis that the aquitard contributes no water from its storage is not always verified. This condition ($S' = 0$), which represents the foundation of Walton's method, can only be considered valid for:

$$\beta = \frac{r}{4B} \cdot \left(\frac{S'}{S}\right)^{0.5} < 0.01. \quad (4.18)$$

In the other cases it is necessary to replace Walton's function $W(u, \frac{r}{B})$ (Eq. 3.22 [18]) with Hantush's, $H(u, \beta)$ [20]:

$$H(u, \beta) = \int_u^\infty \frac{e^{-y}}{y} \cdot \operatorname{erfc} \left(\beta \cdot \left(\frac{u}{y(y-u)}\right)^{0.5} \right) dy \quad (4.19)$$

where erfc is the complementary error function (see 12.1.1 for the definition of this function and Fig. 12.3 for its shape).

4.3 Recovery Tests

A recovery test is a particular kind of aquifer test during which the increase in the water level (or decrease of residual drawdown) is measured. Residual drawdown measurements begin after interrupting the pump at the end of a well pumping period at a constant discharge (see Fig. 4.1b).

For the interpretation of the test, Theis' recovery method is normally used, which is based on the superposition principle: the well is assumed to continue abstracting the same constant discharge Q even after the interruption of the pump at time t , and at this time an imaginary recharge well, placed at the same point, is assumed to start feeding an equal flow as the pumping well; hence, interpretation of the test requires the superposition of two Theis curves [40]. Theis' recovery method is based on the same assumptions as Theis' equation, and is, therefore, theoretically only valid for confined aquifers. However, Neuman [36] demonstrated that it can

be applied also to unconfined aquifers, provided that only late recovery data are considered [30]. In the case of leaky aquifers, instead, Theis' recovery method can only be used for the determination of transmissivity if short times are considered [30]; alternatively, Hantush (as quoted by [30]) formulated an equation to express the residual drawdown, subsequently used by Vandenberg [42] to outline a method for the derivation of hydrodynamic parameters.

The residual drawdown, s' , in the well, at the time $t + t'$, after the pump has been shut down can be derived by employing Theis' recovery method [40] and by applying Cooper and Jacob's logarithmic approximation of the well function [7]. The storativity is assumed to be constant and equal before and after the interruption of the pump, and the transmissivity is considered to be constant.

$$s'(t + t') = \frac{1}{4\pi T} \cdot \left[Q \ln 2.25 \frac{(t + t') T}{S r^2} - Q \ln 2.25 \frac{t' T}{S r^2} \right] = \frac{Q}{4\pi T} \cdot \ln \left(\frac{t + t'}{t'} \right) \quad (4.20)$$

where t is the duration of the pumping phase, and t' the time interval following the interruption of the pump (recovery phase), see Fig. 4.1b. Equation (4.20) can be re-written changing the logarithms to base 10:

$$s'(t + t') = 0.183 \cdot \frac{Q}{T} \cdot \log \left(\frac{t + t'}{t'} \right). \quad (4.21)$$

According to this method, to interpret a recovery test the following procedure should be used (see Fig. 4.16):

- (a) the displacement data acquired during the recovery phase should be plotted with a semilogarithmic scale. In particular, the recovery levels s' are plotted with a linear scale, while the ratio $\frac{t'}{t+t'}$ is plotted with a log-scale;
- (b) the straight segment of the recovery curve is identified, after excluding the points that correspond to the early recovery phase;
- (c) the drawdown, $\Delta s'$, that corresponds to one logarithmic cycle is calculated on the straight segment;
- (d) the transmissivity, T , is calculated using the following relations:

$$T = \frac{Q}{4\pi \Delta s'} \quad \text{if natural logarithms were used;}$$

$$T = 0.183 \cdot \frac{Q}{\Delta s'} \quad \text{if logarithms to base 10 were used.}$$

Recovery tests during which water levels are measured in the active well represent a methodological tool for the quantification of the potential permeability damage near the well itself, assessed through a sound and commonly used procedure in the petroleum industry. This method, however, can only be applied to confined and unconfined aquifers, excluding leaky aquifers. Parameters related to permeability damage in the area close to a well can also be determined through the interpretation

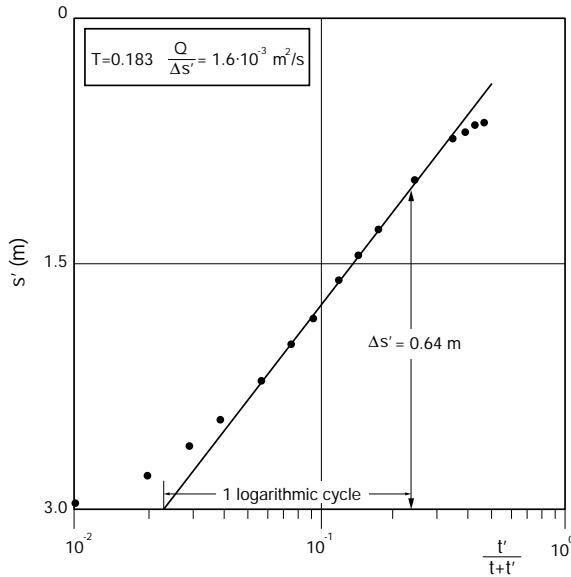


Fig. 4.16 Recovery test interpretation

of data acquired during a slug test *via* the KGS method (see Sect. 4.4.4). An innovative approach for the interpretation of stepdrawdown test and recovery test for the determination of hydrodynamic parameters is described in Sethi (2011) [39].

4.4 Slug Test

Slug tests induce an instantaneous variation of the static water level in a well or piezometer, and subsequently measure the recovery over time of the undisturbed level in the same well.

It is, therefore, a single-well test, carried out in unsteady state regime with the objective of determining the hydraulic conductivity of the aquifer in close proximity to the active well [16].

The test can be conducted by abruptly increasing the static water level via the injection of a known volume of water in the well, and subsequently monitoring the drawdown caused by the flow from the well towards the aquifer (slug injection test). Such operating condition offers an accurate result only if the undisturbed water level is above the screen: in this case, the flow from the well to the aquifer will involve—as it should—only the saturated portion of the formation [3]. Conversely, if the undisturbed level is within the screened portion of the well, a slug test with declining head would cause water to flow not only towards the saturated portion of

the aquifer, but also towards the unsaturated zone, thus determining a greater decline rate and, eventually, an overestimation of the hydraulic conductivity.

Alternatively, a sudden decline of the static level can be induced by extracting a known volume of water, followed by the recording of the consequent water level rise, caused by the flow from the aquifer towards the well (slug withdrawal test) [4]. The second method is more commonly used due to its simpler implementation and more reliable interpretation (see Fig. 4.1c) [16, 30].

A slug test has the undeniable advantage over traditional aquifer tests of being very simple and quick to carry out. This is also reflected in significantly lower costs: in particular, slug tests do not involve the use of pumps or sophisticated equipment, nor of distinct active and observation wells [3, 11]. And since a pump doesn't have to be installed, slug tests can also be carried out in small-diameter wells. Owing to the simplicity of their execution they can be repeated over time and thus provide useful information about potential variations of the hydraulic conditions close to the well [4, 30]. In addition, slug tests can be used in systems in which pumping would not be advisable, such as low permeability aquifers in which the well could dry, or contaminated aquifers, where the pumped water would have to be treated [16].

On the other hand, the flow induced by a slug test is very small. Therefore, the response to the sudden water level perturbation, and the hydraulic conductivity that can be derived from it, are strongly influenced by the hydraulic conditions present in the proximity of the well (e.g., effects of the perforation method, geometry of the well, possible permeability damage).

In other words, slug tests aren't as reliable as traditional multi-well aquifer tests, which remain the most recommended method for characterizing an aquifer, and are the only one which allows the determination of the aquifer's hydraulic behavior. Nevertheless, execution simplicity and low cost make slug tests a valuable tool for the evaluation of the spatial variability of the aquifer's hydrodynamic parameters, which can be assessed by conducting a slug test in every piezometer of the monitoring network [4, 30, 38].

4.4.1 Interpretation Models

A number of two-dimensional mathematical models, both analytical and semi-analytical, to interpret slug tests have been developed over the years, starting in the '50s, the most commonly used being Hvorslev's [23], Cooper, Bredehoeft and Papadopoulos' [8], and Bouwer and Rice's [3] methods; the latter two are illustrated in the following sections.

In the mid '90s, a research team of the Kansas Geological Survey (KGS) presented a three-dimensional semi-analytical method for the interpretation of slug tests conducted in partially penetrating or partially completed wells in confined and unconfined aquifers [24]. This model, which incorporates the concept of aquifer storage, is known as the KGS model, and represents the most advanced currently available interpretation method.

Nevertheless, we will start by describing Bouwer and Rice's method since it still is, to date, the most commonly used. This will provide the tools to understand its theoretical framework and its limitations.

4.4.2 Bouwer and Rice's Method

Let us consider a well or a piezometer completed in an unconfined aquifer, with the geometry depicted in Fig. 4.17.

Bouwer and Rice's theory is founded on the following assumptions [3]:

- the aquifer is homogeneous and isotropic, and, therefore, there is no permeability damage in the proximity of the well;
- groundwater flow obeys Darcy's law;
- the aquifer is unlimited in all directions;
- the aquifer's storage is negligible;
- hydraulic head losses due to flow through the screen are negligible;
- the water table does not fluctuate in time;
- the flow caused by the hydraulic head variation is exclusively horizontal (the virtual horizontal planes crossing the top and bottom of the screen act as impermeable boundaries).

Under these hypotheses, the discharge that flows through the well screen, for a generic variation, s , of the water level relative to the undisturbed level, can be expressed by

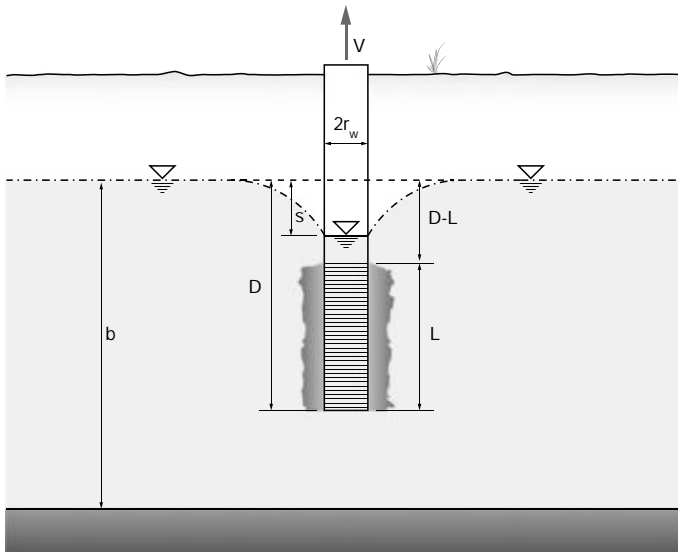


Fig. 4.17 Geometry parameters of a well completed in an unconfined aquifer

using a quasi-steady state approach and adapting Thiem's equation (Eq. 3.13 in Sect. 3.1.2) to the geometry under consideration:

$$Q = 2\pi K_r L \cdot \frac{s}{\ln\left(\frac{R_e}{r_d}\right)}, \quad (4.22)$$

where L is the length of the screen, R_e represents the effective radial distance beyond which the head variation s is dissipated, while r_d is the radial distance beyond which the aquifer is undisturbed (i.e., beyond which the original petrophysical properties are unmodified by the perforation and completion of the well) [3, 30].

For the principle of mass conservation, the discharge, Q , can also be expressed as a function of the rate of variation of the water level inside the well or piezometer whose radius is r_w :

$$Q = -\pi r_w^2 \cdot \frac{ds}{dt}. \quad (4.23)$$

Setting the two expressions equal to each other, the following differential equation is obtained:

$$\frac{ds}{s} = -\frac{2K_r L}{r_w^2 \ln\left(\frac{R_e}{r_d}\right)} dt, \quad (4.24)$$

which, integrated keeping into account the boundaries, leads to the following solution:

$$\ln \frac{s_0}{s} = \frac{2K_r L}{r_w^2} \cdot \frac{t}{\ln\left(\frac{R_e}{r_d}\right)}. \quad (4.25)$$

Bouwer and Rice's solution indicates that the water level variation s increases semi-logarithmically with time (see Fig. 4.18); therefore, ideally, the points $\ln(s)$ versus t should align along a straight line whose slope, m , is proportional to the hydraulic conductivity of the formation.

m can be determined simply by selecting two points on this straight line and calculating:

$$m = \frac{\ln s_0 - \ln s}{t - t_0},$$

and thus [3]:

$$K_r = \frac{r_w^2 \ln(R_e/r_d)}{2 \cdot L} \cdot m. \quad (4.26)$$

The only problem arising in the application of the above solution is related to the determination of the effective radius, R_e , which is a function of the following parameters linked to the geometry of the well (refer to Fig. 4.17):

$$R_e = f(L, D, b, r_d).$$

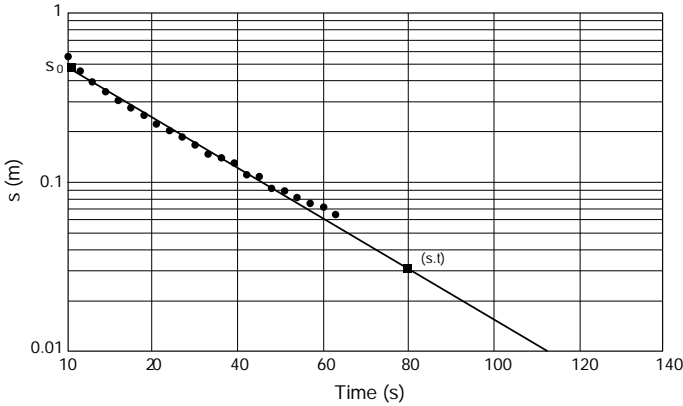


Fig. 4.18 Interpretation of a slug test with Bower and Rice’s method

Bouwer and Rice solved this issue by using an electrical analogy, which allowed them to define R_e as a function of the constants A , B , and C as follows [3]:

Partially penetrating wells ($D < b$)

$$\ln \frac{R_e}{r_d} = \left\{ \frac{1.1}{\ln \left(\frac{D}{r_d} \right)} + \frac{A + B \ln \left[\frac{b-D}{r_d} \right]}{\frac{L}{r_d}} \right\}^{-1} \quad (4.27)$$

Fully penetrating wells ($D = b$)

$$\ln \frac{R_e}{r_d} = \left\{ \frac{1.1}{\ln \left(\frac{b}{r_d} \right)} + \frac{C}{\frac{L}{r_d}} \right\}^{-1} \quad (4.28)$$

The values of A , B , and C are plotted as a function of the ratio $\frac{L}{r_d}$ in Fig. 4.19.

4.4.2.1 Duration of a Slug Test

In highly permeable formations, the time for the water level to recover its undisturbed value can be very short, requiring the use of automatic measurement and recording devices [3].

During the test planning phase, it is therefore important to be aware of the order of magnitude of its duration. This can be obtained by calculating the necessary time to recover 90% of the initial water level displacement by introducing the order of magnitude expected for the hydraulic conductivity in Eq. (4.25):

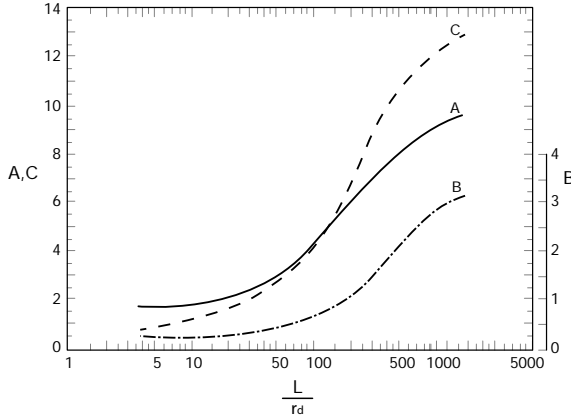


Fig. 4.19 Plot for the determination of the dimensionless parameters A, B and C for the calculation of the effective radius R_e (modified from [3])

$$t_{90\%} = 1.15 \cdot \frac{r_w^2}{K_r \cdot L} \cdot \ln \left(\frac{R_e}{r_d} \right). \tag{4.29}$$

4.4.2.2 Deviation from Ideal Behavior

Influence of Storage

Amongst their founding hypotheses, both Bouwer and Rice’s [3] and Hvorslev’s [23] methods neglect storage. However, in reality, all aquifers are characterized by a certain storage capacity, which causes the experimental data, $\ln s$ versus t , not to align along a straight line, but to exhibit a curvature even in perfectly executed slug tests (see Fig. 4.20).

Thus arises the problem of identifying the straight line that best approximates the semi-logarithmic theoretical model. Butler [4] recommends selecting the linear behavior, in particular, in the range $s/s_0 = 0.15$ to 0.25 .

Effect of the Gravel Pack

Apart from the curvature deriving from storage, two distinct linear segments can often be identified when plotting the recovery of head data, the first of which (AB) is much steeper than the second (BC) (Fig. 4.21). This can be caused by the gravel (or filter) pack and/or the development in proximity to the well, which created an area with high permeability that favors a much faster response to the instantaneous perturbation (AB segment). Then, once the transient regime starts affecting the undisturbed area of the aquifer, a second linear section—relevant for hydraulic conductivity calculations—can be identified (BC segment).

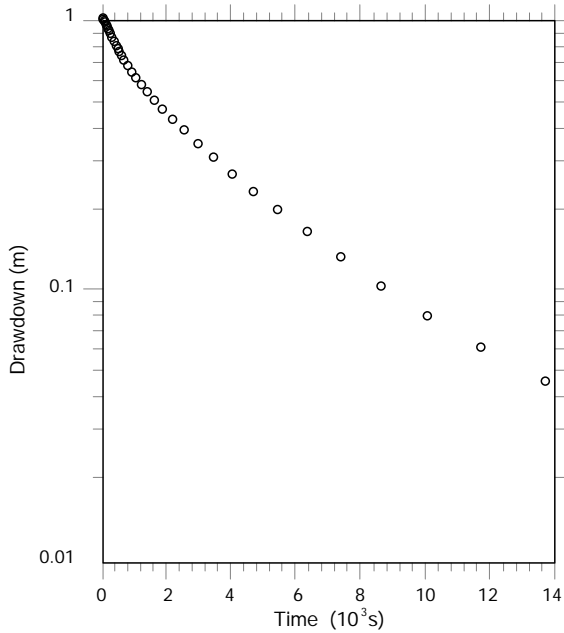


Fig. 4.20 Influence of the aquifer's storage on the linearization of experimental data in a semi-logarithmic plot

The double linearization occurs mainly when both static level and displacement fall within the screened section, whereas it should not appear when the displacement is outside the screen [2].

Effect of the Size of the Well and of the Length of the Screen

Theoretically, the diameter of the well or piezometer and the length of the screen should not have any impact on the interpretation of a slug test.

In practice, however, a couple of useful considerations on the design and interpretation of the test should be made [2]:

- the values of r_d and L should be such that the ratio L/r_d falls within the range 5–1500, for which the values of the parameters A, B and C are available;
- the greater the values of r_d and L , the more significant the value of the obtained hydraulic conductivity, because it corresponds to a greater aquifer volume;
- in the case of piezometers with a small diameter (such as 5 cm), the derivable hydraulic conductivity is only representative of a small portion of aquifer, and is, therefore, more susceptible to spatial variations. In addition, in this case, the uncertainties about the size of the gravel pack and/or the developed area have a greater numerical influence on the determination of the hydraulic conductivity.

Effect of the Aquifer Type

Although Bouwer and Rice's analysis refers to unconfined aquifers [3], Bouwer

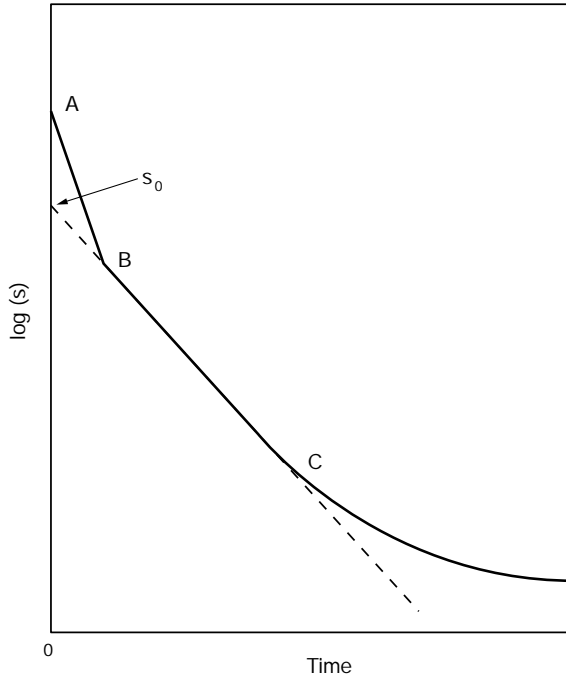


Fig. 4.21 Schematic representation of the double linearization (modified from [2])

subsequently extended its applicability also to the other types of hydraulic behavior (confined and leaky aquifers) [2]. Theoretically, the greater the distance between the top of the screen and the impermeable or semi-permeable layer that overlies the aquifer, the more reliable the obtainable results are likely to be.

4.4.3 Cooper, Bredehoeft and Papadopoulos' Method

Despite having been developed earlier (1967), Cooper, Bredehoeft and Papadopoulos' method [8] offers the additional advantage of taking into account the storage capacity of the formation; on the other hand, it can only be applied to confined, homogeneous, isotropic and unlimited aquifers.

The assumptions are that the well is fully penetrating (i.e., screened over the entire saturated thickness, see Fig. 4.22) and that Darcy's law is valid.

Under these hypotheses, the equation governing the behavior of the system is the classical two-dimensional groundwater flow equation for a radial coordinate system:

$$\frac{\partial^2 h}{\partial r^2} + \frac{1}{r} \frac{\partial h}{\partial r} = \frac{S}{T} \frac{\partial h}{\partial t}, \tag{4.30}$$

with the following boundary conditions:

$$h(r_w, t) = s(t) \text{ for } t > 0, \tag{4.31}$$

$$h(\infty, t) = 0 \text{ for } t > 0, \tag{4.32}$$

$$h(r, 0) = 0 \text{ for } r > r_w, \tag{4.33}$$

$$\text{(mass balance)} \quad 2\pi r_w T \frac{\partial h}{\partial r}(r_w, t) = \pi r_c^2 \frac{\partial s}{\partial t} \text{ for } t > 0 \tag{4.34}$$

$$s(0) = s_0 = \frac{V}{\pi r_c^2}, \tag{4.35}$$

where h is the hydraulic head relative to the null value set at $r = \infty$ (or the generic displacement in the aquifer), r_w is the radius of the screened casing, r_c is the radius of the unslotted casing where the instantaneous water level displacement is induced by injecting or extracting a volume V of water (Fig. 4.22). Of course, in wells or piezometers completed with a single casing of constant diameter, $r_w = r_c$.

Under these hypotheses, Cooper, Bredehoeft and Papadopulos obtained the following solution by applying the Laplace transform [8]:

$$\frac{s}{s_0} = F(\alpha, \beta), \tag{4.36}$$

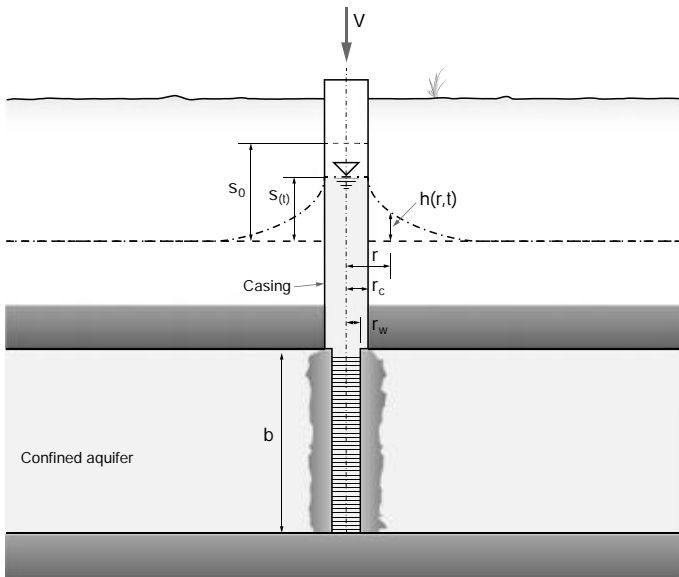


Fig. 4.22 Definition of the parameters describing the geometry of a well completed in a confined aquifers

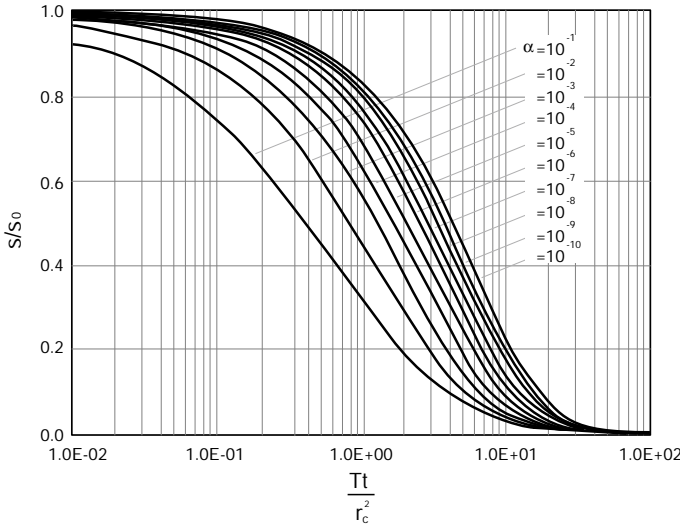


Fig. 4.23 Cooper, Bredehoeft and Papadopoulos' type curves for the interpretation of a slug test

being: $\alpha = \frac{r_w^2}{r_c^2} S$, $\beta = \frac{T-t}{r_c^2}$, and $F(\alpha, \beta)$ a complex integral:

$$F(\alpha, \beta) = \frac{8\alpha}{\pi^2} \int_0^\infty \exp\left(-\beta \frac{u^2}{\alpha}\right) \frac{1}{u\Delta(u)} du, \tag{4.37}$$

where $\Delta(u)$ is:

$$\Delta(u) = [u J_0(u) - 2\alpha J_1(u)]^2 + [u Y_0(u) - 2\alpha Y_1(u)]^2, \tag{4.38}$$

where J_0 and Y_0 , J_1 and Y_1 are zero and first order Bessel functions of the first and second kind, respectively.

The numerical values of s/s_0 for different values of α and β have been tabulated and plotted by Cooper et al. [8] and by Papadopoulos et al. [38], and are depicted in Fig. 4.23.

The interpretation of a slug test with Cooper, Bredehoeft, Papadopoulos' method can be carried out with a type curve matching method analogous to the one used for the interpretation of aquifer tests, see Fig. 4.24 [8, 30]:

- plot the normalized displacement values s/s_0 over time on a semilogarithmic graph (linear scale for the normalized displacement, logarithmic for time), having the same scale as the available Cooper, Bredehoeft and Papadopoulos's type curves;
- superimpose the type curves and the experimental plot;
- translate the experimental curve only along the x-axis until the best match with one of the type curves is identified;
- identify the value of α for the best match curve;

- having fixed the superimposition, select any match point, characterized by an x value (log-scale) equal to t^* (for the experimental curve) and β^* for the type curve;
- calculate the two unknowns:

$$T = \beta \frac{r_c^2}{t^*}, \quad (4.39)$$

$$S = \alpha \frac{r_c^2}{r_w^2}. \quad (4.40)$$

When applying Cooper, Bredehoeft and Papadopulos's method a few limitations emerge:

- the shape varies only slightly between type curves; hence, often there is not a unique good match with the experimental curve. If this does not influence significantly the determination of the transmissivity, T , it has a major impact on the determination of the storativity, S : one order of magnitude variation of α (and thus S) does not significantly change the geometry of the type curve [11, 16, 30, 38];
- Cooper, Bredehoeft and Papadopulos's solution assumes a perfectly radial flow, a condition that is verified only for fully penetrating wells or piezometers, which is rarely the case in confined aquifers.

The induced error is, however, negligible when the screen is at least twenty fold the well radius, a condition which is generally satisfied.

4.4.4 The KGS Method

In 1994 a research team of the Kansas Geological Survey proposed a rigorous semi-analytical solution for the interpretation of a slug test conducted in a partially penetrating and/or completed well, using a three-dimensional model that includes the effect of the aquifer's storage [24]. Their model considers two distinct boundary conditions for the top of the formations: no flow (like Cooper, Bredehoeft and Papadopulos's method) and constant hydraulic head (like Bouwer and Rice's method); their solutions can, therefore, be applied to the interpretation of slug tests carried out both in confined and unconfined aquifers.

To summarize, the KGS method considers:

- the aquifer's storage;
- the well-aquifer mass balance;
- the partial penetration of the well or piezometer;
- the formation's anisotropy, if present;
- the permeability damage in proximity of the well;
- confined and unconfined aquifers.

The broad range of applicability of the solutions comes to the cost of a greater complexity compared to the methods examined earlier; however, the application of the KGS method was facilitated by the development of the AQTESOLV software [13].

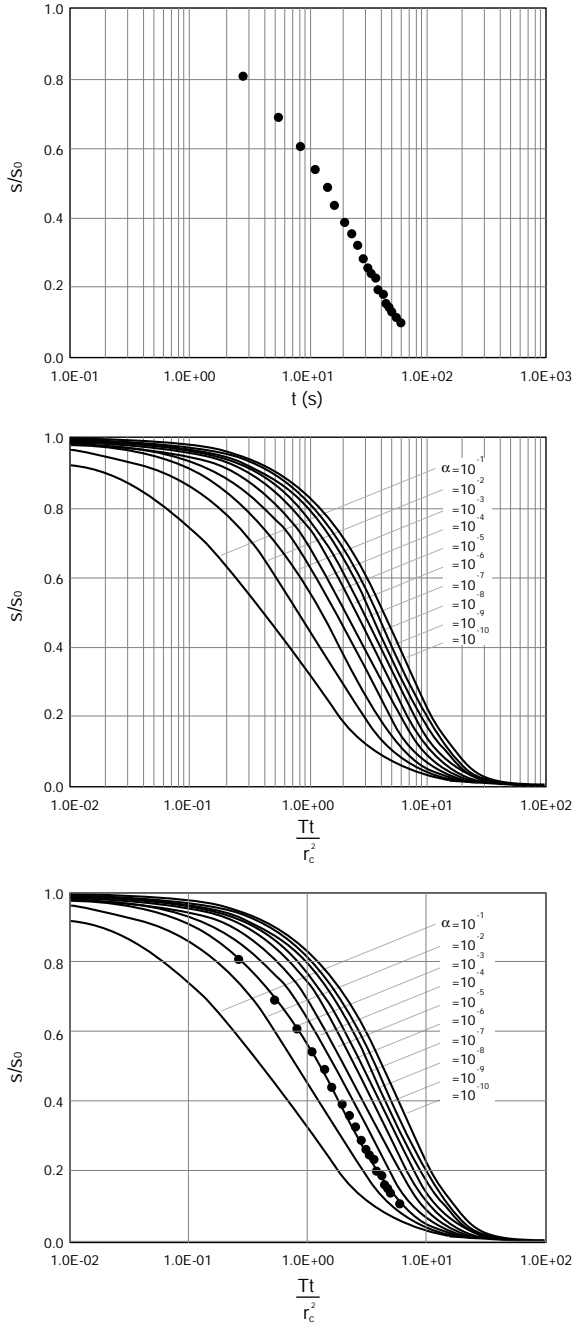


Fig. 4.24 Slug test interpretation procedure with Cooper, Bredehoeft and Papadopolos' method by type curve matching

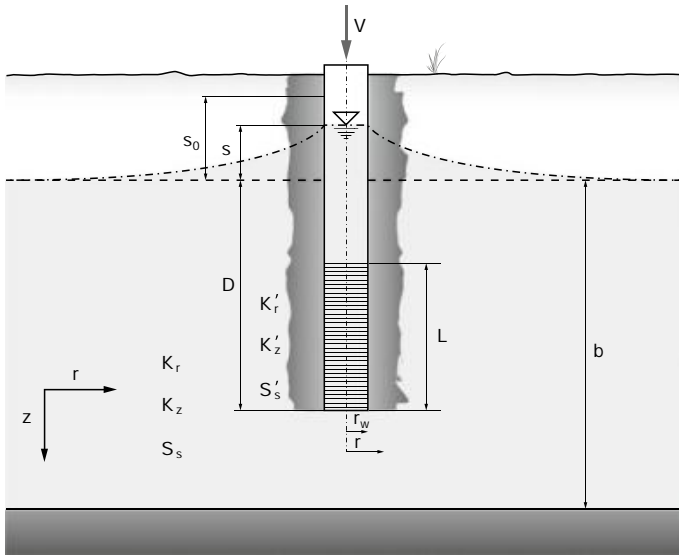


Fig. 4.25 Parameters defining the geometry of a well or borehole relative to the KGS method

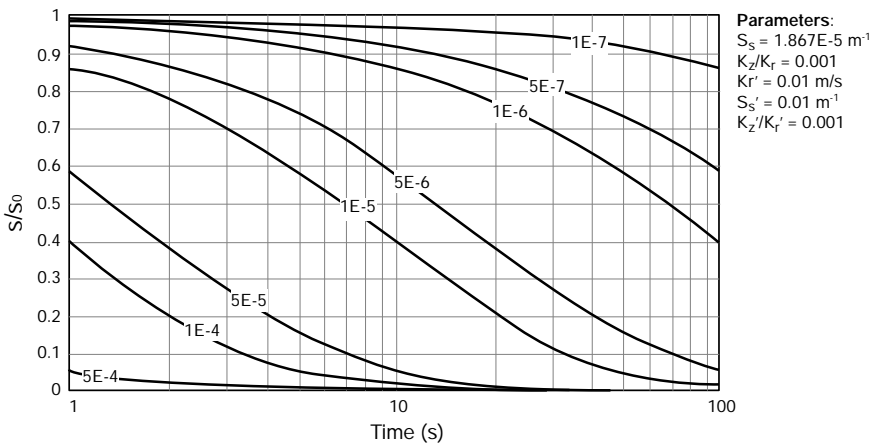


Fig. 4.26 Family of type curves of a given well geometry according to the KGS method

In general terms (refer to Fig. 4.25), the dimensionless displacement, s/s_0 , can be expressed as:

$$\frac{s}{s_0} = f(K_r, K_z, S_s, K'_r, K'_z, S'_s, L, D, b),$$

where the prime-decorated parameters refer to the annulus around the well where formation damage (skin effect) can be present.

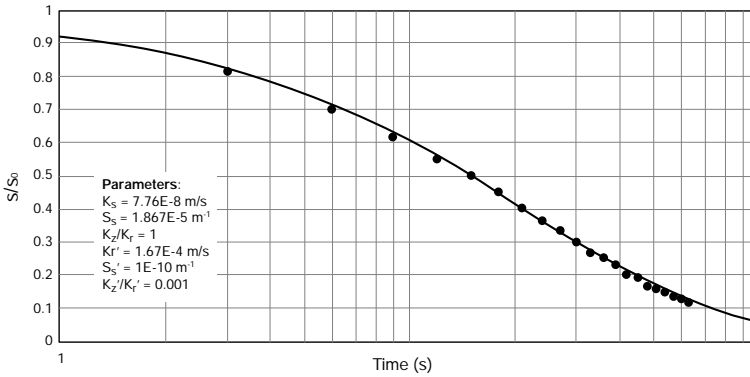


Fig. 4.27 Example of slug test interpretation with the KGS method, using the AQTESOLV software program [13]

The dimensionless displacement is, therefore, dependent on nine parameters, three of which (L , D , and b) are known, provided that the geometry of the completed well/piezometer is known. Figure 4.26 shows a family of type curves for a given completion geometry.

The interpretation of a slug test with the KGS method uses the type curve matching procedure, via non-linear fitting of the experimental curve with one of the type curves generated by the above mentioned software program (see Fig. 4.27) [13].

4.5 Other Methods for the Determination of Parameters Characterizing an Aquifer

Even though aquifer tests are the most reliable tool for the determination of an aquifer’s hydrodynamic parameters, the number of tests that can be carried out is sometimes insufficient to obtain a significant distribution of values. It is, therefore, important to keep in mind that there are other methods available.

4.5.1 Determination of Hydraulic Conductivity or Transmissivity

The hydraulic conductivity or the transmissivity of an aquifer (deriving one from the other is immediate) represent the most important hydrodynamic parameters, since they can affect the flow directions and rates in both steady and transient regimes. Alternative methods to transient regime aquifer tests (see Sects. 4.1–4.4) that are available for the estimation of these parameters are described below.

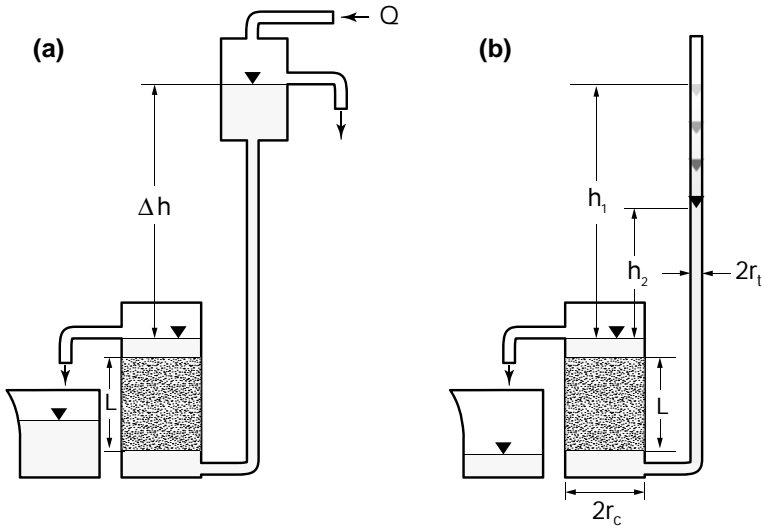


Fig. 4.28 a Constant and b falling head permeameters [16, 41]

Laboratory Measurement with a Constant or Falling Head Permeameter

The hydraulic conductivity can also be measured in the laboratory in a sample of the aquifer formation collected during well drilling.

The intrinsic limitation of this kind of method lies in the collection of a representative sample, and in the challenge of reproducing in the laboratory the stress conditions existing on site. Regardless of these considerations, the measurement is made with a device called permeameter, with which a flow of water is induced through the sample, and discharge and hydraulic head are then measured.

There are two types of permeameters: with constant or variable head (see Fig. 4.28) [41].

Constant head permeameters are usually used to measure the hydraulic conductivity of granular, mainly sandy-gravelly, sediments. The sample is placed in a cylinder of known cross-sectional area and, after carefully saturating it with water, a flow is induced through it as a result of a constant hydraulic head difference. The hydraulic conductivity can be derived through the direct application of Darcy's law [41]:

$$K = \frac{V_w}{t} \frac{L}{A \cdot \Delta h}, \quad (4.41)$$

after measuring the volume of water, V_w , that flowed through the sample during the time t , as a result of the hydraulic head difference, Δh , across the sample with cross-sectional area, A , and length, L .

The falling head permeameter, instead, is usually used to measure the hydraulic conductivity of fine loose samples or consolidated samples.

After saturating the sample as above, the tall column is filled with water up to a generic height, h_1 . After opening the stopcock and allowing water to flow through

the sample, the time for the water level in the column to drop to the generic height, h_2 , is measured.

The water discharge through the sample is, for the law of mass conservation, the same that flows across the section of the column. Therefore [16]:

$$Q = -\pi r_t^2 \frac{dh}{dt} = \pi r_c^2 K \frac{h}{L},$$

from which the following can be derived, by separating the variables and integrating:

$$-\left(\frac{r_t}{r_c}\right)^2 L \int_{h_1}^{h_2} \frac{dh}{h} = K \int_0^t dt,$$

and, thus

$$K = \left(\frac{r_t}{r_c}\right)^2 \frac{L}{t} \ln \frac{h_1}{h_2}. \quad (4.42)$$

In (4.42), r_t represents the radius of the column, and r_c the radius of the cylindrical sample holder.

For clay-like materials, characteristic of aquicludes, not even the falling head permeameter is suitable for hydraulic conductivity measurements, and indirect geotechnical measurements are used.

Correlation with the Specific Capacity

If correctly executed, this method provides a quite precise estimate of the transmissivity. For its application we refer the reader to Sect. 5.4.4 (Eqs. 5.9 and 5.10) because understanding of the well loss equation (Eq. 5.1) is required.

Correlation with the Granulometry

The great variability range of hydraulic conductivity in soils has already been mentioned. From a theoretical point of view, it can be explained with one among the many models that describe a porous medium, the simplest of which compares the medium to a bundle of capillary tubes [29]. All these models lead to relations of this kind [1, 15, 27, 31]:

$$K \propto d^2,$$

where d is an equivalent diameter, often assigned the value of d_{10} (the size of the sieve through which only 10% in weight of the sediment grains pass).

This implies that the main factor, albeit not the only one, controlling a soil's permeability is its granulometry. From homogeneous clays ($10^{-5} \leq d_{10} \leq 10^{-4}$ cm), to gravel ($d_{10} \approx 1$ cm), d_{10} spans 4–5 orders of magnitude, and permeability, consequently, spans 8–10.

In addition, it emerges that small granulometry variations correspond to significant hydraulic conductivity variations.

One of the most simple expressions correlating hydraulic conductivity and aquifer granulometry is Hazen's formula [22]:

$$K = 100 \cdot d_{10}^2, \quad (4.43)$$

valid for d_{10} expressed in cm and K in cm/s.

Hazen's formula is, in general, valid for uniformly graded materials, $U = d_{60}/d_{10} \leq 2$); for well-graded material, d_{50} is often used instead:

$$K = 100 \cdot d_{50}^2. \quad (4.44)$$

The literature reports numerous alternative correlations that keep into account other parameters, such as porosity, in addition to the equivalent diameter [1, 5, 26, 28, 29, 43]. However, since only a preliminary order of magnitude for the hydraulic conductivity can be derived from these correlations, Hazen's formula is sufficient for this objective.

When even a particle size distribution curve is unavailable for the formation of interest, one must resolve to tables such as the one in Fig. 1.14, in Chap. 1.

Lefranc Test

This is a very commonly used test, especially in the field of geotechnics, but in most instances it provides unreliable results because the conditions underlying its interpretation are not respected during execution. Lefranc tests are carried out while drilling boreholes for geotechnical or hydrogeological investigations, and consist in inducing flow from the well towards the formation (injection test) or the other way round (pumping test), depending on whether the water level in the borehole rises or falls relative to the undisturbed level. During a Lefranc test, the same operating conditions used in the lab with a permeameter are used in the field. Therefore two types of tests can be carried out: *constant head tests*, in which the injected (or extracted) water discharge necessary to maintain a constant water level displacement in the borehole relative to the surrounding formation is measured; or *falling head tests*, in which the decline (or rise) rate of the water level in the borehole is measured after provoking an instantaneous displacement [6].

Regardless of the selected operating conditions, a Lefranc test is interpreted with Darcy's law; thus, the test should be carried out only in saturated formations, and the flow should be laminar. These conditions are often disregarded also due to the high hydraulic gradients used during the test which induce non Darcyan flow.

When the investigated formation is such that the uncased borehole's wall might collapse, the execution of the test must be preceded by a careful preparation of the screened section, as follows:

- the borehole should be drilled with casing until the depth of interest is reached;
- an impermeable plug should be placed at the bottom of the borehole, with the goal of preventing preferential flow paths during the test, in particular through the gap between the borehole and the casing;
- a second inner tube with a smaller diameter which passes through the impermeable plug should be installed;
- the inner tube should be elevated to the bottom end of the plug, and at the same time the draining section (*test cavity*) should be created, by placing suitable granular filter material under the stopper.

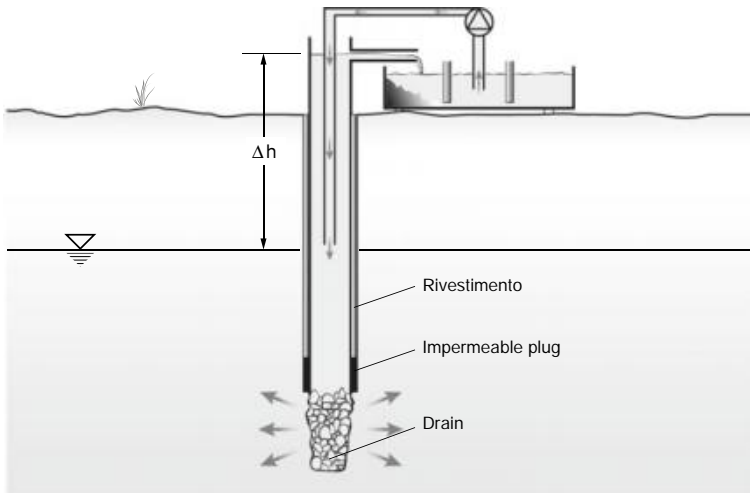


Fig. 4.29 Schematic of a constant head Lefranc test with water injection

If the formation is sufficiently stable, it isn't necessary to place the plug and install the inner tube, and the test can be carried out simply with the outer casing and a screen placed at the bottom of the borehole.

Constant Head Tests

The operating conditions of constant head Lefranc tests are depicted in Fig. 4.29; they are the least frequently used tests because they require equipment (i.e., a reservoir and a pumping system) often unavailable to the companies that conduct them.

Once a steady state is reached following the creation of a hydraulic head variation, Δh , Darcy's law can be applied [6]

$$Q = K A \frac{\Delta h}{L} = K F \Delta h,$$

to calculate the hydraulic conductivity:

$$K = \frac{Q}{F \cdot \Delta h}. \quad (4.45)$$

For this calculation, the constant discharge, Q , and displacement, Δh , values have been measured, and the shape factor, $F = A/L$, which depends on the shape and the size of the cavity, has to be known (Fig. 4.30 and Table 4.5).

Variable Head Tests

They are carried out following the schematic in Fig. 4.31 and are more frequently used because they do not require particular equipment. They can be interpreted by measuring the time it takes the water level within the casing to drop from h_1 to h and using the same conceptual approach as in falling head permeameters [6].

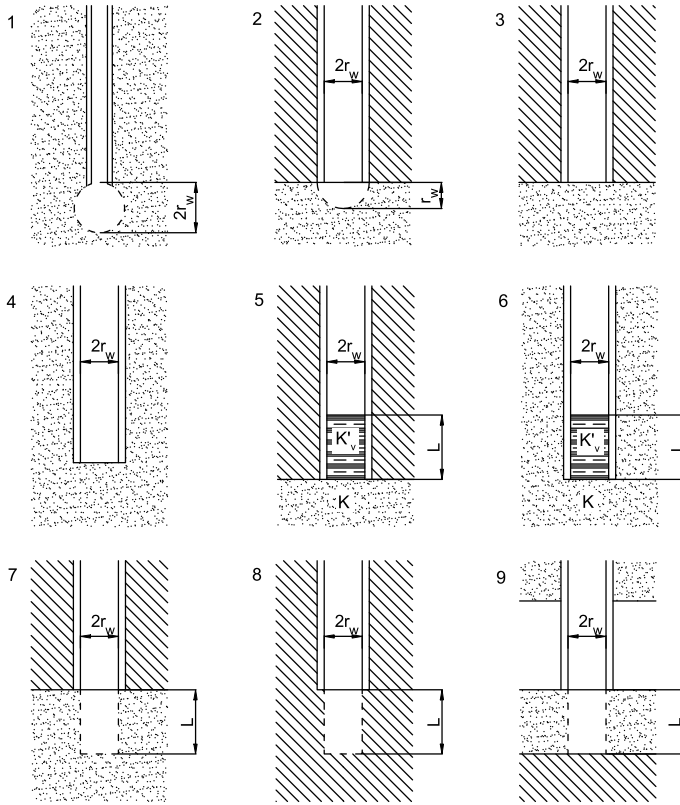


Fig. 4.30 Intake sections according to Hvorslev [23]

Table 4.5 Shape factors, F , suggested by Hvorslev [23] and Mathias and Butler [32]

Intake section as in Fig. 4.30	F
1 Spherical soil bottom in homogeneous soil	$4\pi r_w$
2 Hemispherical soil bottom at impervious boundary	$2\pi r_w$
3 Flush bottom at impervious boundary	$4r_w$
4 Flush bottom in uniform soil	$5.5r_w$
5 Soil in casing at impervious boundary	$\frac{4r_w}{1 + \frac{4LK_h}{\pi r_w K_v}}$
6 Soil in casing in uniform soil	$\frac{5.5r_w}{1 + \frac{5.5LK_h}{\pi r_w K_v}}$
7 Well point or hole extended at impervious boundary	$\frac{2\pi r_w}{\sinh[\tanh^{-1}(r_w/L)] \cdot \ln\{\coth[0.5 \tanh^{-1}(r_w/L)]\}}$
8 Well point or hole extended in uniform soil	$\frac{4\pi r_w}{\sinh[\tanh^{-1}(2r_w/L)] \cdot \ln\{\coth[0.5 \tanh^{-1}(2r_w/L)]\}}$
9 Hole fully penetrating a confined aquifer	$\frac{2\pi L}{\ln(\frac{K_c}{r_w})}$

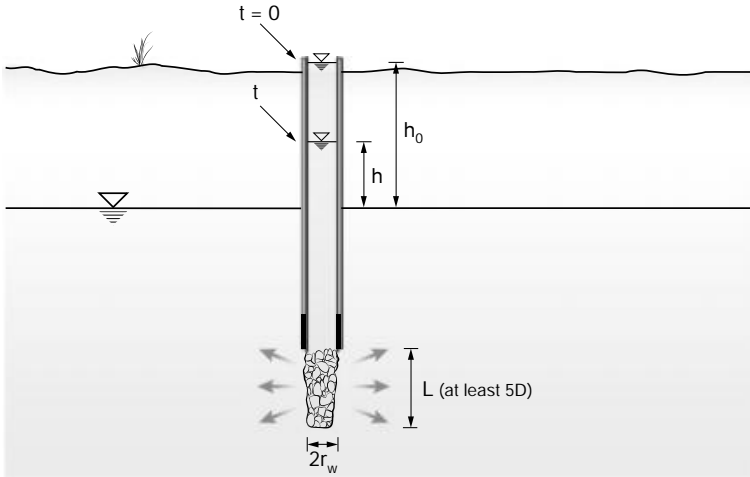


Fig. 4.31 Schematic of a variable head Lefranc test with water injection

For the law of mass conservation:

$$Q = -\pi r_w^2 \frac{dh}{dt} = FK h \quad \text{from which, separating the variables and integrating:}$$

$$-\pi r_w^2 \int_{h_1}^h \frac{dh}{h} = FK \int_0^t dt \quad \text{and, thus:} \quad K = \frac{\pi r_w^2}{Ft} \ln \frac{h_1}{h}, \quad (4.46)$$

where r_w is the inner radius of the casing.

In order to avoid errors in the measurement of time, t , it is recommended to use a head drop of at least $h = 0.2h_1$.

Single-Well Point Dilution Tests

These can be particularly useful for the determination of the horizontal hydraulic conductivity at a particular depth of the aquifer, rather than the average hydraulic conductivity of the entire saturated thickness, derived from the interpretation of an aquifer test.

From a practical point of view, the test consists in the isolation of the aquifer level of interest with two packers placed in the well or piezometer (henceforth simply referred to as wells), and injecting a pulse (also known as slug dose) of a known mass of tracer in the isolated water volume, as depicted in Fig. 4.32.

The interpretation of the test is based on the *point dilution* principle, and requires the measurement of the tracer’s concentration over time, at the point of injection in the well [12].

If the isolated well portion has a small enough volume, mixing of the tracer with groundwater within this volume can be considered instantaneous and complete (any vertical flow can be neglected). Therefore, the tracer’s mass variation within the well portion of interest can be assumed, for the principle of mass conservation, to be equal

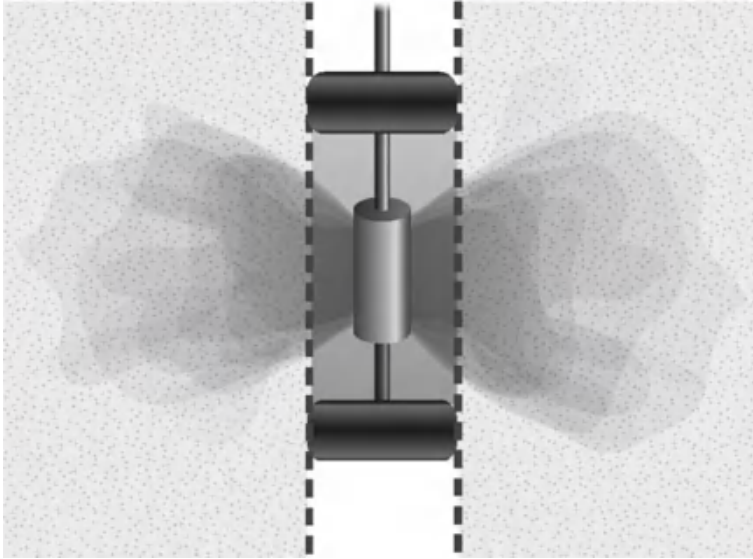


Fig. 4.32 Schematic of a dilution test with two packers

to the tracer mass transported out of the well by the water flow, in the infinitesimal time interval considered. In mathematical terms, this can be formulated as follows:

$$dM = -V_w \cdot dC = Q C \cdot dt = 2r_w h v' C \cdot dt,$$

with C being the tracer’s concentration; r_w the well radius; Q the discharge of the tracer transferred to the aquifer; h the portion of well affected by the tracer test; v' the water velocity at the well’s axis; $V_w = \gamma \cdot \pi r_w^2 h$ the volume of the well portion affected by the tracer test; γ a volume reduction factor that keeps into account the volume occupied by the probe measuring tracer concentration.

By separating the variables and integrating, one obtains [12]:

$$\int_{C_0}^C \frac{dC}{C} = -\frac{2r_w}{\gamma \pi r_w^2} \cdot v' \cdot \int_{t_0}^t dt \quad \text{and thus:}$$

$$v' = \frac{\gamma \pi r_w}{2(t - t_0)} \cdot \ln \frac{C_0}{C}, \tag{4.47}$$

with C_0 being the concentration of the tracer at time t_0 .

Solution (4.47) indicates that the tracer concentration decreases semi-logarithmically (see Fig. 4.33).

Since a well can be considered a medium with a much higher hydraulic conductivity than the surrounding porous medium, water velocity inside the well, v' , is most certainly greater than the average filtration velocity, q , of water in the aquifer.

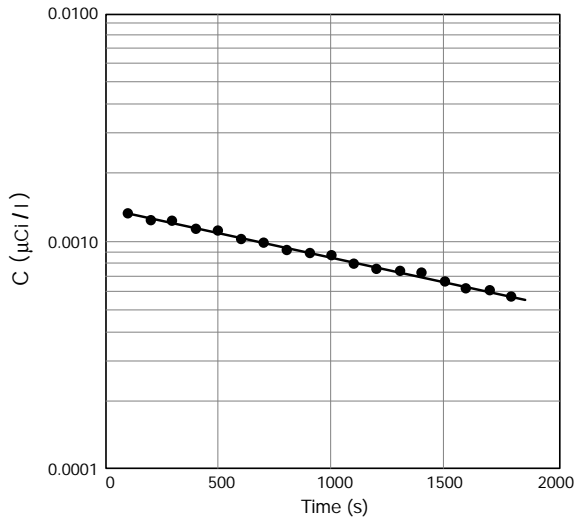


Fig. 4.33 Radioactive tracer point dilution during a single-well test

Therefore:

$$q = \frac{v'}{\alpha},$$

with α being a factor greater than 1, that keeps into consideration the distortion of the flow lines induced by the presence of the well. This distortion depends on the characteristics of the system through which the tracer has to flow (the well screen, the gravel pack placed between the casing and the uncased borehole, the aquifer) and is equal to [12]:

$$\alpha = 8 \cdot \left\{ \left(1 + \frac{K}{K_d} \right) \cdot \left[\left(1 + \frac{r_w^2}{r_e^2} \right) + \frac{K_d}{K_{eq}} \cdot \left(1 - \frac{r_w^2}{r_e^2} \right) \right] + \left(1 - \frac{K}{K_d} \right) \cdot \left[\left(\frac{r_w}{r_d} \right)^2 + \left(\frac{r_e}{r_d} \right)^2 \right] + \frac{K_d}{K_{eq}} \cdot \left[\left(\frac{r_w}{r_d} \right)^2 - \left(\frac{r_e}{r_d} \right)^2 \right] \right\}^{-1}$$

where r_w and r_e are the inner and outer well radius, respectively, r_d the outer radius of the gravel pack, K_{eq} the equivalent hydraulic conductivity of the screened section (this information should be provided by all suppliers), K_d the hydraulic conductivity of the gravel pack, and K the hydraulic conductivity—the problem unknown—, see Fig. 4.34.

Overall, the filtration velocity in the porous medium can be determined with the equation:

$$q = \frac{\gamma \pi r_w}{2\alpha(t - t_0)} \cdot \ln \frac{C_0}{C} = Ki, \tag{4.48}$$

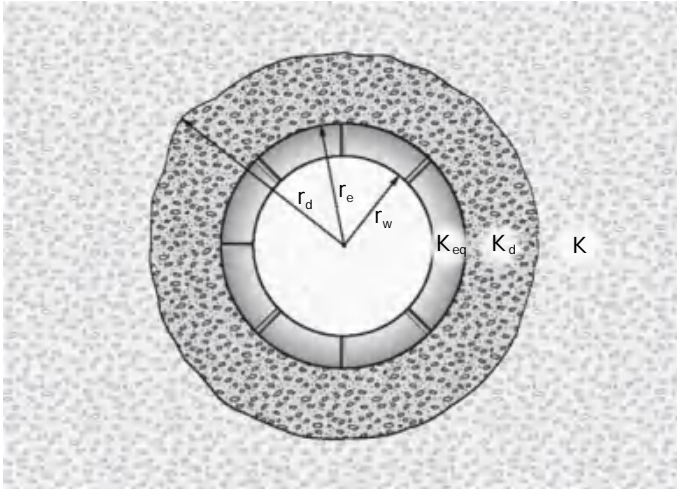


Fig. 4.34 Physical and geometry parameters for the calculation of the correction factor α

from which the hydraulic conductivity in the interval of interest can be obtained:

$$K = \frac{\gamma \pi r_w}{2 \alpha i} \cdot \left(\frac{\ln C_0 - \ln C}{t - t_0} \right). \tag{4.49}$$

It is worth remarking that when applying Eq. (4.49):

- the term between brackets represents the slope of the straight part of the semi-logarithmic graph, $\ln C$ versus t , plotting the data acquired during the test (it is possible that the data do not align along a straight line during the initial phase);
- the parameter α is a function of the hydraulic conductivity, K , whose calculation is the objective of the dilution test. Therefore, solving Eq. (4.49) follows an iterative procedure.

Interpretation of the Flow Net

The value of transmissivity in a certain area can be derived from its value in a contiguous area, obtained—for example—through an aquifer test, by analyzing the flow net.

Let us consider the schematic in Fig. 4.35. The law of mass conservation imposes that the discharge within a flow channel delimited by two contiguous flow lines is constant:

$$Q = A_1 K_1 i_1 = A_2 K_2 i_2.$$

But since $A = L \cdot b$, the above equation becomes:

$$L_1 T_1 i_1 = L_2 T_2 i_2,$$

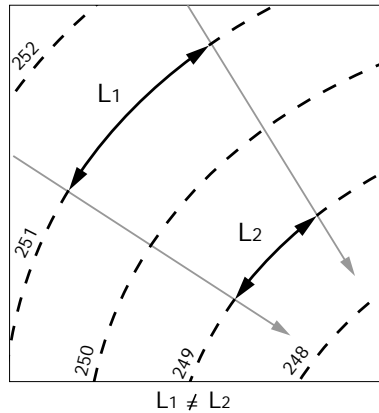


Fig. 4.35 Flow net schematic

from which, knowing the transmissivity in area 1 and the potentiometric distribution in the area under investigation, the transmissivity in the contiguous area 2 can be obtained:

$$T_2 = T_1 \cdot \frac{i_1}{i_2} \frac{L_1}{L_2}. \quad (4.50)$$

If the equipotential lines were approximated with straight lines, the flow lines would be parallel to each other and, consequently, L_1 would be equal to L_2 and Eq. (4.50) could be further simplified to:

$$T_2 = T_1 \cdot \frac{i_1}{i_2}. \quad (4.51)$$

4.5.2 Determination of the Storativity

The value of storativity, S , affects the hydraulic behavior of an aquifer only during transient regimes. The following possible alternatives to aquifer tests in transient regime (refer to Sects. 4.1–4.4) are available for its determination.

Application of the Analytical Definition

If experimental data is unavailable, the elastic storativity can be obtained by applying its analytical definition:

$$S = g\rho_w b \cdot (c_f + nc_w). \quad (4.52)$$

Equation (4.52) highlights the dependence of the value of S on the saturated thickness, b , on the depth at which the aquifer is found (a parameter which influences

compressibility values of the formation, c_f , and of water, c_w), on the porosity, and on water density.

Given that, from a practical point of view, the density is constant and the total porosity of an aquifer has a limited range of variability, the storativity value essentially depends on the saturated thickness, b , and the depth, which affects the compressibility values.

Van der Gun Correlation

Van der Gun elaborated a formula to calculate the elastic storativity, S , of a confined or leaky aquifer based on its dependence on the depth and thickness of the aquifer itself [17]:

$$S = 1.8 \cdot 10^{-6} \cdot (d_2 - d_1) + 8.6 \cdot 10^{-4} \cdot (d_2^{0.3} - d_1^{0.3}), \quad (4.53)$$

where d_1 and d_2 (expressed in meters) represent the depths of the top and bottom of the aquifer, respectively.

Correlation with the Lithology

When there are no other options, the order of magnitude of the storativity can be estimated by correlations available in the literature that correlate the specific storage, S_s and the formation's lithology, see the in Table 1.5 in Chap. 1.

Once the value of S_s has been obtained, the storativity can be directly derived:

$$S = S_s \cdot b.$$

Needless to say, this approach completely overlooks the influence of the aquifer's depth.

4.5.3 Determination of the Specific Yield

This parameter influences the hydrodynamic behavior of unconfined aquifers. Beside aquifer tests conducted in transient regime, the specific yield, S_y , can be estimated in the laboratory or via correlation with the lithology. Since the value of the specific yield is comparable to the effective porosity, the methods used to determine the latter parameter (see Sect. 4.5.4) also provide an estimate of S_y .

Laboratory Drainage Tests Under Gravity

The specific yield can be determined in the laboratory by draining an aquifer sample, previously saturated, under gravity. The test must occur in an environment with controlled humidity, to avoid losses to evaporation, and should last long enough for equilibrium to be reached (for fine material, this could mean months). If we add the difficulty of obtaining a sample representative of the entire aquifer and of reproducing in the laboratory real physical conditions, it is very clear why this kind of test, although conceptually very simple, is hardly ever used, except for particular cases.

Correlation with the Lithology

Correlations with other parameters, such as the lithology of the aquifer formation, have been proposed for the estimation of S_y . An example of such correlations is offered in Table 1.4 in Sect. 1.5.1 [25].

4.5.4 Determination of the Effective Porosity

The effective porosity, n_e , which can be assimilated to S_y , is an important parameter because it affects water's seepage velocity in all aquifer types. As for the other described parameters, a few options for its determination are illustrated, as alternatives to aquifer tests in transient state. Below, the available options for its determination are illustrated.

Multiple-Well Tracer Tests

These are probably the most reliable method, albeit the most expensive, for the determination of the effective porosity.

A multi-well tracer test consists in the measurement of the concentration over time of a tracer in one or more observation wells located downgradient of the well where a pulse of tracer was injected. Its main purpose is to determine the seepage velocity at the tested level in the aquifer. The curve describing the evolution of the tracer's concentration in an observation well or piezometer is called *breakthrough curve*.

Once a breakthrough curve has been acquired in an observation point located downgradient of the injection well, the seepage velocity can be derived through the following relation:

$$v = \frac{d}{t_a},$$

where d is the distance between the injection and the observation points, and t_a is the time it took the tracer to travel this distance (arrival time). Therefore, knowing the hydraulic conductivity of the tested aquifer level, and the hydraulic gradient between the injection and observation points at the time of the test, the effective porosity can be obtained:

$$n_e = \frac{Ki}{v} = \frac{Ki}{d} \cdot t_a. \quad (4.54)$$

The only critical aspect in the interpretation of a tracer test is the determination of the arrival time, since the tracer does not cross the observation point instantaneously, but is characterized by a first arrival time, t_c (before which the concentration is equal to zero), by a phase during which the concentration increases progressively up to a time, t_m , with maximum concentration, and a third phase with progressively decreasing concentration, which ends with the complete disappearance of the tracer at time, t_f , see Fig. 4.36.

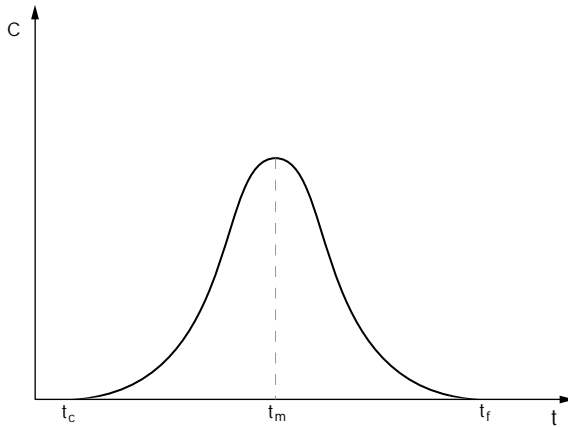


Fig. 4.36 Symmetrical tracer breakthrough curve

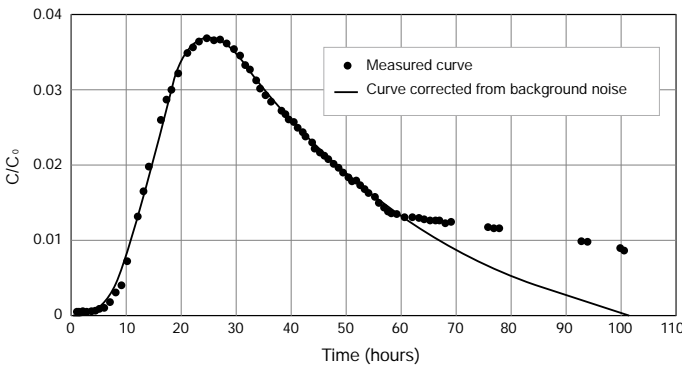


Fig. 4.37 Asymmetrical breakthrough curve and background noise correction

If the tracer was indeed introduced through a pulse injection—thus almost instantaneously, the breakthrough curve will have a Gaussian bell curve shape, with a basically symmetrical distribution, as depicted in Fig. 4.36.

In this case, the arrival time is assumed to be the average time, coinciding with the maximum concentration time t_m :

$$t_a = t_m = \frac{t_c + t_f}{2}.$$

In most cases, however, the breakthrough curve is asymmetrical: in this case, the time corresponding to the barycenter of the tracer plume is used as the arrival time. This time is obtained by transforming the instantaneous concentration breakthrough curve into a cumulative concentration curve, and identifying the time corresponding to a cumulated concentration equal to 50%, see Figs. 4.37 and 4.38.

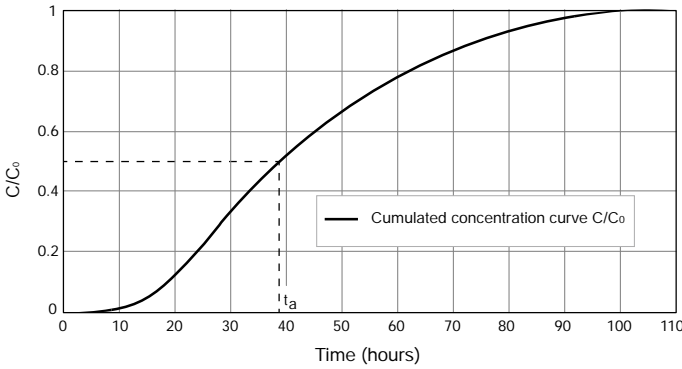


Fig. 4.38 Cumulated breakthrough curve for the estimation of the tracer’s arrival time

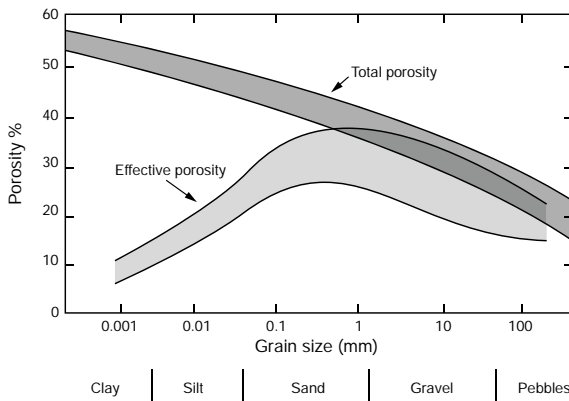


Fig. 4.39 Variation range of total and effective porosity as a function of granulometry and lithology (modified from [9])

The transformation of the instantaneous breakthrough curve into a cumulated breakthrough curve can be obtained by dividing the former into a set of n time intervals Δt_i and applying the following:

$$\left(\frac{C}{C_0}\right)_{cum} = \frac{\sum_{i=1}^m \left[\left(\frac{C}{C_0}\right)_i \Delta t_i\right]}{\sum_{i=1}^n \left[\left(\frac{C}{C_0}\right)_i \Delta t_i\right]} \quad \text{con } m = 1, 2, \dots, n. \quad (4.55)$$

Correlations with the Granulometry

When other options are unavailable, a tentative value of the effective porosity can be obtained through a correlation with the granulometry of the aquifer formation, such as that depicted in Fig. 4.39.

References

1. J. Bear, *Dynamics of Fluids in Porous Media* (Courier Corporation, 1972)
2. H. Bouwer, The Bouwer and Rice slug test | an update. *Groundwater* **27**, 304–309 (1989)
3. H. Bouwer, R.C. Rice, A slug test for determining hydraulic conductivity of unconfined aquifers with completely or partially penetrating wells. *Water Resour. Res.* **12**, 423–428 (1976)
4. J.J.J. Butler, *The Design, Performance, and Analysis of Slug Tests* (CRC Press, Boca Raton, 1997)
5. P.C. Carman, Fluid flow through granular beds (English). *Trans. Inst. Chem. Eng.* **75**, S32–S48 (1937)
6. R.P. Chapuis, M. Soulié, G. Sayegh, Laboratory modelling of field permeability tests in cased boreholes. *Can. Geotech. J.* **27**, 647–658 (1990)
7. H.H. Cooper, C.E. Jacob, A generalized graphical method for evaluating formation constants and summarizing well-field history. *Eos Trans. Am. Geophys. Union* **27**, 526–534 (1946)
8. H.H. Cooper, J.D. Bredehoeft, I.S. Papadopoulos, Response of a finite-diameter well to an instantaneous charge of water. *Water Resour. Res.* **3**, 263–269 (1967)
9. E. Custodio, M.R. Llamas, *Hidrologia subterránea* (Ed. Omega, 1996)
10. A. Di Molfetta, Determinazione delle caratteristiche idrodinamiche degli acquiferi e produttive dei pozzi mediante prove di pompaggio, Italian. IGEA 13–30 (1995)
11. P.A. Domenico, F.W. Schwartz, *Physical and Chemical Hydrogeology* (Wiley, New York, 1998)
12. W. Drost, D. Klotz, A. Koch, H. Moser, F. Neumaier, W. Rauert, Point dilution methods of investigating ground water flow by means of radioisotopes. *Water Resour. Res.* **4**, 125–146 (1968)
13. G.M. Duffield, *AQTESOLV for Windows User's Guide* (HydroSOLVE, Inc., Reston, VA, 2000)
14. J. Ferris, D. Knowles, R. Brown, R. Stallman, Theory of aquifer tests, USGS Numbered Series 1536-E (U.S. Government Print. Office, 1962)
15. C.W. Fetter, *Contaminant Hydrogeology (English)*, 2nd edn. (Waveland Press Inc., Long Grove, 2008)
16. C.W. Fetter, *Applied Hydrogeology (English)*, 4th edn. (Pearson Education, Long Grove, 2014)
17. R.A. Freeze, J.A. Cherry, *Groundwater* (Prentice-Hall, 1979)
18. M.S. Hantush, C.E. Jacob, Non-steady radial flow in an infinite leaky aquifer. *Eos Trans. Am. Geophys. Union* **36**, 95–100 (1955)
19. M.S. Hantush, Hydraulics of wells, in *Advances in Hydroscience*, vol. 1, ed. by Ven Te Chow. *Advances in Hydroscience* (Academic Press, New York, 1964), pp. 281–442
20. M.S. Hantush, Modification of the theory of leaky aquifers. *J. Geophys. Res.* **65**, 3713–3725 (1960)
21. M.S. Hantush, Drawdown around a Partially Penetrating Well. *Trans. Am. Soc. Civ. Eng.* **127**, 268–283 (1961)
22. A. Hazen, *Some Physical Properties of Sands and Gravels: With Special Reference to Their Use in Filtration* (1892)
23. M.J. Hvorslev, *Time Lag and Soil Permeability in Ground-water Observations* (Waterways Experiment Station, Corps of Engineers, U.S. Army, 1951)
24. Z. Hyder, J.J. Butler, C.D. McElwee, W. Liu, Slug tests in partially penetrating wells. *Water Resour. Res.* **30**, 2945–2957 (1994)
25. A. Johnson, *Specific Yield: Compilation of Specific Yields for Various Materials*. USGS Numbered Series 1662-D (U.S. Government Printing Office, Washington, D.C., 1967)
26. P.J. Kamann, R.W. Ritzi, D.F. Dominic, C.M. Conrad, Porosity and permeability in sediment mixtures. *Groundwater* **45**, 429–438 (2007)
27. M. Kasenow, *Determination of Hydraulic Conductivity from Grain Size Analysis* (Water Resources Publication, 2002)
28. C.E. Koltermann, S.M. Gorelick, Fractional packing model for hydraulic conductivity derived from sediment mixtures. *Water Resour. Res.* **31**, 3283–3297 (1995)
29. J. Kozeny, Ueber kapillare Leitung des Wassers im Boden. *Sitzungsber Akad. Wiss., Wien* **136**, 271–306 (1927)

30. G.P. Kruseman, N.A. de Ridder, *Analysis and Evaluation of Pumping Test Data*, Publication 47 (International Institute for Land Reclamation and Improvement, Wageningen, Netherlands, 1994)
31. O.M. Lopez, K.Z. Jadoon, T.M. Missimer, Method of relating grain size distribution to hydraulic conductivity in dune sands to assist in assessing managed aquifer recharge projects: Wadi Khulays dune field, Western Saudi Arabia. *Water* **7**, 6411–6426 (2015)
32. S.A. Mathias, A.P. Butler, An improvement on Hvorslev's shape factors. *Géotechnique* **56**, 705–706 (2006)
33. A.F. Moench, Computation of type curves for flow to partially penetrating wells in water-table aquifers. *Groundwater* **31**, 6 (1993)
34. S.P. Neuman, Supplementary comments on 'theory of flow in unconfined aquifers considering delayed response of the water table' (English (US)). *Water Resour. Res.* **9**, 1102–1103 (1973)
35. S.P. Neuman, Effect of partial penetration on flow in unconfined aquifers considering delayed gravity response. *Water Resour. Res.* **10**, 303–312 (1974)
36. S.P. Neuman, Analysis of pumping test data from anisotropic unconfined aquifers considering delayed gravity response. *Water Resour. Res.* **11**, 329–342 (1975)
37. P.S. Osborne, Superfund technology support center for groundwater (Robert S. Kerr Environmental Research Laboratory), *Suggested Operating Procedures for Aquifer Pumping Tests*, technical report (United States Environmental Protection Agency, Office of Research and Development, Office of Solid Waste and Emergency Response, 1993)
38. S.S. Papadopoulos, J.D. Bredehoeft, H.H. Cooper, On the analysis of 'slug test' data. *Water Resour. Res.* **9**, 1087–1089 (1973)
39. R. Sethi, A dual-well step drawdown method for the estimation of linear and non-linear flow parameters and wellbore skin factor in confined aquifer systems. *J. Hydrol.* **400**, 187–194 (2011)
40. C.V. Theis, The relation between the lowering of the Piezometric surface and the rate and duration of discharge of a well using ground-water storage. *Eos Trans. Am. Geophys. Union* **16**, 519–524 (1935)
41. D.K. Todd, *Ground Water Hydrology* (Wiley, New York, 1959)
42. A. Vandenberg, Determining aquifer coefficients from residual drawdown data. *Water Resour. Res.* **11**, 1025–1028 (1975)
43. C.-B. Wang, W.-X. Zhang, Synthesizing nanoscale iron particles for rapid and complete dechlorination of TCE and PCBs. *Environ. Sci. Technol.* **31**, 2154–2156 (1997)

Chapter 5

Well Testing



Abstract In order to effectively and sustainably exploit an aquifer, having determined its hydrodynamic characteristics and behavior (through aquifer tests, as described in Chap. 4) is not sufficient. It is, in fact, necessary to conduct a well test to derive information on the production and efficiency of a water supply system. Operationally, they are step-drawdown tests, consisting in a succession of at least three pumping stages, each with an increased discharge and lasting until a pseudo-steady state drawdown is achieved. The aim of these tests is to correlate each stabilized drawdown value in the well to its corresponding pumping rate, and to discern between head losses attributable to the aquifer system and those deriving from the water supply system (e.g., well design and construction characteristics, formation damage close to the well, non-darcyan flow close to the well and within the screen slots). Step-drawdown test interpretation is based on Rorabaugh's empirical equation. According to this method, the stabilized drawdown measured in a well as a result of pumping a constant discharge is the sum of a linear term, representing the total head losses resulting from the laminar component of flow, and an exponential term, representing the head losses due to inertial flow in the proximity of the well and to turbulent flow through the screen slots. This chapter provides the means to estimate such terms and how to use them to determine the productivity (quantified by its specific capacity) and efficiency of a water supply well.

The analytical solutions of the groundwater flow equation, presented in Chap. 3, are used for the description of flow in porous media and for the interpretation of aquifer tests. They provide information on the characteristics of the aquifer, but completely disregard the existence of a water supply system and its construction characteristics. Hence, no information about production and efficiency of a water supply system can be derived from aquifer tests. The assessment of these features is, instead, the main goal of *well testing*. Well tests (or well-performance tests) aim at experimentally determining the relation between well discharge and the corresponding stabilized drawdown in the well. This relation keeps into account hydraulic head losses attributable both to the aquifer system and to the characteristics of well design, construction, and deterioration over time, as well as to formation damage close to the well and to non-darcyan flow close to the well and within the screen slots. This

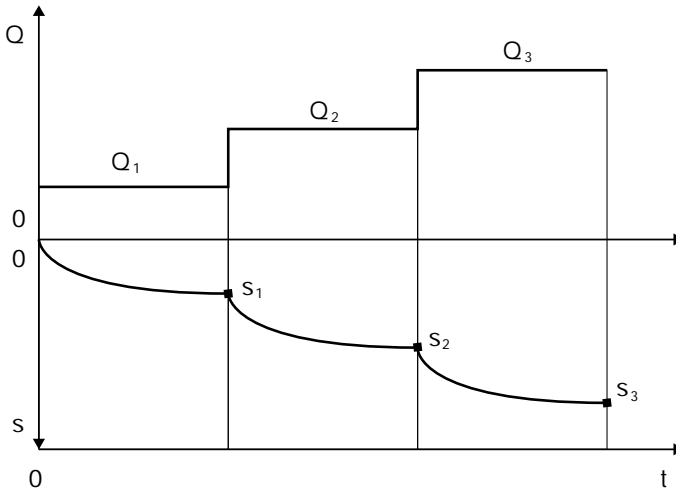


Fig. 5.1 Operating conditions of a step-drawdown test

information can be used to determine the efficiency of a well and thus its potential for exploitation.

5.1 Operating Conditions of a Well Test

Given their specific focus, well tests employ only the active well; from an operating standpoint, they consist in a succession of at least three pumping stages with a stepwise discharge increase, and in measuring the corresponding pseudo-steady state drawdown (see Fig. 5.1); tests that follow this procedure are called *step-drawdown tests* [7]. The discharge range should be as broad as possible ($Q_{\max}/Q_{\min} \geq 3$) and should include the pumping rate planned for the production system [5].

For practical applications, a system is considered to have reached a pseudo-steady state when the drawdown does not vary for at least thirty minutes.

5.2 Theoretical Foundations and Interpretation of Step-Drawdown Tests

The interpretation of a step-drawdown test is based on Rorabaugh's empirical equation [10]:

$$s_m = BQ + CQ^n, \quad (5.1)$$

according to which the stabilized drawdown measured in a well as a result of pumping a constant discharge is the sum of a linear and an exponential term, the latter to the

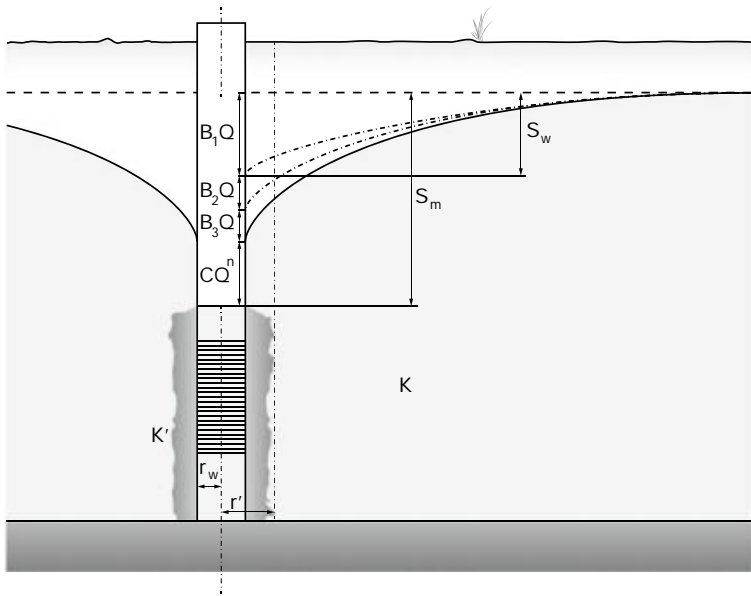


Fig. 5.2 Schematic representation of head losses in a real well: s_m is the stabilized drawdown measured in a well in response to pumping a constant discharge Q , s_w is the drawdown that would be measured if the well had an ideal behavior

power of $n \geq 2$ [7]. In the particular case of $n = 2$ Rorabaugh's equation coincides with the frequently used Jacob equation [4]. The latter, however, does not always accurately describe the water-production behavior of a well.

The linear term of (5.1) expresses the total head losses resulting from the laminar component of flow, and is constituted of the three following elements:

- $B_1 Q$ represents the drawdown due to linear aquifer-losses, which varies as a function of time during the transient regime and becomes a constant once the pseudo-steady state is reached (see Fig. 5.2);
- $B_2 Q$ represents the head losses due to partial penetration and completion of the well;
- $B_3 Q$ represents the head losses due to altered permeability regions potentially present in the proximity of the well relative to the rest of the formation.

Therefore, since $B = B_1 + B_2 + B_3$, if the well is fully penetrating ($B_2 = 0$) and the formation is perfectly homogeneous even in the proximity of the well ($B_3 = 0$), then $B = B_1$.

The non-linear term CQ^n , in turn, represents the head losses due to inertial flow in the proximity of the well, and to turbulent flow of water through the screen slots, with C being the well-loss constant (see Fig. 5.2).

Therefore, with reference to Eq. (5.1), interpretation of a step-drawdown test entails determining experimentally parameters B , C and n , that quantify the well

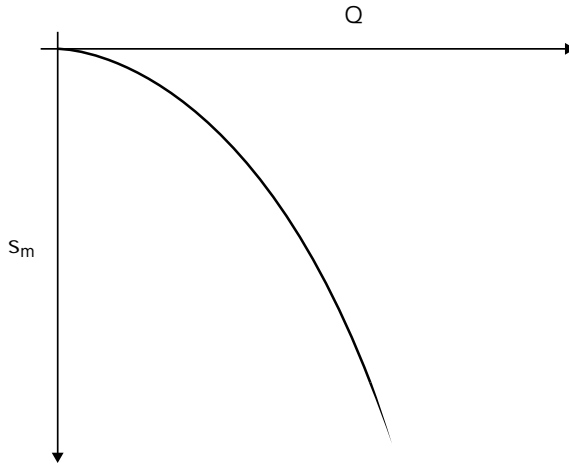


Fig. 5.3 Head loss versus discharge curve for a well

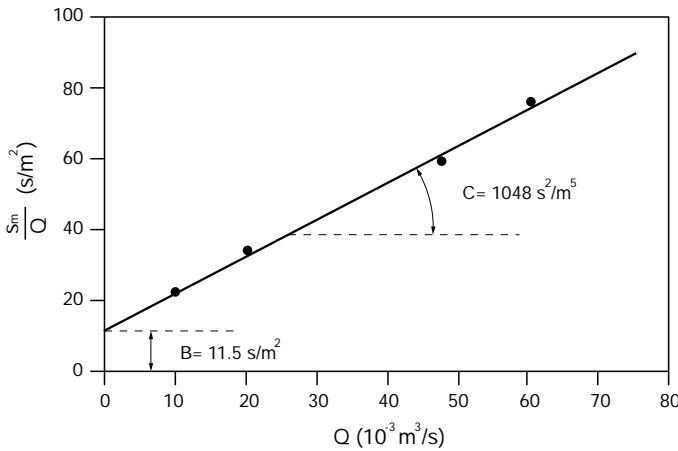


Fig. 5.4 Determination of Jacob's equation's parameters (Rorabaugh's equation with $n = 2$)

loss equation. This equation allows to predict the drawdown induced by a certain discharge, or, *viceversa*, what discharge will cause a certain drawdown. The relation between head loss and discharge of a well is depicted in Fig. 5.3.

The interpretation of a step-drawdown test is very simple, and can be carried out by verifying whether the collected data ($s_m - Q$ couples for every discharge step) align when plotted on a Cartesian diagram as $\frac{s_m}{Q}$ vs Q : if they do, then $n = 2$. Conversely, if the data don't align, $n \neq 2$ so they should be plotted on a logarithmic plot as $(\frac{s_m}{Q} - B)$ vs Q . In the former case the solution can be found directly (see Fig. 5.4); whereas in the latter, the value of B , which is a component of the y-axis variable, has to be found through iterative attempts (see Fig. 5.5) or non-linear fitting. The

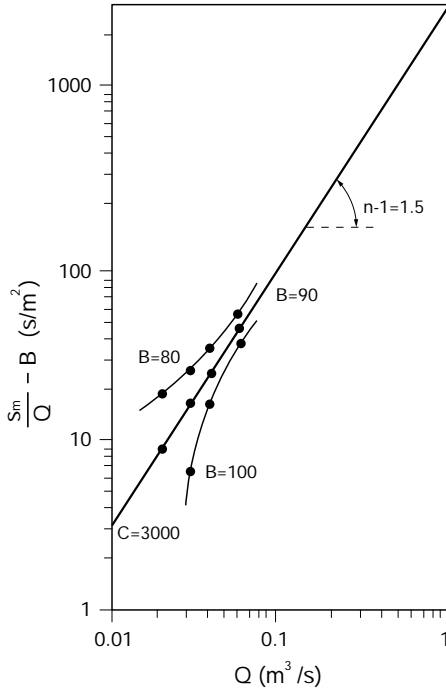


Fig. 5.5 Determination of Rorabaugh’s equation’s parameters ($n \neq 2$)

most likely value of B is, of course, the one that determines the best data alignment; smaller values render the curve more concave, while greater values make it convex. By applying the method of least squares to the regression line, the problem can be solved numerically, rather than graphically.

5.3 Well Productivity and Efficiency

The productivity of a well is not quantified by the discharge it is capable of producing (which can be maintained incorrectly and dangerously high), but by its *specific capacity*:

$$q_{sp} = \frac{Q}{s_m}, \tag{5.2}$$

obtained by dividing the pumped discharge, Q , by the corresponding pseudo-steady state drawdown, s_m .

Clearly, the greater the specific capacity, the better the well. However, the specific capacity alone isn’t sufficient to describe the influence of the well construction characteristics: however high, the specific capacity of a real well will always be smaller than an ideal well constructed by the book.

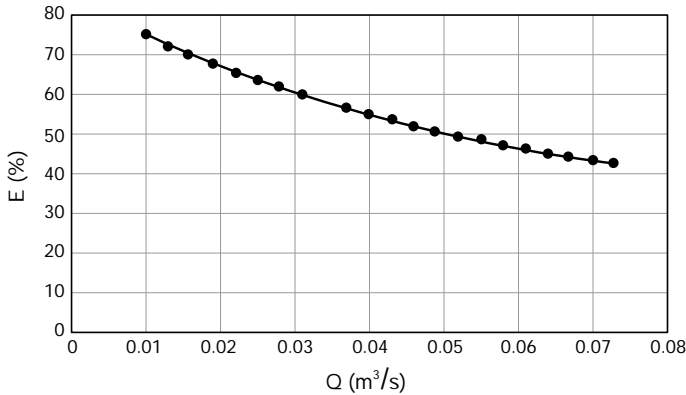


Fig. 5.6 Well efficiency as a function of pumped discharge

As a consequence, the concept of *well efficiency* needs to be introduced, defined as the ratio between a well's specific capacity measured in pseudo-steady state conditions and the specific capacity it would have in the same conditions if its behavior were ideal (i.e., laminar flow, fully penetrating well, constant permeability even inside the well).

Hence, with reference to Fig. 5.2, the well efficiency can be described as [7]:

$$E = \frac{Q/s_m}{Q/s_w} \cdot 100 = \frac{s_w}{s_m} \cdot 100 = \frac{B_1 Q}{BQ + CQ^n} \cdot 100. \quad (5.3)$$

In addition to carrying out and interpreting a step-drawdown test for the determination of B , in order to be able to apply Eq. (5.3) B_2 and B_3 have to be determined, so that $B_1 = B - B_2 - B_3$ can be derived.

Its definition in Eq. (5.3) highlights that well efficiency decreases as the discharge increases, in particular due to the increasing role played by head losses resulting from turbulent flow (see Fig. 5.6).

A constant decline of a well's efficiency during the course of its operating life can be attributed to a decrease in the saturated thickness of unconfined aquifers (groundwater overexploitation) or, more often, to clogging of the slotted screens in aquifers of any type.

Equation (5.3) can be used to monitor the evolution of well efficiency during its operating life, and/or to compare its behavior with that of other wells drilled in the same aquifer.

Conversely, it is not recommended to use Eq. (5.3) to compare the production behavior of wells completed in different aquifers or located very far from each other: a small aquifer transmissivity yields a high value of B_1 , which could mask, to a variable extent, the effects of poor completion and of inadequate development of a well on its own efficiency.

Table 5.1 Walton's criterion for the assessment of well efficiency characteristics [13]

C values s^2/m^5	Assessment
$C < 1900$	Properly developed well
$1900 < C < 3800$	Poor quality well
$3800 < C < 15200$	Clogged or deteriorated well
$C > 15200$	Well damaged beyond repair

A wrong definition of well efficiency is sometimes found in specialized literature:

$$E = \frac{BQ}{BQ + CQ^n} \cdot 100.$$

Using this equation leads to the paradoxical conclusion that the greater the permeability damage close to the well (commonly called *skin effect*), or the smaller the screen, the greater the well efficiency.

In the above paragraphs, the role and importance of the various factors that affect well efficiency have been illustrated, but these do not provide an absolute criterion for assessing whether a well was constructed by the book or not. According to Walton [13], a parameter that fulfills this scope, albeit partially, is the the well-loss constant, C , (see Table 5.1), which in an ideal well should be equal to zero (i.e., no turbulent flow).

Walton's criterion is well suited to assess whether a well was constructed appropriately with respect to the effectiveness of the screens and to the role played by the head losses due to turbulent flow. However, a well with a low value of C was not necessarily completed perfectly (there could be a permeability drop close to the well, or the completion geometry could be erroneous); conversely, it is certainly true that a well characterized by a high value of C was either not completed properly, or deteriorated over time.

This criterion is always valid for wells completed in aquifers with porosity permeability (or intergranular permeability), whereas it cannot be applied to fractured aquifer formations, for which:

$$s_w \propto Q^2,$$

and for which, therefore, a high value of C depends on the specificities of the flow characteristics.

5.4 Estimation of the Coefficients B_2 and B_3

5.4.1 Estimation of the Coefficient B_2

The effects of partial well penetration or completion have been analyzed by many authors; Custodio and Lamas [2] review a wide set of algorithms that allow the calculation of the additional head loss resulting from partial completion, depending on the aquifer type.

One of the most general methods was proposed by the TNO institute of geosciences in The Netherlands (in [2]); it was originally derived for confined aquifers, but is also applicable to leaky aquifers as long as $B \gg b$, and to unconfined aquifers provided that $s_m \ll b$. It can be demonstrated that:

$$B_2 = \frac{1}{2\pi T} \cdot \frac{1 - \delta}{\delta} \cdot \left[\ln \frac{4b}{r_w} - F(\delta, \varepsilon) \right], \quad (5.4)$$

where (see Fig. 5.7):

$\delta = \frac{L}{b}$ is the relative length of the screen,

$\varepsilon = \left| \frac{2a + L - b}{2b} \right|$ is its eccentricity,

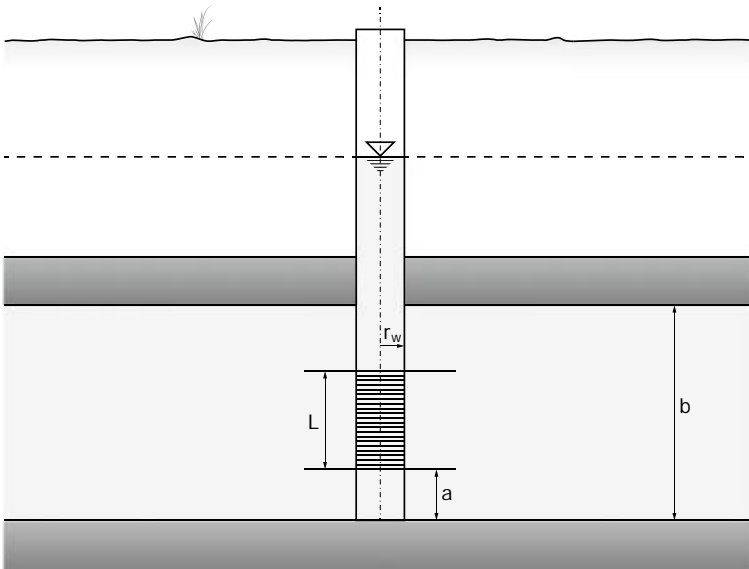


Fig. 5.7 Geometry parameters that characterize a partially completed well

$$F(\delta, \varepsilon) = \frac{1}{\delta(1-\delta)} \cdot [2H(0.5) - 2H(0.5 - 0.5\delta) + 2H(\varepsilon) - H(\delta - 0.5\varepsilon) - H(\varepsilon + 0.5\delta)] \tag{5.5}$$

$$H(x) = \int_u^x \ln \frac{\Gamma(0.5 - u)}{\Gamma(0.5 + u)} du, \tag{5.6}$$

and Γ is the gamma function. The dimensionless function $F(\delta, \varepsilon)$ is plotted in Fig. 5.8.

Another interesting approach can be derived from Brons–Marting’s findings [1], widely used in the petroleum industry and according to which the additional head loss due to a partial completion of a well is quantified by means of a geometric damage coefficient S_b (*pseudo-skin factor*), which depends—of course—on the geometry characteristics of the completion.

This coefficient is linked to the parameter B_2 through the following relation:

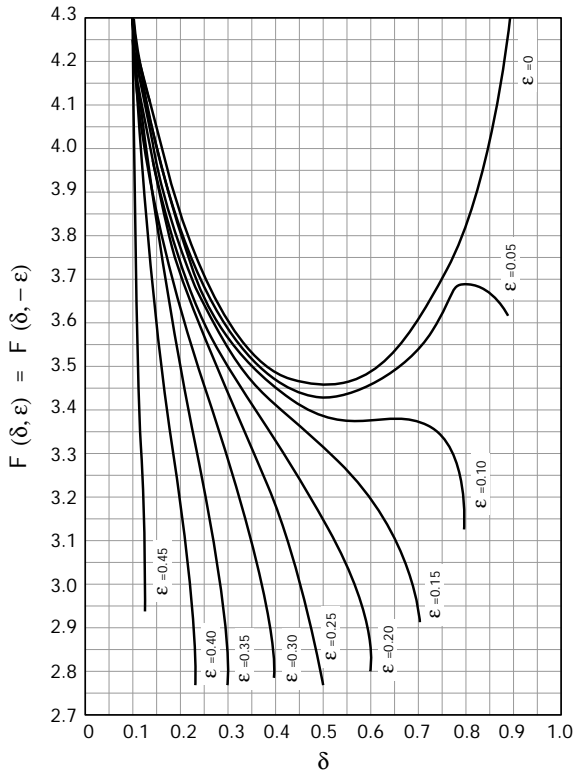


Fig. 5.8 Dimensionless function $F(\delta, \varepsilon)$ (modified from [2])

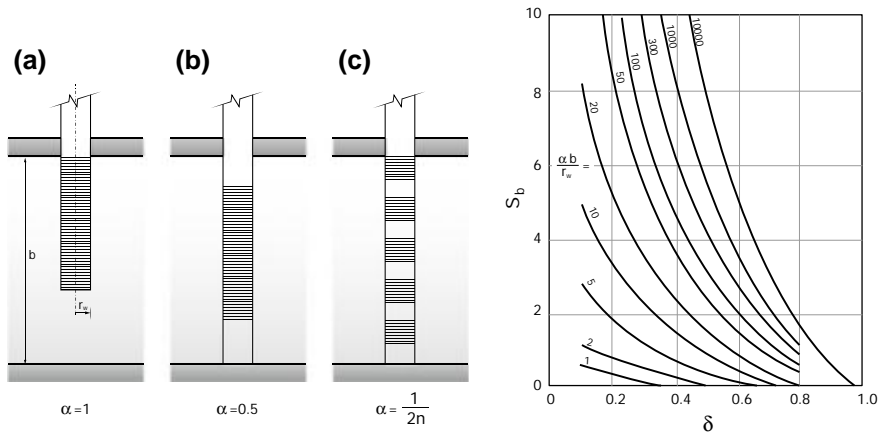


Fig. 5.9 Geometry damage coefficient relative to a few frequently used completion schemes (modified from [1])

$$B_2 = \frac{1}{2\pi T} \cdot S_b. \tag{5.7}$$

The values of S_b can be deduced using Fig. 5.9, as a function of the relative length of the screen δ and of the group $\frac{\alpha b}{r_w}$, with α being a dimensionless geometry coefficient that is equal to: 1 in the case of a single screen at the top or bottom of the aquifer; 0.5 in the case of a screen located in the middle of the aquifer thickness (eccentricity = 0); and $\frac{1}{2n}$ in the case of n screens uniformly distributed along the saturated thickness of the aquifer.

The diagram in Fig. 5.9 is, therefore, particularly useful when the completion design of the well comprises multiple screened sections distributed along the depth of the aquifer, a rather frequent situation that is not addressed by the TNO method.

5.4.2 Estimation of the Coefficient B_3

The value $B_3 Q$ represents the additional drawdown induced by the permeability damage in the proximity of the well. It is a function of the skin coefficient, S_k (deriving from the formation damage, or skin effect), often used in the petroleum field, according to the following relation:

$$B_3 = \frac{1}{2\pi b} \left(\frac{1}{K'} \ln \frac{r'}{r_w} - \frac{1}{K} \ln \frac{r'}{r_w} \right) = \frac{1}{2\pi T} S_k = \frac{1}{2\pi T} \frac{K - K'}{K'} \ln \frac{r'}{r_w}, \tag{5.8}$$

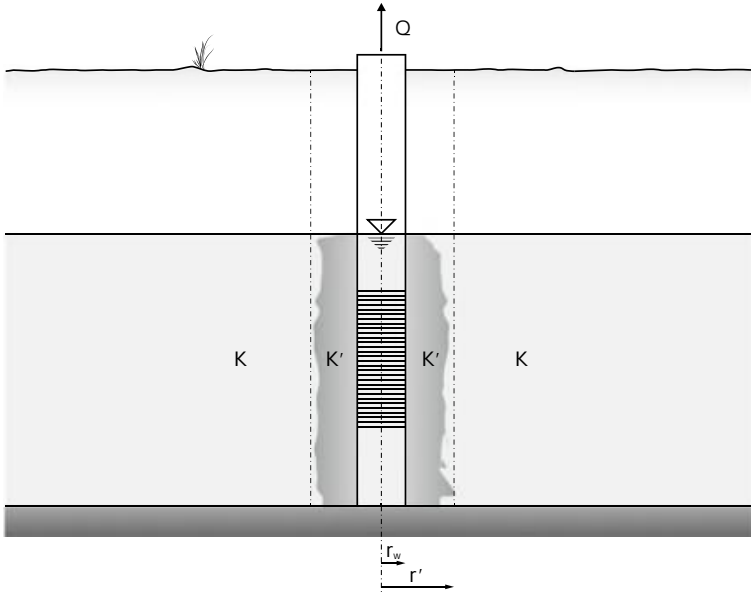


Fig. 5.10 Skin effect in close proximity to the well

with K' being the hydraulic conductivity between the well radius r_w and the radius r' , and K the average hydraulic conductivity of the aquifer, characterizing it for $r > r'$, see Fig. 5.10.

To determine S_k , and consequently B_3 , the values of K' and r' have to be estimated (through, for example, a slug test interpreted with the KGS method, see Sect. 4.4.4) or by a multiwell drawdown test as described in [11].

In most cases, however, given the significantly greater permeabilities that characterize aquifer systems compared to oil fields, if a well is drilled and developed properly, there shouldn't be a residual skin effect, and B_3 should tend to zero.

5.4.3 Calculation of B_2 and B_3

From Eqs. (5.4), (5.7) and (5.8) it is clear that determining B_2 and B_3 requires the introduction of a transmissivity value.

For this sole purpose, a first approximation value deduced from correlations (5.9) and (5.10) can be used, where the specific capacity is calculated as:

$$q_{sp} = \frac{Q}{s_m - C Q^n}.$$

This is justified numerically by the smaller weight of the $(B_2 + B_3) Q$ group relative to the $B_1 Q + C Q^n$ group in Eq. (5.11).

5.4.4 Correlation Between Specific Capacity and Transmissivity

The importance of well tests grew significantly with the extension of their applicability to the estimation of transmissivity, by correlating it to the specific capacity [3]. This is particularly useful if we consider that the number of constant discharge aquifer tests that can be conducted is always limited by the availability of one active well and one piezometer, at the very least; and this is too small and often insufficient for a spatial characterization of transmissivity.

An aquifer's transmissivity is related to the specific capacity of a well completed within the same aquifer by relations such as [9]:

$$T = 1.2 q_{sp} \quad \text{for confined and leaky aquifers,} \quad (5.9)$$

$$T = q_{sp} \quad \text{for unconfined aquifers.} \quad (5.10)$$

Since the above correlations derive from the application of the respective diffusion equations, specific capacity values should be calculated using the drawdown, s_w , that would be measured if the well had an ideal behavior.

Such drawdown can be determined from the value, s_m , measured in the well, by using this equation (see Fig. 5.2):

$$s_w = s_m - (B_2 + B_3) Q - C Q^n, \quad (5.11)$$

whose application entails carrying out and interpreting a well test (to obtain the values of C and n), and being able to determine the values of the coefficients B_2 and B_3 .

5.5 Recent Developments in the Interpretation of Step-Drawdown Tests

Although the application of Rorabaugh's method for the interpretation of step-drawdown tests is still widespread in the field, it should be noted that in recent years other approaches have been developed, aimed at the determination of well characteristics (i.e., well loss and efficiency), or of hydrodynamic parameters, such as transmissivity [6, 8, 9, 11, 12]. In addition, some recent works extend the applicability of the interpretation to heterogeneous aquifers [5].

References

1. F. Brons, V.E. Marting, The effect of restricted fluid entry on well productivity. *J. Pet. Technol.* **13**, 172–174 (1961)
2. E. Custodio, M.R. Llamas, *Hidrología Subterránea* (Ed. Omega, 1996)
3. A. Di Molfetta, Determinazione della trasmissività degli acquiferi mediante correlazione con la portata specifica, Italian. *IGEA* **1**, (1992)
4. C.E. Jacob, Drawdown test to determine effective radius of artesian well. *Trans. Am. Soc. Civ. Eng.* **112**, 1047–1064 (1947)
5. G.H. Karami, P.L. Younger, Analysing step-drawdown tests in heterogeneous aquifers. *Q. J. Eng. Geol. Hydrogeol.* **35**, 295–303 (2002)
6. M.W. Kawecki, Meaningful interpretation of step-drawdown tests. *Ground Water* **33**, 23–32 (1995)
7. G.P. Kruseman, N.A. de Ridder, *Analysis and evaluation of pumping test data*, Publication 47. (International Institute for Land Reclamation and Improvement, Wageningen, Netherlands, 1994)
8. A. Louwyck, A. Vandenbohede, L. Lebbe, Numerical analysis of stepdrawdown tests: parameter identification and uncertainty. *J. Hydrol.* **380**, 165–179 (2010)
9. R. Mace, Estimating Transmissivity Using Specific-Capacity Data. Geological Circulars (University of Texas at Austin, Bureau of Economic Geology, 2001)
10. M.I. Rorabaugh, *Graphical and Theoretical Analysis of Step-drawdown Test of Artesian Well* (American Society of Civil Engineers, Reston, 1953)
11. R. Sethi, A dual-well step drawdown method for the estimation of linear and non-linear flow parameters and wellbore skin factor in confined aquifer systems. *J. Hydrol.* **400**, 187–194 (2011)
12. G. Van Tonder, J.F. Botha, J. Van Bosch, A generalised solution for step-drawdown tests including flow dimension and elasticity. *Water SA* **27**, 345–354 (2001)
13. W.C. Walton, Selected analytical methods for well and aquifer evaluation. Technical Report No. 49 (Illinois State Water Survey, 1962)

Chapter 6

Optimization of a Water Supply System



Abstract In the previous chapter, the methods available for assessing the productivity and efficiency of a well were illustrated. However, a water supply system extends beyond the aquifer-well system, and is composed also of water transmission, treatment, storage and distribution elements. In this chapter, methods for the estimation of head losses occurring from the pumping well along the pipe network that transfers water to the treatment plant, before distribution to consumers, are illustrated. Along this network, there are distributed head losses, in straight pipes, and local head losses, in valves, bends and outlets into reservoirs. Commonly used empirical equations for the calculation of these losses and a method for identifying the optimal operating pumping rate are provided, based on a comparison between pump-related and system head losses. Furthermore, other aspects that need to be kept in mind in the design and long term maintenance of a highly efficient water supply system are highlighted.

The discharge provided by a water supply system is the result of the productivity features of a complex system, which comprises: the aquifer, the pumping well, the submersible pump, the aqueducts or water pipes that carry the water to the water tanks or towers.

Often, the elements of this supply system are designed and analyzed by experts with different training backgrounds, and who consider the component of their expertise as if it were stand-alone: this results in supply systems that operate far from optimally.

It is, therefore, useful to have a method to analyze the correlation between discharge and head-loss in the supply system, in order to optimize the operating conditions and be able to manage the water resources appropriately. Therefore, after briefly illustrating the main components of a water supply system and their respective head losses, the behavior of the entire system will be analyzed with the goal of identifying the conditions for optimal operation.

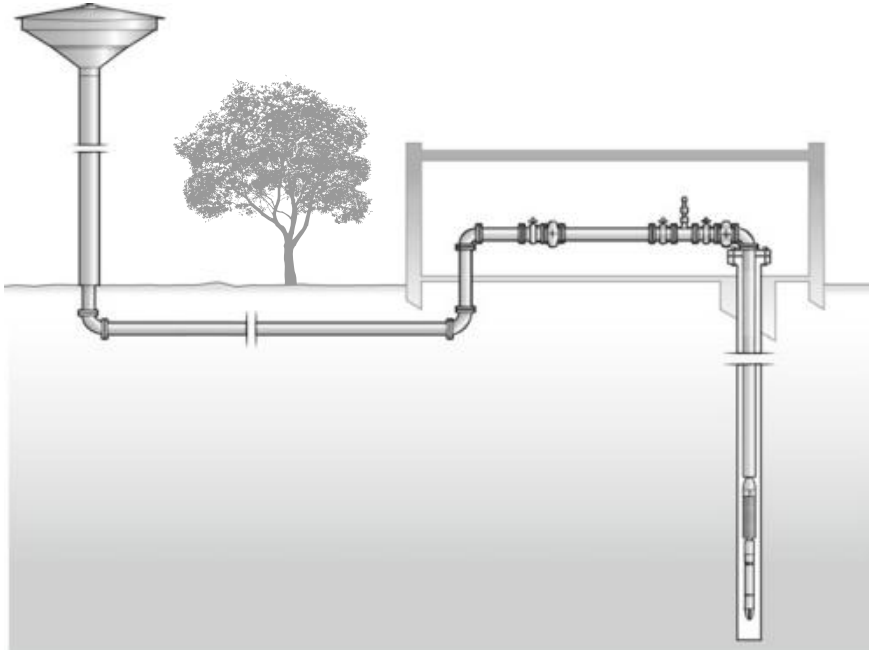


Fig. 6.1 Schematic depiction of a water supply system

6.1 Water Supply System Description

According to the definition used by the Organisation for Economic Co-operation and Development (OECD), a water supply system is “a system for the collection, transmission, treatment, storage and distribution of water from source to consumers, for example, homes, commercial establishments, industry, irrigation facilities and public agencies for water-related activities (fire-fighting, street flushing and so forth)” [6]. In this chapter, we will only consider the part of the system prior to treatment and to the distribution network that brings water to consumers (i.e., the part comprising collection, transmission and storage).

If we consider water flow and its head losses, a water supply system can be broken up into three main sub-systems, as depicted in Fig. 6.1:

- (a) the first is the well-aquifer system, composed of the aquifer itself (i.e., the water source), the filter through which the water enters the well, and the pump with its discharge pipe;
- (b) the second is the water pipe network—including pipe sections, pipe bends and elbows, valves, and fittings—that transfers the water from the well head to the storage tank;
- (c) the third is the storage tank itself.

6.2 Assessment of Head Losses in the System

For a constant discharge to be supplied from the aquifers to the storage tank of a generic system, a submersible pump -usually a multistage centrifugal pump powered by an electric motor- has to be installed in the well. The pump has to be capable of overcoming all the head losses, be they concentrated or distributed along the circuit, as well as the topographic elevation difference between the dynamic level in the well and the higher level in the storage tank.

6.3 Head Losses in the Well-Aquifer Sub-system

The hydraulic head losses in the well-aquifer sub-system are quantified by the pseudo-steady drawdown measured in the well as a result of pumping a constant discharge. According to Rorabaugh's equation, it can be expressed as the sum of a linear and an exponential term, with $n \geq 2$ (see Chap. 5):

$$\Delta H = BQ + CQ^n.$$

A novel approach for the simultaneous determination of the characteristic curve of the well and of the hydrodynamic parameters of an aquifer has been recently described in the literature [8].

6.4 Head Losses in the Pipe Network

The head losses in the pipe network result from the sum of a series of distributed and local losses that occur along the different elements that compose the network itself: straight pipe sections, bends and fittings of various angles, check valves, gate valves, etc. Various methods are available in the literature for the calculation of these contributions [4]; however, since the aim of this chapter is simply to illustrate a procedure for the optimization of a water supply system, in the following sections only a few of such methods are described, all recognized by the S.I., unless otherwise specified.

6.4.1 *Distributed Head Losses*

Distributed head losses in straight pipes can be calculated through practical formulas valid for turbulent flow in rough pipes. For example, Chezy's formula adapted to circular pipes can be used, selecting one of the many available empirical resistance

coefficients; the use of Kutter's coefficient results in the following formula [4, 7]:

$$\Delta H = L \cdot 0.000649 \cdot \left(1 + \frac{2m}{\sqrt{d}}\right)^2 \cdot \frac{Q^2}{d^5}, \quad (6.1)$$

where: d is the inner diameter of the pipe, L its length, and $2m$ a roughness coefficient that accounts for its stage of wear ($2m = 0.35$ for new smooth pipes; $2m = 0.55$ for operational pipes).

6.4.2 Local Head Losses

As depicted in Fig. 6.1, the pump's check valve, other check valves, gate valves, pipe bends, and the pipe's outlet into the tank, are considered local head losses. A mathematical formula is given for each of them, under the hypothesis of pipes that have a limited length. If, instead, pipes longer than a few thousand fold their diameter are considered, inlet and outlet losses, as well as the other local head losses can be considered negligible relative to distributed head losses [3].

The Pump's Check Valve

In most instances, the pump's check valve is not installed on the pump used for purging the well and to conduct pumping tests. Therefore, the interpretation of these tests disregards it. This valve is, instead, mounted on the discharge line of the definitive pump, between the pump itself and the discharge pipe.

It is a spring-assisted in-line (or disk) check valve, whose diameter coincides with that of the vertical discharge pipe.

The corresponding local head loss can be calculated as a function of the kinetic term, $v^2/2g$ [5], of which it has the same dimensions:

$$\Delta H = [0.55 + 4(B_t/d_0 - 0.1) + 0.155/(C_m/d_0)^2] \cdot (v^2/2g), \quad (6.2)$$

where: B_t is the width of the seat, C_m the vertical spring deflection, d_0 the inner diameter of the body of the valve, all expressed in consistent units (see Fig. 6.2).

Check Valves

Other check valves, either of the swing or *hydrostop* type, are usually mounted at the well head to avoid water hammers that might occur at each activation of the pumping system (see Fig. 6.3) [1].

An alternative to the practical formulas suggested in manuals, that indicate head losses equal to 15–20 m of straight pipe, a formula found in [5] that expresses the head loss as a function of the kinetic term, can be used:

$$\Delta H = (0.0032d + 1.187) \cdot (v^2/2g), \quad (6.3)$$

with d being the inner diameter of the pipe, expressed in millimeters.

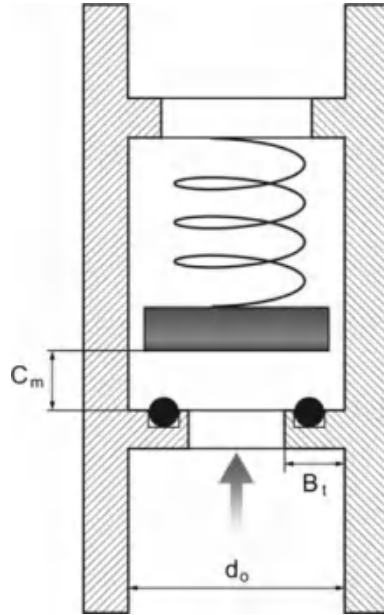


Fig. 6.2 Schematic drawing of the geometry of a pump's check valve

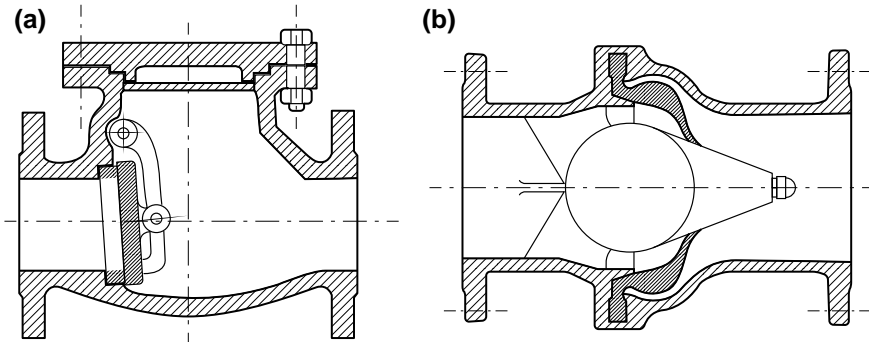


Fig. 6.3 Check valves to prevent water hammers: **a** swing check valve; **b** hydrostop type valve

Gate Valves

Another alternative to the practical formulas available in manuals (that indicate head losses equivalent to 5–10 m of straight pipes) [1, 4]. This formula refers to the confined flow through a straight pipe whose cross section widens from contracted to normal, provided that the velocity of water in the normal cross-section area is, on average, 70% of its velocity in the contracted cross-section. The resulting head drop, expressed as a function of the kinetic term, is:

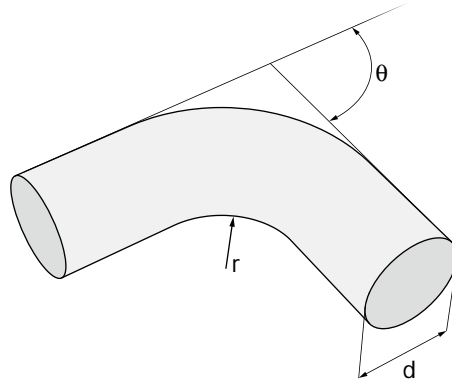


Fig. 6.4 Geometry of a pipe bend with fitting

$$\Delta H = (1/0.7 - 1)^2 \cdot v^2/2g = 0.18 \cdot v^2/2g. \quad (6.4)$$

For pipe diameters that fall within the range commonly used in water transport networks, the coefficient equal to 0.18 in Eq. (6.4) varies within the range 0.15–0.20, which doesn't produce significant differences in the assessment of the overall head loss values. Hence, further refinement of the mathematical formula isn't necessary.

Pipe Bends with Fittings

If θ is the angle between the axes of two pipe sections connected by a fitting, and R is the ratio between the inner diameter, d , and the radius of curvature of the pipe, r (see Fig. 6.4), and if the fitting is smooth and with a circular cross-section, the following formula, proposed by Idel'cik, can be used to determine the head drop [5]:

$$\Delta H = v^2/2g \cdot [(-0.000037\theta^2 + 0.0140\theta + 0.0411) \cdot (3.348R^2 + 0.999) + (0.020 + 0.0035 \cdot R \cdot \theta)] \quad (6.5)$$

where θ is expressed in sexagesimal degrees, and R is dimensionless.

Miter Bends

If we define β as the angle of a miter bend (the angle between the axes of two pipe sections connected by cutting their ends and joining them, see Fig. 6.5), the head loss can be expressed as follows, as a function of the kinetic term [4]:

$$\Delta H = 4 \cdot [\sin(\beta/2)]^2 \cdot v^2/2g. \quad (6.6)$$

Alternatively, the more rigorous Weisbach's formula, can be used [5]:

$$\Delta H = ([\sin(\beta/2)]^2 + 2 [\sin(\beta/2)]^4) \cdot v^2/2g. \quad (6.7)$$

Pipe Outlet into the Tank

The head loss resulting from the outlet of the pipe into the tank can be considered equal to that of a severed pipe stretch with the same inner diameter and length equal

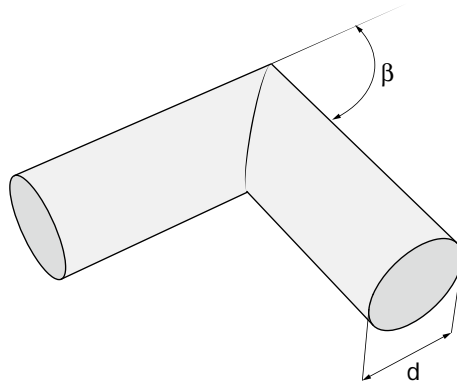


Fig. 6.5 Geometry of a miter bend

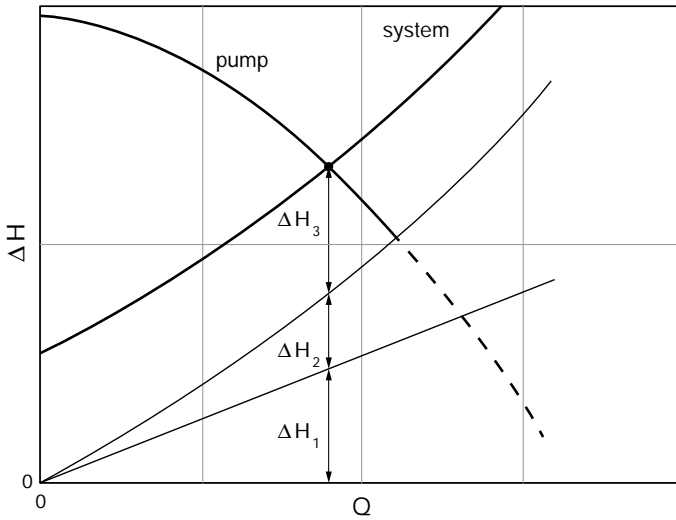


Fig. 6.6 Identification of the operating conditions of a water supply system by intersecting the system curve, $\Delta H = \Delta H_1 + \Delta H_2 + \Delta H_3$, with the pump performance curve

to forty times the diameter. This assumption is shared by all the main hydraulic texts in regard to medium-roughness tube; to solve problems such as the one under consideration, the assumption can be extended with reasonable approximation to all piping used for water delivery [4].

6.5 Optimization of the Productive Capacity of the System

A water supply *system curve* graphically describes the relation between the overall head losses in the system, ΔH , and the supplied discharge, Q . This curve (see Fig. 6.6) can be obtained as the sum of three terms: ΔH_1 (losses in the well-aquifer subsystem), ΔH_2 (losses in the water pipe network), ΔH_3 (elevation).

Except for elevation, which is obviously independent of the discharge, these terms can be derived as a function of discharge with the formulas illustrated in Sects. 6.3 and 6.4.

A possible operating point for the system can be identified by intersecting the system curve and the performance curve of one of the pumps that can be installed in the well (see Fig. 6.6). In almost all cases, centrifugal pumps with a vertical axis and electric motor are installed in potable water wells; their operating features are characterized by two curves that correlate pump head with supplied discharge (see Fig. 6.7).

As a consequence, the point of intersection in Fig. 6.6 is only one of the possible operating conditions. The best operating condition should simultaneously:

- (a) satisfy the supply demand, never producing less than a minimum acceptable discharge value;
- (b) be compatible with the productive capacity of the well-aquifer system, without trespassing a maximum discharge value;
- (c) correspond to the pump with the lowest power requirement and highest efficiency.

Once it has been verified that points (a) and (b) are respected, the optimization procedure requires comparing the intersection point of the system curve with the performance curves of various pumps, whose respective efficiency values need to be assessed.

Figure 6.8 illustrates an example of the procedure for the optimization of the production capacity of a water supply system.

6.6 Changes Over Time

Optimization conditions can vary over time due to a number of factors, the most important ones being:

- (a) clogging of the well screen slots;
- (b) development of inorganic scales in the discharge pipe;
- (c) lowering of the water table due to overuse of the aquifer.

The deviation from optimal operating conditions that results from the three above-mentioned causes is illustrated in Fig. 6.9.

Due to the frequent occurrence of such deteriorating phenomena, the operating conditions of a water supply system should undergo periodical checks: deviations

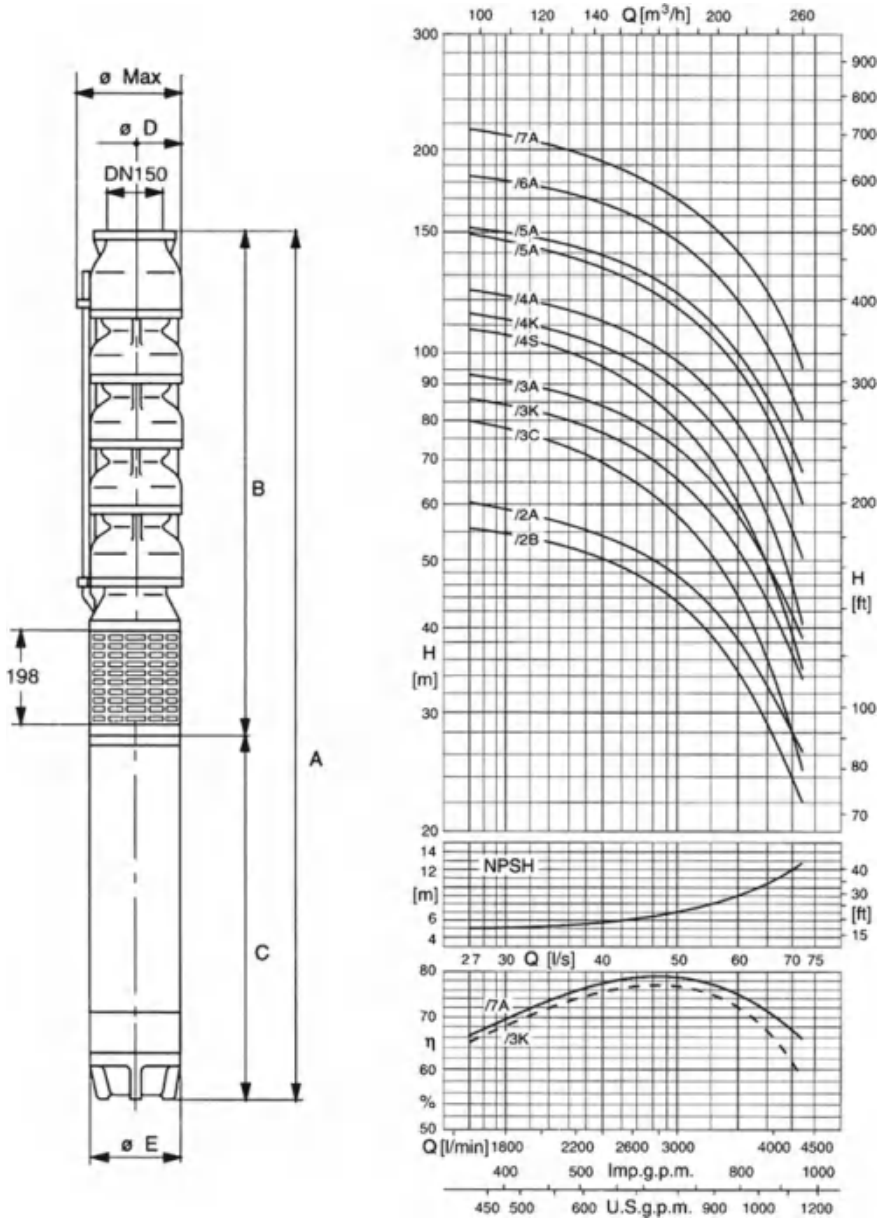


Fig. 6.7 Pump hydraulic head, Net Positive Suction Head (NPSH), and efficiency curves for a group of centrifugal pumps with vertical axis (modified from [2])

from the best efficiency can result in a significant rise in energy consumption, potentially higher than what would be necessary to replace the entire pumping system.

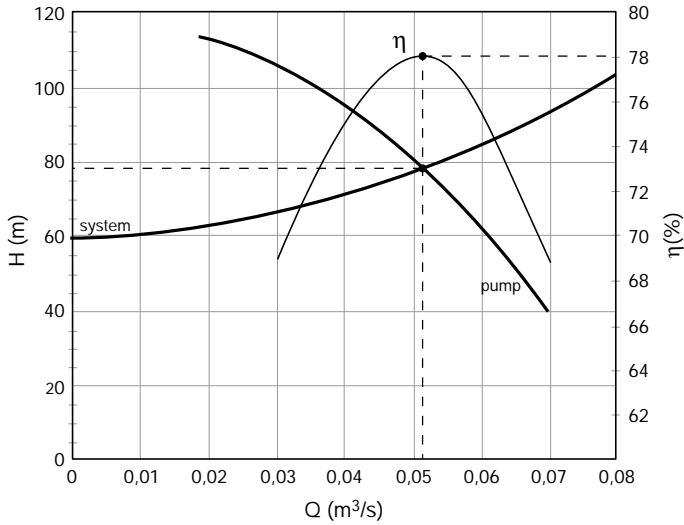


Fig. 6.8 Optimization of a water supply system

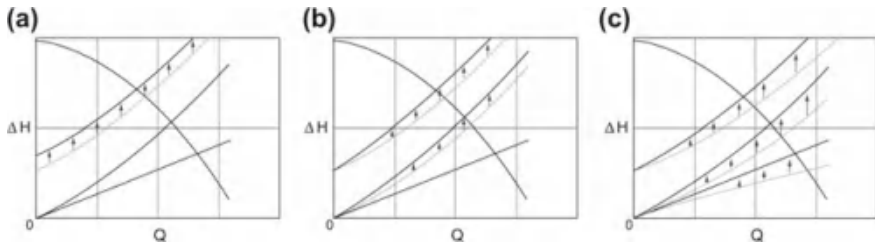


Fig. 6.9 Deviation from optimal operating conditions due to: **a** clogging of the screen slots of the well; **b** deposition of scales in the discharge pipe; **c** lowering of the water table due to overuse of the aquifer

References

1. G.J. Blower, *Plumbing: Mechanical Services* (Pearson Education, London, 2006)
2. Caprari, *Catalogue A96401G/3000/04-05* (2005)
3. Y.A. Çengel, J.M. Cimbala, *Fluid Mechanics: Fundamentals and Applications* (McGraw-Hill Education, New York, 2006)
4. G. De Marchi, *Idraulica* (Hoepli, Milano, 1977)
5. I.E. Idel'chik, *Handbook of Hydraulic Resistance* (Hemisphere Pub. Corp., 1986)
6. OECD, OECD Glossary of Statistical Terms - Water Supply System Definition (2001), <http://stats.oecd.org/glossary/detail.asp?ID=2913>
7. Oppo, Perdite di carico nelle condotte in pressione - Basi di calcolo, http://www.oppo.it/calcoli/canali/perd_carico_cond_pressione.html
8. R. Sethi, A dual-well step drawdown method for the estimation of linear and non-linear flow parameters and wellbore skin factor in confined aquifer systems. *J. Hydrol.* **400**, 187–194 (2011)

Chapter 7

Aquifer Vulnerability and Contamination Risk



Abstract Water supply systems must be designed in such a way to ensure groundwater extraction sustainability. In addition, the quality of pumped water must also be guaranteed, and this entails protecting the groundwater source from contamination. To do so, it is necessary to identify the physical and hydraulic characteristics of the soil, the unsaturated medium and the aquifer itself that influence the migration of contaminants spilled at the surface towards the aquifer, and hence potentially towards sensitive targets (i.e., drinking water pumping wells). The susceptibility of an aquifer to become polluted following a contaminant spill is called vulnerability, and its assessment is the focus of this chapter. Of the four categories of vulnerability assessment methods, i.e., overlay, index and statistical methods, and process-based simulation models, this chapter presents examples of the former two, which are of easier implementation and are widely used. Overlay methods define aquifer vulnerability on the basis of groundwater circulation and rely on the superposition of maps of the hydrogeologic, structural and morphologic setting. Index methods, instead, are based on the assignment of scores (sometimes weighed) to sets of parameters that are likely to affect the degree of vulnerability. Specific methods of these two categories described in detail in this chapter are the one developed by the Bureau de Recherches Géologiques et Minières in France, the Italian CNR-GNDICI and SINTACS methods, the US-EPA DRASTIC method and the British GOD method. The suitability of different methods is discussed, and how vulnerability assessment can be used to determine the risk of contamination is presented. On this basis, an example of contamination risk reduction strategies is illustrated.

The physical characteristics of the soil, the unsaturated medium, and the aquifer affect the way contaminants spilled at the land surface penetrate the unsaturated zone, reach the saturated zone, and propagate in it. Such effects and the diversity of their outcomes have to be taken into account when identifying the measures for the protection of groundwater resources.

The *intrinsic vulnerability* (henceforth simply called vulnerability) is defined as the propensity, or susceptibility, of an aquifer to become contaminated from an external source and, consequently, to become a vehicle of undesirable substances [5, 13, 21]. The greater the vulnerability, the more likely is a contaminant released at the surface to reach an aquifer. The intrinsic vulnerability is only descriptive of the environmental setting and how this can favor the migration of a generic contaminant

towards the groundwater; it does not consider, instead, the features of individual contaminants, in particular their transport properties, including reactivity. These aspects are accounted for by the *specific vulnerability*, which describes the vulnerability of an aquifer to an individual contaminant or a particular group of contaminants [18]. In this chapter only the intrinsic vulnerability will be illustrated; however, the risk assessment procedure which is closely related to vulnerability assessment and is described in Chap. 16 also takes into account specific contaminant behaviors.

In principle, the methods available for vulnerability estimation are based on the identification of the fundamental mechanisms that favor contaminant transport in an aquifer and the most significant parameters that characterize them [15].

Contamination processes essentially follow three phases:

- contaminant transfer from the surface to the subsurface;
- transport across the unsaturated zone;
- transport and spreading in the aquifer itself.

Vulnerability assessment methods are essentially distinguished by the level of detail used when approaching these phases, which can be quantified by the number of parameters used to characterize them.

In general:

- transport from the surface to the subsurface is characterized by the soil properties and by the variables that govern the surface hydrologic balance and, ultimately, the effective infiltration (precipitations, temperature, soil morphology and use);
- penetration across the unsaturated zone is characterized by the depth to groundwater and by the hydraulic conductivity of the unsaturated medium;
- finally, transport in the aquifer itself mainly depends on the hydraulic behavior of the aquifer, its hydraulic conductivity and the hydraulic gradient.

7.1 Vulnerability Assessment Methods

The methods for assessing the vulnerability of an aquifer can be grouped into the following categories [3, 5, 13, 15, 16, 18, 21]:

- overlay methods (i.e., based on hydrogeologic settings);
- index methods;
- statistical methods;
- process-based simulation models.

The latter two methods are typically employed for the analysis of single contamination events and heavily rely on the availability of large datasets on the site of interest. In this chapter, we will focus only on overlay and index methods, which were the earliest to be developed, are simpler to implement, and are still extensively used.

7.1.1 Overlay Methods

These include those methods that define aquifer vulnerability on the basis of groundwater circulation. They are based on map superposition, so they generally apply to vast territories and focus on the hydrogeologic, structural and morphologic setting. They are, therefore, suitable for large to very large scale mapping. The goal of the map determines which parameters will be considered but, in general, vulnerability is defined in qualitative terms.

These methods can be applied when there is geographically sparse information on the site, and they provide a general and preliminary assessment.

Two examples of such methods were developed in Europe, specifically in France and in Italy, i.e., the BRGM and the CNR-GNDICI methods, respectively [1, 6].

7.1.1.1 The BRGM Method

The method developed by the Bureau de Recherches Géologiques et Minières [1] deserves mention because it was one of the first vulnerability assessment attempts.

The method is principally based on the identification of groundwater flow mechanisms; in this sense, geological formations can be classified according to their lithological and permeability characteristics:

- *Alluvial deposits*: they are important groundwater storage rock formations due to the potential water exchange with surface water, and for their high vulnerability.
- *Formations that allow very rapid contaminant spreading*: limestone and dolostone karstic rocks, for example, belong to this category. In these formations water circulates at a remarkable velocity and does not undergo attenuation mechanisms that are, conversely, common in intergranular porosity.
- *Formations that allow rapid contaminant spreading*: the formations that belong to this group (limestones, dolostones, basalts, etc.) display flow velocities that depend on the degree of fracturing.
- *Formations in which contaminants spread slowly*: contaminants are transported slowly through these rocks (fine sands, sandstones, etc.) and may undergo filtration; however, contamination is persistent due to reduced groundwater recharge.
- *Formations characterized by variable velocity of contaminant propagation*. These can be both loose and compact rocks with medium permeability, in which areas with low and high permeability alternate (flysch, morains, clayey-sandy formations, etc.).

On top of this, unconfined aquifers are intrinsically very vulnerable. For such aquifers, the following zones can be defined:

- high piezometric head zones, where aquifer recharge areas are located;
- zones recharged by irrigation with surface waters;
- zones partially protected by low permeability surface cover;
- zones with leakage and infiltration of surface water from streams and rivers.

A qualitative representation of the vulnerability can be obtained by overlaying the above described elements on a map. The same map can be amended by including human elements of risk present in the area (e.g., landfills, farms, factories, etc.).

7.1.1.2 The CNR-GNDCI Method

This mapping method defines a unified legend to represent the elements that determine the intrinsic vulnerability as well as those that, instead, indicate the presence of risk factors in the area [6].

The method considers the following elements:

- *Aquifer characteristics.* These are grouped in six vulnerability classes (from very low to extremely high) based on the presence and type of surface covering, the depth to water table, and the position of the potentiometric surface relative to rivers, as well as on the mechanisms of water circulation through different lithotypes.
- *Elements of the hydraulic structure.* The elements of the hydraulic structure reported on the map (e.g., watersheds, boundaries, potentiometric features) allows for a quick evaluation of the geometry of the aquifer, the direction of flow and hence the spatial and temporal evolution of potential contaminations.
- *Actual state of groundwater contamination.* Representing areas whose water quality is degraded allows to define the transition of aquifer vulnerability from potential to real, and to identify zones that need remediation interventions.
- *Actual and potential sources of groundwater pollution. Hazard hotspots,* defined as any activity, settlement or artifact that could directly or indirectly generate real or potential groundwater degradation factors, are represented with a specific symbol.
- *Potential groundwater pollution sinks.* This category includes natural (e.g., sink-holes) and man-made (e.g., quarries) elements that could amplify the intrinsic vulnerability of an aquifer, by reducing or nullifying the self-cleansing capability of soil.
- *Elements reducing or preventing contamination.* These are constructions or plants designed to reduce the contamination load affecting an aquifer in a specific area or to monitor it, with the goal of reducing the social and economic effects of potential accidental episodes.
- *Main contamination targets.* These are the main sensitive targets in terms of water exploitation, which include water supply systems (wells, springs, surface water points of supply) that could be compromised by the contamination of the surrounding area.

The observation of a map created according to the CNR-GNDCI method offers a full, albeit qualitative, view of both the intrinsic vulnerability of the area under consideration and the existing risk factors.

7.1.2 Index Methods

These are quantitative methods and are the most employed nowadays. They are based on the assignment of a score to a few parameters that affect the degree of vulnerability of an aquifer.

They can be used when medium data density is available; nevertheless, a method of varied complexity and proportional to the amount of available information can be applied to each case.

Internationally, the most used methods are GOD, a simple scoring method, and DRASTIC, a weighted scoring method [2, 14]. However, several others, each emphasizing different parameters or applicable to specific systems, have been proposed, including SINTACS, developed in Italy and illustrated in Sect. 7.1.2.3, SEEPAGE, EPIK, and AVI [7, 12, 15, 20].

Simple scoring methods are based on the assignment of a certain score to a set of chosen parameters. The score is selected within a fixed range established according to the variation window of the parameter. There is a variety of data that can be used, and it is possible to decide to assign a greater importance to the physical and chemical characteristics of the soil or to the main hydrogeological parameters. The GOD method is the most commonly used among the fixed scoring methods, due to its simple and pragmatic structure, and is particularly useful for plain systems, such as the Po Plain in northern Italy.

In weighted scoring methods, instead, the influence of each parameter is hampered or enhanced by a numerical coefficient (i.e., the weight) that can vary according to land use or to the hydrogeological characteristics of the aquifer.

7.1.2.1 The GOD Method

The GOD method, which stands for Groundwater confinement, Overlying strata, Depth to groundwater, considers the intrinsic vulnerability to be the result of the combined effect of a series of components, the most important being [14]:

- the aquifer's hydraulic behavior;
- the lithology and permeability characteristics of the unsaturated medium, which influence the infiltration velocity and the natural attenuation properties of the crossed soils;
- the depth to the water table for unconfined aquifers or the depth to the top of the aquifer for confined ones.

Foster [14] developed a very simple procedure based on these parameters that allows to assess the intrinsic vulnerability of an aquifer objectively. This vulnerability is calculated as the product of three coefficients, each of which corresponds to one of the illustrated components. The product of the three coefficients quantifies the intrinsic vulnerability of a specific area of the aquifer under consideration and is comprised between 0 and 1: the lower limit indicates no vulnerability, the upper limit means extreme vulnerability, see Fig. 7.1.

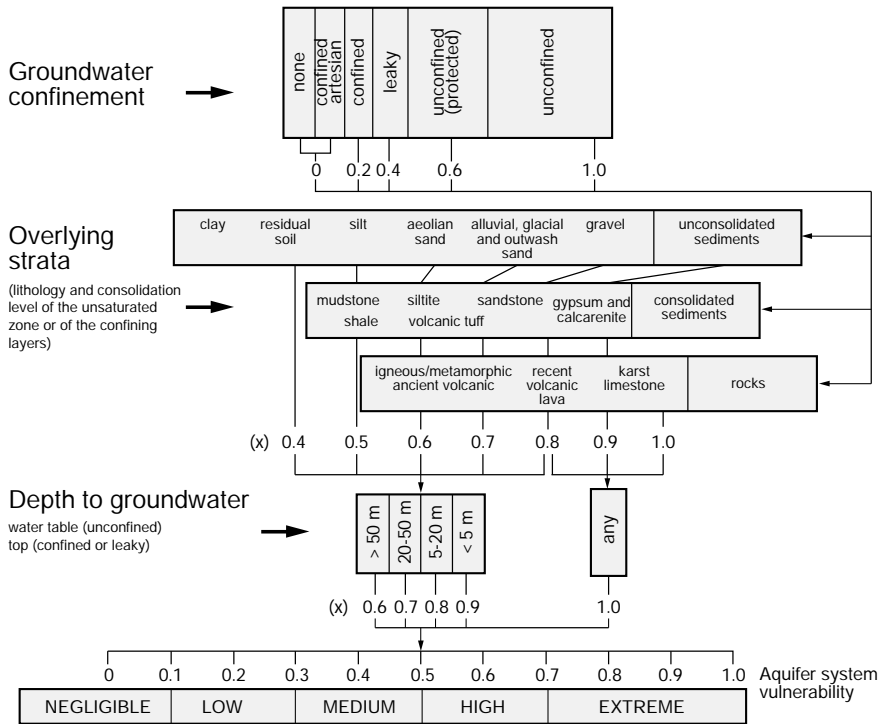


Fig. 7.1 Table for vulnerability assessment with the GOD method (modified from [14])

The main virtues of this method are its simplicity and the ease of acquisition of the required data.

7.1.2.2 The DRASTIC Method

The method, developed by the US-EPA, takes its name from the seven parameters scored for the vulnerability assessment:

- *D* (Depth to groundwater);
- *R* (net Recharge);
- *A* (Aquifer media);
- *S* (Soil media);
- *T* (Topography);
- *I* (Impact of the vadose zone media)
- *C* (hydraulic Conductivity).

Each parameter is attributed a score from 1 to 10 according to the characteristics of the area (see Figs. 7.2, 7.3, 7.4, 7.5, 7.6, 7.7, 7.8); this score is multiplied by a coefficient

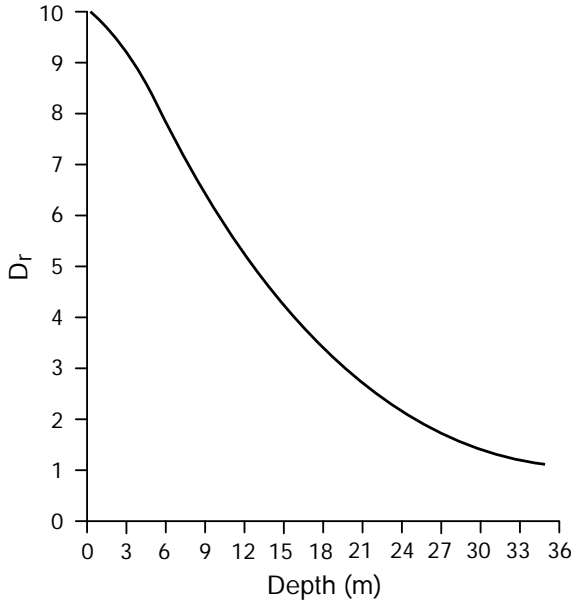


Fig. 7.2 Values of the parameter D_r as a function of the depth to water (for unconfined aquifers) or of the depth of the confining upper layer (confined aquifers) (modified from [2])

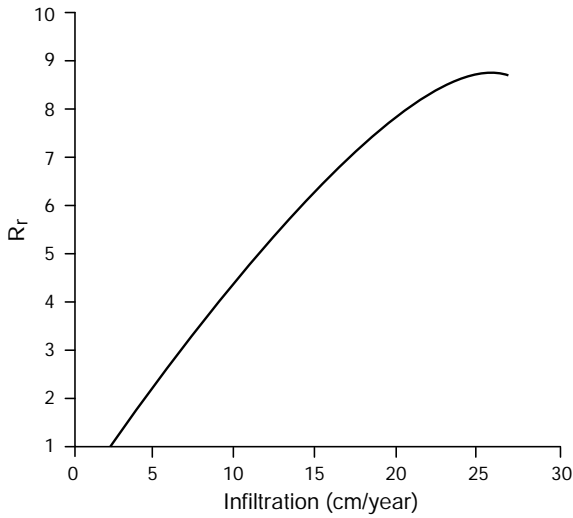


Fig. 7.3 Values of the parameter R_r as a function of the effective infiltration (modified from [2])

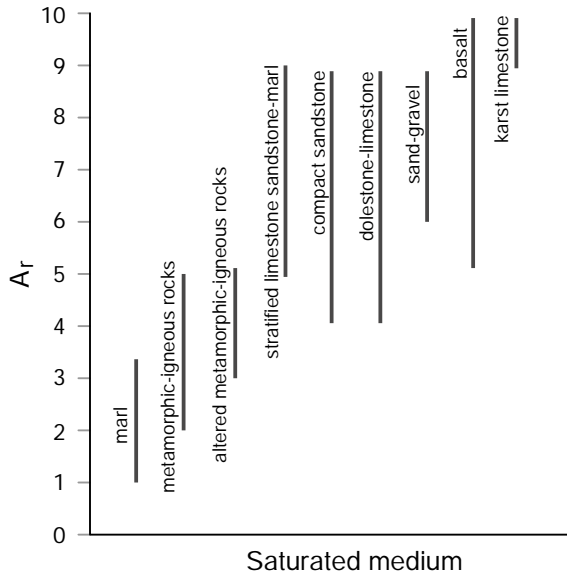


Fig. 7.4 Values of the parameter A_r as a function of the aquifer's lithology (modified from [2])

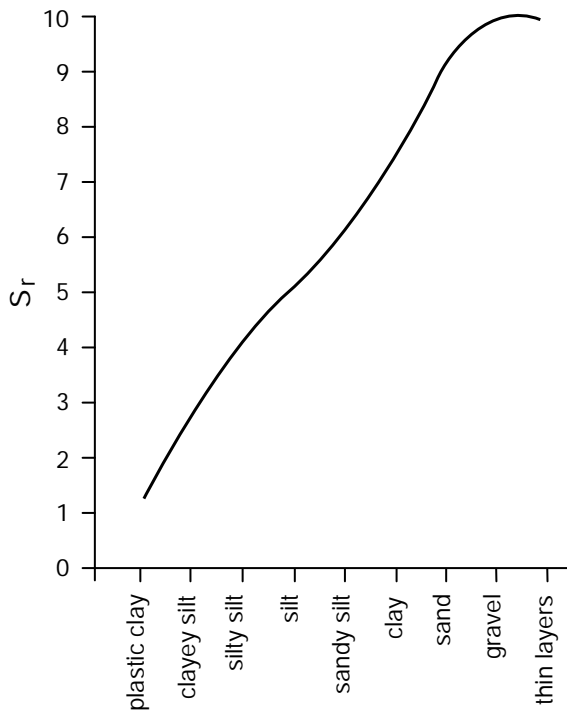


Fig. 7.5 Values of the parameter S_r as a function of the soil type (modified from [2])

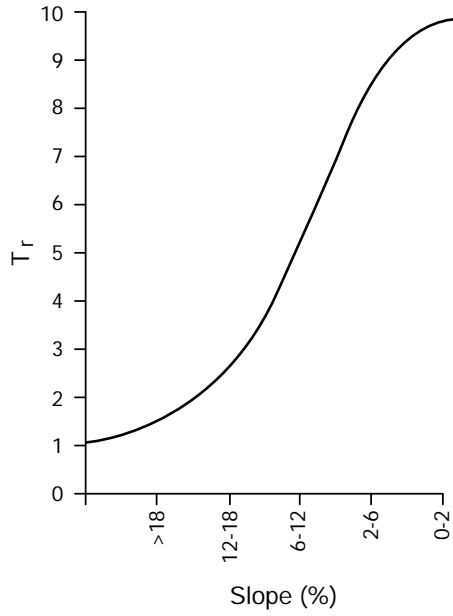


Fig. 7.6 Values of the parameter T_r as a function of the slope of the surface topography (modified from [2])

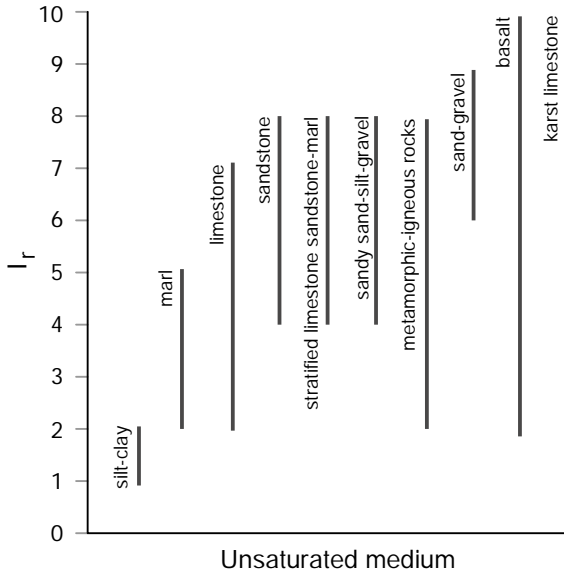


Fig. 7.7 Values of the parameter I_r as a function of the characteristics of the vadose zone (modified from [2])

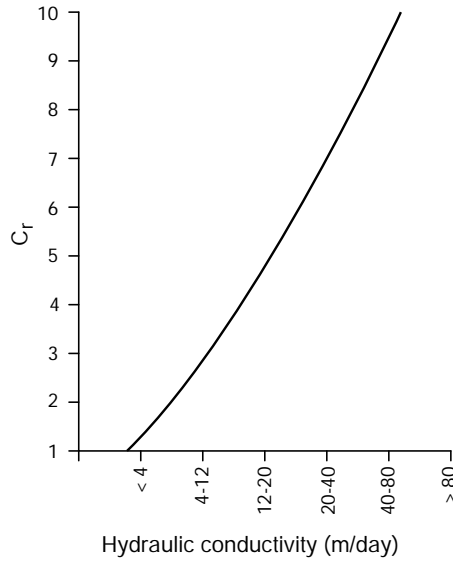


Fig. 7.8 Values of the parameter C_r as a function of hydraulic conductivity (modified from [2])

Table 7.1 Weights used by the DRASTIC method as a function of different soil use (DRASTIC b for areas affected by intensive agriculture)

	DRASTIC a	DRASTIC b
D	5	5
R	4	4
A	3	3
S	2	5
T	1	3
I	5	4
C	3	2

or weight depending on whether the area isn't (DRASTIC a) or is (DRASTIC b) used for intensive agricultural activities, in which case the diffuse presence of pesticides has to be considered (see Table 7.1).

As shown in Table 7.1 only the last four parameters have different weights.

If D_r , R_r , A_r , S_r , T_r , I_r , and C_r indicate the values attributed to each parameter, respectively, on the basis of the characteristics of the considered area (see Figs. 7.2, 7.3, 7.4, 7.5, 7.6, 7.7, 7.8), and D, R, A, S, T, I, and C indicate the value of the corresponding weight, the value of the vulnerability can be calculated as follows:

$$V = D_r \cdot D + R_r \cdot R + A_r \cdot A + S_r \cdot S + T_r \cdot T + I_r \cdot I + C_r \cdot C, \quad (7.1)$$

and will be comprised between 23 and 230 or between 26 and 260 in the absence or presence of intensive agriculture, respectively. The absolute value thus obtained, in some cases, does not give a clear indication of the degree of vulnerability of the area; therefore, to overcome this inconvenience, the value can be divided by the maximum value (i.e., 260), thus yielding an index expressed using decimals or percentages, which favor the immediate comparison of values obtained from close areas.

A closer analysis of the DRASTIC method allows to understand the importance given to the different parameters. For instance, for an area such as the Po Plain, partially used for intensive agriculture:

- for the transfer from the surface to the subsurface:
 - the net **R**echarge has a weight equal to 4;
 - the **T**opography has a weight of 3;
- for the infiltration across the vadose zone:
 - the **S**oil media parameter has a weight of 5;
 - the **D**epth to water has a weight of 5;
 - the **I**mpact of the vadose zone media has a weight of 4;
- for the transport and spreading in the aquifer
 - the **A**quifer media parameter has a weight of 3;
 - hydraulic **C**onductivity has a weight of 2.

Despite clearly offering a more analytical approach than GOD, DRASTIC still significantly simplifies the complex process of contaminant spreading. In particular, it focuses more on the vadose than the saturated zone; specifically, in terms of weights of the parameters:

- those that concern the infiltration across the vadose zone, i.e., *S*, *D*, and *I* are equal to 5, 5, and 4, respectively;
- those that refer to the transfer across the soil surface, *R* and *T*, are equal to 4 and 3, respectively;
- finally, those that refer to the aquifer itself, *A* and *C* are equal to 3 and 2, respectively.

It is worth noting that the complex propagation, dilution and attenuation phenomena occurring in the aquifer once the contaminant has reached it are ignored. The only parameters that are considered are the hydraulic conductivity and the lithology of the solid matrix.

7.1.2.3 The SINTACS Method

SINTACS takes its name from the initials in Italian of the seven parameters considered [7]:

- S—**S**oggiacenza: depth to water;
- I—**I**nfiltrazione efficace: effective infiltration;
- N—effetto di autodepurazione del **N**on saturo: attenuation in the vadose zone;
- T—**T**ipologia della copertura: surface cover;
- A—caratteristiche idrogeologiche dell'**A**cquifero: hydrogeologic characteristics of the aquifer;
- C—**C**onducibilità idraulica dell'**a**cquifero: hydraulic conductivity of the aquifer;
- S—**S**clività della **S**uperficie topografica: slope of the topography.

SINTACS employs a method analogous to DRASTIC, assigning a score to single parameters according to specific experience-based diagrams (with a score range of 1–10) [7]. Table 7.2 summarizes the values that can be attributed to individual parameters based on the diagrams.

The specific value of SINTACS is that it involves the use of weight strings that can be applied alternatively or in parallel, and conceived in such a way to enhance or hamper the influence of single parameters, consistently with the hydrogeological and impact situations present in the considered area. This allows to modulate the use of the methodology according to actual local features.

The five weight classification strings employed by SINTACS are:

- area subjected to normal impact: this includes all the situations concerning areas with small topographic gradient (plains, mountain feet, etc.) where the vadose zone is mainly composed of rocks with intergranular permeability, where there are no particular situations of human impact and where the land is poorly used or transformed;
- significantly impacted area: it includes situations analogous to the previous case, but affected by significant impacts due to diffuse sources of potential contamination (e.g., land treatment with pesticides, industrial activities, etc.);
- areas that undergo draining: this includes areas subjected to continuous or frequent draining from surface water to groundwater, resulting in a significant reduction or in the disappearance of the depth to groundwater due to the contact established between the aquifer and the surface draining network, be the latter natural or artificial (e.g., surface irrigation by flooding);
- areas subjected to karst processes: aquifers in karst systems are characterized by flow paths with high permeability and very short migration time;
- areas with fractured aquifers: the rock formation is characterized by fracture -but not karst- permeability.

The sets of weights that correspond to the different described scenarios are listed in Table 7.3.

As can be noted, the line of normal impact emphasizes the depth to groundwater and the properties of the unsaturated medium, which are the parameters related to the effective ability of the contaminant to reach the aquifer. In significantly impacted areas, in addition to the two mentioned parameters, the influence of the surface cover is also accentuated, in order to keep into account both soil protection and effective infiltration, since irrigation practices represent a relevant mechanism of contaminant transport.

Table 7.2 Scores that the SINTACS method assigns to the different parameters according to their individual type or variation range [7]

Score	S	I	N	T
SINTACS	Depth to groundwater (m)	Effective infiltration (mm/a)	Vadose zone lithology	Soil type
10	0.00–1.50	–	Karst limestone	Thin, absent, clean gravel
9	1.50–3.00	>215	Coarse gravel, gravel and pebbles	Clean sand
8	3.00–5.00	215–180	Gravel and sand	Sandy, peaty
7	5.00–7.50	180–150	Sand	Clayey-sandy
6	7.50–10.00	150–120	Gravel and sand with clay, conglomerates	Loamy sand
5	10.00–13.00	120–95	Alternating	Loamy sand-silt
4	13.00–21.00	95–75	Clayey gravel, sand + clay	Loamy silt
3	21.00–30.00	75–55	Peat	Loamy-silty-clayey
2	30.00–60.00	55–30	Clay + silt + peat	Humic
1	>60.00	<30	Clay	Clayey

Score	A	C	S
SINTACS	Aquifer lithology	Aquifer's hydraulic conductivity (m/s)	Surface topography (%)
10	Karst limestone	$>4 \cdot 10^{-3}$	0–2
9	Fracture limestone, coarse alluvial deposits	$4 \cdot 10^{-3} - 7 \cdot 10^{-4}$	3–4
8	Medium-fine alluvial deposits	$7 \cdot 10^{-4} - 3 \cdot 10^{-4}$	5–6
7	Coarse morain, sandstone, conglomerates	$3 \cdot 10^{-4} - 8 \cdot 10^{-5}$	7–9
6	Pyroclastic rocks, alternating flysch	$8 \cdot 10^{-5} - 3 \cdot 10^{-5}$	10–12
5	Medium-fine marl	$3 \cdot 10^{-5} - 8 \cdot 10^{-6}$	13–15
4	Fractured metamorphic rocks	$8 \cdot 10^{-6} - 2 \cdot 10^{-6}$	16–18
3	Fractured plutonites	$2 \cdot 10^{-6} - 6 \cdot 10^{-7}$	19–21
2	Silt, peat	$6 \cdot 10^{-7} - 3 \cdot 10^{-8}$	22–25
1	Marl, clay	$<3 \cdot 10^{-8}$	>26

Table 7.3 SINTACS parameters and sets of weights defined by the fourth release of the method [7]

Parameter or criterion	Weights assigned to each parameter in the different scenarios				
	Area with normal impact	Significantly impacted area	Area subjected to draining	Area subjected to karst processes	Area with fractured aquifers
S —depth to groundwater	5	5	4	2	3
I —effective infiltration	4	5	2	3	4
N —unsaturated medium	4	5	4	5	3
T —surface cover	5	4	4	1	3
A —aquifer type	3	2	5	5	5
C —hydraulic conductivity	2	2	2	5	4
S —surface topography	3	3	5	5	4

In areas subjected to draining, with small to absent depth to groundwater, the lithology and hydraulic conductivity of the aquifer are assigned the maximum weight.

In karst areas, great importance is given to infiltration and to the lithologic properties and hydraulic conductivity of the aquifer. In this case, also the surface topography becomes relevant because, beside affecting the level of infiltration, it can cause stagnation areas from which contaminants present on the soil surface can penetrate the aquifer more easily.

In fractured aquifers, the parameters assigned the greatest weight are the aquifer's hydraulic conductivity and, secondly, the surface topography.

On the basis of what presented above, the vulnerability of a single cell of land (subarea) is calculated, analogously to the DRASTIC method, as the sum of the scores attributed to each parameter by their respective weights:

$$V = \sum_{i=1}^7 P_i \cdot w_i, \quad (7.2)$$

where P_i and w_i represent, respectively, the score (with a range 1–10) and the weight (dependent on the chosen line) attributed to each parameter.

Formula (7.2) provides vulnerability values comprised between 26 and 260 that can be normalized by dividing them by the maximum obtainable value (i.e., 260) and expressed as percentages.

7.2 Comparison of Different Vulnerability Assessment Methods

Comparisons of the results obtained by applying different vulnerability assessment methods to the same area are available in the literature [8, 9, 17].

The comparison studies are reasonably consistent and allow to make a few general considerations [15, 21]:

- all methods identify unequivocally high and very high vulnerability areas, while the definition of intermediate levels is strongly dependent on the method, i.e., on the considered criteria;
- in terms of appropriate protection, zonation into homogeneous subareas is strongly influenced by the knowledge of the hydrogeological structures; in particular, all methods must define the areas on the basis of the aquifer's hydraulic behavior;
- referring to relatively simple classifications based on controllable and comparable methodologies is preferable, for the achievement of consistent and standardized results;
- if the area is not well characterized, it is preferable to use simple methods that employ known and reliable parameters, rather than to adopt approaches that require a greater number of parameters whose values have to be hypothesized or made up.

Overall, vulnerability maps can be a useful tool for large scale applications such as land use planning and legislation implementation. Conversely, they are unsuitable at the small scale due to the ample space for arbitrary and subjective choices based on indirect evaluations of few variables of the problem, rather than on the actual reconstruction of physical phenomena.

7.3 Contamination Risk

In everyday language, the terms risk and hazard are often used interchangeably. However, this cannot be done in scientific or technical language, which require a correct and appropriate use of terminology.

A *hazardous event* is one caused by natural or anthropogenic factors that could have negative effects (such as contamination) on a certain area.

Hazard expresses the probability of occurrence of a hazardous event (e.g., contamination) of a certain extent, in a specific portion of land and time interval.

The *scenario* is the situation in which a hazardous event can occur: any life situation can potentially be a scenario for a certain hazard to materialize. A road, a radioactive compound, an electrical switch represent scenarios for, respectively, speed, radioactivity, electricity; while accidental spills in the environment, industrial use, storage are examples of hazard scenarios for chemical substances.

Given certain premises (scenario and hazard), a *causal event* causes a situation of potential hazard to translate into an actual hazardous event, thus causing dam-

age. Intersections, type of radiation, presence of humidity, or exposure of humans to chemical substances (via the various penetration paths into the organism) the presence of free flames, are examples of potential causal events of the above mentioned situations.

The *risk of contamination*, R_t , of groundwater resources expresses the probability of groundwater quality degradation following the occurrence of a hazardous situation in a site having specific vulnerability characteristics. In analytical terms, the total contamination risk can be expressed as:

$$R_t = H \cdot V \cdot D, \quad (7.3)$$

where H is the contamination event hazard, V the intrinsic vulnerability of the site and, in particular, of the aquifer that has to be protected, and D is the expected damage caused by the contamination incident.

If we define hazard as the probability, p , that a contamination event, characterized by a certain intensity or magnitude, M , occur in a specific time interval and a specific area, decreasing the risk of groundwater contamination implies reducing the value of the parameters of the following expression:

$$R_t = p \cdot M \cdot V \cdot D, \quad (7.4)$$

where, clearly, the intrinsic vulnerability V constitutes an unvariable constant.

The economic parameter, D , in expression (7.4), i.e. the expected damage of a contamination event, can be broken down into two aliquots:

- the total cost (C_t), resulting from the implementation of remediation interventions (C_r) and from damage compensations (C_c) to third parties (for example: harvest losses, work interruption, etc.). Indirect costs of social unrest deriving from the lack of availability of the natural resource for a certain time, instead, aren't considered. Therefore, the total cost is expressed by the following relation: $C_t = C_r + C_c$;
- the value of the loss of the resource, defined as residual risk, R_r . The residual risk can be expressed as the product of the economic value of the aquifer exposed to the contamination by the fraction of water resource that cannot be recovered, including potential limitations to its exploitation after the restoration intervention.

The analytical definition expressed by Eq. (7.4) is conceptually very important for engineers, despite being difficult to quantify: if the expected environmental damage, D , is hard to quantify, it is almost impossible to calculate the hazard, H . The probability of occurrence of a contamination event cannot be estimated scientifically, due to the lack of historical data and because the majority of groundwater contamination incidents remain unknown.

Think of, for instance, the difference relative to the seismic risk: in this context there is information available on a number of events that occurred at least in the past 2000 years.

Several approaches have been proposed to estimate the hazard indirectly, by using parameters such as solid and/or liquid waste production, pesticide and fertilizer use in agriculture, etc., but they yielded modest results.

The most important thing from an engineering perspective is not, however, the absolute value of the contamination risk, but the definition of the design and management interventions that have to be implemented to reduce the risk.

7.4 An Example of Contamination Risk Reduction

Waste management through landfill disposal has significantly developed over the course of the past decades, evolving from a primitive technology (uncontrolled dumping of waste into a pit) to a complex industrial plant in which chemical, physical and biological processes are monitored.

In this process, driven by technological development and applied research, a crucial role was played by the interventions aimed at reducing and controlling emissions into the environment and, in particular, of leachate seeping towards aquifers. Indeed, the risk of groundwater resources contamination has always been, also for the general population, the determining factor in accepting a landfill or not.

The safeguard of groundwater resources from potential degradation connected to waste disposal must be a priority during the planning, design, management, and post-operation stages of a landfill.

Once the site has been selected, reduction of the contamination risk can be achieved by identifying design and management measures to decrease the probability of a contamination incident, the magnitude of the event and/or, finally, the expected damage caused by groundwater contamination (see Fig. 7.9).

7.4.1 *Reduction of the Probability of Occurrence of the Event*

Decreasing the occurrence probability of a contamination event that follows the draining of leachate from the bottom of a landfill is tightly connected to the installation of an effective *bottom lining*, a barrier system composed of the natural geological barrier (if present), a custom-built impermeable liner, and a leachate drainage and collection system.

The presence of a natural geological barrier influences the choice of the site, by affecting the intrinsic vulnerability; hence, it is by focusing on the design and construction of the artificial liner that the probability of leachate draining out of the landfill can be reduced.

An effective impermeable liner is composed by a *composite barrier*, formed by coupling a compact mineral material (clay) and a geomembrane [4, 10, 19].

The geomembrane, that should be mechanically and chemically compatible with the leachate in order to ensure durability, should be spread in direct contact with the

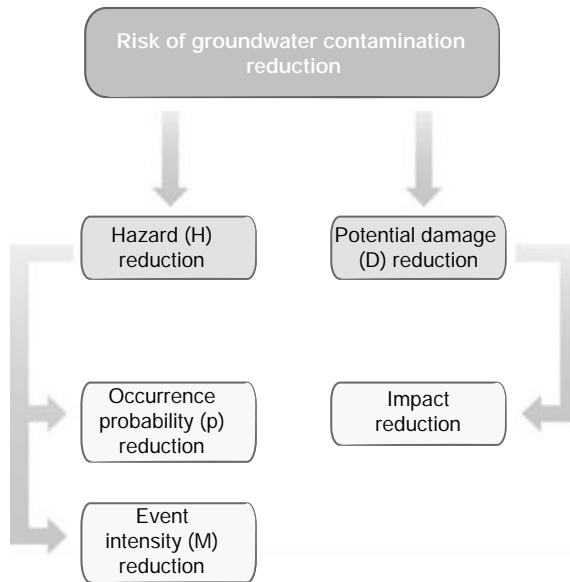


Fig. 7.9 Potential measures for groundwater contamination risk reduction

compacted mineral layer, without interposing a draining layer, since this would favor spreading of the contamination in case of rupture of the membrane itself.

In particularly vulnerable sites or in the presence of hazardous waste, it might be necessary to employ a double composite barrier to reduce the occurrence probability of a contamination event. In this case, a monitoring system can be interposed between the two liners to verify the effectiveness of the first one.

7.4.2 Reducing the Intensity of the Event

The magnitude of a contamination event affecting groundwater resources depends on the volume of leachate present in the landfill. Therefore, the reduction the intensity of the incident can be achieved through a series of design and management measures aimed at decreasing such volume.

The main design measures are: the creation of a suitable leachate drainage, collection, and extraction system; the hydraulic division of the landfill in independent sectors; the construction of an effective surface cap.

The drainage and collection system should prevent leakage of the leachate and contribute to the effectiveness of the landfill's hydraulic barrier. Drainage systems have to be conceived and designed to favor quick conveyance of the leachate towards the collection pipes. Their purpose is, in fact, to minimize the accumulation of leachate and the formation of suspended leachate lenses within the pile of waste. Design

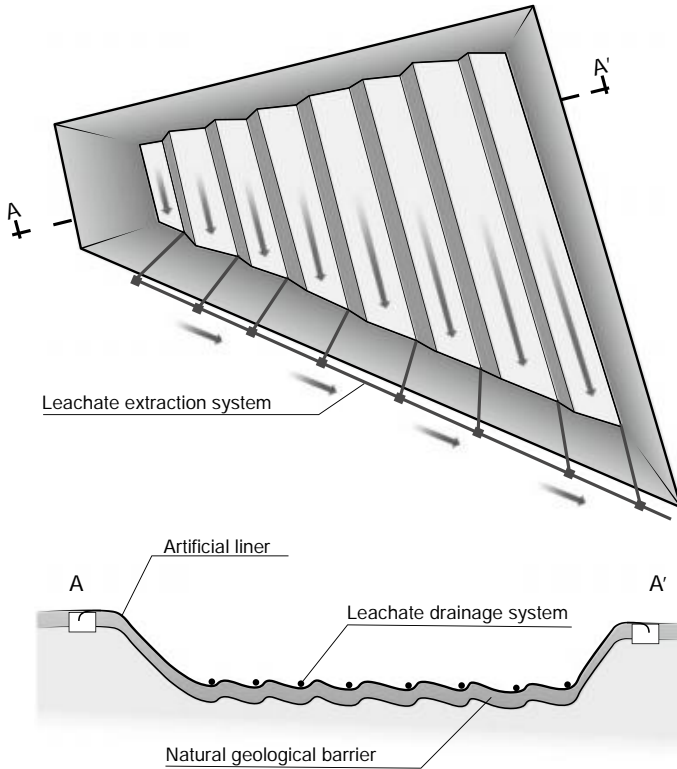


Fig. 7.10 Parceling of the bottom of the landfill in hydraulically independent sectors

choices should aim at avoiding clogging of the drainage system, keeping in mind that the conveyance tubes are the only component of the system that can be inspected and, if necessary, restored.

Leachate collection and removal wells have to be easily accessible and placed so that they are protected during waste compaction, and they mustn't affect the impermeability of the lining system. Therefore, although there are other solutions, the preferable technical choice consists in constructing wells within the body of the landfill, placed along the sides of the pit.

A design criterion that should be mandatory is to shape the bottom of the pit in various hydraulically independent sectors (see Fig. 7.10).

First of all, this prevents the rainwater that falls into sectors not yet occupied by waste from mixing with the leachate during normal landfill operation, thus reducing management costs. In case of an accident, the volume of leachate that could potentially be released into the underlying aquifer is limited to what is contained in the sector affected by the rupture of the liner. Consequently, the greater the hydraulic parceling of the pit, the smaller is the magnitude of the potential accident.

Surface capping of the landfill also plays an important role in reducing the volume of leachate formed: among others, it serves the function of limiting rainwater infiltration, due regard being had to the requirements of the biological degradation of waste.

Also the surface cap is a composite barrier, whose various layers have a different composition to smoothen the waste surface, drain biogas towards the collection points, prevent emissions to the atmosphere and reduce infiltration in the waste, drain rainwater, and allow the environmental restoration of the area. The slopes of the final capping have to promote surface run-off of water and must account for settling phenomena of the body of waste.

The design measures considered up to here can, however, be jeopardized if they are not followed by a strict protocol involving frequent leachate removal from the landfill to avoid its accumulation on the bottom liner and, in general, to minimize its overall volume in the landfill itself.

7.4.3 Reducing Potential Damage

If we assume that, despite all the design measures considered, a groundwater contamination event might occur, reducing the expected damage involves implementing a series of measures to contain the volume of groundwater resources potentially affected.

Specifically, this can be achieved by designing (a) a monitoring network to ensure timely detection of the degradation process, and (b) a hydraulic barrier composed of a system of purging wells, whose activation ensures the containment of the portion of aquifer affected by the contamination incident. For the implementation of both these measures a full hydrogeological, hydrodynamic, and hydrodispersive characterization of the aquifer of interest is necessary.

The hydraulic barrier has to be designed and planned in such a way that, upon activation, groundwater contamination detected by the monitoring network will not affect the area outside the plant.

An effective system of purging wells or recovery wells has thus to be installed at the landfill site, downgradient relative to the direction of flow. Their number and position should ensure full interception of the contamination front resulting from a potential rupture of the impermeable lining.

The necessary number and position of the purging wells can be determined with varying degrees of precision, depending on the level of experimental characterization of the aquifer. In particular, the design of the purging system can derive from:

- groundwater flow simulations, based on the hydrogeological and hydrodynamic characterization of the system. This implies the simplifying assumption that contaminant transport occurs exclusively according to advective processes (see Chap. 10). The design solution should ensure that the contamination front caused by the rupture of the impermeable lining at any point of the landfill bottom is included within the capture zone of the purging wells (see Fig. 7.11);

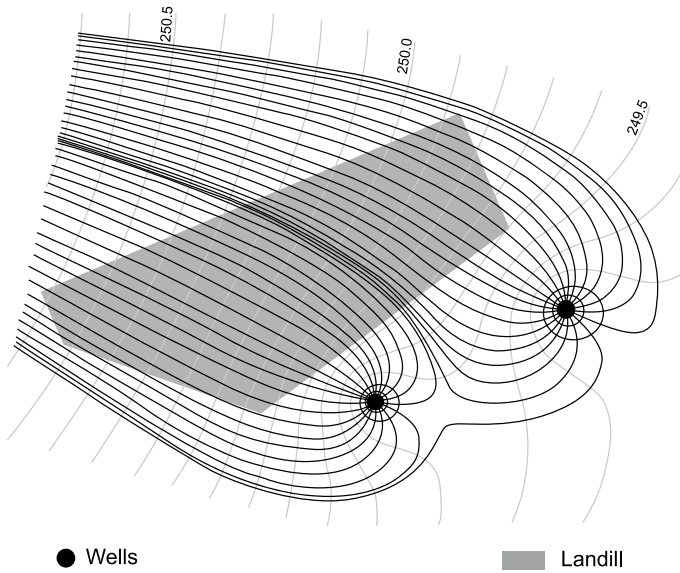


Fig. 7.11 Location of purging wells based on the simulation of the advective process alone (flow model)

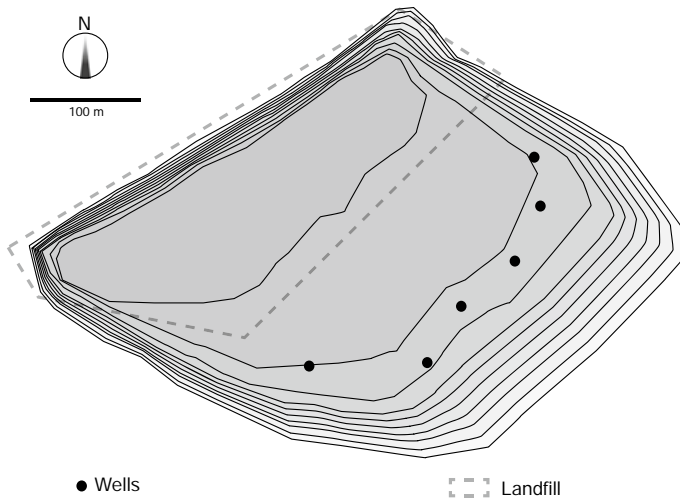


Fig. 7.12 Effectiveness assessment of a purging well system via a flow and transport model of the landfill area: distribution of equal concentration curves (modified from [11])

- simulation of flow and transport processes in the aquifer, when data from a hydrodispersive characterization are available. This model, closer to the actual evolution of the potential event, can include the analysis of the main hydrological, physico-chemical, and possibly biological processes that govern the evolution of the contamination plume. Figure 7.12 shows an example of this approach. The resulting concentration should be compared to the threshold values.

References

1. M. Albinet, J. Margat, Cartographie de la vulnérabilité à la pollution des nappes d'eaux souterraines. *Bull BRGM* **2**, 13–22 (1970)
2. L. Aller, T. Bennett, J. Lehr, R. Petty, G. Hackett, DRASTIC: standardized system for evaluating groundwater pollution potential using hydrogeologic settings. *J. Geol. Soc. India* **29**, (1987)
3. ASTM, D6030 - 15 standard guide for selection of methods for assessing groundwater or aquifer sensitivity and vulnerability, Technical report, West Conshohocken, PA (1999)
4. J.R. Boulding, J.S. Ginn, *Practical Handbook of Soil, Vadose Zone, and Ground-Water Contamination: Assessment, Prevention, and Remediation*, 2nd edn. (CRC Press, Boca Raton, 2004)
5. B.W. Burval, Group, Aquifer vulnerability, in *Groundwater Resources in Buried Valleys* (Leibniz Institute for Applied Geosciences (GGA Institut). Hannover **149–156**, (2006)
6. M. Civita, Una metodologia per la definizione e il dimensionamento delle aree di salvaguardia delle opere di presa delle sorgenti normali. *Bollettino dell'Associazione Mineraria Subalpina* **25**(4), 423–440 (1988)
7. M. Civita, M. De Maio, Sintacs. Un sistema parametrico per la valutazione e la cartografia della vulnerabilità degli acquiferi all'inquinamento. Metodologia e automatizzazione, *Quaderni di tecniche di protez. ambient.* (Pitagora, Bologna, 1997)
8. M. Civita, C. De Regibus, Sperimentazione di alcune metodologie per la valutazione della vulnerabilità degli acquiferi. *Acts of the Second National Conference* **3**, 63–72 (1995)
9. A. Corniello, D. Ducci, P. Napolitano, Comparison between parametric methods to evaluate aquifer pollution vulnerability using a GIS: an example in the 'Piana Campana'. *Southern Italy* **1**, 1721–1726 (1997)
10. J.W. Delleur, *Handbook of Groundwater Engineering* (CRC Press, Boca Raton, 2006)
11. A. Di Molfetta, L. Gautero, Il monitoraggio delle acque sotterranee in siti pericolosi: impostazione metodologica, strumenti e costi. *IGEA* **37–46**, (1997)
12. N. Doeriger, P.-Y. Jeannin, F. Zwahlen, Water vulnerability assessment in karst environments: a new method of defining protection areas using a multi-attribute approach and GIS tools (EPIK method). *Environ. Geol.* **39**, 165–176 (1999)
13. M.J. Focazio, *Assessing Ground-Water Vulnerability to Contamination: Providing Scientifically Defensible Information for Decision Makers* (U.S. Department of the Interior, U.S. Geological Survey, 2002)
14. S.S.D. Foster, *Fundamental Concepts in Aquifer Vulnerability, Pollution Risk and Protection Strategy: International Conference, 1987, Noordwijk Aan Zee, the Netherlands Vulnerability of Soil and Groundwater to Pollutants* (Netherlands Organization for Applied Scientific Research, The Hague, 1987)
15. R.C. Gogu, A. Dassargues, Current trends and future challenges in groundwater vulnerability assessment using overlay and index methods. *Environ. Geol.* **39**, 549–559 (2000)
16. J.E. Liggett, S. Talwar, Groundwater vulnerability assessments and integrated water resource management. *Streamline Watershed Manag. Bull.* **13**, (2009)

17. S. Stevenazzi, M. Masetti, G.P. Beretta, Groundwater vulnerability assessment: from overlay methods to statistical methods in the Lombardy Plain area. *Acque Sotterranee - Ital. J. Groundw.* **6**, (2017)
18. C. Stumpp, A.J. Żurek, P. Wachniew, A. Gargini, A. Gemitzi, M. Filippini, S. Witczak, A decision tree tool supporting the assessment of groundwater vulnerability. *Environ. Earth Sci.* **75**, 1057 (2016)
19. US EPA, Multi-phase extraction: state-of-the-practice, Reports and Assessments (1999), <https://www.epa.gov/remedytech/multi-phase-extraction-state-practice>
20. D. Van Stempvoort, L. Ewert, L. Wassenaar, Aquifer vulnerability index: a GIS - compatible method for groundwater vulnerability mapping. *Can. Water Resour. J./Revue canadienne des ressources hydriques* **18**, 25–37 (1993)
21. P. Wachniew, A.J. Zurek, C. Stumpp, A. Gemitzi, A. Gargini, M. Filippini, K. Rozanski, J. Meeks, J. Kværner, S. Witczak, Toward operational methods for the assessment of intrinsic groundwater vulnerability: a review. *Crit. Rev. Environ. Sci. Technol.* **46**, 827–884 (2016)

Chapter 8

Well Head Protection Areas



Abstract In the previous chapter, methods for the assessment of the vulnerability of aquifers to contamination are illustrated as a first step towards the protection of groundwater resources. Here, static and dynamic protection measures of sources of water for human consumption are presented. Static protection entails the definition of areas of land around the water source that must be subjected to specific safeguard measures and land use limitations. Such areas can be defined via geometric methods (i.e., defining the area arbitrarily, such as by drawing a circle of set radius around the pumping well) or via the time of travel approach. The latter method takes into account the aquifer type and its hydrodynamic parameters, in particular using the groundwater flow velocity to delineate protection areas defined by the time it takes a contaminant to reach the drinking water extraction well. Dynamic protection entails the establishment of a monitoring network along the perimeter of previously defined protection areas. Practical guidance is provided for appropriately designing this network in terms of monitoring-well positioning and sampling frequency.

One of the main approaches employed for the protection of sources of water for human consumption is the definition of protection areas around the abstraction points. Such areas are regulated at a national and international level. For example, the European Commission provides guidance for the establishment of *Drinking Water Protected Areas* and *Safeguard zones* as a strategy for the Water Framework Directive implementation [3]; the US-EPA, instead, imposes the definition of *Wellhead Protection Areas* to ensure the quality of water abstracted for human consumption is preserved [7]. Defining protection areas (*static protection*) by imposing safeguard measures and limitations to land use does not fully address the issue of protecting drinking water extraction wells, but simply prevents contamination events from occurring within the zones thus delineated. Ensuring the protection of drinking water abstractions also from contamination incidents occurring outside the protection zones would entail the creation of a monitoring network along their perimeter and periodically assessing the quality of the groundwater abstracted from the wells for human consumption (*dynamic protection*).

8.1 Approaches for the Definition of Protection Areas

The *geometric method* is the easiest approach for the delineation of a portion of land for the safeguard of groundwater resources. It consists in drawing a circle of arbitrary radius around the drinking water abstraction well. Since this criterion does not consider in any way the groundwater hydrodynamics, it is usually employed to define a zone of absolute safeguard (with very strong limitations on land use) in the immediate proximity of the well [6, 10].

The *time of travel* approach, instead, consists in the definition of protection areas whose shape and size are defined by the time it takes a contaminant to spread in the subsurface; hence, this method depends on the groundwater flow velocity and, consequently, on the aquifer type and its hydrodynamic parameters [2]. The availability of information and knowledge of the hydrogeology of the site affect the level of accuracy that can be achieved in the calculation of the time of travel. In fact, depending on the amount of available data, analytical or numerical approaches may be employed [8, 10, 11].

According to the time of travel approach, protection areas are zones delineated by isochrones. *Isochrones* are lines that connect points that share the same time of travel, i.e., the time it takes a contaminant to reach the well, regardless of the migration path [5, 9, 13].

8.1.1 Analytical Definition of the Protection Area of a Single Well in a Confined Aquifer

In the case of a single well pumping at a constant rate, Q , from a homogeneous and isotropic aquifer of thickness b , characterized by uniform hydraulic gradient i , effective porosity n_e , and $q = Ki$, the isochrones can be determined analytically with the following expression [1]:

$$t_D = -y_D - \ln \left[\cos(x_D) - \frac{y_D}{x_D} \sin(x_D) \right], \quad (8.1)$$

where:

$$x_D = \frac{2\pi bv}{Q} x, \quad (8.2)$$

$$y_D = \frac{2\pi bv}{Q} y, \quad (8.3)$$

$$t_D = \frac{2\pi bv^2}{Qn_e} t. \quad (8.4)$$

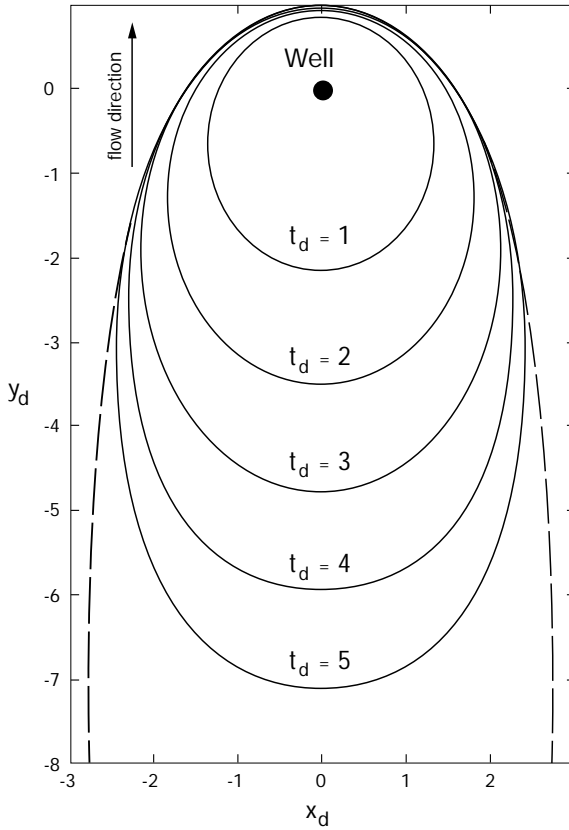


Fig. 8.1 Isochrones in a dimensionless Cartesian coordinate system for an aquifer whose direction of flow is parallel to the y -axis. The dashed line indicates the groundwater divide [4]

Equation (8.1) is valid for confined aquifers, and only under certain circumstances for unconfined aquifers.

Figure 8.1 shows the solutions of Eq. (8.1) for $t_D = 1, 2, 3, 4, 5$ in a dimensionless Cartesian coordinate system where the y axis is parallel to the direction of flow.

8.1.2 General Application of the Time of Travel Criterion

The use of the time of travel method to define the protection areas of a well-field requires the use of a mathematical method, be it analytical or numerical, capable of simulating the flow in the aquifer system.

The problem is essentially solved by determining the isochrones by analyzing the travel times along different flow lines. These represent the migration paths followed

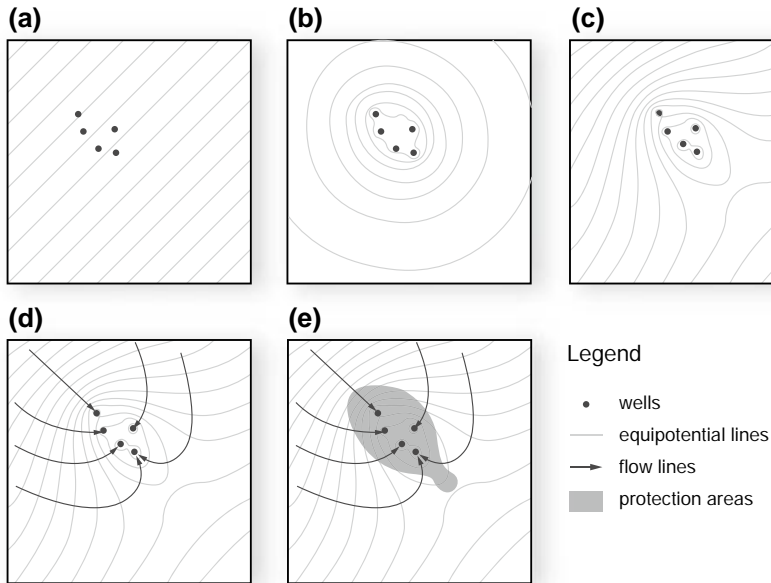


Fig. 8.2 Schematic of the procedure to calculate the protection areas with the time of travel approach

by water molecules (modified by the activation of the wells) and are perpendicular to the equipotential lines (under the assumption that the porous medium is isotropic).

Clearly, employing a mathematical model (either analytical such as WHPA software, or numerical like MODFLOW/MODPATH or FEFLOW) presupposes that the type and the hydrodynamic parameters of the aquifer system in question are known. These have to be priorly determined by carrying out and interpreting appropriate aquifer tests. Once the aquifer has been characterized, the approach for the definition of the protection areas entails the following steps:

- generation of a potentiometric map of the aquifer under consideration (see Fig. 8.2a);
- calculation of hydraulic head variations induced by all the wells pumping the aquifer at operation rate and the consequent seepage velocities, based on the hydrodynamic parameters obtained experimentally (see Fig. 8.2b);
- calculation of the potentiometric levels in dynamic conditions by subtracting the drawdown in every point of the investigated domain (see Fig. 8.2c);
- tracing of a sufficient number of flow lines (see Fig. 8.2d);
- calculation of the travel times to the well along each flow line: a series of nodes have to be identified on every flow line starting from the well by moving upgradient by steps of length Δl and calculating the travel time Δt :

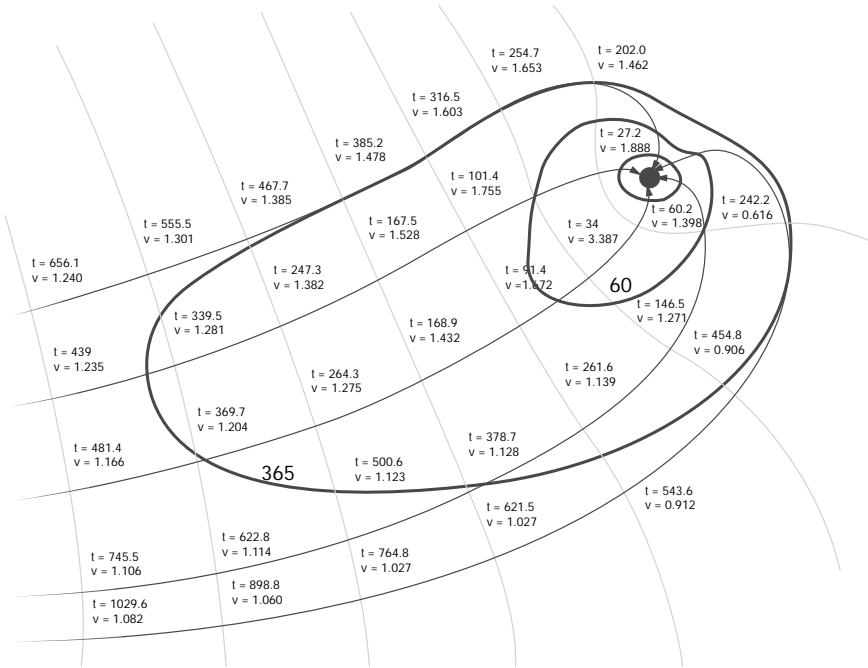


Fig. 8.3 Example of protection areas definition using the time of travel method. Times are expressed in days, velocities in meters per day

$$\Delta t = \frac{\Delta l \cdot n_e}{K \cdot i}$$

- connection of points on the various flow lines that have equal time of travel to obtain the isochrones (see Fig. 8.2e). An automatic approach for the delineation of wellhead protection areas in complex scenarios is described in [13].

The last phase is best described in Fig. 8.3, that shows how every node at the intersection between equipotential lines and flow lines is characterized by specific values of velocity and of time of travel. The travel time is directly proportional to the effective porosity, n_e . Large n_e values determine reduced seepage velocities; thus, the extension of the protection area corresponding to a specific time of travel is smaller. This highlights the importance of determining n_e with a reasonable degree of accuracy.

Figure 8.4 shows an example of protection area definition with the time of travel method.

The only transport mechanism considered by the time of travel approach is advection. However, it is possible to include also the hydrodynamic dispersion in the calculation [12].

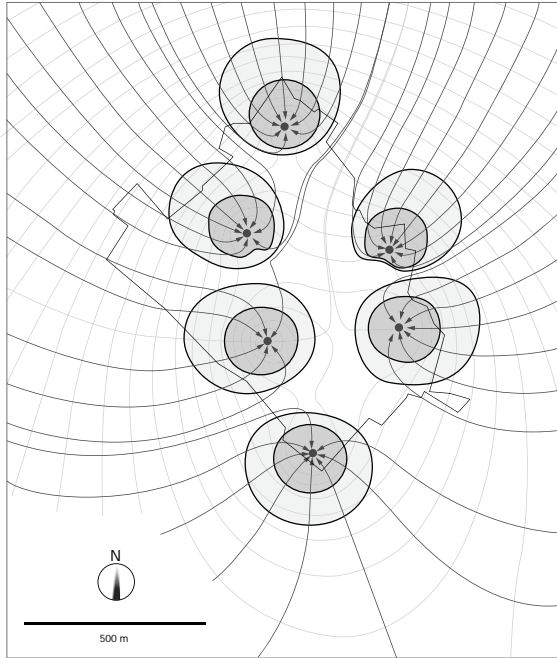


Fig. 8.4 Delineation of protection areas around a wellfield with the time of travel method

8.2 Dynamic Protection

Dynamic protection entails the creation of a monitoring network along the perimeter of previously defined protection areas. A regular assessment plan has then to be established to ensure the quality of the groundwater resources abstracted for human consumption is not deteriorating.

Monitoring networks are composed of a series of piezometers or wells screened only in the aquifer of interest. Clearly, a groundwater supply system might require multiple distinct monitoring networks, each with its own depth, characteristics and position, according to the different exploited aquifers. In other words, each supply system needs to have a monitoring network with its own set of wells for each separately exploited aquifer. The diameter of the monitoring wells should allow unhindered periodic sampling of groundwater for analysis.

The main issue is deciding the distance (interaxis) between two monitoring wells along the perimeters of the protection area. The optimal solution is a compromise between monitoring the quality of each flow line (infinite number of wells) and the available budget for contamination prevention (number of wells tending to zero). A reasonable compromise can be identified by keeping in mind that:

- the arrival front of a potential contaminant, represented by the distance between the two most outer flow lines that converge towards an extraction well that needs protection, must be monitored;

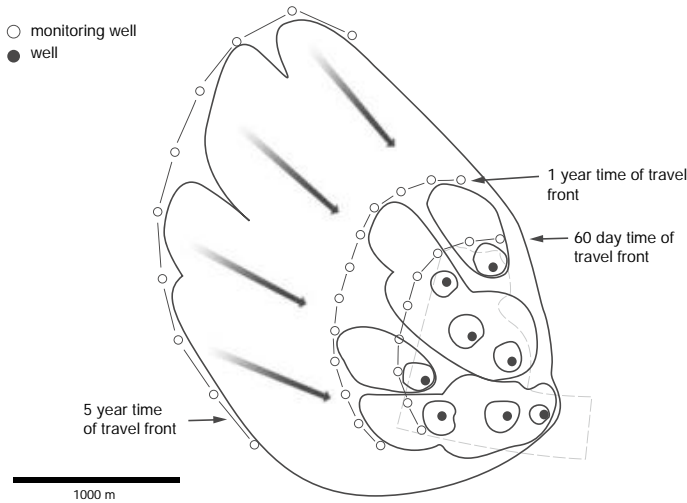


Fig. 8.5 Possible monitoring network configuration, composed of three monitoring barriers placed along the 60 day, one year and five year arrival fronts

- the width of this front is a function of the time of travel that characterizes the protection area, and it varies according to a configuration that depends on the potentiometric profile, the hydrogeological characteristics of the aquifer, the sampling amount, and the distribution density of the abstraction wells;
- the interaxis between two monitoring wells should be chosen accounting for the contamination risk and, therefore, the hazard features of human settlements present upgradient of the supply systems that need protection and of the vulnerability of the aquifer of interest.

Figure 8.5 shows an example of a potential monitoring network, based on the construction of three monitoring barriers placed along the 60-day, one-year and five-year arrival fronts.

Another crucial aspect for the effectiveness of the monitoring system is the definition of the frequency of sampling and analysis. Also for this parameter the optimal solution is a compromise between maximum and minimum sampling frequency, the former allowing the detection of contamination as soon as it reaches the monitoring network, the latter corresponding to the time of arrival that characterizes the protection area.

In the quest for this compromise, two aspects should be kept in mind:

- the optimal frequency should not surpass the capacity of the analytical devices;
- the frequency should be sufficiently smaller than the arrival time, in order not to eliminate the safety and notice margin, which is the main goal of the creation of protection areas.

References

1. J. Bear, M. Jacobs, On the movement of water bodies injected into aquifers. *J. Hydrol.* **3**, 37–57 (1965)
2. A. Ceric, H. Haitjema, On using simple time-of-travel capture zone delineation methods. *Ground Water* **43**, 408–412 (2005)
3. E. Commission, *Common Implementation Strategy for the Water Framework Directive - Guidance No 16: Groundwater in Drinking Water Protected Areas*. Technical Report (European Commission, 2007)
4. P. Cordero, R. Sethi, A. Di Molfetta, Determinazione delle aree di salvaguardia di pozzi ad uso idropotabile mediante criterio cronologico. Technical report (Politecnico di Torino for Regione Piemonte, Torino (Italy), 2005)
5. A. Di Molfetta, G. Bortolami, Valutazione delle aree di protezione di impianti idropotabili: aspetti tecnici e normativi. *Bollettino dell'Associazione Mineraria Subalpina* **4** (1989)
6. M. Doveri, M. Menichini, A. Scozzari, Protection of groundwater resources: worldwide regulations and scientific approaches, in *Threats to the Quality of Groundwater Resources*. The Handbook of Environmental Chemistry (Springer, Berlin, Heidelberg, 2015), pp. 13–30
7. US EPA, *Guidelines for Delineation of Wellhead Protection Areas (English)* (BiblioGov, Place of publication not identified, 1987)
8. M.N. Fienen, J. Luo, P.K. Kitanidis, Semi-analytical homogeneous anisotropic capture zone delineation. *J. Hydrol.* **312**, 39–50 (2005)
9. S. Franzetti, A. Guadagnini, Probabilistic estimation of well catchments in heterogeneous aquifers. *J. Hydrol.* **174**(1–2), 149–171 (1996)
10. T. Harter, *Delineating Groundwater Sources and Protection Zones* (2002)
11. W. Kinzelbach, M. Marburger, W.-H. Chiang, Determination of groundwater catchment areas in two and three spatial dimensions. *J. Hydrol.* **134**, 221–246 (1992)
12. T. Tosco, R. Sethi, Comparison between backward probability and particle tracking methods for the delineation of well head protection areas. *Environ. Fluid Mech.* **10**, 77–90 (2010)
13. T. Tosco, R. Sethi, A. Di Molfetta, An automatic, stagnation point based algorithm for the delineation of Wellhead Protection Areas. *Water Resour. Res.* **44** (2008). <https://doi.org/10.1029/2007WR006508>

Chapter 9

Groundwater Contaminants



Abstract Aquifer contamination occurs following a release of chemical compounds in groundwater exploited for human consumption which poses a health risk to the consumers. There is a variety of anthropogenic causes of contamination, spanning from discharge of wastewater to the ground, to industrial or mining activities, from accidental spills to agricultural activities. The wide range of sources of contamination is reflected on the extremely broad and diverse set of contaminants, including biological, chemical and radioactive constituents. This chapter is dedicated to the chemical, physical and toxicological classification and characterization of chemical contaminants. Chemically, compounds can be broadly categorized as inorganic (e.g., metals, certain anions and cations, metalloids) or organic (i.e., containing at least one organic carbon). The main organic groups are described, including hydrocarbons, halogenated hydrocarbons, phenols, chlorobenzenes, nitroaromatic compounds, and a class of recently identified hazardous compounds, named emerging organic contaminants, is presented. A physical characterization of contaminants is essential for the prediction of their behavior once they are released to the ground and migrate either across the unsaturated zone towards the saturated medium, or directly in the aquifer. The most important physical characteristics affecting contaminant migration and illustrated in this chapter are physical state, miscibility with water, mass density, solubility in water and volatility. Finally, a toxicological classification of contaminants is provided, which categorizes them as threshold or non-threshold compounds, depending on whether their health effects are manifested only above a certain concentration or are independent of the exposure level (i.e., they induce genetic mutations which lead to cancer development). This classification lays the foundations for the definition of threshold concentration values in drinking water prescribed by national and international health agencies and regulatory authorities. A comparison of the guideline or regulatory values defined by the WHO, the US-EPA, the EU and the Italian law is provided.

Access to safe and clean drinking water, i.e., water that “does not represent any significant risk to health over a lifetime of consumption, including different sensitivities that may occur between life stages”, is essential to life and has been recognized as a basic human right by the United Nations General Assembly, in 2010 [1]. Despite this fact, there has been little consideration for the preservation of water—and in particular groundwater—resources, often leading to their degradation. The degradation of

the natural quality of groundwater as a result of natural processes or, notably, human activity is defined as *groundwater contamination* [6].

Contamination occurs when a constituent (i.e., *contaminant*), or a mixture of constituents, is released in groundwater exploited for human consumption and poses a risk to the affected population's health. Major anthropogenic sources of contamination are: direct discharge of wastewater to the ground; accidental release of contaminants from storage or disposal sites, or from means of transportation or transmission (e.g., septic tanks, landfills, impoundments, storage tanks or containers, pipelines, trucks); agricultural activities (e.g., pesticide and fertilizer applications, animal feeding operations); mining activities; oil and gas production related activities; industrial activities (e.g., chemical and petrochemical industry, metal plating and cleaning industries, nuclear industry) [6].

Such activities can release a variety of contaminants, which may be biological (i.e., microorganisms, including parasites, bacteria and viruses), chemical (including organic and inorganic compounds) or radioactive (i.e., radionuclides) [13, 28]. These can be released directly into an aquifer, in the case of sources buried at water table depth, or at the surface, from which they can infiltrate into the ground until they reach the groundwater.

In this text we only focus on chemical contaminants and the following chapters are dedicated to the description of contaminant propagation in groundwater. However, before discussing the different and complex phenomena that control transport, it is essential to stress that the results of such processes depend primarily on the contaminants' features. Therefore, given the large number of compounds that can pollute water as a consequence of human activity, understanding propagation mechanisms must be preceded by an attempt at classifying contaminants according to their characteristics.

Contaminant classification criteria depend on the considered properties, but a full characterization of propagation mechanisms and their consequences on human health requires, at the very least, a chemical, physical and toxicological description (see Table 9.1).

Table 9.1 Main description criteria for groundwater contaminants

Description criterion	Property
Chemical	Composition
Physical	Physical state
	Miscibility
	Density
	Solubility
Toxicological	Volatility
	Toxicity
	Carcinogenicity

9.1 Chemical Classification

The first broad chemical classification categorizes contaminants as organic or inorganic.

9.1.1 Inorganic Contaminants

The main inorganic contaminants found in groundwater are metals and metalloids (in particular, arsenic) [5], whose origin can be found in industrial effluents, municipal or industrial solid waste landfills, and mine drainage.

Due to their tendency to accumulate in the body, many metals consumed via oral intake can exhibit toxic (e.g., barium, cadmium, copper, lead, mercury, uranium), and in some cases carcinogenic (e.g., chromium(VI), arsenic), effects in humans even when present at very low concentrations [2, 25, 26, 28]. Other common inorganic contaminants are cations and anions (e.g., nitrates and nitrites, mainly of agricultural origin; sulfates; fluorides; and cyanides), and radionuclides (e.g., uranium, radium, plutonium).

Table 9.2 lists the main inorganic contaminants and the threshold concentration values defined by the WHO, US-EPA, EU, and the Italian legislation (see Sect. 9.3.2 for further details on regulation of contaminants in ground- and drinking water).

9.1.2 Organic Contaminants

The majority of groundwater-resource contamination incidents involves organic compounds, resulting from the worldwide surge in human consumption of hydrocarbons and their derivatives, as well as the synthesis of novel chemicals, in recent decades [6].

A substance is considered an organic compound if it contains at least one carbon atom of organic origin. Carbon atoms can form four covalent bonds and are also capable of forming double or triple bonds with other atoms.

9.1.2.1 Hydrocarbons

Hydrocarbons are the most simple organic compounds existing in nature because they are composed exclusively of carbon and hydrogen. They are extracted from natural reservoirs in the form of complex mixtures of liquid (*crude oil* or *petroleum*) or gaseous compounds, even though they can also be found in a solid or semi-solid form.

Table 9.2 Inorganic contaminants and threshold concentrations in water for human consumption according to the WHO, US-EPA, EU and Italian (D.Lgs. 31/01) guidelines or directives, and in groundwater according to the Italian legislation (D.Lgs. 152/06) [9, 13, 19, 20, 28]

	WHO	US-EPA	EU (Dir. 98/83/EC)	Italy (D.Lgs. 31/01)	Italy (D.Lgs. 152/06)
Chemical	Threshold concentration values ($\mu\text{g/L}$)				
Metals and metalloids					
Aluminium		50–200 ^d			200
Antimony	20	6	5	5	5
Silver		100 ^d			10
Arsenic	10 ^{b,e}	10	10	10	10
Barium	700	2000			
Beryllium		4			4
Cadmium	3	5	5	5	5
Chromium (total)	50 ^c	100	50	50	50
Iron		300 ^d			200
Mercury	6	2	1	1	1
Nickel	70		20	20	20
Lead	10 ^{b,e}	TT-Cu/Pb ^a ; Action Level = 15	10	10	10
Copper	2000	TT-Cu/Pb ^a ; Action Level = 1300	2000	1000	1000
Selenium	40 ^c	50	10	10	10
Manganese		50 ^d			50
Thallium		2			2
Uranium	30 ^c	30			
Zinc		5000 ^d			3000
Inorganic contaminants					
Boron	2400		1000	1000	1000
Cyanides (free)		200	50	50	50
Fluorides	1500	4000	1500	1500	1500
Fluoride		2000 ^d			
Nitrites	3000	1000	500	500	500
Nitrates	50000	10000	50000	50000	50000
Sulfates		250000 ^d			250000

^aLead and copper are regulated by a treatment technique that requires systems to control the corrosiveness of their water. If more than 10% of tap water samples exceed the action level, water systems must take additional steps

^bCalculated guideline value is below the achievable analytical quantification level

^cSignificant scientific uncertainties regarding derivation of health-based guideline value

^dNational secondary drinking water regulations

^e Calculated guideline value is below the level that can be achieved through practical treatment methods

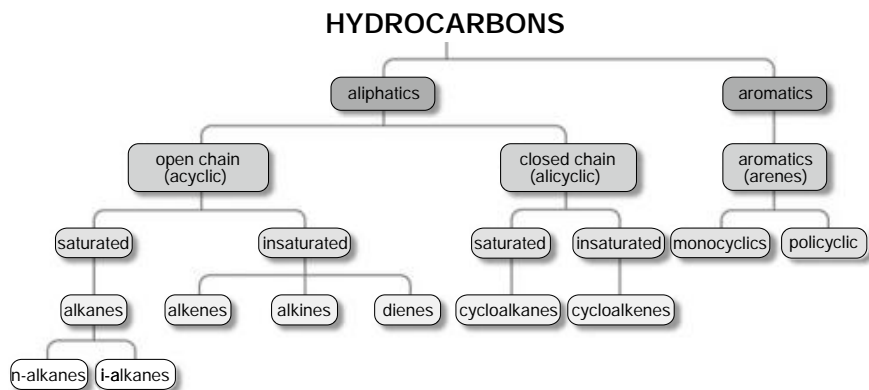


Fig. 9.1 Hydrocarbon classification

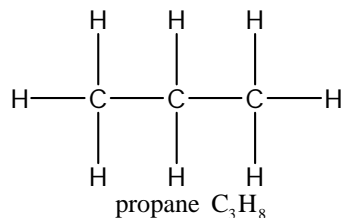
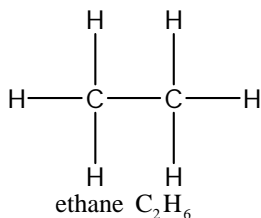
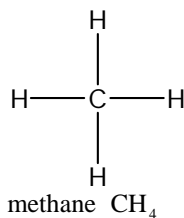
The full classification of hydrocarbons may appear quite complicated (see Fig. 9.1), but the primary parameter to keep into consideration is the presence or absence of at least one benzene ring, which yields *aromatic* or *aliphatic* hydrocarbons, respectively.

Within these categories, hydrocarbons can be *saturated* (when each carbon atom only shares single bonds with the other atoms) or *unsaturated* (when the molecule also contains double or triple bonds); *open-chained* (when the carbon atoms do not form a ring) or *cyclic* (when they do). Finally, hydrocarbons are also identified by the general formula of the group they belong to, by their molecular formula, and, in the presence of isomers (i.e., compounds that have the same molecular formula but different molecular structure, and, therefore, different properties), by their structural formula.

There are four main types of hydrocarbons: alkanes, cycloalkanes, aromatic hydrocarbons, and alkenes. The majority of crude oil components belong to the first three categories, whereas alkenes are mainly products of oil refining.

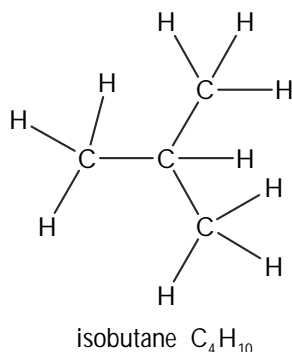
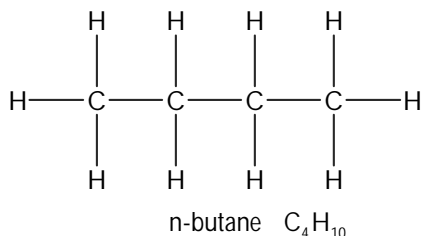
Alkanes

Alkanes (also called paraffins) are characterized by the general formula C_nH_{2n+2} and include the hydrocarbons most commonly found in crude oil: methane, ethane, propane, butane, etc.



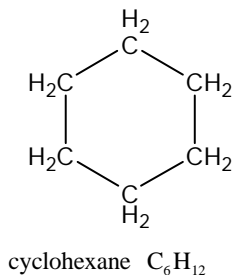
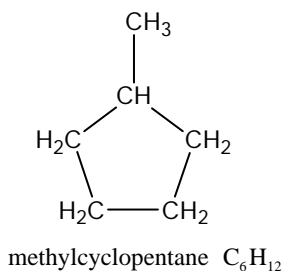
They are open-chain, saturated aliphatic hydrocarbons.

As the number of carbon atoms increases, also the number of compounds with isomers increases, the first being butane:



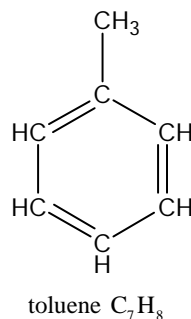
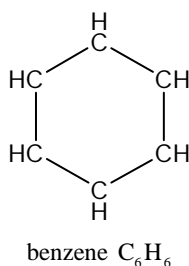
Note that, despite being branched, the structure of isobutane is open-chained (called *branched chain*).

Cycloalkanes Cycloalkanes (also called naphthenes or, when they have more than 20 carbon atoms, cycloparaffins) are characterized by the general formula C_nH_{2n} and are cyclic saturated aliphatic hydrocarbons. Typical examples of this type of compound are: methylcyclopentane, ethylcyclohexane, 1, 1, 3-trimethylcyclohexane.



Aromatic hydrocarbons Aromatic hydrocarbon (or arene) molecules are characterized by the presence of at least one benzene ring, comprising six carbon atoms joined in a ring. The six electrons shared in the six C–C bonds are delocalized over the ring; this delocalization is typically represented by a circle inside the carbon hexagon ring in the structural formula of benzene, although it is also sometimes represented by alternating single and double bonds between the six carbon atoms. Aromatic hydrocarbons have an unsaturated cyclic structure and are not characterized by a general formula. Due to the presence of unsaturated bonds, they react easily with other compounds and incorporate other elements or groups in the benzene ring, thus yielding a great variety of aromatic compounds.

Benzene is, of course, the basic compound of the aromatic group and, with toluene, ethylbenzene, and xylene (in its *ortho*, *meta* and *para* isomeric forms), constitutes the BTEX chemicals, among the most important components of refined petroleum products.

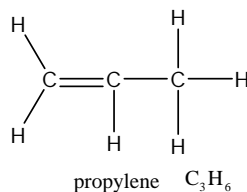
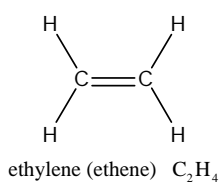


BTEX chemicals are monocyclic (or mononuclear) aromatic hydrocarbons (i.e., their molecules only contain one benzene ring).

Other aromatic compounds can have multiple benzene rings joined to each other (see Fig. 9.2) and are called polycyclic aromatic hydrocarbons (PAHs).

Alkenes

Alkenes (also called *olefines* or *olefins*) are not natural components of petroleum, but are generated during crude oil refining. Their general formula is C_nH_{2n} and are open-chained unsaturated aliphatic hydrocarbons. The most common substances in this group are ethene (or ethylene) and propene (or propylene):



9.1.2.2 Halogenated Aliphatic Hydrocarbons

These are amongst the most common groundwater contaminants and derive from aliphatic hydrocarbons by substitution of one to four hydrogen atoms with the same number of halogen atoms (chlorine, bromine, fluorine). In particular, chlorinated aliphatic hydrocarbons (commonly known as *chlorinated solvents*) represent an environmentally very relevant contaminant group, due to their broad past industrial use. Figure 9.3 shows the structural formula of the main chlorinated solvents, deriving from ethene, ethane and methane. Table 9.3 summarizes name, common name, commercial acronym, and main sources of these products.

9.1.2.3 Phenols

Benzene is also building block for phenols; in these molecules a hydrogen atom is replaced by a hydroxyl group OH^- . If, in addition to this substitution, other hydrogen


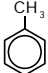
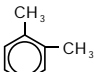
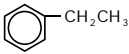

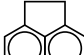
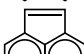

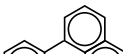
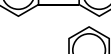

Name	Structure	Molecular weight	Solubility in water	Soil-water partition coefficient
Benzene		78.11	1780 mg/L	97
Toluene		92.1	500 mg/L	242
Xilene		106.17	170 mg/L	363
Ethylbenzene		106.17	150 mg/L	622
Naphthalene		128.16	31.7 mg/L	1,300
Acenaphthene		154.21	7.4 mg/L	2,580
Acenaphthylene		152.2	3.93 mg/L	3,814
Fluorene		166.2	1.98 mg/L	5,835
Fluoranthene		202	0.275 mg/L	19,000
Phenanthrene		178.23	1.29 mg/L	23,000
Anthracene		178.23	0.073 mg/L	26,000

Fig. 9.2 Structure and property of a few monocyclic and polycyclic aromatic hydrocarbons [16]

atoms are replaced by chlorine atoms or by nitro groups ($-\text{NO}_2$), chlorophenols or nitrophenols are formed, respectively (see Fig. 9.4).

9.1.2.4 Chlorobenzenes

Chlorobenzenes are chlorinated aromatic hydrocarbons, derived by direct substitution of one to six hydrogen atoms with the same number of chlorine atoms, yielding chlorobenzene to hexachlorobenzene, respectively.

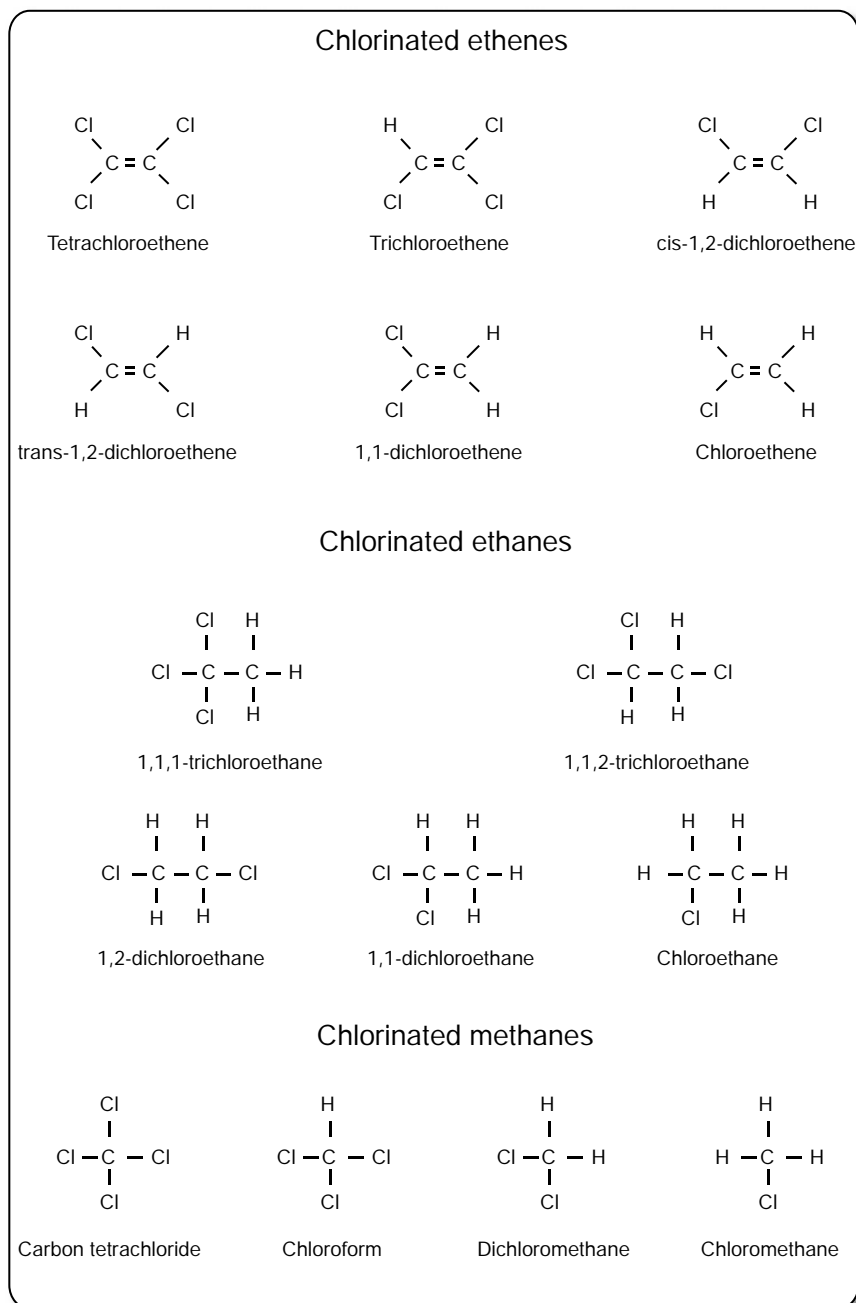


Fig. 9.3 Molecular structure of the main chlorinated aliphatic hydrocarbons

Table 9.3 Name, common name, abbreviation and most frequent sources of main chlorinated aliphatic hydrocarbons

Name	Common name	Abbreviation	Most frequent source
Chlorinated ethenes			
Tetrachloroethene	Perchloroethene	PCE	Solvent containing waste
Trichloroethene	—	TCE	Solvent containing waste, PCE degradation
Cis-1,2-dichloroethene	—	Cis-DCE	Solvent containing waste, PCE and TCE degradation
Trans-1,2-dichloroethene	—	Trans-DCE	Solvent containing waste, PCE and TCE degradation
1,1-dichloroethene	Vinylidene dichloride	1, 1-DCE	Solvent containing waste, 1, 1, 1-TCE degradation
Chloroethene	Vinyl chloride	VC	PVC production residues, PCE and 1, 1, 1-TCA degradation
Chlorinated ethanes			
1,1,1-trichloroethane	Methyl chloroform	1,1,1-TCA	Solvent containing waste
1,1,2-trichloroethane	Vinyl trichloride	1,1,2-TCA	Solvent containing waste
1,2-dichloroethane	Ethylene dichloride	1,2-DCA	PVC production residues, 1,1,2-TCA degradation
1,1-dichloroethane	Ethylidene dichloride	1,1-DCA	1,1,1-TCA degradation
Chloroethane	—	CA	Refrigerant waste, tetraethyllead production residue, 1,1,1-TCA and 1,1,2-TCA degradation
Chlorinated methanes			
Carbon tetrachloride	Tetrachloromethane	CT	Solvent containing waste, fire extinguisher waste
Trichloromethane	Chloroform	CF	Solvent containing waste, hospital waste, CT degradation
Dichloromethane	Methylene chloride	DCM	Solvent containing waste, CT degradation
Chloromethane	Methyl chloride	—	Refrigerant waste, CT degradation

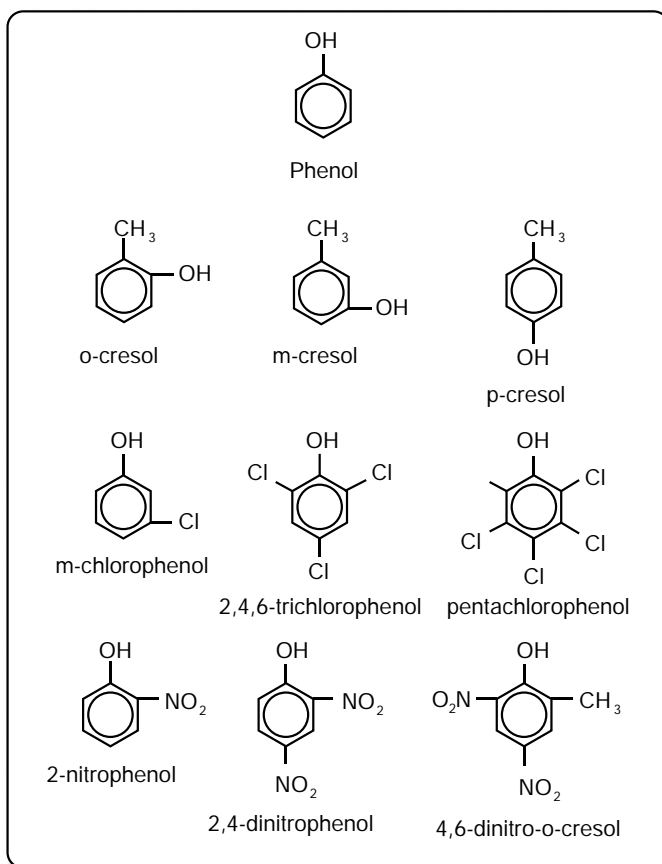


Fig. 9.4 Molecular structure of the main phenols [16]

9.1.2.5 Nitroaromatic Compounds

These chemicals are characterized by one or multiple nitro groups bound to their aromatic ring structure. These compounds are still widely used in the explosive and pesticide industries, among others [27].

9.1.2.6 Emerging Organic Contaminants

These are synthetic organic compounds (SOCs), some of which may fall within the above described categories, that have only recently been recognized by the scientific community to represent potential health hazards. Typically, they are recently developed products or chemicals newly discovered in the environment, which may

Table 9.4 Organic contaminants and threshold concentrations in water for human consumption according to the WHO, US-EPA, EU, and Italian (D.Lgs. 31/01) guidelines or directives, and in groundwater according to the Italian legislation (D.Lgs. 152/06) [9, 13, 19, 20, 28]

Chemical	WHO	US-EPA	EU (Dir. 98/83/EC)	Italy (D.Lgs. 31/01)	Italy (D.Lgs. 152/06)
Threshold concentration values ($\mu\text{g/L}$)					
Aromatic organic compounds					
Benzene	10 ^c	5	1	1.5	1
Ethylbenzene	300 ^e	700			50
Styrene	20 ^e	100			25
Toluene	700 ^e	1000			15
Xylene (para)	500 ^e	10000			10
Di(2-ethylhexyl) phthalate	8	6			
Polycyclic aromatic compounds					
PAH (any)			0.1	0.1	
Benzo[a]pyrene	0.7 ^c	0.2	10	0.01	0.01
Carcinogenic chlorinated aliphatic compounds					
Trichloromethane	300				0.15
VC	0.3 ^c	2	0.5	0.5	0.5
1,2-DCA	30 ^c	5	3	3	3
1,1-DCE		7			0.05
TCE	20 ^g	5	10	10	1.5
PCE	40	5	10	10	1.1
Hexachlorobutadiene	0.6				0.15
Non-carcinogenic chlorinated aliphatic compounds					
CT	4	5			
DCM	20	5			
1,2-DCE	50	70			60
1,2-Dichloropropane	40 ^g	5			0.15
1,1,2-TCA					0.2
Carcinogenic halogenated aliphatic compounds					
Total Trihalomethanes	1	80	100	30	
Tribromomethane	100				0.3
1, 2-Dibromoethane	0.4 ^{g,c}	0.05			10 ⁻³
Dibromochloromethane	100				0.13
Bromodichloromethane	60 ^c				0.17
Chlorinated benzenes					
Chlorobenzene		100			40
1,2-Dichlorobenzene	1000 ^e	600			270
1,4-Dichlorobenzene	300 ^e	75			0.5
1,2,4-Trichlorobenzene		70			190
Hexachlorobenzene		1			0.01
Phenols and chlorophenols					
2,4,6-Trichlorophenol	200 ^{e,c}				5
Pentachlorophenol	9 ^{g,c}	1			0.5
Pesticides used in agriculture					
Pesticides			0.1	0.1	

(continued)

Table 9.4 (continued)

	WHO	US-EPA	EU (Dir. 98/83/EC)	Italy (D.Lgs. 31/01)	Italy (D.Lgs. 152/06)
Alachlor	20 ^c	2			0.1
Aldrin	0.03				0.03
Atrazine	100	3			0.3
gamma-Hexachlorocyclohexane	2	0.2			0.1
Chlordane	0.2	2			0.1
DDD, DDT, DDE	1				0.1
Dieldrin	0.03				0.03
Endrin	0.6	2			0.1
2, 4-Dichlorophenoxyacetic acid	30	70			
1, 2-Dibromo-3-chloropropane	1	0.2			
Methoxychlor	20	40			
Simazine	2	4			
2, 4, 5-TP (Silvex or Fenoprop)	9	50			
Total pesticides			0.5	0.5	0.5
Dioxines and furans					
Sum PCDD, PCDF					4·10 ⁻⁶
Carbofuran	7	40			
Other compounds					
PCBs		0.5			0.01
Acrylamide	0.5 ^c	TT-wt ^a	0.1	0.1	0.1
Chemicals used in water treatment					
Bromate	10 ^{d,c}	10	10	10	
Monochloramine	3000	MRDLG ^b = 4			
Chlorine	5000	MRDLG ^b = 4			
Chlorite	700 ^d	1000		300	
Epichlorohydrin	0.4 ^g	TT-wt ^a	0.1	0.1	
Monochloroacetate	20				
Dichloroacetate	50 ^{e,c}				
Trichloro-acetate	200				
Chlorine dioxide		MRDLG ^b = 0.8			

^aEach water system must certify, in writing, to the state (using third-party or manufacturer's certification) that when acrylamide and epichlorohydrin are used to treat water, the combination (or product) of dose and monomer level does not exceed the levels specified, as follows: Acrylamide = 0.05% dosed at 1 mg/L (or equivalent); Epichlorohydrin = 0.01% dosed at 20 mg/L (or equivalent)

^bMaximum Residual Disinfectant Level Goal (MRDLG)—The level of a drinking water disinfectant below which there is no known or expected risk to health. MRDLGs do not reflect the benefits of the use of disinfectants to control microbial contaminants

^cFor non-threshold substances, the guideline value is the concentration in drinking-water associated with an upper-bound excess lifetime cancer risk of 10⁻⁵

^dCalculated guideline value is below the achievable analytical quantification level

^eConcentrations of the substance at or below the health-based guideline value may affect the appearance, taste or odour of the water, leading to consumer complaints; P, provisional guideline value because of uncertainties in the health database

^fCalculated guideline value is likely to be exceeded as a result of disinfection procedures

^gSignificant scientific uncertainties regarding derivation of health-based guideline value

be SOC transformation or degradation byproducts. Emerging organic contaminants include, among others, pharmaceuticals, illegal drugs, personal care products, food preservatives and additives, and engineered nanomaterials [3, 4, 8, 21–24].

Table 9.4 lists the main organic contaminants and the threshold concentration values defined by the WHO, US-EPA, EU, and the Italian legislation (see Sect. 9.3.2 for further details on regulation of contaminants in ground- and drinking water).

9.2 Physical Characteristics

Contaminants can be classified based on the physical properties that affect their behavior once they enter in contact with groundwater. The most important among these are physical state, miscibility with water, mass density, solubility in water, and volatility.

9.2.1 Physical State

The vast majority of contaminants of anthropic origin are liquid at ambient temperature and pressure, as well as under the thermodynamic conditions encountered in aquifers. The only exceptions are a few contaminants that are naturally found as gases, the most common being methane, ethane, ethene, and their chlorinated derivatives chloromethane, chloroethane, and vinyl chloride.

9.2.2 Miscibility

In order to analyze the behavior of a contaminant in an aquifer, the first thing to assess is whether it is miscible with water or not. A substance (*solute*) is completely miscible with water (*solvent*) if they form a single phase and are no longer physically distinguishable.

The majority of inorganic contaminants are completely miscible with groundwater although this is affected by local geochemical conditions, whereas the majority of organic contaminants, being hydrocarbons or their derivatives, constitute an immiscible phase (think about the behavior of a drop of oil in a glass of water).

All compounds that are immiscible with water are generically called NAPLs (*Non Aqueous Phase Liquids*).

It is important to note that even immiscible substances have a certain solubility in water, ranging from few μg (e.g., benzopyrene, $1.2 \mu\text{g/l}$) to hundreds of grams per liter (e.g., dioxane, 430 g/l). When a contaminant is present in an aquifer at a higher concentration than its solubility, the fraction that exceeds the solubility concentration behaves as a separate liquid phase from water.

It is worth stressing the significance of miscibility, given that saturation of the porous medium with a single phase is one of the conditions for Darcy's law validity, which is the base for all quantitative interpretations of groundwater flow.

9.2.3 Density

Even though the components of NAPL mixtures are very different from each other and could be categorized much more systematically, the easiest classification, which also happens to be the most relevant for practical purposes, is based on their density relative to water:

- Light NAPLs (LNAPLs) are those compounds with a smaller density than water and that, therefore, tend to float on the water table;
- Dense NAPLs (DNAPLs) have a greater density than water and tend to penetrate deep within the saturated area.

LNAPLs (Light Non Aqueous Phase Liquids)

LNAPLs are substances deriving principally from the production, refining and transport of petroleum products. The most common causes of aquifer contamination with LNAPLs are: rupture of pipelines; petrol tankers overturning; leakage from storage tanks containing different kinds of petrols, diesel, kerosene and other similar substances. The most important LNAPLs are the BTEX chemicals (benzene, toluene, ethylbenzene and xylene), which are aromatic hydrocarbons present in fuels, and their derivatives.

DNAPLs (Dense Non Aqueous Phase Liquids)

Most polycyclic aromatic hydrocarbons, halogenated aromatic and aliphatic hydrocarbons, and pesticides are DNAPLs.

As a consequence, DNAPLs are associated to a wide range of human activities and industrial plants, in the chemical, metallurgical, textile, drycleaning, and mechanical sectors, among others.

Their high density and small viscosity favor the penetration of these substances in the soil and within aquifers, even through the smallest pores.

Furthermore, they are very persistent in soil, they are biodegraded very slowly, if at all, and some intermediate metabolites are more toxic than the original substance.

9.2.4 Solubility

Solubility in water represents the concentration of a dissolved contaminant when the solution is in equilibrium with the pure contaminant phase, under specific temperature and pressure conditions.

Solubility is a parameter of significant importance for its implications on the migration and final fate of a contaminant. High solubility values result in, for example:

- fast dissolution and transport in the aquifer;
- modest sorption to the solid phase;
- limited bioaccumulation;
- fast biodegradation.

The solubility of contaminants in water is variable and ranges across many orders of magnitude. In particular, NAPLs display a very low solubility in water, which, however, is still orders of magnitude greater than the guideline values recommended by the WHO or the threshold concentrations set by the European or American legislations [9, 13, 28].

The *effective solubility*, s_e , of a component of a NAPL mixture can be determined by multiplying its molar fraction by its pure phase solubility:

$$s_{e,i} = x_i \cdot s_i \quad (9.1)$$

with x_i being the molar fraction of compound i in the NAPL mixture, and s_i its solubility in water when pure.

9.2.5 Octanol-Water Partition Coefficient

The *octanol-water partition coefficient*, K_{ow} , is the ratio between the concentrations of a compound in a system composed of two immiscible liquid phases, i.e., octanol and water (C_{oct} and C_w , respectively), in a state of equilibrium [10]:

$$K_{ow} = \frac{C_{oct}}{C_w} \quad (9.2)$$

It is a coefficient of great importance for the understanding of the chemical distribution of a compound in a system composed of an aqueous and an oil phase. It is also used to calculate the water-solid partition of an organic contaminant in an aquifer (see Sect. 10.4).

Note that the solubility range of chemical substances in octanol is rather limited. The great variability of the octanol-water partition coefficient (i.e. $10^{-3} < K_{ow} < 10^7$) can thus be attributed to the broad range of solubility in water. It is, therefore, generally preferred to refer to the logarithm of the partition coefficient.

9.2.6 Vapor Pressure

It is the pressure exerted by the vapor of a compound in equilibrium with its pure liquid phase. This parameter is important to establish the volatilization rate of a pure phase or of a mixture of compounds. Combined with other properties such

as solubility, it allows to estimate the water-air partition coefficient. Compounds with high vapor pressure values (1 mm Hg at 25 °C) are qualified as *Volatile Organic Compounds* (VOCs).

The dependence of vapor pressure, P_{vp} , on temperature, T , can be expressed as follows, according to the Antoine equation:

$$\log_{10} P_{vp} = A - \frac{B}{T + C}, \quad (9.3)$$

where A , B , and C are three compound-specific coefficients found in respective tables [29, 30].

9.2.7 Henry's Constant

In conditions of equilibrium between an aqueous solution of a certain compound and the surrounding air, Henry's constant represents the ratio between the partial pressure, p_a , of the compound in the gas phase and its concentration in the liquid phase (i.e., the groundwater phase), C_w :

$$H = \frac{p_a}{C_w}. \quad (9.4)$$

In this case, Henry's constant is expressed in atm · m³/mol. The dimensionless Henry's constant is often used, by converting the partial pressure to molar concentration, C_a , through the ideal gas law:

$$H_c = \frac{H}{RT} = \frac{C_a}{C_w},$$

where R is the universal gas constant, 8.2 · 10⁻⁵ atm · m³/mol · K; T the absolute temperature of the gas in K; and C_a the concentration of the generic compound in the gas phase.

An estimate of Henry's constant can be obtained by dividing the compound's vapor pressure by its water solubility at the same temperature.

The relation between Henry's constant and temperature can be described through the following empirical expression:

$$H = \exp\left(A - \frac{B}{C + T}\right), \quad (9.5)$$

where A , B , and C are three constants available in the literature.

Table 9.5 summarizes the values of the main properties of the most common NAPL contaminants.

Table 9.5 Main properties of selected NAPL compounds

Family/compounds	Formula	Relative density –	Solubility (mg/l)	K_{ow} –	Vapor pressure (mm Hg)	Henry's constant –
BTEX						
Benzene	C_6H_6	0.879	1750	130	60	0.2288
Ethylbenzene	C_8H_{10}	0.867	152	1400	7	0.3249
Toluene	$C_6H_5CH_3$	0.866	535	130	22	0.26
o-Xilene	$C_6H_4(CH_3)_2$	0.880	175	890	5	0.2173
Polycyclic aromatic hydrocarbons						
Acenaphthene	$C_{12}H_{10}$	1.069	3.42	10000	0.01	0.31796
Benzopyrene	$C_{20}H_{12}$	1.35	0.0012	1.15×10^6	–	4.6602×10^{-5}
Benzoperylene	$C_{22}H_{12}$	–	0.007	3.24×10^6	–	5.7737×10^{-6}
Naphtalene	$C_{10}H_8$	1.145	32	2800	0.23	0.0199
methylnaphtalene	$C_{10}H_7CH_3$	1.025	25.4	13000	–	–
Ketones						
Acetone	CH_3COCH_3	0.791	Inf	0.6	89	0.0010
Methyl ethyl ketone	$CH_3COCH_2CH_3$	0.805	2.68×10^5	1.8	77.5	0.0053
Halogenated aliphatic hydrocarbons						
Bromodichloromethane	$CHBrCl_2$	2.006	4400	76	50	8.4543
Bromoform	$CHBr_3$	2.903	3010	250	4	0.0240
Tetrachloromethane	CCl_4	1.594	757	440	90	–
Chloroform	$CHCl_3$	1.49	8200	93	160	0.1398
Chloroethane	CH_3CH_2Cl	0.903	5740	35	1000	0.2103
1,1-Dichloroethane	$C_2H_4Cl_2$	1.176	5500	62	180	0.6351
1,2-Dichloroethane	$C_2H_4Cl_2$	1.253	8520	30	61	0.0494
1,1-Dichloroethene	$C_2H_2Cl_2$	1.250	2250	69	495	–
Cis-1,2-Dichloroethene	$C_2H_2Cl_2$	1.27	3500	5	206	1.3155
Trans-1,2-Dichloroethene	$C_2H_2Cl_2$	1.27	6300	3	265	0.2194
Hexachloroethane	C_2Cl_6	2.09	50	39800	0.4	–
Dichloromethane	CH_2Cl_2	1.366	20000	19	362	0.0903
1,1,2,2-Tetrachloroethane	$CHCl_2CHCl_2$	1.600	2900	250	5	0.0824
Tetrachloroethene	C_2Cl_4	1.631	150	390	14	0.7588
1,1,1-Trichloroethane	CCl_3CH_3	1.346	1500	320	100	0.7093
1,1,2-Trichloroethane	$CH_2ClCHCl_2$	1.441	4500	290	19	0.0305
Trichloroethene	C_2HCl_3	1.466	1100	240	60	0.4135
Vinyl chloride	C_2H_2CHCl	0.908	2670	24	266	3.5467
Halogenated aromatic hydrocarbons						
Chlorobenzene	C_6H_5Cl	1.106	466	690	9	0.1525
2-Chlorophenol	C_6H_5ClOH	1.241	29000	15	1.42	0.0161
p-1,4-Dichlorobenzene (1,4)	$C_6H_4Cl_2$	1.458	79	3900	0.6	0.0659
Hexachlorobenzene	C_6Cl_6	2.044	0.006	1.7×10^5	1×10^{-5}	0.0618

(continued)

Table 9.5 (continued)

Family/compounds	Formula	Relative density —	Solubility (mg/l)	K_{ow} —	Vapor pressure (mm Hg)	Henry's constant —
Pentachlorophenol	$C_6 O H C l_5$	1.978	14	1.0×10^5	1×10^{-4}	8.2482×10^{-5}
1,2,4-Trichlorobenzene	$C_6 H_3 C l_3$	1.446	30	20000	0.42	0.0585
2,4,6-Trichlorophenol	$C_6 H_2 C l_3 O H$	1.490	800	74	0.012	—
PCB						
Aroclor 1254		1.5	0.012	1.07×10^6	7.7×10^{-5}	—
Others						
Phenol	$C_6 H_6 O$	1.071	93000	29	0.2	1.6373×10^{-5}
2,6-Dinitrotoluene	$C_6 H_3 (N O_2)_2 C H_3$	1.283	1320	100	—	—
1,4-Dioxane	$C_4 H_8 O_2$	1.034	4.31×10^5	1.02	30	—
Nitrobenzene	$C_6 H_5 N O_2$	1.203	1900	71	0.15	—
Tetrahydrofuran	$C_4 H_8 O$	0.888	0.3	6.6	131	—

9.3 Contaminant Toxicity and Regulatory Framework

Ensuring protection of drinking water supplies (including groundwater) is a key aspect of public health management. As such, it is the responsibility of national agencies to provide a safe drinking water framework. This should include targets and standards for water quality, and enforceable legislation and policies for the achievement and surveillance of such targets.

Water quality targets are usually expressed as guideline concentrations of individual constituents, which should not be exceeded in drinking water or in drinking water sources. Their values are aimed at ensuring that long term exposure to equal or smaller concentrations of a certain compound presents no health risk for the consumers. They are typically based on toxicological and health data, determined through studies conducted preferentially on human populations or, alternatively, on laboratory animals. In Sect. 9.3.1 the most commonly used toxicological classification of contaminants, used for the determination of guideline values, is presented.

9.3.1 Toxicological Classification

The potential health repercussions on a population exposed to a certain contaminant through drinking water are assessed by some of the major international health and environmental research agencies, including World Health Organization (WHO) agencies (e.g., the Joint Meetings on Pesticide Residues (JMPR), the International

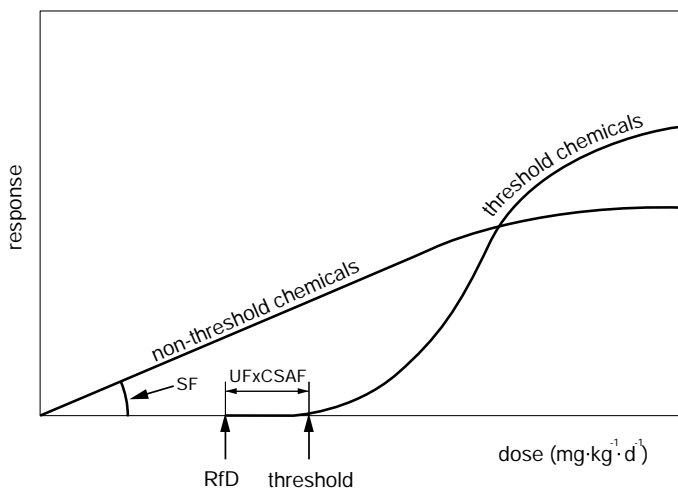


Fig. 9.5 Comparison of dose-response curves of a threshold and of a non-threshold chemical; TDI: tolerable daily intake, UF: uncertainty factor, CSAF: chemical-specific adjustment factor, SF: slope factor

Table 9.6 Potential carcinogenic risk categories of chemical substances according to the IARC [28]

Category	Behavior
Group 1:	The agent is carcinogenic to humans
Group 2A:	The agent is probably carcinogenic to humans
Group 2B:	The agent is possibly carcinogenic to humans
Group 3:	The agent is not classifiable as to its carcinogenicity to humans
Group 4:	The agent is probably not carcinogenic to humans

Agency for Research on Cancer (IARC), the Joint FAO/WHO Expert Committee on Food Additives (JECFA) and the Integrated Risk Information System (IRIS) of the American Environment Protection Agency (EPA). These agencies classify chemical substances on the basis of their dose-response relationship (i.e., “threshold” and “non-threshold” chemicals, see Fig. 9.5), and of their potential carcinogenic risk for humans. Table 9.6 shows the carcinogenic risk categories used by the IARC and, by extension, by the WHO [28]; very similar classes are also used by the EPA [12].

The use of nanomaterials is continuously increasing as the number of studies related to their toxicological effects. If on one side they can be beneficial in removing some classes of contaminants on the other side they can be toxic and/or carcinogenic.

Table 9.7 Uncertainty factor UF values according to the WHO guidelines for drinking water quality [28]

UF	Source of uncertainty
1–10	Interspecies variation (extrapolation from experimental animals to humans)
1–10	Intraspecies variation (accounting for individual variations within human)
1–10	Adequacy of studies or database
1–10	Nature and severity of effect

Threshold Chemicals

It is generally assumed that for most kinds of toxicity there is a threshold concentration below which there will be no health effect. Based on this assumption, a *reference dose*, RfD , (or *tolerable daily intake*, TDI as defined by the WHO) can be determined. The RfD is defined as the “amount of substance in food and drinking water, expressed on a body weight basis (milligram or microgram per kilogram of body weight), that can be ingested over a lifetime without appreciable health risk, and with a margin of safety”, and is calculated as follows [11, 28]:

$$RfD = \frac{NOAEL \text{ or } LOAEL \text{ or } BMDL}{UF \text{ and/or } CSAF} \left[\frac{\text{mg}}{\text{kg} \cdot \text{d}} \right]$$

where $NOAEL$ is the No-Observed-Adverse-Effect Level, $LOAEL$ is the Lowest-Observed-Adverse-Effect Level, $BMDL$ is the lower confidence limit on the benchmark dose, UF is an Uncertainty Factor, and $CSAF$ is a Chemical-Specific Adjustment Factor.

The choice between $NOAEL$, $LOAEL$ and $BMDL$ depends on the availability and quality of experimental data, while UFs are applied if there are sources of uncertainty (see Table 9.7) in the establishment of the RfD , and their value is determined through expert judgment of the available scientific data. $CSAFs$, instead, are mainly applied as uncertainty factors to account for inter- or intraspecies variations, but instead of taking on a default value, they are based on experimentally derived toxicokinetic and toxicodynamic data [28].

Non-threshold Chemicals

Substances that induce mutations to the genetic material of somatic cells which lead to the development of cancer are defined as genotoxic carcinogenic chemicals. Theoretically, genotoxic effects can occur at any level of exposure, hence the term *non-threshold chemicals*. Non-threshold chemicals are typically assumed to have a linear dose-response behavior (with slope SF , i.e., the *slope factor*), which can be derived from high dose exposure experiments conducted on animals [12, 28].

It should be noted that certain chemicals may exert a carcinogenic effect via indirect mechanisms rather than genotoxicity; in this case, a RfD can generally be defined and such compounds are classified as threshold chemicals.

9.3.2 Regulation of Contaminants in Groundwater

International or national health authorities, such as the World Health Organization (WHO) or the United States Environmental Protection Agency (US EPA), use the dose-response classification of chemicals to define health targets. These can represent benchmarks for regulators at a local level (as in the case of the WHO guideline values), or enforceable concentration limits (as in the case of the US EPA targets) for either surface, ground-, or drinking-water. The WHO recommendations for the definition of a full framework for safe drinking water are compiled in the “Guidelines for drinking-water quality” [28]. This document provides guideline values for constituents with confirmed or probable toxicity, or that are causing concern at an international level, and whose occurrence in drinking water is not unlikely. Guideline values (*GVs*) for threshold chemicals are derived from their *RfD* according to the following:

$$GV = \frac{RfD \cdot BW \cdot P}{CR} \left[\frac{\text{mg}}{\text{l}} \right]$$

where *BW* is the body weight (assumed to be 60 kg, by default), *P* is the fraction of the *RfD* allocated to drinking-water, and *CR* is the contact ratio, i.e., the daily drinking-water consumption (the default value is 2 l).

For non-threshold chemicals, instead, guideline values represent the concentration that would result in one additional case of cancer per 10⁵ people ingesting that dose of chemical for 70 years. In other words, it represents the concentration of chemical that would cause a lifetime cancer risk increase of 10⁻⁵ [28].

The European Commission (EC) adopts the WHO guideline values, corroborated by the opinion of the Scientific Committee on Health and Environmental Risk (SCHER), as reference quality standards for drinking water. As per the Drinking Water Directive (DWD) [9], each country of the European Union should use them for the definition of enforceable threshold values in drinking water within its territories. The threshold should be no greater than the parametric values listed in Annex I of the directive [9] and should be adapted to local circumstances, such as environmental, social, economic and cultural issues, and priorities that may affect exposure [28]. It should be noted that in addition to the DWD, the EC also specifically regulates groundwater management through the *directive on the protection of groundwater against pollution and deterioration* [14], established within the Water Framework Directive [15]. However, this directive only defines quality standards for nitrates and active substances in pesticides (Annex I of the directive 2000/60/CE) [7, 14].

The US EPA addresses ground- and drinking-water jointly, and sets enforceable standards for drinking water (National Primary Drinking Water Regulations, NPDWR), which are valid at a national level [13]. However, according to the Safe Drinking Water Act, individual states are free to enforce their own drinking water standards, as long as they are at least as stringent as those set by the EPA [17]. The enforceable standards set by the EPA are Maximum Contaminant Levels (MCLs), defined as the “highest level of a contaminant that is allowed in drinking water”. These are set as close as feasible to the Maximum Contaminant Level Goals (MCLGs),

i.e., “the level of a contaminant in drinking water below which there is no known or expected risk to health” [13].

Tables 9.2 and 9.4 compare the WHO guideline values for inorganic and organic compounds with the EPA MCLs and the European Union quality standards for drinking water, as defined by the DWD [9], as well as with the threshold concentrations (Concentrazioni Soglia di Contaminazione—CSC) in ground- and drinking-water set by the Italian legislation in compliance with the European regulations [18–20] for selected groundwater pollutants.

References

1. U.N.G. Assembly, *Resolution 64/292: The Human Right to Water and Sanitation* (2010)
2. ATSDR, ATSDR Toxic Substances Portal (2017). <https://www.atsdr.cdc.gov/substances/index.asp>
3. P. Avetta, D. Fabbri, M. Minella, M. Brigante, V. Maurino, C. Minero, M. Pazzi, D. Vione, Assessing the phototransformation of diclofenac, clofibric acid and naproxen in surface waters: Model predictions and comparison with field data. *Water Res.* **105**, 383–394 (2016)
4. V. Belgiorno, L. Rizzo, *Emerging Contaminants into the Environment: Contamination Pathways and Control*, English (ASTER, Dubai, 2012)
5. P. Bhattacharya, D. Chatterjee, G. Jacks, Occurrence of Arsenic-contaminated groundwater in alluvial aquifers from Delta Plains, Eastern India: Options for safe drinking water supply. *Int. J. Water Resour. Develop.* **13**(1), 79–92 (1997)
6. J.R. Boulding, J.S. Ginn, *Practical Handbook of Soil, Vadose Zone, and Ground-Water Contamination: Assessment, Prevention, and Remediation*, 2nd edn. (CRC Press, New York, 2004)
7. E. Commission, Commission Directive 2014/80/EU of 20 June 2014 amending Annex II to Directive 2006/118/EC of the European Parliament and of the Council on the protection of groundwater against pollution and deterioration Text with EEA relevance, <http://eur-lex.europa.eu/legalcontent/EN/TXT/?uri=CELEX%3A32014L0080>
8. A. Cosenza, C.M. Maida, D. Piscionieri, S. Fanara, F. Di Gaudio, G. Viviani, Occurrence of illicit drugs in two wastewater treatment plants in the South of Italy. *Chemosphere* **198**, 377–385 (2018)
9. Council of the European Union, Council Directive 98/83/EC of 3 November 1998 on the quality of water intended for human consumption (1998), <http://eurlex.europa.eu/legal-content/EN/TXT/?uri=CELEX%3A31998L0083>
10. P.A. Domenico, F.W. Schwartz, *Physical and Chemical Hydrogeology* (Wiley, New York, 1998)
11. US EPA, Risk Assessment Guidance for Superfund (RAGS): Part A (1989). <https://www.epa.gov/risk/risk-assessment-guidance-superfund-ragspart>. Reports and Assessments, reviewed in 2010
12. US EPA, Guidelines for Carcinogen Risk Assessment (2005). <https://www.epa.gov/risk/guidelines-carcinogen-risk-assessment>. Policies and Guidance
13. US EPA, National Primary Drinking Water Regulations | Ground Water and Drinking Water | US EPA (2009). <https://www.epa.gov/ground-water-anddrinking-water/national-primary-drinking-water-regulations#one>
14. European Parliament, Council of the European Union, Directive 2006/118/EC of the European Parliament and of the Council of 12 December 2006 on the protection of groundwater against pollution and deterioration (2006). <http://eur-lex.europa.eu/legalcontent/EN/TXT/?uri=CELEX%3A02006L0118-20140711>

15. European Parliament, Council of the European Union, Directive 2000/60/EC of the European Parliament and of the Council of 23 October 2000 establishing a framework for Community action in the field of water policy (2000). <http://eur-lex.europa.eu/legalcontent/EN/TXT/?uri=CELEX%3A32000L0060>
16. C.W. Fetter, *Contaminant Hydrogeology*, 2nd edn. (Waveland Pr Inc, Long Grove, Ill, 2008)
17. US Government, Safe Drinking Water Act (SDWA) (1974). <https://www.epa.gov/sdwa>. Collections and Lists
18. G. Italiano, D.lgs. 27/2002 Modifiche ed integrazioni al decreto legislativo 2 febbraio 2001, n. 31, recante attuazione della direttiva 98/83/CE relativa alla qualità delle acque destinate al consumo umano (2002). <http://www.parlamento.it/parlam/leggi/deleghe/02027dl.htm>
19. G. Italiano, D.lgs. n. 152/2006 (T.U. ambiente) (2006). <http://www.bosettiegatti.eu/info/norme/statali/20060152.htm>
20. G. Italiano, D.lgs. n. 31/2001 Attuazione della direttiva 98/83/CE relativa alla qualità delle acque destinate al consumo umano (2001). <http://www.camera.it/parlam/leggi/deleghe/01031dl.htm>
21. S.J. Klaine, P.J.J. Alvarez, G.E. Batley, T.F. Fernandes, R.D. Handy, D.Y. Lyon, S. Mahendra, M.J. McLaughlin, J.R. Lead, Nanomaterials in the environment: Behavior, fate, bioavailability, and effects. *Environ. Toxicol. Chem.* **27**(9), 1825–1851 (2008)
22. D.J. Lapworth, N. Baran, M.E. Stuart, R.S. Ward, Emerging organic contaminants in groundwater: A review of sources, fate and occurrence. *Environ. Pollut.* **163**, 287–303 (2012)
23. C. Postigo, D. Barceló, Synthetic organic compounds and their transformation products in groundwater: Occurrence, fate and mitigation. *Sci. Total. Environ., Better Underst. Links Stress., Hazard Assess. Ecosyst. Serv. Water Scarcity* **503**, 32–47 (2015)
24. M. Sgroi, P. Roccaro, G.V. Korshin, V. Greco, S. Sciuto, T. Anumol, S.A. Snyder, F.G.A. Vagliasindi, Use of fluorescence EEM to monitor the removal of emerging contaminants in full scale wastewater treatment plants. *J. Hazard. Mater.* **323**, 367–376 (2017)
25. A.C. Society, Learn About Cancer: Cancer Resources (2017). <https://www.cancer.org/cancer.html>
26. P.B. Tchounwou, C.G. Yedjou, A.K. Patlolla, D.J. Sutton, Heavy metals toxicity and the environment. *EXS* **101**, 133–164 (2012)
27. T. Vincent, G. Carimal, E. Eljarrat, D. Barceló, *Emerging Organic Contaminants in Sludges—Analysis, Fate and Biological Treatment*, vol. 24, 1st edn., *The Handbook of Environmental Chemistry* (Springer, Heidelberg, 2013)
28. WHO - World Health organization, WHO | Guidelines for drinking-water quality, 4th (2011). http://www.who.int/water_sanitation_health/publications/dwq-guidelines-4/en/
29. I. Wichterle, J. Linek, *Antoine Vapor Pressure Constants of Pure Compounds* (Academia, 1971)
30. C. Yaws, H.-C. Yang, To estimate vapor pressure easily. antoine coefficients relate vapor pressure to temperature for almost 700 major organic compounds. *Hydrocarb. Process.* **68**, 65–68 (1989)

Chapter 10

Mechanisms of Contaminant Transport in Aquifers



Abstract This chapter focuses on the mechanisms that govern the propagation of contaminants in aquifers. A qualitative and analytical description of the main hydrological, physico-chemical and biological process is provided. The hydrological mechanisms responsible for the transport and spreading of contaminants derive from the presence and movement of groundwater. The first of such processes is advection, according to which a compound is transported along the main direction of flow at seepage velocity. Molecular diffusion, instead, is responsible for the migration of the contaminant from high to low concentration areas, as a result of thermal agitation of water molecules. The last hydrological process is mechanical dispersion, which is a consequence of microscale heterogeneities present in the porous medium and results in a non-uniform velocity distribution relative to seepage velocity and the emergence of a transverse velocity component. During their migration within an aquifer, chemical compounds can also undergo chemical reactions that can lead to their transformation or degradation. The main reaction models and the most common types of reactions that are likely to occur in groundwater (i.e., acid-base reactions, complexation, hydrolysis, dissolution and precipitation, radioactive decay) are illustrated. Contaminant transformation and degradation can also be biologically mediated, primarily through microbial activity; such reactions are often described through first-order reaction kinetic models or Monod's model. Finally, contaminant concentration in groundwater is also affected by sorption, a process by which compounds are removed from solution and transferred to the solid phase through a partitioning process typically characterized through isotherms. All these processes are described individually in this chapter, although in reality they occur simultaneously. The chapters that follow describe contaminant transport accounting for the concomitance of these processes.

Understanding and describing analytically the transport and propagation processes of one or more contaminants in an aquifer is complex because of the concurrence of several processes, which can be grouped in the three categories that follow [4, 5].

- **Hydrological phenomena:** these result from the presence and movement of groundwater; quantitatively, they are the most relevant phenomena and they include *advection*, *molecular diffusion*, and *mechanical dispersion* (sometimes called *kinematic dispersion*).

- **Chemical and physico-chemical phenomena:** these include chemical reactions, radioactive decay, contaminant hydrolysis and dissolution, sorption to solid surfaces, volatilization.
- **Biological phenomena:** they include all the contaminant degradation and transformation phenomena mediated by microorganisms and plants; these phenomena are called *biodegradation processes*.

Contaminant propagation is also affected by a series of other factors, the most important being related to the nature and properties of the contaminant itself (see Chap. 9), to the aquifers' characteristics (hydraulic conductivity, porosity, degree of heterogeneity), and to the release mechanisms (contaminant source geometry, pulse versus continuous release).

In the following paragraphs the main processes are illustrated, with reference to a contaminant miscible with water or, if immiscible, to its soluble fraction.

10.1 Hydrological Phenomena

As mentioned above, hydrological phenomena comprise advection, molecular diffusion, and mechanical dispersion.

10.1.1 Advection

This process is responsible for groundwater transport of contaminants at seepage (or advective transport) velocity along the flow direction:

$$v = \frac{q}{n_e} = \frac{Ki}{n_e}. \quad (10.1)$$

If we consider a coordinate system (x, y, z) with the x -axis coinciding with the groundwater flow direction, and the other two being perpendicular to it and to each other (such that $v_x = v$; $v_y = 0$; $v_z = 0$), the mass flux, j_A , resulting from advective transport along the x direction across a unit surface characterized by an effective porosity n_e is:

$$j_{A,x} = n_e v C, \quad (10.2)$$

where C is the solute concentration (ML^{-3}).

In the ideal situation in which this were the only ongoing phenomenon, the concentration distribution would shift downgradient unmodified (see Fig. 10.1).

In the case of a continuous source, the contaminant front perpendicular to the direction of propagation would advance in time along the x direction at the average pore velocity, v (i.e., seepage velocity). Immediately upgradient of the front, the

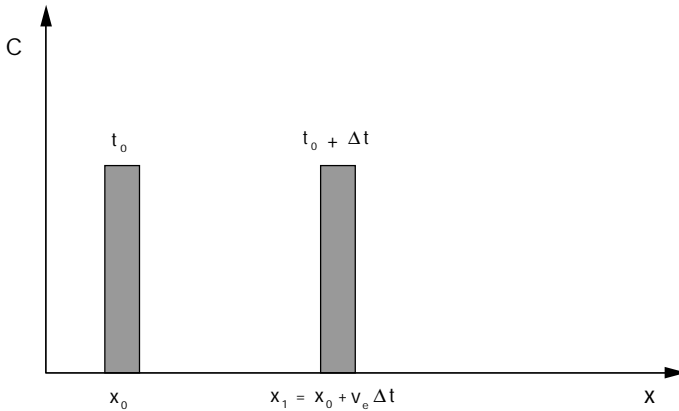


Fig. 10.1 Advective propagation of a contaminant impulse

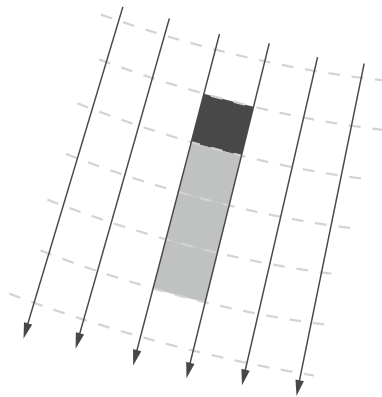


Fig. 10.2 Mass transport due to advection in the case of a continuous source (modified from [5])

concentration would be the same as at the source, while immediately downgradient it would be null. Furthermore, there would be no mass exchange outside the flow channel delimiting the source of contamination (see Fig. 10.2) [4, 5, 7].

10.1.2 Molecular Diffusion

This phenomenon is caused by the thermal agitation of water molecules and results in solute transport from areas with higher to lower concentration.

Hence, a contaminant flow along the concentration gradient direction is generated, whose mass flux in free medium, j_M , is expressed by Fick's law of diffusion:

$$j_{M_i, x_i} = -D_d \frac{\partial C}{\partial x_i}. \quad (10.3)$$

Given that j_M has dimensions $MT^{-1}L^{-2}$, while the concentration C has dimensions ML^{-3} , the molecular diffusion coefficient, D_d , must have dimensions L^2T^{-1} and is, therefore, measured in m^2/s , in the S.I.

The molecular diffusion coefficient is usually very small and is isotropic. Its value is approximately of the order of $10^{-9} m^2/s$, and varies with temperature and with the type of solute [7].

In a porous medium, diffusion is even smaller because of the tortuosity of the paths that water has to cover to bypass the solid grains, which depends on the granulometry of the solid matrix [2]. Therefore, the molecular diffusion coefficient has to be further multiplied by the tortuosity of the porous medium (which is lower than one and can be estimated as the ratio of the length of a microscale flow channel and the length of the porous medium sample), resulting in the following expression: $D_0 = D_d \cdot \tau$ [4, 7, 8]. The diffusion flux in a porous medium is, therefore:

$$j_{M_i, x_i} = -n_e D_0 \frac{\partial C}{\partial x_i}. \quad (10.4)$$

Figure 10.3 shows how, following a pulse injection in a one-dimensional geometry, a normal concentration distribution centered in the source is created along the x -axis: with time, the solute reaches increasingly further distances from the injection point; as a consequence of dilution, the maximum concentration value decreases.

The diffusion process is particularly complex for ionic species (Table 10.1) because while migrating they have to maintain the electroneutrality of the solution.

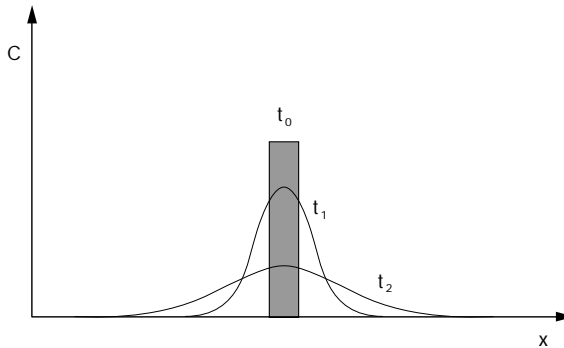


Fig. 10.3 Diffusive transport of a solute introduced with a pulse injection

Table 10.1 Diffusion coefficients of a few ions in water

Cations	D_d ($10^{-9}\text{m}^2/\text{s}$)	Anions	D_d ($10^{-9}\text{m}^2/\text{s}$)
H^+	9.31	OH^-	5.27
Na^+	1.33	F^-	1.46
K^+	1.96	Cl^-	2.03
Rb^+	2.06	Br^-	2.01
Cs^+	2.07	HS^-	1.73
Mg^{2+}	0.705	HCO_3^-	1.18
Ca^{2+}	0.793	SO_4^{2-}	1.07
Sr^{2+}	0.794	CO_3^{2-}	0.955
Ba^{2+}	0.848		
Ra^{2+}	0.889		
Mn^{2+}	0.688		
Fe^{2+}	0.719		
Cr^{3+}	0.594		
Fe^{3+}	0.607		

10.1.3 Mechanical Dispersion

The heterogeneities present in any porous medium observed at the microscale have an impact on transport phenomena. In particular, they are responsible for [5, 7]:

- a non-uniform velocity distribution within a single flow channel;
- variation of velocity from pore to pore;
- transverse velocity components due to the matrix tortuosity.

The combination of these phenomena (see Fig. 10.4) is called mechanical (or kinematic) dispersion and results in:

- a non uniform velocity distribution relative to the seepage velocity;
- a transverse velocity component relative to the flow direction, which increasingly widens the area affected by the contamination.

The analytical description of these phenomena is complex, and is usually solved by applying Fick's law, as in the case of diffusion, for the definition of the mass flux, j_C [4, 5]:

$$j_{C,x} = -n_e D_{C,L} \frac{\partial C}{\partial x}, \quad (10.5)$$

$$j_{C,y} = -n_e D_{C,T} \frac{\partial C}{\partial y}, \quad (10.6)$$

$$j_{C,z} = -n_e D_{C,T} \frac{\partial C}{\partial z}, \quad (10.7)$$

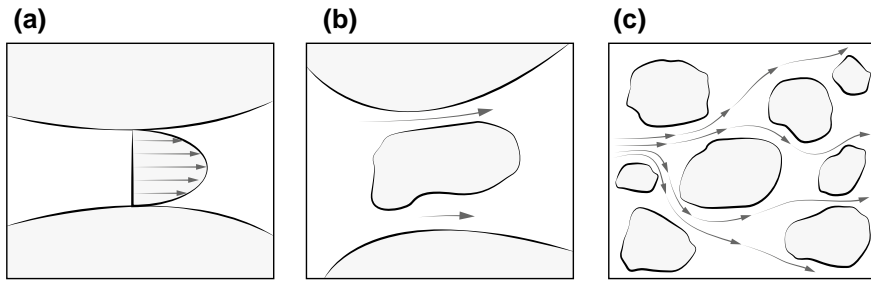


Fig. 10.4 Causes of mechanical dispersion resulting from inhomogeneous velocity distribution at the microscale: **a** distribution profile within an individual pore; **b** effect of different pore diameters; **c** transverse velocity components relative to the main flow direction

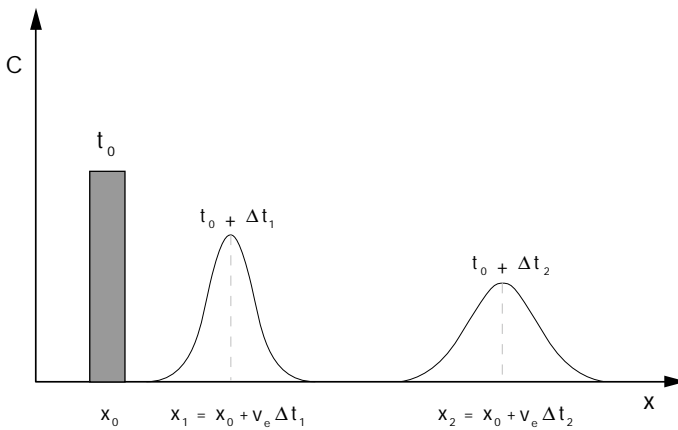


Fig. 10.5 Advective and dispersive propagation of a contaminant introduced through a pulse injection

with $D_{C,L}$ and $D_{C,T}$ being the longitudinal and transverse mechanical dispersion coefficients, respectively, and having set the x -axis parallel to the flow direction (main dispersion axis).

Figures 10.5 and 10.6 show the characteristics of one-dimensional contaminant propagation considering both advection and dispersion, the former referring to a pulse injection, the latter to a continuous source.

Several laboratory experiments have shown that there is a proportionality relation between the mechanical dispersion coefficient and the seepage velocity (see Fig. 10.7):

$$D_{C,L} = \alpha_L v, \tag{10.8}$$

$$D_{C,T} = \alpha_T v. \tag{10.9}$$

The parameters α_L and α_T have the dimensions of length, and are called longitudinal and transverse dispersivity, respectively [17].

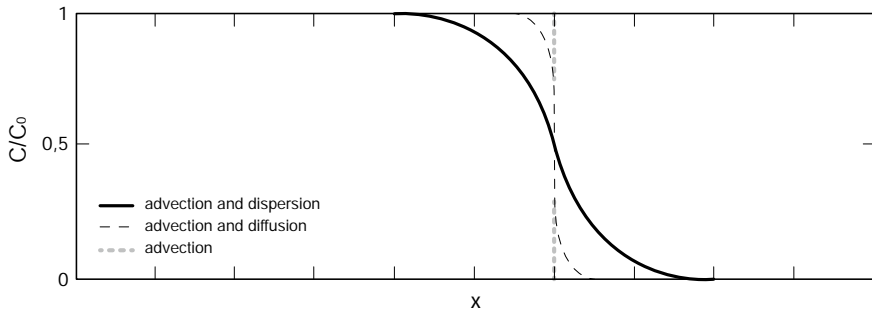


Fig. 10.6 Advective, diffusive, and dispersive contributions to solute transport in one-dimensional flow with a continuous source

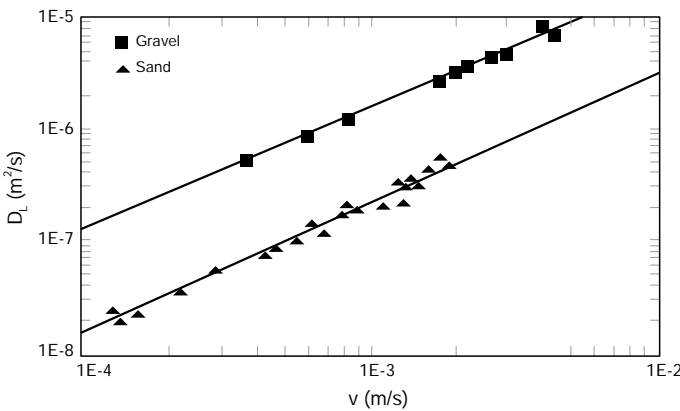


Fig. 10.7 Proportionality relation between dispersion coefficient and seepage velocity (modified from [15])

10.1.4 Hydrodynamic Dispersion

Since molecular diffusion and mechanical dispersion have been expressed with analogous relations, the two phenomena can be combined into a single process called *hydrodynamic dispersion*, that determines the propagation of the contaminant mass flux, j_I , along the three principal dispersion axes. It can be expressed as follows:

$$j_{I,x} = -n_e D_L \frac{\partial C}{\partial x}, \tag{10.10}$$

$$j_{I,y} = -n_e D_T \frac{\partial C}{\partial y}, \tag{10.11}$$

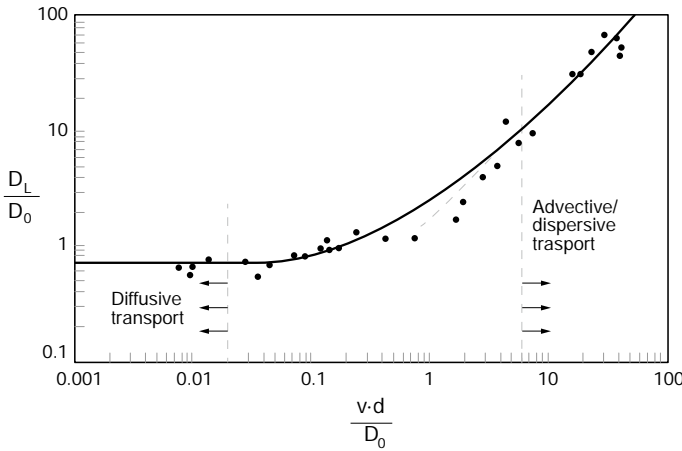


Fig. 10.8 Ratio between the longitudinal mechanical dispersion and the molecular diffusion coefficients as a function of the Peclet number

$$j_{l,z} = -n_e D_T \frac{\partial C}{\partial z}, \tag{10.12}$$

with D_L and D_T being the longitudinal and transverse hydrodynamic dispersion coefficients ($L^2 T^{-1}$), respectively.

Therefore:

$$D_L = D_0 + D_{C,L} = D_0 + \alpha_L v, \tag{10.13}$$

$$D_T = D_0 + D_{C,T} = D_0 + \alpha_T v. \tag{10.14}$$

Figure 10.8 illustrates the evolution of the ratio between the longitudinal mechanical dispersion and the molecular diffusion coefficients (D_L/D_0) as a function of the Peclet number, as determined through tracer experiments; Fig. 10.9 illustrates the evolution of the ratio D_T/D_0 .

The Peclet number, Pe , is a dimensionless number expressing the relative importance of advection relative to diffusion during transport:

$$Pe = \frac{vd}{D_0}, \tag{10.15}$$

with d being a characteristic length of the porous medium (e.g., d_{50}). For low Peclet numbers, the ratio D_L/D_0 is constant, regardless of groundwater velocity (see Fig. 10.8). Under these conditions, molecular diffusion is the main transport mechanism, and dispersion is negligible: this is the case for very fine sediments or for very slow flow velocities. For greater velocities, beyond a transition range, mechanical dispersion is the main cause of mixing and spreading of the plume. For common groundwater velocity values, molecular diffusion effects are usually

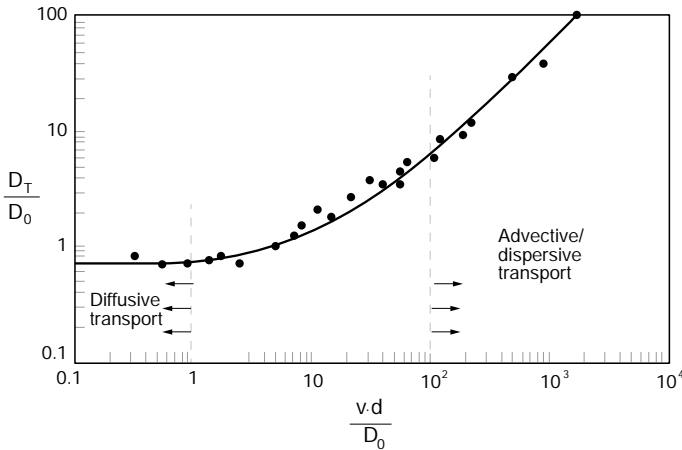


Fig. 10.9 Ratio between the lateral mechanical dispersion and the molecular diffusion coefficients as a function of the Peclet number

negligible compared to those of mechanical dispersion, so:

$$D_L \approx \alpha_L v, \tag{10.16}$$

$$D_T \approx \alpha_T v. \tag{10.17}$$

Also, longitudinal phenomena are usually quantitatively more significant than transverse ones, and typically [4]:

$$\frac{D_T}{D_L} \approx \frac{\alpha_T}{\alpha_L} = \frac{1}{20} \text{ to } \frac{1}{5}. \tag{10.18}$$

Figure 10.10 illustrates the mechanisms of propagation of a contamination phenomenon governed by hydrodynamic dispersion as well as advection: the contaminant mass reaches broader regions of the aquifer due to the lateral widening of the plume and, as a consequence, concentration decreases progressively.

Dispersivity is strongly affected by the broadening of the propagation (see Fig. 10.11). It has been observed that the greater the scale of the phenomenon, the greater the value of dispersivity that allows a correct interpretation of experimental data. This is called the scale effect of hydrodynamic dispersion.

As mentioned above, the mechanical dispersion is a result of heterogeneities that characterize any porous medium at the microscale. Even aquifers that are normally considered homogeneous display significant hydraulic conductivity and porosity variations. In particular, one should keep in mind that the hydraulic conductivity can span a very broad range of values, encompassing nine orders of magnitude. Therefore, the greater the covered distance, the greater the heterogeneities and the

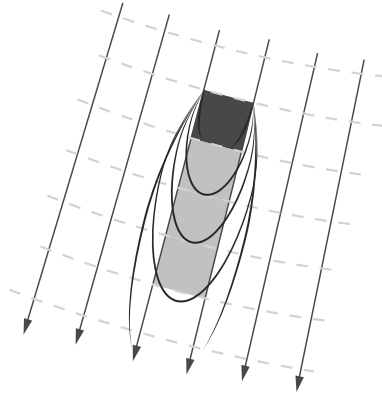


Fig. 10.10 Mass transport resulting from the combination of advective and dispersive flow, in the case of a continuous source

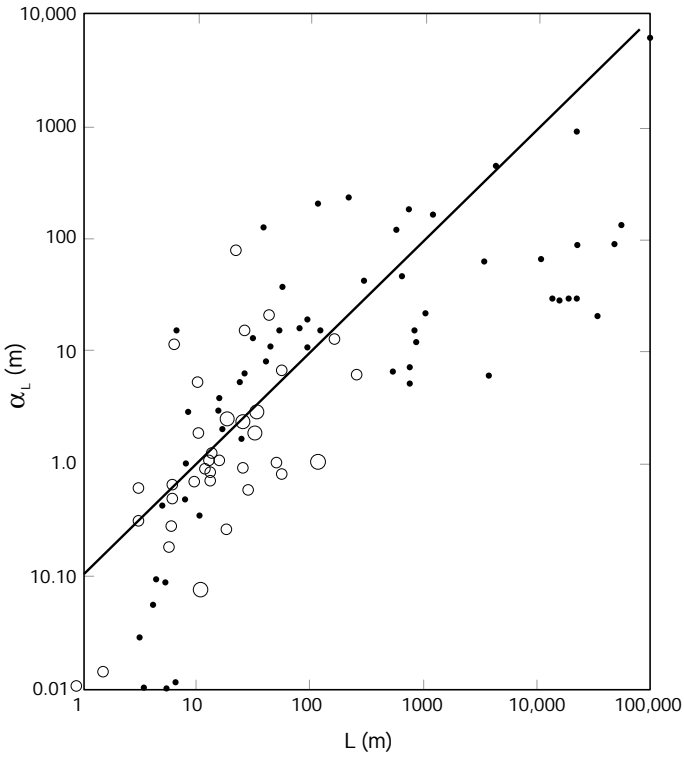


Fig. 10.11 Longitudinal dispersivity as a function of migration distance: scale effect (modified from [9])

Table 10.2 Parameters for the definition of the scale effect, according to several authors

<i>a</i>	<i>L</i>	<i>b</i>	Authors
0.085 ± 0.016 0.199 ± 0.046 0.057 ± 0.014 0.29 0.10	L	0.96 ± 0.6 0.86 ± 0.08 0.94 ± 0.08 0.72 1.00	[11]
0.1	L	1.00	[10]
0.181	L	0.86	[13]
0.177	L	1.00	[1]
0.0175 0.32	L (<100 m) L (>100 m)	1.46 0.83	[12]
0.83	log ₁₀	2.414	[16]

variations of hydraulic conductivity and porosity encountered by flowing groundwater. Even if seepage velocity doesn't change, the deviation from the average value increases and, therefore, so does the hydrodynamic dispersion (macrodispersivity).

Several authors have proposed relations of the following type [4]:

$$\alpha_L = aL^b, \tag{10.19}$$

with *L* being the size of the considered phenomenon, and *a* and *b* parameters related to the aquifer type. Among the most commonly used relations, the simplest is:

$$\alpha_L = 0.1L. \tag{10.20}$$

In Table 10.2 the values of parameters *a* and *b* proposed by a few authors are listed.

10.2 Chemical Phenomena

This paragraph focuses on the chemical processes that can lead to the transformation or disappearance of groundwater contaminants and to the formation of other compounds as reaction products.

10.2.1 Reaction Models

The variations in contaminant concentration resulting from chemical reactions can be described mathematically by equilibrium models, or by kinetic models.

Let us consider a generic reversible reaction, during which compounds A and B react to form compound C :



with a , b and c being the respective number of moles necessary to balance the reaction. The system reaches a chemical equilibrium when the rate of reagent disappearance and product formation equals the rate of the reverse reaction, where the product disappears and the initial reagents are formed again. Under these conditions, the law of mass action, which correlates the activities of reagents and products through an equilibrium constant, K_{eq} , can be applied [5]:

$$K_{eq} = \frac{[C]^\gamma}{[A]^\alpha [B]^\beta}, \quad (10.22)$$

where $[\cdot]$ represents the molar concentration of each compounds, and the exponents (γ , α and β) the correspondent activities. Transport mechanisms determine a distribution of products and reagents which vary from point to point. If the reaction rate is significantly faster than the hydrological transport of the compounds, the system can be assumed to reach instantaneous equilibrium in each point, relative to this reaction, and the correlation between local concentration values of products and reagents can be described by the above equation in every point of the system.

The local equilibrium hypothesis constitutes the foundation of equilibrium models. According to these, the products' concentrations depend exclusively on the reagents' concentrations, and are correlated to the latter through an equilibrium constant. Generally, the values of these constants vary as a function of temperature and can be obtained in the laboratory or derived from in situ measurements.

Equilibrium models are suitable for the simulation of reversible reactions, which occur at a higher rate than contaminant hydrologic transport.

For slow or irreversible reactions, the local equilibrium hypothesis cannot be considered valid, and a kinetic model must be used.

If we refer to reaction (10.21), the rates of appearance or disappearance of products or reagents can be expressed as follows:

$$r_A = -\frac{dC_A}{dt} = k_A C_A^p C_B^q, \quad (10.23)$$

$$r_B = -\frac{dC_B}{dt} = k_B C_A^p C_B^q, \quad (10.24)$$

$$r_C = \frac{dC_C}{dt} = k_C C_C^r, \quad (10.25)$$

where r_A , r_B and r_C represent reagent disappearance and product appearance rates, respectively, and k_A is the kinetic constant.

Both the kinetic reaction constants and the orders of a reaction have to be determined experimentally.

If the order of reaction, p , q or r , is null for one of the compounds, the reaction is called of zero order for that compound. In this case, the reaction rate is independent from the concentration of that chemical substance. If the reaction order, p , q or r , is equal to one for one of the compounds, the reaction kinetics is called of the first order, relative to that compound: in this case, there is a linear relation between the reaction rate and the concentration of that chemical substance.

If none of the exponents, p , q or r , is equal to zero or one, the reaction kinetics is more complex to analyze.

When a compound is present in great excess in the system, the reaction rate can be independent of the concentration of that compound (zero-order kinetics) [3]:

$$\frac{dC_A}{dt} = -k_A, \quad (10.26)$$

which, assuming an initial concentration $C_{A,0}$ in a batch reactor, leads to the expression:

$$C_A = C_{A,0} - k_A t. \quad (10.27)$$

Conversely, if the reaction kinetics depends linearly on reagent A 's concentration, the disappearance of this reagent can be expressed as a first order differential equation [3, 4]:

$$\frac{dC_A}{dt} = -k_A C_A. \quad (10.28)$$

In a batch reactor, the concentration at a generic time, t , is:

$$C_A = C_{A,0} e^{-k_A t}. \quad (10.29)$$

The choice between an equilibrium or kinetic model depends on the considered reaction. Irreversible chemical reactions can only be simulated correctly with a kinetic model: this is the case of radioactive decay, some redox reactions and some reactions involving organic compounds. If the reaction is reversible, its kinetics has to be compared with the flow velocity, to establish whether the local equilibrium hypotheses can be considered valid.

10.2.2 Chemical Reactions

Acid-Base Reactions

These reactions involve substances that act as proton donors and acceptors (i.e., acids and bases, respectively). The strength of individual acids and bases (quantified by the equilibrium constant of their dissociation reaction) and acid-base reactions influence

Table 10.3 Solubility products and dissociation constants at standard conditions (25 °C) for a few important reactions in groundwater

Mineral	Reaction	– log <i>K</i>
Brucite	$Mg(OH)_2 + 2H^+ = Mg^{2+} + 2H_2O$	16.8
–	$Fe(OH)_2 + 2H^+ = Fe^{2+} + 2H_2O$	14.1
Ferrihydrite (am.)	$Fe(OH)_3 + 3H^+ = Fe^{3+} + 3H_2O$	3.0–5.0
Goethite	$FeOOH + 3H^+ = Fe^{3+} + 2H_2O$	1.0
Pyrolusite	$MnO_2 + 4H^+ + 2e^- = Mn^{2+} + 2H_2O$	41.4
Hausmannite	$Mn_3O_4 + 8H^+ + 2e^- = 3Mn^{2+} + 4H_2O$	61.0
Manganite	$Mn_3OOH + 3H^+ + e^- = Mn^{2+} + 2H_2O$	25.3
Pyrocroite	$Mn(OH)_2 + 2H^+ = Mn^{2+} + 2H_2O$	15.2
–	$Ni(OH)_2 + 2H^+ = Ni^{2+} + 2H_2O$	15.5
Calcite	$CaCO_3 = Ca^{2+} + CO_3^{2-}$	8.48
Aragonite	$CaCO_3 = Ca^{2+} + CO_3^{2-}$	8.37
Dolomite (cr.)	$CaMg(CO_3)_2 = Ca^{2+} + Mg^{2+} + 2CO_3^{2-}$	17.1
Dolomite (am.)	$CaMg(CO_3)_2 = Ca^{2+} + Mg^{2+} + 2CO_3^{2-}$	16.5
Siderite (cr.)	$FeCO_3 = Fe^{2+} + CO_3^{2-}$	10.9
Siderite (am.)	$FeCO_3 = Fe^{2+} + CO_3^{2-}$	10.5
Rhodochrosite (cr.)	$MnCO_3 = Mn^{2+} + CO_3^{2-}$	11.1
–	$NiCO_3 = Ni^{2+} + CO_3^{2-}$	6.9
Pyrite	$FeS_2 = Fe^{2+} + 2S^-$	30.2
Pyrrhotite	$FeS = Fe^{2+} + S^{2-}$	17.3
Millerite	$NiS = Ni^{2+} + S^{2-}$	22.0–29.0
	Reaction	– log <i>K</i>
	$H_2O = H^+ + OH^-$	14.0
	$CO_2(g) + H_2O = H_2CO_3$	1.47
	$H_2CO_3 = HCO_3^- + H^+$	6.35
	$HCO_3^- = CO_3^{2-} + H^+$	10.33
	$Ca^{2+} + HCO_3^- = CaHCO_3^+$	1.11
	$Fe^{2+} + HCO_3^- = FeHCO_3^+$	2.0
	$Mg^{2+} + HCO_3^- = MgHCO_3^+$	1.07
	$Mn^{2+} + HCO_3^- = MnHCO_3^+$	1.95

the pH ($-\log_{10}[H^+]$) and the ion chemistry of the system they occur in, hence their great importance in groundwater systems. Table 10.3 lists some of the most significant acid-base dissociation reactions in groundwater, and the corresponding equilibrium (dissociation) constants [5, 6].

Strong acids are rarely present in groundwater and when they are it is attributable to contamination incidents. Small concentrations of strong bases, instead, can be found in aquifers as a result of dissolution of minerals, in particular carbonates and silicates.

The accumulation of cations resulting from the dissolution of carbonates and silicates is generally greater than that of anions resulting from the dissociation of strong acids. Therefore, in natural conditions groundwater tends to be slightly alkaline, with pH ranging from 7 to 8.

pH values are usually smaller in superficial aquifers, because they are more exposed to contamination with acid substances deriving from human activities (e.g., acid rain). pH values below 6 are extremely rare, unless a source of contamination is very close.

Complexation

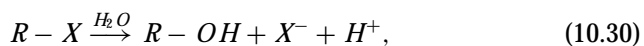
Free metal ions can establish short-range interactions with free anions or neutral molecules, thus forming *complexes*. The metal ion is the central atom of the complex, while the anion or molecule it links to is called *ligand*. Many compounds can act as ligands, including water, organic (e.g., citrate, acetate, oxalate, lactate, amino acids, phenols, carboxylic acids) or inorganic (e.g., carbonate and phosphate ions), natural or synthetic (e.g., ethylenediaminetetraacetic acid (EDTA)) substances [5, 6].

Ligands can form one or multiple bonds with the central metal ion (i.e., mono- or poly-dentate ligands, respectively), thus influencing the stability of the resulting complex. When the ligand is water, it forms the so-called *primary hydration sphere* around the metal ion, and together they constitute a *solvation complex*. Other ligands, instead, can replace water molecules in the primary hydration sphere and establish a direct link with the central atom, thus forming a *complex ion* (or *inner sphere complex*); conversely, when the ligand does not displace water molecules and is attached to the metal ion from outside the hydration sphere, an *ion pair* (or *outer-sphere complex*) is formed [6].

Complexes have distinct chemical and environmental properties from their individual components and are typically soluble. In fact, complexation is extremely important in the environment because it may lead to increased metal solubility, even by several orders of magnitude, thus preventing their precipitation and favoring their transport in groundwater. This is true also for metals such as Cd, Cr, Cu, Pb, U, or Pu, which represent a significant health hazard. Particularly relevant and common environmental ligands are humic and fulvic acids. These are organic acids that do not belong to any specific biochemical category, are widespread in soils and in soil water, and contain many organic functional groups that can potentially bind metal ions [5, 6].

Hydrolysis

Hydrolysis is a reaction that leads to the splitting of two reactants, one of which is water. In groundwater systems, hydrolysis of organic compounds is particularly relevant as it increases their solubility and biodegradability. The transformation they undergo in water is of this kind [5]:



where $R - X$ is a generic organic molecule in which X can be a halogen, or a phosphorus, nitrogen or carbon atom.

Organic Compound Dissolution

Natural hydrocarbons and organic contaminants are typical examples of compounds that can form a separate phase in aquifers. They can migrate in the form of a distinct phase, or dissolve more or less rapidly in water. Organic compounds are very diverse in terms of solubility: some, like methanol, are extremely soluble, while others, like DDT and PCBs, are highly hydrophobic and almost insoluble [5].

However, one should keep in mind that the acceptable concentration thresholds for hydrophobic contaminants are often lower than their solubility.

Dissolution and Precipitation of Solids

Dissolution and precipitation of minerals such as carbonates, silicates, sulfides and hydroxides are among the main processes controlling groundwater geochemistry. They are, in particular, important in that they are responsible for the introduction and removal of metals in or from solution. The dissolution reactions of a few minerals and the deriving solubility products are listed in Table 10.3. It should be kept in mind that when other ions are present in solution, the solubility of a solid is often very different from that measured in pure water.

Radioactive Decay

Radioactive contaminants are subject to natural decay processes. The concentration of radionuclides in an aquifer decreases progressively with time, both in the dissolved and the sorbed phase. Radioactive decay follows a first order kinetics, k , which depends on the radionuclide's half-life according to the relation [4]:

$$t_{1/2} = \frac{0.693}{k} = \frac{\ln 2}{k}. \quad (10.31)$$

Half-life is defined as the time during which 50% of radioactive atoms naturally decays. Table 10.4 lists the half-life values of a few radionuclides.

10.3 Biological Processes: Biodegradation

Subsurface environments host a variety of prokaryotic and eukaryotic microorganisms, which include bacteria, archaea, protozoans, algae and fungi. These organisms are capable of mediating a broad range of chemical reactions that are among the main processes controlling subsurface geochemistry and often have a relevant impact on the fate of contaminants. Microorganisms can drive the alteration or the decomposition into simpler products of chemical compounds via *biotransformation* or *biodegradation* reactions, respectively. These are generally accepted to be prevalent processes in the breakdown of organic compounds in soils and aquifers, and

Table 10.4 Half-life values for a few radionuclides

Radionuclides	Half-life
Barium 140	13 days
Carbon 14	5730 years
Cerium 141	33 days
Cesium 137	30 years
Cobalt 60	5.25 years
Iron 55	2.7 years
Iodine 131	8 days
Krypton 85	10.3 years
Manganese 54	310 days
Lead 210	21 years
Plutonium 239	24300 years
Potassium 40	$\sim 1.4 \cdot 10^9$ years
Radium 226	1620 years
Ruthenium 103	40 days
Silica 32	~ 300 years
Strontium 89	51 days
Strontium 90	28 years
Thorium 230	75200 years
Thorium 234	24 days
Uranium 235	$\sim 7 \cdot 10^6$ years
Uranium 238	$\sim 4.5 \cdot 10^9$ years
Zirconium 95	65 days

are also able to act on and transform inorganic species. Organic compounds can be used by microorganisms as a primary source of energy and carbon, or can be transformed cometabolically alongside other substrates. These transformations mainly entail redox, hydrolysis, and conjugation (i.e., addition of functional groups or hydrocarbon moieties to the molecule) reactions. Often, and most desirably, biodegradation of contaminants yields innocuous organic or inorganic products (e.g., carbon dioxide, water, chlorine); however, in certain instances toxic intermediate products are formed (e.g., vinyl chloride can accumulate during the stepwise microbial dechlorination of PCE or TCE) [3–5].

In order to describe biodegradation processes quantitatively, their kinetics need to be defined. One of the most commonly used models is Monod's, who realized the importance of taking into account microbial growth when describing substrate consumption. This model is formalized as follows [4]:

$$\frac{dC}{dt} = -k(C)C = -k_{\max} \frac{C}{k_c + C} \quad (10.32)$$

where C is the contaminant concentration (ML^{-3}); k is the microorganism growth rate, which is a function of substrate concentration (T^{-1}); k_{\max} is the maximum growth rate (T^{-1}); and k_c is the half-saturation constant (ML^{-3}), which represents the substrate concentration that allows the microorganisms to grow at a rate k equal to half the maximum growth rate, k_{\max} .

For non-limiting concentrations of substrate, $C \gg k_c$ and the term $(k_c + C)$ is approximately equal to C , and thus microbial growth follows a zero-order kinetics relative to the substrate:

$$\frac{dC}{dt} = -k_{\max}. \quad (10.33)$$

Conversely, if $C \ll k_c$, the contaminant disappearance rate is reduced to the expression:

$$\frac{dC}{dt} = -\frac{k_{\max}}{k_c} C, \quad (10.34)$$

which describes a first-order kinetics, that can be solved for solute concentration as follows:

$$C = C_0 e^{-\frac{k_{\max}}{k_c} t}. \quad (10.35)$$

Despite taking into account microbial growth, the Monod model makes many simplifications and does not take into account, for example, death of microorganisms or the simultaneous use of multiple substrates. Developments of the Monod models are available in the literature; however, the number of parameters they involve increases very quickly, rendering their application impractical [4]. Even for the Monod model it is often difficult to determine the parameters in the field and, thus, simpler models are commonly used, with the first-order kinetics model being the most utilized. Nevertheless, it should be kept in mind that it may lead to an overestimation of biodegradation, because it does not take into account the biomass maximum growth limit, nor substrate depletion.

10.4 Physico-Chemical Processes: Sorption

Sorption is defined as the removal of a compound (the *sorbate*) from solution and its transfer to a solid phase (the *sorbent*, which could be a mineral or organic matter) [6, 14]. Although this definition should include also precipitation phenomena (see Sect. 10.2.2), sorption usually only refers to absorption and adsorption processes. *Adsorption* is a surface process that results in the accumulation of a dissolved substance at the solid-solution interface; whereas through *absorption* a solute is incorporated within the solid matrix of a sorbent. Since in most cases it is difficult to establish whether the distribution of a solute between the solid and the aqueous phase is due to adsorption or absorption, the general term sorption is preferentially used [3, 6]. Retention of solutes on or within solids can be physical or chemical in nature. *Phys-*

ical sorption relies on physical forces, which can be attractive (e.g., Van der Waals forces) or repulsive (e.g., hydrophobic bonds can be created between solid surfaces and non-polar organic molecules that are repulsed by polar water molecules). *Chemical sorption* (or *chemisorption*), instead, entails the formation of chemical bonds between sorbate and sorbent and includes ion exchange, protonation, and hydrogen bonding. The most common of these is *ion exchange*, in which an ion is replaced by another ion of same charge at a solid surface site with opposite charge. Since many mineral surfaces are negatively charged, *cation exchange* is more common in natural groundwater environments than *anion exchange* [3]. Sorption is usually fully or partly reversible, and the inverse process (i.e., the release of ions or molecules from a solid surface to the aqueous phase) is called *desorption* [3, 6, 14].

The process that controls the distribution of a contaminant, originally present only in solution, between solution and solid phase through sorption and desorption is called *partitioning*. The contact between water and solid matrix in the aquifer determines a mass exchange between the two phases until equilibrium conditions are reached. Partitioning of a solute between the liquid and solid phases at equilibrium can be determined in the laboratory by putting in contact samples of a dissolved compound at different concentrations with an aquifer sample; subsequently, once equilibrium is reached, the mass of contaminant removed from solution is measured for each different sample. The experimental results are then represented on an isotherm, in which the sorbed contaminant mass per unit solid mass at equilibrium, S , is plotted against its concentration in solution, C , at a specific temperature, T [6].

If the sorption process is sufficiently rapid relative to the flow rate, the sorbed phase can be considered in equilibrium with the solute; the value of S is, in this case, exclusively a function of the concentration, C , and can be derived from the isotherm. If, instead, sorption is slow, the local equilibrium hypothesis is not necessarily valid: to describe the process a kinetic model rather than an equilibrium model will have to be used.

A linear relation, called *linear isotherm*, exists between the sorbed mass per unit solid mass and the dissolved concentration, in particular for small solute concentrations, which is the case in most contamination events (see Fig. 10.12) [4]:

$$S = K_d C, \quad (10.36)$$

where the coefficient of proportionality, K_d ($L^3 M^{-1}$), is known as the *solid-liquid partition coefficient*.

The linear isotherm appropriately represents systems with low solute concentration. However, at higher concentrations the process could deviate from the linear model due to saturation of the solid matrix sorption sites. Under such circumstances, the solid-liquid partition is described more accurately by the Langmuir isotherm (Fig. 10.13), which is based on the assumption that a solid surface has a finite number of sorption sites [5]:

$$S = \frac{\alpha \beta C}{1 + \alpha C}, \quad (10.37)$$

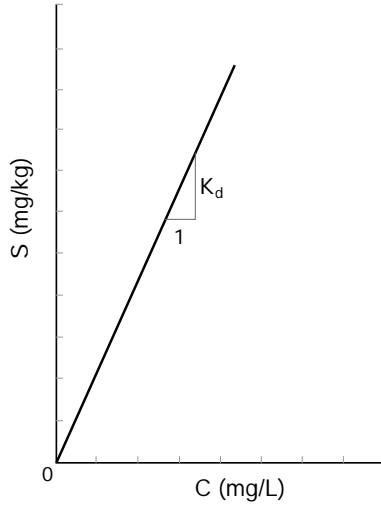


Fig. 10.12 Linear isotherm

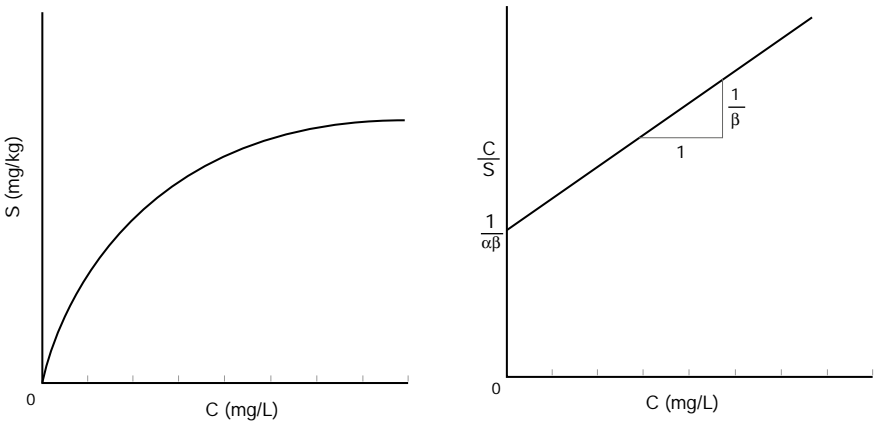


Fig. 10.13 Langmuir isotherm

with α and β being empirical constants.

In other cases, deviation from the ideal model is caused by competition between multiple contaminants for an active sorption site. These circumstances are accounted for by the Freundlich isotherm (Fig. 10.14) [5]:

$$S = KC^{1/N}, \tag{10.38}$$

with K and N being two empirical constants.

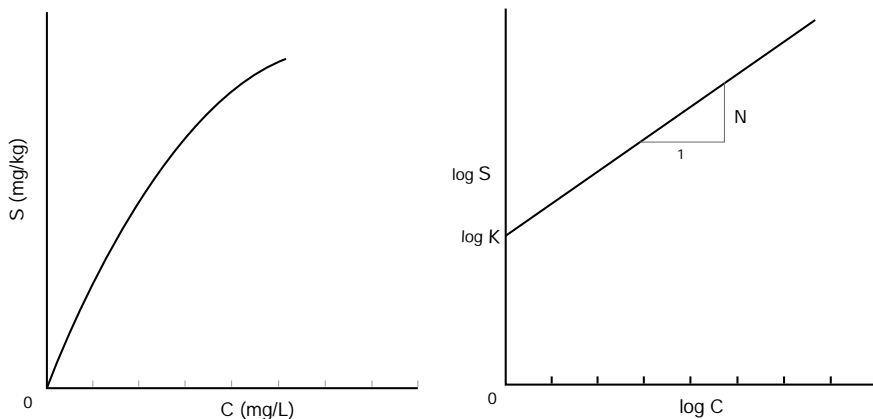


Fig. 10.14 Freundlich isotherm, in linear and logarithmic coordinate systems

Many organic substances dissolved in water tend to sorb to the solid surface of the grains composing the aquifer; this behavior is called *hydrophobic effect*. Hydrophobic compounds can be dissolved in many non-polar organic solvents, but are sparingly soluble in water. When the organic carbon (OC) content of a soil or an aquifer reaches at least 1% in weight, sorption of organic substances occurs almost exclusively on the surface of the organic carbon, and the solid-liquid partition coefficient is equal to [4]:

$$K_d = f_{oc} K_{oc}, \tag{10.39}$$

where f_{oc} is the dimensionless weight fraction of OC in the aquifer relative to the total weight of the solid composing the aquifer, and K_{oc} is the partition coefficient of a generic organic compound between OC and water, ($L^3 M^{-1}$).

The OC in aquifer samples can be measured in the laboratory. It can vary significantly within the same type of material and it ranges between 10^{-2} and 10^{-4} .

K_{oc} can be estimated through its correlation with the octanol-water partition coefficient, K_{ow} :

$$\log K_{oc} = a + b \log K_{ow}, \tag{10.40}$$

where the coefficients a and b depend on the type of contaminant.

An estimate of the value of K_{oc} can also be derived from the solubility S of a certain compound based on an equation analogous (save for the sign) to the previous one:

$$\log K_{oc} = a' - b' \log S. \tag{10.41}$$

The values of the coefficients a , b , a' , b' relative to a few contaminants are available in the literature [7].

Figure 10.15 highlights the direct proportionality between K_{oc} and K_{ow} , and the inverse proportionality between K_{oc} and S .

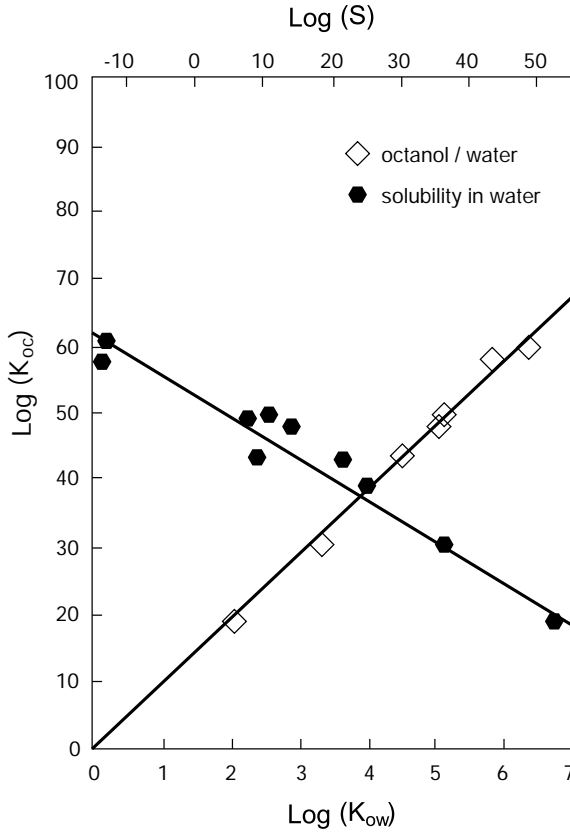


Fig. 10.15 Experimental correlations: K_{oc} versus K_{ow} and K_{oc} versus S (modified from [7])

The sorption of a fraction of the contaminant present in solution to the aquifer’s solid matrix determines a delay in the advancement rate of the contaminant front (see Fig. 10.16). This delay is quantified by the *retardation factor*, R , a dimensionless coefficient defined by the ratio between the water’s seepage velocity, v , and the contaminant’s seepage velocity, v_c :

$$R = \frac{v}{v_c}. \tag{10.42}$$

For a solute with linear equilibrium sorption, the retardation factor, R , depends on the characteristics of the aquifer and of the contaminant, according to the following relation:

$$R = 1 + \frac{\rho_b}{n_e} K_d, \tag{10.43}$$

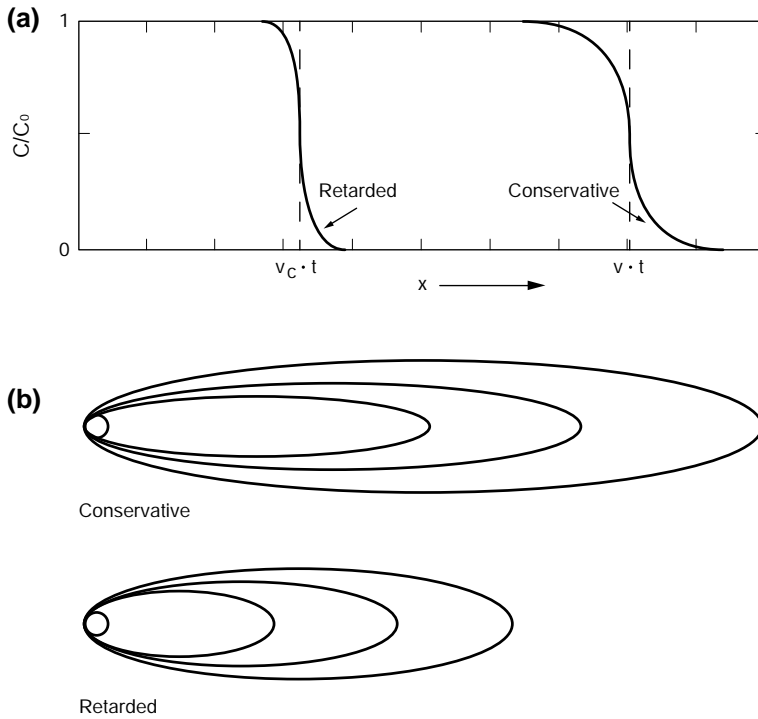


Fig. 10.16 Comparison of propagation of conservative solutes versus solutes subject to sorption, released by a continuous source in a **a** one- or **b** two-dimensional geometry

where ρ_b is the mass density of the aquifer’s solid matrix (usually 1600–2100 kg/m³), n_e the effective porosity, and K_d the partition coefficient relative to a linear isotherm ($M^{-1}L^3$).

10.5 Concomitant Processes

The propagation processes illustrated individually in this chapter, in reality occur simultaneously, with a relative significance that depends on the characteristics of the aquifer and of the contaminant.

Figure 10.17 depicts the possible evolution of a contamination plume in an aquifer in the case of a continuous source: (a) and (b) show the behavior of a conservative contaminant that propagates exclusively under the effect of hydrological processes, whereas (c) and (d) illustrate the behavior of a reactive contaminant undergoing chemical, physico-chemical, linear adsorption, and biological processes (see earlier sections of this chapter and Chaps. 12 and 13).

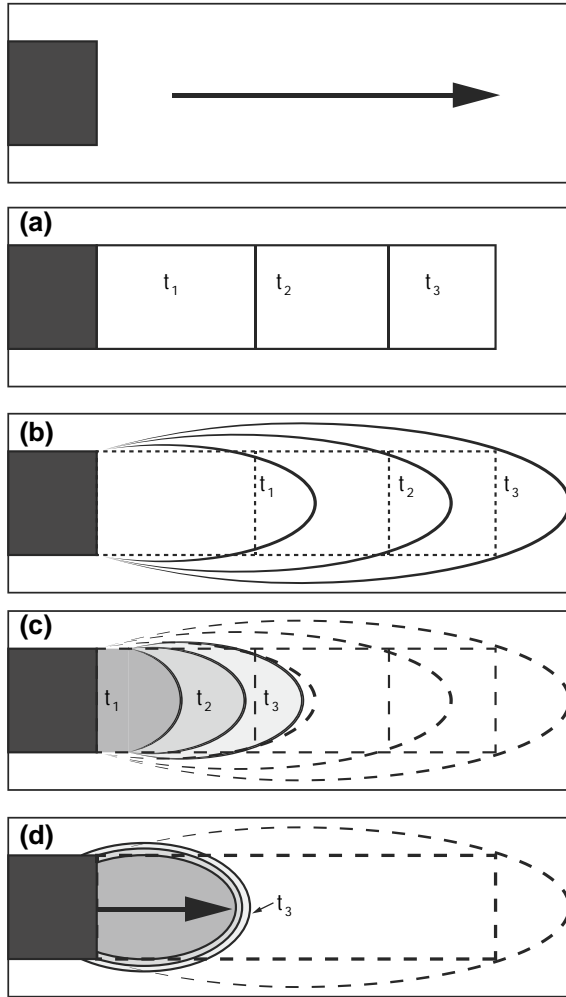


Fig. 10.17 Propagation of a contaminant from a continuous source: **a** only advective flow; **b** advective and dispersive flow; **c** advective and dispersive flow with sorption phenomena; **d** advective and dispersive flow with sorption and biodegradation

References

1. A. Arya, T.A. Hewett, R.G. Larson, L.W. Lake, Dispersion and reservoir heterogeneity. *SPE Reserv. Eng.* **3**, 139–148 (1988)
2. J. Bear, *Dynamics of Fluids in Porous Media* (Courier Corporation, Chelmsford, 1972)
3. J.R. Boulding, J.S. Ginn, *Practical Handbook of Soil, Vadose Zone, and Ground-Water Contamination: Assessment, Prevention, and Remediation*, 2nd edn. (CRC Press, Boca Raton, 2004)
4. J.W. Delleur, *Handbook of Groundwater Engineering* (CRC Press, Boca Raton, 2006)

5. P.A. Domenico, F.W. Schwartz, *Physical and Chemical Hydrogeology* (Wiley, New York, 1998)
6. M.E. Essington, *Soil and Water Chemistry: An Integrative Approach* (CRC Press, Boca Raton, 2004)
7. C.W. Fetter, *Contaminant Hydrogeology*, 2nd edn. (Waveland Press Inc., Long Grove, 2008)
8. R.A. Freeze, J.A. Cherry, *Groundwater* (Prentice-Hall, Upper Saddle River, 1979)
9. L.W. Gelhar, C. Welty, K.R. Rehfeldt, A critical review of data on field-scale dispersion in aquifers. *Water Resour. Res.* (1992)
10. A. Lallemand-Barre, P. Peaudecerf, Recherche des relations entre la valeur de la dispersivité macroscopique d'un milieu aquifère, ses autres caractéristiques et les conditions de mesure. *Bull. Bur. Rech. Geol. Min. Fr.* **2**, 277–284 (1978)
11. A. Mercado, Spreading pattern of injected water in a permeability stratified aquifer. *Artif. Recharg. Manag. Aquifers* **72**, 23–26 (1967)
12. S.P. Neuman, Universal scaling of hydraulic conductivities and dispersivities in geologic media. *Water Resour. Res.* **26**, 1749–1758 (1990)
13. J. Schroter, Mikro- und Makrodispersivität poröser Grundwasserleiter. *Meyniana* **36**, 1–34 (1984)
14. A. Thompson, K.W. Goynes, Introduction to the sorption of chemical constituents in soils — learn science at scitable (2012), <https://www.nature.com/scitable/knowledge/library/introduction-to-the-sorption-of-chemical-constituents-94841002>
15. S. Troisi, *Propagazione di inquinanti in sistemi porosi e fessurati* (Bios, Cosenza, 1996)
16. M. Xu, Y. Eckstein, Use of weighted least-squares method in evaluation of the relationship between dispersivity and field scale. *Ground Water* **33**, 905–908 (1995)
17. A. Zech, S. Attinger, A. Bellin, V. Cvetkovic, P. Dietrich, A. Fiori, G. Teutsch, G. Dagan, A Critical Analysis of Transverse Dispersivity Field Data. *Groundwater* (2018)

Chapter 11

The Mass Transport Equations



Abstract This chapter derives the differential equations of mass transport, distinguishing between conservative solutes (i.e., exclusively undergo hydrological processes) and reactive solutes (i.e., also undergo physico-chemical and/or biological processes). The differential equations are derived by imposing the mass balance of a generic solute in a representative elementary volume during a certain time interval.

In the previous chapter individual hydrological, physico-chemical, chemical, and biological processes that affect the propagation of contaminants in groundwater were described. Transport of solutes is a consequence of these mechanisms acting concertedly. The resulting scenario is extremely complex, and is governed by the continuous interactions taking place in the aquifer between solute and water, solute and solid matrix, and between different solutes.

In Sect. 2.1 the law of mass conservation was applied to a representative elementary volume (REV) to derive the equation that governs groundwater flow in a porous medium. In this chapter, the law of mass conservation will be applied to a generic solute or contaminant present in an aquifer.

11.1 Contaminant Mass Balance

The differential equations of mass transport allow a quantitative description of the propagation of a water-miscible contaminant, or of its soluble fraction, in a porous medium. Mass transport equations are obtained by imposing the mass balance of a generic solute in the REV during the time interval dt :

$$M_{out} - M_{in} = M_i - M_f, \quad (11.1)$$

where M_{out} and M_{in} are the mass of solute flowing in and out, respectively of the control volume, and M_i and M_f are the mass of solute present within the control volume at the beginning and end, respectively, of the considered time interval.

Solutes can be grouped into two categories: conservative solutes, which exclusively undergo hydrological phenomena (or, more precisely, for which other phenomena are negligible), and non-conservative (or reactive) solutes, which also undergo physico-chemical, chemical, and/or biological processes.

11.2 Conservative Solutes

In this case, only advection and hydrodynamic dispersion need to be kept into account. Under these conditions, and assuming a (x, y, z) coordinate system composed by the main dispersivity axes (with the x -axis coinciding with the flow direction, and the others being perpendicular to it and to each other, such that $v_x = v$; $v_y = 0$; $v_z = 0$), Table 11.1 describes the components of solute mass flowing in and out of the aquifer REV (whose volume is $dx \cdot dy \cdot dz$ and which is characterized by a porosity n_e) during the time interval dt .

The solute mass present in the control volume at the beginning of the time interval is:

$$M_i = n_e C dx dy dz, \tag{11.2}$$

while at the end of the interval dt the mass can be expressed as:

$$M_f = \left[n_e C + \frac{\partial}{\partial t} (n_e C) dt \right] dx dy dz. \tag{11.3}$$

By applying the mass balance (Table 11.1) the most general form of the differential equation of mass transport, or *advection-dispersion equation*, can be derived:

Table 11.1 Components of inflowing and outflowing mass during the infinitesimal time interval dt due to advection and hydrodynamic dispersion, with reference to the aquifer REV

Inflowing solute mass (in dt)		
Axis	Advection	Hydrodynamic dispersion
x	$v C n_e dy dz dt$	$- D_x \frac{\partial C}{\partial x} n_e dy dz dt$
y	-	$- D_y \frac{\partial C}{\partial y} n_e dx dz dt$
z	-	$- D_z \frac{\partial C}{\partial z} n_e dx dy dt$
Outflowing solute mass (in dt)		
Axis	Advection	Hydrodynamic dispersion
x	$\left[v C n_e + \frac{\partial}{\partial x} (v C n_e) dx \right] dy dz dt$	$- \left[D_x \frac{\partial C}{\partial x} n_e + \frac{\partial}{\partial x} \left(D_x \frac{\partial C}{\partial x} n_e \right) dx \right] dy dz dt$
y	-	$- \left[D_y \frac{\partial C}{\partial y} n_e + \frac{\partial}{\partial y} \left(D_y \frac{\partial C}{\partial y} n_e \right) dy \right] dx dz dt$
z	-	$- \left[D_z \frac{\partial C}{\partial z} n_e + \frac{\partial}{\partial z} \left(D_z \frac{\partial C}{\partial z} n_e \right) dz \right] dx dy dt$

$$\frac{\partial}{\partial x} \left(D_x \frac{\partial C}{\partial x} n_e \right) + \frac{\partial}{\partial y} \left(D_y \frac{\partial C}{\partial y} n_e \right) + \frac{\partial}{\partial z} \left(D_z \frac{\partial C}{\partial z} n_e \right) - \frac{\partial}{\partial x} (vC n_e) = \frac{\partial}{\partial t} (n_e C). \quad (11.4)$$

If a homogeneous medium is considered, and the effective porosity variations over time are neglected, the previous equation becomes:

$$\frac{\partial}{\partial x} \left(D_x \frac{\partial C}{\partial x} \right) + \frac{\partial}{\partial y} \left(D_y \frac{\partial C}{\partial y} \right) + \frac{\partial}{\partial z} \left(D_z \frac{\partial C}{\partial z} \right) - \frac{\partial}{\partial x} (vC) = \frac{\partial C}{\partial t}. \quad (11.5)$$

If, in addition, the dispersion coefficients are considered constant in space, the differential equation is further simplified to:

$$D_x \frac{\partial^2 C}{\partial x^2} + D_y \frac{\partial^2 C}{\partial y^2} + D_z \frac{\partial^2 C}{\partial z^2} - \frac{\partial}{\partial x} (vC) = \frac{\partial C}{\partial t}. \quad (11.6)$$

Finally, if the flow is uniform, the advection-dispersion equation becomes:

$$D_x \frac{\partial^2 C}{\partial x^2} + D_y \frac{\partial^2 C}{\partial y^2} + D_z \frac{\partial^2 C}{\partial z^2} - v \frac{\partial C}{\partial x} = \frac{\partial C}{\partial t}. \quad (11.7)$$

Equation (11.5) can also be written in the following form:

$$\text{div}(\mathbb{D} \cdot \mathbf{grad} C - \mathbf{v}C) = \frac{\partial C}{\partial t}, \quad (11.8)$$

where

- $-\text{div}(\mathbf{v}C)$ is the advective term;
- $\text{div}(\mathbb{D} \cdot \mathbf{grad} C)$ is the dispersive term;
- \mathbb{D} is the tensor of the hydrodynamic dispersion coefficients:

$$\mathbb{D} = \begin{pmatrix} D_x & 0 & 0 \\ 0 & D_y & 0 \\ 0 & 0 & D_z \end{pmatrix}. \quad (11.9)$$

Keep in mind that (see Chap. 10):

$$D_x = D_0 + \alpha_x v, \quad (11.10)$$

$$D_y = D_0 + \alpha_y v, \quad (11.11)$$

$$D_z = D_0 + \alpha_z v. \quad (11.12)$$

11.3 Reactive Solutes

When the sole hydrological phenomena are considered, all contaminants basically behave in the same way, if the modest influence of molecular diffusion is excluded. Conversely, when physico-chemical processes are taken into account, each contaminant is characterized by a distinct behavior.

As illustrated in the previous chapter, reactions can be described through a kinetic or an equilibrium model, based on the rate of the reaction processes in aqueous phase or of the interactions with the solid phase. An example of chemical equilibrium in a heterogeneous phase is sorption to the surface of the aquifer grains; the process determines a delay in solute transport relative to the groundwater flow rate.

The solute mass balance considered in Sect. 11.2 is unaltered in regard to the inflowing and outflowing mass components, but the initial and final mass components are different. Table 11.2 describes the mass balance components over the time interval dt .

If the variations of the mass density of the aquifer's solid matrix, ρ_b , and of the effective porosity, n_e , over time are considered negligible, and if, for simplicity, sorption is modeled through an equilibrium process characterized by a linear isotherm (see Eq. (10.36)), and the degradation is assumed to follow a first-order kinetics, we obtain the following:

$$\frac{\partial S}{\partial t} = \frac{\partial S}{\partial C} \cdot \frac{\partial C}{\partial t} = K_d \frac{\partial C}{\partial t} \tag{11.13}$$

$$\left(\frac{\partial C}{\partial t} \right)_{\text{deg}} = -\lambda C, \tag{11.14}$$

where S is the sorbed mass per unit solid mass, C is the dissolved concentration, K_d is the solid-liquid partition coefficient, and λ is the degradation reaction rate coefficient.

By applying the mass balance (11.1) the following equation can be derived:

$$\begin{aligned} \frac{\partial}{\partial x} \left(D_x \frac{\partial C}{\partial x} \right) + \frac{\partial}{\partial y} \left(D_y \frac{\partial C}{\partial y} \right) + \frac{\partial}{\partial z} \left(D_z \frac{\partial C}{\partial z} \right) - \frac{\partial}{\partial x} (Cv) = \\ = \left(1 + K_d \frac{\rho_b}{n_e} \right) \frac{\partial C}{\partial t} + \lambda C, \end{aligned} \tag{11.15}$$

Table 11.2 Mass balance components in the time interval dt in the REV, in the presence of sorption and natural degradation processes

	Initial mass	Final mass
Dissolved solute mass	$n_e C \, dx dy dz$	$\left\{ n_e C + \left[\frac{\partial n_e C}{\partial t} - \left(\frac{\partial n_e C}{\partial t} \right)_{\text{deg}} \right] dt \right\} dx dy dz$
Sorbed solute mass	$\rho_b S \, dx dy dz$	$\left[\rho_b S + \frac{\partial}{\partial t} (\rho_b S) dt \right] dx dy dz$

from which the differential advection-dispersion equation for reactive solutes can be derived, considering uniform flow and constant hydrodynamic dispersion coefficients:

$$D_x \frac{\partial^2 C}{\partial x^2} + D_y \frac{\partial^2 C}{\partial y^2} + D_z \frac{\partial^2 C}{\partial z^2} - v \frac{\partial C}{\partial x} - \lambda C = R \frac{\partial C}{\partial t}, \quad (11.16)$$

or:

$$\text{div}(\mathbb{D} \cdot \mathbf{grad} C - \mathbf{v}C) - \lambda C = R \frac{\partial C}{\partial t}, \quad (11.17)$$

where

- $R = 1 + K_d \frac{\rho_b}{n_e}$ is the retardation factor
- $\lambda = \frac{0.693}{t_{1/2}}$ is the reaction rate coefficient for biodegradation

Note that for $R = 1$ and $\lambda = 0$ Eqs. (11.16) and (11.17) coincide with Eqs. (11.7) and (11.8) valid for conservative solutes.

11.4 Initial and Boundary Conditions

In order to be able to solve the differential equations of mass transport, a set of initial and boundary conditions concerning the spatial domain have to be defined. The initial conditions specify the flow domain and the contaminant concentrations at the beginning of the simulation. The boundary conditions describe the interactions between the system and the surrounding area, by specifying the value of the dependent variable (usually concentration), or the value of its first derivative at the domain boundary.

Generally, when solving the transport equations, three types of boundary conditions are used: Dirichlet's (first species; i.e., given concentration), Neumann's (second species; i.e., zero mass flux) and Cauchy's (third species; i.e. given mass flux).

The differential equation of mass transport can be solved analytically only under the assumption that a few simplifying hypotheses are valid. These regard the geometry of the source, contaminant release mechanism, boundary conditions, and flow regime. In all other cases, the differential equation can only be solved numerically.

Chapter 12

Analytical Solutions to the Differential Equation of Mass Transport for Conservative Solutes



Abstract In this chapter, analytical solutions to the differential equation of mass transport for conservative solutes are illustrated. Their derivation relies on a number of simplifying hypotheses, including that: the medium is saturated, homogeneous and isotropic; water has constant density and viscosity, regardless of solute concentration; Darcy's law is valid; flow directions and rates are uniform; transport parameters are constant within the domain; boundary conditions are constant in time. Solutions for one-, two- and three-dimensional geometries are presented, the former being mainly used for the interpretation of laboratory experiments, the latter two being more relevant for practical applications. Pulse and continuous solute release are considered. Notably, in a three-dimensional geometry a pulse input from a point source and a continuous input from a plane source are illustrated. A solution of the differential equation of mass transfer for the former contamination scenario was derived by Baetslé, while Domenico and Robbins proposed a model for the latter.

The differential equation of mass transport can be solved analytically, provided that a few simplifying hypotheses are satisfied: the medium is saturated, homogeneous, and isotropic; water has constant density and viscosity, regardless of solute concentration; Darcy's law is valid; flow directions and rates are uniform; transport parameters are constant within the domain; boundary conditions are constant in time; chemical reactions follow a first order kinetics; sorption between solid and liquid phases has reached a steady state.

In the following paragraphs the main analytical solutions valid for different geometries and boundary conditions are presented, under the assumption that the groundwater contaminants are conservative (or non-reactive) and are, therefore, only subjected to hydrological transport phenomena.

First, solutions for a one-dimensional geometry, mainly used for the interpretation of laboratory experiments, will be introduced; then, solutions for more realistic two- and three-dimensional geometries will be presented. In the latter cases, transverse dispersion mechanisms cannot be neglected, as can be seen in Fig. 12.1, which depicts the following contaminant release scenarios:

- line source, 2D geometry (a);
- point source, 3D geometry (b);
- plane source, 3D geometry (c).

12.1 One-Dimensional Geometry

Equation (11.7) is reduced to the following simplified form:

$$D_x \frac{\partial^2 C}{\partial x^2} - v \frac{\partial C}{\partial x} = \frac{\partial C}{\partial t}. \quad (12.1)$$

12.1.1 Continuous Input

Figure 12.2 shows the laboratory setup for the continuous input of a constant contaminant concentration, C_0 , at the inlet of an initially uncontaminated column packed with porous and permeable material. Initial and boundary conditions for a semi-infinite geometry are:

$$C(x, t = 0) = 0 \quad \text{for } x > 0, \quad (12.2)$$

$$C(x = 0, t) = C_0 \quad \text{for } t > 0, \quad (12.3)$$

$$C(x = \infty, t) = 0 \quad \text{for } t \geq 0. \quad (12.4)$$

The analytical solution of equation (12.1) with boundary conditions expressed by (12.2) to (12.4) was provided by Ogata and Banks [5]:

$$\frac{C(x, t)}{C_0} = \frac{1}{2} \left\{ \operatorname{erfc} \left[\frac{x - vt}{2\sqrt{D_x t}} \right] + \exp \left(\frac{vx}{D_x} \right) \cdot \operatorname{erfc} \left[\frac{x + vt}{2\sqrt{D_x t}} \right] \right\} \quad (12.5)$$

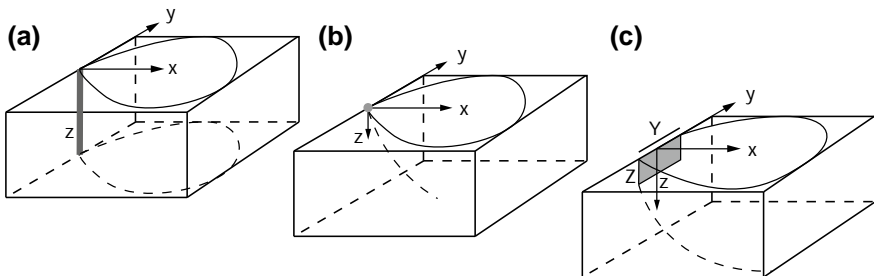


Fig. 12.1 Main contamination source geometries: **a** line source; **b** point source; **c** plane source

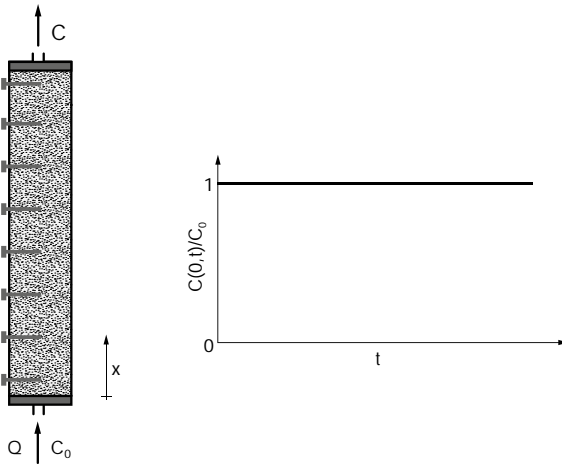


Fig. 12.2 One-dimensional column equipped with sampling ports for continuous input experiments of a constant contaminant concentration C_0

with erfc being the *complementary error function*:

$$\text{erfc}(\beta) = 1 - \text{erf}(\beta)$$

$$\text{erf}(\beta) = \frac{2}{\sqrt{\pi}} \int_0^\beta e^{-y^2} dy \quad \text{error function.}$$

The diagrams of the dimensionless functions $\text{erf}(\beta)$ and $\text{erfc}(\beta)$ are represented in Fig. 12.3, and their values are listed in Table 12.1.

The concentration profile as a function of space and time deriving from the application of solution (12.5) is illustrated in Fig. 12.4.

For typical values encountered in practical applications of v , x , and t : $\text{erfc}\left[\frac{x+vt}{2\sqrt{D_x t}}\right] \rightarrow 0$ and the Ogata–Banks solution can be simplified to:

$$\frac{C(x, t)}{C_0} = \frac{1}{2} \text{erfc}\left[\frac{x - vt}{2\sqrt{D_x t}}\right], \tag{12.6}$$

This is the exact solution that would be obtained by considering a boundless system geometry.

A few important conclusions can be drawn about the evolution of a contamination event with a continuous source of input, by analyzing the simplified Ogata–Banks equation.

Let us consider, to start with, the meaning of the numerator $(x - vt)$ of the argument of complementary error function, erfc . This expression describes the observation point relative to the advective front (vt) . The possible situations can be summarized as follows:

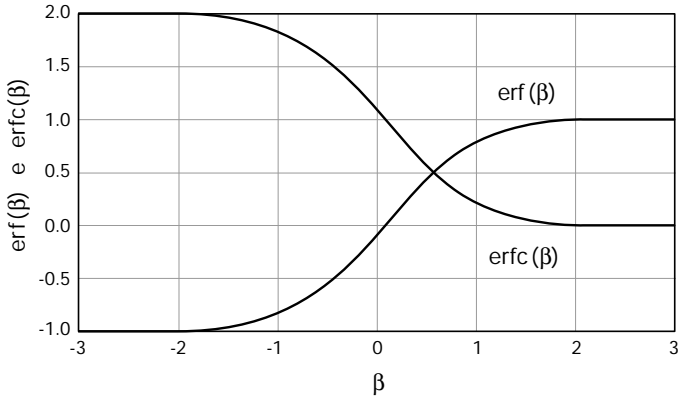


Fig. 12.3 Diagrams of the error function $\text{erf}(\beta)$ and the complementary error function $\text{erfc}(\beta)$

Table 12.1 Values of the dimensionless functions $\text{erf}(\beta)$ and $\text{erfc}(\beta)$ for positive values of the argument. The reader should keep in mind that $\text{erf}(-\beta) = -\text{erf}(\beta)$ and that $\text{erfc}(-\beta) = 1 + \text{erf}(\beta)$

β	$\text{erf}(\beta)$	$\text{erfc}(\beta)$	β	$\text{erf}(\beta)$	$\text{erfc}(\beta)$
0	0	1.0	1.1	0.880205	0.119795
0.05	0.056372	0.943628	1.2	0.910314	0.089686
0.1	0.112463	0.887537	1.3	0.934008	0.065992
0.15	0.167996	0.832004	1.4	0.952285	0.047715
0.2	0.222703	0.777297	1.5	0.966105	0.033895
0.25	0.276326	0.723674	1.6	0.976348	0.023652
0.3	0.328627	0.671373	1.7	0.983790	0.016210
0.35	0.379382	0.620618	1.8	0.989091	0.010909
0.4	0.428392	0.571608	1.9	0.992790	0.007210
0.45	0.475482	0.524518	2.0	0.995322	0.004678
0.5	0.520500	0.479500	2.1	0.997021	0.002979
0.55	0.563323	0.436677	2.2	0.998137	0.001863
0.6	0.603856	0.396144	2.3	0.998857	0.001143
0.65	0.642029	0.357971	2.4	0.999311	0.000689
0.7	0.677801	0.322199	2.5	0.999593	0.000407
0.75	0.711156	0.288844	2.6	0.999764	0.000236
0.8	0.742101	0.257899	2.7	0.999866	0.000134
0.85	0.770668	0.229332	2.8	0.999925	0.000075
0.9	0.796908	0.203092	2.9	0.999959	0.000041
0.95	0.820891	0.179109	3.0	0.999978	0.000022
1.00	0.842701	0.157299			

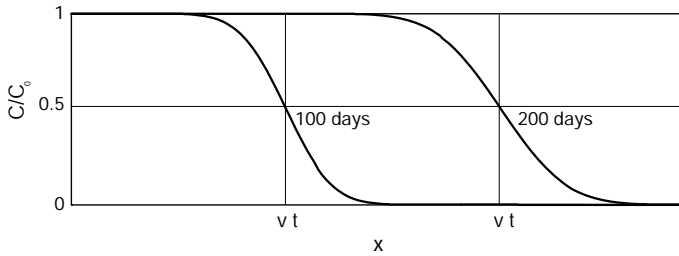


Fig. 12.4 Concentration profile in a one-dimensional geometry given a continuous input as a function of space and time

- $x = vt$: the observation point coincides with the position of the advective front. Hence, $\text{erfc}(0) = 1$ and so $C = 0.5 C_0$: in correspondence of the advective front, the concentration is half the injected concentration, and this value ($0.5 C_0$) migrates at the groundwater seepage velocity;
- $x \gg vt$: the observation point is far ahead of the advective front; the argument of the function erfc is equal or greater than 2; therefore $\text{erfc}(\beta) = 0$ and $C = 0$. In other words, at this point there is no trace of the contamination;
- $x > vt$: the observation point is a little ahead of the advective front; the argument β of the function erfc is positive and comprised between 0 and 2. Hence, the value of the function erfc is between 1 and 0, so $0 < C < 0.5 C_0$. Contaminant present at a concentration smaller than $0.5 C_0$ is attributable to the longitudinal dispersion;
- $x \ll vt$: the observation point is far behind the advective front. It is sufficient for β to be equal to -2 , for $\text{erfc}(\beta)$ to be equal to 2 and thus $C = C_0$;
- $x < vt$: the observation point is close behind the advective front: $-2 < \beta < 0$. Therefore, $1 < \text{erfc}(\beta) < 2$ and so $0.5 C_0 < C < C_0$.

Longitudinal dispersion transfers part of the contaminant mass ahead of the advective front; its effect increases with the distance from the source of contamination and, hence, with time. Dimensionally, the denominator of the erfc function is a length and expresses the role of the longitudinal dispersion: it can be considered a measure of the dispersion of the contaminant mass in the proximity of the advective front, in correspondence of which $C/C_0 = 0.5$.

12.1.2 Pulse (or Instantaneous) Input

The analytical solution to differential equation (12.1) describing a pulse contaminant input in the origin and considering an infinitely long column, was derived by Sauty [6]:

$$C(x, t) = \frac{m}{An_e\sqrt{4\pi D_x t}} \cdot \exp\left[-\frac{(x - vt)^2}{4 D_x t}\right], \tag{12.7}$$

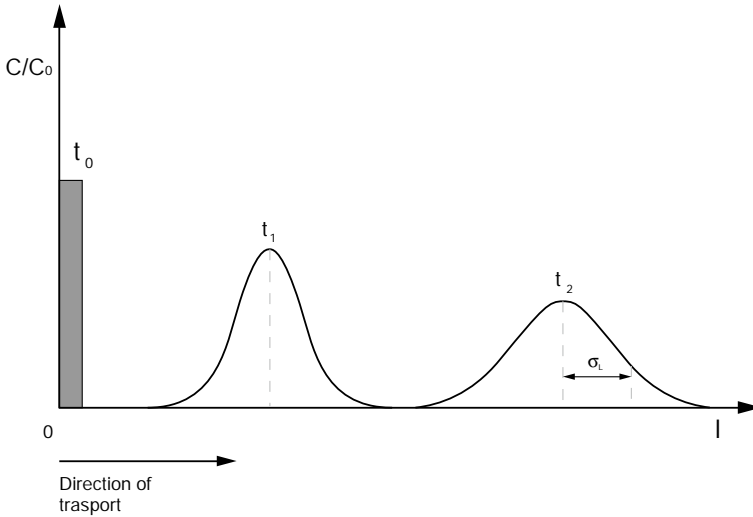


Fig. 12.5 Concentration distribution as a function of space and time for a pulse input in a one-dimensional geometry

where m is the solute mass input at time t_0 , and A is the cross-sectional area of the column.

Since the solute is, by hypothesis, conservative, the total mass remains constant during the propagation of the pulse. This mass is proportional to the area below the Gaussian curve, as depicted in Fig. 12.5. The maximum concentration is found at the advective front:

$$C_{\max} = \frac{m}{An_e\sqrt{4\pi D_x t}} \quad (12.8)$$

The dimensions of the plume increase with time due to the evolution of the standard deviation:

$$\sigma_x = \sqrt{2D_x t}.$$

12.2 Two-Dimensional Geometry

There are several solutions of the equation of mass transport in a two-dimensional geometry. These can be used to simulate the propagation of contaminants released from sources in aquifers with a relatively small thickness, under the hypothesis that the solute is well mixed along the entire saturated thickness and that the vertical

concentration gradient is negligible. The source is assumed to be linear, vertical, and to have length equal to the aquifer depth (see Fig. 12.1b).

The differential equation of mass transport can be thus written as follows:

$$D_x \frac{\partial^2 C}{\partial x^2} + D_y \frac{\partial^2 C}{\partial y^2} - v \frac{\partial C}{\partial x} = \frac{\partial C}{\partial t}. \quad (12.9)$$

12.2.1 Vertical Line Source, Pulse Input

In this case, the aquifer is assumed to have an infinite extension in both the x and y direction. The contaminant is introduced in a single pulse in the point $(0, 0)$. The analytical solution to differential equation (12.9) was provided by Wilson and Miller [7]:

$$C(x, y, t) = \frac{m}{4\pi b n_e t \sqrt{D_x D_y}} \cdot \exp \left[-\frac{(x - vt)^2}{4D_x t} - \frac{y^2}{4D_y t} \right], \quad (12.10)$$

where m (M) is the mass injected along the thickness b .

Figure 12.6 shows the concentration distribution of a conservative contaminant on the horizontal flow plane, following a pulse input. Naturally, the maximum concentration will be found along the longitudinal flow direction, in correspondence of the center of the contaminant plume ($x = vt$, $y = 0$):

$$C_{\max} = \frac{m}{4\pi b n_e t \sqrt{D_x D_y}}. \quad (12.11)$$

The size of the plume increases over time, following the evolution of the standard deviation:

$$\sigma_x = \sqrt{2D_x t}; \quad \sigma_y = \sqrt{2D_y t}.$$

12.2.2 Vertical Line Source, Continuous Input

Also in this case the aquifer is assumed to extend infinitely in both the x and the y directions. The contaminant is released into the aquifer, in the point $(0, 0)$, with known discharge and concentration. Also for this case, the analytical solution to differential equation (12.9) was derived by Wilson and Miller [7]:

$$\frac{C(x, y, t)}{C_0} = \frac{Q}{4\pi b n_e \sqrt{D_x D_y}} \cdot \exp\left(\frac{x}{B}\right) \cdot W\left(u, \frac{r}{B}\right), \quad (12.12)$$

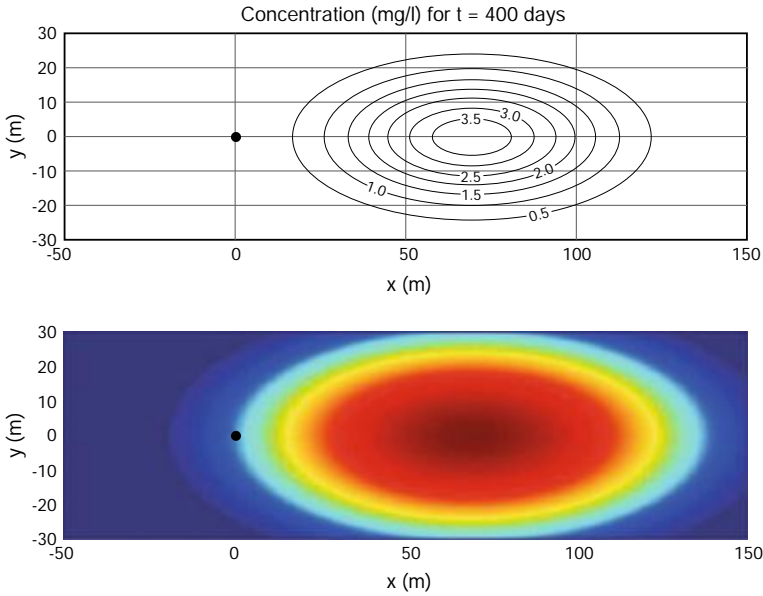


Fig. 12.6 Conservative solid transport in a two-dimensional geometry following a pulse input in $x = 0, y = 0$ (modified from [8])

where:

$$B = \frac{2D_x}{v} = 2\alpha_x, \tag{12.13}$$

$$u = \frac{r^2}{4D_x t}, \tag{12.14}$$

$$r = \sqrt{x^2 + \frac{D_x}{D_y} y^2} = \sqrt{x^2 + \frac{\alpha_x y^2}{\alpha_y}} \tag{12.15}$$

and Q is the injected volume discharge under the assumption that the natural groundwater flow is not affected.

The dimensionless function $W(u, \frac{r}{B})$ that appears in Eq. (12.12) is the same as the one used to describe the hydrodynamic behavior of a semi-confined aquifer (see Sect. 3.2.1); the meaning of the variables in the argument is clearly different, however.

The steady state solution ($t \rightarrow \infty$) was derived by Bear [2]:

$$\frac{C(x, y)}{C_0} = \frac{Q}{2\pi b n_e \sqrt{D_x D_y}} \cdot \exp\left(\frac{x}{B}\right) \cdot K_0\left(\frac{r}{B}\right), \tag{12.16}$$

where K_0 is the modified Bessel function of the second kind and order zero. Figure 12.7 shows the steady state concentration distribution in the x, y plane.

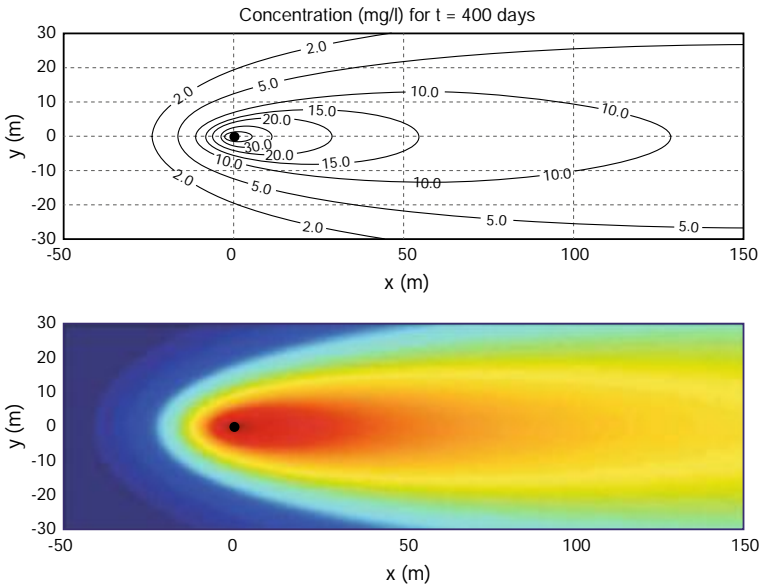


Fig. 12.7 Transport of a conservative solute in a two-dimensional geometry with a continuous input in $x = 0, y = 0$

12.3 Three-Dimensional Geometry

The differential equation of mass transport, or advection-dispersion equation, is:

$$D_x \frac{\partial^2 C}{\partial x^2} + D_y \frac{\partial^2 C}{\partial y^2} + D_z \frac{\partial^2 C}{\partial z^2} - v \frac{\partial C}{\partial x} = \frac{\partial C}{\partial t}, \tag{12.17}$$

having taken the x axis as the longitudinal axis coinciding with the groundwater flow direction.

12.3.1 Point Source, Pulse Input

In this case, the aquifer is considered unlimited in the three directions x, y and z . The contaminant is introduced in a single pulse in the point $(0, 0)$. Baetsl derived the analytical solution [1]:

$$C(x, y, z, t) = \frac{m}{8(\pi t)^{3/2} n_e \sqrt{D_x D_y D_z}} \cdot \exp \left[-\frac{(x - vt)^2}{4 D_x t} - \frac{y^2}{4 D_y t} - \frac{z^2}{4 D_z t} \right] \tag{12.18}$$

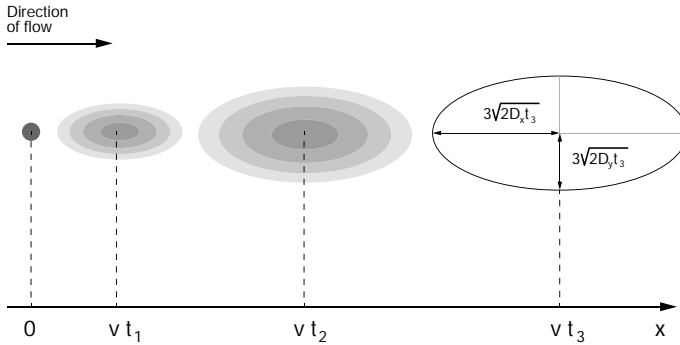


Fig. 12.8 Evolution over time and in space of a contaminant plume deriving from a point source with pulse input

where m is the released mass.

Naturally, the maximum concentration will be found along the longitudinal flow direction, in correspondence of the center of the contaminant plume, and will have coordinates and value:

$$\begin{aligned}
 y &= 0, \\
 z &= 0, \\
 x &= vt, \\
 C_{\max} &= \frac{m}{8(\pi t)^{3/2} n_e \sqrt{D_x D_y D_z}}. \tag{12.19}
 \end{aligned}$$

The size of the plume increases over time (see Fig. 12.8), following the evolution of the standard deviation:

$$\sigma_x = \sqrt{2D_x t}; \quad \sigma_y = \sqrt{2D_y t}; \quad \sigma_z = \sqrt{2D_z t}.$$

The plume delimited by $3\sigma_x$, $3\sigma_y$, $3\sigma_z$ contains 99.7% of the contaminant mass.

The Baetsl solution is perfect for the analysis of contamination incidents that involve an almost instantaneous point release, such as tanker overturnings, quick leaks from a tank, etc.

12.3.2 Plane Source, Continuous Input

This analytical solution, known as Domenico and Robbins' model, refers to a vertical plane source of width Y and height Z , in a semi-unlimited aquifer (see Fig. 12.1) [4]:

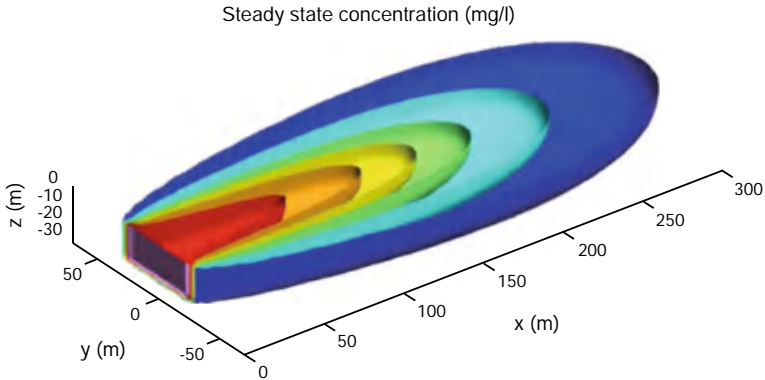


Fig. 12.9 Three-dimensional evolution of a contaminant plume released from a plane source with continuous input (modified from [8])

$$\frac{C(x, y, z, t)}{C_0} = \frac{1}{8} \operatorname{erfc} \left[\frac{x - vt}{2\sqrt{D_x t}} \right] \cdot \left\{ \operatorname{erf} \left[\frac{y + Y/2}{2\sqrt{\frac{D_y x}{v}}} \right] - \operatorname{erf} \left[\frac{y - Y/2}{2\sqrt{\frac{D_y x}{v}}} \right] \right\} \cdot \left\{ \operatorname{erf} \left[\frac{z + Z}{2\sqrt{\frac{D_z x}{v}}} \right] - \operatorname{erf} \left[\frac{z - Z}{2\sqrt{\frac{D_z x}{v}}} \right] \right\} \quad (12.20)$$

Figure 12.9 shows the three-dimensional concentration distribution obtained from Domenico and Robbins' solution.

Along the vertical symmetry plane $y = 0$ the following can be obtained (for $\operatorname{erf}(-\beta) = -\operatorname{erf}(\beta)$):

$$\frac{C(x, y, z, t)}{C_0} = \frac{1}{4} \operatorname{erfc} \left[\frac{x - vt}{2\sqrt{D_x t}} \right] \cdot \operatorname{erf} \left[\frac{Y}{4\sqrt{\frac{D_y x}{v}}} \right] \cdot \left\{ \operatorname{erf} \left[\frac{z + Z}{2\sqrt{\frac{D_z x}{v}}} \right] - \operatorname{erf} \left[\frac{z - Z}{2\sqrt{\frac{D_z x}{v}}} \right] \right\} \quad (12.21)$$

And, analogously, along the x -axis ($y = 0, z = 0$):

$$\frac{C(x, y, z, t)}{C_0} = \frac{1}{2} \operatorname{erfc} \left[\frac{x - vt}{2\sqrt{D_x t}} \right] \cdot \operatorname{erf} \left[\frac{Y}{4\sqrt{\frac{D_y x}{v}}} \right] \cdot \operatorname{erf} \left[\frac{Z}{2\sqrt{\frac{D_z x}{v}}} \right] \quad (12.22)$$

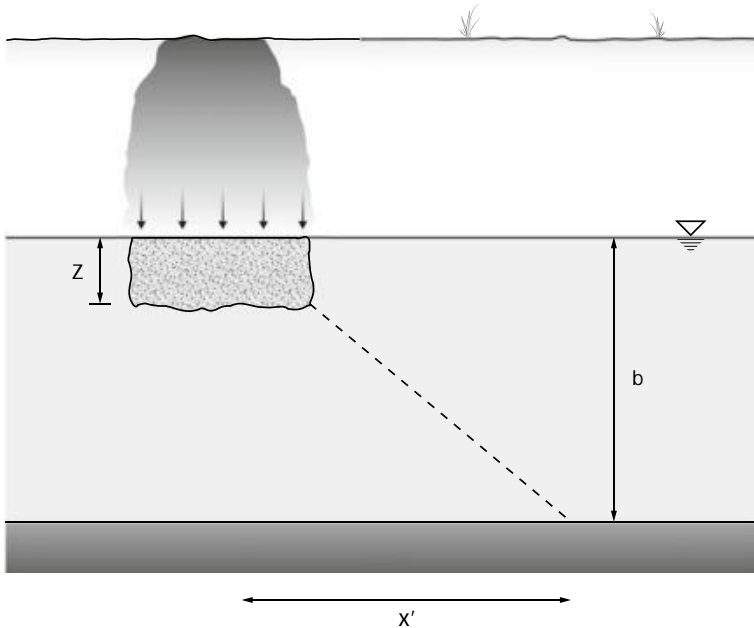


Fig. 12.10 Vertical dispersion of a contaminant limited by the achievement of the base of the aquifer

For D_y and D_z that tend to zero $\text{erf}(\infty) = 1$, which yields once again the Ogata-Banks solution.

If the saturated thickness of the aquifer is small, within a short distance and time the entire vertical section of the aquifer will be affected by the contamination plume (see Fig. 12.10).

To a first approximation, the distance x' at which the entire saturated thickness is contaminated is equal to [3]:

$$x' = \frac{(b - Z)^2}{\alpha_z}. \quad (12.23)$$

Domenico and Robbins' solution is, of course, only valid for $x \leq x'$. For $x > x'$ it is necessary to use the constant value x' in the denominator of the argument of the erf function.

References

1. L. Baetslé, Migration of radionuclides in porous media, *Progress. Nuclear Energy Series XII, Health Physics* (Pergamon Press, London, 1969), pp. 707–730
2. J. Bear, *Dynamics of Fluids in Porous Media* (Courier Corporation, 1972)

3. P.A. Domenico, V.V. Palciauskas, Alternative Boundaries in Solid Waste Management. *Ground Water* **20**, 303–311 (1982)
4. P.A. Domenico, G.A. Robbins, A New Method of Contaminant Plume Analysis. *Ground Water* **23**, 476–485 (1985)
5. A. Ogata, R. Banks, A solution of the differential equation of longitudinal dispersion in porous media, USGS Numbered Series 411-A (1961)
6. J.-P. Sauty, An analysis of hydrodispersive transfer in aquifers. *Water Resour. Res.* **16**, 145–158 (1980)
7. J.L. Wilson, P.J. Miller, Two-dimensional plume in uniform groundwater flow. *J. Hydraul. Eng.* **104**, 503–514 (1978)
8. V. Zolla, Analisi dei fenomeni di contaminazione da Fe, Mn e Ni nelle acque sotterranee mediante applicazione di modelli numerici, Italian, thesis dissertation in environmental engineering (Politecnico di Torino, Torino, 2004)

Chapter 13

Analytical Solutions of the Differential Equation of Mass Transport for Reactive Solutes



Abstract Having provided a few analytical solutions for conservative solutes in the previous chapter, here the focus is on reactive solutes. The underlying hypotheses considered to be verified in order to obtain such solutions are the same as in the case of conservative solutes, with the additional requirement that: natural degradation can be described by first-order kinetics and the sorption isotherm is linear. Solutions for continuous and pulse releases are provided for one-, two-, and three-dimensional geometries, with line sources being considered in 2D geometries, and point and plain sources being hypothesized in 3D geometries.

As previously anticipated, reactive (or non-conservative) solutes are those substances for which physico-chemical and biological phenomena that occur concomitantly to propagation in groundwater cannot be ignored.

A few analytical solutions of the differential equation of mass transport, valid under the hypothesis that the following conditions are respected, are illustrated in the next paragraphs:

- the medium is saturated, homogeneous and isotropic;
- Darcy's law is valid;
- the flow is uniform;
- water density and viscosity are constant and independent of solute concentration;
- natural degradation can be described by first-order kinetics;
- the sorption isotherm is linear.

In the following sections a few analytical solutions to the differential equation of mass transport are illustrated.

13.1 One-Dimensional Geometry

Despite very rarely being representative of real situations, one-dimensional geometries are useful for educational purposes. The simplified structure of the equations that describe them highlight more clearly the importance and role of the concomitant

phenomena that contribute to contaminant transport, sorption and degradation. In the present chapter, degradation and sorption are first treated individually; then, the behavior of compounds undergoing both processes at the same time is investigated.

13.1.1 Continuous Input

Let us consider the system in Fig. 12.2, where the x axis coincides with the longitudinal direction of flow.

13.1.1.1 Solutes That Undergo Degradation

In this case, the differential equation that governs mass transfer of a contaminant undergoing degradation only in the liquid phase is:

$$D_x \frac{\partial^2 C}{\partial x^2} - v \frac{\partial C}{\partial x} - \lambda C = \frac{\partial C}{\partial t}, \quad (13.1)$$

where the boundary conditions are those expressed by (12.2)–(12.4).

The analytical solution for (13.1) was found by Bear [2]:

$$\begin{aligned} \frac{C(x, t)}{C_0} = & \frac{1}{2} \exp \left[\frac{vX}{2D_x} (1 - U) \right] \cdot \operatorname{erfc} \left(\frac{x - Ut}{2\sqrt{D_x t}} \right) + \\ & + \frac{1}{2} \exp \left[\frac{vX}{2D_x} (1 + U) \right] \cdot \operatorname{erfc} \left(\frac{x + Ut}{2\sqrt{D_x t}} \right), \end{aligned} \quad (13.2)$$

where $U = \sqrt{1 + \frac{4\lambda D_x}{v^2}}$.

This can be approximated as follows:

$$\frac{C(x, t)}{C_0} = \frac{1}{2} \exp \left[\frac{vX}{2D_x} (1 - U) \right] \cdot \operatorname{erfc} \left(\frac{x - Ut}{2\sqrt{D_x t}} \right). \quad (13.3)$$

The steady state solution, instead, is:

$$C(x) = C_0 \exp \left[\frac{vX}{2D_x} (1 - U) \right]. \quad (13.4)$$

In the previous equations, λ represents the degradation coefficient, a function of the compound's half-life: $\lambda = \frac{0.692}{t_{1/2}}$.

Figure 13.1 depicts the behavior of a contaminant undergoing biodegradation compared to a conservative solute.

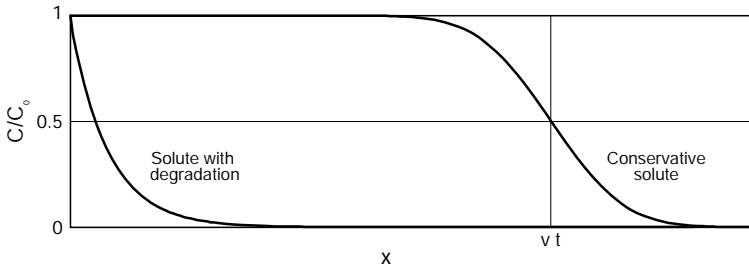


Fig. 13.1 Comparison of the concentration distribution of a conservative solute and a solute subject to degradation, in the case of continuous input of a constant concentration in $x = 0$

13.1.1.2 Solutes That Sorb to the Solid Matrix

The differential equation of reference is:

$$\frac{D_x}{R} \frac{\partial^2 C}{\partial x^2} - \frac{v}{R} \frac{\partial C}{\partial x} = \frac{\partial C}{\partial t} \quad (13.5)$$

and the boundary conditions are those expressed by (12.2)–(12.4).

The analytical solution of Eq. (13.5) is:

$$\frac{C(x, t)}{C_0} = \frac{1}{2} \left\{ \operatorname{erfc} \left[\frac{x - v_c t}{2\sqrt{D_c t}} \right] + \exp \left(\frac{v_c x}{D_c} \right) \cdot \operatorname{erfc} \left[\frac{x + v_c t}{2\sqrt{D_c t}} \right] \right\} \quad (13.6)$$

In the previous equation, $v_c = \frac{v}{R}$ and $D_c = \frac{D_x}{R}$ are the velocity and the hydrodynamic dispersion of a compound subjected to retardation (i.e., $(v_c < v)$), respectively. The solution coincides with the Ogata–Banks equation, except for the replacement of v with v_c , and of D_x with D_c .

Figure 13.2 shows the concentration distribution of a conservative contaminant compared to a contaminant subject to sorption: at the same time point the latter is delayed relative to the former.

13.1.1.3 Solutes That Undergo Degradation and Sorption

The differential equation describing the transport of these solutes is:

$$\frac{D_x}{R} \frac{\partial^2 C}{\partial x^2} - \frac{v}{R} \frac{\partial C}{\partial x} - \frac{\lambda}{R} C = \frac{\partial C}{\partial t} \quad (13.7)$$

with the same boundary conditions expressed in (12.2)–(12.4).

The nonsteady state analytical solution of (13.7) coincides with solution (13.2) but for the replacement of v with $v_c = \frac{v}{R}$ and of D_x with $D_c = \frac{D_x}{R}$:

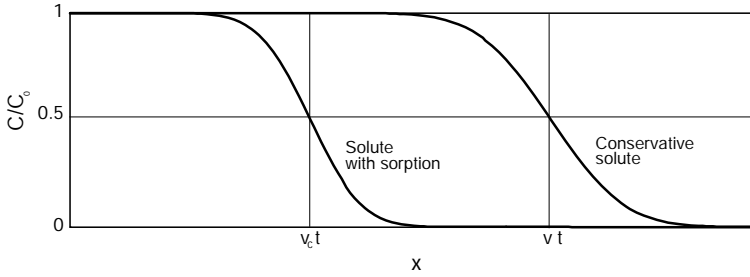


Fig. 13.2 Comparison of the concentration distribution of a conservative solute and one undergoing sorption, in the case of a continuous input of a constant concentration in $x = 0$

$$\frac{C(x, t)}{C_0} = \frac{1}{2} \exp \left[\frac{vX}{2D_x} (1 - U) \right] \cdot \operatorname{erfc} \left(\frac{x - Uvt/R}{2\sqrt{D_x t/R}} \right) + \frac{1}{2} \exp \left[\frac{vX}{2D_x} (1 + U) \right] \cdot \operatorname{erfc} \left(\frac{x + Ut/R}{2\sqrt{D_x t/R}} \right), \quad (13.8)$$

where: $U = \sqrt{1 + \frac{4\lambda D_x}{v^2}}$.

The approximate solution is:

$$\frac{C(x, t)}{C_0} = \frac{1}{2} \exp \left[\frac{vX}{2D_x} (1 - U) \right] \cdot \operatorname{erfc} \left(\frac{x - Uvt/R}{2\sqrt{D_x t/R}} \right). \quad (13.9)$$

The steady state solution is:

$$C(x) = C_0 \exp \left[\frac{vX}{2D_x} (1 - U) \right]. \quad (13.10)$$

Figure 13.3 compares the behavior of a solute that undergoes degradation, sorption or both with that of a conservative solute.

13.1.2 Pulse Input

The approximate solution to Eq. (13.7) for a contaminant introduced via a pulse input and that undergoes both degradation and sorption is:

$$C(x, t) = \frac{m}{An_e \sqrt{4\pi D_x R t}} \cdot \exp \left[-\frac{\lambda}{R} t - \frac{(x - vt/R)^2}{4D_x t/R} \right], \quad (13.11)$$

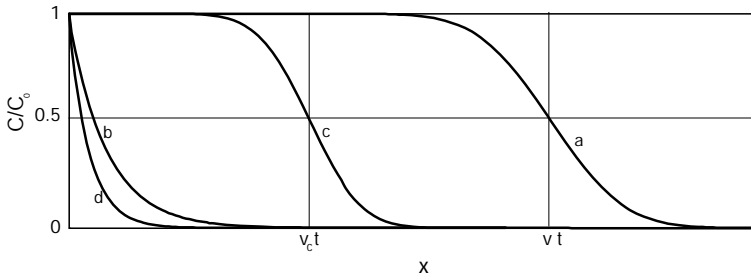


Fig. 13.3 Concentration distribution of contaminants subjected to unidirectional propagation following a continuous constant input in $x = 0$: **a** conservative (or non-reactive) contaminant; **b** contaminant undergoing degradation; **c** contaminant sorbing to the solid matrix; **d** contaminant subjected to natural degradation and sorption

where m is the contaminant mass injected at time t_0 and A the cross-sectional area of the column. Figure 13.4 shows the distribution of a reactive solute relative to a conservative one.

Since the solute is reactive, the portion of its mass present in the aqueous phase decreases during the propagation of the pulse. At the advective front, the maximum concentration is:

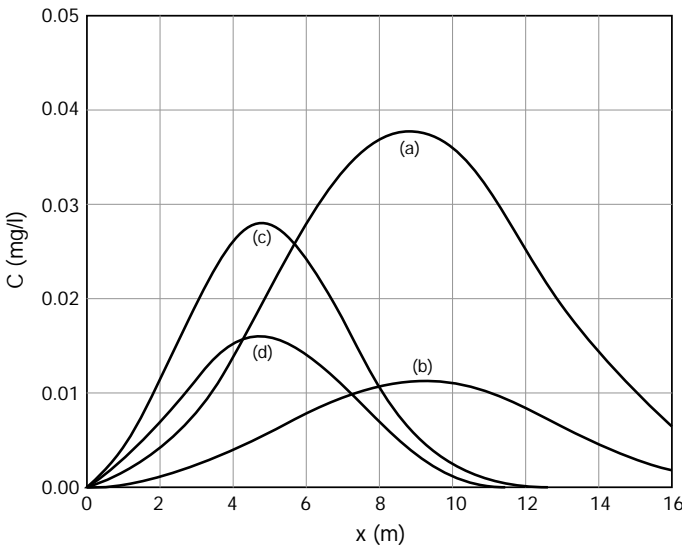


Fig. 13.4 Concentration distribution of contaminants propagating unidirectionally following a pulse input: **a** conservative (or non reactive) contaminant; **b** contaminant undergoing biodegradation; **c** contaminant undergoing sorption; **d** contaminant undergoing both biodegradation and sorption (modified from [5])

$$C_{\max} = \frac{m}{An_e\sqrt{4\pi D_x R t}} \cdot \exp\left[-\frac{\lambda}{R}t\right]. \quad (13.12)$$

13.2 Two-Dimensional Geometry

The differential equation that governs mass transport in a two-dimensional geometry is:

$$D_x \frac{\partial^2 C}{\partial x^2} + D_y \frac{\partial^2 C}{\partial y^2} - v \frac{\partial C}{\partial x} - \lambda C = R \frac{\partial C}{\partial t}. \quad (13.13)$$

13.2.1 Line Source, Pulse Input

The aquifer is assumed to extend infinitely in both the x and y directions. The contaminant is introduced with a pulse in the point $(0, 0)$ and undergoes biodegradation and sorption. The analytical solution to differential equation (13.13) is:

$$C(x, y, z, t) = \frac{m}{4\pi bn_e t \sqrt{D_x D_y}} \cdot \exp\left[-\frac{\lambda}{R}t - \frac{(x - vt/R)^2}{4D_x t/R} - \frac{y^2}{4D_y t/R}\right]. \quad (13.14)$$

The maximum concentration will be found at the advective front, with coordinates (x, y) and value (C_{\max}) equal to:

$$\begin{aligned} x &= v_c t = \frac{v}{R}t, \\ y &= 0, \\ C_{\max} &= \frac{m}{4\pi bn_e t \sqrt{D_x D_y}} \cdot \exp\left[-\frac{\lambda}{R}t\right]. \end{aligned} \quad (13.15)$$

13.2.2 Line Source, Continuous Input

The aquifer is assumed to extend infinitely in both the x and y directions. The contaminant is released into the aquifer, in the point $(0, 0)$, with known discharge and concentration. The analytical solution to the differential equation for a solution undergoing biodegradation and sorption (13.13) is:

$$\frac{C(x, y, t)}{C_0} = \frac{Q}{4\pi bn_e \sqrt{D_x D_y}} \cdot \exp\left(\frac{x}{B}\right) \cdot W\left(u, \frac{r}{B}\right), \quad (13.16)$$

where:

$$B = \frac{2D_x}{v} = 2\alpha_x, \quad (13.17)$$

$$u = \frac{r^2}{4D_x t} \cdot \frac{R}{U^2}, \quad (13.18)$$

$$r = \sqrt{\left(x^2 + \frac{D_x}{D_y} y^2\right) U^2} = \sqrt{\left(x^2 + \frac{\alpha_x}{\alpha_y} y^2\right) U^2}, \quad (13.19)$$

$$U = \sqrt{1 + \frac{2\lambda B}{v}} \quad (13.20)$$

and Q is the volume discharge injected. The dimensionless function $W(u, \frac{r}{B})$ that appears in Eq. (13.16) is the same as the one used to describe the hydrodynamic behavior of a semi-confined aquifer (see Sect. 3.2.1); the meaning of the variables in the argument is clearly different, however.

The steady state solution ($t \rightarrow \infty$) that applies to this case was determined by Bear [3]:

$$\frac{C(x, y)}{C_0} = \frac{Q}{2\pi bn_e \sqrt{D_x D_y}} \cdot \exp\left(\frac{x}{B}\right) \cdot K_0\left(\frac{r}{B}\right), \quad (13.21)$$

where K_0 is the modified Bessel function of the second kind and order zero.

13.3 Three-Dimensional Geometry

A three-dimensional geometry reflects real contaminant-transport phenomena. The differential equation of transport is:

$$D_x \frac{\partial^2 C}{\partial x^2} + D_y \frac{\partial^2 C}{\partial y^2} + D_z \frac{\partial^2 C}{\partial z^2} - v \frac{\partial C}{\partial x} - \lambda C = R \frac{\partial C}{\partial t}. \quad (13.22)$$

As for conservative solutes, also in this case there are two analytical solutions of interest for practical applications.

13.3.1 Point Source, Pulse Input

The general solution of (13.22) was determined by Baetslé [1]:

$$C(x, y, z, t) = \frac{m}{8(\pi t)^{3/2} n e \sqrt{\frac{D_x D_y D_z}{R}}} \cdot \exp \left[-\frac{\lambda}{R} t - \frac{(x - vt/R)^2}{4D_x t/R} - \frac{y^2}{4D_y t/R} - \frac{z^2}{4D_z t/R} \right], \quad (13.23)$$

where m is the contaminant mass released instantaneously and λ is the biodegradation coefficient.

For $R = 1$ and $\lambda = 0$ Eq. (13.23) coincides with (12.18), valid for conservative solutes.

The concentration peak, see Fig. 12.8, is always at the center of the contamination plume, and has coordinates (x, y, z) and value (C_{max}) equal to:

$$\begin{aligned} x &= v_c t = \frac{v}{R} t, \\ y &= 0, \\ z &= 0, \\ C_{max} &= \frac{m}{8(\pi t)^{3/2} n e \sqrt{\frac{D_x D_y D_z}{R}}} \cdot \exp \left(-\frac{\lambda}{R} t \right). \end{aligned} \quad (13.24)$$

13.3.2 Plane Source, Continuous Input

Domenico determined the general solution of Eq. (13.22) [4]:

$$\begin{aligned} \frac{C(x, y, z, t)}{C_0} &= \frac{1}{8} \exp \left[\left(\frac{vX}{2D_x} \right) (1 - U) \right] \cdot \operatorname{erfc} \left[\frac{x - Uvt/R}{2\sqrt{D_x t/R}} \right] \cdot \\ &\cdot \left\{ \operatorname{erf} \left[\frac{y + \frac{y}{2}}{2\sqrt{\frac{D_y x}{v}}} \right] - \operatorname{erf} \left[\frac{y - \frac{y}{2}}{2\sqrt{\frac{D_y x}{v}}} \right] \right\} \cdot \\ &\cdot \left\{ \operatorname{erf} \left[\frac{z + Z}{2\sqrt{\frac{D_z x}{v}}} \right] - \operatorname{erf} \left[\frac{z - Z}{2\sqrt{\frac{D_z x}{v}}} \right] \right\}, \end{aligned} \quad (13.25)$$

where $U = \sqrt{1 + \frac{4\lambda D_x}{v^2}}$. The maximum concentration value can be found along the x axis, by setting $y = 0$ and $z = 0$ in the previous equation, which results in:

$$\frac{C(x, y, z, t)}{C_0} = \frac{1}{4} \exp \left[\left(\frac{vx}{2D_x} \right) (1 - U) \right] \cdot \operatorname{erfc} \left[\frac{x - Uvt/R}{2\sqrt{D_x t/R}} \right] \cdot \operatorname{erf} \left[\frac{Y}{4\sqrt{\frac{D_y x}{v}}} \right] \cdot \operatorname{erf} \left[\frac{Z}{2\sqrt{\frac{D_z x}{v}}} \right]. \quad (13.26)$$

References

1. L. Baetslé, Migration of radionuclides in porous media, *Progress in Nuclear Energy Series XII, Health Physics* (Pergamon Press, London, 1969), pp. 707–730
2. J. Bear, *Dynamics of Fluids in Porous Media* (Courier Corporation, Chelmsford, 1972)
3. J. Bear, M. Jacobs, On the movement of water bodies injected into aquifers. *J. Hydrol.* **3**, 37–57 (1965)
4. P.A. Domenico, An analytical model for multidimensional transport of a decaying contaminant species. *J. Hydrol.* **91**, 49–58 (1987)
5. C.W. Fetter, *Contaminant Hydrogeology*, 2nd edn. (Waveland Press Inc., Long Grove, 2008)

Chapter 14

Transport of Immiscible Fluids



Abstract The previous Chapters described the transport of miscible compounds in aquifers. Here, mechanisms of immiscible compound (also called non-aqueous phase liquid, NAPL) transport and propagation is presented. To do so, relevant properties of a multi-phase system (i.e., wettability, interfacial tension and capillary pressure, effective and relative permeability, drainage and imbibition) are illustrated. Migration of NAPLs in the subsurface is then qualitatively described, separately discussing the behavior of light- and dense-NAPLs. Light-NAPLs spilled at the surface that reach the saturated zone tend to accumulate and float on the water table and spread horizontally, progressively releasing their soluble fraction into the groundwater. Dense-NAPLs are denser than water, so if they reach the saturated zone they tend to displace groundwater from the pores, penetrating vertically in the aquifer. Depending on the volume of the release, Dense-NAPL contamination may affect the entire saturated thickness, and the compound may move along base of the aquifer. As for light-NAPL, also dense NAPLs present as a pure phase act as a continuous source of contaminant by releasing their soluble fraction into the groundwater. Finally, a quantitative approach to immiscible compound transport is provided, allowing for the estimation of mass distribution in the different phases in the saturated and unsaturated zones.

In the previous chapters the analytical solutions that describe the transport of both conservative and reactive miscible contaminants in groundwater were illustrated.

In some cases, however, aquifers are contaminated with water-immiscible substances. These are organic compounds, often found in multi-component mixtures; a typical example are hydrocarbons and chlorinated organic solvents (see Chap. 9).

These substances are generically grouped under the term NAPLs (Non Aqueous Phase Liquids); they exhibit different properties and behavior from soluble contaminants (tracers), which are completely miscible with groundwater.

14.1 Properties of a Solid–Liquid Multiphase System

Understanding groundwater contamination by a NAPL is more complex than an analogous contamination by a perfectly miscible compound. In addition to knowing the properties of the contaminant itself, it is necessary to know a few fundamental characteristics of multi-phase systems in aquifers, namely:

- wettability;
- interfacial tension and capillary pressure;
- effective and relative permeability;
- drainage and imbibition.

14.1.1 Wettability

In a porous medium occupied by multiple immiscible phases it is necessary to consider the forces acting at the separation surfaces (*interfaces*) between fluids, and between each fluid and the solid phase (the grains composing the aquifer).

Wettability expresses the tendency of a fluid to be attracted to a solid surface in preference to another immiscible fluid. It is quantified by the contact angle, ϕ , measured within the fluid under consideration, and formed by the tangent to the interface between the fluids and the solid surface. A fluid is defined as *wetting* if $\phi < 90^\circ$ (perfectly wetting for $\phi = 0$), while it represents the *non-wetting* phase if $\phi > 90^\circ$, see Fig. 14.1.

Although wettability is a specific property of each mineral-fluid system, water is always the wetting fluid relative to NAPLs and air on mineral grains, with $\phi_{water} < \phi_{NAPL} < \phi_{air}$. However, certain immiscible contaminants may be wetting relative to water and air if the solid phase is composed of organic matter (e.g., peat, humus); in addition, the wetting characteristics of many contaminants remain uncertain [5, 6].

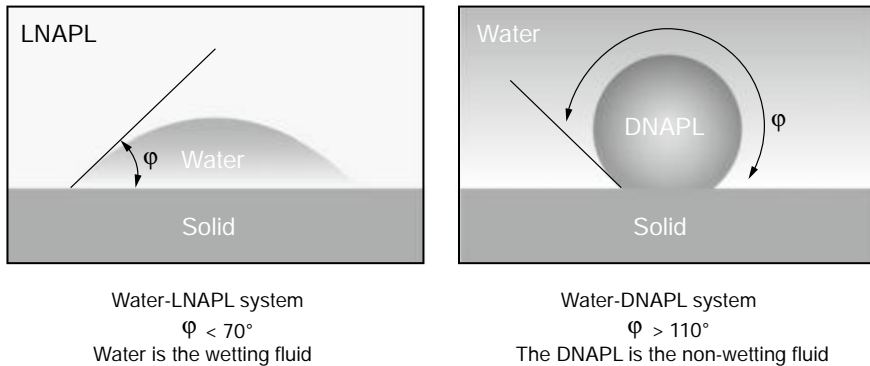


Fig. 14.1 Configurations of NAPL wettability

14.1.2 Interfacial Tension and Capillary Pressure

The forces acting at the interface between the various phases are a result of molecular actions and are called *capillary forces* because one of their most obvious manifestations is the behavior of a fluid in a capillary tube.

One of the characteristic properties of every fluid is its *surface tension*, defined as “the force acting on a liquid surface that results in a minimum liquid surface area. It is produced by the unbalanced inward pull exerted on the layer of surface molecules by molecules below the liquid surface” [7]. The term *surface tension*, that expresses the tendency of a fluid to reduce the contact area, is generally used only for liquids in contact with their vapor or, in practical terms, with air. The surface tension of water (in an air–water multiphase system) is 0.0726 N/m [6].

When there are separation surfaces between two or more liquids, or between liquid and solid, the term *interfacial tension*, σ , is used. The water–hydrocarbon interfacial tension is in the order of 0.03 N/m; the variation range of σ for the majority of NAPLs is between 0.015 and 0.050 N/m [5, 6].

Capillary pressure, p_c , is defined as the pressure difference at the interface between two immiscible fluids: in particular, it is the pressure difference measured between the non-wetting, p_{nw} , and the wetting phase, p_w [2, 6]:

$$p_c = p_{nw} - p_w. \quad (14.1)$$

If we consider a capillary tube of radius r , the capillary pressure can be calculated by applying the Laplace–Plateau law [2]:

$$p_c = \frac{2\sigma \cos \varphi}{r}. \quad (14.2)$$

In practical terms, the capillary pressure can be seen as a measure of the pressure that a non-wetting fluid needs to exert in order to displace a wetting fluid that fills a pore; or, alternatively, of the ease with which a wetting fluid fills a porous medium and repulses a non-wetting fluid [2, 5].

14.1.3 Effective and Relative Permeability

Darcy’s law regulates the flow of a single conservative fluid in a fully saturated porous medium in laminar flow conditions [6]:

$$\mathbf{q} = -\frac{k}{\mu}(\nabla p + \rho g \nabla z), \quad (14.3)$$

where \mathbf{q} is the flow velocity of the fluid, k (L^2) is the absolute (or intrinsic) permeability of the porous medium, μ and ρ are the fluid's dynamic viscosity and density, respectively; the z -axis is assumed to be directed upwards.

As long as the hypotheses underlying Darcy's law are respected, the absolute permeability depends exclusively on the porous medium (see Sect. 1.6).

When contamination events are characterized by the saturation of the porous medium with multiple immiscible phases, Darcy's law has to be generalized to account for a multi-phase flow.

If the saturation of a generic fluid is less than one, the *effective permeability* of the porous medium for that fluid is smaller than the intrinsic permeability and is a function of the saturation values of the different phases. When two or more immiscible fluids are present, the effective permeability is always smaller than the absolute permeability k .

The concomitant flow of the various phases occurs with discharges defined by Darcy's law, but according to the following generalized form [1, 5]:

$$\mathbf{q}_i = -\frac{k_i}{\mu_i} (\nabla p_i + \rho_i g \nabla z), \quad (14.4)$$

where \mathbf{q}_i is the flow velocity of the phase i , k_i (L^2) its effective permeability, and μ_i and ρ_i are its dynamic viscosity and density, respectively.

The values of effective permeability can vary significantly due to the infinite combinations of possible saturations between different phases; therefore, for simplicity, relative permeability is used.

Relative permeability is defined as the ratio of the effective permeability of a particular fluid and the absolute permeability of the medium where flow is occurring [6]:

$$k_{r,i} = \frac{k_i}{k}. \quad (14.5)$$

Therefore, in addition to the effective permeability, also relative permeabilities are non-linear functions of saturation, and their values vary between zero and a threshold value smaller than one: they represent the ratio between the discharge of the fluid under consideration at a generic value of saturation and the discharge that would be measured if saturation were equal to one. Figure 14.2 shows the evolution of relative permeability as a function of saturation.

The following statements can be derived by observing the curve [5, 6]:

- For each of the two phases a *residual saturation* can be defined, below which there is no flow and the effective permeability (and thus also the relative permeability) is null. The two threshold saturations are called residual saturation of the wetting and of the non-wetting phase, respectively.
- In the case of the wetting phase, it is called *irreducible* or *pendular saturation* because the fluid wets the rock in the form of pendular rings that are not interconnected; for values greater than equilibrium, one refers to *funicular saturations*,

because the pendular rings join and the fluid acquires phase continuity and can flow.

- Analogously, for the non-wetting phase the residual saturation is called *insular saturation*, because the fluid is split up into discontinuous blobs that cannot flow through pore constrictions; above equilibrium values the saturation is, again, called funicular.
- The sum of the relative permeabilities of two phases flowing concomitantly is smaller than one: in other words, the flow of one phase reduces the flow capability of the other.

The residual saturation of a NAPL varies between 0.1 and 0.2 and between 0.1 and 0.5 in the unsaturated and the saturated zones, respectively.

14.1.4 Imbibition and Draining

While penetrating a porous medium, immiscible fluids tend to displace (and replace) one another via dynamic processes, i.e. imbibition and draining. *Imbibition* is the displacement of the non-wetting phase by the wetting fluid (e.g., water percolating through the unsaturated zone); conversely, *draining* is the displacement of the wetting fluid by the non-wetting phase (e.g., penetration of a NAPL in an aquifer) [5, 6].

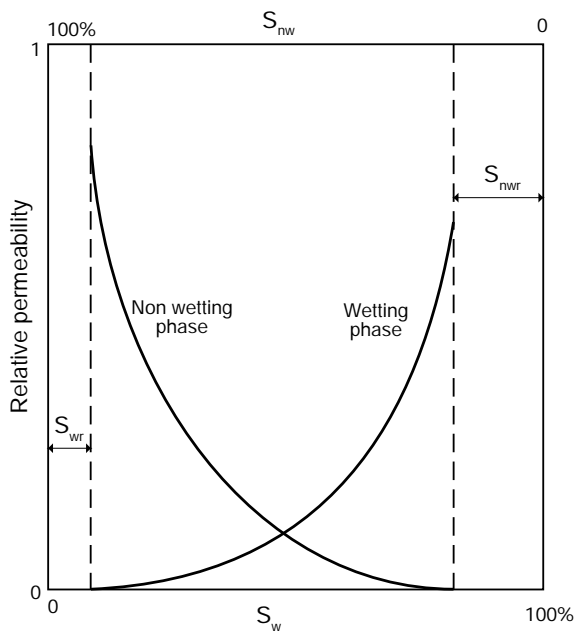


Fig. 14.2 Relative permeabilities in a multiphase system as a function of the fluids saturations. S_w and S_{wn} are the saturations of the wetting and non-wetting phases, respectively; S_{wrf} and S_{wnr} are the residual saturations of the wetting and non-wetting phases, respectively

Draining only starts happening in the presence of a 100% saturation of the wetting phase, i.e. in a saturated uncontaminated aquifer. For a DNAPL particle to displace water, a threshold capillary pressure (also called *displacement* or *entry pressure*) has to be overcome, the value of which is all the greater the smaller the aquifer permeability (and the smaller r). As saturation decreases, capillary pressure increases, and so does the pressure that needs to be applied to displace water in increasingly smaller pores. When the capillary pressure is too high, drainage (and thus contamination) stops: not all the water is replaced and its saturation at the end of the draining process is called *residual water saturation* or *residual wetting-phase saturation*, S_{wr} , or—mainly in the petroleum field—*irreducible water saturation*. For this saturation value, p_c tends to infinity [6].

The imbibition process starts with a gradual decrease in saturation in the non-wetting fluid (Fig. 14.3, *main imbibition curve*). However, as can be observed, the imbibition curve does not overlap with the drainage curve; this deviation is called *hysteresis*. When the capillary pressure decreases to zero, not all the DNAPL has been displaced: a certain amount, the *residual saturation of the non-wetting phase*, S_{nwr} , remains definitively trapped in the porous medium. An additional draining process drives the system along the so-called *main* (or *secondary*) *drainage curve*

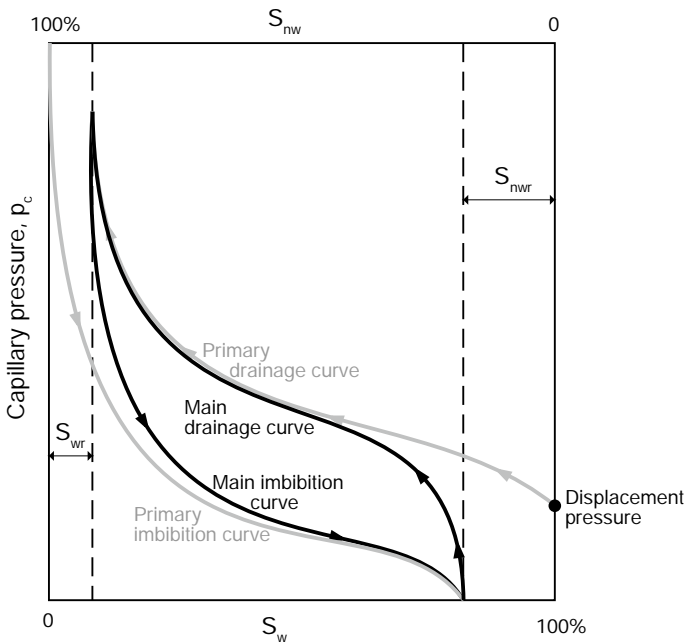


Fig. 14.3 Capillary pressure curves during draining and imbibition processes in a multiphase system. S_w and S_{nw} are the saturations of the wetting and non-wetting phases, respectively; S_{wr} and S_{nwr} are the residual saturations of the wetting and non-wetting phases, respectively (modified from [6])

that is distinct from the primary curve due to the fact that at this point the aquifer is already contaminated with a NAPL. Paths corresponding to intermediate saturation values (i.e., comprised between the residual saturation of the individual phases) are found between the primary drainage and imbibition curves [4, 6].

14.2 Qualitative Models of NAPL Behavior in the Ground

Let us consider the release of a NAPL on the soil surface or in superficial ground. With time, the substance will percolate through the unsaturated zone and toward the water table under the force of gravity.

In the unsaturated zone, water is the wetting phase, while air and the NAPL are the non-wetting phases; the NAPL is wetting relative to air in regard to the film of water surrounding the grains of the solid matrix.

Once the threshold pressure is overcome, the NAPL moves from pore to pore displacing air (or, more generically, soil gases) and water present in the center of the pores; it is incapable, however, of displacing the film of water around the solid grains. The NAPL will continue to move until its saturation in the unsaturated zone reaches its residual value, S_{nwr} .

If the contaminant spill is not continuous, the volume of free substance decreases progressively, because a part of it is trapped as S_{nwr} in the previously drained pores. If the release was relatively small, migration through the unsaturated zone might stop before the water table is reached, assuming that the entire volume introduced is distributed in the unsaturated pores at a saturation value of S_{nwr} .

While they migrate towards the water table, NAPLs also tend to spread laterally due to the contrasting action of capillary pressures and to the presence of levels with looser or denser packing, or with reduced hydraulic conductivity [6].

If the released volume is large enough for the contaminant to reach the capillary fringe and the water table, the density of the NAPL has to be considered in order to describe its behavior.

14.2.1 Behavior of LNAPLs

Following a spill, LNAPLs percolate through the unsaturated medium till they reach the capillary fringe. Here, water saturation increases progressively to unity and, concomitantly, LNAPL's relative permeability decreases. As water saturation increases, buoyancy forces become relevant and the lighter fluids (e.g., BTEX and other fuels) accumulate and float on the water table.

Right below the source, LNAPLs rest on the water table in a typical *pancake* configuration that concerns the capillary fringe and the top of the saturated zone.

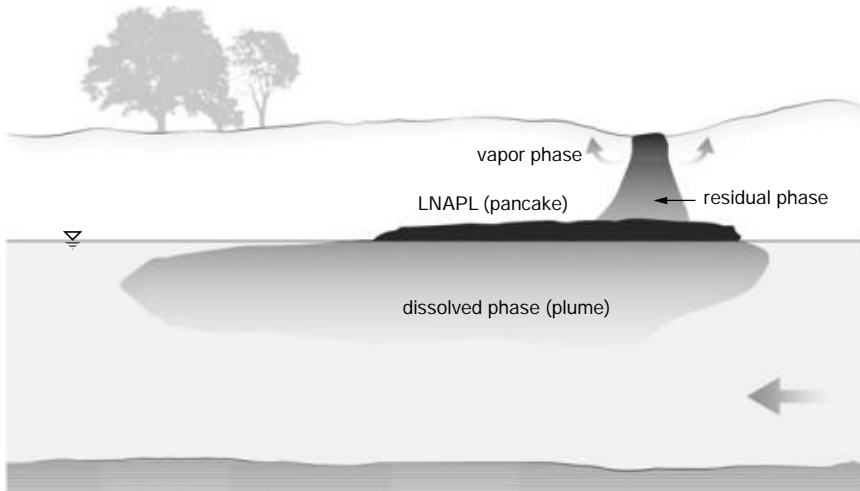


Fig. 14.4 LNAPL behavior in the ground

As depicted in Fig. 14.4, the pancake spreads also upgradient, although of course it mainly develops along the groundwater flow direction.

The water flowing in contact with the LNAPL brings the soluble fractions of the mixture into solution, forming a plume that develops in the flow direction. BTEX compounds, which represent a significant human health hazard, are among the components that are, albeit partly, solubilized [6].

The spatial distribution of contaminants strongly depends on the release conditions. The release of a significant amount of LNAPL in a short time determines quick percolation with significant lateral spreading, which leads to the formation of an upside-down cone containing the contaminant at its residual saturation. In addition, when a large volume of LNAPL reaches the capillary fringe in a short time, it causes a depression in the water table, the extent of which depends on the amount and density of the product. In these cases, the compound is mainly dispersed in the capillary fringe, where it moves until it reaches its residual saturation, and its relative permeability equals zero [5].

Conversely, in the case of small releases distributed over time, the contaminant moves mainly along paths with higher permeability; the extent of lateral spreading and the amount of immobilized product at its residual saturation are considerably smaller; therefore, the majority of the introduced contaminant reaches the water table.

14.2.2 Behavior of DNAPLs

The defining feature of DNAPLs is that their density is greater than water. They cross the unsaturated zone with less lateral spreading than LNAPLs, unless they encounter

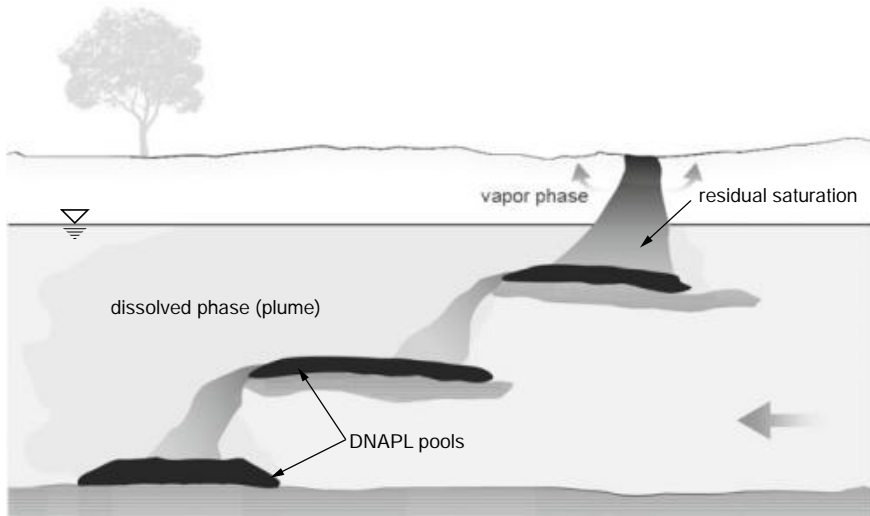


Fig. 14.5 DNAPL behavior in the ground in the case of significant release or continuous input

layers with reduced permeability. Once they reach the water table, they tend to displace water due to their greater density. If the introduced volume is significant or the input is continuous, the displacement can affect the entire saturated thickness of the aquifer, and DNAPLs can accumulate on the underlying impermeable layer. Once they reach the base of the aquifer, they tend to move in the direction of the topographic slope, which might not coincide with the groundwater flow direction. In the capillary fringe and in the aquifer DNAPLs spread laterally until they reach their residual saturation (see Fig. 14.5) [5, 6, 8]. These zones at residual saturation, as in the case of LNAPLs, represent a permanent source of contaminants dissolved in water.

If, instead, the DNAPL volume is limited and the source isn't continuous, the compound probably won't reach the base of the aquifer, and will stop at the depth at which it reaches the residual saturation. Figure 14.6 illustrates this situation.

The final configuration of a DNAPL contamination is strongly conditioned by the degree of heterogeneity of the aquifer, as well as the spill conditions [5, 6].

14.3 Secondary Contamination Due to NAPLs

NAPLs represent both a direct and a secondary source of contamination. Regardless of their presence in the ground as a free product or at residual saturation, they are capable of releasing gaseous compounds via volatilization in the unsaturated zone and liquid components by solubilization in the saturated zone.

The process of secondary contamination is worsened by effective infiltration, which carries the most soluble components of the released contaminant from the unsaturated area to the aquifer.

Even though in absolute terms the solubility of these compounds is not high (see Table 9.5), it is still much greater than the threshold values for human consumption, which are extremely low (of the order of $\mu\text{g/l}$).

The soluble fraction of a NAPL behaves like a miscible contaminant, and is, therefore, subject to the hydrological, physico-chemical, and biological processes described in Chap. 10. Therefore, the size and features of the contamination plume depend on the characteristics of the aquifer and of the contaminant.

14.4 Quantitative Approach

After highlighting the numerous factors that affect the evolution of a NAPL contamination process, a simplified geological model (i.e., homogeneous and isotropic medium) can be used to derive a few quantitative relations to solve simple problems concerning groundwater contamination with immiscible compounds.

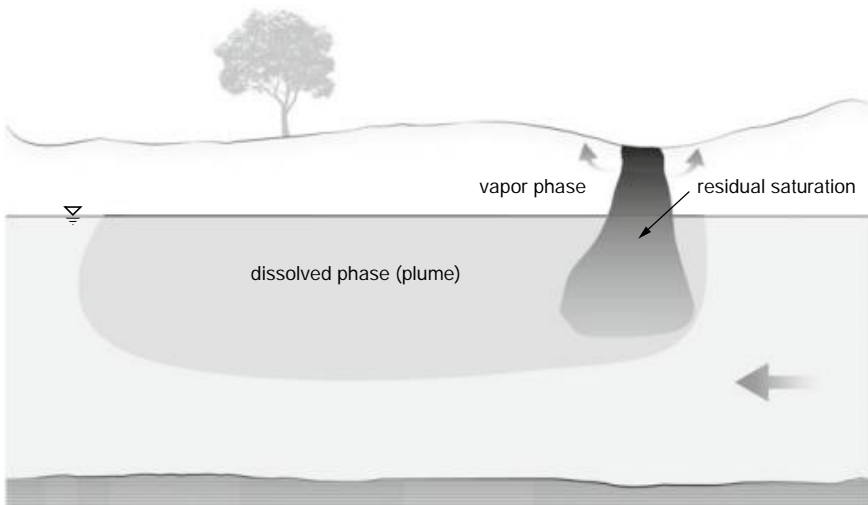


Fig. 14.6 Behavior of a DNAPL in the case of a small volume spill

14.4.1 Geometrical and Temporal Characterization

There are a few simple relations that characterize a NAPL contamination from a spatial and temporal point of view. If we indicate with V_{spill} the released volume of NAPL, and with S_{nwr} its residual saturation, the volume of the portion of aquifer affected by the contamination is:

$$V_{res} = \frac{V_{spill}}{nS_{nwr}}, \quad (14.6)$$

and the depth of the contaminated portion of aquifer:

$$L = \frac{V_{res}}{A}, \quad (14.7)$$

where A is the surface of the source of contamination.

The time required to dissolve an accumulated mass, M , of DNAPL exiting from the source zone with a groundwater concentration, C , is:

$$t = \frac{M}{vn_e C A_{tran}} \quad (14.8)$$

where A_{tran} is the cross-section of the DNAPL, measured perpendicularly to the groundwater flow direction.

14.4.2 NAPL Mass Distribution

A NAPL contamination event has, as primary and secondary effect, the distribution of the compound's (or compounds') mass in different phases.

In the unsaturated zone, four different phases can coexist: NAPL in its pure state (as a free product or at residual saturation), dissolved in the water present in the vadose zone, as a vapor, and sorbed to the grains composing the geological formation.

In the saturated zone, instead, three different phases can be found: pure NAPL, dissolved in water and sorbed to the solid matrix.

The distribution of mass in these phases depends on the parameters that control volatilization, dissolution and sorption processes [3].

14.4.2.1 Distribution in the Unsaturated Zone

The mass of NAPL dissolved in the aqueous phase is given by the product of the effective solubility, s_e , and the volume of water present in the unsaturated zone:

$$M_w = s_e \cdot S_{wr} \cdot V_v = s_e \cdot S_{wr} \cdot n \cdot V_b, \quad (14.9)$$

with S_{wr} being the residual water saturation, V_v the porous volume, and V_b the bulk volume.

Therefore, the mass per unit volume is:

$$\frac{M_w}{V_b} = s_e \cdot S_{wr} \cdot n = s_e \cdot \theta_{wr}, \quad (14.10)$$

where $\theta_{wr} = S_{wr} \cdot n$ is the residual water content.

The mass sorbed to the solid surface, M_s , is:

$$M_s = K_d \cdot C_w \cdot (\rho_b \cdot V_b), \quad (14.11)$$

and, therefore, the mass per unit volume:

$$\frac{M_s}{V_b} = \rho_b \cdot K_d \cdot C_w = \rho_b \cdot K_{oc} \cdot f_{oc} \cdot C_w. \quad (14.12)$$

When a pure NAPL phase is present, the dissolved concentration, C_w , should be replaced by the effective solubility, s_e .

The mass of NAPL present as a pure phase, M_N , is, of course, given by the product of its density, ρ_N , by its volume, V_N ; thus:

$$M_N = \rho_N \cdot V_N = \rho_N \cdot S_{nr} \cdot n \cdot V_b, \quad (14.13)$$

and the mass per unit volume is:

$$\frac{M_N}{V_b} = \rho_N \cdot S_{nr} \cdot n = \rho_N \cdot \theta_{nr}, \quad (14.14)$$

where θ_{nr} is the residual NAPL content.

Finally, the mass of NAPL in the gaseous phase, M_g , is given by the product of the molecular weight, P_{mol} , and the number of moles, N_{mol} , present in the considered volume:

$$M_g = N_{mol} \cdot P_{mol} = \frac{p_v \cdot V_b \cdot \theta_a}{z \cdot R \cdot T} \cdot P_{mol}, \quad (14.15)$$

so the mass per unit volume is:

$$\frac{M_g}{V_b} = \frac{p_v \theta_a}{R \cdot T} \cdot P_{mol}, \quad (14.16)$$

having assumed $z = 1$ at almost atmospheric pressure.

By applying the above formulas to a practical case, it emerges clearly that most of the mass is present in the pure state at residual saturation and, to a lesser extent, sorbed to the solid matrix.

This is unfortunate because these are the two most difficult forms of contamination to remediate, whereas it would be easier to get rid of vapors (by extraction) or of the dissolved phase (by pumping or other techniques, see Chap. 17 for further detail) [5, 6].

14.4.2.2 Distribution in the Saturated Medium

When a DNAPL accesses the aquifer, its mass distributes in three phases: pure, dissolved, and sorbed to the solid surface:

$$\frac{M_N}{V_b} = \rho_N \cdot S_{nwr} \cdot n = \rho_N \cdot \theta_{nwr}, \quad (14.17)$$

$$\frac{M_w}{V_b} = C_w \cdot (1 - S_{nwr}) \cdot n = C_w \cdot (n - \theta_{nwr}), \quad (14.18)$$

$$\frac{M_s}{V_b} = \rho_b \cdot K_d \cdot C_w. \quad (14.19)$$

Only (14.18) is different from the unsaturated zone. Of course, the total mass is the sum of the individual phases.

14.5 Concluding Remarks

Addressing groundwater contamination with NAPLs is complex because the pollutant is almost always composed of a mixture of compounds, each of which has a specific behavior that can be significantly different from the others.

According to the typical behavior of multiphase systems in porous media (capillary pressure, residual saturation, relative permeabilities), NAPLs remain trapped at their residual saturation both in the unsaturated and the saturated medium. This is one of the reasons why NAPLs are hard to identify in many *in situ* investigations.

In many cases, the presence of a NAPL can be visually confirmed by observing whether hydrocarbons are present as a free phase in wells, floating on the water, or whether they impregnate extracted soil cores.

In other cases, however, the presence of NAPLs is difficult to confirm because hydrocarbons trapped at their residual saturation in the soil pores do not flow towards monitoring wells and are hard to observe directly in the cores. Sometimes, even when direct investigation methods are available (such as the analysis of concentrations in the soil), not all doubts can be dispelled.

The mass of NAPL present in the form of residual saturation is usually much greater than the dissolved mass forming the typical *plume*. Suffice to think that the concentration of dissolved hydrocarbons is measured in ppm or ppb (i.e., 1 g of hydrocarbon per 10^6 or 10^9 g of water, respectively), while the residual NAPL phase is defined in terms of saturation as a percentage of the porous volume.

The importance of the dissolved phase is tied only to the potentially high migration rate. However, it should be highlighted that large amounts of NAPL in the ground can invalidate any groundwater remediation attempt, because they become sources that release soluble fractions of contaminant into the groundwater and feed the aquifer contamination for an extremely long time.

On the other hand, capillary forces (related to the immiscibility of fluids) hinder, or make impossible, the complete removal of a NAPL that has penetrated the ground. For example, the exploitation of an oilfield usually leaves behind two thirds of the resources present in the reservoir: sophisticated assisted recovery techniques can yield between 40 and 70% of the oil, under optimal operating conditions. These values are acceptable in oilfield exploitation, but are utterly insufficient in the environmental field.

In order for an aquifer contaminated with hydrocarbons to recover its potable use, no less than 99% of the NAPL should be removed, since the maximum allowed concentrations are in the order of ppb.

This limit is definitely unattainable with conventional techniques (pumping), and possibly also with more advanced techniques. The results that can be achieved are in any case tied to the nature of the solid matrix, the type of contamination, and the amount of available resources (see Chap. 17).

References

1. K. Aziz, A. Settari, *Petroleum Reservoir Simulation*. English, OCLC: 839733832 (Elsevier Applied Science, London, 1979)
2. J. Bear, *Dynamics of Fluids in Porous Media* (Courier Corporation, North Chelmsford, 1972)
3. J.R. Boulding, J.S. Ginn, *Practical Handbook of Soil, Vadose Zone, and Ground-Water Contamination: Assessment, Prevention, and Remediation*, 2nd edn. (CRC Press, Boca Raton, 2004)
4. H.J. Diersch, *FEFLOW Finite Element Subsurface Flow & Transport Simulation System - Reference manual* (WASY GmbH, 2002)
5. P.A. Domenico, F.W. Schwartz, *Physical and Chemical Hydrogeology* (Wiley, New York, 1998)
6. A. Mayer, S.M. Hassanizadeh, *Soil and Groundwater Contamination: Nonaqueous Phase Liquids-Principles and Observations, Water Resources Monograph 17* (American Geophysical Union, Washington, D.C., 2005)
7. T.M. Pankratz, *Environmental Engineering Dictionary and Directory* (CRC Press, Boca Raton, 2000)
8. F. Schuille, *Dense Chlorinated Solvents in Porous and Fractured Media: Model Experiments* (Lewis Publishers, Boca Raton, 1988)

Chapter 15

Characterization of a Contamination Event



Abstract This chapter provides a methodological approach for the characterization of a contamination event. This includes an examination of both the unsaturated (i.e., soil, soil gas and pore water) and the saturated media (i.e., soil and groundwater), and is structured around three main phases, i.e., collection and organization of existing data, development of a conceptual model, verification of the hypotheses made in the conceptual model through targeted investigations and sampling. After illustrating different strategies available for defining the sampling design, sampling techniques for the different phases of the unsaturated and saturated media are described. In the unsaturated medium, soil sampling can be carried out through rotary or direct push techniques; active and passive sampling methods are available for the collection of soil gas samples; lysimeters or filter-tip samplers can be used for sampling pore water. Sampling of the saturated medium should allow to obtain a three-dimensional reconstruction of the contaminated areas. Hence, recommendations on the spatial distribution of monitoring wells, on the available options for vertical sampling and on well-purging prior to sampling are provided. These aspects are fundamental for ensuring the collection of representative samples. Subsequently, the most important aspects that need to be kept into account when planning a sampling campaign are illustrated, in particular as regards sampling rate, sample collection method, sampling devices (e.g., bailers, pumps). On site measurement of water quality parameters is also considered, and the possibility of filtering samples during collection is discussed. Quality assurance and control protocols aimed at ensuring accuracy, precision and defensibility of acquired data are then illustrated. Finally, a brief overview of sample storage, blank collection and sampling materials is provided.

In this chapter a methodological approach is offered for the characterization of contamination in the unsaturated medium, which includes soil, soil gas, and pore water, and in the saturated medium, i.e., in groundwater and soil. The full approach entails [7]:

- the physical characterization of the affected environmental components (e.g., determination of the aquifer's hydraulic behavior and hydrodynamic parameters);
- the characterization of the contamination itself (i.e., determination of the type of contamination and its extension in each environmental component; measurement

of contamination levels and identification of values exceeding acceptable thresholds; identification of hotspots).

However, since the first point has already been thoroughly addressed in Chap. 4, the present chapter is focused on the characterization of the contamination, structured in the following phases [16].

- Collection and organization of existing data. All information regarding the site, previously carried out operations, stocked materials, and surrounding environment needs to be recovered.
- Development of a preliminary conceptual model. Specific characteristics of the site are described in terms of: source of contamination; degree and extension of the contamination of surface and subsurface soil, of surface and ground-water, on the site and in the affected surrounding area; potential migration paths from the sources of contamination to the environmental targets and the population. This schematic representation of the site represents the foundation for appropriately planning detailed characterization investigations and remediation interventions.
- Planning and carrying out investigations aimed at: verifying all the hypotheses made in the conceptual model based on previously available data.

15.1 Sampling Design

The number, location, and timing of sampling points should be planned in order to meet the predetermined contamination characterization objectives, such as the assessment of the level and spatial distribution of contaminants in the various environmental components. To this aim, a sampling design strategy must be developed such that the collected data is representative of the area of investigation and appropriate for the intended application; furthermore, minimal resource expenditure should be a goal.

The investigated area and the ensemble of individual items of interest it comprises represent the *target population* (e.g., the part of an aquifer that is thought to be affected by a contaminant spill); the part of the target population that can be accessed for sampling and data collection is called *sampled population* (e.g., the part of land above the aquifer that is not occupied by buildings) and the individual items of this population that could potentially be sampled are the *sample units*. *Blank samples* are, instead, those collected in areas neighboring the area of interest, which are unaffected by the contamination. Samples have to be collected in all investigated environmental components and their number varies as a function of the characteristics of the area, but should always be equal or greater than three.

There are several sampling design strategies, which fall into two main categories: probabilistic and judgmental [7, 11]. When a probabilistic sampling design method is employed, sampling units are selected randomly or in a deterministic way, and the data collected from them can be used to draw statistical inferences about the

sampled population and, by extension, about the target population with a calculable degree of uncertainty. Conversely, in judgmental sampling design, expert knowledge or professional judgment are used to choose sampling units and interpret collected data; in this case, therefore, precision of the interpretations cannot be established. A description of the most relevant probabilistic sampling design strategies and further details about judgmental sampling design follow [7].

- *Judgemental sampling.* Sampling design is based on the conceptual model developed from knowledge of the site and on professional judgment. This method can be used for the actual sampling strategy, or as a preliminary step in a more complex sampling procedure. It is most effective when the site has been previously characterized; on the contrary, it may be problematic in the case of complex situations or of scarce information on the history of the site.
- *Systematic and regular grid sampling.* The position of the first sampling unit is set randomly, and all the following are established according to a regularly spaced network of locations (Fig. 15.1). A simple strategy for the definition of a square sampling grid is the identification of the distance between two neighboring lines of the grid. This distance can be calculated, for example, as follows:

$$G = \sqrt{A/n},$$

where G is the distance to be defined, A is the surface area of the site under consideration, and n is the number of sampling units [3].

- *Simple random sampling.* The location of the sampling units is randomly selected from a list of all possible sampling units or by randomly determining their geographical coordinates (Fig. 15.2). This method is particularly useful when the target population is known to be relatively homogeneous and there are no hot spots (or they can be excluded).
- *Stratified sampling.* In this case the sampling units are identified after dividing the sampled population into non-overlapping strata, or sub-populations, that are considered to be more homogeneous (Fig. 15.3). The identification of the sub-populations is based on prior knowledge of the site or on expert judgment. An advantage of this method is that it provides structure to the investigation, by ensuring that sampling occurs in homogeneous areas; this reduces the variability between sampling units (within the same sub-population) and the overall accuracy of the estimates. However, often, operational complexity hinders the classification of the sampling units into distinct and separate strata, which is necessary for employing stratified sampling.
- *Ranked set sampling.* By combining simple random sampling with the professional judgment of a field investigator, this method increases the chances of selecting significant samples and reduces the number of samples to be analyzed with expensive methods, favoring the use of on site analysis with portable, more cost effective instruments. The first step consists in randomly sampling m sets of units and analysing r samples per selected set with fast and inexpensive procedures. The r samples are then ranked based on the collected data. Professional judgment is

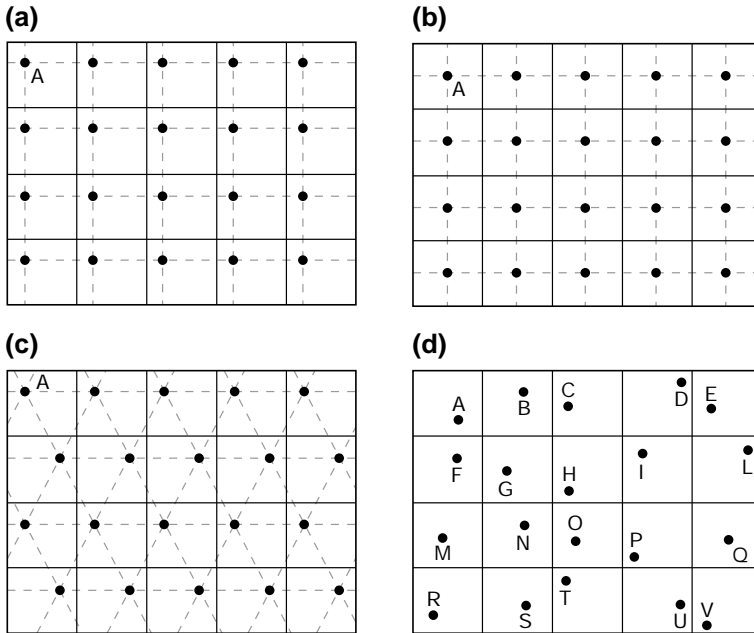


Fig. 15.1 Different systematic or grid sampling designs: **a** square aligned grid; **b** centered square grid; **c** triangular grid; **d** unaligned grid

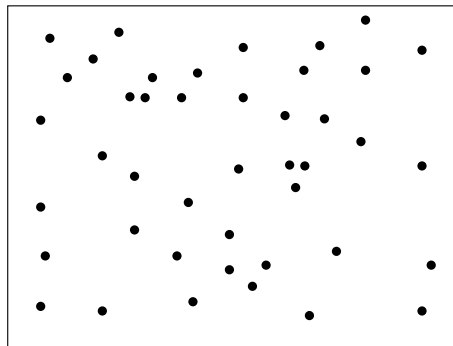


Fig. 15.2 Simple random sampling

used to select one unit per set and precision measurements are conducted on the chosen sample to estimate the parameters of the population it belongs to.

- *Adaptive cluster sampling.* Unlike the previous method, this is an effective and economical method for the definition of the position and extension of the contamination plume. First, sampling units with contaminant concentration exceeding a certain threshold are identified via random sampling. Then, additional rounds of analysis are employed to determine the concentration values in the proximity of the

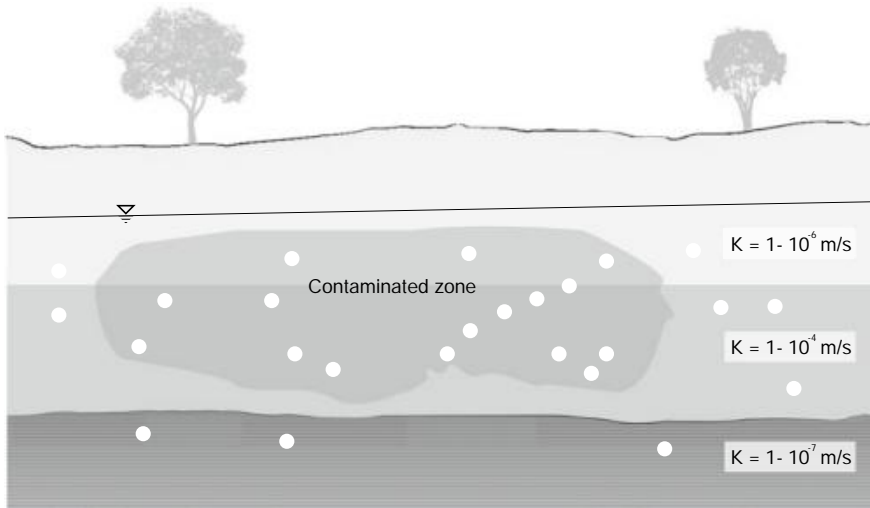


Fig. 15.3 Stratified sampling based on the hydraulic conductivity of the aquifer

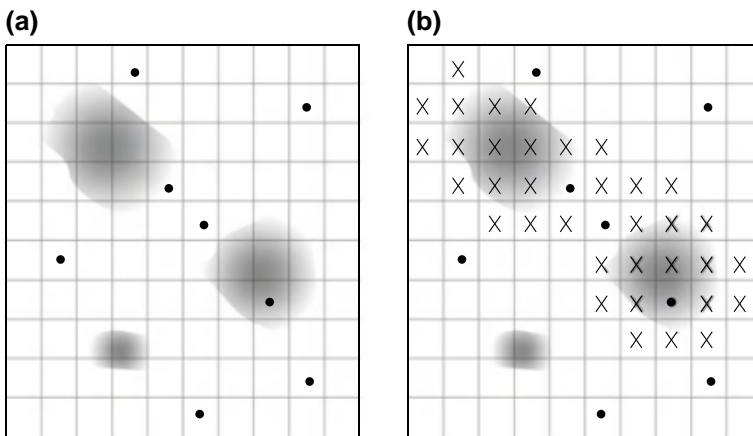


Fig. 15.4 Adaptive cluster sampling: **a** initial sampling; **b** final sampling result

locations of the sampling units identified in the previous round. Adaptive cluster sampling allows a more accurate estimation of the average concentration of a certain contaminant in a site and the delineation of the boundaries of contamination plumes (Fig. 15.4).

- *Composite sampling.* Technically, this is not a sampling design strategy but, rather, a sampling and measurement method. It consists in physically combining volumes of material from different sampling units to obtain a single homogeneous sample. This method can only be used if mixing of samples is not expected to generate a bias in the measurements (e.g., loss of volatile fractions of a contaminant), and

is recommended when analysis expenses are unreasonably higher than sampling costs. Compositing can only be used if the spatial distribution of the measured property is not required, since such information is lost.

15.2 Sampling the Unsaturated Medium

Characterizing the contamination of the unsaturated medium entails describing qualitatively and quantitatively the pollution event, in terms of contaminant typology, spatial distribution, and concentration.

In the unsaturated medium a contaminant can be found:

- in the gaseous phase;
- as a free phase;
- dissolved in water;
- sorbed to the soil.

A thorough understanding of a contamination event requires, therefore, collecting soil, soil-gas, and pore-water samples for laboratory analysis.

15.2.1 Minimum Number of Sampling Points

Table 15.1 offers guidance in planning the number of necessary sampling points in the saturated and unsaturated media, depending on the size of the investigated site.

15.2.2 Soil Sampling

Soil sampling techniques used to characterize the contamination are similar to those used in geotechnics, although the precautions that need to be taken to ensure representativity of the sample are different, as the final goal of the investigation is distinct.

Table 15.1 Recommended number of surface material, soil and backfill material sampling points

<i>Site surface area (m²)</i>	<i>Number of sampling points</i>
<10,000	At least 5 points
10,000–50,000	5–15 points
50,000–250,000	15–60 points
250,000–500,000	60–120 points
>500,000	At least 2 points every 10,000 m ²

In the context of the characterization of a contamination event, the main goal of soil sampling is to collect the most representative sample of the chemical, physical, and biological properties of the encountered soil horizons and to detect the presence of pollutants, if any. A correct characterization approach takes into account the borehole drilling phase as well as sample recovery. In fact, it is crucial to proceed with dry sampling techniques (without perforating fluids) that minimize overheating.

There are two types of techniques that can be used for soil sampling for environmental data collection and analysis:

- rotary techniques: the most widely used in environmental sampling. Although drilling is sometimes possible during sampling, these methods require the use of water for the advancement of the tubings;
- direct push techniques: they were developed in recent years specifically for environmental sampling; they don't require the use of perforating fluids during drilling nor sampling.

In the following paragraphs the main dry drilling techniques for soil sample collection, and the most important volatile organic compound (VOC) sampling methods are illustrated.

15.2.3 Rotary Techniques

A rotary sampler penetrates the soil by means of a set of rotating and pushing rods that connect it to the surface.

The penetration speed can be increased by circulating a perforating fluid inside the rods (*direct circulation*), or in the annular space (i.e., the space between the borehole wall and the outer casing, *reverse circulation*). Even though the use of perforating fluid promotes drill cutting removal during bit penetration, wellbore wall stability, and bit cooling and lubrication, it is counterproductive for the collection of a representative and undisturbed sample. Drilling fluid, composed mainly of water or of a mixture of water and mud, tends to penetrate inside the sample, compromising the results of analytical measurements.

For this reason, it is preferable to drill the borehole without drilling fluids (i.e., dry drilling), or, if impossible, only with water.

Rotary techniques are not hindered by any limitations in terms of perforation diameter, depth or type of soil.

15.2.4 Direct Push or Drive Drilling Methods

Direct push systems (pioneered by Geoprobe® [17, 18]) use dry drilling to drive a sampler into the ground and collect discrete soil samples and soil gases in the unsaturated medium and groundwater in the saturated medium. The operating principle

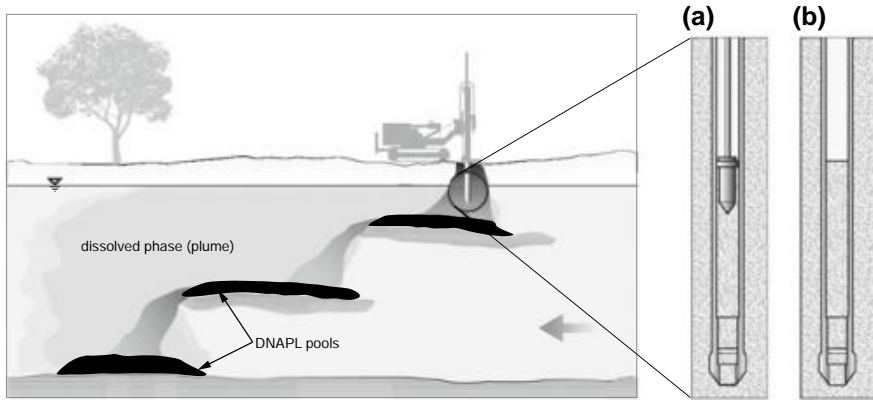


Fig. 15.5 Direct push rigs for soil sampling: **a** piston sampler; **b** open drive sampler

of direct push systems is similar to penetrometers used in geotechnics: a hydraulic hammer drives a set of rods to the desired depth in the ground. A sampler tailored for the environmental component to be collected is installed at the end of the rods.

Direct push rigs allow the recovery of soil cores with a diameter smaller than 2" by means of open drive samplers or piston samplers (Fig. 15.5). An outer casing can be used to prevent the borehole walls from collapsing and cross-contamination of the sample. Contact of the sample with the atmosphere and external agents is minimized by using plastic liners that can be sealed with custom caps.

Direct push systems have the advantage of being cost effective, as well as being fast and yielding high quality samples. Owing to their versatility, in recent years they have become widely used in the environmental field.

15.2.5 Soil Sampling for Volatile Compound Analysis

Traditional soil sample quartering and storage techniques are unsuited for the analysis of VOCs due to their significant volatility and interaction with the container. Lewis et al. [13] highlighted the impossibility of obtaining reliable analytical results from soil quartering with 125 ml plastic or glass containers.

It is preferable to recover samples directly in the vials used for chemical analysis. Sample treatment should be specific to the planned analysis method (purge and trap, headspace, etc.).

The most appropriate operating procedure is to use a *sub-corer* (Fig. 15.6), which is basically a plastic syringe deprived of its rubber piston used to remove a small aliquot of the soil core immediately after its extraction. This sub-sample should then be directly transferred to a vial sealed with stoppers with inert septa.

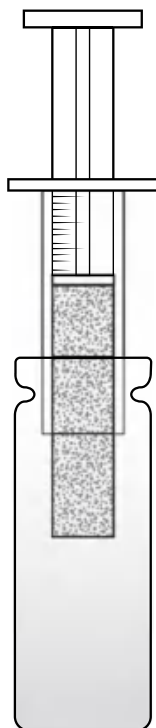


Fig. 15.6 Sub-corer for VOC-contaminated soil sampling

15.2.6 Soil Gas Sampling

Soil gas sampling is usually carried out near municipal waste landfills to assess biogas migration in the unsaturated medium. In addition, this method can be used to screen for the potential presence of volatile contaminants in the subsurface, and to investigate their spatial distribution.

The ability of this technique to detect contaminants is limited by the physical and chemical characteristics of the compounds. In particular, vapor pressure and Henry's constant, indicators of the tendency of a compound to partition to the gaseous phase, play an important role. In the case of active sampling (Sect. 15.2.6.1), vapor pressure should be greater than 0.5 mmHg; if the compound is present in the pore water or dissolved in groundwater, Henry's constant should be at least 0.1.

There are other factors, independent of the contaminant's characteristics, that limit the use of this technique, such as soil water content (that should be smaller than 80%), and the presence of low permeability horizons.

In the following paragraphs two common soil gas sampling techniques are described: active and passive sampling.

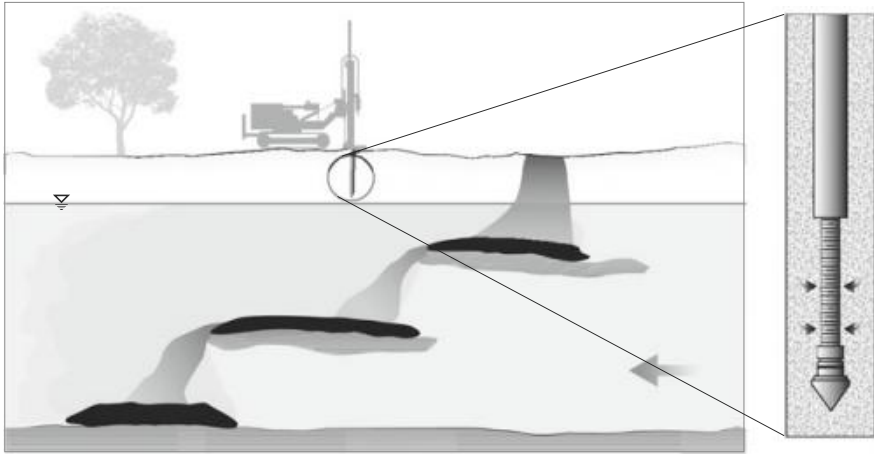


Fig. 15.7 Direct push system for soil gas sampling

15.2.6.1 Active Sampling

Active sampling consists in introducing pointed tip probes or permanent probes (analogous to piezometers) in the unsaturated medium and subsequently extracting soil gases with electric or manual vacuum pumps.

Pointed-tip probes can be driven into the ground manually or by direct-push methods (e.g., Geoprobe, Enviprobe), see Fig. 15.7. When proceeding manually, probes are usually no longer than two meters. With direct push systems, instead, probes can be driven up to thirty meters into the ground.

After pushing the tip at the desired depth, before starting the actual sampling, it is recommended to purge sampling units and tubing. Purging volume and discharge depend on soil permeability and on the volume of the probe and of the tubings.

While purging, it is worth checking there are no leaks at the joints of the setup or short-circuiting with the surface. This may occur when there are preferential paths that connect the sampler with the atmosphere, causing a decrease in contaminant concentration and an increase in the concentration of atmospheric gases, such as oxygen.

Soil gases can be collected with manual vacuum pumps or syringes, simply by connecting them to the sampler tubing. Gas analysis can be carried out directly on site with more or less sophisticated methods, ranging from colorimetric test kits, to portable flame ionization detectors (FIDs), photoionization detectors (PIDs), infrared (IR) detectors, or portable gas chromatographs (GCs).

Conversely, if the analyses are conducted in the laboratory, samples need to be collected either as a gas phase in appropriate steel, glass, or Tedlar containers or as a solid phase, after allowing the contaminant to sorb onto an apt support, such as activated carbon (Fig. 15.8).

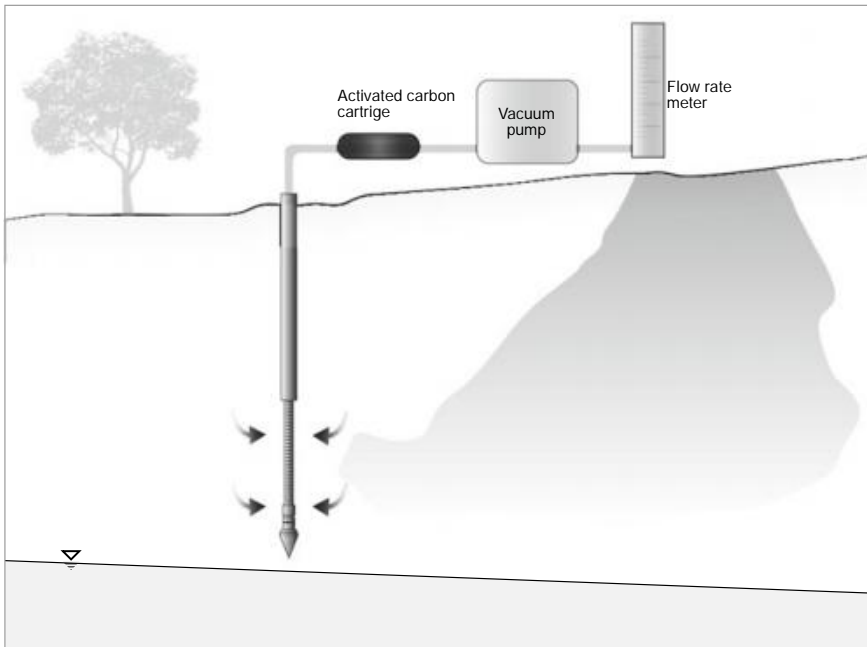


Fig. 15.8 Soil gas sampling by sorption to activated carbon cartridges

15.2.6.2 Passive Sampling

In contrast to active methods, passive sampling relies on natural contaminant flow through the soil towards a sampler composed of a sorbing material (generally activated carbon).

The sorbing material is placed inside containers, usually made of glass, positioned in boreholes with the open end facing downwards (see Fig. 15.9). The boreholes, backfilled with native material, are usually no deeper than two meters. Passive samplers are removed after allowing enough time for gases to sorb, generally from two to thirty days.

15.2.7 Pore Water Sampling

In some cases, pore water sampling can be of significant importance for the assessment of the degree of contamination of the unsaturated zone.

Pore water can be extracted on site through direct methods, or in the laboratory through indirect techniques applied to soil samples (e.g., centrifugation, high-pressure squeezing). Some studies have, however, revealed that each technique is best

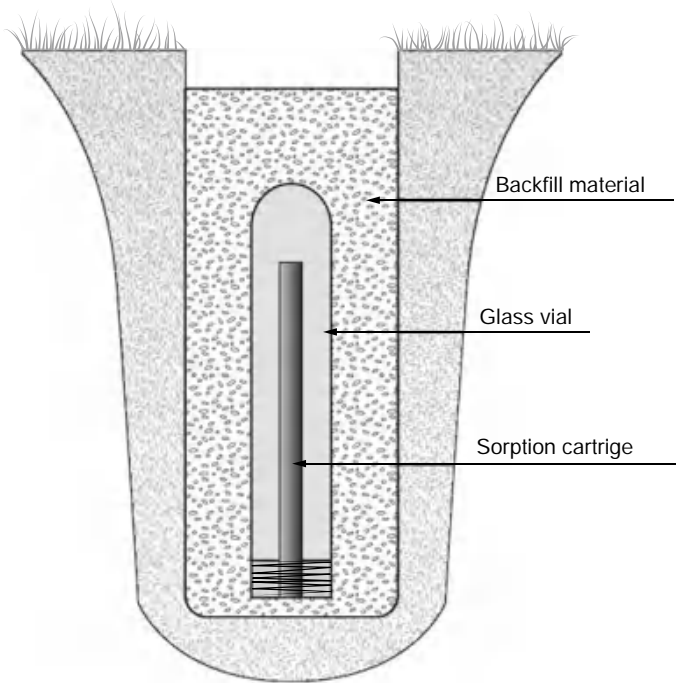


Fig. 15.9 Soil gas passive sampler

suited for sampling a different type of liquid. In particular, on site extraction can only recover fluids withheld at pressures up to 60 kPa, while laboratory techniques can recover liquids trapped at significantly greater pressures. Generally, however, pore-water samples recovered via on site techniques are considered more representative than those extracted in the laboratory.

The most common on site pore-water sampling methods are suction lysimeters and filter tip samplers (BAT samplers).

On site pore fluid sampling has to be carried out with competence, and caution must be used during the interpretation of laboratory results. Pore water is recovered by creating a negative pressure within the sampler and is, therefore, poorly suited for the collection of samples containing volatile compounds. Furthermore, sampler material can react with some contaminants or cause selective sampling.

15.2.7.1 Lysimeters

Lysimeters are composed of a porous cup placed at the end of a tube. The tube is usually made of PVC or stainless steel; while the porous cup can be made of ceramics, nylon, PTFE, or sintered metals.

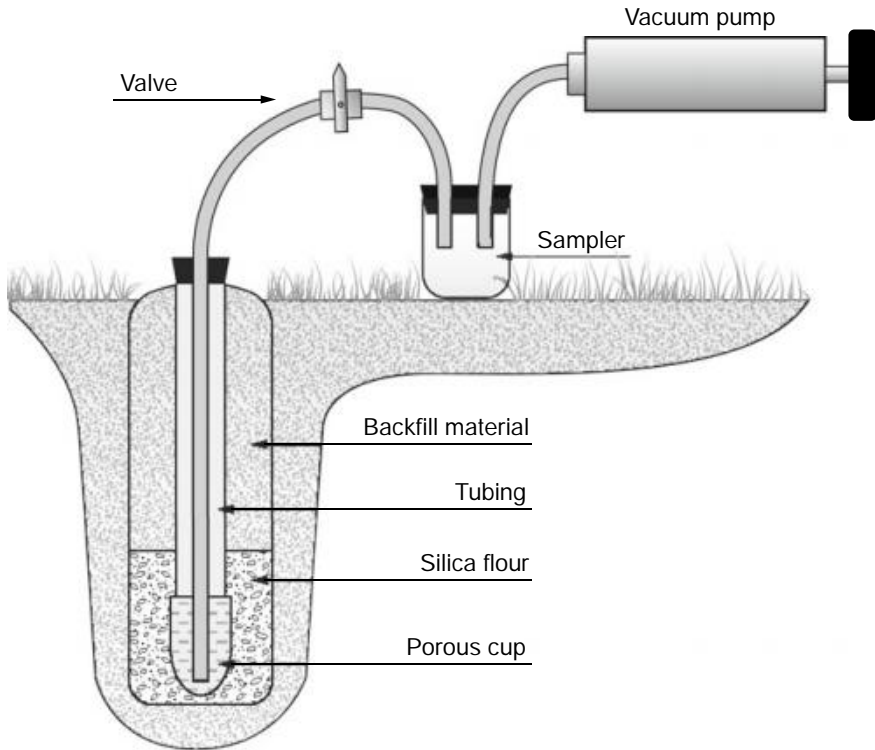


Fig. 15.10 Suction lysimeter

Lysimeters work by creating a negative pressure inside the sampler; this determines a head drop relative to the surrounding soil and the establishment of a gradient that drives water into the sampler. Pore water is collected in the lysimeter tubing and recovered at the surface through a connection tube. Flow through the porous cup can be extremely slow, so it is necessary to maintain the vacuum in the lysimeter for a long time, to ensure a sufficient amount of liquid is collected [5].

There are two types of lysimeters: suction and pressure-vacuum lysimeters.

Suction lysimeters are composed of a porous cup placed at the bottom end of a capped tube that reaches the surface (Fig. 15.10). Initially, vacuum is created inside the lysimeter with a manual pump connected to the porous cup with a small tube. After enough time has elapsed for the liquid to enter the lysimeter, the sample is collected by sucking it with the pump. Suction lysimeters are used to recover samples at depths smaller than two meters.

Pressure-vacuum lysimeters have a cylindrical body with a diameter of about 2" and approximately thirty centimeters long (Fig. 15.11). They are a two line system with two tubes connecting the lysimeter to the surface; one is the return line, which reaches the bottom of the lysimeter, while the other is the vacuum/pressure line,

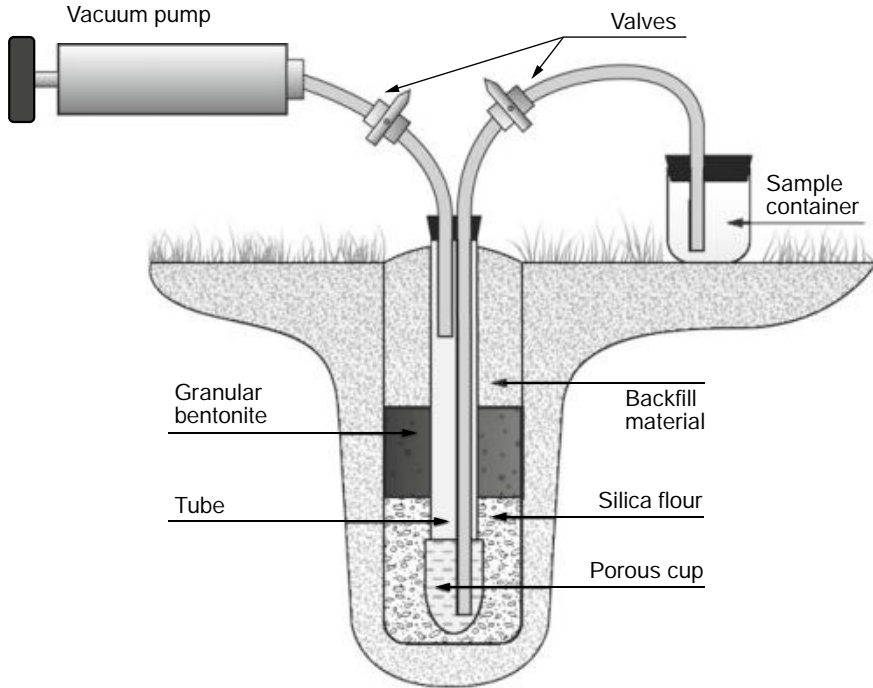


Fig. 15.11 Pressure-vacuum lysimeter

which ends in the upper part of the lysimeter. During sampling, negative pressure is applied to the lysimeter by connecting a vacuum pump to the vacuum/pressure line, while keeping the return line closed by means of a valve. The vacuum/pressure line is then closed as well, letting the pore fluid enter the lysimeter. After allowing sufficient time, the valves on both lines are opened, and a positive pressure is applied to the lysimeter through the vacuum/pressure line, pushing the collected sample up the return line. Generally, it isn't possible to reach depths greater than about twenty meters with vacuum/pressure-vacuum lysimeters. At greater depths, the pressure required to push the sample to the surface tends to push it back through the porous cup. This can be prevented by using a double chamber lysimeter with a check valve.

15.2.7.2 Filter Tip (or BAT) Samplers

Filter tip samplers are similar to suction lysimeters, but are distinct in that they do not have a pressure line that reaches the surface. Samples are drawn through the filter tip into a sample vial due to a preemptively created vacuum in the sampler. As shown in Fig. 15.12, the sampler is lowered from the surface into a previously drilled hole

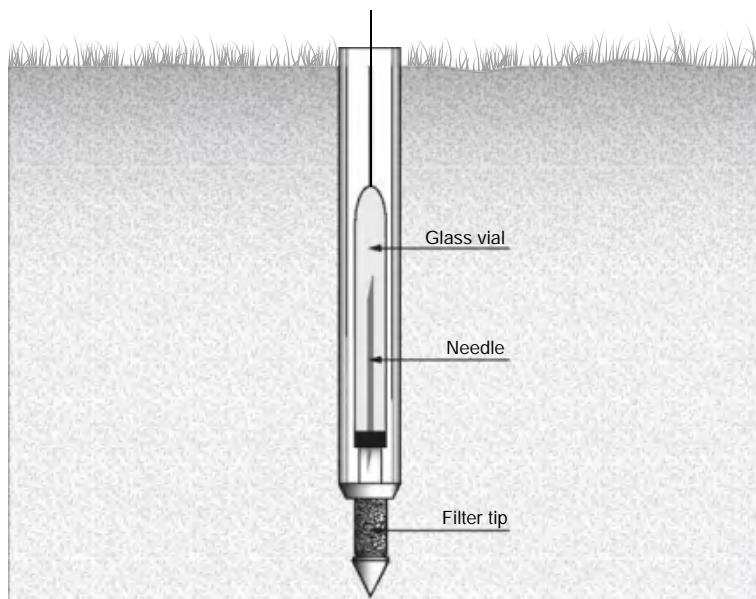


Fig. 15.12 Filter tip (or BAT) sampler

using a weighted cable. The weight of the cable drives a hypodermic needle, aligned with the sampler filter tip, through the vial septum, breaking it [5, 9].

The greatest limitation of this method is the long time required for the collection of a sufficient sample volume.

15.3 Sampling the Saturated Medium

The distribution of a contaminant in an aquifer depends on multiple factors, the most important being related to the contaminant's nature (density, miscibility with groundwater, viscosity), the aquifer's characteristics (hydraulic conductivity, porosity, heterogeneity), the type and conditions of contaminant spill (source geometry), and to the onset of biodegradation processes [4, 5, 10].

In the following sections the most appropriate techniques and methods for the identification of the type and extension of a contamination event in an aquifer system are described.

Groundwater monitoring points should allow the reconstruction and delimitation of contaminated areas and must include monitoring wells positioned upgradient of the affected area for the determination of background values. Monitoring wells, characterized by diameters ranging from 1" to 4", can be installed with destructive (non-core) drilling or with continuous core drilling and should cross the entire saturated thickness of the aquifer system. Usually, wells are screened above the water

table to allow LNAPLs to enter the well, in such a way that they can be sampled or measured. Conversely, for the determination of the vertical contaminant distribution, wells selectively screened at various depths or multilevel monitoring wells should be used.

15.3.1 Vertical Sampling

It is particularly important to determine the three-dimensional distribution of the contamination when the contaminants' nature and their interaction with the aquifer leads to the formation of concentration layers along the vertical axis. This is the case, for example, of compounds that are immiscible with groundwater.

For such contaminants, an effective sampling campaign should be aimed at identifying all substances and the spatial distribution of their dissolved and free phase concentrations, keeping into account also the potential presence of degradation products. Therefore, only a sampling protocol that includes sample collection at various pre-established depths can be considered appropriate.

Discrete vertical sampling can follow two distinct approaches:

- multilevel monitoring wells;
- point *direct push* techniques.

15.3.2 Multilevel Monitoring Wells

There are significant advantages in using multilevel, rather than traditional, sampling systems. With this method it is possible to determine the three-dimensional distribution and the level of contamination, by monitoring the evolution of the concentration of each compound with depth in each observation point. It is, furthermore, possible to better understand the local flow conditions, since the hydraulic head can be measured at various depths.

Multilevel monitoring can be carried out according to the following methods (Fig. 15.13):

- *Double packer following completion.* After completing a well, two packers are placed inside it to isolate a portion of aquifer. This system is not recommended since cross-contamination events and fluid circulation within the filter pack cannot be prevented. Furthermore, their installation is slow and laborious.
- *Piezometer clusters.* Several small diameter, screened piezometers are completed in separate boreholes at different depths. This is an expensive method because it increases drilling costs.
- *Nested piezometers.* Multiple piezometers, separated by annular bentonite seals and concrete, are installed inside a single borehole. Their greatest limitation is the difficulty of ensuring perfect hydraulic isolation of the monitored intervals;

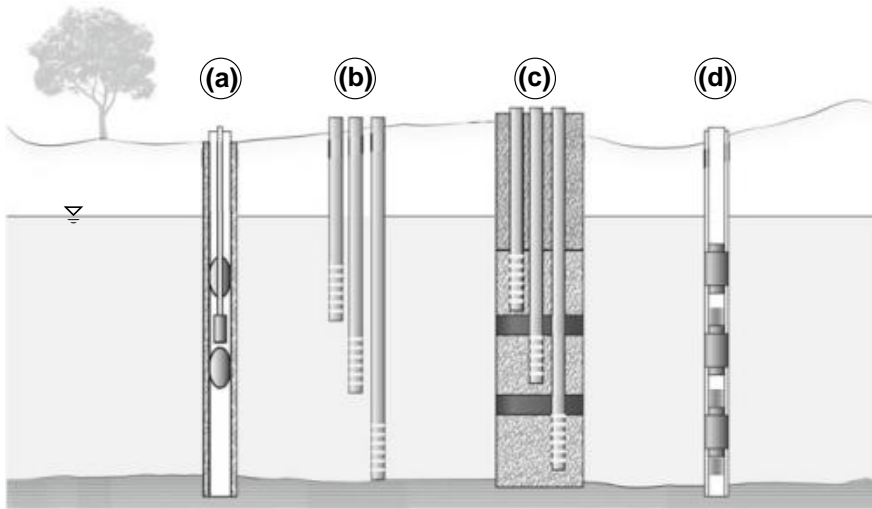


Fig. 15.13 Multilevel measurement systems inside piezometers: **a** double packer; **b** piezometer cluster; **c** nested piezometers; **d** multilevel systems

furthermore, purging can last very long because of the wide diameter of the filter pack surrounding the group of casing pipes.

- *Multilevel (or multi-port) systems.* They are generally composed of an alternating sequence of packers and monitoring ports (such as CMT by Solinst) aligned inside a casing string, and are sometimes equipped with submersible pumps to bring water samples to the surface (such as Flute system). They can be removed relatively easily from the borehole in which they are installed and have the advantage of requiring minimal purge volumes.

15.3.3 Direct Push Techniques

Direct push systems enable discrete groundwater sampling by means of a screened stainless steel tube advanced directly in the aquifer formation to the depth of interest (Fig. 15.14).

These techniques allow instantaneous water sample extraction from the observation points, and offer the following advantages:

- speedy sampling;
- extremely low sampling cost;
- no perforating fluids or drill cuttings;
- direct sampling with minimal purging possible;
- multilevel sampling along the aquifer thickness;
- piezometer cluster installation possible.

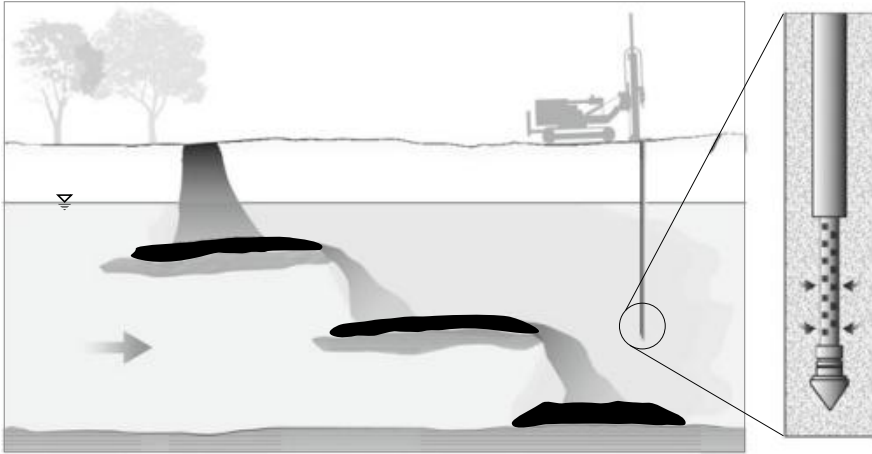


Fig. 15.14 Direct-push (percussion) technique for the vertical characterization of contamination in an aquifer system

The only limitation of this method is the sampling depth, which normally cannot be greater than 30–40 m, and the diameter of the sampling pipe, which is 1.5" for groundwater collection.

Water is normally sampled by means of inertial or tiny submersible bladder pumps.

15.4 Purging

Prior to sampling the well should be purged in order to collect a fresh and representative groundwater sample while minimizing disturbance to the natural groundwater flow.

To this end, standing water present in the well must be removed since it is characterized by different physico-chemical equilibria than the aquifer because of its interactions with well casing material and the atmosphere.

The actual sampling phase can only occur after the well has been purged. The purging technique should be selected according to the following factors [14]:

- purge volume;
- possibility of using the same equipment for purging and sampling;
- diameter of the observation point (well or piezometer);
- depth to groundwater;
- simplicity of decontamination and disassembling operations;
- transportability;
- need for an external power supply;
- cost.

A crucial aspect during purging is the pumping rate: if excessive, it can result in increased sample turbidity, drying up of the piezometer, supernatant free phase recovery or sample dilution; conversely, with exceedingly low rates the operation might end up taking too long or not being carried out adequately.

Usually, pumping rates do not exceed few liters per second. We refer to *low-flow purging* when rates are smaller than 0.5 l/min.

The choice of purge volumes and duration is usually based on the criteria illustrated in the following sections: the first three concern traditional purging, while the last regards low-flow purging.

15.4.1 Well Volume Based Criterion

According to this criterion, 1–20 well volumes should be purged. Well volume includes the amount of sitting water present above and below the screen in the well casing pipe, but not the water in the filter pack.

Even though a unique criterion cannot be established, purging 3–5 well volumes is generally considered sufficient to ensure sample significance [16].

The advantage of this approach lies in its operational simplicity, even though purging volume and time may be significant in the case of large monitoring wells.

15.4.2 Criterion Based on Physico-Chemical Parameters Stabilization

This approach consists in monitoring parameters such as specific conductance, pH, temperature and Eh until they stabilize, while purging a well.

Once the observed parameters reach stability, the pumping rate is reduced to allow sampling.

The greatest challenge consists in identifying the most suitable parameter for establishing that all standing water has been eliminated. Some authors have suggested that the most significant parameters are dissolved oxygen (DO) and specific conductance, whereas pH and temperature are less reliable because they stabilize very quickly. It is recommended to measure these parameters with multiparametric probes, either submerged or coupled to a flow-through cell (see Sect. 15.7) [14, 16].

15.4.3 Well Storage and Hydrodynamic Parameters Based Criterion

This criterion is based on the fact that the percentage of water that derives from the aquifer system increases with pumping time, and depends on the well's storativity and on the aquifer's hydrodynamic characteristics.

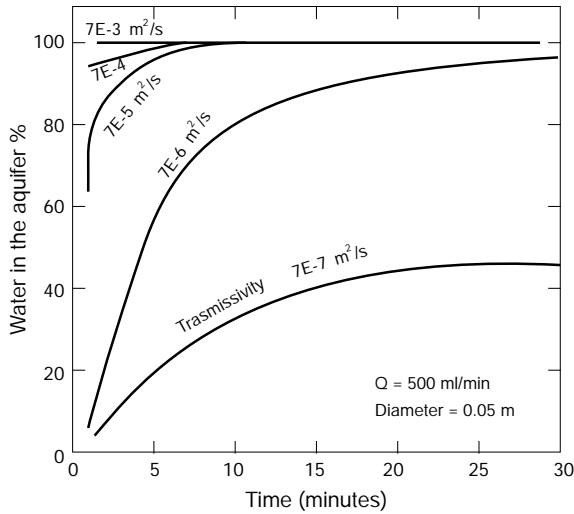


Fig. 15.15 Percentage of water deriving from the aquifer as a function of time and for different transmissivity values (modified from [12])

Given the formation transmissivity, the well diameter, and the purge pumping rate, it is possible to calculate the necessary purge time to obtain significant samples (Fig. 15.15).

15.4.4 Low-Flow Purging and Physico-Chemical Parameters Stabilization

Low-flow purging is based on the assumption that only the volumes of water above and below the screens are *standing*, while at the screen level water is in direct contact with the aquifer [16]. By purging at extremely low pumping rates ($<0.5 \text{ l/min}$) and inducing minimal drawdown ($<0.1 \text{ m}$), it is possible to collect groundwater directly, without it mixing with standing water [16].

After lowering the pump in the piezometer very slowly and with great care, to avoid mixing of groundwater with standing water, and after placing it in the middle of the screened section, it is possible to initiate the *low-flow purging*, which should last until the physico-chemical parameters stabilize.

Owing to the small pumping rates, this method minimizes purging volumes, aquifer disturbance, contaminant stripping and mobilization of suspended solids. It is particularly effective in wells with small diameters, characterized by short screens [16].

Such small pumping rates can only be achieved with peristaltic or bladder pumps.

15.5 Sampling

Sampling is aimed at collecting a sample that reflects the physico-chemical composition of groundwater as closely and consistently as possible (i.e., accurately and precisely, respectively).

Groundwater temperature, pressure, dissolved gas content, and redox state at sampling depth are usually different from surface conditions; therefore, a number of preventive measures need to be taken during sample collection in order to minimize its alteration. In addition, one should also keep in mind that the sampling system itself can alter the sample, due to its functioning mechanism or to the materials it is made of.

In particular, samplers that introduce air or inert gases to lift the sample and that induce significant pressure variations or turbulence, should be avoided. Systems that apply a positive pressure to the discharge pipe are preferable to those that suck the sample, to minimize volatilization.

The choice of materials should be aimed at limiting transfer to and from the sample (e.g., additive release, sorption and desorption, physical or chemical degradation). Furthermore, the following factors should be considered when selecting the sampling device:

- type of contaminant being sampled;
- possibility of regulating sampling discharge;
- possibility of in-line sample filtration;
- diameter of the sampling point;
- depth to groundwater;
- simplicity of decontamination and disassembling operations;
- transportability;
- necessity of an external power supply;
- cost.

The main sampling systems are reviewed in Sect. 15.6.

15.5.1 Sampling Rate

When samples are collected by means of a pumping system, the pumping rate has to be chosen with care.

A good rule of thumb is to sample groundwater at a lower pumping rate than the purging discharge. A small sampling discharge is essential for minimizing aquifer disturbance and ensuring the sample is representative. However, it should not be so low that sample containers are not efficiently filled and that exposure to atmospheric conditions is not minimized. To avoid having to use two distinct purging and sampling systems, it is preferable to use a pump whose pumping rate is adjustable [14].

An effective technique is considered to be *low-flow sampling*, which uses an extremely low sampling rate (<0.3 l/min) in order to minimize aquifer disturbance, contaminant stripping, and mobilization of suspended solids. The use of valves that could create rapid pressure variations (*orifice effect*) to achieve these flow rates, thus affecting sample quality, is discouraged [16].

15.5.2 Sample Collection

Transferring the sample to a container for transport to the laboratory is a very delicate phase, given the need to obtain significant analytical results.

Therefore, it is advisable to:

- make sure there are no sources of contamination close by (e.g., operating engines, exhausts), before opening the container;
- open the container just before sampling;
- minimize turbulence, shaking, volatilization, exposure to the atmosphere, and heating of the water sample;
- fill the container completely, minimizing the headspace, if VOCs have to be measured;
- filter the sample and add preservatives immediately after collection, if necessary;
- stopper the container;
- label the sample unambiguously.

In-line sampling is a particularly effective sample collection technique that minimizes contact with the atmosphere. This solution, depicted in Fig. 15.16, consists in filling the sampling container by means of a tube submersed in the liquid itself. A second tube is used to eliminate excess liquid. If the container is transparent, the degree of turbidity of the sample can be evaluated visually, to decide whether to continue or interrupt the purging phase.

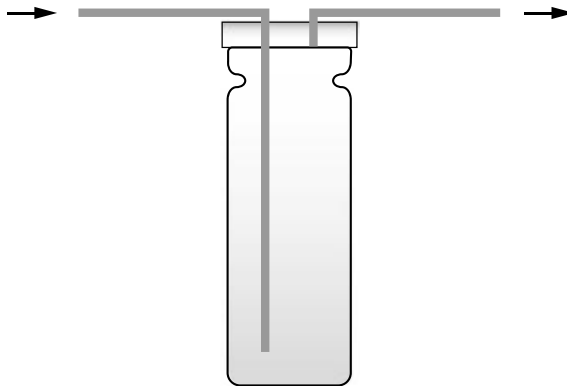


Fig. 15.16 In-line sampling

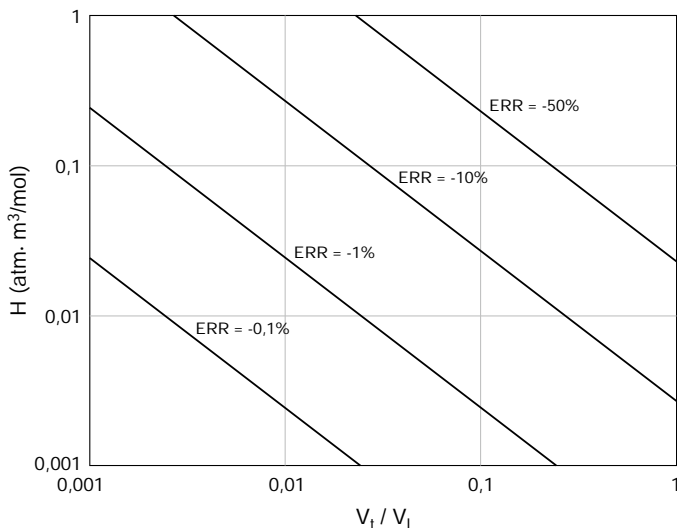


Fig. 15.17 Pankow's diagram; H represents Henry's constant and V_t/V_l the ratio between headspace and solution volume (modified from [15])

As previously mentioned, headspace and air bubbles should be minimized in the container. This is particularly important when volatile compounds have to be measured: in such cases, it is recommended to fill the container to the brim maintaining a convex meniscus.

In this regard, Pankow's diagram (see Fig. 15.17) provides the magnitude of the error in the determination of the concentration of a volatile compound whose Henry's constant is H . The error is represented as a function of the ratio between headspace and aqueous solution volume [15].

15.6 Sampling and Purging Mechanisms

Sampling and purging devices can be classified based on their functioning mechanism:

- *grab samplers;*
- *positive displacement pumps;*
- *submersible centrifugal pumps;*
- *suction lift pumps;*
- *inertial lift pumps.*

Grab samplers, such as bailers and syringe samplers, can be used to collect relatively deep samples without using pumping systems.

Table 15.2 Groundwater sampling and purging system classification

<i>Grab samplers</i>	Bailer Syringe sampler Thief sampler
<i>Positive displacement pumps</i>	(Low flow) Submerged centrifugal pump Bladder pump Gas-drive pump Piston pump Gear-drive pump Progressing cavity pump
<i>Suction lift pumps</i>	Surface centrifugal pump Peristaltic
<i>Inertial pumps</i>	With check valve

Positive displacement systems include all submersible pumps that exert a positive pressure on the discharge pipe, and thus on the fluid, avoiding volatile compound stripping. They work by alternatively filling a compartment with fluid at the inlet, and emptying it at the outlet. This category includes bladder (or diaphragm) pumps, gas displacement pumps, plunger or piston pumps, gear-drive pumps, and progressing cavity (or helical rotor) pumps [14].

Submersible centrifugal pumps push the fluid by means of rotation of impellers. For environmental sampling applications, they should be used at low flow rates, at which they function according to the positive displacement mechanism. Conversely, at high rates, turbulence and cavitation can be generated, making them unsuitable for sampling [2]. Submersible centrifugal pumps are the most commonly used for sampling due to the continuous and pulsation-free flow they induce, the broad range of flow rates, which are also easily adjustable, and their contained cost.

Suction lift pumps are surface pumps (i.e., situated at ground level) and function by applying a vacuum to an intake line. Their main drawbacks are their limited lift capability (<10 m) and the risk of stripping volatile compounds. The most common suction lift pumps are surface centrifugal pumps and peristaltic pumps, which utilize impellers and rotors, respectively, to create suction.

Finally, inertial pumps use inertia to draw water into a tube and to the surface [14].

Table 15.2 classifies the pumps that can be used for sampling and purging groundwater; in the following paragraphs the most commonly used systems are illustrated in greater detail.

15.6.1 Bailers

Bailers are hollow tubes that are lowered in extraction or monitoring wells with a cable. Bailers vary greatly in terms of style, size, materials and complexity. Generally, they are one to two meters long, although they could basically have any length.

The sampling tube material should be chemically inert, typical examples being stainless steel, PVC, and fluorocarbons. Particular care must be taken when selecting the recovery cable material, which shouldn't be made of natural fabrics or adsorbing materials.

While sampling, the bailer should be lowered and extracted with great care, to avoid hitting the well casing or causing groundwater mixing by oscillating the sampler.

To avoid aerating the sample excessively, bottom-discharge bailers can be used [14, 16].

Advantages

- supernatant free phase can be sampled in static conditions (without purging);
- can be made of basically any material, provided it's inert;
- inexpensive, disposable ones available;
- easy to use;
- no limitations in terms of diameter or depth of the well;
- light and portable;
- easy to decontaminate;
- no external power supply required.

Limitations

- can cause VOC losses or alteration of redox-sensitive samples;
- sample quality strongly dependent on the operator's expertise;
- not suitable for purging;
- possible sample losses at the valves;
- generally slow, although possible, in-line sampling.

15.6.2 Submersible Centrifugal Pumps

Submersible centrifugal pumps were originally developed to be installed in water supply wells. Recently, smaller models that can be installed in monitoring wells with a diameter greater than 2" have been developed and have proved commercially very successful (see Fig. 15.18). Submersible pumps operating at low flow rates, unlike surface ones, exert a positive pressure on the discharge pipe and on the fluid, thus preventing stripping [2].

Centrifugal pumps for environmental sampling use water rather than hydrocarbon oils as lubricants, and are usually made of highly inert materials such as stainless steel, PTFE, or Viton, which are suitable also for VOC sampling.

Pumps whose discharge can be adjusted according to purging or sampling requirements are commercially available.

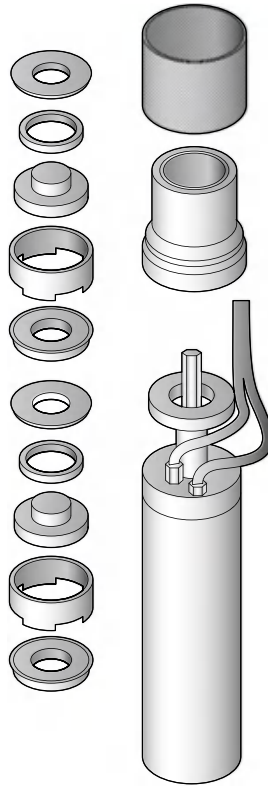


Fig. 15.18 Components of an axial centrifugal pump used for groundwater sampling

Advantages

- high quality samples collected at low discharges;
- adjustable pumping rate with some models;
- medium to high lift capabilities;
- a few models are made of inert materials;
- in-line sample filtration possible.

Limitations

- models that cannot pump low discharges are unsuited for VOC-containing sample collection;
- external power source required;
- complex decontamination process;
- limited transportability: although the smallest pumps are portable, the whole sampling system is usually bulky and heavy.

15.6.3 Bladder Pumps

Bladder pumps are submersible positive displacement pumps and are among the most effective for trace metal and VOC sampling.

Bladder pumps operate in two stages (Fig. 15.19). First, a flexible chamber (bladder) fills through a check valve at the bottom of the pump due to hydrostatic pressure. As soon as the chamber is full, the bottom valve closes and prompts the injection of gas between the body of the pump and the water-containing chamber. The latter is compressed, releasing the water through a check valve at the top of the bladder into the discharge pipe.

The lift capability of the pump is directly related to the gas injection pressure in the space around the bladder.

Pumps that can be lowered in monitoring wells with a diameter as small as 3/4" and whose pumping rate can be adjusted to purging or sampling requirements (suitable also for *low-flow purging* or *sampling*) are available. Recently, Geoprobe, developed a manual mechanical bladder pump able to sample from wells as small as 1/2".

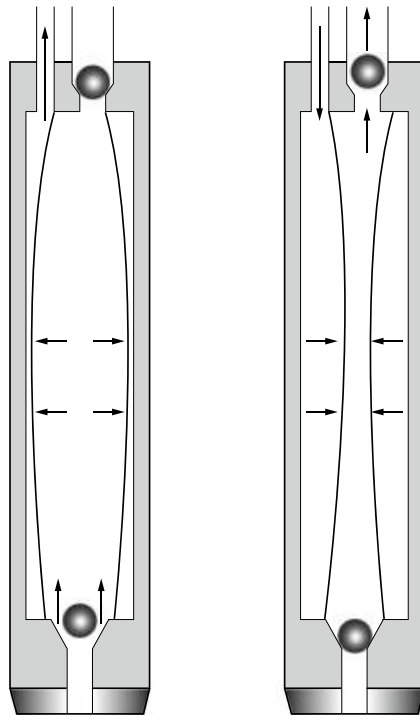


Fig. 15.19 Operating phases of a bladder pump: filling and emptying of the chamber

Advantages

- high quality samples collected at low discharges;
- no contact between sample and compressed gas or mechanics of the pump;
- bladder can be made of virtually inert materials;
- adjustable pumping rate;
- in-line sample filtration possible;
- some models have a very high lift capability;
- pump not damaged by drying out.

Limitations

- limited transportability: although the smallest pumps are portable, the whole sampling system is usually bulky and heavy;
- compressed air and a control system necessary;
- possibly slow deep-well purging and sampling;
- complex decontamination process;
- bladder can break;
- training necessary for pump operation.

15.6.4 Peristaltic Pumps

Peristaltic pumps are suction lift pumps: a rotor compresses a flexible tube (usually made of PVC or silicone rubber) creating a reduced pressure at one of its ends that sucks well-water to the surface (Fig. 15.20).

In theory, suction systems should be able to lift water up to 9.7 m, but actually they are rarely able to exceed an 8 m lift. Due to the application of suction, they aren't suitable for VOC sampling, unless they are coupled to a sampling device that limits volatile stripping. Conversely, they are extremely useful for sampling small-diameter wells, or in all situations that require in-line sample filtration [14, 16].

Peristaltic pumps whose discharge rate can be adjusted to purging or sampling requirements (also suitable for *low-flow purging* and *sampling*) are commercially available.

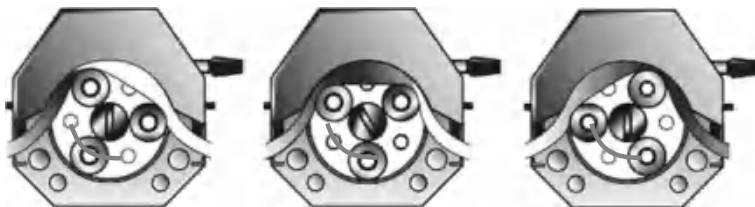


Fig. 15.20 Operation phases of a peristaltic pump

Advantages

- in-line sample filtration possible and quick;
- portable and easy to use;
- any material, even highly chemically inert ones, can be selected to produce the squeezable tube;
- adjustable discharge;
- no contact between sample and pump parts;
- can be used in wells of any diameter (even $<1/4''$);
- can be powered by battery;
- easy decontamination.

Limitations

- suction can cause VOC volatilization;
- usually lift does not exceed 8 m.

15.6.5 Inertial Lift Pumps

Inertial lift pumps (also called *tubing-check-valve pumps*) are suitable also for purging and sampling wells with a very small diameter. They are composed of a tube equipped with a check valve at one end, which is submerged in water. By applying a reciprocating motion to the tube, water is drawn to the surface for sample collection (see Fig. 15.21). This can be done manually or, if constant pumping rates are required or if water has to be lifted from great depths, the sampling tube can be coupled to an electric motor or a combustion engine [14].

Samples collected with this method are very turbid due to the reciprocating motion inside the monitoring well [16].

Advantages

- can be made of basically any material;
- inexpensive, disposable ones available;
- easy to use;
- no limitations in terms of well diameter;
- light and portable;
- no external power supply required.

Limitations

- possible increase in groundwater turbidity;
- not suitable for purging large volumes of water;
- not suitable for sampling deep wells;
- possible but complex in-line sample filtration.

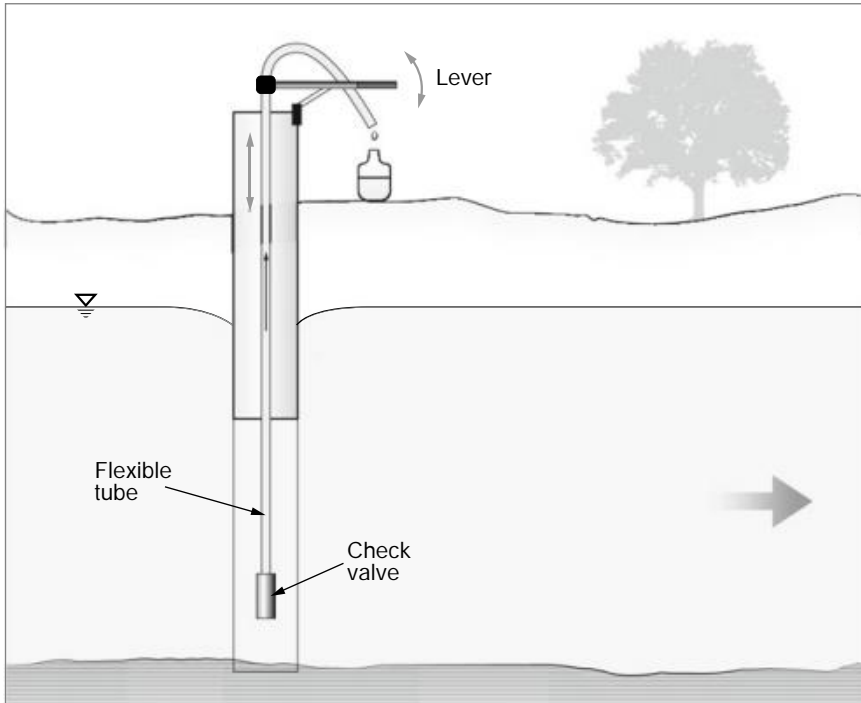


Fig. 15.21 Inertial pump with check valve

15.7 On Site Measurement of Water Quality Parameters

Many physico-chemical parameters characterizing water undergo abrupt changes during extraction from the sampling point and following exposure to oxygen and atmospheric pressure. The main parameters that are likely to change are specific conductance, pH, dissolved oxygen, Eh, alkalinity, and temperature.

Since there is no way of stabilizing these parameters, they have to be measured on site and avoiding contact with air. To do this, multiparametric probes can be lowered directly in the well or can be coupled to a flow-through cell (Fig. 15.22). Readings should be made while purging the observation point.

If submersible probes are used, it is necessary to ensure that there is sufficient water circulation by placing the pump's suction tube close to the electrodes. However, their use is limited by small sampling point diameters.

When lowering the probes in the well is impossible or undesirable, a flow-through cell can be used. The operating principle of a flow-through cell is very simple. It is composed of a container with an inlet and an outlet, as well as a space for the sensors. During the purging phase, the pumped water flows through the cell, wetting the sensors without entering in contact with the air.

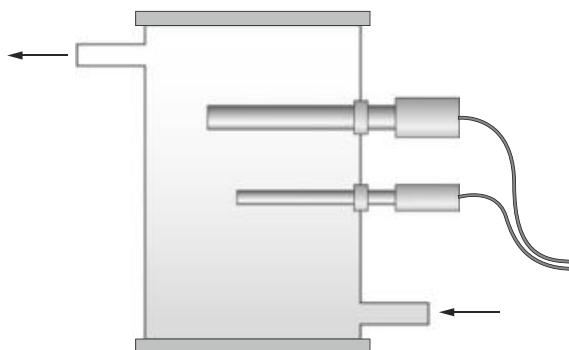


Fig. 15.22 Schematic representation of a flow-through cell

When the above-described direct measurements cannot be made, it is advisable to carry them out immediately after collecting the sample. In all other cases, it is necessary to specify, along with the analytical results, that the measurements were not conducted on site.

15.8 Sample Filtration

Drilling, completing, developing, purging, and sampling a monitoring well tend to mobilize colloids and suspended solids that normally wouldn't be carried by natural flow. Artificially mobilized material may have adsorbed contaminants on its surface or be fully or partially composed of inorganic compounds (mainly metals).

Solid and colloid suspension can be limited by thoroughly completing monitoring wells and by using low flow purging and sampling techniques. In all other cases, filtering the sample can eliminate the majority of suspended solids and colloids that were artificially mobilized, even though also the fraction transported due to the natural aquifer gradient is likely to be removed.

In addition, depending on the selected techniques and devices, filtration could also alter some of the physico-chemical parameters, such as dissolved metal concentration, partial pressure and concentration of dissolved gases, pH, and redox potential. Sample aeration can cause oxidation and precipitation of dissolved metals such as iron. Furthermore, filtration can also remove low-mobility compounds that tend to be adsorbed on suspended solids, such as PCBs.

There is, therefore, an open debate regarding sample filtration: according to one position, filtration affects the representativity of the sample, while the other claims that geochemical studies of contaminated sites should focus on the determination of the concentration of compounds actually dissolved in water, rather than the apparent concentration resulting from sorption onto suspended solid material.

There is no single right answer to this debate: in some cases filtration is necessary, in others it affects the accuracy of the analytical results. For metal analysis,

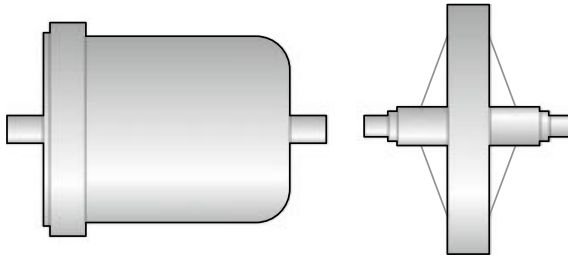


Fig. 15.23 In-line filters for water sampling

filtered and unfiltered samples can be collected, to determine their dissolved and total concentration, respectively. Nevertheless, in certain circumstances the collection of unfiltered samples is the only available option, due to operational hurdles in the field (long-lasting and difficult on site filtration).

For the sake of completeness, we would like to mention the three techniques available for on site filtration:

- vacuum (or suction) filtration;
- positive pressure filtration;
- in-line filtration.

It is important to understand how each of these methods may affect sample chemistry.

Vacuum and pressure filtration entail transferring the collected water from one container to another through a filter. Water is generally filtered through a glass, cellulose, or another inert material microfiber membrane with a pore size of $0.45 \mu\text{m}$.

In the case of vacuum filtration, the sample is “sucked” through the filter, whereas in pressure filtration it is “pushed” by gas or mechanically. The main issues with these systems are the aeration and oxygenation of the sample, and gas stripping and alteration of their partial pressure.

In-line filtration was developed to solve these issues. In this case, a membrane or filter cartridge (Fig. 15.23) is applied directly to the discharge line of the sampling system, such that the out-flowing water can be collected without additional transfers or entering in contact with other gases. Clearly, this method cannot be used unless sufficiently low pumping rates can be achieved.

15.9 Quality Control

Quality assurance (QA) and quality control (QC) measures that should be taken throughout all sampling phases to ensure accuracy, precision and defensibility of acquired data are listed below [6, 8].

The following information, documents and protocols should always accompany any sampling campaign:

- field log: site location, operation times, goal of the activities, and any additional information necessary to unambiguously describe what was done;
- sample labeling record. Unique sample names should be coupled with information on: sampling time, location, depth and temperature; required analysis; sampling containers, their material, volume, capping system, and level of cleanliness;
- number of sampling points, of sub-samples, and of replicates;
- sample volume, determined by the number and kind of parameters to be measured (hence, by the kind of analytical protocols that need to be followed);
- analytical measurement precision;
- safety measures and protective equipment for workers in relation to eye and skin contact, inadvertent ingestion, inhalation and radiation hazards, as well as to equipment-associated hazards;
- sampling equipment cleaning and decontamination protocols (products and methods to be used);
- sample container, transport, and storage method description;
- sample labeling with permanent markers, which should also be included in the sampling report written according to the applicable legislation;
- sampling and analysis protocol, including a detailed description of the procedures;
- data processing, presentation, and storage information.

In the following paragraphs we illustrate some of the main aspects of quality control of a sampling program and the subsequent sample analysis.

15.10 Equipment Cleaning and Decontamination

The main goal of decontaminating the equipment is to minimize the risk of introducing external contaminations or of cross-contaminating different sampling points. The American Society for Testing and Materials details a list of decontamination procedures for contaminated sample contacting equipment in the ASTM D 5088-15a standard [1]:

Minimal Decontamination Procedure

- Wash sample contacting equipment with a detergent solution.
- Rinse thoroughly with control water. Control rinse water should have known chemical composition; potable (tap) water can be used for remove heavy mud and dirt, or to rinse off other solutions.

Rigorous Decontamination Procedure (to Meet the Sampling or QA/QC Objectives)

- “Wash with detergent solution, using a brush made of inert material to remove any particles or surface film. For equipment that, because of internal mechanism or tubing, cannot be adequately cleaned with a brush, the decontamination solutions should be circulated through the equipment.

- Rinse thoroughly with control water.
- If required, rinse with an inorganic desorbing agent (may be deleted if samples will not undergo inorganic chemical analysis). This rinse should only be used on non-metal surfaces and only after cleaning with detergent wash has been found inadequate.
- Rinse with control water.
- Rinse with deionized water.
- Allow equipment to air dry in a clean environment prior to next use. The use of heating, such as placing the equipment in an oven can also be beneficial and can be a part of the decontamination process.
- Wrap equipment for transport with inert material (aluminum foil or plastic wrap) to avoid direct contact with potentially contaminated material.
- Sampling Equipment used for “Classic Parameters” analyses (such as nutrients, oxygen demand, certain inorganics, sulfides, pH, flow measurements, etc.) where the samples will not be for analysis for trace organic or inorganic constituents may use an abbreviated cleaning between sampling points. For routine water quality sampling of classical parameters, buckets, dredges, sample tubes, etc., should be rinsed with tap, control, or deionized water before use and between sampling locations. Flow measuring equipment such as velocity meters and stream gauging equipment should be rinsed with the tap or control water prior to and after use [1].”

The choice of the appropriate detergent solution to be used in the above protocol mainly depends on the type of contaminant and on the equipment material that needs decontamination. A few common examples are: non-phosphate detergents (such as Liquinox or Detergent 8); sodium bicarbonate or carbonate; trisodium phosphate; calcium hypochlorite; hydrochloric or nitric acid; citric, tartaric, oxalic acids; and organic solvents (e.g., isopropanol, acetone, methanol, hexane, or ethanol). Some of these detergents are toxic themselves; therefore, they must be handled and disposed of with care [1].

15.11 Sample Storage

If water, soil, or gas samples are not analyzed on site immediately after collection, some precautions need to be taken to prevent the analysis from being compromised due to sample alteration [5]. To this end, specific sample storage procedures need to be followed: samples should be placed in containers made of appropriate materials for the collected environmental component and the contaminant to be analyzed.

Soil samples are generally stabilized by storing them at 4°C. Water samples, instead, require more sophisticated preservation methods, including:

- pH control;
- addition of chemical compounds;
- temperature control;
- protection from light.

Physico-chemical properties of water begin to change as soon as the sample is extracted from the aquifer; chemical, physical, and biological processes that alter the quality and representativity of the sample include:

- sorption and desorption;
- complexation;
- acid-base reactions;
- redox reactions;
- precipitation;
- photodegradation;
- gas stripping and solution;
- biodegradation.

The laboratory conducting the analyses must identify the most suitable preservation method for each parameter and each environmental component.

15.12 Blanks and Replicates

The function of replicates is to determine and assess the reliability and variability of the laboratory analyses results. They are obtained by splitting a sample into two or three fractions, labeled as different samples and subsequently analyzed separately.

Blank preparation, instead, is very important for the quality control procedure of a groundwater sampling campaign. There are several kinds of blank, among which [10, 14, 16]:

- *Trip blanks.* Their purpose is to reveal any contamination of the containers or of the samples during the trip or storage. The analysis laboratory prepares them with ultrapure water; they are then carried to the sampling point with all the other empty containers. These blanks remain in the transport container or in the refrigerators throughout the duration of sampling, without being opened, and are then sent back to the laboratory with the other samples. Usually, these blank are used to identify the presence of volatile contaminants.
- *Field blanks.* They are used to identify sample contamination during collection. They are prepared like the trip blanks, but are exposed to air at the sampling point, like the samples.
- *Equipment blanks.* They are used to assess the effectiveness of decontamination operations and contaminant removal from purging, sampling, and measurement equipment. Ultrapure water from the laboratory is circulated through the equipment and collected at the outlet.

Table 15.3 Materials ordered by decreasing chemical inertia

PTFE (Teflon)
Rigid PVC
Flexible PVCe
Stainless steel (316 and 304)
Viton
Polyethylene
ABS
Common steel alloys
Silicone rubber

15.13 Materials

The choice of the materials used during construction, purging, and sampling of the observation point is very important. The materials the equipment (i.e., instrument body, rotors, tubings, fittings, containers) is made of have to be highly inert with respect to physico-chemical attack and degradation that could result from contact with contaminants. This requirement is important to ensure reliable and accurate analytical results, as well as to guarantee that the equipment is maintained and protected in the long term. A few materials are listed in order of decreasing chemical inertia in Table 15.3 [9, 14].

References

1. ASTM, D5088-15A standard practice for decontamination of field equipment used at waste sites, Technical report D5088-15A, West Conshohocken, PA (2015)
2. J.R. Boulding, *EPA Environmental Assessment Sourcebook* (CRC Press, Boca Raton, 1996)
3. E. de Fraja Frangipane, G. Andreottola, F. Tatano, *Terreni contaminati: identificazione, normativa, indagini, trattamento* (CIPA, Milano, 1994)
4. A. Di Molfetta, R. Sethi, Caratterizzazione di acquiferi contaminati, *Indagini in sito per la caratterizzazione meccanica ed ambientale del sottosuolo*, vol. 18.09 (2001), pp. 1–62
5. P.A. Domenico, F.W. Schwartz, *Physical and Chemical Hydrogeology* (Wiley, New York, 1998)
6. US EPA, EPA QA/R-5, EPA requirements for quality assurance project plans (Policies and Guidance, 2001), <https://www.epa.gov/quality/epa-qar-5-eparequirements-quality-assurance-project-plans>
7. US EPA, Guidance for choosing a sampling design for environmental data collection (ProQuest, UMI Dissertation Publishing, 2002)
8. US EPA, Quality assurance, quality control, and quality assessment measures — monitoring and assessment — US EPA (2012), <https://archive.epa.gov/water/archive/web/html/132.html>
9. M.E. Essington, *Soil and Water Chemistry: An Integrative Approach* (CRC Press, Boca Raton, 2004)
10. C.W. Fetter, *Applied Hydrogeology*, 4th edn. (Pearson Education, Long Grove, 2014)
11. C. Giasi, P. Masi, *Considerazioni sulle modalità di campionamento nella caratterizzazione dei siti contaminati* (Ranieri Editore, Milano, 2001)

12. J.P. Gibb, R.A. Griffin, R.M. Schuller, *Procedures for the Collection of Representative Water Quality Data from Monitoring Wells*, Article; Article/Report 7 (Illinois State Water and Geological Surveys, Champaign, 1981)
13. T.E. Lewis, A.B. Crockett, R.L. Siegrist, Soil sampling and analysis for volatile organic compounds. *Environ. Monit. Assess.* **30**, 213–246 (1994)
14. D.M. Nielsen, G. Nielsen, *The Essential Handbook of Ground-Water Sampling* (CRC Press, Boca Raton, 2006)
15. J.F. Pankow, Magnitude of artifacts caused by bubbles and headspace in the determination of volatile compounds in water. *Anal. Chem.* **58**, 1822–1826 (1986)
16. R.W. Puls, M.J. Barcelona, Low-flow (minimal drawdown) ground-water sampling procedures, Technical report EPA/540/S-95/504 (Technology Innovation Office, Office of Solid Waste and Emergency Response, US EPA, Washington, 1996)
17. www.geoprobe.com. Geoprobe Systems
18. www.carsico.it. Carsico s.r.l

Chapter 16

Human Health Risk Assessment



Abstract The focus of this chapter is human health risk assessment, which quantifies the human or environmental toxicological effects deriving from the release of a contaminant at a source and its migration towards exposed receptors. Essentially, this entails a quantitative description of the relations in the system “source—pathway—receptor”. The procedure of risk assessment consists in a sequence of steps, starting from site assessment investigations, through the definition of a conceptual model (i.e., identification of potential receptors and migration and exposure pathways, selection of constituents of concern), the determination of concentrations at the point of exposure, actual risk calculation, to a risk management decision making stage (i.e., uncertainty assessment, risk acceptability evaluation, determination of the maximum acceptable concentration levels at the source and the selection of appropriate interventions). The risk assessment itself can be carried out at an increasing degree of detail, through a tiered approach, illustrated in the chapter. A relevant focus of this chapter is the calculation of the concentration at the point of exposure via the determination of the natural attenuation factor. This factor is the cumulative result of the contaminant concentration attenuation in the course of its migration from the source to the point of exposure (e.g., partitioning between environmental components, attenuation in the unsaturated medium, dilution in the aquifer or in rivers, volatilization). Having determined the concentration at the point of exposure, the calculation of the rate of exposure is presented. With these two parameters it is then possible to calculate the risk deriving the exposure to carcinogenic or threshold compounds, following a contamination event. The carcinogenic risk is quantified by the incremental lifetime cancer risk, which is a function of the slope factor (defined in Chap. 9); the non-carcinogenic risk, instead, is quantified by the hazard quotient, which is a function of the reference dose (also defined in Chap. 9). Once the risk has been calculated, its acceptability can be evaluated according to the local legislation, and measures to manage it can be put into place.

The unbalance between the increasing number of environmental contamination incidents and the limited availability of resources for its restoration has prompted the development of an objective support tool for the management of contaminated sites.

Such a tool should allow to quantitatively assess the human health risk related to a contamination event.

Human health risk assessment is the scientifically and technically most advanced approach for the evaluation of the degree of contamination of a site and for the definition of intervention priorities at the site itself (protection, remediation, or restoration). One of its most striking features is its ability to quantify human health and environmental hazards related to the release of contaminants and to provide support in the development of strategies to manage individual risks by employing rigorous methods, thus preventing the waste of economic resources in situations that do not pose any actual human health risk.

Risk assessment is, therefore, particularly useful when: (i) threshold concentration values defined by the local legislation are exceeded in one or multiple environmental components and the required remediation interventions are hindered by technical or economic limitations; (ii) ownership of areas previously exploited for potentially risky activities is transferred to a new buyer and their interest must be protected; (iii) disused industrial areas, in which production processes that were not regulated by appropriate environmental legislation used to be carried out, must be rehabilitated.

In particular, risk analysis is used by the European and American legislation for the definition of threshold concentrations that must be achieved through the remediation of contaminated sites [3, 8, 15]. In the general context mentioned above, risk assessment is especially interesting for evaluating the potential health risk associated to the degradation of groundwater resources, which, besides being the topic of this book, are also the most vulnerable environmental component. A Risk Based Corrective Action (RBCA) procedure starts from the quantification of risk and the development of a strategy to support the management and remediation of contaminated sites [2, 5].

16.1 Definition of Human Health Risk

In everyday language the term “risk” is hard to define appropriately and significant efforts have been made to agree upon a single unambiguous definition of the term (see Sect. 7.3).

When referring to the environment, in particular to groundwater resources, it is important to make a distinction between the concepts of contamination risk and of human health risk.

As extensively addressed in Sect. 7.3, groundwater *contamination risk* expresses the probability of quality deterioration of groundwater resources after the occurrence of a hazardous situation at a site characterized by specific vulnerability characteristics.

Human health risk, instead, quantifies the human or environmental toxicological effects resulting from the presence of a source of contamination whose emissions or spills can reach potentially exposed targets (receptors) via various migration pathways. Therefore, evaluating the human health risk entails a quantitative description

of the relations in the “source—pathway—receptor” system. It should be noted that according to the implementation strategies for the Water Framework Directive (WFD) defined by the European Commission, *risk* is understood as the risk of not achieving the environmental objectives of the WFD, rather than directly as the risk of human health being affected [3]. In this chapter, the classic interpretation of risk for human health and the environment is considered.

The evaluation process of the human health risk is called *human health risk assessment*; for brevity, henceforth we will refer to it as *risk assessment (RA)* [6]. This procedure is an absolute evaluation, specific to the site in question and independent from situations that can be found in different contexts. It should, therefore, not be confused with the numerous available relative risk assessment methods, which are based on the assignment of weights and scores to rank the examined sites by hazard level.

16.2 Features of Risk Assessment

The procedures for RA and RBCA were first developed in the US in the late '80s [13] and subsequently standardized by [1, 2]. RA is based on a tiered approach structured in various phases.

16.2.1 Phases

The RA approach is structured in a logical sequence of phases progressing from site assessment investigations to risk management decision making. In particular, the following steps can be identified (see Fig. 16.1):

- site characterization;
- definition of the conceptual model;
- determination of concentrations at the point of exposure;
- risk calculation;
- decision assessment.

Site assessment includes all the environmental investigations required to characterize the source of contamination and the environmental components affected by the pollution. Based on the obtained results and on the history of the site, a conceptual model can be developed, which identifies potential receptors and migration and exposure pathways, and in which a set of *constituents of concern (COCs)*, used as parameters representative of the contamination, are selected.

In order to determine the concentration values at the points of exposure (POEs), it is necessary to be able to simulate the migration processes of the various COCs that lead to the POEs from the source. This, combined with the assessment of the

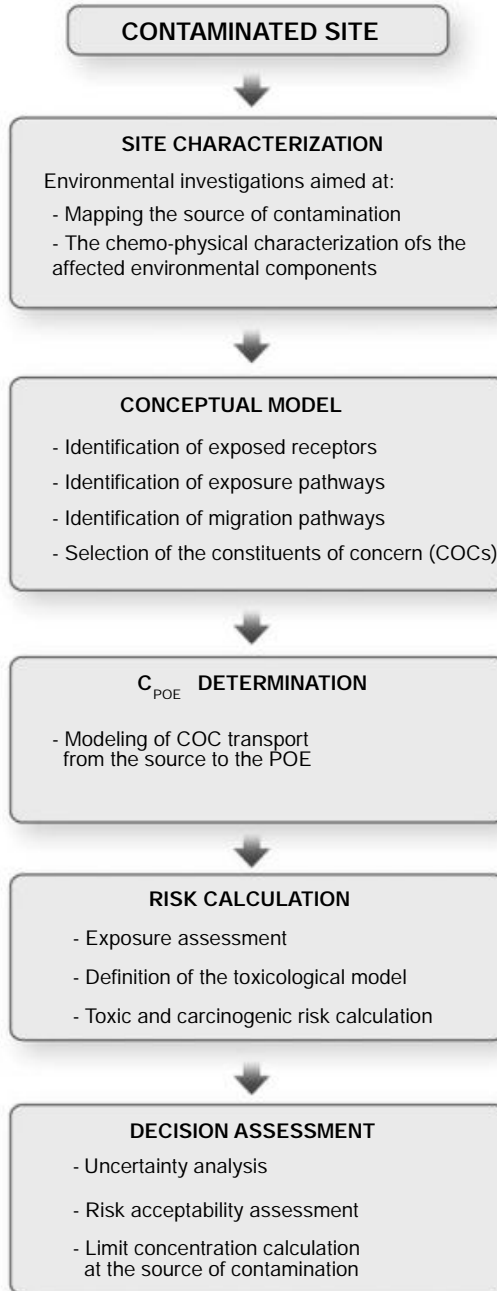


Fig. 16.1 Schematic of the phases of risk assessment

exposure rate and of the toxicological properties of the COCs, allows to calculate the toxic or genotoxic (carcinogenic) risk.

The last phase consists in the decision assessment related to risk management. This phase includes an uncertainty assessment, a risk acceptability evaluation, the determination of the maximum acceptable concentration levels at the source, and the selection of appropriate interventions [2, 3, 16].

16.2.2 Risk Assessment Tiers

RA is a tiered approach which can be carried out at increasing levels of detail, which depend on the need and on the information that is available [3, 16]. In particular, the ASTM E2081 standard [2], an improved version of the previous ASTM E 1739 standard, defines the so called Risk-Based Corrective Action (RBCA), structured in three tiers, see Fig. 16.2.

The first tier essentially consists in comparing the site contamination with screening concentration values. It is aimed at identifying the potential need for emergency interventions, particularly for provisional safety measures, and it consists in the collection of concentration values on site and in comparing them with the *screening levels*. These threshold values are conservatively defined as those concentration levels that do not pose risks for human health and the environment.

On this basis, Risk-Based Screening Levels (RBSLs) and Soil Screening Levels (SSLs) have been determined by the ASTM and US EPA, respectively [1, 2, 13]. As an example of a European implementation of a similar approach, the Italian legislation defined threshold contaminant concentrations (CSC–Concentrazioni Soglia di Contaminazione) as screening levels. These values were defined considering the entire nation, different land uses, the environmental and toxicological behavior of substances, and the most critical exposure pathways according to the principles of RA [10, 11]. If the screening levels are not exceeded, a monitoring program can be put in place, but no remediation action is required. Conversely, if some of the values are exceeded, the site is considered *potentially contaminated* and the need for an intervention is established through a more detailed risk assessment.

The second tier consists in a simplified risk assessment, in which part of the input data are derived from targeted on-site investigations, whereas missing information is obtained from validated and up-to-date databases or from the literature, favoring conservative data in order to ensure that calculations promote environment and human health protection. Concentrations deriving from second tier RA are less conservative and closer to reality, because data deriving from the actual risk scenario and analytical models is used.

User friendly computer programs are available for the implementation of second tier RA, among which the most commonly used are “RBCA Toolkit for Chemical Releases” and “BP–RISC”, which follow the RBCA approach defined in the ASTM manual PS 104 [7, 9].

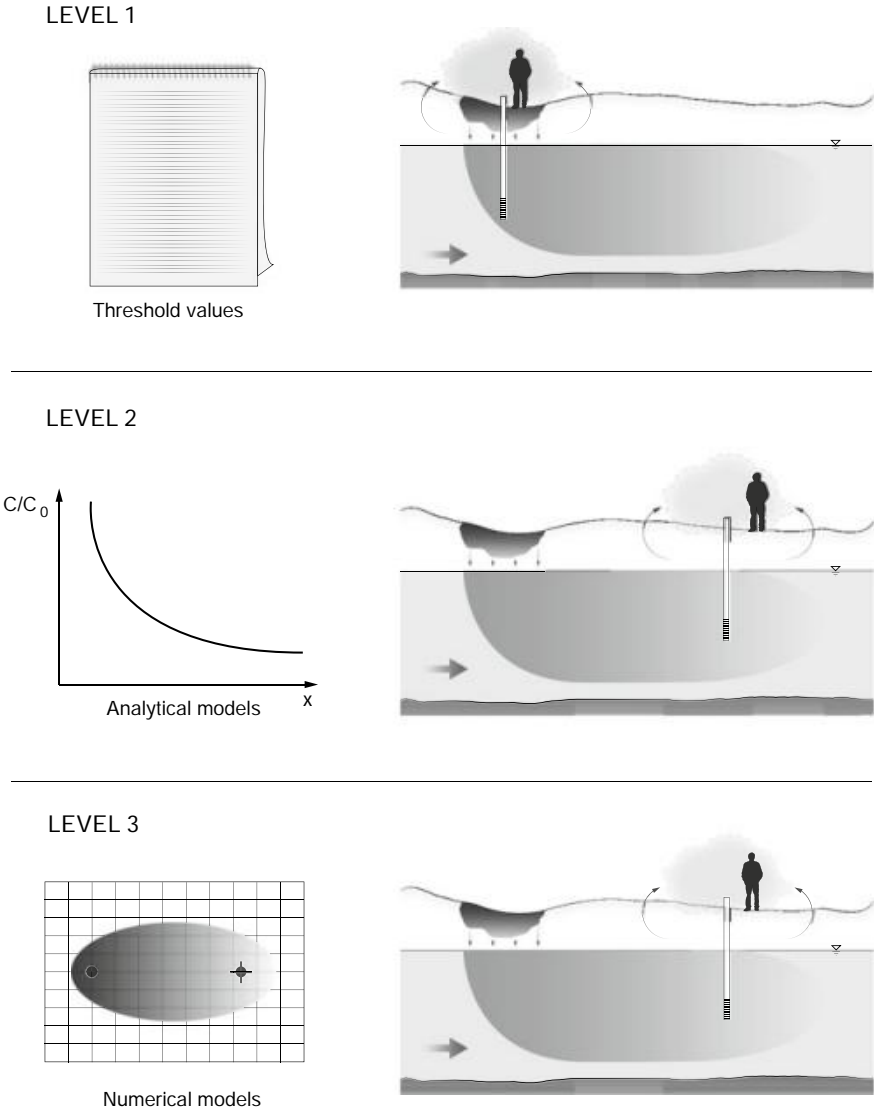


Fig. 16.2 Schematic of the three levels of detail of risk assessment according to the RBCA approach

The third tier represents an even more detailed appraisal of risk, based on more sophisticated computational methods (mainly numerical and probabilistic models). These require a sufficient amount of site-specific chemical, physical and biological data to carry out a full experimental system characterization.

In addition to quantifying the risk, second and third tier RA can be used to define the acceptability levels, in a process called *backward analysis* (i.e., the maximum

concentration that can be tolerated for each contaminant present in the source, beyond which the risk becomes unacceptable). In this case, these threshold values defined within the RBCA procedure are called *Site-Specific Target Levels* (SSTLs). Unlike the levels set in first tier RA (e.g., RBSLs), they are site-specific because they are derived from the parameters of the contamination scenario under consideration. Overall, they represent the target concentrations of a remediation intervention in a contaminated site.

Clearly, further stages of assessment should not be excluded and can follow an improvement in the experimental characterization of the site, to achieve a RA that is increasingly closer to reality and less conservative.

16.3 Risk Assessment Development

16.3.1 Characterization Plan

Prior to conducting the risk assessment of a site, the physical and environmental settings of the latter have to be characterized, see Chap. 15.

The reliability and scientific soundness of the RA process and its results are strongly reliant on the amount and quality of the data available for the characterization of the site of interest. Although, on the one hand, a thorough investigation can be resource consuming, on the other hand it offers a clear economic advantage in the downstream design stage of the remediation intervention, should it prove necessary.

Based on the data obtained during site assessment and on the site history, a conceptual model can be defined by identifying the receptors, potential routes of exposure, migration pathways of the contaminants released at the source, and by selecting the COCs.

The identification of possible receptors and of the pathways of exposure must consider present and future land use, since contaminant release is a dynamic phenomenon.

Once receptors and pathways of exposure have been identified, the conceptual model requires the definition of all the actual migration pathways that the contaminants can follow to reach the POEs. The transport pathways of contaminants subjected to an RA study can be summarized in the following categories: groundwater, surface water, air, soil, and food chain. Depending on the specific environmental context where the site of interest lies, not all pathways are necessarily “active”. It should be noted that the scenario *groundwater–drinking water ingestion* is, in most cases, the most serious, in particular when release of mobile contaminants occurs.

Data analysis of a detailed risk assessment applied to all the chemical compounds detected in a potentially contaminated site would be excessively costly and would unnecessarily complicate the results of the evaluation.

It is, therefore, important to focus on the COCs, i.e., a group of substances that can be considered representative of the total impact of the source of contamination, in terms of toxic and genotoxic risk.

Hence, the choice of the COCs for a specific site represents one of the crucial aspects of RA, in particular when the contamination event involves the concomitant presence of multiple compounds.

Generally, the selection is based on the following factors [2]:

- presence of compounds that exceed the threshold concentration defined by the local legislation in one or multiple environmental components;
- presence of compounds that exceed the natural background levels;
- compounds directly related to the activities carried out at the site detected in one or more environmental components;
- toxicity level;
- mobility and persistence level.

16.3.2 Calculation of the Concentration at the Point of Exposure

A receptor can be exposed to a compound at the source (direct exposure) or at a distance from it (indirect exposure): in the former case, the concentration that describes the source is the value that should be used in the RA; in the latter, the mechanisms of contaminant migration from the source to the POE have to be modeled. The modeling process develops in sequential steps, the output of each representing the input for the following.

Eventually, the process results in the determination of the *natural attenuation factor* (*NAF*), i.e., the ratio between the concentration of the COC at the source and at the POE (C_{POE}), in steady state conditions. The value of the *NAF* and, consequently, of C_{POE} depends on the specific migration path followed by the contaminant.

In the following paragraphs the individual modeling stages are introduced. Here, the focus is exclusively the contamination of water resources; it must be stressed, however, that risk assessment must consider all possible migration paths within the different environmental components and all exposure pathways. The deterministic analytical approach described below is based on the ASTM standard PS 104 [2].

16.3.2.1 Release in the Unsaturated Medium

Groundwater quality degradation starts with a spill from a source present in the soil and the subsequent formation.

Leachate is composed of a mix of compounds whose concentration is governed by the soil-leachate partition coefficient, K_{sw} . This parameter is defined as the ratio

between the concentration of a generic component in the leachate and in the mass of soil at the source, in steady state conditions [5]:

$$K_{sw} = \frac{C_{soil}}{C_{leach}}. \quad (16.1)$$

Assuming that:

- (a) the equilibrium between the concentrations in the leachate and in the soil at the source is achieved instantaneously;
- (b) decay processes in the soil and in the leachate are negligible;
- (c) the mass present at the source is infinitely large relative to the release potential to the leachate;

the partition coefficient can be calculated from the total mass of the generic contaminant, M_T , contained in the volume, V_b , of the polluting source:

$$M_T = M_{leach} + M_s + M_g = (\theta_w + \rho_b K_d + H\theta_a) C_{leach} V_b, \quad (16.2)$$

thus, the concentration of the generic compound at the source is:

$$C_{soil} = \frac{M_T}{\rho_b V_b} = \frac{(\theta_w + \rho_b K_d + H\theta_a)}{\rho_b} C_{leach}, \quad (16.3)$$

and the soil-leachate partition coefficient becomes [14]:

$$K_{sw} = \frac{\theta_w + \rho_b K_d + H\theta_a}{\rho_b} \left[\frac{L^3}{M} \right], \quad (16.4)$$

where ρ_b is the soil bulk density; θ_w the volumetric water content; θ_a the volumetric air content ($\theta_a = n - \theta_w$); n the total porosity; H Henry's constant; K_d the partition coefficient for organic compounds ($K_d = K_{oc} \cdot f_{oc}$, with f_{oc} being the fraction of organic carbon and K_{oc} being the partition coefficient of a compound between organic carbon and water).

Based on expression (16.1) the concentration of an individual contaminant in the leachate is:

$$C_{leach} = \frac{C_{soil}}{K_{sw}}, \quad (16.5)$$

provided that it doesn't exceed the solubility limit:

$$C_{leach} \leq x_i S_i, \quad (16.6)$$

where x_i is the molar fraction of a generic contaminant initially present at the source and S_i its solubility in water, and provided that the mass of the contaminant in the leachate does not exceed, during the entire exposure duration, ED , the mass of the same contaminant at the source:

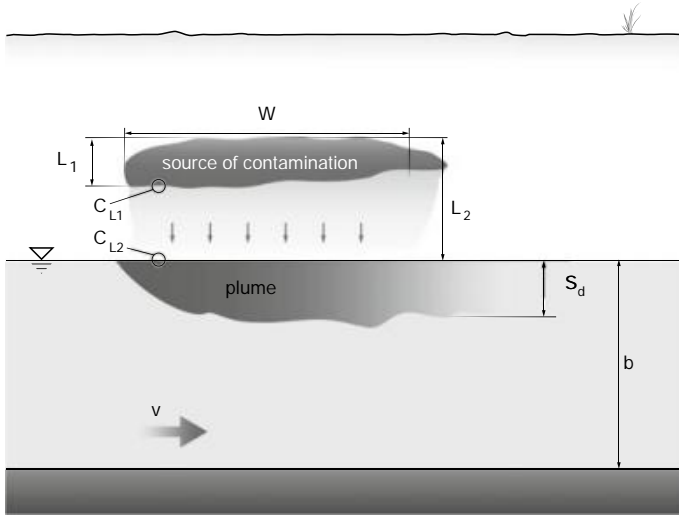


Fig. 16.3 Schematic of release processes from the source to the water table

$$M_{leach} \leq M_{soil}. \tag{16.7}$$

The latter condition (see Fig. 16.3) translates into the inequality:

$$C_{leach} \cdot (I_{eff} \cdot ED) \cdot A \leq C_{soil} \cdot A \cdot L_1 \cdot \rho_b, \tag{16.8}$$

or:

$$C_{leach} \leq \frac{C_{soil} \cdot L_1 \cdot \rho_b}{I_{eff} \cdot ED}, \tag{16.9}$$

where I_{eff} is the effective infiltration occurring at the site of interest, and L_1 and A are the thickness and horizontal area, respectively, of the the source of contamination.

Based on the above, the smallest value among those obtained from Eqs. (16.5), (16.6) and (16.9) will clearly have to be used as C_{leach} .

Equation (16.4), describing the partition between the different phases at equilibrium, and representing the ASTM release model, is a very conservative solution that yields an overestimation of the leachate’s composition, and hence of the RA. If leaching tests have been carried out, the experimental results can be directly used instead of Eq. (16.4).

In the case of RA of a solid waste landfill, this first step ends once the specific composition of the leachate, used as the starting datum for the procedure, has been determined.

16.3.2.2 Attenuation in the Unsaturated Medium

Once the leachate is formed, it flows vertically towards the water table under the effect of gravity and of capillary forces. This flow causes the contaminant mass to spread across the volume of unsaturated medium that separates the source of contamination from the water table, resulting in a decrease in concentration.

If the depth to groundwater, L_2 , is significantly greater than the thickness of the source of contamination, L_1 (see Fig. 16.3), it is worth considering attenuation processes that may lead to a decrease in contaminant concentration as they cross the unsaturated zone. This decrease can be quantified through the so called *Soil Attenuation Model (SAM)* [4].

If volatilization and biodegradation processes are neglected, and if the law of mass conservation is applied to each contaminant:

$$M_T = (\theta_w + \rho_b K_d + H\theta_a) \cdot C_{leach} \cdot A \cdot L = \text{constant}, \quad (16.10)$$

then:

$$C_{l_2} = C_{l_1} \frac{L_1}{L_2}, \quad (16.11)$$

where C_{l_1} and C_{l_2} are the concentrations in the leachate at depths L_1 and L_2 , respectively.

C_{l_2} represents, therefore, the maximum concentration of a contaminant when it reaches the water table. Actually, this value decreases in time, as the concentration of each compound at the source decreases. The SAM model, however, assumes that this concentration remains constant in time, consistently with the conservative assumption that the mass present at the source is infinitely greater than its release potential.

Even biodegradation, not considered until now, can play an important role during the migration of some organic compounds across thick unsaturated media. In this case, natural biodegradation can be simulated with an exponential decay model of the first order by using the dimensionless BioDegradation Factor, *BDF*, which can be calculated as follows:

$$BDF = \exp \left[-\lambda_v (L_2 - L_1) \frac{\theta_w + \rho_b K_d + H\theta_a}{I_{eff}} \right], \quad (16.12)$$

where λ_v is the biodegradation coefficient in the vadose zone, $[T^{-1}]$.

It follows that the concentration of a contaminant in the leachate that mixes with groundwater can be expressed as:

$$C_{l_2} = \frac{C_{soil}}{K_{sw} \cdot BDF} \cdot \frac{L_1}{L_2}, \quad (16.13)$$

which can be reduced to:

$$C_l = \frac{C_{soil}}{K_{sw} \cdot LAF}, \quad (16.14)$$

by including all the attenuation factors that act on contaminants in the unsaturated medium in the *Leachate Attenuation Factor (LAF)*. Clearly, overlooking the attenuation processes occurring in the unsaturated medium (i.e., $LAF = 1$) results in significantly more conservative results of the RA.

16.3.2.3 Leachate Dilution in the Mixing Zone

Once the leachate has crossed the entire unsaturated medium, it mixes with the groundwater at the water table.

At steady state a groundwater and leachate mixing zone is established, in which concentrations are diluted according to a dimensionless Leachate Dilution Factor (*LDF*), defined as [5, 16]:

$$LDF = \frac{C_l}{C_0}, \quad (16.15)$$

where C_0 is the contaminant concentration in the mixing zone below the source of contamination.

A very simple conceptual model (box model) can be used to quantify the *LDF*, by evaluating the mass dilution in the mixing zone located right below the source of contamination.

Referring to the schematic in Fig. 16.3 and defining S_w as the width of the contamination front determined in the mixing zone perpendicularly to the direction of flow, S_d as the thickness of the mixing zone, v as the groundwater seepage velocity, and n_e as the effective porosity, the following can be derived:

leachate volume discharge entering the mixing zone, $I_{eff} W S_w$

uncontaminated water volume discharge entering the mixing zone, $v n_e S_d S_w$

overall liquid volume discharge present in the mixing zone, $v n_e S_d S_w + I_{eff} W S_w = (v n_e S_d + I_{eff} W) S_w$

Consequently, the leachate dilution factor in the mixing zone (which is proportional to the discharge) is equal to:

$$LDF = 1 + \frac{v n_e S_d}{I_{eff} W} = 1 + \frac{K i S_d}{I_{eff} W}, \quad (16.16)$$

where K is the hydraulic conductivity of the contaminated aquifer, i the average piezometric gradient in the mixing zone and W the width of the source along the direction of flow.

A correct estimation of the thickness, S_d , of the mixing zone isn't straightforward. If a specific estimate isn't available, the following algorithm can be used:

$$S_d = \sqrt{2\alpha_z W} + b \cdot \left[1 - e^{-\frac{i_{eff} \cdot W}{K i b}} \right], \quad (16.17)$$

where b is the saturated thickness of the aquifer and α_z the vertical dispersivity, provided that $S_d \leq b$.

To summarize, the concentration of a contaminant in the mixing zone of an aquifer can be derived from its concentration at the source by applying the following expression [14]:

$$C_0 = \frac{C_{soil}}{LAF \cdot K_{sw} \cdot LDF}. \quad (16.18)$$

If monitoring wells have been installed and used to sample contaminated groundwater from the aquifer, below the source, and if the concentration distribution can be considered to have reached a steady state relative to the duration of the phenomenon (e.g., the site is an old illegal waste dump), the measured concentration values can be used instead of the above described calculations. Thus, they become the starting values for the RA.

16.3.2.4 Dilution and Attenuation in the Aquifer

The aquifer contamination that occurred in the mixing zone due to the leachate that percolated from the source of contamination in the soil is further diluted and attenuated due to transport and dispersion phenomena in the aquifer itself.

This decrease in concentration is quantified through the dimensionless *Dilution Attenuation Factor* (DAF), defined as the ratio between the concentration of the compound in the mixing zone, C_0 , and in the aquifer, downgradient of the mixing zone, C_{gw} [5]:

$$DAF = \frac{C_0}{C_{gw}}. \quad (16.19)$$

The DAF can be determined analytically or numerically.

Domenico's is one of the most commonly used analytical solutions, due to the fact that it applies to boundary conditions that describe with sufficient accuracy the dispersion of a compound released from a source of non-negligible dimensions via continuous injection (see Sect. 13.3.2). This solution describes the non-steady three-dimensional concentration distribution resulting from a continuous release from a plane source positioned perpendicularly to the direction of flow of the aquifer, with transversal and vertical dimensions, S_w and S_d , respectively (see Fig. 16.4).

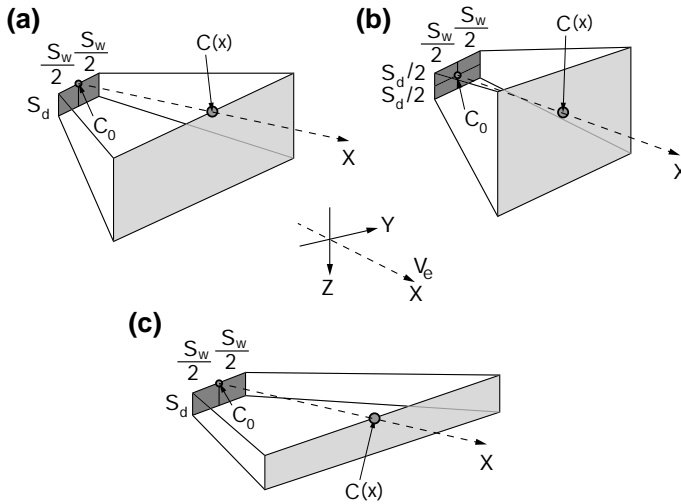


Fig. 16.4 Possible effects of vertical dispersion on the geometry of contamination resulting from the continuous release from a plane source: **a** only downward-directed vertical dispersion; **b** vertical dispersion directed both up- and down-ward; **c** no vertical dispersion (the contaminant reached the base of the aquifer in the mixing zone)

In addition to the hydrological processes (i.e., advection and hydrodynamic dispersion), the solution accounts for the potential natural decay of a contaminant, which can be described with a first order reaction kinetics (radioactive decay, biodegradation, hydrolysis), and for potential sorption of the contaminant to the surface of the solid grains, which can be described by a linear isotherm (see Sect. 13.3.2).

In the more realistic hypothesis that contaminant dispersion occurs along two transverse (+y and -y) and one vertical (+z) direction, as well as along the direction of flow, x (see Fig. 16.4a), if we indicate with C_0 the concentration at the plane source, with α_x, α_y and α_z , respectively, the longitudinal, transverse and vertical dispersivity, with R_i the retardation factor of a generic compound, and with λ_i its decay coefficient, in steady state conditions the highest concentration value will be found along the x axis:

$$\frac{C(x)}{C_0} = \exp \left\{ \left(\frac{x}{2\alpha_x} \right) \left[1 - \sqrt{1 + \frac{4\lambda_i\alpha_x R_i}{v}} \right] \right\} \cdot \operatorname{erf} \left[\frac{S_w}{4\sqrt{\alpha_y x}} \right] \cdot \operatorname{erf} \left[\frac{S_d}{2\sqrt{\alpha_z x}} \right]. \tag{16.20}$$

Here degradation is assumed to occur both in the liquid and in the sorbed phase (for degradation only in the liquid phase $R_i = 1$).

Should the inclusion of both directions of vertical dispersion (+z e -z) be preferable for the contaminant at hand, analogously to the two transverse directions (see Fig. 16.4b), Eq. (16.20) becomes:

$$\frac{C(x)}{C_0} = \exp \left\{ \left(\frac{x}{2\alpha_x} \right) \left[1 - \sqrt{1 + \frac{4\lambda_j \alpha_x R_i}{v}} \right] \right\} \cdot \operatorname{erf} \left[\frac{S_w}{4\sqrt{\alpha_y x}} \right] \cdot \operatorname{erf} \left[\frac{S_d}{4\sqrt{\alpha_z x}} \right]. \quad (16.21)$$

Finally, if the aquifer thickness is small and entirely affected by the contamination since the mixing phase (Fig. 16.4c), there will be no vertical dispersion and Eq. (16.20) becomes:

$$\frac{C(x)}{C_0} = \exp \left\{ \left(\frac{x}{2\alpha_x} \right) \left[1 - \sqrt{1 + \frac{4\lambda_j \alpha_x R_i}{v}} \right] \right\} \cdot \operatorname{erf} \left[\frac{S_w}{4\sqrt{\alpha_y x}} \right]. \quad (16.22)$$

Since $C(x)$ is the highest contaminant concentration that can be found in the aquifer downgradient of the mixing stage, in the procedure to calculate risk, C_{gw} is set equal to $C(x)$.

When the above described boundary conditions and/or the geometry of the source of contamination are not suitable to describe the real system, the differential equation must be solved numerically to describe the hydrologic, physico-chemical and biological processes involved in the event under investigation.

Whatever the approach eventually used, the dispersivity parameters play an important role; these are, however, difficult to determine experimentally. If specific values are not available, conservative values recommended by default by the RBCA approach are [7]:

$$\begin{aligned} \alpha_x &= 0.1 L, \\ \alpha_y &= 0.33 \alpha_x, \\ \alpha_z &= 0.05 \alpha_x. \end{aligned}$$

Many correlations for the estimation of dispersivity parameters according to the scale, L , of the examined event are available in the literature (see Sect. 10.1.4).

16.3.2.5 Dilution in a River

If the considered aquifer is drained by a river, as depicted in Fig. 16.5, the hypothetical groundwater contamination undergoes an additional dilution process, quantified by the dimensionless River Dilution Factor (RDF , or groundwater to surface water dilution factor). The RDF is defined as the ratio between the contaminant concentration in the groundwater upgradient of the mixing zone with the river, C_F , and its concentration in the river, C_r [5]:

$$RDF = \frac{C_{gw}}{C_r}. \quad (16.23)$$

If we refer to the schematic in Fig. 16.5, RDF can be calculated via the discharge balance in the mixing zone, through the following equation:

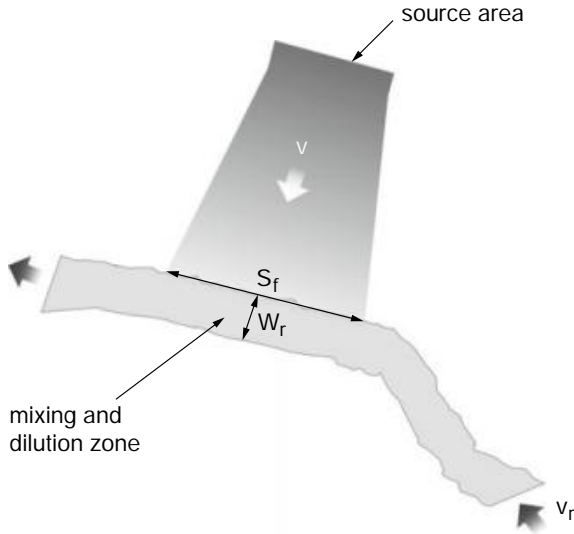


Fig. 16.5 Contamination plume dilution in a river

$$RDF = 1 + \frac{Q_r}{v n_e S_f b_r} = 1 + \frac{v_r W_r}{v n_e S_f}, \quad (16.24)$$

where b_r , Q_r , v_r , and W_r are, respectively, the width of groundwater-to-surface water discharge, the river discharge, the river water velocity, and the river width in dry spell conditions; and S_f is the thickness of affected groundwater to surface water discharge.

Equation (16.24) is applicable if the contaminant concentration in the river (C_{r0}) upstream of the mixing area is equal to zero.

If, instead, $C_{r0} \neq 0$, the RDF is equal to:

$$RDF = \frac{C_{gw} [v n_e S_f b + Q_r]}{C_{gw} v n_e S_f b + C_{r0} Q_r} = \frac{C_{gw} [v n_e S_f + v_r W_r]}{C_{gw} v n_e S_f + C_{r0} v_r W_r}. \quad (16.25)$$

16.3.2.6 Vapor Volatilization in Outdoor Environments

Volatile compounds present in the groundwater can migrate across the unsaturated zone and towards the surface as vapors (Fig. 16.6a). In outdoor environments, vapors mix with the air above the source of contamination. The process can be described quantitatively through the dimensionless outdoor Volatilization Factor (VF_{out}), defined as the ratio between the contaminant concentration in the atmosphere at the POE, C_{POE} , and its concentration in the groundwater, C_F [5]:

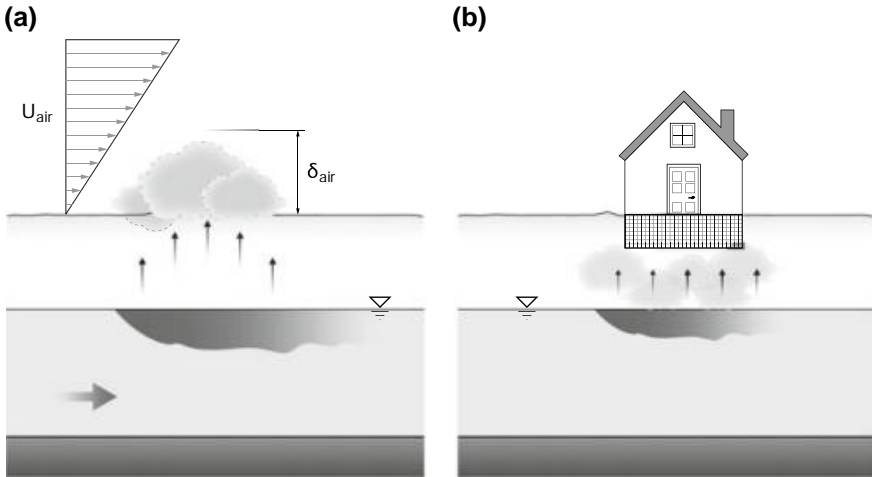


Fig. 16.6 Vapor volatilization in out- and in-door environments

$$VF_{out} = \frac{C_{POE}}{C_F}. \quad (16.26)$$

VF_{out} can be estimated with the following equation:

$$VF_{out} = \frac{H}{1 + \frac{U_{air} \delta_{air} L_{GW}}{D_{ws}^{eff} W}} \cdot 10^3. \quad (16.27)$$

U_{air} is the average air velocity 2 m above the surface; δ_{air} is the elevation of the mixing zone in the atmosphere; L_{GW} is the depth to groundwater; W is the length of the source in the main wind direction; D_{ws}^{eff} is the diffusion coefficient of the contaminant, expressed as a function of the characteristics of the capillary fringe and of the vadose zone via the following equation:

$$D_{ws}^{eff} = (h_{cap} + h_v) \cdot \left(\frac{h_{cap}}{D_{cap}^{eff}} + \frac{h_v}{D_s^{eff}} \right)^{-1}. \quad (16.28)$$

In Eq. (16.28), h_{cap} is the thickness of the capillary fringe, h_v is the thickness of the unsaturated zone, and D_{cap}^{eff} is the effective diffusion coefficient in the capillary fringe. The latter parameter can be expressed as:

$$D_{cap}^{eff} = D_a \cdot \frac{\theta_{a, cap}^{3.33}}{n^2} + \frac{D_w}{H} \cdot \frac{\theta_{w, cap}^{3.33}}{n^2}, \quad (16.29)$$

where D_s^{eff} is the effective diffusion coefficient in the unsaturated zone, in turn expressed as:

$$D_s^{eff} = D_a \cdot \frac{\theta_a^{3.33}}{n^2} + \frac{D_w}{H} \cdot \frac{\theta_w^{3.33}}{n^2}. \quad (16.30)$$

D_a is the diffusion coefficient in air, D_w is the diffusion coefficient in water, $\theta_{a, cap}$ is the air content in the capillary fringe, and $\theta_{w, cap}$ is the water content in the capillary fringe.

16.3.2.7 Vapor Volatilization in Indoor Environments

Volatilization in indoor environments occurs when there is a building above the contaminated portion of the aquifer. The volatile fraction of contaminants can infiltrate within buildings through cracks in the foundations or walls (Fig. 16.6b). This phenomenon is quantitatively described by the dimensionless indoor Volatilization Factor, VF_{in} , defined as the ratio between the contaminant concentration in indoor air at the POE, C_{POE} , and in the aquifer, C_F [5]:

$$VF_{in} = \frac{C_{POE}}{C_F}. \quad (16.31)$$

A model proposed by Johnson e Ettinger [5, 12] is used to estimate VF_{in} :

$$VF_{in} = \frac{H \frac{D_w^{eff}}{L_{GW} L_b ER}}{1 + \frac{D_w^{eff}}{L_{GW} L_b ER} + \frac{D_w^{eff} L_{crack}}{D_{crack}^{eff} L_{GW} \eta}}, \quad (16.32)$$

where L_b is the ratio between indoor volume and infiltration surface area; ER is the indoor air circulation rate; L_{crack} is the thickness of the foundations; η is the surface fraction of the cracks in the foundations; D_{crack}^{eff} is the effective diffusion coefficient of the contaminant through the cracks, expressed by the following equation:

$$D_{crack}^{eff} = D_a \cdot \frac{\theta_{a, crack}^{3.33}}{n^2} + \frac{D_w}{H} \cdot \frac{\theta_{w, crack}^{3.33}}{n^2}. \quad (16.33)$$

In the previous equation $\theta_{a, crack}$ and $\theta_{w, crack}$ are the air and water content in the cracks of the foundations, respectively.

16.3.2.8 Overall Attenuation Factor

The degradation of water resources undergoes an overall attenuation measured by the Natural Attenuation Factor (NAF), defined as:

$$NAF = \frac{\text{contaminant concentration at the source}}{\text{contaminant concentration at the point of exposure}} = \frac{C_{soil}}{C_{POE}}. \quad (16.34)$$

Based on the previous paragraphs, if exposure by ingestion of contaminated water is considered, the value of the NAF can be derived from the following [5, 16]:

$$NAF = K_{sw} \cdot LAF \cdot LDF \cdot DAF \cdot RDF. \quad (16.35)$$

Dimensionally, $NAF = [L^3/M]$.

Clearly, if exposure does not occur via water taken from a river, but directly from an aquifer, RDF can be set equal to 1 in Eq. (16.35).

If, instead, exposure occurs by inhalation of vapors migrating from the groundwater, the NAF can be calculated as

$$NAF = \frac{K_{sw} \cdot LAF \cdot LDF}{VF}, \quad (16.36)$$

where $VF = VF_{out}$ if exposure happens outdoors, or $VF = VF_{in}$ if it happens indoors.

16.3.2.9 Concentration at the Point of Exposure

Based on the definition of the natural attenuation factor, which summarizes all the attenuation mechanisms that could occur during the migration of the contaminants from the source to the point of exposure, the concentration at the POE is:

$$C_{POE} = \frac{C_{soil}}{NAF}. \quad (16.37)$$

If a monitoring network is available at the point of exposure to measure the concentrations of the groundwater contaminants, these values can be used directly to determine of the resulting health risk. In this case, risk assessment will be more reliable because all uncertainties associated with the simulation of complex physical, chemical and biological processes influencing the transport and spreading of the contamination are eliminated.

16.4 Toxicological Models and Parameters

The potential harmful effects on the health of a population exposed to contaminants at the POE can be defined through the data published by the US EPA Integrated Risk Information System (IRIS) and other international or local research and health institutes. In Italy, for example, the National Institute of Health (ISS—Istituto Superiore di Sanità) and the National Institute for Prevention and Safety at Work (ISPESL—

Istituto Superiore per la Prevenzione e la Sicurezza sul Lavoro) made a database available which describes the main physico-chemical and toxicological properties of the main contaminants.

Human health risk assessment considers the chronic toxicity of compounds, evaluating the risks that environmental contamination with a certain substance (or group of substances) can cause on the health of individuals following chronic exposure. The US Environmental Protection Agency groups substances in six hazard categories. However, the most relevant classification for risk assessment classifies toxic compounds as non-carcinogens and carcinogens (or threshold and non-threshold chemicals, respectively), according to the dose-response model they follow (see Sect. 9.3).

The toxicological parameters used in risk analysis are the reference dose, *RfD*, for non-carcinogenic substances and the slope factor, *SF*, for carcinogens.

16.5 Risk Assessment

The human health risk represents the risk increment the receptor is subjected to as a result of the exposure to a specific situation of environmental contamination.

The value of risk is clearly correlated to the concentration value of the contaminant at the POE, the exposure rate and the toxicological features of the compound.

16.5.1 *Determination of the Concentration at the Point of Exposure*

The risk assessment procedure entails the identification of all the actual migration paths that COCs can follow to reach the POE. Exposure of the receptor can occur at the source of contamination or at a certain distance from it. In the former case (i.e., direct exposure), the concentration of the contaminant at the point of compliance coincides with the concentration assumed as representative of the source. Conversely, indirect exposure can only be calculated by modeling the mechanisms that drive contaminant migration from the source to the point of compliance, as discussed in Sect. 16.3.2 in regard to groundwater.

A deterministic approach to the calculation of concentrations at the POE implies the use of analytical or numerical models. Analytical models (second level analysis) are clearly easier to deal with, but they make a few simplifying assumptions on certain aspects of the physical model: the characteristics of the medium (it is considered homogeneous and isotropic), the geometry of the source of contamination and the boundary conditions.

Numerical models (third level analysis), instead, take into account the heterogeneities of the system and include generic source geometries and boundary condi-

tions. However, they require a more detailed knowledge of the physical system and, therefore, a more thorough characterization phase.

Whatever the model, the result consists in the calculation of the *NAF* for each exposure pathway, defined as the ratio between the concentration of the COC at the source, C_s , and at the POE, C_{POE} , in steady state conditions. Naturally, for direct exposure *NAF* is equal to 1.

16.5.2 Rate of Exposure

For each migration pathway, every individual receptor enters in contact with the contaminant at a specific *exposure rate*, i.e., the average amount of each environmental medium (water, air, soil) in-taken per body weight unit per day of exposure.

The exposure rate, E , can thus be calculated with the following formula [5]:

$$E = \frac{CR \cdot EF \cdot ED}{BW \cdot AT}, \quad (16.38)$$

where CR is the contact factor, i.e., the amount of each environmental component (water, air, soil) ingested, inhaled, or touched per unit of time or event (dimensionally, it is L^3/T for water and air, M/T for soil; usually it is expressed in l/d or m^3/d or mg/d); EF is the exposure frequency, it is dimensionless but is normally expressed as days per year; ED exposure duration [T], usually expressed in years; BW is the average body weight value during the period of exposure [M]; AT is the period during which exposure is averaged, [T], usually expressed in days.

Hence, dimensionally, the exposure rate is expressed in:

- $L^3 M^{-1} T^{-1}$ for air or water migration pathways;
- T^{-1} for migration through soil.

Considering the units normally used in practical applications, E is measured in:

- $\frac{l}{kg \cdot d}$ for water,
- $\frac{m^3}{kg \cdot d}$ for air,
- $\frac{mg}{kg \cdot d}$ for soil.

Table 16.1 lists the exposure rates suggested by the US-EPA guidelines or, when not available, by other international references. The rate of exposure is a standard parameter, independent of the local situation of risk under assessment. Its value depends on the type of land use at the investigated site (residential or industrial-commercial) and on the safety factor adopted in the estimation. In this regard, Table 16.1 cites two values:

- *MLE* (Most Likely Exposure), which represents the statistically most likely mean exposure rate for an average population sample;
- *RME* (Reasonable Maximum Exposure), which represents the maximum reasonably possible exposure rate: in other words, the maximum exposure rate endured by 95% of the exposed population. This value is used for conservative estimations.

It is worth noting that for carcinogenic compounds the exposure rate is averaged over the mean lifetime ($AT = 70 \text{ years} \times 365 \text{ days/year}$), while for non-carcinogenic substances it is averaged over the actual duration of exposure ($AT = ED \times 365$).

An individual receptor's *average daily intake* of a substance per body weight unit at the POE is given by the multiplying the exposure rate by the expected or measured concentration of the single component at the POE. Dimensionally, it is expressed as [T^{-1}], but it can also be measured in $\frac{\text{mg}}{\text{kg}\cdot\text{d}}$.

16.5.3 Risk Calculation

For risk calculation, it is necessary to differentiate between carcinogenic and non-carcinogenic toxic substances.

16.5.3.1 Carcinogenic Risk

The increase in the chance of developing cancer during lifetime due to the exposure to a single substance is given by the product of the average daily intake (calculated for a lifetime) by the slope factor, *SF*, of the dose-effect correlation [16]:

$$ILCR = C_{POE} \cdot E \cdot SF = \frac{C_s}{NAF} \cdot E \cdot SF. \quad (16.39)$$

ILCR (Incremental Lifetime Cancer Risk) is a dimensionless parameter that quantifies the number of cancer events that can probably be detected in an exposed population; such events are the excess relative to the cancer incidence normally affecting an analogous, but not exposed, population (control population). Risk is generally considered acceptable if *ILCR* is smaller than 10^{-5} [15].

The risk calculated with the previous expression should be interpreted as the upper 95% confidence limit (i.e., there is only a 5% chance that the actual risk is higher than the estimate).

Cumulative effects deriving from exposure to multiple toxic and/or carcinogenic compounds are not fully understood yet. If more detailed information is lacking, a conservative approach is adopted, consisting in summing the risk values of all the *N* COCs considered for all the *M* exposure pathways. The carcinogenic risk is therefore:

Table 16.1 Standard exposure rate values used in the RBCA procedure (modified from [5])

		CR	EF (giorni/anno)	ED (anni)	BW (kg)	SA (cm ²)	AF (mg/cm ² /d)	DA	Exposure (E)		
									Equation	Value for carcinogens	Value for non-carcinogenic substances
Residential use											
Potable water ingestion	MLE	1.4 l/d	350	8	70	-	-	-	$\frac{CR \times EF \times ED}{BW \times AT}$	0.0022 l/kg/d	0.019 l/kg/d
	RME	2 l/d	350	30	70	-	-	-	$\frac{CR \times EF \times ED}{BW \times AT}$	0.012 l/kg/d	0.027 l/kg/d
Soil and particulate ingestion	MLE	25 mg/d	350	8	70	-	-	-	$\frac{CR \times EF \times ED}{BW \times AT}$	0.039 mg/kg/d	0.34 mg/kg/d
	RME	100 mg/d	350	30	70	-	-	-	$\frac{CR \times EF \times ED}{BW \times AT}$	0.59 mg/kg/d	1.4 mg/kg/d
Volatile particle inhalation	MLE	Total = 18 m ³ /d Indoor = 12 m ³ /d	350	8	-	-	-	-	$\frac{CR \times EF \times ED}{BW \times AT}$	0.028 m ³ /kg/d	0.25 m ³ /kg/d
	RME	Total = 20 m ³ /d Indoor = 15 m ³ /d	350	30	-	-	-	-	$\frac{CR \times EF \times ED}{BW \times AT}$	0.12 m ³ /kg/d	0.27 m ³ /kg/d
Skin contact with soil	MLE	-	40	9	70	5000	0.2	Organics: 0.04 Metals: 0.001	$\frac{SA \times AF \times DA \times EF \times ED}{BW \times AT}$	0.008 mg/kg/d	0.063 mg/kg/d
	RME	-	350	30	70	5800	1.0	Organics: 0.04 Metals: 0.001	$\frac{SA \times AF \times DA \times EF \times ED}{BW \times AT}$	1.4 mg/kg/d	3.2 mg/kg/d

(continued)

Table 16.1 (continued)

	CR	EF (giorni/anno)	ED (anni)	BW (kg)	SA (cm ²)	AF (mg/cm ² /d)	DA	Exposure (E)		
								Equation	Value for carcinogens Value for non-carcinogenic substances	
Commercial/industrial use										
Potable water ingestion	MLE	250	4	70	-	-	-	$\frac{CR \times EF \times ED}{BW \times AT}$	0.0056 l/kg/d	0.0098 l/kg/d
	RME	250	25	70	-	-	-	$\frac{CR \times EF \times ED}{BW \times AT}$	0.0035 l/kg/d	0.0098 l/kg/d
Soil and particulate ingestion	MLE	250	4	70	-	-	-	$\frac{CR \times EF \times ED}{BW \times AT}$	0.028 mg/kg/d	0.49 mg/kg/d
	RME	250	25	70	-	-	-	$\frac{CR \times EF \times ED}{BW \times AT}$	0.17 mg/kg/d	0.49 mg/kg/d
Volatile particle inhalation	MLE	250	4	70	-	-	-	$\frac{CR \times EF \times ED}{BW \times AT}$	0.011 m ³ /kg/d	0.20 m ³ /kg/d
	RME	250	25	70	-	-	-	$\frac{CR \times EF \times ED}{BW \times AT}$	0.070 m ³ /kg/d	0.20 m ³ /kg/d
Skin contact with soil	MLE	40	4	70	5000	0.2	Organics: 0.04 Metals: 0.001	$\frac{SA \times AF \times DA \times EF \times ED}{BW \times AT}$	0.0036 mg/kg/d	0.063 mg/kg/d
	RME	250	25	70	5800	1.0	Organics: 0.04 Metals: 0.001	$\frac{SA \times AF \times DA \times EF \times ED}{BW \times AT}$	0.81 mg/kg/d	2.3 mg/kg/d

CR = contact ratio; EF = exposure ratio; ED = exposure duration; BW = body weight; SA = surface area; AF = soil to skin adherence factor; DA = dermal adsorption

$$ILCR_T = \sum_{i=1}^N \sum_{j=1}^M ILCR_{ji}. \quad (16.40)$$

16.5.3.2 Non-carcinogenic Risk

The risk for non-carcinogenic substances is expressed by an index called hazard quotient, HQ , determined by dividing the average daily intake (calculated for the actual duration of exposure) by the reference dose [16]:

$$HQ = \frac{C_{POE} \cdot E}{RfD}. \quad (16.41)$$

The hazard quotient indicates by how many times the average daily intake exceeds the reference dose. The HQ is a dimensionless parameter.

Thus, HQ does not express a probability, but the ratio between the actual exposure level and the threshold level that does not cause toxic effects on the population.

Clearly, if $HQ < 1$ there is no risk; if, conversely, $HQ \geq 1$ sensitive members of the population could start manifesting pathological, non-carcinogenic, effects.

Analogously to carcinogenic compounds, the total hazard index, HI , is calculated by summing the contributions of all the N COCs considered for all the M active exposure routes:

$$HI = \sum_{i=1}^N \sum_{j=1}^M HQ_{ji}. \quad (16.42)$$

This sum approach is valid if there is no antagonistic or synergistic interaction between the different chemical substances considered. It should also be noted that the risks deriving from different exposure pathways should only be summed if the same individual(s) are very likely to be exposed at the POE via different routes.

16.5.4 Acceptability Criteria

Human health protection standards entail the following criteria:

Carcinogenic Risk

Increased probability of developing a cancer during lifetime due to the exposure to contamination should not exceed the range 10^{-6} – 10^{-4} .

For example, the Italian legislation considers an individual risk (related to a single contaminant) smaller 10^{-6} (1 additional case of cancer per million exposed individuals), and a cumulative risk (due to the concomitant effects of multiple substances) smaller than 10^{-5} to be acceptable.

Toxic Risk

The individual or cumulative hazard quotient should not exceed the threshold limit of 1.0.

16.6 Risk Management

Based on the results of the risk assessment, there can be two distinct outcomes:

- The level of risk calculated at all POEs and for all COCs can be considered acceptable; therefore, no intervention is necessary other than the construction of a monitoring network to verify that the risk remains acceptable in the medium and long term, even upon changes of the boundary conditions.
- The cumulative risk exceeds the acceptability standards; an intervention among the following three is necessary:
 - site remediation via removal of the source of contamination or at least reduction of the concentration of the compounds responsible for the situation of risk;
 - permanent containment or immobilization, by acting on the mechanisms and/or possibility of contaminant migration, in order to reduce the mass that can reach the POE from the source (e.g., solidification, capping, physical containment barriers, hydraulic containment, etc.);
 - intervention on the receptors, for example by modifying the use of the site (e.g., from residential to commercial/industrial).

If the first option is selected, it is necessary to define per each COC the residual concentration beyond which the risk becomes unacceptable (see Fig. 16.7).

It is worth noting that risk assessment is a bidirectional process, as illustrated in Fig. 16.8 [2]. If the goal is to calculate the risk caused by the presence of a source of contamination, a relational system of the type:

concentration \Rightarrow exposure \Rightarrow toxicity \Rightarrow risk, is developed (direct analysis).

Conversely, when the goals of a remediation interventions have to be defined (residual concentration or site-specific acceptability levels), the opposite relation has to be developed (backward analysis):

risk \Rightarrow toxicity \Rightarrow exposure \Rightarrow concentration.

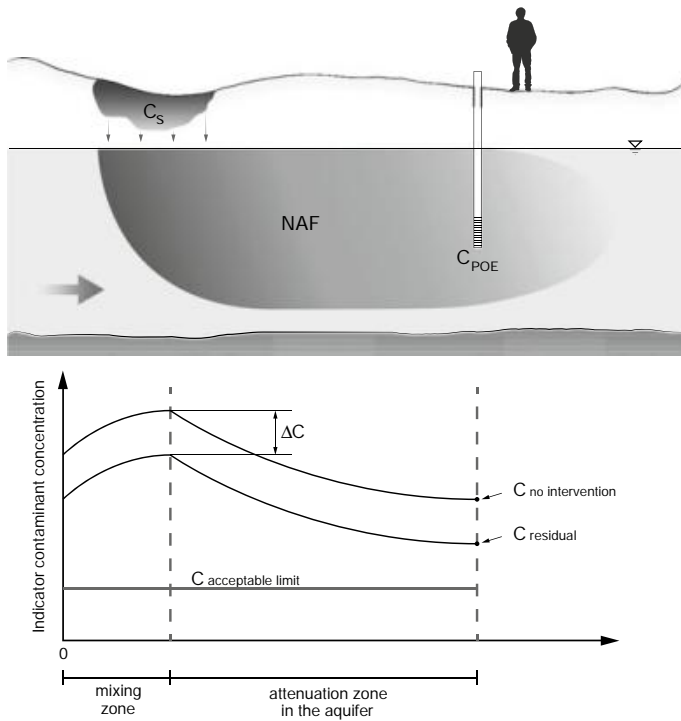


Fig. 16.7 Reduction of the level of contamination of an aquifer with the goal of achieving a residual concentration curve which ensures an acceptable health risk, despite being greater than the threshold value

16.7 Concluding Remarks

Human health risk assessment is the most effective tool available for the evaluation of the contamination status of a site and of the intervention priorities, with the goal of making safe, remediating and restoring the contaminated area.

The procedure is very flexible and can be approached at various levels of detail, according to the quality and amount of data available for the characterization of the affected site and environmental component. In addition, it can be used both for calculating the risk and for determining the remediation objectives through the calculation of residual concentrations.

The standard application procedure is deterministic, and is based on the attribution of a conservative value to input parameters, in order to derive the maximum potential risk for exposed receptors. Given the significant likelihood of overestimating the actual risk a subject undergoes, when the deterministic approach indicates that acceptability levels have been exceeded, it is good practice to couple risk assessment with a probabilistic approach, which assigns a probability distribution to the input parameters.

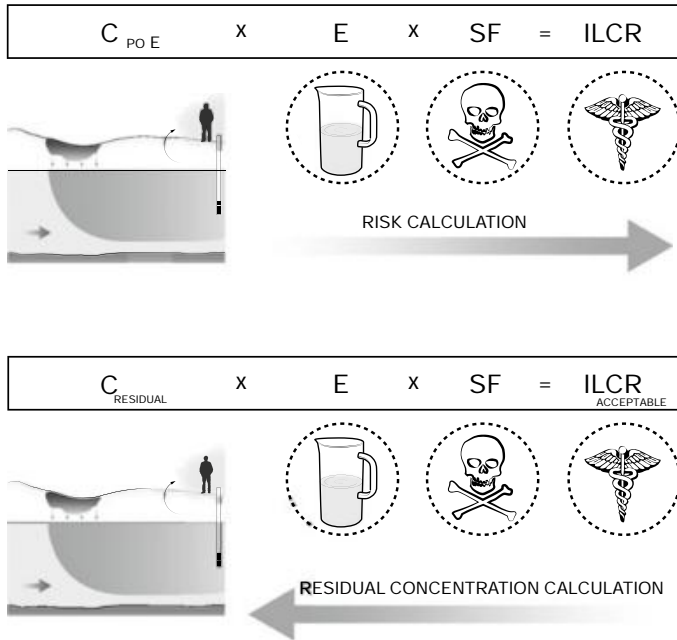


Fig. 16.8 Schematic of the bidirectional principle for the application of the risk assessment procedure (application to a monitored underground waste dump)

Regardless of the level of detail and the methodological approach employed, it is crucial to stress the importance of an appropriate characterization plan, which should allow to define the geometry and features of the source of contamination, and the properties of the environmental components involved in contaminant migration. In addition, expertise is also essential for a correct application of the method, in order to quantify the risk having understood the implicit hypotheses and assumptions underlying different choices in the course of the procedure.

References

1. ASTM, E1739 - 95(2015) standard guide for risk-based corrective action applied at petroleum release sites, Technical report, West Conshohocken, PA (1995)
2. ASTM, E2081 - 00(2015) standard guide for risk-based corrective action, Technical report, West Conshohocken, PA (2000)
3. E. Commission, Common implementation strategy for the water framework directive - guidance document No 26 on risk assessment and the use of conceptual models, Technical report, European Commission (2010)
4. J.A. Connor, R.L. Bowers, S.M. Paquette, C.J. Newell, Soil attenuation model (SAM) for derivation of risk-based soil remediation standards, in *Proceedings of the 1997 Petroleum*

- Hydrocarbons and Organic Chemicals in Ground Water: Prevention, Detection, and Remediation* (1997)
5. J.A. Connor, R.L. Bowers, J.P. Nevin, R.T. Fisher, Guidance manual for risk-based corrective action tool kit for chemical releases, Technical report, Groundwater Service, Inc., 2211 Norfolk, Suite 1000, Houston (2007)
 6. A. Di Molfetta, I. Aglietto, La procedura di analisi di rischio sanitario ambientale. *IGEA* **12**, 67–78 (1999)
 7. G. Environmental, RBCA software tool kit for chemical releases version 2.6 (2014)
 8. US EPA, Guidelines for carcinogen risk assessment, Policies and Guidance (2005), <https://www.epa.gov/risk/guidelines-carcinogen-risk-assessment>
 9. GroundwaterSoftware.com, BP RISC: human health risk assessment and biodegradation software (2011)
 10. G. Italiano, D.lgs. n. 31/2001 Attuazione della direttiva 98/83/CE relativa alla qualità delle acque destinate al consumo umano (2001), <http://www.camera.it/parlam/leggi/deleghe/01031dl.htm>
 11. G. Italiano, D.lgs. n. 152/2006 (T.U. ambiente) (2006), <http://www.bosettiegatti.eu/info/norme/statali/20060152.htm>
 12. P.C. Johnson, R.A. Ettinger, Heuristic model for predicting the intrusion rate of contaminant vapors into buildings. *Environ. Sci. Technol.* **25**, 1445–1452 (1991)
 13. US EPA, Risk assessment guidance for superfund (RAGS): part A, en, Reports and Assessments, reviewed in 2010 (1989), <https://www.epa.gov/risk/risk-assessment-guidance-superfund-rags-part>
 14. I. Verginelli, R. Baciocchi, Role of natural attenuation in modeling the leaching of contaminants in the risk analysis framework. *J. Environ. Manag.* **114**, 395–403 (2013)
 15. WHO - world health organization, WHO – guidelines for drinking-water quality, 4th edn. (2011), http://www.who.int/water_sanitation_health/publications/dwq-guidelines-4/en/
 16. T. Tosco, R. Sethi, Human health risk assessment for nanoparticle contaminated aquifer systems. *Environ. Pollut.* **239**, 242–252 (2018)

Chapter 17

Remediation of Contaminated Groundwater



Abstract In order to decrease the health risk deriving from a contamination event, a number of cleanup and corrective actions, collectively called remediation, can be implemented. Remediation can be applied directly at the site of contamination (in situ) or off site (ex situ), in which case the contaminated environmental component is physically extracted and treated in dedicated facilities at the surface. There are three main remedial approaches, generally categorized as: containment, which aims at preventing the migration of the contamination and hence the exposure of sensitive targets; active restoration, which entails removing or treating the contamination; and natural attenuation, which relies on naturally occurring biological, chemical and physical degradation or transformation processes that convert contaminants into harmless compounds. This Chapter reviews the main containment and remedial strategies available for the management of a groundwater contamination event, and provides valuable information to support the choice of the most suitable approach. The presented strategies include: free product recovery for light non-aqueous phase liquid removal; vacuum enhanced extraction; subsurface containment; pump and treat; air- and bio-sparging; permeable reactive barriers; in situ flushing; in situ oxidation; in situ bioremediation. Applicability, design options and operating conditions, as well as advantages and drawbacks of the presented methods are illustrated.

Cleanup or corrective actions aimed at the reduction of health or environmental risks caused by the exposure to contaminated aquifers are collectively called *remediation*. The goal of remediation interventions can be to fully restore the site's background conditions or to reduce contaminant concentrations below threshold values set on the basis of technology limitations or of health or risk standards. The final protection level achieved is often dictated, at least in part, by the costs involved in the action. Several remediation approaches exist and they fall under the general categories of containment, active restoration, and natural attenuation responses. *Containment* essentially aims at preventing the migration and spreading of the contamination, and avoiding exposure of sensitive targets. *Active restoration* comprises contaminant removal and/or treatment technologies. *Natural attenuation*, instead relies on the degradation or transformation of contaminants into harmless compounds via biological, chemical, and physical processes naturally occurring at the contaminated site [5, 7, 17, 23, 26]. There is a broad array of containment and active restoration techniques, which can be classified according to various criteria. For instance, according to the con-

taminated environmental component (soil or groundwater), to the localization of the treatment (in situ and ex situ), to the type of contaminant (metals, cyanides, LNAPLs, DNAPLs, radionuclides, etc.), to the mechanisms and techniques used (oxidation, reduction, biodegradation, volatilization, flow, etc.) [7].

In regard to the localization of the treatment, remediation measures can be:

- in situ: the polluted environmental component is treated directly on site, without being removed;
- ex situ: the contaminated environmental component is extracted (i.e., soil is excavated, water is pumped) and is either treated at the surface, at the same site (i.e., *on site*), or transported to a remote site for treatment *off site*.

Even though both ex situ and in situ approaches for the treatment of contaminated soil have specific benefits and drawbacks, in situ approaches tend to be favored [41]. This is due to the fact that extracting the contaminated medium is usually considerably expensive, entails managing contaminated material at the surface, and exposes workers to health hazards and other environmental components to potential contamination. Nevertheless, in certain instances ex situ techniques can be more efficient at contaminant removal due to the more effective contact between contaminated material and decontaminating agent, and are generally more easily monitored [40, 41].

When treating groundwater, direct in situ, or occasionally on site, interventions are basically the only viable option. Contaminated aquifer remediation approaches can also be classified according to their objective:

- *Source control*. Its main goal is the removal or containment of the source of contamination or of compounds present as a separate phase.
- *Plume treatment*. Its aim is to treat and contain the dissolved contaminant plume to prevent it from reaching points of exposure.
- *Polishing*. This is typically a final step following more aggressive remediation interventions (e.g., direct treatment of the source).

In many practical cases, these also correspond to sequential phases of a restoration intervention [7].

In the following paragraphs, the operational principles, main features, advantages, and limitations of various techniques for contaminated groundwater remediation are illustrated.

17.1 Free Product Recovery

Free product recovery intervenes directly on the source of contamination to remove the so called *LNAPL pancake*. Several techniques are available for its implementation:

- free product removal with skimming systems;
- free product recovery with water table depression;
- vacuum enhanced extraction.

17.1.1 Free Product Removal with Skimming Systems

The simplest way of recovering free product is to employ direct methods that do not involve the extraction of groundwater.

A *skimmer*, which is a device capable of separating the oil phase and collecting it in a specific container, is lowered down a monitoring well (diameter greater than 2") or trench intersecting the source of contamination. Such devices offer no hydraulic control over contaminant migration, so they are often used as an initial measure anticipating further remedial actions and are best suited for LNAPL accumulations of limited size and thickness [48]. The most common types of skimming systems are [67]:

- *Floating skimmers*. They have a hydrophobic membrane that only allows the collection of the oil phase. Therefore, their operation is based on the surface tension difference between the liquid phases. The hydrophobic screen's selectivity is effective only at shallow depths and in the absence of solid precipitates. Regular maintenance and reconditioning of the membrane is necessary.
- *Pneumatic pump skimmers*. Both water and oil phases are collected and are subsequently separated by means of density sensitive float valves. They are most effective when the density of the floating oil phase is significantly smaller than water. Furthermore, solid particles and debris can hinder LNAPL recovery, as well as interfering with pneumatic valve functioning.
- *Belt skimmers*. They employ a belt of oil-adsorbent material (see Fig. 17.1), which is cycled down the monitoring well to soak up the oil phase. The NAPL is then extracted at the surface by squeezing it through two rollers. The advantage of this system is that it doesn't require a pumping system.

17.1.2 Free Product Recovery with Water Table Depression

By creating a depression of the water table, the free product is drawn towards the pumping well and can thus be recovered. There are two possible configurations for this approach [48, 67]:

- *single pump system*: groundwater and oil phase are simultaneously collected with the same pump (Fig. 17.2). The two phases have to be separated in a second stage;
- *dual pump system*: a first pump is used for drawing water, while another pump and a skimmer are used to recover the oil phase (Fig. 17.3). This method prevents phase mixing and downgradient separation is unnecessary. However, since a fraction of the contaminant is dissolved, it is rarely possible to discharge the pumped water without treatment.

Optimizing these systems entails minimizing the water pumping rate while maximizing free product recovery. Limiting water table depression is essential for reducing

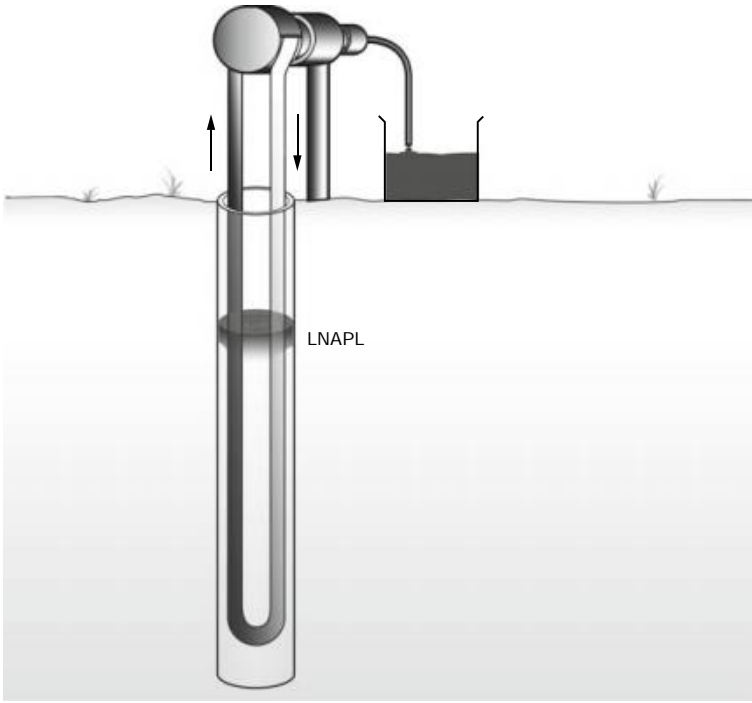


Fig. 17.1 Belt skimmer

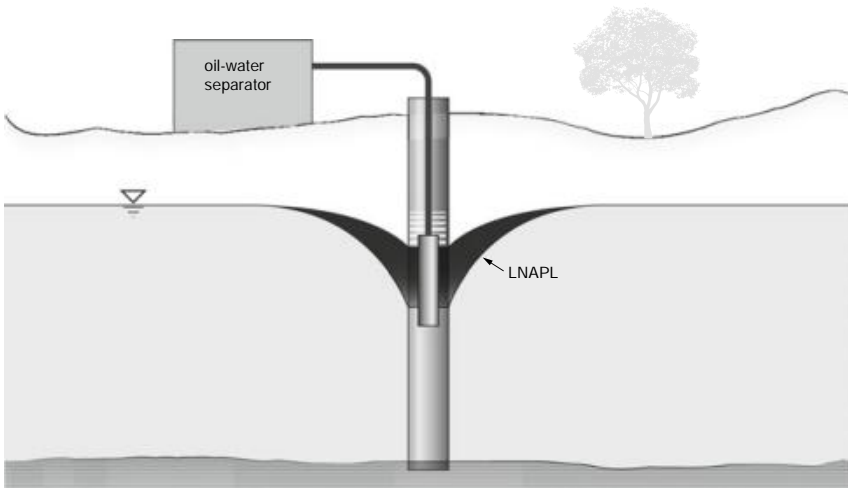


Fig. 17.2 Free product recovery with water table depression. Single pump system

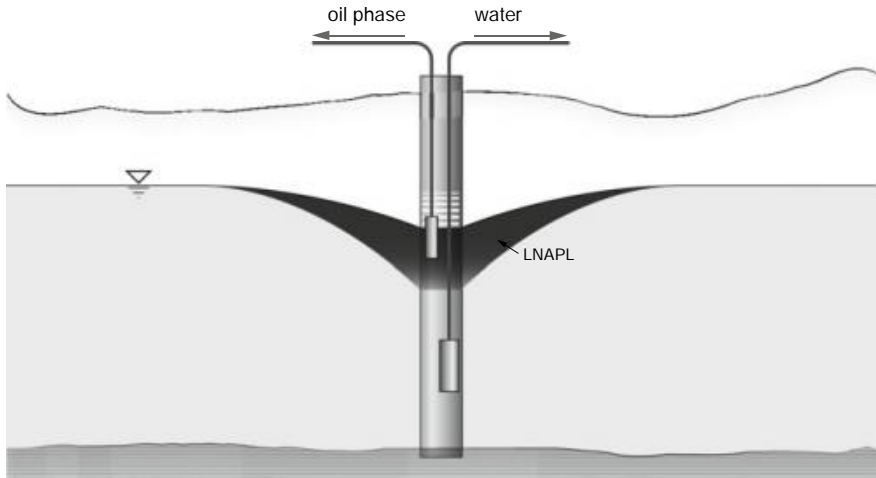


Fig. 17.3 Free product recovery with water table depression. Dual pump system

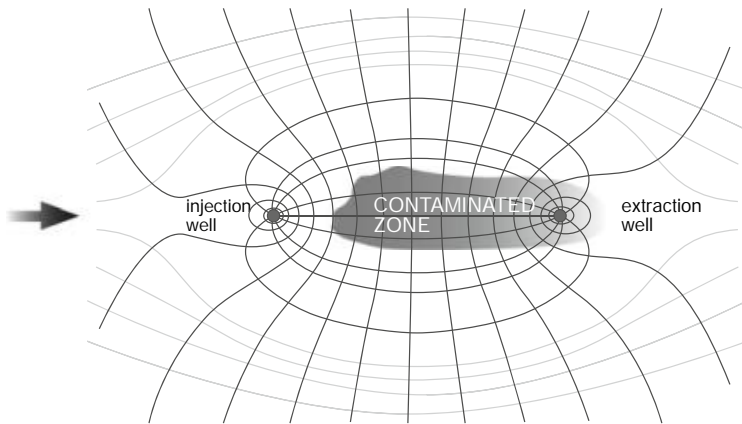


Fig. 17.4 Hydraulic confinement of an aquifer portion by means of a system composed of a pumping and an injection well

energy and treatment expenses as well as for preventing the free product from reaching deep aquifer layers (i.e., smearing), where it would accumulate at its residual saturation and become a long term source of soluble contamination.

Soluble contaminant hydraulic confinement and quickened recovery can be achieved by installing two wells in the direction of flow, one for water extraction and the other, upgradient, for treated water re-injection (see Fig. 17.4). Free product recovery via water table depression is a relatively versatile and cheap method; however, it has the disadvantage of causing smearing of the contaminant and of requiring extracted water treatment.

17.1.3 Vacuum Enhanced Extraction

Vacuum enhanced extraction, or multi-phase extraction (MPE), utilizes similar configurations to recovery methods with water table depression; however, by applying vacuum, the capture zone is increased and more fluid can be drawn to the well. Furthermore, it offers the advantages of being able to avoid smearing and of remediating volatile compounds from the vadose zone, in addition to the free product [48, 67].

In MPE, sealed recovery wells are employed; a portion of the screened section of the well extends above the water table, and the bottom of the drop tube of the vacuum pump is at or below the water table. There are three main configurations for MPE [41, 69]:

- *single pump system*: in this design, a single pump is used to draw both liquid and vapor phase;
- *dual pump system*: here, a submersible and a vacuum pump are used to extract separately the liquid and vapor phases, respectively;
- *bioslurping*: this system has the same configuration as the single pump method, except that the drop tube is set at, or just below, the liquid-gas interface and is the most effective in free product recovery. This design has the additional advantage of drawing significant volumes of air from the unsaturated medium, contributing to the oxygenation of the contaminated aquifer and thus promoting aerobic contaminant biodegradation [23].

In all cases, phase separation is carried out in a dedicated tank at the surface.

17.2 Subsurface Containment

Containment techniques are designed to prevent the contamination from spreading by avoiding clean groundwater from flowing across the contaminated zone and/or by preventing polluted groundwater from migrating. Therefore, they aren't actual remediation strategies, but they serve as safety measures. Containment can be achieved by hydrodynamic means or through physical methods [7, 41].

Hydrodynamic containment consists in isolating the contaminated portion of aquifer or the source of contamination by installing a system of pumping and injection wells that strategically modify the local flow regime and inhibit mixing of fresh and contaminated groundwater [17, 23, 48].

Physical containment methods, instead, aim at imposing a physical barrier or wall to confine the source of contamination in situ in order to prevent spreading of additionally released contaminant. Their effectiveness relies on the continuity (i.e., lack of leaks) of the barrier, and on its resilience to physical and chemical degradation [17].

There are several technologies available to achieve physical containment of contamination, listed below [7, 17, 23, 26, 48, 52, 72].

- *Slurry trench walls*: a bentonite slurry is poured into a trench during its excavation to provide support to the trench walls, and is subsequently solidified by the addition of another material such as native soil or cement. Slurry walls can be constructed in such a way to surround the entire source of contamination or to prevent groundwater from flowing across it. Impermeability, resistance to degradation and integrity of these cutoff walls can be improved by inserting a geomembrane, thus yielding *composite slurry walls*.
- *Sheet piling*: reinforced concrete or steel piles interlocked along the edges are driven into the soil to create a continuous barrier. The joints between individual piles should be sealed with impermeable material to avoid leaking of the confined contaminant.
- *Grouting and jet grouting*: this technique consists in the injection under pressure of *grout* (i.e., a stabilizing material such as cement, bentonite or silicate grouts) into the porous medium. The grout penetrates the formation from the injection point and solidifies, thus reducing the permeability of the medium and forming so called *grout curtains*. In the case of jet grouting, the grout is injected at very high pressures and while it penetrates it damages soil structure and mixes with it.
- *Solidification and stabilization*: these methods employ various strategies to stabilize the contaminated portion of aquifer. For example, additives (such as cement, asphalt, organic polymers) can be mixed with soil, or electricity can be used to generate heat and melt the soil to vitrify it.

In some cases, a bottom horizontal barrier can be created in addition to the perimetral one (for example by grouting through drill holes); this could be necessary when the impermeable layer that underlies the aquifer is particularly deep [7].

Clearly, impermeable barriers permanently modify flow in the contaminated aquifer; in some cases, mitigation measures may therefore be necessary. If the perimetral barriers are anchored in a low permeability confining layer, precipitation events may cause the contaminated water enclosed in the containment system to overflow. To avoid this situation, it is necessary to create a surface seal (e.g., made of clay, natural soil mixed with stabilizers, bentonite, synthetic membranes) that prevents or limits effective infiltration; this, in addition, prevents the escape of toxic vapors. Alternatively, a pumping system can be installed to maintain a constant water level within the confinement area. In the latter case, extracted water has to be treated before disposal [17, 26].

Given its installation costs, the requirement of hydrodynamic monitoring, and the fact that the source of contamination is not removed, containment via vertical barriers should only be considered in extreme cases as an emergency human health safety measure. Surface barriers (capping) are, instead, used more frequently for their effective reduction of the amount of infiltrating precipitations, which contribute to the transport of the soluble contaminant fraction to the aquifer.

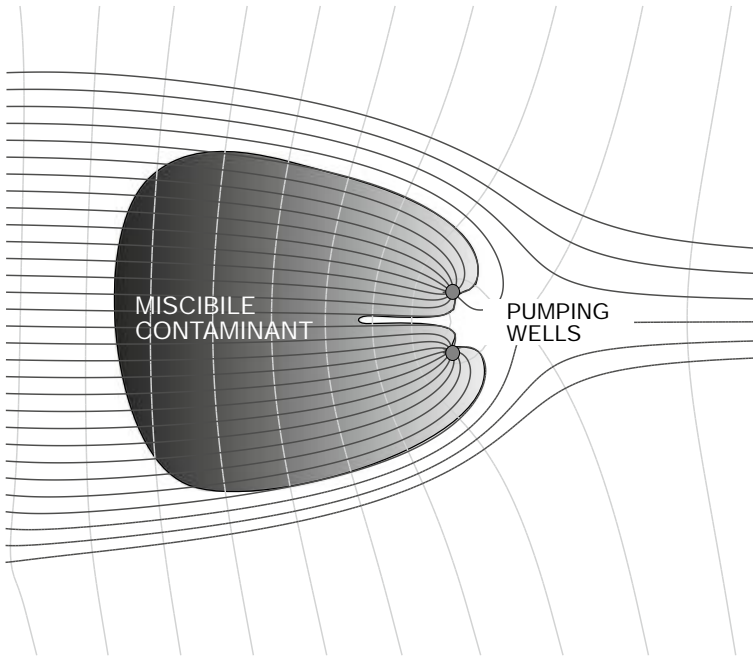


Fig. 17.5 Pump and treat for the removal of a perfectly miscible contaminant

17.3 Pump and Treat

This is a well established and one of the most commonly used aquifer remediation strategies. As the name suggests, it consists in completing a certain number of pumping wells in the polluted aquifer to extract water and transport it to a dedicated facility for contaminant separation and treatment. Treated water is then discharged for disposal or further use [7].

This technique is used to remove miscible contaminants present as plumes or the soluble fraction of a NAPL contaminant (Fig. 17.5); clearly, this method is not suitable for removal of NAPLs present at residual saturation.

Pump and treat systems (henceforth called P&T) can be used as a strategy for contaminant removal, as well as for hydraulic containment of the plume, which doesn't require the removal of a significant mass of contaminant. The latter application is used as a security measure, as it doesn't remove the source of contamination nor does it prevent the plume from spreading as soon as pumping is discontinued [17, 23].

17.3.1 Design of a P&T System

The main objective of any P&T system is the hydraulic control of the contamination plume, which is achieved when the dissolved contaminant carried by the groundwater

flow is contained within the *capture zone* of the extraction wells, i.e., the portion of aquifer whose flow is directed towards the pumping well(s) [23, 26].

Critical aspects are:

- determination of the total water pumping rate and of the number, location, depth and discharge of each well;
- calculation of the volume of water necessary for the remediation of the contaminated area and achievement of target concentrations;
- assessment of the effectiveness and efficiency of the intervention the plan should aim at maximizing efficiency and minimizing costs.

In most cases, P&T design is supported by numerical modeling, which simulates the hydrodynamic behavior of the aquifer affected by the contamination, and the flow paths followed by the contaminant molecules. Nevertheless, in particularly simple cases, the design can rely on the application of analytical solutions. Whatever the approach, the main aspect of the design is the identification of the capture zone.

Its shape and extension depend on multiple factors, including aquifer type, hydraulic gradient, hydraulic conductivity, pumping rate, formation heterogeneity and/or anisotropy, and well completion geometry.

The capture zone should not be confused with the area of influence, which represents the portion of aquifer whose piezometric surface is affected by a pumping well. It cannot, therefore, be determined from the radius of influence. The capture zone extends mainly upgradient of the well(s), including only a small downgradient portion of the aquifer, as illustrated in Fig. 17.6.

17.3.1.1 Single Well Design

Let us consider a steady state flow regime in a homogeneous and isotropic confined aquifer, characterized by a uniform hydraulic gradient, i . The equation describing the profile of the flow line separating the groundwater that flows towards a completed well extracting at a constant pumping rate, Q , and the groundwater that continues flowing downgradient is [26]:

$$x = \frac{-y}{\tan(2\pi \cdot K \cdot b \cdot i \cdot y/Q)}. \quad (17.1)$$

x and y in Eq. (17.1) are the coordinates in a Cartesian reference system whose origin is the pumping well, as depicted in Fig. 17.7.

As evident from Fig. 17.7, the downgradient extension of the capture zone is defined by the *stagnation point*, x_0 , characterized by zero gradient and whose coordinate is [7, 17, 26]:

$$x_0 = \frac{-Q}{2\pi \cdot K \cdot b \cdot i}. \quad (17.2)$$

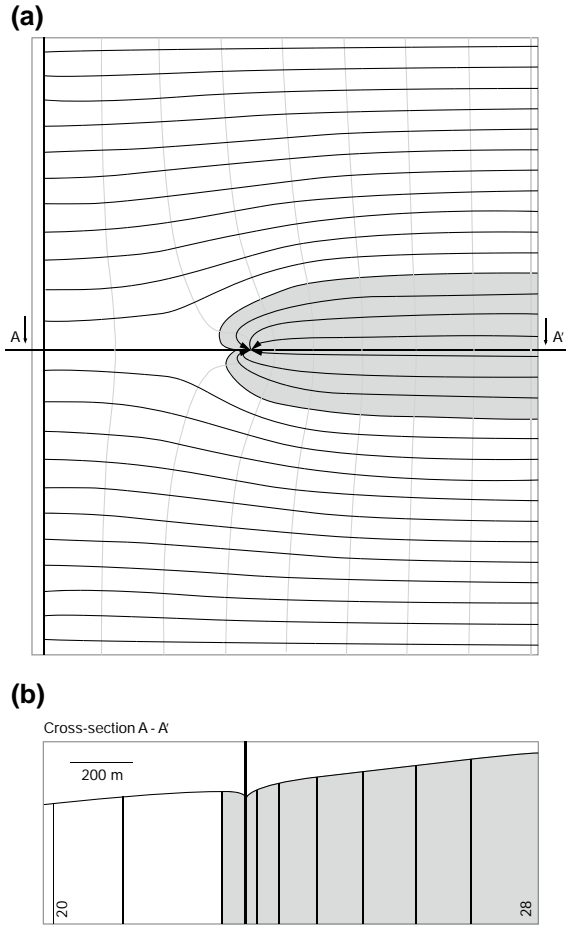


Fig. 17.6 Capture zone of a completed well (P1) pumping 10 l/s from an homogeneous and isotropic unconfined aquifer with a hydraulic gradient of 0.005 and hydraulic conductivity of 0.0001 m/s, in steady state conditions. **a** Plan view; **b** cross-sectional view, simulated with Visual MODFLOW v.2.8.2 (modified from [46])

while its maximum upgradient width is derived as x tends to infinity and is twice y_{\max} , defined as:

$$y_{\max} = \pm \frac{Q}{2 \cdot K \cdot b \cdot i} \tag{17.3}$$

For unconfined aquifers, instead, hydraulic head values in two wells located along the groundwater flow direction have to be known. If we define h_1 and h_2 as the up- and down-gradient heads referred to the bottom of the aquifer, respectively, and d as the distance between the two isolines, the capture zone can be described as follows [29]:

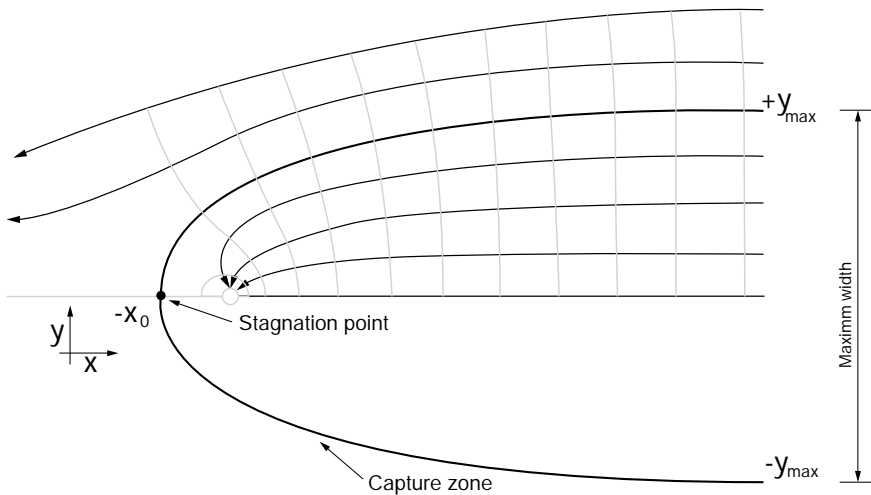


Fig. 17.7 Flow field generated by a pumping well in an aquifer characterized by a uniform flow regime (modified from [26])

$$x = \frac{-y}{\tan[\pi \cdot K \cdot (h_1^2 - h_2^2) \cdot y / (Q \cdot d)]} \tag{17.4}$$

Its maximum width, obtained for x that tends to infinity, can be expressed as:

$$y_{\max} = \pm \frac{Q \cdot d}{K \cdot (h_1^2 - h_2^2)} \tag{17.5}$$

while the position of the stagnation point relative to the well is

$$x_0 = \frac{-Qd}{\pi K (h_1^2 - h_2^2)} \tag{17.6}$$

The above equations do not consider the vertical coordinate; therefore, they can only be applied when a two-dimensional analysis is sufficient, i.e., when the wells are screened over the entire saturated thickness of the aquifer.

17.3.1.2 Multiple Aligned Wells Design

The capture zone created by a single well, even when exploited at its maximum, won't be, in most cases, big enough to capture the entire contamination plume. In such cases, additional wells have to be installed to create a larger capture zone. The determination of the maximum discharge rate of the wells require the performance of step-drawdown tests as described in Sects. 5.1–5.3.

Table 17.1 Capture zone geometry features created by 2, 3 or 4 pumping wells in uniform flow conditions (modified from [36])

Number of pumping wells	Optimal distance D between neighboring wells	Width of the capture zone along the line of wells	Maximum width of the capture zone
2	$\frac{Q}{\pi bq}$	$\frac{Q}{bq}$	$2 \frac{Q}{bq}$
3	$1.26 \frac{Q}{\pi bq}$	$1.5 \frac{Q}{bq}$	$3 \frac{Q}{bq}$
4	$1.20 \frac{Q}{\pi bq}$	$2 \frac{Q}{bq}$	$4 \frac{Q}{bq}$

The maximum distance, D , between n completed wells that ensures full capture of the contamination plume can be calculated analytically by applying the complex potential theory. This solution is valid under the hypothesis that the wells are aligned perpendicularly to the direction of flow and that each of them extracts the same discharge, Q ; as above, the aquifer is assumed to be confined, homogeneous and isotropic, with constant thickness and hydraulic gradient, and under steady state conditions with Darcian velocity, q [36]. The features of the capture zone are summarized in Table 17.1.

Given the spatial distribution of contaminant concentration and the groundwater flow direction and rate, Javandel and Tsang [36] developed a method to determine the ideal number, discharge, and position of pumping wells for the removal of a contamination plume, by means of a set of type curves defining the capture zones created by 1, 2, 3, or 4 wells for different values of Q/bq (see Fig. 17.8).

The procedure entails the following steps:

1. preparation of a concentration map at the same scale as the type curves, indicating groundwater flow direction and the threshold concentration contour line;
2. superposition of the concentration map with the single well type curves aligning the flow direction, and identification of the type curve that captures the entire plume and of the corresponding value of Q/bq ;
3. calculation of the discharge, Q , by multiplying Q/bq by the aquifer thickness, b , and the flow velocity, q ;
4. if the obtained discharge is sustainable for the pumping well and the aquifer (see Chap. 5 on well testing), the optimal well number is one, and its ideal position coincides with that of the type curve well;
5. conversely, if the well cannot produce the discharge, Q , steps 2 to 4 have to be repeated using an increasing number of wells (up to four) until the optimal number is identified. It should be noted that the location of the wells can be derived directly from the type curves in the superposition position, while the distance between the wells depends specifically on the selected curve (i.e., in other words on the value of the parameter Q/bq) and is determined based on the relations in Table 17.1. Furthermore, due to the superposition of the effects induced by the presence of

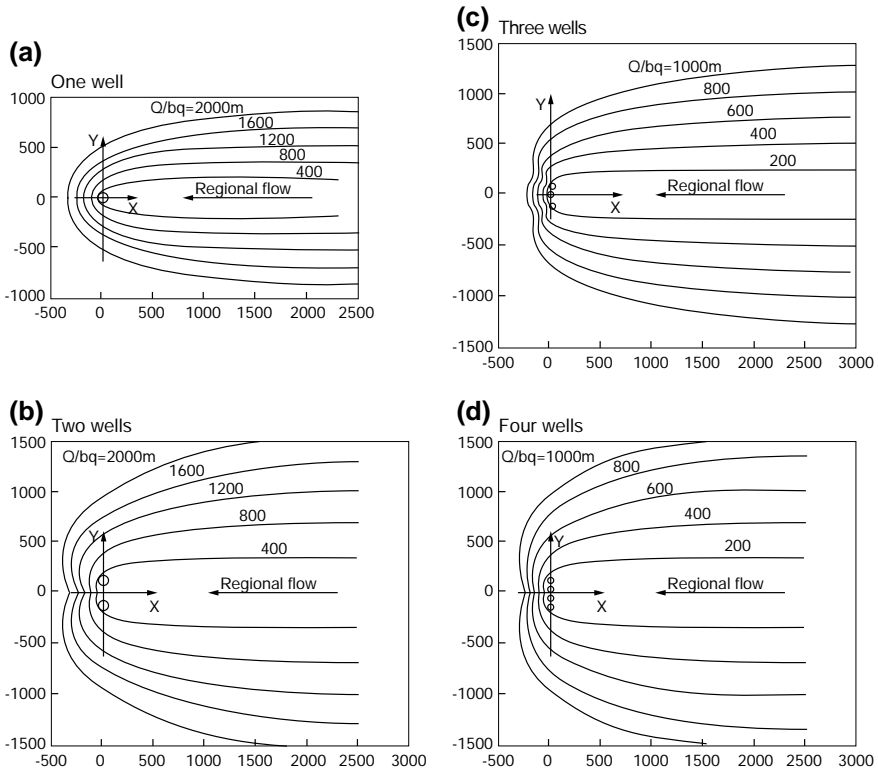


Fig. 17.8 Type curves representing capture zones created by **a** 1; **b** 2; **c** 3; **d** 4 pumping wells for various values of the parameter Q/bq (modified from [36])

multiple wells, isn't possible to pump from each well the same discharge that would be extracted from a single well for the same threshold drawdown.

Finally, because of the assumptions underlying this simple model, it cannot be applied to unconfined, heterogeneous, anisotropic aquifers, nor in the presence of recharge boundaries or partially penetrating wells.

17.3.1.3 General Cases

As previously mentioned, none of the described analytical solutions is suitable for the design of P&T interventions in most real contamination source or plume geometries. In such cases, a numerical model has to be used to describe flow directions and rates, and the paths followed by groundwater and contaminants (MODFLOW/MODPATH and Feflow are the most commonly used tools) [18, 31]. Figure 17.9 depicts a real-case design of a P&T system. It is worth remembering that numerical models are indispensable to account not only for the size or particular geometry of a contam-

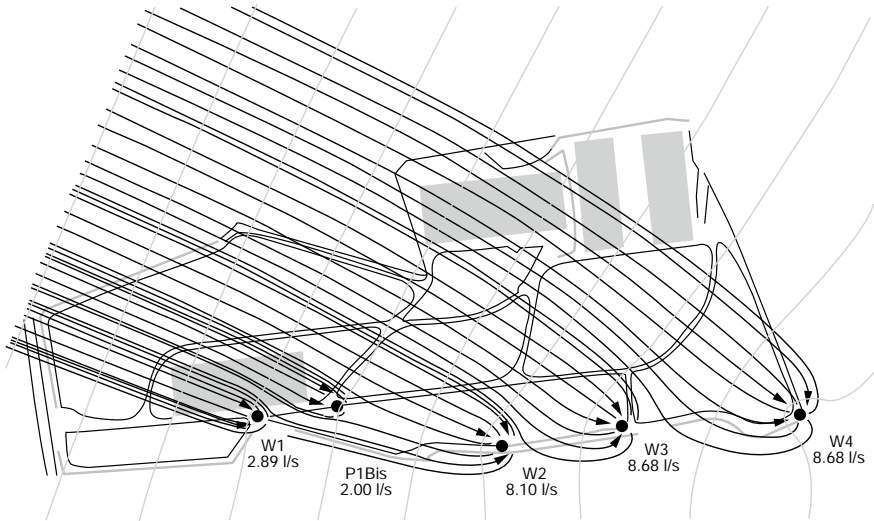


Fig. 17.9 Real example of a P&T intervention plan

ination plume, but also for all conditions that do not respect the ideal hypotheses for which an analytical solution exists. Heterogeneous and/or anisotropic aquifers, nonuniform hydraulic gradient, partially penetrating wells, nonuniform distribution of the contaminant along the saturated thickness, different pumping rates at different wells are a few examples of frequently occurring situations that impose the use of numerical models.

For example, Fig. 17.10 shows how the capture zone of a partially penetrating well is limited on the vertical plane. Figure 17.11, instead, shows that horizontal anisotropy can cause the capture zone not to be wide enough.

17.3.1.4 Integrated Systems

In some cases, pumping wells can be combined with other approaches, such as impermeable barriers, injection wells, or trench drains, to improve the efficiency and effectiveness of the system.

Installing low-permeability physical barriers coupled with a pumping system can promote the accomplishment of both containment and remediation objectives. Impermeable barriers enhance groundwater control by preventing uncontaminated and contaminated water from mixing, by limiting the migration of the pollutant towards unaffected areas, and by avoiding additional contaminant release into the plume. Furthermore, they favor the generation of a stable, inward-directed hydraulic gradient, a necessary feature for contaminated flow containment; they reduce the aggressiveness of the P&T system by allowing the use of lower pumping rates; and they simplify capture zone monitoring operations.

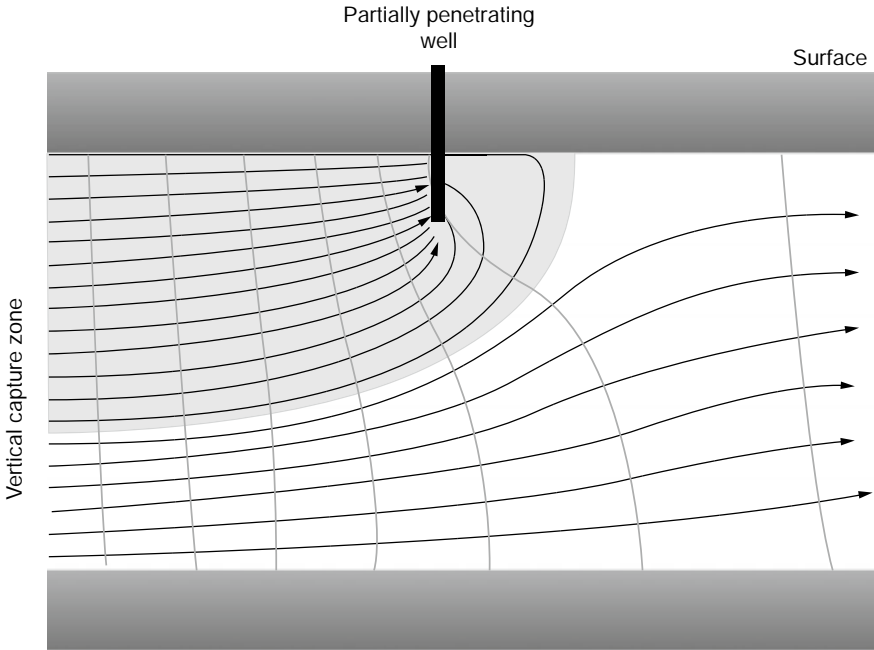


Fig. 17.10 Capture zone of a partially penetrating well

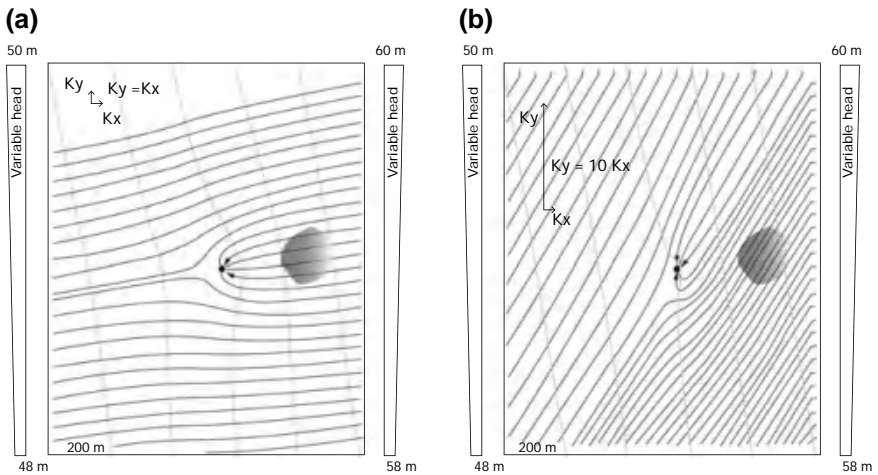


Fig. 17.11 Visual Modflow (v.2.8.2) simulation of the effect of anisotropy on the pumping intervention: steady state flow in **a** isotropic ($K_x = K_y = K_z = 0.0001$ m/s) and **b** anisotropic ($K_x = K_z = 0.0001$ and $K_y = 0.0001$ m/s) confined aquifer (modified from [46])

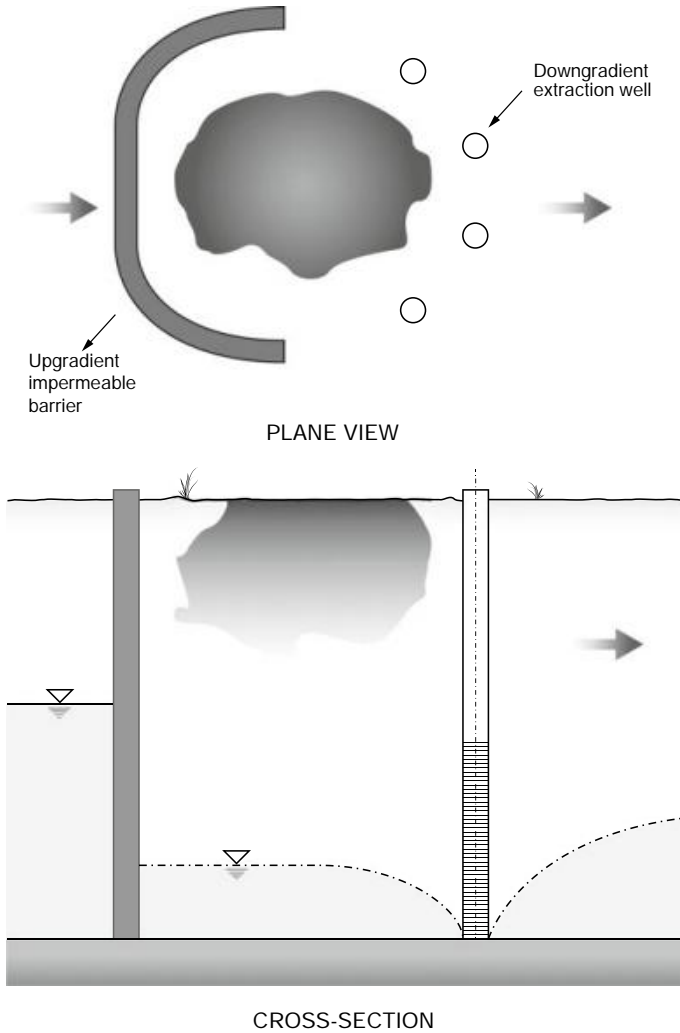


Fig. 17.12 Extraction wells coupled with an upgradient impermeable barrier (modified from [42])

Low permeability vertical barriers can be placed up- or down-gradient of the contaminated matrix, or can fully encircle it, and can, in addition, be used to isolate the source of contamination from the rest of the contaminated area. Coupling upgradient barriers with downgradient wells (see Fig. 17.12), prevents clean water from flowing through the polluted section of aquifer and spreading the contaminant. This reduces the amount of water that needs to be extracted and treated to achieve the desired residual concentration, and allows the use of low pumping rates for hydraulic containment.

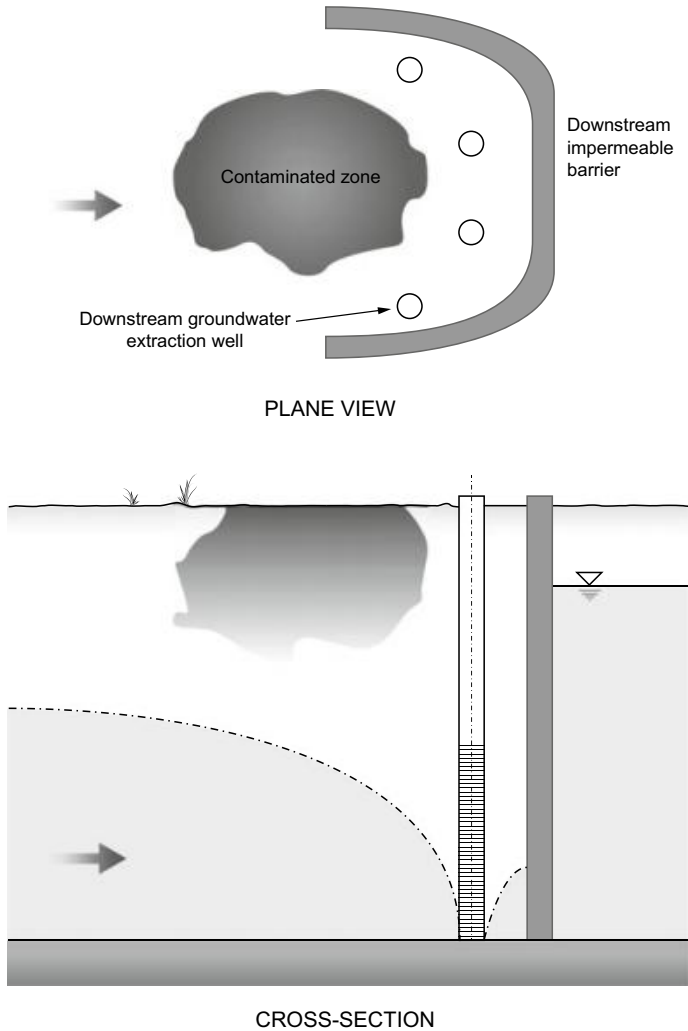


Fig. 17.13 Pumping wells coupled with downgradient impermeable barrier

Conversely, coupling downgradient barriers with pumping wells (as shown in Fig. 17.13) limits the extraction of uncontaminated water present downgradient and the volume of water to be treated, thus accelerating remediation and reducing costs.

Finally, the source zone can be totally enclosed in containment barriers, preventing further migration of contaminants and favoring the achievement of remediation objectives within a reasonable time frame.

For containment barriers to be effective and to prevent water from circumventing them, they have to be keyed into the impermeable layer that underlies the aquifer. The capture system can also be combined with surface capping to limit precipitation infiltration, and thus further reduce pumping requirements [17, 23, 26, 48].

It is worth to employ such systems, from both a technical and an economic point of view, when, for example:

- the capability of treating captured water is limited;
- they reduce treatment costs, when these are greater than confinement costs;
- aquifer thickness is small;
- the initial hydraulic gradient is relatively high;
- the base of the aquifer is quite steep;
- porous medium permeability is high;
- the aquifer is heterogeneous.

Another example of integrated systems is the coupling of extraction and injection wells.

Injecting clean water into the aquifer increases the hydraulic gradient, and thus the flow velocity within the contaminated zone. This causes increased leaching of the contaminated matrix and migration of the pollutants towards the pumping wells. Furthermore, placing recharge wells upgradient causes the flow of uncontaminated water to diverge around the source of contamination or the plume, whereas placing them downgradient prevents further spreading of the plume.

The effluent from the treatment plant or water deriving from another supply can be injected above or below the potentiometric surface through wells, trenches, drains, or infiltration basins, and can be controlled by maintaining a certain piezometric level or by pumping specific discharges.

A *doublet* configuration is particularly effective for the hydraulic confinement of the contaminated zone and for circulation of contaminated water within the injection/extraction cell (Fig. 17.14) [56]. Treatment of the captured water may not achieve the target concentrations during the first round, and can be re-introduced in the contaminated matrix, without causing additional impact. Of course, the position of the wells, and injection and pumping rates have to be chosen with great care on the basis of a thorough site characterization. The design of the intervention should aim at minimizing the volume of water to be treated and, most importantly, at avoiding the migration of part of the re-injected water downgradient of the cell, which could cause the need to increase the pumping rate. Double-cell configurations require smaller discharges than doublets, and allow maintenance of the inner wells without compromising the hydraulic containment.

17.3.2 Flushing Water Volume

In order for a P&T system to be effective, the amount of water that needs to be flushed through the contaminated area has to be estimated. This parameter is usually described in terms of pore volumes (*PVs*). The *pore volume* is defined as the volume of water found within the contamination plume, and is calculated as follows:

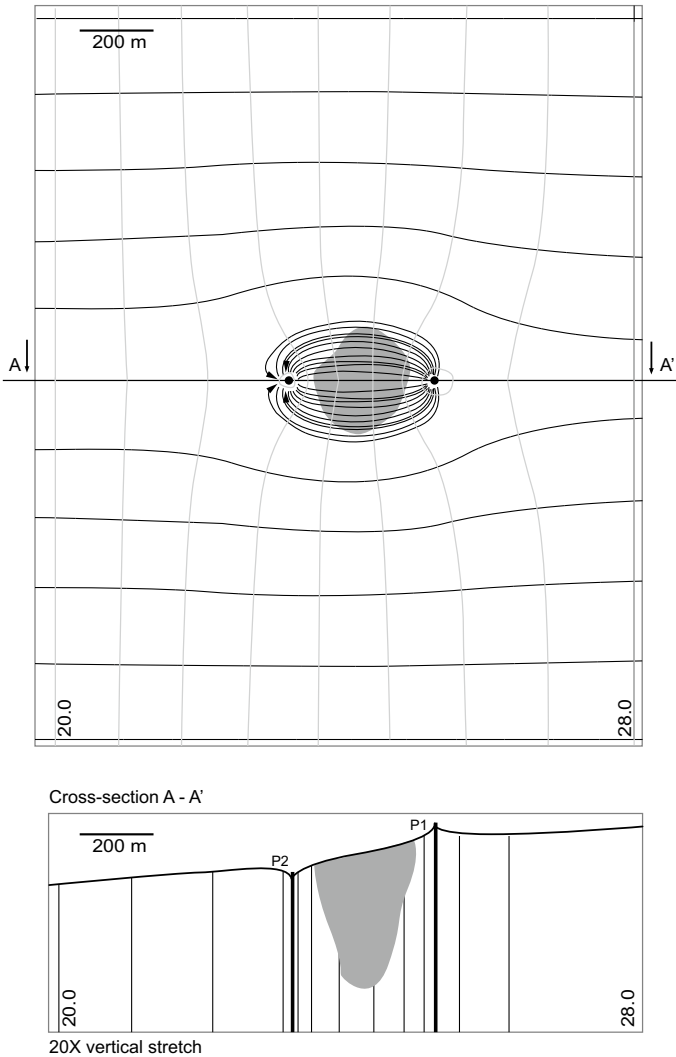


Fig. 17.14 Hydraulic containment of the contaminated zone by means of a doublet system, simulated with Visual Modflow v.2.8.2. in steady state conditions: homogeneous and isotropic unconfined aquifer ($K = 0,0001 \text{ m/s}$) with an initial hydraulic gradient of 0,005; well P2 pumps 10 l/s, while P1 recharges the same discharge

$$PV = \int_A b \cdot n_e \cdot dA, \tag{17.7}$$

where b is the plume thickness, n_e the effective porosity of the formation, and A the area of the plume.

For uniform thickness and effective porosity:

$$PV = B \cdot n_e \cdot A, \quad (17.8)$$

where B represents the average thickness of the plume.

Under certain simplifying assumptions, the theoretical number of PVs required for the achievement of remediation goals can be approximated through simple relations with the *retardation factor* (R), defined as:

$$R = \frac{v}{v_c}$$

where v is the groundwater seepage velocity and v_c the average linear velocity of the dissolved contaminant.

In particular, assuming linear, reversible, and instantaneous sorption processes and the absence of solid contaminants, and neglecting dispersion phenomena, the relation between R and the number of PVs (NPV) is linear:

$$NPV = -R \cdot \ln \left(\frac{C_{wt}}{C_{wo}} \right), \quad (17.9)$$

where C_{wt} is the target contaminant concentration and C_{wo} is the initial aqueous-phase contaminant concentration [14, 15, 17].

Clearly, the linear sorption assumption is only useful for very simple systems, but in most real case scenarios can lead to major underestimation of P&T flushing-water volumes and thus of remediation times. For example, this assumption doesn't hold for most inorganic contaminants, which exhibit nonlinear sorption isotherms. It also doesn't hold if part of the pore space is unavailable to fluid flow, or when slow contaminant diffusion rates from low to high permeability areas hinders contaminant removal.

Therefore, in most cases, it is necessary to resort to modelling for the estimation of NPV , or to the assessment of contaminant concentration evolution as a function of extracted PVs during operation. The parameters that need to be taken into account during NPV evaluation are the target concentration levels, the initial distribution of the contamination, and the chemical and physical phenomena that may affect the remediation intervention.

When designing or running a P&T system, a useful indicator of the aggressiveness of the intervention is the number of PVs withdrawn per year, calculated as:

$$NPV_a = \frac{Q_a}{PV}, \quad (17.10)$$

where Q_a is the total annual discharge.

Another important parameter defining a P&T system that should be calculated, is the time required to pump one PV of groundwater from the contaminated zone.

However, it is often difficult to obtain a sufficiently detailed site characterization to allow an accurate estimate of restoration time, in particular due to the difficulty of quantifying the initial distribution of contaminant mass and of predicting the extent of tailing phenomena (see Sect. 17.3.4) [14].

17.3.3 Performance of a P&T System

In general, a P&T intervention is considered effective if it captures the entire contamination plume while extracting the smallest possible amount of water. An oversized system would lead to excessive groundwater resource impoverishment, as well as increasing contaminated water extraction and treatment costs.

The efficiency of a remediation design including one or multiple capture wells can be assessed by calculating the ratio between the maximum width of the contamination front, L , and the maximum width of the well capture zone, F ($F = 2y_{max}$), known as *hydraulic efficiency*:

$$E_i = \frac{L}{F}. \quad (17.11)$$

Clearly, E_i cannot be greater than one, because if L were greater than F , the system would be undersized and it would be impossible to fully remove the contamination plume. However, this definition only keeps into account advection, neglecting hydrodynamic dispersion, which broadens the area affected by the contamination and causes a progressive decrease of concentration.

Another method to assess the performance of a pumping system is the *Hydrochemical efficiency*, E_{id} [38], determined by comparing the average pollutant concentration, $\bar{C}_P(t)$, in the water extracted during the time t (calculated as the ratio between the contaminant mass removed during that time and the water volume pumped in the same time interval) with the average concentration, \bar{C}_0 , present in the contaminated area at time $t = 0$ [38]:

$$E_{id}(t) = \frac{\bar{C}_P(t)}{\bar{C}_0}, \quad (17.12)$$

with:

$$\bar{C}_P(t) = \frac{\int_0^t C_P(\tau) \cdot Q(\tau) \cdot d\tau}{\int_0^t Q(\tau) \cdot d\tau} = \frac{\text{extracted mass}}{\text{extracted volume}}. \quad (17.13)$$

Two alternative configuration designs can be compared by calculating the hydrochemical efficiency for the time, t_p , at which the same percentage of the total initial mass of contaminant present in the aquifer is removed: the most efficient option is the one characterized by a greater value of $\bar{C}_P(t_p)$. During design, the evolution of solute concentration in the well is obtained by considering the sole advection phenomenon, but the same procedure can be followed including the other mechanisms that govern transport.

Please note that this assessment method is valid only for pulse sources of contamination or in those cases in which the source has already been removed.

When contaminant injection doesn't occur in a pulse, the released mass isn't constant; in fact, it increases over time (e.g., landfill leachate seepage). In this case, it is preferable to use a different method to assess the capability of a P&T system to remove contaminated groundwater. The efficiency of a P&T system is defined as the total mass of contaminant, $M_P(t)$, extracted from the capture wells in a certain time interval, and the total mass, $M_S(t)$, released at the source during the same time:

$$\eta(t) = \frac{M_P(t)}{M_S(t)} = \frac{\int_0^t C_P(\tau) \cdot Q_P(\tau) d\tau}{\int_0^t C_S(\tau) \cdot Q_S(\tau) d\tau} = \frac{\text{extracted mass}}{\text{released mass}}. \quad (17.14)$$

In the previous equation, $C_P(\tau)$ and $Q_P(\tau)$ are the solute concentration and the extracted discharge at the well at time τ , while $C_S(\tau)$ and $Q_S(\tau)$ are, respectively, the solute concentration released at the source and the discharge of the groundwater that has flowed through it at time τ .

In order to be able to compare different pumping system patterns, however, it is necessary for the mathematical model to simulate a source that releases into the aquifer the same contaminant mass in the time interval t , regardless of the design option and the flow conditions resulting from the various configurations. In addition, for the comparison to be more significant, the parameter η should be assessed once the source is exhausted and all the contaminant mass present in the porous medium has been removed.

In the case of a continuous source of contamination, the efficiency of a remediation intervention can also be estimated accurately by the ratio between the mass discharge extracted by the well at the time t , $\dot{M}_P(t)$ and the mass discharge released by the source at the same time, $\dot{M}_S(t)$:

$$\varepsilon(t) = \frac{\dot{M}_P(t)}{\dot{M}_S(t)} = \frac{C_P(t) \cdot Q_P(t)}{C_S(t) \cdot Q_S(t)} = \frac{\text{extracted mass discharge}}{\text{released mass discharge}}, \quad (17.15)$$

where $C_P(t)$ and $Q_P(t)$ are, respectively, the solute concentration in the pumped water and the volume discharge extracted from the well at the same time t , and $C_S(t)$ and $Q_S(t)$ are, respectively, the solute concentration released by the source and the volume discharge of the groundwater flowing through it.

By using the previous definition of efficiency, it is possible to say that if the mass extracted by the well is equal to that released by the source throughout the duration of the intervention, all the mass of contaminant will be removed by the same well. Furthermore, if the capture well is placed within the contamination plume, during the initial pumping phases the capture flow rate could be greater than the injected flow rate. Therefore, the efficiency could be greater than one. Conversely, the efficiency η remains smaller than one.

17.3.4 Potential P&T Limitations

Two phenomena representing serious drawbacks of P&T systems have been revealed by monitoring contaminated sites during and after pumping: *tailing* and *rebound* (Fig. 17.15). *Tailing* refers to the progressive decrease in the ability of the system to remove the contaminant as the pumping operation proceeds. *Rebound*, instead, is the rapid increase of contaminant concentration in solution upon pumping discontinuation [7, 14, 26].

Both these mechanisms can cause the residual contaminant concentration in the groundwater to exceed the target levels and thus be responsible for the failure of the restoration intervention. Furthermore, the asymptotic decrease of the concentration towards a value greater than zero and than the acceptable limit determines the system to operate for a significantly longer time: without this phenomenon the intervention would only last the necessary time to pump a volume equal to the volume of the contamination plume.

The extent of the influence of these mechanisms depends on the physical and chemical characteristics of the contaminant, as well as on the properties of the aquifer and its solid matrix.

Site characterization should aim at identifying the causes of *tailing* and *rebound*, which include:

- desorption of the fraction of contaminant associated with the surface of the aquifer's solid grains;
- dissolution of precipitated contaminant;

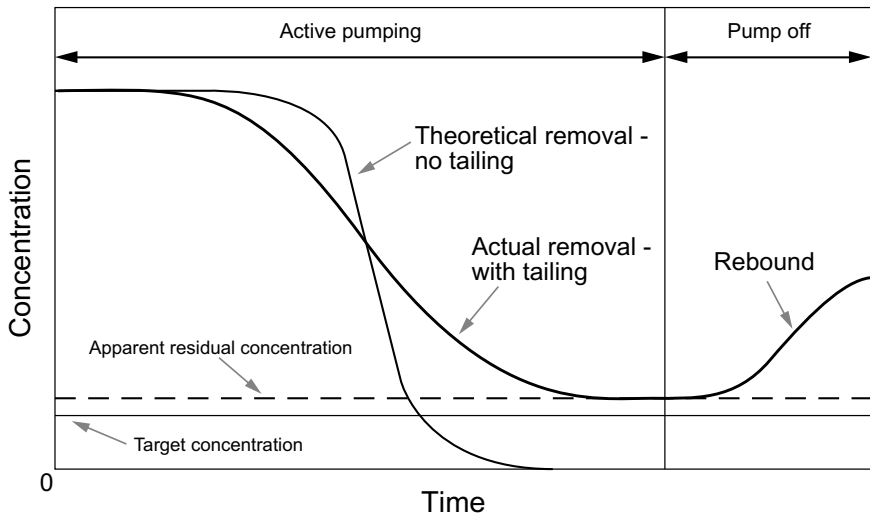


Fig. 17.15 *Tailing* and *rebound* effects on the evolution of the concentration of dissolved contaminant in the groundwater, as a function of pumping time or extracted volume (modified from [14])

- back diffusion from low to high permeability zones;
- groundwater velocity variations.

Rebound can also occur when pumping is interrupted once the threshold concentration has been achieved without having removed the source of contamination from the aquifer.

17.3.5 Extracted Water Treatment Technology

Once the contaminated water has been drawn to the surface, it has to undergo a series of physical, chemical, and/or biological processes to reduce pollutant concentration to acceptable values. Physical treatments include volatilization (e.g., air or steam stripping), filtration or ultrafiltration (through membranes), adsorption, physical separation (e.g., by density), and incineration. Chemical approaches, instead, include precipitation of contaminants, redox reactions, or ion exchange. Finally, contaminated water can be treated in bioreactors (e.g., with activated sludge, in aerated surface impoundments, via anaerobic digestion) or in slurry phase systems [7, 17].

The best treatment technology of a given site is evaluated and selected based on technical and economic considerations. The key parameters driving the choice are the discharge, the composition of the solution, and the initial and target concentrations.

The discharge that needs treating is directly related to the extracted discharge, in turn defined by the restoration targets. Target concentrations, instead, essentially depend on the final destination of the treated water, a few possibilities being: release into surface water bodies, transfer to another treatment plant, re-injection into the same aquifer, and direct use. Usually, transfer to a pre-existing plant is the least restrictive option, although every system requires concentration and discharge values to fall within specific and pre-determined ranges. Discharge into a surface water body or re-injection into the aquifer, instead, require specific authorizations and more stringent treatments.

If the water is contaminated by a mixture of compounds, one specific technology might not be suitable for the full treatment, but can be considered as a pre-treatment or as a polishing step in a chain process. In some situations, differential treatment of groundwater extracted from different areas of the site can have some benefits: for example, when groundwater with a high contaminant load is pumped at the source, and scarcely contaminated water is extracted downgradient.

Once the technical applicability of the potential methods for plume treatment has been established, their efficiency, feasibility, and costs have to be assessed. The efficiency is calculated based on the design discharge value, the level of treatment required by each component and the reliability of the method. Due to the scarcity of available data, the latter is difficult to estimate for innovative technologies. Therefore, without reliable information on performance, it is recommended to conduct laboratory analysis and pilot studies to identify critical data and potential issues that could arise. The treatment time can be estimated from pilot studies results. The feasibility of

a given method, instead, depends on technical/administrative aspects characterizing the site. These include the possibility of obtaining necessary permits, the limitations related to space availability, storage and disposal possibilities, the availability of required equipment and experienced workers, the environmental impact, and the relationship with the local community. Finally, cost assessment entails estimating investment costs, annual management costs, and the duration of the treatment [14].

Treatment strategies should be designed and implemented considering that feeding flow conditions, such as discharge and composition, could potentially change during the life cycle of a P&T system. Such an approach ensures a better performance at lower costs.

As for pumping operations, also treatment optimization requires a thorough monitoring activity over time.

17.4 Air Sparging and Biosparging

Air sparging (AS), also known as *in situ volatilization* or *in situ air stripping*, is a remedial technology that extends to the saturated zone the possibilities and potential of *soil vapor extraction* (SVE), used in the unsaturated zone. In fact, AS is most effective when used in combination with SVE.

It consists in injecting pressurized air below the water table through a system of vertical wells to enable the transfer of volatile contaminants from the liquid and sorbed phase to the gas phase (Fig. 17.16). When combined with SVE, contaminated vapors are extracted from the unsaturated zone and treated at the surface. If there

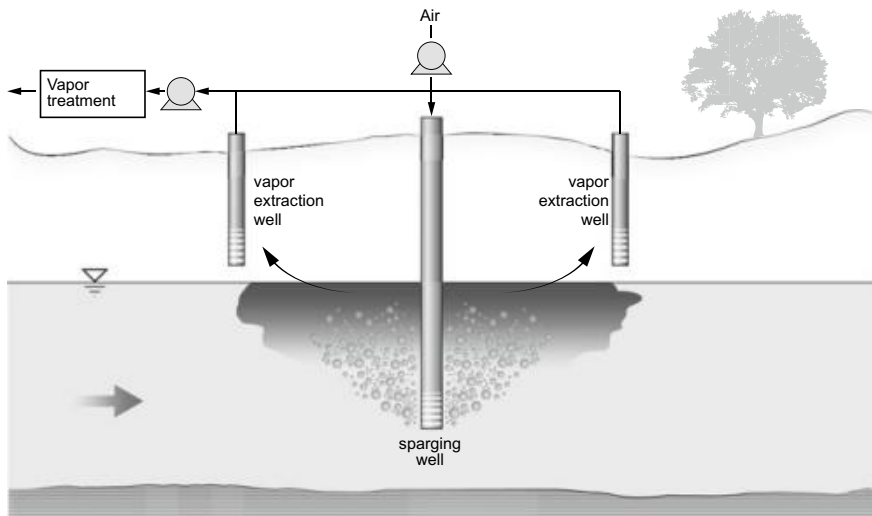


Fig. 17.16 Air sparging

is a chance vapors might migrate towards the surface or in underground structures, thus representing a source of risk, coupling of AS with a vapor capture system is necessary [17, 41, 51]. Furthermore, AS should not be used in confined aquifers, as the volatilized phase would remain trapped below the upper confining layer [68].

There are three main mechanisms contributing to contaminant removal via AS:

- dissolved contaminant stripping from the water phase;
- direct volatilization of the contaminant sorbed to the solid matrix or trapped in pores as a pure phase;
- aerobic contaminant biodegradation.

The ability of an air sparging system to remove a dissolved contaminant exclusively by stripping strongly depends on the compound's Henry's constant and on the manner in which air partitions in the unsaturated and saturated media. Direct volatilization, instead, is related to the compound's vapor pressure. Finally, aerobic biodegradation depends on the type of contaminant, on the presence of appropriate microbial communities, and on nutrient availability [51, 68].

In the case of petroleum hydrocarbons, volatilization and stripping mechanisms dominate the early phases of the remedial intervention, while biodegradation tends to become effective in the long term [51].

If contaminant biodegradation is promoted and prioritized over volatilization and stripping, the process is called biosparging (BS). From an operational standpoint, AS and BS technology can be combined and it is possible to switch from the former to the latter simply by reducing the operating air injection rate.

17.4.1 Design and Aim

The design of an air/bio sparging system depends on the aims set for the intervention:

- source remediation;
- dissolved contaminant removal;
- contamination plume containment.

Air sparging is one of the most effective remedial technologies available for submerged sources of contamination with volatile and biodegradable compounds [41]. In most cases, removal of the source of contamination is followed by remediation of the plume by natural attenuation processes.

In order to target the dissolved contaminant, a network of injection wells should be completed such that the superposition of the areas of influence of the individual wells fully encompasses the plume (see Fig. 17.17).

If the aim is to contain the contamination plume, the system has to be designed in order to maximize efficiency in a limited space, and the wells will be mainly placed perpendicularly to the direction of flow.

The classic air sparging system can be modified to meet specific needs by:

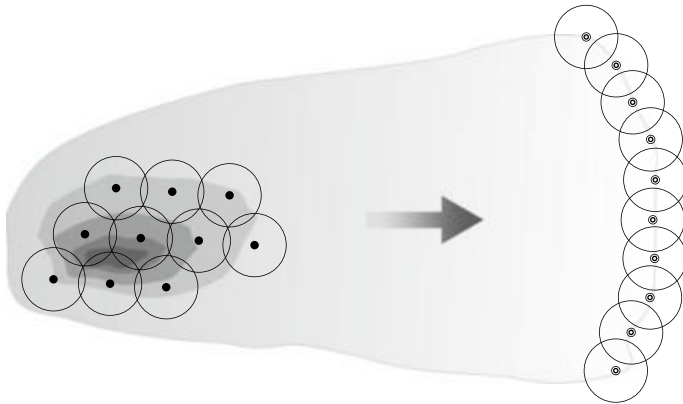


Fig. 17.17 Localization of air sparging wells for source remediation and plume containment

- directional drilling;
- injecting additional nutrients to promote biodegradation;
- replacing air with nitrogen to reduce iron oxide formation in aquifers with high iron concentration;
- injecting additional gases, such as ozone or oxygen, or replacing air with oxygen to increase O_2 availability for biodegradation processes.

17.4.2 Applicability

AS and BS applicability strongly depends on the characteristics of the contaminant and of the polluted porous medium. It is appropriate to use these remedial technologies when the contaminant:

- is present as pure NAPL trapped inside pores and is characterized by a vapor pressure value greater than 0.5–1 mmHg;
- is dissolved in groundwater and has a Henry's constant value greater than $1 \cdot 10^{-5} \frac{\text{atm} \cdot \text{m}^3}{\text{mol}}$;
- has a low aerobic biodegradation half-life (see Table 17.2 and Fig. 17.18).

Air sparging is usually limited to the treatment of contaminated areas no deeper than 15–20 m, relative to the water table. Installation and operation costs of the air injection system increase considerably with the depth of the contamination.

The effectiveness of air sparging interventions essentially depends on the possibility of affecting broad portions of the contaminated aquifer with a uniform air flow. To this end, the contaminated site should be homogeneous, to prevent the air from following preferential flow paths. Low permeability layers hinder the vertical migration of air, reducing the effectiveness of the treatment (Fig. 17.19) [23, 68]. Laboratory experiments have shown that in such conditions the injected air tends

Table 17.2 Examples of air sparging applicability to contaminants [51]

Contaminant	Stripping H (atm · m ³ /mol)	Volatilization τ (mmHg)	Aerobic biodegradation $t_{1/2}$ (h)
Benzene	$5.5 \cdot 10^{-3}$	95.2	240
Toluene	$6.6 \cdot 10^{-3}$	28.4	168
Xilene	$5.1 \cdot 10^{-3}$	$5.1 \cdot 10^{-3}$	
Ethylbenzene			
TCE			
PCE			
Petrol	High	High	High
Fuel oils	Low	Very low	Moderate

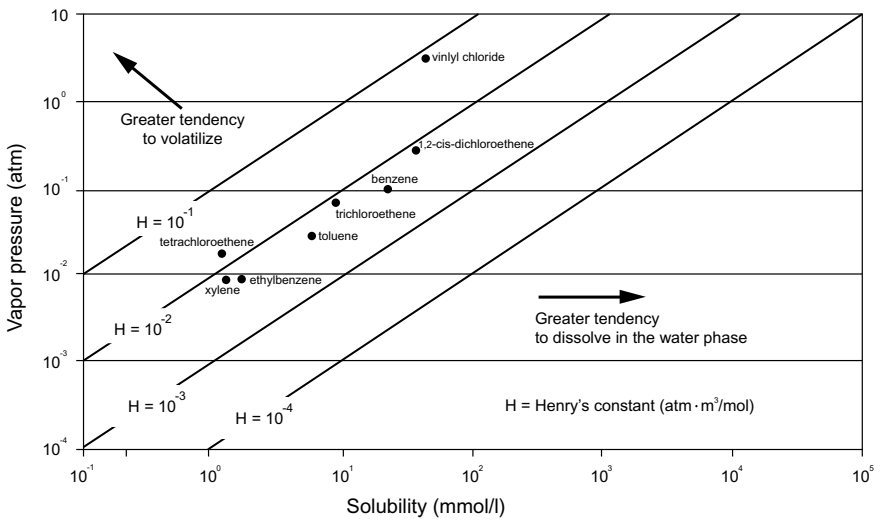


Fig. 17.18 Relation between vapor pressure, solubility and Henry's constant of a few volatile organic compounds

to accumulate below the low permeability lenses, subsequently moving horizontally. It is reasonable to assume that inside an aquifer this behavior could cause the contamination plume to spread. Similarly, also high permeability layers can favor horizontal migration of air, causing spreading of the plume. Furthermore, horizontal air movement makes capturing the stripped contaminants more difficult, and can lead to situations of potential hazard, if the vapors reach building foundations or other underground structures.

Vertical permeability of soil is directly proportional to the effective porosity and to the average grain size of the sediment; it is recommended to use air sparging in saturated zones with hydraulic conductivity greater than 10^{-5} m/s.

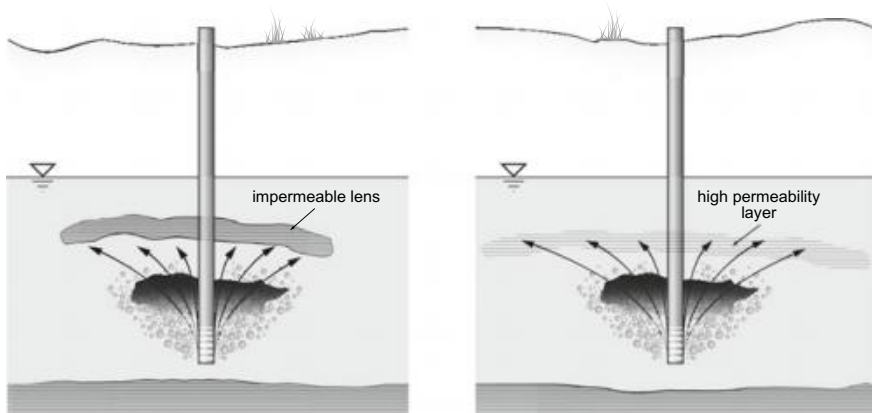


Fig. 17.19 Limitations to AS applicability attributable to the presence of layers characterized by strong permeability heterogeneities relative to the aquifer (modified from [51])

17.4.3 Dynamics of the Process

The mechanism of air flow through saturated media are not fully understood; it is, therefore, difficult to predict the performance of an AS intervention. In the early days of this technology, it was thought that injected air moved vertically in the form of bubbles; currently, instead, it is generally agreed that air migrates through preferential channels and paths [23]. Upon injection, air causes the water table to rise (a process sometimes called *mounding*). While this may be problematic because it could cause lateral spreading of the contamination, it normally only occurs during an early transient stage of injection, during which the freshly introduced volume of air causes an expansion of the injection region (Fig. 17.20). Subsequently, the formation of preferential flow paths allows air to start migrating towards the vadose zone. This second transient phase causes the water table mound to contract and eventually become negligible (Fig. 17.21), and lasts until the achievement of a steady state, i.e., equilibrium between injected and migrating air [51].

During the transient phases some of the most relevant causes for water mixing occur, i.e., groundwater displacement due to the introduction of air and capillary interactions between air and water. During steady state, water mixing still happens, albeit to a smaller extent, due to air-induced shear stresses, evaporative water loss, thermal convection, and migration of fine material. Water mixing in AS is crucial for its contribution to the transport of the mass of contaminant out of the aquifer and to the introduction of oxygen in the polluted zone. It is, therefore, preferable to extend the duration of the nonsteady phase to maximize water mixing. Transient phase duration is correlated to the porosity of the medium; hence, AS tends to be more effective in more permeable media. Furthermore, pulse injections of air or cyclic variations of air flow rate cause long lasting transient phases and improved groundwater mixing [41, 51, 68].

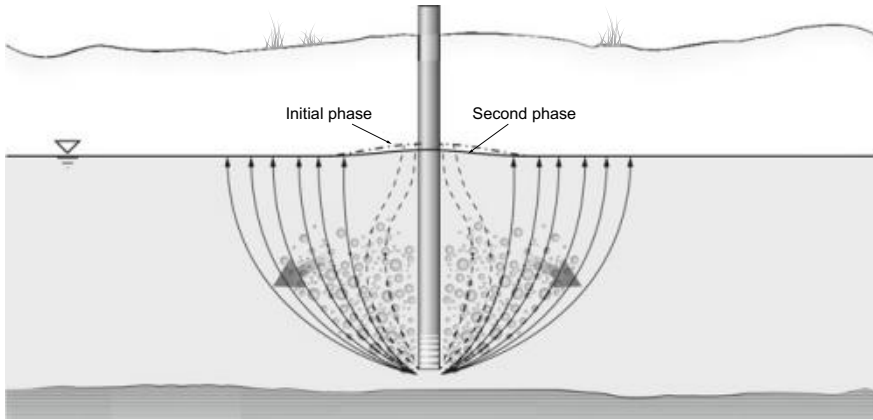


Fig. 17.20 Initial injection phase and consequent groundwater mounding

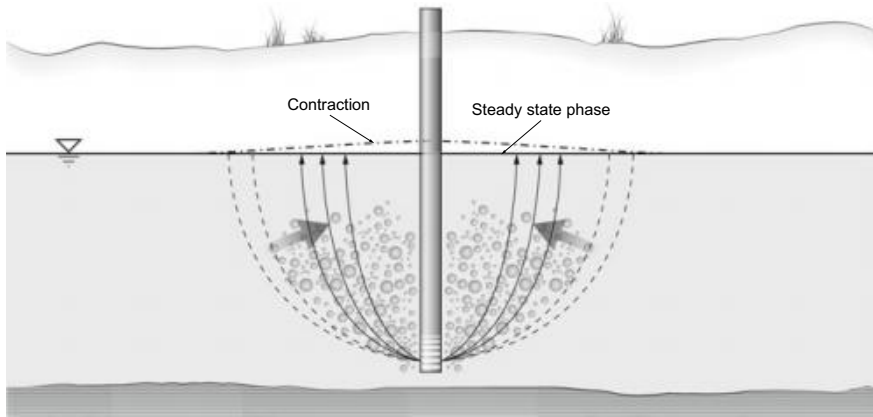


Fig. 17.21 Contraction of the injection zone and achievement of steady state conditions

17.4.4 Air Sparging System Design

There are several parameters that should be considered when designing an air sparging system.

- **Size of the area of influence:** sparging wells should be spaced in order to generate overlapping zones of influence, to ensure full coverage of the contaminated area. It is difficult to define the radius of the area of influence of an AS well: although there are many methods available (e.g., measurement of the lateral extension of the water table mound; measurement of dissolved oxygen or redox potential variations; measurement of soil gas pressure; determination of the head space pressure in saturated zone probes, which is a reliable and cost effective method; use of tracers; geophysical methods, such as the measurement of electricity resistivity changes,

which is the most reliable of available methods), many of them tend to be imprecise and overestimate the zone of influence [23, 51].

- Injection depth: it should be at least 30–50 cm below the lowest detected contaminated point; however, since it depends on the geological structure of the subsurface, injection of air below low-permeability layers should be avoided. Injection depth affects air sparging pressure and flow rate in that greater depths determine greater areas of influence; therefore, higher air flow rate and pressure will be necessary at greater depths to achieve the desired air saturation [51].
- Injection pressure and flow rate: it has to be sufficient to overcome the hydrostatic pressure of the water column above the screens, (p_h), the threshold pressure for water displacement from the aquifer formation (p_a), and the pressure drop in the tubings, the well, the screens, and the filter pack, (p_d). Therefore, injection pressure should be at least equal to the sum of these components: $p_i = p_h + p_a + p_d$. The injection pressure should be calculated accurately, since the common belief that high injection pressures yield equally high operation efficiencies is unfounded. In fact, excessive injection pressures can lead to formation fractures and thus create preferential migration paths that actually reduce contaminant removal efficiency [51, 68].
- Injection method: air can be injected continuously or by pulses. Pulsing injection is preferable because it increases the area of influence of AS, and because it increases mixing in the aquifer due to the cyclic formation and collapse of air channels.
- Sparging well construction method: injection points must be appropriately sealed to avoid short-circuiting up the well bore. Their diameters usually have a diameter ranging from 1 to 4"; although the size should not impact the effectiveness of the AS intervention, the employment of smaller wells, coupled to direct push drilling techniques, contributes to minimizing installation costs [51].

17.5 Permeable Reactive Barriers

Permeable reactive barriers (PRBs) are an established remedial technology that has attracted significant interest since the 1990s. In Sect. 17.5.6 the design and construction of the first PRB built in Italy are presented as a case study [20].

PRBs are based on a relatively simple principle: a wall of reactive material is placed in the aquifer in order to intercept the contamination plume while it migrates under the effect of the natural gradient. The reactions that ensue lead to the degradation or immobilization of the contaminant within the barrier while it flows through it (see Fig. 17.22).

PRBs can be designed according to the following two configurations (Fig. 17.23) [7, 41, 50]:

- continuous trenches that extend across the entire or part of the saturated thickness;
- funnel and gate systems that use low permeability barriers to direct (funnel) groundwater flow from the contaminated region towards a permeable treatment zone (gate).

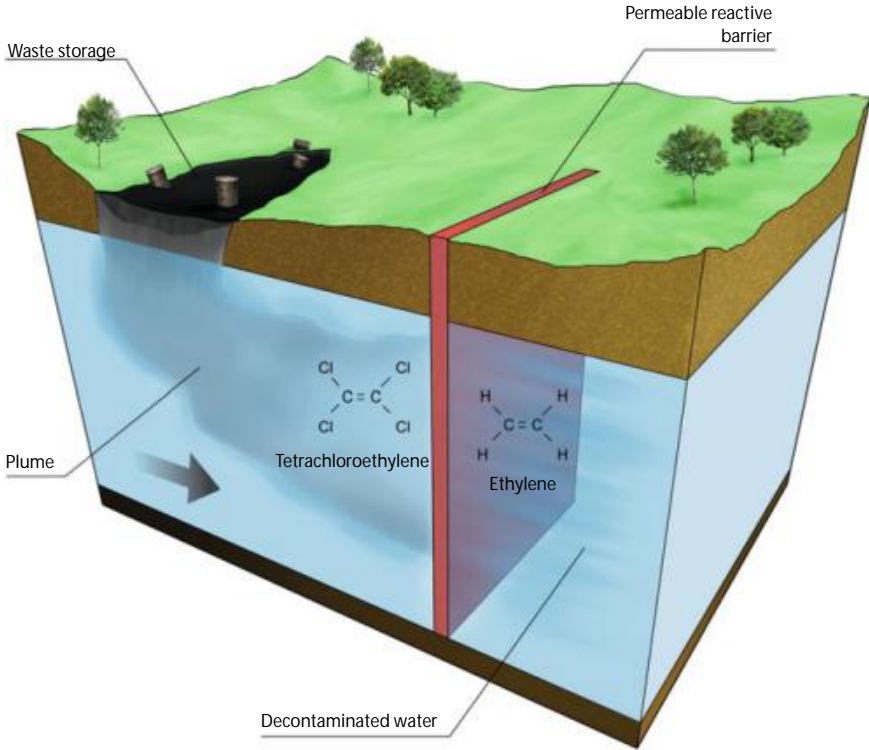


Fig. 17.22 Continuous permeable reactive barrier configuration

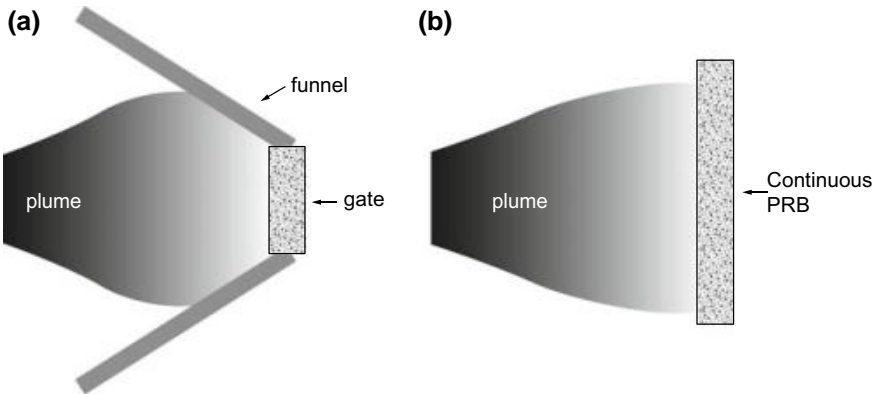


Fig. 17.23 Permeable reactive barrier configurations: a funnel e gate; b continuous trench

Table 17.3 Contaminants that can be treated with Fe⁰ PRBs

Organic compounds		Inorganic compounds			
Methanes	Carbon tetrachloride Trichloromethane	Trace metals	Nickel Lead Uranium Technetium Iron Manganese Selenium Copper Cobalt Cadmium Zinc		
Ethanes	Hexachloroethane 1,1,1-trichloroethane 1,1,2-trichloroethane 1,1-dichloroethane				
Ethenes	Tetrachloroethene Trichloroethene Cis-1,2-dichloroethene Trans-1,2-dichloroethene 1,1-dichloroethene Vinyl chloride 1,3-dichloropropene				
Propanes	1,2,3-trichloropropane 1,2-dichloropropane			Anionic contaminants	Sulfates Nitrates Phosphates Arsenic
Others	Hexachlorobutadiene 1,2-dibromoethane freon 113 N-nitrosodimethylamine				

PRBs are in situ treatment systems that can operate for years at extremely low management costs.

A key aspect of PRB design is that the permeability of the reactive material cannot be lower than that of the aquifer, to avoid flow line diversion around the barrier itself.

Several processes contributing to the removal, elimination or attenuation of contamination can occur at the treatment zone [6, 41]:

- chemical reactions;
- physical separation;
- biodegradation;
- sorption.

There is a wide range of reactive materials (e.g., solid organic material, zeolite, zero valent iron, slag, augmented microorganisms) that can be used in PRBs for the transformation of a few contaminants into non-toxic species. The most commonly used is zero valent iron (ZVI or Fe⁰, see Tables 17.3, 17.4, and 17.5), which is particularly effective for the removal of chlorinated solvents and can also immobilize heavy metals such as chromium and uranium [34, 41].

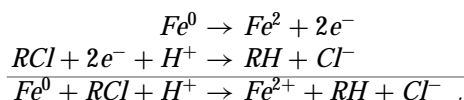
Chlorinated solvents are removed from groundwater via a redox process during which Fe⁰ is oxidized to Fe²⁺ while the halogenated hydrocarbons are reduced, thus losing chlorine ions:

Table 17.4 Contaminants that cannot be treated with Fe^0 PRBs

Organic compounds	Inorganic compounds
Dichloromethane	Chlorine
1, 2-dichloroethane	Perchlorate
Chloroethane	
Chloromethane	

Table 17.5 Compounds whose treatability with Fe^0 PRBs is unknown

Organic compounds	Inorganic compounds
Chlorobenzenes	Mercury
Chlorophenols	
A few pesticides	
PCB	



In the overall reaction each molecule acquires two electrons (donated by an iron atom) and a proton (present in the groundwater) per chlorine lost. Theoretically, the process should ensue according to a series of chain reactions that lead to the progressive dehalogenation of the chlorinated substance until it is reduced to an alkane or alkene.

However, other by-products have been observed: in particular, during the degradation of tetrachloroethylene (PCE) and trichloroethylene (TCE) compounds that are not predicted by the above reaction, such as acetylene, can be detected, in addition to ethene and ethane. This suggests that two main reaction mechanisms must exist (Fig. 17.24) [34]:

- *sequential hydrogenolysis*: two electrons and a proton attack the solvent molecule causing the elimination of a chlorine ion and the formation of a compound with a lower degree of saturation;
- *β -reductive dechlorination*: two electrons are transferred from the iron to the chlorinated ethene, leading to the loss of two chlorine ions Cl^- from the molecule and the formation of a triple bond; intermediate products (chloroethylene or acetylene) are quickly transformed by hydrogenolysis and finally hydrogenated.

Some of the intermediate products of the first reaction, specifically *cis*-DCE and vinyl chloride (VC) are degraded at a slower rate than TCE itself. Conversely, the chloroacetylene produce during β -reductive dechlorination has a very short life and its reduction to ethene is fast. Several studies have demonstrated that the degradation process mainly occurs via β -reductive dechlorination and, therefore, the production of toxic byproducts such as VC is minimal [24, 73].

Generally, perhalogenated hydrocarbons tend to be reduced more quickly than those that are less halogenated; in addition, dechlorination of carbon-saturated compounds (e.g., carbon tetrachloride) is faster than that of insaturated substances (e.g., TCE or VC).

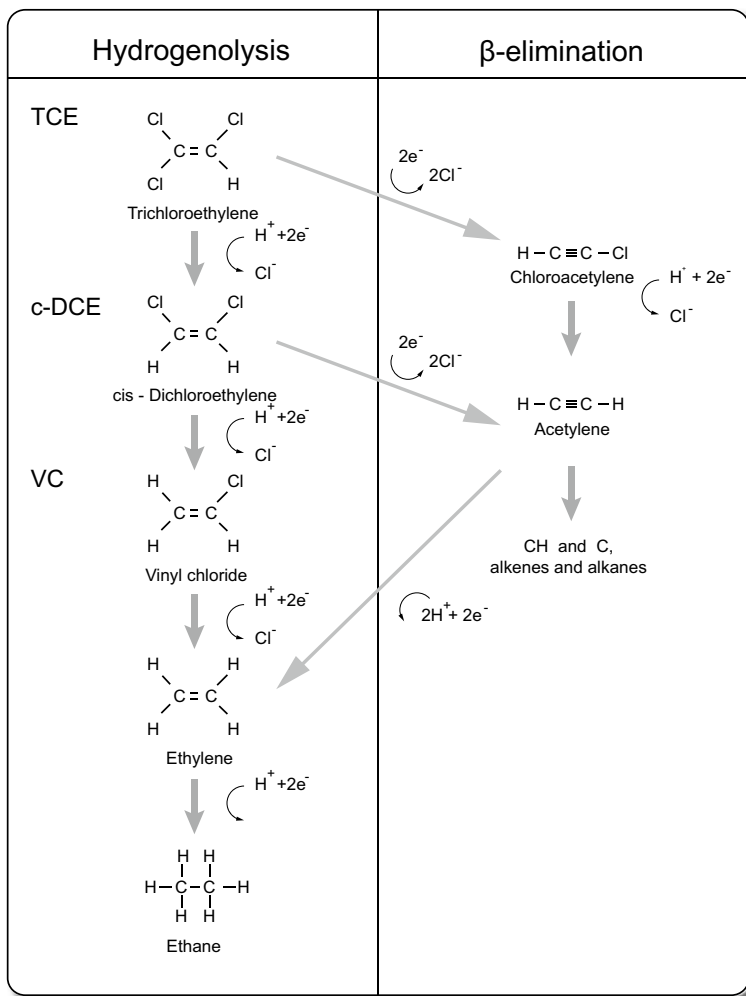


Fig. 17.24 Main TCE degradation pathways in a Fe^0 permeable reactive barrier

17.5.1 Laboratory Tests

The goal of laboratory tests is to determine:

- the ideal reactive material for the treatment cell;
- the degradation constants relative to the contaminant removal reactions;
- the predicted duration of the reactive barrier.

The reactive material to be employed in the permeable barrier should be chosen according to the following parameters:

- *reactivity*: a filling material that is likely to achieve a high degradation constant value is preferable. In the case of Fe^0 the reactivity increases with its specific surface area (i.e., with decreasing particle size);
- *stability*: the time during which the reactive material continues to fulfill its function;
- *availability and cost*: these parameters have to be optimized, without forgetting the reactivity of the material;
- *hydraulic conductivity*: it has to be greater than, or at least comparable with, that of the aquifer system, in order to ensure the capture of the contamination plume and prevent flow lines from being diverted;
- *environmental compatibility*: naturally, the reactive medium cannot be an additional source of groundwater contamination.

Following these guidelines, zerovalent iron is the most widely used reactive medium in pilot- and full-scale barriers. Several manufacturers make it commercially available with varying characteristics in terms of purity and degradation ability [34, 41].

Laboratory tests for the determination of degradation kinetics can be carried out in batch or through column experiments.

The batch mode observes the evolution of the contaminants' concentration over time in a closed shaking reactor, and is generally only used as a preliminary investigation of the degradation kinetics. Batch tests have the advantage of being quick, cheap, and simple. However, they have some drawbacks related to the fact that shaking the reactor modifies many transport mechanisms making it poorly representative of contaminant degradation in not-shaken systems. In addition, the reactive material to contaminant solution ratio is significantly smaller than what can be achieved in column experiments or in practical applications.

The main advantage of running column experiments is that they offer the possibility of determining degradation kinetics in closer conditions to those found in the field (Fig. 17.25). Despite being more expensive and demanding than batch tests, column experiments usually provide more realistic results, and provide information on the duration and long term performance of the reactive material.

Samples can also be collected along the length of the column to monitor the variations of the ionic composition and of properties such as redox potential and pH, and to investigate the formation of precipitates, as well as to observe the evolution of the contaminants' concentration [34].

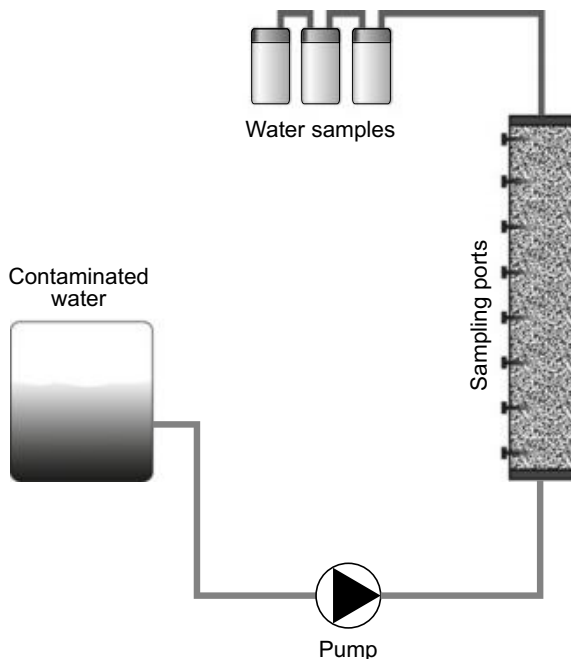
Both batch and column experiments can be performed with:

- deionized water amended with contaminants;
- clean groundwater amended with contaminants;
- contaminated groundwater.

To extend the experimental results to the field it is often necessary to apply corrective factors that keep into account the operating conditions of the reactive material, such as:

- temperature: groundwater temperature usually ranges between 10 and 15 °C, significantly lower than ambient laboratory temperature. Therefore, laboratory exper-

Fig. 17.25 Column experiments for the determination of degradation kinetics



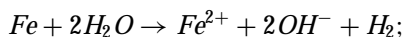
iments overestimate the degradation kinetics, which have to be corrected with a coefficient derived with the Arrhenius equation [1, 35];

- bulk density: real reactive cells have a smaller bulk density than that measured in the laboratory due to the different sedimentation conditions of the material. Hence, the reactive surface can be smaller in the field than in the column, imposing the application of another correction of the kinetics.

The longevity of a barrier can be investigated with column experiments by applying greater flow rates than those found in the field, to accelerate aging processes and pore clogging due to the formation of precipitates.

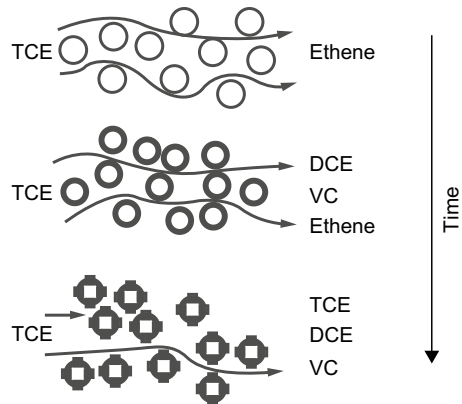
In the case of a Fe^0 barrier, effectiveness can decrease over time due to several undesirable chemical reactions:

- iron oxidation in contact with water: the kinetics of this reaction is, in any case, smaller than that of chlorinated solvent degradation:



- iron oxidation by dissolved oxygen: high oxygen concentrations in the groundwater can oxidize the first centimeters of the barrier and create problems related to the precipitation of iron hydroxides. This situation can be avoided with a few simple measures in the system design;

Fig. 17.26 Possible consequences of reactive material coating in PRBs



- pH increase: dehalogenation processes in the reactive zone consumes protons resulting in an excess of hydroxyl ions and an increase in the pH of the water, sometimes exceeding 9. A direct consequence of the increase in pH is that precipitate formation and accumulation on the metal surface (coating) becomes more likely, leading to reduced metal reactivity and shorter residence time of the contaminated water within the reactive barrier (Fig. 17.26).

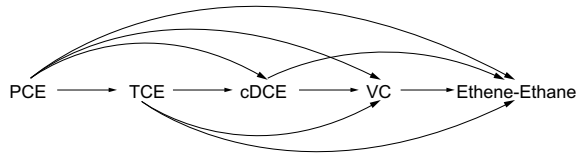
As well as the above mentioned tests, it is also possible to carry out several other specific studies to determine additional parameters. These include:

- determination of the *specific surface area* (m^2/g), an important parameter that contributes to the calculation of the degradation kinetics;
- determination of the hydraulic conductivity and of the porosity of the reactive material, which are used in numerical flow and transport models;
- microbiological analysis of the reactive material and of the groundwater to quantify microbially-driven degradation;
- tracer tests for the observation of the effects of reduced hydraulic conductivity and porosity as a consequence of hydroxide precipitation and pore clogging;
- measurement of the oxidation state of the surface of the reactive material.

17.5.2 Design of a PRB

To appropriately design a permeable barrier, in particular its reactive *gate*, it is recommendable to carry out a three-dimensional simulation assuming a transient regime. The simulation should include advection, hydrodynamic dispersion, sorption to the solid matrix, and network degradation reactions (see Fig. 17.27), according to a system of partial differential equations that can be summarized with the following expression [58]:

Fig. 17.27 Network degradation pathways of a few chlorinated ethenes



$$\begin{aligned}
 R_i \frac{\partial C_i}{\partial t} + v \frac{\partial C_i}{\partial x} - D_x \frac{\partial^2 C_i}{\partial x^2} - D_y \frac{\partial^2 C_i}{\partial y^2} - D_z \frac{\partial^2 C_i}{\partial z^2} &= \\
 &= \sum_{j=1}^{i-1} y_{i/j} \lambda_j C_j - \lambda_i C_i + \sum_{j=i+1}^n y_{i/j} \lambda_j C_j
 \end{aligned}
 \tag{17.16}$$

where C_i is the concentration of the substance i (ML^{-3}); $y_{i/j}$ the yield coefficient, which can be described as the mass of product i formed per unit mass of the species j ; λ_i the first order degradation kinetics constant of the species i (T^{-1}); v the groundwater seepage velocity (LT^{-1}); D_x, D_y, D_z the hydrodynamic dispersion coefficients ($L^2 T^{-1}$); and n the total number of species involved in the network degradation process.

Usually, during the preliminary stages of the permeable gate design, a one-dimensional geometry is considered, and a few mechanisms, such as sorption, hydrodynamic dispersion, and chain degradation reactions are neglected. In a transient regime, the simplified differential equation for each contaminant is:

$$\frac{\partial C}{\partial t} = -v_{gate} \frac{\partial C}{\partial x} - \lambda C,
 \tag{17.17}$$

where v_{gate} represents the average seepage velocity within the gate of the barrier. The same equation in the steady state, which is what is used for design, is:

$$v_{gate} \frac{\partial C}{\partial x} = -\lambda C,
 \tag{17.18}$$

whose solution describes the evolution of the concentrations within the barrier as function of space:

$$C = C_{in} e^{-\lambda \frac{x}{v_{gate}}}.
 \tag{17.19}$$

Once the contaminant concentration in the water outflowing from the reactive gate has been defined, the thickness can be calculated as (Fig. 17.28):

$$S = -\frac{v_{gate}}{\lambda} \ln \left(\frac{C_{out}}{C_{in}} \right),
 \tag{17.20}$$

Fig. 17.28 Simplified schematic of a permeable reactive barrier

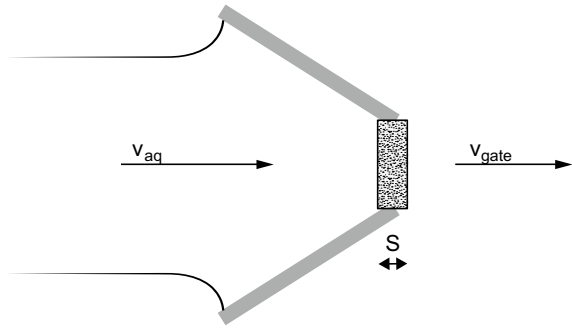


Table 17.6 Characteristics of commercial zero-valent iron

Filling porosity	ε	0,5
Bulk density	ρ_b	2600 kg m ⁻³
Specific surface area	a	7-1000 m ² kg ⁻¹
Gate hydraulic conductivity	K_g	5 · 10 ⁻⁴ ms ⁻¹

the residence time of water inside the permeable gate is:

$$t_p = \frac{S}{V_{gate}} = -\frac{1}{\lambda} \ln \left(\frac{C_{out}}{C_{in}} \right), \tag{17.21}$$

and the mass of iron filling the barrier is equal to:

$$W = SA\rho_b = -\frac{A\rho_b V_{gate}}{\lambda} \ln \left(\frac{C_{out}}{C_{in}} \right). \tag{17.22}$$

In the previous equations C_{in} indicates the concentration of the generic contaminant entering the gate and C_{out} the target concentration after treatment.

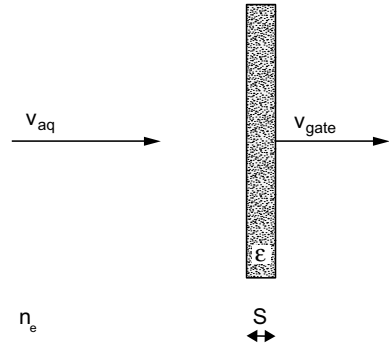
Table 17.6 lists a few characteristic parameters of a typical commercial zerovalent iron.

Usually, the seepage velocity within the gate can only be calculated with a flow model, capable of describing the changes that the natural flow field undergoes due to the PRB construction. In the case of continuous trench reactive barriers (Fig. 17.29), the model can be avoided and the seepage velocity inside the gate can be expressed as a function of that in the aquifer, v , according to a water discharge balance that yields the following relation:

$$V_{gate} = \frac{Vn_e}{\varepsilon}, \tag{17.23}$$

where n_e and ε represent the effective porosity of the aquifer and of the reactive gate, respectively. By using this relation, the equations expressing the gate thickness and the mass of iron can be reformulated as follows:

Fig. 17.29 Simplified schematic of a continuous trench PRB



$$S = -\frac{vn_e}{\lambda\varepsilon} \ln\left(\frac{C_{out}}{C_{in}}\right), \tag{17.24}$$

$$W = SA\rho_b = -\frac{A\rho_b vn_e}{\lambda\varepsilon} \ln\left(\frac{C_{out}}{C_{in}}\right) = -\frac{A\rho_b Ki}{\lambda\varepsilon} \ln\left(\frac{C_{out}}{C_{in}}\right), \tag{17.25}$$

where K is the hydraulic conductivity of the aquifer [LT^{-1}] and i is the hydraulic gradient.

A model delving into greater depth could keep into account the byproducts formed inside the barrier during contaminant degradation. The contaminant removal process involves the formation of a series of intermediary products, themselves toxic, that have to remain within the barrier sufficiently long to be degraded. The thickness of the barrier should be determined in such a way to ensure a sufficiently long water residence time for contaminants and byproducts to be abated to concentrations below the cleanup target values (Fig. 17.30).

Despite the possibility of using Eqs. (17.24) and (17.25) for continuous trench reactive barriers, it is advisable to use at least a two-dimensional numerical flow (and possibly transport) model, for a more accurate design.

17.5.3 Technical Solutions for Constructing a Permeable Reactive Barrier

Once the location, the configuration, and the physical dimensions of the reactive barrier have been determined, the most suitable technology for its construction has to be selected. The factors that ultimately contribute to this decision are:

- depth of the excavation;
- permeability of the gate;
- soil characteristics and geotechnical constraints;
- disposal of contaminated soil removed during trench excavation;
- site accessibility and availability of space at the surface for the construction site;
- costs.

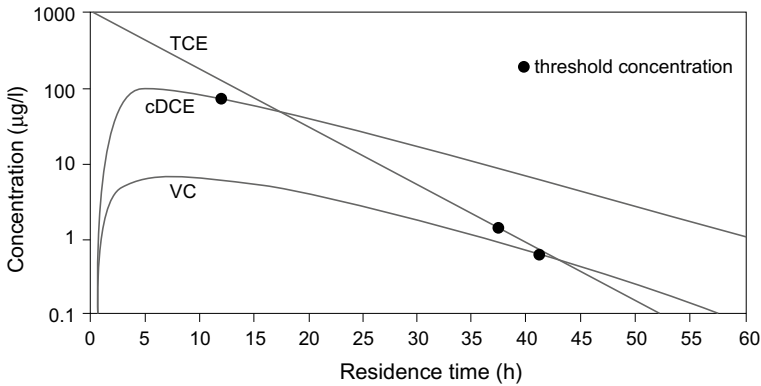


Fig. 17.30 Residence time determination using a sequential degradation model (modified from [28])

In general, the size and geometry of the barrier must be able to capture the entire contamination plume even upon variations of the flow conditions or in the presence of external oscillations (e.g., water table oscillations, recharge processes, pumping).

If the contamination doesn't affect the entire saturated thickness, a *hanging barrier* can be installed, thus limiting the excavation depth to the superficial part of the aquifer. Conversely, if the contamination is distributed across the entire saturated thickness of the aquifer, or if it affects the deepest layers, the barrier has to reach the underlying impermeable bed. Properly placing the reactive cell and keying it into the impermeable base are important measures for the prevention of over- and under-flow processes. Clearly, the deeper the barrier, the more technical issues are likely to arise in regard to the excavation and trench support, also affecting construction costs.

The permeability of the cell must be greater than the aquifer, to avoid circumvention phenomena, and to favor the flow of contaminated water through the reactive barrier. On the other hand, higher hydraulic conductivities usually correspond to a smaller specific surface area of the reactive material (hence, reduced reactivity), which has to be counteracted by increasing the thickness of the reactive gate.

A set of tests have to be performed to assess the geotechnical characteristics of the soil: continuous core drilling surveys coupled to penetration tests (SPT), plate loading tests, as well as lab tests to determine shear resistance and deformation parameters of collected samples. In addition, an appropriate slurry to support the trench wall has to be identified. During permeable gate installation, a biodegradable slurry can be added as the trench is excavated. This liquid shoring is then replaced by the reactive material, and any residual trace of biopolymer can be subsequently eliminated.

Site accessibility and space availability for installation operations should not be neglected when selecting the construction technology, since excavation generally implies the use of cumbersome heavy vehicles. The excavated soil and the water extracted to depress the water table have to be disposed of, or treated, in off-site plants or in dedicated on-site facilities.

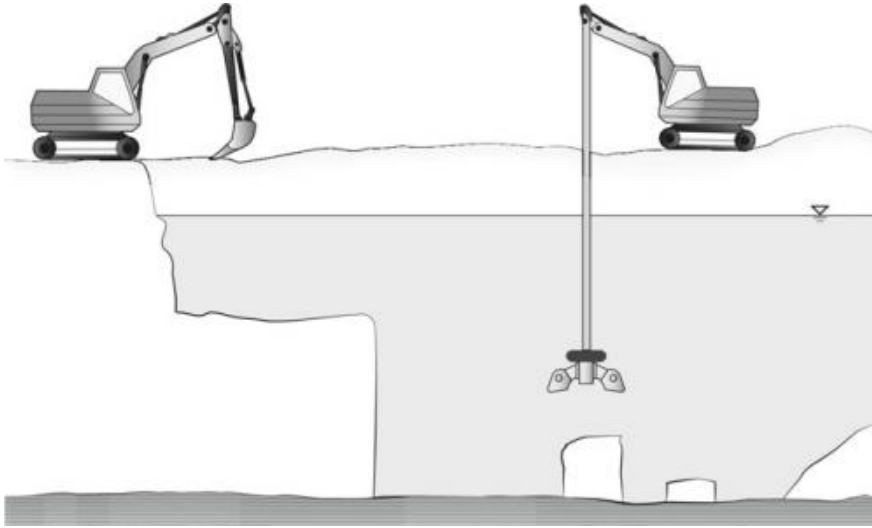


Fig. 17.31 Conventional trenching techniques (modified from [27])

17.5.3.1 Permeable Reactive Zone Emplacement

In this section a few conventional or innovative technologies are described for the construction of the trench for the emplacement of the reactive material [34]:

- *Conventional trenching techniques.* Backhoe or clamshell-bucket excavators are usually used for digging the trench (Fig. 17.31). Sheet piling can be employed to shore the trench during gate installation; additionally, a dewatering system can also be used when excavating deep below the water table. Alternatively, biopolymer shoring can be used: the trench is filled with a biodegradable slurry that prevents the soil from caving in and that is subsequently eliminated without affecting the permeability of the reactive zone. Clamshell-bucket excavators can be used to dig depths up to 50–60 m.
- *Continuous chain trenching.* This technique employs a trencher equipped with a digging chain to cut the ground and excavate a continuous trench 30–60 cm wide (Fig. 17.32), immediately backfilled with the reactive material or with a continuous layer of HDPE to ensure its impermeability. They can reach a depth of about 10–15 m.
- *Excavation techniques with caissons.* Caissons are used to stabilize borehole walls during excavation. Cylindrical caissons with a diameter of the order of 2 m are driven into the soil for the creation of the gate(s). Once the caisson is installed, the soil within it can be replaced with reactive material. This is an economical solution limited by the maximum achievable depth, which is around 15 m, depending on the lithology.

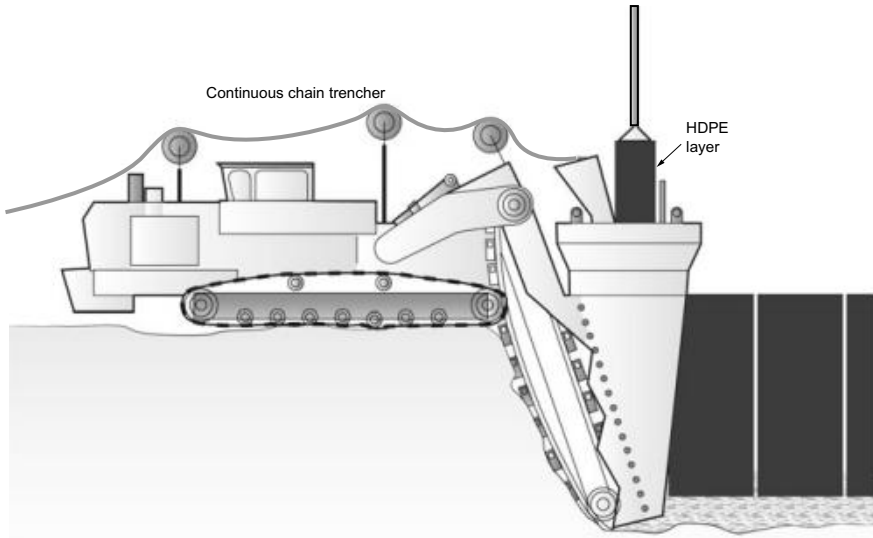


Fig. 17.32 Continuous chain trenching (modified from [27])

- *Mandrel-driven installment.* This method is similar to the use of sheet piles or caissons in that it uses an external prop to shore the borehole. However, in this case the excavating machine doesn't remove the soil, but creates space for the gate by driving a hollow tube with a special shoe. Once the borehole has been drilled, it can be filled with the reactive material and the tube can be extracted.

17.5.3.2 Construction of Low Permeability Walls

For the construction of a funnel-and-gate type barrier, low-permeability vertical walls have to be installed to assist with routing the flow towards the reactive gate.

Table 17.7 gives an overview of the construction systems used to install vertical containment walls.

The most commonly used systems for installing PRBs are essentially those used for subsurface containment (see Sect. 17.2):

- *Cement-bentonite slurry walls.* This is the most common barrier type, constructed with an alternate panel or continuous excavation method. This type of wall can be constructed in a single phase (one-phase), directly injecting the final cement-bentonite slurry during excavation, or as a two-phase process, replacing the trench stabilizing slurry with the final one at the end of the excavation. These walls are normally 0.6–1 m thick, and reach maximum depths of about 30–40 m when normal

Table 17.7 List of systems for the construction of impermeable vertical barriers. *S* indicates the thickness of the wall, *L* the maximum depth (modified from [47])

Technology	Conventional name	Impermeable material	Size	
			S (m)	L (m)
Trenching, removal of soil and replacement with impermeable slurries	One-phase slurry walls	Cement-bentonite slurries	0.4–1.6	100–170
	Two-phase slurry walls	Cement-bentonite slurries	0.4–1.6	40–70
	Geomembrane composite wall	Cement-bentonite slurry and geomembrane	0.4–1.6	20–50
	Secant pile wall	Cement-bentonite or grout slurry	0.4–1.5	20–40
Soil displacement and injection of impermeable slurries or emplacement of sheet piles and prefabricated panels	Thin slurry diaphragm	Cement-bentonite slurries with inert materials or additives	0.05–0.3	10–35
	Thin diaphragm with geomembrane	Cement-bentonite slurry and geomembrane	>0.002	10–40
	Sheet-piles	Steel	0.02	20–30
	Emplaced diaphragms and prefabricated panels	Grout	>0.4	15–25
In situ soil permeability reduction	Injections	Cement-bentonite slurries, silicates, cement slurries with or without filler	1.5–2.5	20–80
	Jet-grouting	Bentonite slurries with cement	0.15–2.5	20–70
	Soil mixing	Lime, cement, bentonite	0.8–1.5	30–60
	Freezing	Liquid nitrogen with freezing plant	>0.7	50–100

equipment is used; with modern chain trenchers significantly greater depths can be reached.

- *Soil-bentonite slurry walls.* This kind of diaphragm wall, mainly used in the USA, is excavated by continuous trenching and by shoring the trench with bentonite slurries, and subsequently filling it with a soil-bentonite slurry. They are usually 0.8–1.5 m thick and 20–30 m deep.
- *Composite slurry walls.* A continuous trench is excavated in the presence of cement-bentonite or soil-bentonite slurries, and a plastic liner with leakproof seams is inserted before the solidification of the impermeable slurry. This type of wall can reach depths up to approximately 50 m.
- *Thin slurry diaphragm walls.* They can be installed with various methodologies: pre-emplacment by vibration of metal sheet piles or prefabricated concrete panels, and subsequent filling of the cavities thus formed in the ground with bentonite slurries.

- *Soil mixing barriers.* The barrier is constructed by driving a hollow auger that can inject an additive, such as powdered bentonite and/or cement, and simultaneously mix it with the soil. Continuity of the barrier is ensured by a certain degree of overlap between the columns. The overall permeability of the system is strongly affected by the soil type.
- *Jet grouting barriers.* It is one of the most versatile and used technologies, and consists in the injection of bentonite or cement slurries directly in the ground. Minimum permeability strongly depends on the characteristics of the treated soil, on the distance between injection points and the type of injection. Maximum achievable depths are around 70 m.
- *Sheet piles.* This methodology is generally used for urgent interventions because it can be implemented very quickly. The sheet piles can be installed with vibratory or drop hammers that drive them directly into the soil. Unless the joints between the sheet piles are specifically sealed, they are likely to leak.

17.5.4 Monitoring Network

Once the barrier has been installed, a monitoring phase begins and is meant to [7, 34]:

- ensure the plume is adequately captured and treated, by verifying that: contaminant concentrations downgradient of the PRB are below the threshold values, there are no toxic byproducts, there isn't an under- or overflow problem, actual capture zone and residence time within the gate are consistent with the predictions. A set of monitoring wells up- and downgradient, as well as within the reactive zone of the barrier have to be installed to carry out these verifications;
- assess the longevity of the barrier through geochemical and potenziometric studies that could indicate pore clogging in the reactive material, or by analyzing samples collected in the permeable treatment zone.

To this end, it is necessary to emplace a multilevel (if possible) monitoring network, within and outside the permeable barrier, so that the spatial and temporal variation of geochemical and contamination properties of water can be evaluated. A few possible monitoring network configurations are illustrated in Fig. 17.33:

- (a) monitoring wells are about ten centimeters into the gate, aligned perpendicularly to the direction of flow; with this pattern it is possible to observe concentration variations due to heterogeneities of the medium;
- (b) monitoring points are located outside of the barrier to monitor the degradation of the contaminant and the formation of byproducts, if any;
- (c) some of the monitoring wells are placed upgradient and along the thickness of the barrier to investigate the kinetics of contaminant abatement;
- (d) a few monitoring wells are installed up- and down-gradient of the funnel to avoid barrier circumvention or leak problems.

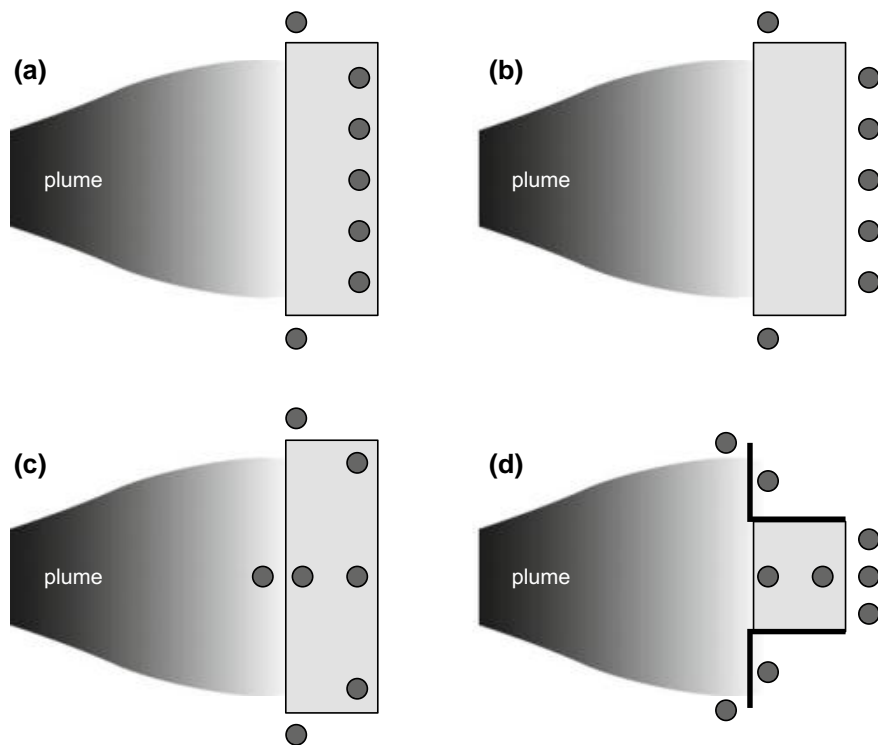


Fig. 17.33 Various monitoring network configurations for a PRB

When sampling monitoring wells located close to the barrier, a few precautions need to be taken, such as symmetrical sampling relative to the flow direction and the use of small purge volumes to avoid creating artificial gradients or drawing untreated water.

Tracer tests, generally conducted with sodium bromide, are used to detect flow velocity heterogeneities within the reactive gate, and to identify the capture zone. An alternative to tracer tests is represented by the use of submersible probes, which, lowered in monitoring wells within the reactive gate, take targeted measurements of the three-dimensional velocity vector.

Reactive material samples can be collected with vertical borings of increasing depth along the thickness of the gate. Air contact must be avoided during sample extraction; it is recommended to introduce new reactive material to replace extracted samples.

17.5.5 Iron Microparticles and Nanoparticles

Millimetric zerovalent iron is an established reactive material used in permeable reactive barriers to treat aquifers contaminated from a plane source or one that is difficult to identify.

Fig. 17.34 Electron micrograph of zerovalent iron nanoparticles



In the late 1990s, Zhang and Wang [75] proposed to use, instead, micro- or nanoscale iron particles (NZVI). The small particle diameter (ranging from 10 to 100 nm for NZVI, see Fig. 17.34, and from 100 nm to 100 μm for microscale zerovalent iron, MZVI) makes it possible to inject the reactive material in the aquifer at significantly greater depths than those achievable with PRB excavation [59, 65]. During nanoremediation, a reactive zone (RZ) is formed which enables direct treatment of the source, rather than only of the plume, thus reducing remediation time.

Their small size causes particles to have a high specific surface area and, consequently, high reactivity [10, 53, 78]. Under the simplifying hypothesis that the contaminant is subjected to first order degradation kinetics in contact with zerovalent iron, the influence of the specific surface area can be expressed as follows:

$$\frac{dC_{TCE}}{dt} = -kC_{TCE} = -(k_{SA} \cdot ssa \cdot C_{Fe}) \cdot C_{TCE} \quad (17.26)$$

where k represents the first-order pseudokinetics constant (T^{-1}), ssa the specific surface area (L^2M^{-1}), C_{Fe} the concentration of iron per water volume (ML^{-3}), C_{TCE} the contaminant concentration (ML^{-3}), k_{SA} the degradation kinetics constant per unit specific surface area and unit zerovalent iron concentration (LT^{-1}). This expression highlights how the overall degradation kinetics increases linearly with the specific surface area, for equal normalized degradation kinetics, k_{SA} , and zerovalent iron concentration, C_{Fe} ; micro- and nano-scale iron are, therefore, more reactive than millimetric iron.

Due to their tendency to aggregate and sediment, the particles have to be stabilized by means of, for example, biopolymers [61]. These natural compounds confer a non-newtonian shear thinning rheological behavior to iron suspensions which allows for particle stabilization under static conditions, and minimizes injection pressure into the aquifer [16, 74].

The most suitable techniques for the injection of these fluids in the subsurface consist in the emplacement of multi-depth injection systems (e.g. PIM by Carsico), or of spot injection points by means of direct push systems. In most cases, direct

injection in traditional monitoring wells is not recommended unless the aquifer is characterized by high hydraulic conductivity.

Particle mobility during permeation injection can be predicted by means of colloidal transport numerical models [3, 62–64], also useful for the design of the intervention and the estimation of the radius of influence (ROI). Novel approaches have been developed in order to tune the mobility of the particles [4] in order to better control the geometry and position of the RZ.

17.5.6 A Case Study: The Permeable Reactive Barrier in Avigliana

In this section we describe the design and construction procedure of the first zero valent iron permeable reactive barrier installed in Italy, specifically in Avigliana (close to Torino) in October 2004.

The area of the intervention is located in a part of land close to the Dora Riparia river. In the past, the site was used for the disposal and storage of materials deriving from machining operations and foundries (Fig. 17.35).

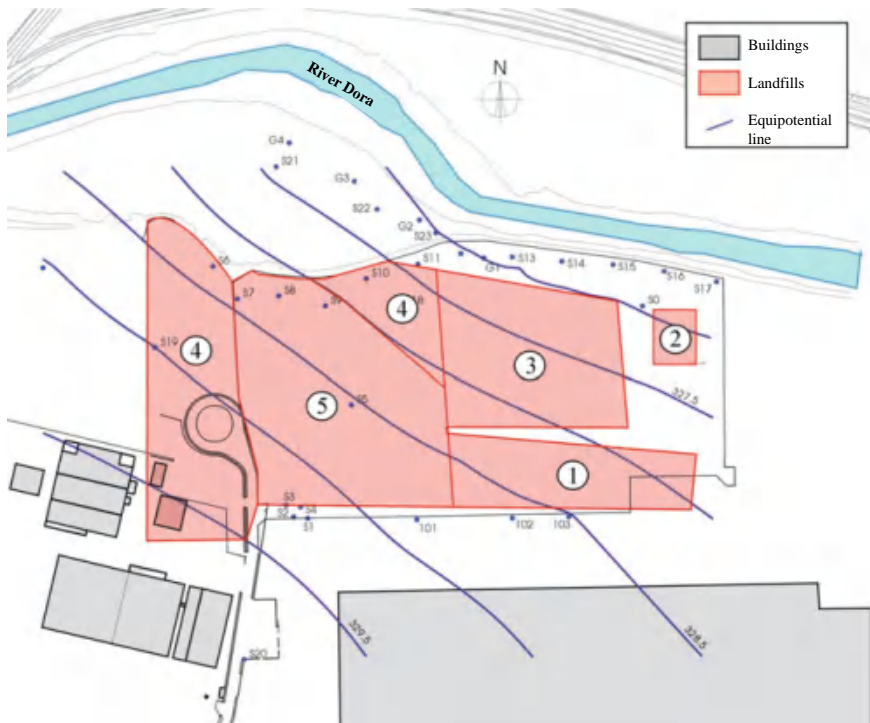


Fig. 17.35 Plane view of the site and average piezometric level of the surface aquifer

In the area of interest, the saturated thickness of the surface aquifer ranges from 9 to 11 m, and progressively decreases with increasing vicinity to the Dora Riparia river, which represents the aquifer's draining axis. The groundwater flow direction is SW-NE and the average hydraulic gradient is about 1.1%. Average hydraulic conductivity, derived from pumping tests, Lefranc tests and slug tests, is equal to $1.8 \cdot 10^{-4}$ m/s.

The contamination affecting the different environmental components was characterized with direct push tools, by sampling soil, soil gases, and groundwater from 73 points. In addition, groundwater samples were collected from the permanent monitoring network, composed of 28 monitoring wells, 4 of which are multilevel.

The analysis results revealed the presence of two groundwater contamination plumes, containing chlorinated solvents at concentrations exceeding the threshold limits imposed by the Italian law (D.M. 471/99) (Fig. 17.36). The contaminants present at the highest concentration were perchloroethylene, trichloroethylene, and their biodegradation products (area 1, TCE: 130 $\mu\text{g/l}$, cDCE: 130 $\mu\text{g/l}$; area 2, PCE: 56 $\mu\text{g/l}$, TCE: 36 $\mu\text{g/l}$).

The goals of the approved intervention were: (a) remediation (including the set up of safety measures) of the chlorinated solvent contamination in area 1, by means



Fig. 17.36 Delimitation of the areas contaminated by chlorinated solvents according to the Italian legislation (D.M. 471/99)

of a zero-valent iron PRB; (b) the permanent containment and implementation of safety measures in area 2, by sealing the surface via impermeable capping.

The remediation aim was to achieve a total carcinogenic chlorinated solvent concentration of $30 \mu\text{g/l}$ downgradient of the barrier; this threshold value was established via site-specific third tier risk assessment.

17.5.6.1 Barrier Design

Design of the barrier entailed defining its configuration, its location and orientation, and its geometry (height, length, thickness), verifying the capture zone, and calculating the amount of zero-valent iron necessary for contaminant treatment [19].

Among the configuration options, the continuous trench barrier was selected. This configuration ensures minimal interference with natural groundwater flow, and limits installation costs.

Based on geochemical characterization, on numerical flow simulations (Fig. 17.37), and on the intervention objectives, the length of the barrier was set to be 120 m, and the depth of the excavation about 14 m from the surface, to be adjusted in such a way that the barrier would penetrate the underlying silty-clay impermeable

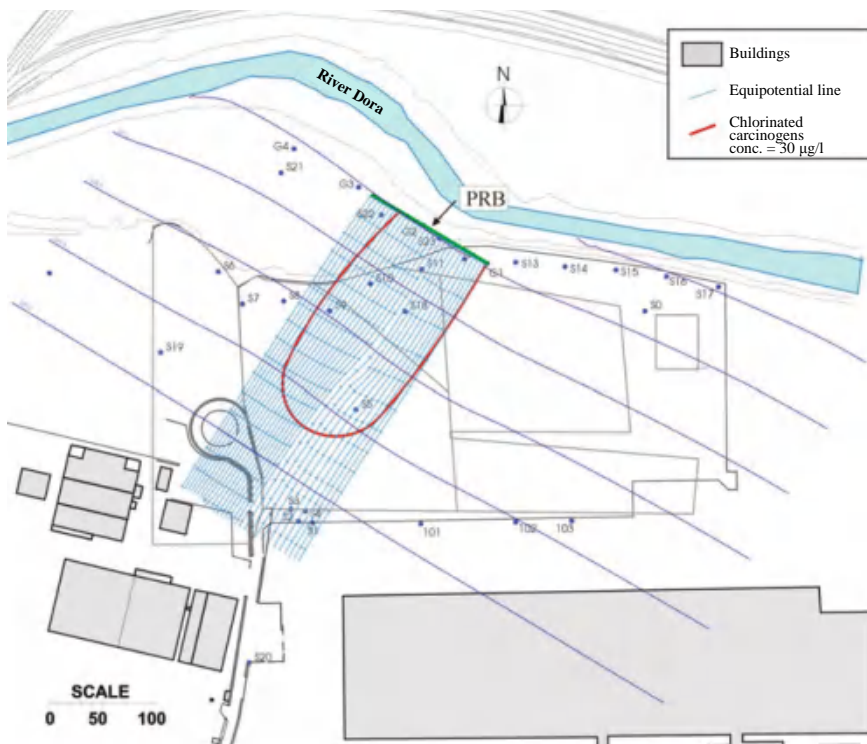


Fig. 17.37 Estimation of the capture zone of the barrier with a numerical flow model

layer by at least 60 cm. The reactive section of the barrier was therefore set to be 9.16–11.16 m high.

The location of the barrier was defined in order to be (Fig. 17.37):

- perpendicular to the flow lines, to minimize its length;
- as downgradient as possible, to ensure the interception of all contamination sources;
- in a position that would prevent the excavation from affecting the impermeability of close landfills.

The thickness of the barrier was calculated after carrying out a column degradation experiment. A 100 cm long plexiglass column with an inner diameter of 5 cm and four sampling ports was used. The column was packed with 5846 g of iron (Gotthart Maier Metallpulver), characterized by a grain size distribution in the range of 0.5–3 mm. The test was conducted after sampling groundwater from a monitoring well in the site close to the tentative position of the barrier. The collected water was further contaminated in the laboratory to achieve easily measurable concentrations, and was then injected in the column. The experiment lasted 60 days, until an almost steady state was reached.

Degradation kinetics and half-lives were calculated using nonlinear fitting of the experimental data (Table 17.8). Half-lives were corrected by applying a multiplication factor of 3, to keep into account temperature differences between the field (10.8 °C) and the laboratory (22 °C).

The thickness of the barrier was determined using a steady state first-order degradation kinetics model. The maximum average concentration between those measured in the two most contaminated monitoring wells was used as the input concentration for the barrier design.

With a residence time of 28 h a total concentration of carcinogenic chlorinated aliphatic compounds of 12.8 µg/l could be achieved, which is well below the target threshold value, 30 µg/l. This corresponds to a design assumption of an additional safety factor greater than two, that keeps into account the uncertainties about the values of hydraulic conductivity, effective porosity, concentration, etc.

The thickness of the zero-valent iron gate was calculated to be 0.5 m on the basis of the characteristics of the iron and of the hydrogeology, derived from in situ tests. Since the minimum thickness of the excavation equipment is 0.6 m, the difference had to be compensated by amending the iron with 17% in volume of sand.

Table 17.8 Half-lives before and after temperature correction

	$t_{1/2}$ No correction h	$t_{1/2}$ Correction (x3) h
TCE	0.74	2.2
cDCE	8.4	25.2
1, 1-DCE	1.5	4.5
1, 2-DCP	20.5	61.5
VC	8.2	24.6

17.5.6.2 Construction of the Barrier

The continuous trench PRB was created using a hydraulic clamshell-bucket excavator (Fig. 17.38) and a biopolymer slurry to ensure wall stability until filling with zero-valent iron [20].

The reactive barrier is 120.3 m long, and is divided in 17 panels, each 7 m long on average, 11.9–13.8 m deep, and 60 cm thick. The barrier was built in panels to avoid excessive excavation times, potentially compromising the stability of the slurry. The operational stages entailed (Fig. 17.39):

- the excavation of a trench with the same length as a panel;
- the emplacement of a steel temporary separation tubing, acting as a plug to prevent intercommunication between neighboring panels;



Fig. 17.38 Hydraulic clamshell-bucket crane used to excavate the barrier trench

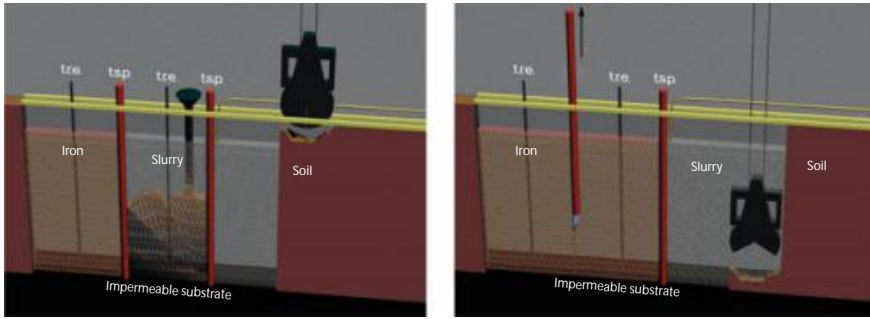


Fig. 17.39 Zero-valent iron PRB panel construction procedure; t.r.e.: PVC pipes for enzyme recirculation; t.s.p.: steel temporary separation tubings

- the installation of a micro-fissured PVC pipe to recirculate enzymes;
- slurry displacement within the trench by means of the reactive iron-sand mixture;
- biopolymer slurry disruption through the injection of enzymes;
- filling of the upper portion of the barrier with sand and capping of the trench with three layers of compacted clay, each 20 cm thick.

The German company Gotthart Maier Metallpulver GmbH supplied 1700 t of zero-valent iron used as a reactive material.

17.5.6.3 Economic Assessment and Monitoring

Installing the barrier cost approximately 1 400 800 euro, which comprise the following.

- Data acquisition costs for design: characterization of land topography, and of the site lithostratigraphy and hydrogeology; determination of degradation kinetics with column experiments; numerical investigation of flow.
- Costs of the actual construction of the barrier: zero-valent iron, biodegradable polymer and enzyme supply; trench excavation; work-site preparation; slurry production; royalties for the EnvironMetal Process (E. T. I.) patent.
- Monitoring costs after barrier installment: equipment for the additional monitoring wells; sample analysis to verify the achievement of remediation and safety goals.

The unitary treatment cost, estimated to be 0.62 Euro per cubic meter of treated water (under the hypothesis of 30 years of operation), is smaller than the unitary values associated to alternative technologies for treating the site.

Monitoring confirmed the successful operation of the barrier and a degradation capability greater than that estimated in the laboratory [79].

17.6 In Situ Flushing

This technique consists in flushing an aqueous solution through a contaminated soil or aquifer. The flushing solution can be introduced through vertical or horizontal injection wells, trenches, infiltration galleries, or aboveground spray irrigation, and infiltrates the contaminated porous medium under the effect of a hydraulic gradient. The contaminant-carrying flushing solution (i.e., the *elutriate*) is then recovered downgradient through extraction wells or trenches, and treated at the surface. Treated elutriate can be disposed of by discharging it in superficial waters or in the sewers, or it can be recirculated in the flushing system (Fig. 17.40).

The flushing solution can be plain water, sometimes amended with surfactants, acids, bases, reductants, chelating or complexing agents, or cosolvents to enhance the mobility or solubility of the contaminants. Despite still being widely used as a flushing fluid, water is only effective in dissolving a limited number of contaminants, such as hexavalent chromium, chlorides, and sulfates, and flushing times are often too long. Deployment of hydrochloric, sulfuric, and nitric acid is, instead, more successful in the mobilization of metals, because of re-dissolution of precipitates and limitation of sorption. Using organic acids can be advantageous due to their biodegradability. It is also possible to use solutions of chelating ligands for metal removal (e.g., citric acid, gluconate, glycine, EDTA) [41, 55, 70].

However, most commonly, water amended with surfactants or cosolvents (or a mix of the two) is used, which is effective in treating organic contaminants, in particular hydrophobic ones.

Surfactant molecules are composed of a hydrophilic head and a hydrophobic tail, the latter normally being a long hydrocarbon chain (Fig. 17.41). In virtue of their specific characteristics, surfactants arrange at the water-NAPL interface reducing

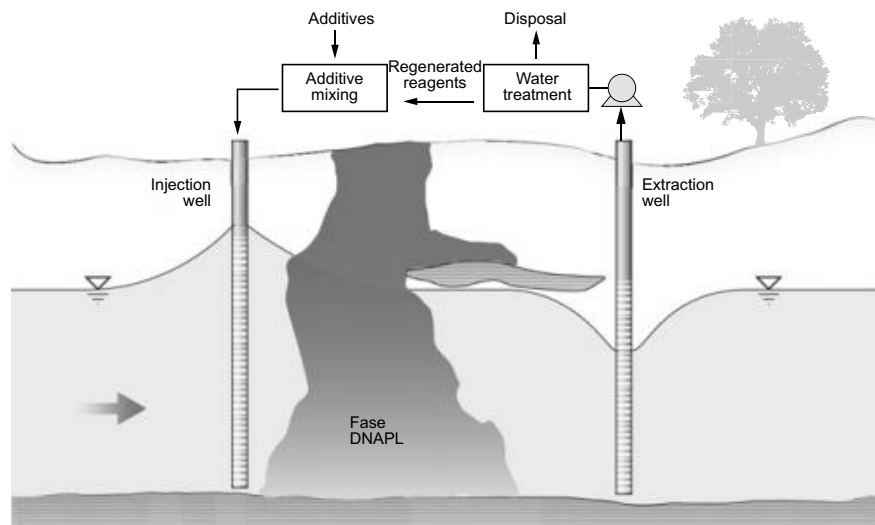


Fig. 17.40 In situ flushing with injection and extraction wells

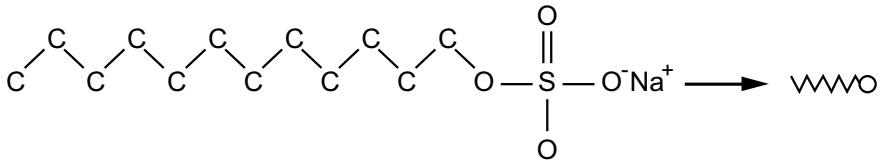


Fig. 17.41 Surfactant monomer

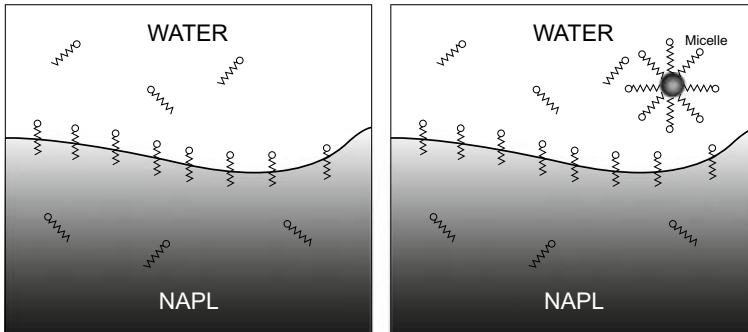


Fig. 17.42 Micelle formation upon achievement of the critical micellar concentration

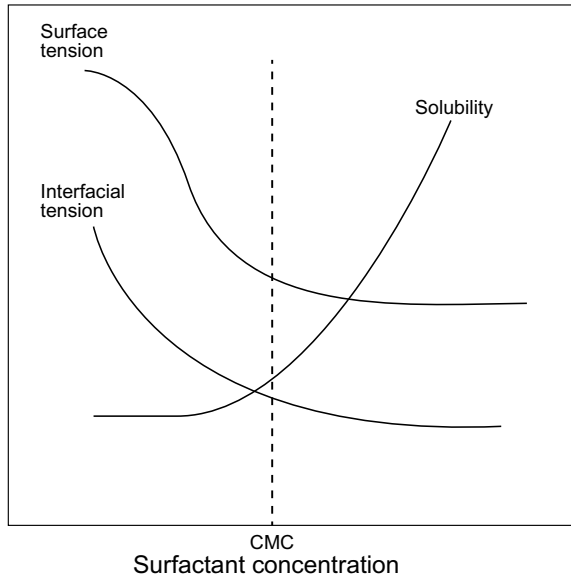
surface tensions, thus increasing NAPL solubility in water. Furthermore, as surfactant concentration increases and overcomes the *critical micelle concentration (CMC)*, *micelles* of NAPL encircled by a single layer of surfactant molecules and surrounded by water begin to form. The formation of these stable droplets enhances contaminant mobility and prevents its adhesion to the soil (Fig. 17.42). Figure 17.43 shows how the solubility of the organic compound in the aqueous phase, and consequently the removal of contaminant present at the residual saturation, increases significantly for surfactant concentration values higher than the CMC. The solubility value includes molecules present in the water as well as those trapped in the micelles.

There are *non-ionic*, *anionic*, and *cationic* surfactants. The latter are rarely used because they tend to sorb to negatively charged soil surfaces, while non-ionic and anionic surfactants are preferred also because they are generally less toxic than cationic surfactants [70]. Another important feature of surfactants is their *hydrophile-lipophile balance (HLB)*, used to describe their affinity towards the aqueous or the organic phase. Surfactants with a small HLB value should be excluded because they tend to lead to the formation of reverse micelles (i.e., water droplets surrounded by NAPL).

Based on the above information, it is clear that the surfactant should be chosen and dosed carefully, according to the type of contaminant and the physico-chemical characteristics of the contaminated medium (e.g., temperature, salinity), in order to optimize the flushing intervention.

Also alcohols can be used for in situ flushing. Alcohols are miscible both in water and in NAPLs, capable of increasing the solubility of the organic phase in water and of decreasing the water-NAPL surface tension. They can be used:

Fig. 17.43 Qualitative evolution of a few parameters as a function of surfactant concentration



- at low concentrations (1–5%): in this case, the alcohol increases the NAPL solubility of many organic contaminants due to the so-called *cosolvent effect*. Large amounts of flushing solution have to be delivered to the contaminated area for the achievement of significant results. The presence of alcohol in water also decreases contaminant sorption to the aquifer solid matrix;
- at high concentrations: the alcohol partitions between the aqueous phase and the NAPL, affecting the viscosity, density, solubility, and interfacial tension of the NAPL. If the dose is sufficient, the interfacial tension can be reduced to zero. In this way, a single fluid phase is created, characterized by a density that depends on the relative proportions of water, alcohol, and NAPL.

In addition to the selection of the most appropriate flushing solution, in situ flushing effectiveness depends on a number of factors, relating to both the contaminant and the site (see Table 17.9). In general, this technology tends to be more successful in homogeneous and highly permeable soils that do not exhibit strong alkalinity or acidity. One of its main advantages is that extracted fluids can be re-used and that, other than the installation of the extraction system, it is quite simple to implement and does not involve excavation. Furthermore in situ flushing is not limited by the depth of the contamination.

The greatest limitation of in situ flushing is that it might cause an uncontrolled mobilization of the contaminants. For this reason, flushing interventions are often implemented after installing a containment wall downgradient, although even in this case it is difficult to prevent the vertical expansion of the contaminated region. Furthermore, great care has to be taken in the preventive assessment of potential

Table 17.9 In situ flushing screening table [55]

Site-related critical factors	Success likelihood		
	Low	Moderate	High
Main contaminant phase	Vapor	Liquid	Dissolved
Hydraulic conductivity (m/s)	$<10^{-7}$	10^{-7} – 10^{-5}	$>10^{-5}$
Soil specific surface area (m ² /kg)	>1	0.1–1.0	<0.1
TOC (%)	>10	1–10	<1
pH	Can interact with the additives and should be considered when choosing the materials		
Cationic exchange capacity (CEC)	High	Moderate	Low
Clay content	Can influence the mobility of some contaminants and the circulation of the flushing solution		
Fractures in the geological formation	Present	–	Absent
Contaminant-related critical factors	Success likelihood		
	Low	Moderate	High
Solubility in water (mg/l)	<100	100–1000	>1000
Sorption to the soil (mg/kg)	>10000	100–10000	<100
Vapor pressure (mmHg)	>100	10–100	<10
Viscosity (cPoise)	>20	2–20	<2
Density (g/cm ³)	<1	1–2	>2
K_{ow}	–	–	10–1000

reactions between different contaminants and extraction agents, in order to avoid the formation of toxic vapors or of products that are more toxic than those originally present [41, 55].

17.7 In Situ Oxidation

In situ oxidation consists in the injection of strong oxidants in the unsaturated medium or directly into the aquifer to target the source of contamination directly. It is a relatively quick and inexpensive technology, whose effectiveness depends on the characteristics and concentrations of the contaminants. A few limitations derive, however, from the uncertainty related to some of the intermediate degradation reactions and to the final products, whose toxicity has to be assessed.

Successful in situ oxidation relies on the appropriate choice of the oxidant and of the delivery mechanism, depending on the contaminant type and the subsurface conditions. It is worth mentioning a few contaminants that can be chemically oxidized: BTEX (benzene, toluene, ethylbenzene, xylene); a few chlorinated solvents, such as PCE (tetrachloroethylene), TCE (trichloroethylene), VC (vinyl chloride); polycyclic aromatic hydrocarbons; and other organic molecules [66, 70, 76].

Table 17.10 Redox potentials of the main oxidizers

Oxidant	Redox potential (V)
Hydroxyl radical	2.80
Sulfate radical	2.60
Ozone	2.07
Persulfate ion	2.01
Hydrogen peroxide	1.70
Permanganate ion	1.68

The oxidizing agents most frequently used and commercially available are:

- potassium or sodium permanganate (KMnO_4 or NaMnO_4 , respectively);
- Fenton's reagent ($\text{H}_2\text{O}_2 + \text{Fe(II)}$);
- ozone (O_3);
- persulfate ($\text{S}_2\text{O}_8^{2-}$).

The redox potentials of the active species formed in the aquifer and the treatable contaminants are listed in Tables 17.10 and 17.11, respectively.

Potassium permanganate is capable of oxidizing contaminants directly, without the addition of catalysts, and is effective within a broad pH range, as well as being extremely stable. The oxidation generally leads to the formation of carbon dioxide and manganese oxide.

The manganese introduced in the form of permanganate can precipitate or form manganese dioxide, a natural soil mineral. Excessive manganese precipitation can, however, lead to a reduction in the permeability of the medium, which can limit the distribution of the oxidant over time. Compared to other commonly used oxidants, permanganate's redox potential is not very high and can, therefore, require a long time for contaminant removal.

Potassium permanganate is usually available in 3–4% aqueous solutions, while sodium permanganate is available in 40% aqueous solutions. Typical injection concentrations are around 25% and depend on the temperature and on the ionic composition in water. The dose is determined through laboratory and in situ pilot tests, and as a function of the hydrogeological features of the site.

Fenton's reaction, instead, is obtained by combining hydrogen peroxide and ferrous iron. The presence of iron catalyzes the formation of hydroxyl radicals that have an oxidation potential significantly higher than hydrogen peroxide. The hydroxyl radical is an oxidizing agent capable of non-selectively degrading contaminant molecules, and is second only to fluorine in terms of oxidizing capability. The effectiveness of this compound is also tied to the formation of a few reducing compounds that contribute to contaminant degradation.

Commercially available Fenton solutions are H_2O_2 solutions in water (5–35%). The initial amount of H_2O_2 and iron ions is based on the level of contamination and the volume of soil and groundwater to be treated; importantly, the stoichiometric ratio between H_2O_2 and Fe^{2+} is calculated during laboratory investigations.

Table 17.11 Contaminants treatable with various oxidants (acronyms: BTEX: benzene, toluene, ethylbenzene, xylene; CF: chloroform; CM: chloromethane; CT: carbon tetrachloride; DCE: dichloroethene; MTBE: methyl tert-butyl ether; PAHs: polycyclic aromatic hydrocarbons; PCBs: polychlorinated biphenyls; PCE: tetrachloroethene; TCA: trichloroethane; TCE: trichloroethene; VC: vinyl chloride)

Oxidant	Degradable contaminants	Persistent contaminants	Recalcitrant contaminants
Fenton	TCA, PCE, TCE, DCE, VC, BTEX, chlorobenzene, phenols, MTBE, explosives	DCA, CM, PAHs, CT, PCBs	CF, pesticides
Ozone	PCE, TCE, DCE, VC, BTEX, chlorobenzene, phenols, MTBE, explosives	DCA, MC, PAHs	TCA, CT, CF, PCBs, pesticides
Permanganate	PCE, TCE, DCE, VC, BTEX, PAHs, phenols, explosives	Pesticides	Benzene, TCA, CT, CF, PCBs
Activated persulfate	PCE, TCE, DCE, VC, BTEX, chlorobenzene, phenols, MTBE	PAHs, explosives, pesticides	PCBs

Sometimes it is necessary to inject a greater amount of oxidizing solution due to heterogeneities that limit the contact with the contaminant, and to a delayed decomposition of H_2O_2 to hydroxyl radicals, which could reduce the reagent-contaminant contact time.

Fenton solutions are relatively cheap and very aggressive, but only function at low pH values (2–4). To overcome this limitation, some of the commercial products use a chelating agent to maintain the iron in solution also at circumneutral pH values [70, 76].

Early applications of in situ chemical oxidation through Fenton's reaction employed high concentrations of hydrogen peroxide in water (35–50%), to generate heat and volatilize residual contaminant concentrations. The drawback of this approach is that at such concentrations the reaction can become uncontrolled, and temperatures can rise excessively, potentially leading to explosions. It is, therefore, preferable to use relatively low concentrations (8–10%), that cause limited temperature increases [70].

Ozone is characterized by high oxidation capability and can, therefore, be conveniently used in situ chemical oxidation. It is injected through vertical or horizontal wells and causes direct contaminant oxidation. It is currently used to degrade contaminants such as PAHs, BTEX compounds, VOCs and can oxidize chemicals such as phenols to less toxic forms. Since it is an unstable molecule, it is particularly indicated for the treatment of contaminants whose aerobic degradation is favored by the increase of oxygen, such as petroleum-derived hydrocarbons. Ozone gas is generated on site through an electrical process, using oxygen or air as a substrate, which yield, respectively, ozone concentrations of about 5% or 1%. Since the ozone generator has to be built on site, ozone oxidation costs are quite high.

Persulfate is the most recently tested oxidant. Its oxidation potential is greater than hydrogen peroxide, but it reacts very slowly unless a catalyst, such as ferrous iron or heat, are used. Above 40 °C persulfate releases sulfate free radicals and becomes very reactive. Under these conditions it is able to degrade many organic contaminants [66, 70].

The concentration and amount of oxidizing solution that have to be injected essentially depend on the mass of contaminant, on the hydrogeological characteristics of the site, and on the specific type of reagent employed. One should keep in mind that the injection of an excessive amount of reagent could spread the contamination inside the aquifer.

The oxidizing solution is usually injected in various spots, through wells specifically constructed with traditional technologies (like monitoring wells) or through small diameter wells installed using the Geoprobe technology. The injection points should provide adequate coverage of the contaminated area, to ensure optimal contact between reagent and contaminant in the whole remediation area. For the oxidation mechanism to be effective, it is crucial for the oxidizing agent to enter in contact with the contaminant. Detailed knowledge of the subsurface and in particular of the degree of heterogeneity of the aquifer system is, therefore, essential [70, 76].

17.8 In Situ Bioremediation

In situ bioremediation (ISB) technologies are based on the natural biodegradation of contaminants in the subsurface. Biodegradation is the microbe-mediated biochemical transformation of contaminants, which leads to the destruction of organic compounds, typically resulting in the accumulation of harmless products (e.g., carbon dioxide, water, chlorine, methane), or to the conversion of inorganics to less toxic or mobile forms (e.g., reduction of chromium (VI) to chromium (III)) [41, 71].

The objective of bioremediation interventions is to control and stimulate microbial activity to create optimal environmental conditions for biodegradation processes, although in certain instances stimulation isn't necessary and biodegradation can occur naturally (i.e., *natural attenuation* or *intrinsic remediation*) [41, 54]. Preliminary investigations are necessary to understand the microbial processes responsible for contaminant degradation and to determine the physical, chemical and hydrological conditions present in the site of interest. Bioremediation can then be promoted by delivering substrates into the ground that favor microbial activity (i.e., *biostimulation*) or by introducing microorganisms that are capable of driving the desired reaction (i.e., *bioaugmentation*). Following stimulation, the contaminated site must be tightly monitored, to make sure remediation is ensuing as predicted [17, 23].

Subsurface environments host a variety of prokaryotic as well as eukaryotic microorganisms capable of transforming contaminants; these include mainly fungi, archaea and bacteria. In this text we will only refer to the reactions mediated by bacteria and archaea, due to their predominance.

Although individual species are sometimes capable of fully degrading certain contaminants, biodegradation is usually carried out by microbial communities, with single species specializing in few basic steps which, combined, can lead to the full mineralization of organic substrates. Mutual microbial interaction results from the adaptation of the species to the chemical and physical conditions of the environment they occupy. For this reason, biodegradation mediated by indigenous species

is significantly more successful than that obtained with bioaugmentation, as foreign species may not adapt well to the environmental conditions of the contaminated site.

Microbial diversity and the fact that consortia, rather than individual species, contribute to biodegradation make it a very versatile process, which can involve diverse reactions (e.g., hydrolysis, oxidation, reduction, dehalogenation, decarboxylation) and which is applicable to a broad range of contaminants, including VOCs and semi-VOCs, fuels, pesticides, herbicides, and PAHs [17, 41].

ISB is, therefore, a very promising technique whose main advantages are:

- permanent elimination of organic contaminants: biological processes can degrade most organic compounds, preventing the use of interventions that only result in the transfer of these substances between different environmental components;
- possibility of direct on site installation of systems necessary for the process;
- cost effectiveness relative to other technologies;
- lack of risks or costs related to the transport of contaminated material;
- minimal site disturbance;
- potential for integration with other remedial technologies;
- positive impact on public opinion.

There are, however, also a few limitations associated to bioremediation [17, 41]:

- not all contaminants are susceptible to biodegradation;
- detailed and long-term monitoring necessary;
- potential formation of toxic byproducts;
- potential formation of unknown products;
- requires multidisciplinary skills;
- strongly dependent on site specificities (i.e., an approach that works on one site might not work on another).

17.8.1 Factors Contributing to Biodegradation

Bioremediation relies on the ability of microorganisms to degrade contaminants, and its effectiveness depends on a number of factors, including compound biodegradability, microbial metabolism, site hydrology, and environmental conditions [7]. Essentially, for biodegradation to take place, it is necessary for microorganisms expressing the enzymes that catalyze the transformation of the contaminant of interest to be present in the indigenous microbial community, and for these microorganisms to have the necessary resources to grow and drive the reaction.

17.8.1.1 Microbial Growth

Microbial growth depends on several factors, illustrated in the paragraphs that follow [71].

Table 17.12 Microbial classification

Microbial classification	Energy source	Carbon source (substrate)
Autotrophs		
Photoautotrophs	Light	CO ₂
Chemolithotrophs	Oxidation-reduction reactions of inorganic compounds	CO ₂
Heterotrophs	Oxidation-reduction reactions of organic compounds	Organic carbon

Carbon and energy source. Microorganisms can be categorized according to the type of metabolism they strive on, with increasing levels of detail. The most general classification divides microbes in those that carry out respiration and those that live on fermentation. Regardless of whether they respire or ferment, in order to duplicate, microorganisms require a source of carbon, for biomass synthesis, and a source of energy, to support all the reactions involved in growth and survival (see Table 17.12). The carbon source can be organic, supporting a *heterotrophic* metabolism, or inorganic (i.e., CO₂), which supports *autotrophic* growth. Microbes are extremely versatile in terms of carbon source, a few typical compounds that they can use being organic acids (e.g., pyruvate, lactate) and simple sugars (e.g., glucose, saccharose, lactose).

Energy, instead, is harnessed from a sequence of redox reactions during which electrons are transferred from an electron donor (which coincides with the carbon source in heterotrophic growth) to a terminal electron acceptor (TEA) via a series of intermediary electron acceptors. In respiration, electron donor and acceptor are distinct, while in fermentation they coincide, which causes this kind of metabolism to have a significantly lower energy yield.

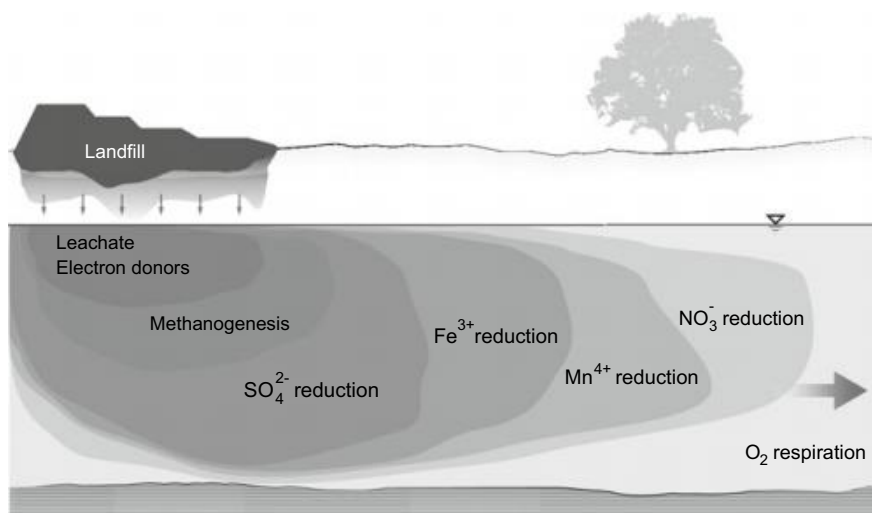
Terminal electron acceptor. There are a variety of electron acceptors that can be used in microbial metabolisms. The ability to use a certain TEA is often used as a way of classifying microorganisms. Different TEAs provide different energy yields and determine the type of metabolism, and consequently the degradation reactions that a certain species can carry out (see Table 17.13). The main electron acceptors are: O₂, NO₃⁻, Mn⁴⁺, Fe³⁺, SO₄²⁻, CO₂, and organic compounds.

Higher energy yielding electron acceptors present in the environment are consumed earlier. This determines the formation of a succession of so-called *redox zones*.

These have been widely documented in contaminated aquifers, where the pollutant is used as the electron donor for microbial growth [2, 9, 11, 44]. Figure 17.44 illustrates the typical redox zonation that follows leachate release from a landfill. Close to the source of contamination high energy yield electron acceptors have been consumed and methanogenesis prevails (via CO₂ reduction: this is a very specialized process that yields little energy and can only be carried out by some archaeal species); a sequence of progressively more thermodynamically favorable redox zones

Table 17.13 Types of microbial metabolisms and respective electron acceptors

Metabolism type	Electron acceptor	Energy yield
Aerobic respiration	O_2	High
Anaerobic respiration		↑
Nitrate reduction	NO_3^-	
Manganese reduction	Mn^{4+}	
Iron reduction	Fe^{3+}	
Sulfate reduction	SO_4^{2-}	
Methanogenesis (carbon dioxide reduction)	CO_2	
Fermentation	Organic compounds	Low

**Fig. 17.44** Redox zonation in an aquifer following leachate seepage from a landfill

(i.e., sulfate, iron, manganese, and nitrate) ensue as distance from the source increases up to the natural oxic conditions. Figure 17.45 depicts the results of a 1D simulation (performed using RT3D transport code, [13]) of the redox zonation of an aquifer contaminated with organic compounds.

Nutrients. Carbon, oxygen, nitrogen, hydrogen and phosphorous are the main cell structure building blocks; however, microorganisms also require a set of micronutrients (e.g., S, K, Ca, Fe, Cu, Co) for biosynthesis and survival. When one of these elements is limiting, microbial growth slackens.

When planning a bioremediation intervention, the availability of C, N, and P has to be considered, while the other elements are normally present in adequate concentrations in most soils and aquifers.

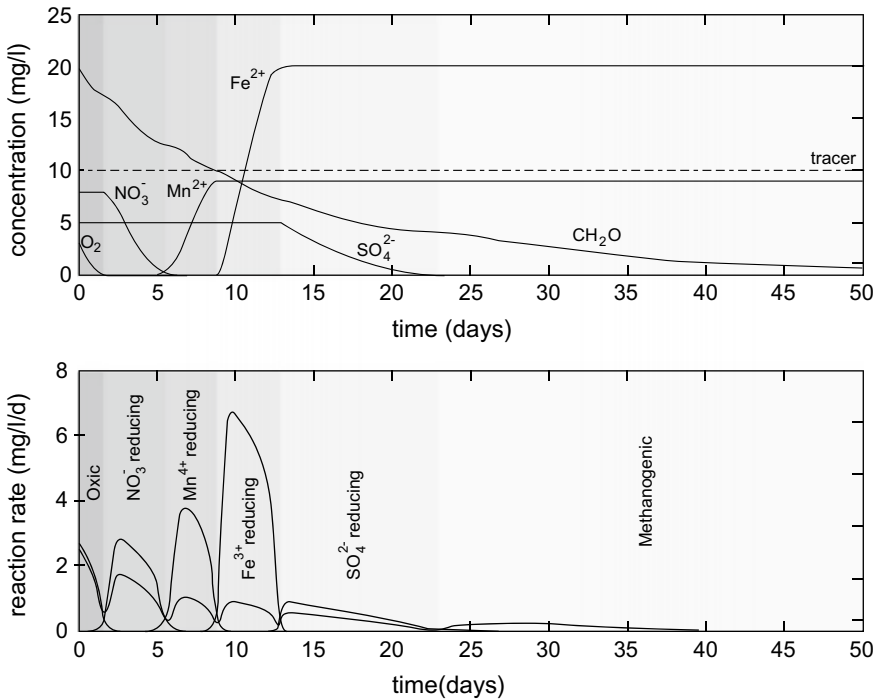


Fig. 17.45 1D simulation of the redox zonation of an aquifer contaminated with organic compounds (modified from [21])

Environmental conditions. For microorganisms to grow, the environmental conditions have to be favorable to their metabolic activity. Therefore, for a bioremediation project to be successful, the environmental conditions have to be checked, in particular moisture, temperature, pH, salinity, and redox potential. In addition to the fundamental role of water in cells, moisture is the most important parameter because it affects contaminant availability, transfer of gas phases, and the level of toxicity of the contaminants. Temperature influences the rate of degradation and should, therefore, be kept into account when implementing a bioremediation approach. pH influences the cellular activities of the microorganisms and the equilibria of the redox reactions they catalyze. The optimal pH for most bacteria is circumneutral. However, while some microorganisms are very sensitive to pH changes, others can survive in a broad pH range (e.g., from pH 4 to pH 10); furthermore, some species preferentially, or necessarily, grow at extreme pH values (i.e., obligate acidophiles typically require the pH to be below 2, whereas obligate alkaliphiles grow optimally at pH 10 or 11). Similarly, while most microbial species grow optimally at fresh water salinity levels, some are tolerant to or require high salt concentrations (brackish [77] or saline water, which could be present in groundwaters affected by marine intrusion),

i.e., halotolerant or halophilic species, respectively. Finally, the soil redox potential dictates which biochemical reactions are thermodynamically favorable and, hence, can occur in that specific environment.

17.8.1.2 Contaminants

Not all organic compounds are readily biodegradable, so bioremediation is not always a viable approach. It is therefore crucial to conduct a preliminary assessment of the properties of the contaminants. Some compounds are recalcitrant to biologic degradation, and others, persistent substances, are degraded so slowly that a bioremediation approach would be inefficient and unfeasible. Biodegradability is strongly influenced by the molecular structure of the compound and, in general, natural substances (e.g., fuels) tend to be more readily degradable than synthetic chemicals (e.g., chlorinated solvents, chlorofluorocarbons) [17]. In particular, recalcitrant or persistent compounds are often characterized by one or more of the following properties:

- presence of halogens in their molecular structure;
- highly branched molecular structure;
- scarce water solubility;
- complex and/or highly symmetrical molecular structure.

In addition to their structural properties, the concentration of organic contaminants is also important. A biodegradable compound may be toxic beyond a certain concentration and inhibit microbial activity, thus becoming persistent.

Those compounds, instead, that can undergo microbe-mediated degradation can be transformed via a four general mechanisms [71]:

- *Aerobic oxidation*: the contaminant is the carbon and energy source in aerobic respiration, and the electron acceptor is, therefore, O_2 . This process is most effective for non-halogenated light hydrocarbons (e.g., BTEX, diesel)
- *Anaerobic oxidative degradation*: as in the previous process, the contaminant is degraded via oxidation in a respiratory metabolism. However, the reaction occurs in anoxic environments and the electron acceptor isn't, therefore, O_2 : typical alternative TEAs are sulfate, nitrate, and iron.
- *Anaerobic reductive degradation*: the contaminant is the electron acceptor in an anaerobic respiratory metabolism, and its reduction leads to its detoxification. Reductive dechlorination (during which chlorine atoms in chlorinated compounds are replaced by hydrogen atoms) is an example of this mechanism. Also inorganic contaminants, such as heavy metals and radionuclides, can be transformed via this process (e.g., reduction of Cr(VI) to Cr(III), or U(VI) to U(IV)).
- *Fermentation*: the contaminant is both the donor and acceptor of electrons during degradation. The products of this processes (e.g., hydrogen gas, acetate, formate) can be used as substrates for growth by other microbial species.

- *Cometabolism*: the contaminant does not contribute in any way to microbial growth, and is transformed fortuitously via metabolic reactions originally meant to operate on different substrates.

17.8.2 Biodegradation of Organic Contaminants

As already widely discussed, aquifer contamination with organic contaminants is an extremely widespread environmental issue. Halogenated aliphatic hydrocarbons and petroleum products (in particular their most soluble fraction, i.e., BTEX) are among the most commonly encountered compounds in groundwater. Under suitable environmental conditions, both halogenated aliphatic hydrocarbons and BTEX are susceptible to biodegradation reactions, which may belong to a variety of metabolic pathways (i.e., aerobic or anaerobic respiration, fermentation, cometabolism).

17.8.3 Biodegradation of Petroleum Products

Some microorganisms are capable of degrading petroleum products and, in particular, their most soluble fraction, composed of BTEX chemicals, which are ubiquitous in the soil and in aquifers. These microbial species are capable of using hydrocarbon molecules as a source of carbon and energy: the organic compound is oxidized while an electron acceptor is simultaneously reduced.

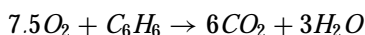
In the presence of oxygen BTEX chemicals undergo aerobic biodegradation, with oxygen being the electron acceptor.

Under anaerobic conditions, degradation of BTEX compounds can follow various anaerobic oxidation pathways, in which the electron acceptor can be, for instance, nitrate, ferric iron, or sulfate.

The degradation reactions of benzene, a common petroleum product, in the presence of different electron acceptors are illustrated below.

Aerobic Conditions

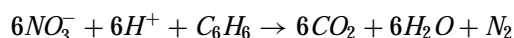
Aerobic Respiration



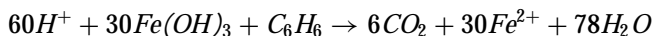
0.32 mg/l of degraded benzene per mg/l of O₂ consumed.

Anaerobic Conditions

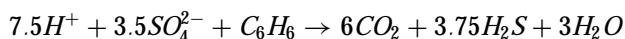
Denitrification



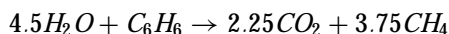
0.21 mg/l of degraded benzene per mg/l of NO₃⁻ consumed.

Iron (III) Reduction

0.045 mg/l of degraded benzene per mg/l of Fe^{2+} produced.

Sulfate Reduction

0.22 mg/l of degraded benzene per mg/l of sulfate consumed.

Degradation in Methanogenic Environments

1.3 mg/l of degraded benzene per mg/l of methane produced. It should be noted that microbes do not convert benzene to methane directly; however, anaerobic benzene degradation may yield the substrates for microbially-mediated methane synthesis.

For the degradation of organic contaminants, microorganisms sequentially use different electron acceptors according to their energy yield.

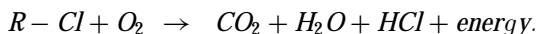
17.8.4 Biodegradation of Chlorinated Organic Compounds

Chlorinated aliphatic hydrocarbons (CAHs) and some halogenated aromatic compounds can be biodegraded via direct or cometabolic aerobic or anaerobic oxidation, or via anaerobic reductive dechlorination (RD). In general, more chlorinated compounds (e.g., PCE or TCE) are more oxidized so reductive treatments are more effective, while oxidative and reductive degradation of less chlorinated compounds (e.g., DCE or VC) can be equally successful [71].

17.8.4.1 Direct Aerobic Oxidation

In oxic environments, some CAHs can be oxidized directly by microorganisms that use such compounds as electron donors and as substrates for growth. Bacteria gain nourishment and energy for cell growth and maintenance from contaminant degradation. The electrons donated from the CAH via oxidation reactions are transferred to oxygen, the electron acceptor, which is thus reduced to water.

The reaction can be summarized as:



Direct aerobic oxidation only works for CAHs containing up to a maximum of two chlorine atoms; therefore, compounds that can be targeted with this method are: DCE, DCA, VC, CA, MC and CM. Direct aerobic oxidation is a fast process that leads to contaminant mineralization (i.e., the conversion of an organic compound to inorganic components).

There are many bacterial species capable of carrying out aerobic oxidation (e.g., *Pseudomonas spp.*, *Rhodomonas spp.*). Since they are considered ubiquitous, it isn't necessary to resort to bioaugmentation for a bioremediation intervention based on direct aerobic oxidation. However, microbial activity can be stimulated by adding oxygen. Oxygen solubility in water is limited: the concentration of dissolved oxygen in water in equilibrium with atmospheric air is about 10 mg/l. Therefore, only low contaminant concentrations can be treated and usually oxygen is the limiting factor for in situ treatment of contaminated aquifers in aerobic conditions. Thus, it can be amended by exploiting the transportability of oxygen in groundwater. Oxygen can be delivered dissolved in water, via sparging or by deploying oxygen releasing compounds (ORC, such as calcium or magnesium peroxide, hydrogen peroxide, or ozone) [17, 71].

17.8.4.2 Cometabolic Aerobic Oxidation

In some cases, certain organic compounds that cannot be used as sources of carbon or energy can, nevertheless, be transformed by microorganisms via so-called cometabolic processes.

Contaminants degraded through aerobic cometabolic processes are oxidized fortuitously by bacteria that grow aerobically on other substrates. Cometabolic reactions are catalyzed by non-specific enzymes capable of acting on multiple substrates (oxygenase enzymes, such as methane, toluene or ammonia monooxygenase) [30].

In the case of chlorinated solvent contamination, there are bacterial communities capable of cometabolically oxidizing CAHs using methane, propane, ethene, propene, toluene, phenol, cresol, ammonia, isoprene and isopropylbenzene, as substrates for growth. The metabolic pathways of these compounds involve the synthesis of several enzymes capable of fortuitously attacking contaminant molecules.

Chlorinated solvents that can be degraded via aerobic cometabolism are: TCE, DCE, VC, TCA, DCA, CF, and MC. Aerobic degradation of DCE and VC was found to be particularly effective [33]; these compounds are often found in sites contaminated with CAHs as byproducts of anaerobic reduction of PCE and TCE (see Sect. 17.8.4.3).

However, not all CAHs can be degraded cometabolically in the presence of oxygen: PCE and CT, for example, are persistent in such conditions.

Other CAHs have been identified to be recalcitrant to aerobic cometabolic degradation, such as chlorinated solvents characterized by an asymmetrical distribution of chlorine atoms in their molecular structure. An example of such compounds is 1, 1-DCE, originating from the abiotic dehydrohalogenation of 1, 1, 1-TCA, a common CAHs contaminant [22, 30, 71].

17.8.4.3 Anaerobic Reductive Dechlorination

Many aliphatic and aromatic halogenated compounds (including PCE, halogenated dioxines, PCBs) can be transformed and mineralized in situ by indigenous microbial communities under anaerobic conditions. The main transformation mechanism of chlorinated organics in anaerobic environments is reductive dehalogenation (or dechlorination, RD). It consists in the elimination of chlorine atoms from the molecule, and can occur via two pathways: α - and β -elimination. α -elimination (or hydrogenolysis, see Fig. 17.24), the most common pathway, consists in the sequential replacement of a chlorine in the halogenated molecule with a hydrogen, with a net gain of two electrons and a proton. β -elimination, instead, consists in the simultaneous removal of two adjacent chlorine atoms, through the acquisition of two electrons and the formation of a double bond between the two carbon atoms, which results in an unsaturated molecule [37].

During reductive dechlorination, halogenated molecules are used as electron acceptors; they are reduced with the electrons released from the oxidation of a primary substrate, the electron donor. The primary substrate can either be an organic compound or hydrogen gas.

RD is effective with most halogenated aliphatic hydrocarbons by progressively converting compounds from more to less chlorinated. It is efficient, in particular, in reducing chlorinated ethenes or ethanes to ethene or ethane, respectively, via sequential reactions.

RD can be a direct or a cometabolic process:

- *Direct mechanism.* Microorganisms use the chlorinated compound as a TEA and gain energy from the reaction. Usually, the electron donor in the redox reaction that leads to the dehalogenation of chlorinated organics is hydrogen gas, often provided indirectly from the fermentation of organic substrates. Chlorinated solvents or aromatics are used by the bacteria as the electron acceptor for respiration; for this reason, this process is also referred to as *dehalorespiration*. A number of bacterial species, belonging to the Firmicutes, Proteobacteria, and Chloroflexi phyla, have been isolated and found capable of direct RD using, in particular, PCE or TCE as TEAs. In most cases, however, individual strains are unable to carry out the full dechlorination pathway that yields non-toxic ethene as a final product, and complete dechlorination may occur only through complementary microbially-driven steps [12, 25, 32, 39, 57, 60]. In fact, only one species of dehalorespiring bacteria capable of fully reducing PCE and TCE to ethene has been identified, i.e., *Dehalococcoides mccartyi* strain 195 (previously *D. ethenogens* 195) [37, 43, 49].
- *Cometabolism.* In the anaerobic cometabolic process, enzymes responsible for the reduction of other TEAs, such as sulfate and carbon dioxide, can fortuitously attack and dehalogenate chlorinated solvents [30]. Cometabolic RD can be carried out by many methanogens and sulfate reducers. These microorganisms are unable to fully reduce PCE and TCE to ethene, and the reduction is interrupted at DCE [45].

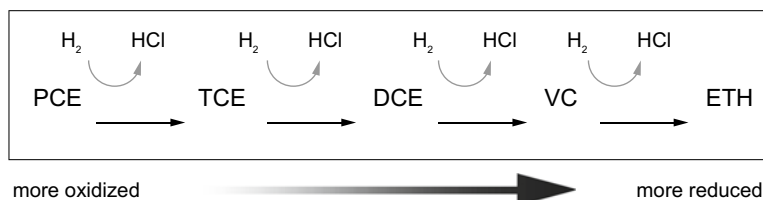
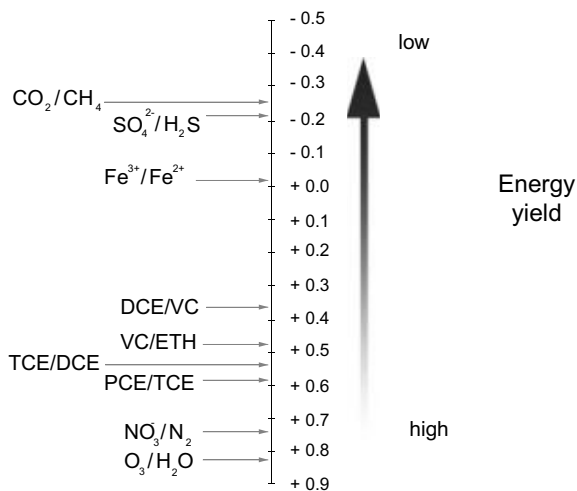


Fig. 17.46 Anaerobic reductive dechlorination of PCE (modified from [54])

Fig. 17.47 Redox potentials (in volts) associated to the reduction of potential electron acceptors (modified from [54])



The most important RD reaction is the sequential degradation of PCE to TCE, to DCE (in particular, the 1, 2-cisDCE isomer is usually formed), to VC, and finally to ETH. The rate of the intermediate transformations in the reduction process from PCE to ethene isn't constant. This is due to the different oxidation states and redox potentials of the molecules involved in the process (Fig. 17.46): due to their lower chlorine content, the oxidation state of carbon is progressively smaller in DCE, VC, and ETH, relative to PCE and TCE.

Among the available substrates, microorganisms select those that yield the greatest energy. The favored electron acceptor is determined by the amount of energy that a microorganism can gain by coupling its reduction to a given oxidation reaction. Since PCE and TCE are more oxidized, they are stronger electron acceptors and are degraded more quickly; in particular, the reduction of PCE to TCE has a higher energy yield than the other partial reactions. Therefore, in the absence of oxygen and nitrate, PCE is the preferred TEA, and is reduced rapidly (Fig. 17.47). The reduction of less chlorinated compounds instead yields significantly less energy, hence they compete with other electron acceptors (e.g., sulfate). The result of this competition between various electron acceptors is the inhibition or slowing down of the reductive dehalogenation of less chlorinated CAHs.

Not only is the degradation rate different for different CAHs, but in many cases dehalorespiring bacteria lack the necessary enzymes to reduce CAHs beyond DCE, and even *D. mccartyi* 195 only reduces VC cometabolically, without gaining any benefit from it [43]. This often causes the accumulation of the least chlorinated compounds (DCE and VC) in the contaminated site. This phenomenon is concerning, particularly because vinyl chloride is more toxic and hence more hazardous than the original compounds (PCE and TCE), and can be addressed by bioaugmenting the site with *D. mccartyi* 195 and stimulating its growth, or by employing oxidative techniques for the removal of DCE and VC once PCE and TCE have been removed [8, 71].

17.8.4.4 Anaerobic Oxidation

Contaminated aquifers are often anoxic environments, in which microbial degradation is based on processes that don't require the presence of oxygen. Anaerobic reductive dechlorination, described above, represents a particularly effective bio-transformation pathway for highly chlorinated solvents, such as PCE and TCE. Less chlorinated CAHs, such as DCE or VC, instead, can be removed by anaerobic oxidation in, for instance, iron reducing and methanogenic environments [8]. This mechanism entails the oxidation of chlorinated compounds in the absence of oxygen. Some bacteria can use CAHs as electron donors, sources of energy and carbon for cell growth and maintenance [71].

17.8.5 Enhanced in Situ Bioremediation

Enhanced in situ bioremediation (EISB) aims at monitoring and stimulating microbial activity in order to create the optimal conditions for bioremediation to occur, and includes both bioaugmentation and biostimulation treatments [17, 41]. Microbial growth can be enhanced essentially by amending the subsurface with [71]:

- *Substrates* needed by indigenous microorganisms, such as sources of carbon and energy (electron donors), which are sometimes limiting for cell growth and maintenance. Under certain conditions, the contaminant itself constitutes the substrate used by the microorganisms.
- *Microorganisms*. Specific microbial communities can be inoculated or, if naturally present at the site, cultivated to increase cell density and accelerate the processes of contaminant removal.
- *Nutrients*. In addition to micronutrients, microbes also need appropriate amounts of nitrogen and phosphorous.
- *Electron acceptors*. Since aerobic degradation processes are usually faster, it can be useful to replenish the contaminated area with oxygen, where it is lacking. Oxygen can be delivered to the aquifer by means of:

- biosparging: it consists in the injection of air below the water table to achieve oxygen concentrations of 8–10 mg/l in the point of injection;
- pure oxygen dissolved in water. With this system, which is the most commonly employed, concentrations that exceed saturation can be achieved (e.g., 40 mg/l);
- water amended with hydrogen peroxide. Hydrogen peroxide (H_2O_2) is a highly soluble compound that breaks down into water and molecular oxygen. This method enables the achievement of high dissolved oxygen concentrations. For instance, a 500 mg/l solution of hydrogen peroxide in water yields a dissolved oxygen concentration of 235 mg/l. The main limitations of this method are the high cost of H_2O_2 and its toxicity towards some microbial species;
- oxygen releasing compounds (ORC). These products are specific formulations of manganese or calcium peroxide, or ozone, that release oxygen over time, when put in contact with groundwater.

The distribution of these components in the subsurface can be carried out with the following systems [71]:

- *Injection and extraction systems.* This configuration, also called *active circulation approach*, establishes a recirculation of contaminated groundwater: it is extracted from an area downgradient of the plume, replenished of the necessary biostimulants, and finally re-injected upgradient. The recirculation cell thus formed is an extremely effective way of mixing the amended substances in the plume (Figs. 17.48 and 17.49).

This generates an area of active treatment through which the contaminated water is recirculated multiple times. The recirculation system is not completely closed: some upgradient groundwater enters the recirculation cell, while part of the water escapes the treatment zone downgradient of the cell. The flow rate of groundwater entering and exiting the recirculation cell depends on the pumping discharge, the hydraulic gradient, the hydraulic conductivity of the aquifer and the angle between the injection/extraction system and the groundwater flow direction.

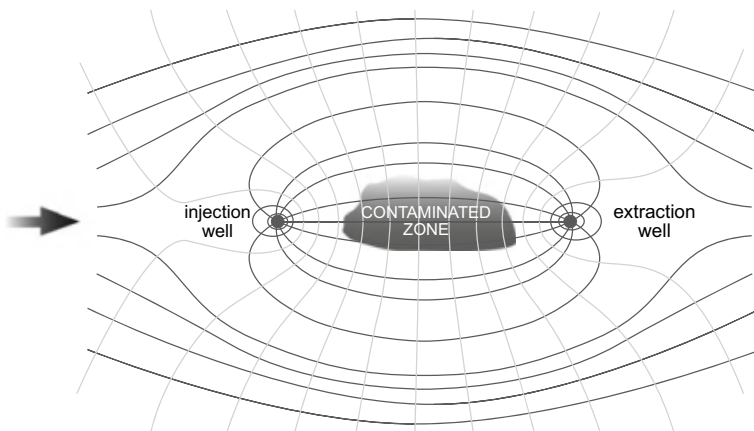


Fig. 17.48 Hydraulic confinement of the contaminated area

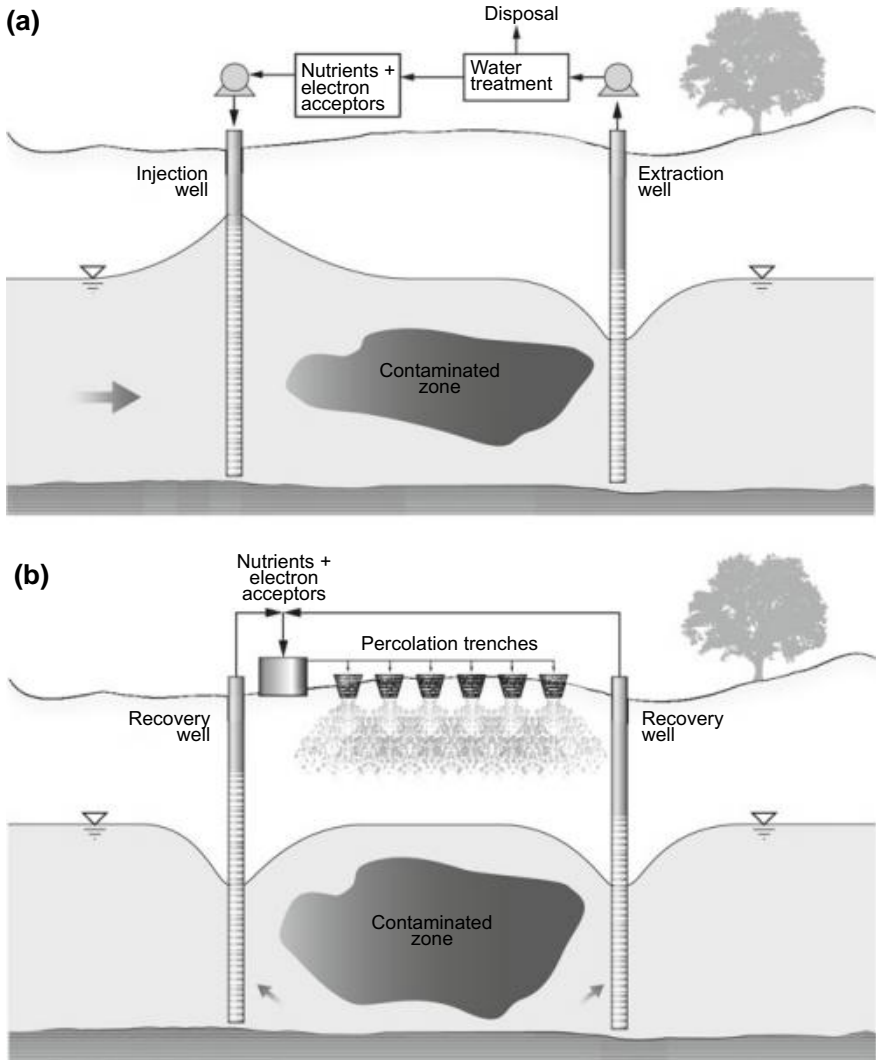


Fig. 17.49 Bioremediation with (a) an injection/extraction system or (b) percolation trenches

In many cases it is necessary to create multiple recirculation cells, installing an upgradient and a downgradient line of injection and extraction wells, respectively, perpendicular to the groundwater flow direction. Injection/extraction systems are usually created installing vertical wells; however, it is possible to use trenches and horizontal wells. Closed or almost closed cell recirculation systems are ideal for the treatment of portions of plume that are characterized by high concentrations of dissolved contaminants, or in areas that contain the source of contamination.

- *Single injection systems.* Substrates, nutrients and/or electron acceptors dissolved in water can be introduced through single wells. The variations to the natural groundwater flow induced by the injection are usually modest. These systems are useful for reducing already low levels of contamination in aquifers, or for polishing interventions.
- *Biosparging.* These gas-phase injection systems can be used to stimulate direct aerobic oxidation and cometabolic aerobic oxidation of contaminants. Oxygen gas (or air) and some substances used as primary substrate during cometabolic aerobic oxidation (such as methane), can thus be distributed in the aquifer.
- *Passive systems.* They don't involve recirculation or active injection. The substances needed to enhance and stimulate microbial processes are distributed in the contaminated aquifer via passive wells or permeable reactive barriers.

References

1. S. Arrhenius, Über die Dissociationswärme und den Einfluss der Temperatur auf den Dissoziationsgrad der Elektrolyte. *Zeitschrift für Physikalische Chemie* **4U**, 96–116 (1889)
2. M.J. Baedecker, W. Back, Hydrogeological Processes and Chemical Reactions at a Landfill, en. *Ground Water* **17**, 429–437 (1979)
3. C. Bianco, T. Tosco, R. Sethi, A 3-dimensional micro- and nanoparticle transport and filtration model (MNM3D) applied to the migration of carbon-based nanomaterials in porous media, eng. *J. Contam. Hydrol.* **193**, 10–20 (2016)
4. C. Bianco, J.E. Patiño Higuera, T. Tosco, A. Tiraferri, R. Sethi, Controlled Deposition of Particles in Porous Media for Effective Aquifer Nanoremediation, eng. *Sci. Rep.* **7**, 12992 (2017)
5. D. Bolster, M. Barahona, M. Dentz, D. Fernandez-Garcia, X. Sanchez-Vila, P. Trinchero, C. Valhondo, D.M. Tartakovsky, Probabilistic risk analysis of groundwater remediation strategies. *Water Resour. Res.* **45**(6), 74 (2009)
6. D.W. Blowes, C.J. Ptacek, S.G. Benner, C.W.T. McRae, T.A. Bennett, R.W. Puls, Treatment of inorganic contaminants using permeable reactive barriers. *J. Contam. Hydrol.* **45**(1–2), 123–137 (2000)
7. J.R. Boulding, J.S. Ginn, *Practical Handbook of Soil, Vadose Zone, and Ground-Water Contamination: Assessment, Prevention, and Remediation, Second Edition*, en, 2nd edn. (CRC Press, USA, 2004)
8. P.M. Bradley, Dichloroethene and vinyl chloride degradation potential in wetland sediments at Twin Lakes and Pen Branch, Savannah River National Laboratory, South Carolina, U.S. Geological Survey open-file report 2007-1028. Title from PDF title screen (viewed on Mar. 14, 2007). Includes bibliographical references (p. 12). (U.S. Geological Survey, Savannah River National Laboratory, Reston, Va (US), 2007)
9. A. Brun, P. Engesgaard, T.H. Christensen, D. Rosbjerg, Modelling of transport and biogeochemical processes in pollution plumes: Vejen landfill, Denmark. *J. Hydrol.* **256**, 228–247 (2002)
10. D. O'Carroll, B. Sleep, M. Krol, H. Boparai, C. Kocur, Nanoscale zero valent iron and bimetallic particles for contaminated site remediation. *Adv. Water Resour.* **51**, 104–122 (2013)
11. F.H. Chapelle, P.B. McMahon, N.M. Dubrovsky, R.F. Fujii, E.T. Oaksford, D.A. Vroblesky, Deducing the distribution of terminal electron- accepting processes in hydrologically diverse groundwater systems, en. *Water Resour. Res.* **31**, 359–371 (1995)
12. D. Cheng, J. He, Isolation and characterization of “Dehalococcoides” sp. Strain MB, which dechlorinates tetrachloroethene to trans-1,2- Dichloroethene, en. *Appl. Environ. Microbiol.* **75**, 5910–5918 (2009)

13. T.P. Clement, Y. Sun, B.S. Hooker, J.N. Petersen, Modeling multispecies reactive transport in ground water. *Groundwater Monit. Rem.* **18**(2), 79–92 (1998)
14. R.M. Cohen, J. Mercer, R.M. Greenwald, M.S. Beljin, Design guide-lines for conventional pump-and-treat system, EPA Ground Water Issue (United States Environmental Protection Agency, Office of Research and Development, Office of Solid Waste and Emergency Response, Washington, DC, 1997)
15. R. Cohen, A.H. Vincent, J. Mercer, C.R. Faust and C. Spalding, Methods for monitoring pump-and-treat performance. Research report, Rep. EPA/600/R-94/123 102 pp. (1994)
16. S. Comba, R. Sethi, Stabilization of highly concentrated suspensions of iron nanoparticles using shear-thinning gels of xanthan gum. *Water Res.* **43**, 3717–3726 (2009)
17. J.W. Delleur, *Handbook of Groundwater Engineering*, en (CRC Press, USA, 2006)
18. H.-J. Diersch, *FEFLOW: Finite element modeling of flow, mass and heat transport in porous and fractured media* (Springer, 2014)
19. A. Di Molfetta, R. Sethi, Barriere reattive permeabili, Italian, in Bonifica di siti contaminati. Caratterizzazione e tecnologie di risanamento, L. Bonomo, Collana di istruzione scientifica (McGraw-Hill Education, 2005)
20. A. Di Molfetta, R. Sethi, Clamshell excavation of a permeable reactive barrier, en. *Environ. Geol.* **50**, 361–369 (2006)
21. A. Di Molfetta, M. Rolle, R. Sethi, Modello cinetico per la descrizione della zonazione redox in acquiferi contaminati a valle di discariche. *Siti Contaminati* **3**, 98–111 (2004)
22. M.E. Dolan, P.L. McCarty, Methanotrophic chloroethene transformation capacities and 1,1-dichloroethene transformation product toxicity, eng. *Environ. Sci. Technol.* **29**, 2741–2747 (1995)
23. P.A. Domenico, F.W. Schwartz, *Physical and Chemical Hydrogeology*, en (Wiley, New York, 1998)
24. M. Elsner, M. Chartrand, N. VanStone, G. Lacrampe Couloume, B. Sherwood Lollar, Identifying abiotic chlorinated ethene degradation: characteristic isotope patterns in reaction products with nanoscale zero-valent iron. *Environ. Sci. Technol.* **42**, 5963–5970 (2008)
25. D.E. Fennell, I. Nijenhuis, S.F. Wilson, S.H. Zinder, M.M. Häggblom, Dehalococoides ethenogenes strain 195 reductively dechlorinates diverse chlorinated aromatic pollutants, eng. *Environ. Sci. Technol.* **38**, 2075–2081 (2004)
26. C.W. Fetter, *Applied Hydrogeology, English*, 4th edn. (Pearson Education, Long Grove, Ill, 2014)
27. A.R. Gavaskar, Design and construction techniques for permeable reactive barriers. *J. Hazard. Mater.* **68**, 41–71 (1999)
28. R.W. Gillham, J. Vogan, L. Gui, M. Duchene, J. Son, *Iron barrier walls for chlorinated solvent remediation*, en, in *In Situ Remediation of Chlorinated Solvent Plumes, SERDP/ESTCP Environmental Remediation Technology* (Springer, New York, NY, 2010), pp. 537–571
29. S. Grubb, Analytical model for estimation of steady-state capture zones of pumping wells in confined and unconfined aquifers, en. *Ground Water* **31**, 27–32 (1993)
30. T.C. Hazen, Cometabolic bioremediation, en, in *Handbook of Hydro-Carbon and Lipid Microbiology*, ed. by K.N. Timmis (Springer, Berlin, 2010), pp. 2505–2514
31. A.W. Harbaugh, E.R. Banta, M.C. Hill, M.G. McDonald, MODFLOW-2000, The U. S. Geological Survey Modular Ground-Water Model-User Guide to Modularization Concepts and the Ground-Water Flow Process. *Open-file Report* (U.S. Geological Survey, 2000), pp. 134
32. C. Holliger, G. Schraa, A.J. Stams, A.J. Zehnder, A highly purified enrichment culture couples the reductive dechlorination of tetrachloroethene to growth, en. *Appl. Environ. Microbiol.* **59**, 2991–2997 (1993)
33. G.D. Hopkins, L. Semprini, P.L. McCarty, Microcosm and in situ field studies of enhanced biotransformation of trichloroethylene by phenolutilizing microorganisms. *Appl. Environ. Microbiol.* **59**, 2277–2285 (1993)
34. ITRC, Permeable Reactive Barrier: Technology Update, Technical report (The Interstate Technology and Regulatory Council (ITRC) PRB Technology Update Team, 2011)

35. IUPAC, Compendium of Chemical Terminology (the "Gold book"), 2nd edition (Compiled by A. D. McNaught and A. Wilkinson. Blackwell Scientific Publications, Oxford, 1997)
36. I. Javandel, C.-F. Tsang, Capture-zone type curves: a tool for aquifer cleanup, en. *Ground Water* **24**, 616–625 (1986)
37. B.-E. Jugder, H. Ertan, M. Lee, M. Manefield, C.P. Marquis, Reductive dehalogenases come of age in biological destruction of organohalides. *Trends Biotechnol.* **33**, 595–610 (2015)
38. W. Kinzelbach, *Groundwater modelling: an introduction with sample programs in BASIC, First*. Developments in Water Science, vol. 25 (Elsevier, Amsterdam, 1986)
39. L.R. Krumholz, R. Sharp, S.S. Fishbain, A freshwater anaerobe coupling acetate oxidation to tetrachloroethylene dehalogenation, eng. *Appl. Environ. Microbiol.* **62**, 4108–4113 (1996)
40. S. Kuppusamy, T. Palanisami, M. Megharaj, K. Venkateswarlu, R. Naidu, *Ex-situ remediation technologies for environmental pollutants: a critical perspective*, en, in *Reviews of Environmental Contamination and Toxicology*, vol. 236 (Springer, Cham, 2016), pp. 117–192
41. S. Kuppusamy, T. Palanisami, M. Megharaj, K. Venkateswarlu, R. Naidu, *In-situ remediation approaches for the management of contaminated sites: a comprehensive overview*, en, in *Reviews of Environmental Contamination and Toxicology*, vol. 236 (Springer, Cham, 2016), pp. 1–115
42. M.D. LaGrega, P.L. Buckingham, J.C. Evans, *Hazardous Waste Management, English*, Reissue edn. (Waveland Pr Inc, Long Grove, Ill., 2010)
43. F.E. Löffler, K.M. Ritalahti, S.H. Zinder, *Dehalococcoides and Reductive Dechlorination of Chlorinated Solvents*, en, in *Bioaugmentation for Groundwater Remediation, SERDP ESTCP Environmental Remediation Technology* (Springer, New York, 2013), pp. 39–88
44. D.R. Lovley, J.C. Woodward, F.H. Chapelle, Stimulated anoxic biodegradation of aromatic hydrocarbons using Fe(III) ligands, en. *Nature* **370**, 128–131 (1994)
45. J.K. Magnuson, R.V. Stern, J.M. Gossett, S.H. Zinder, D.R. Burris, Reductive dechlorination of tetrachloroethene to ethene by a two component enzyme pathway. *Appl. Environ. Microbiol.* **64**, 1270–1275 (1998)
46. L. Maldi, *Pump and Treat come metodo di trattamento di acquiferi contaminate da metalli, Italian, PhD master thesis* (Politecnico di Torino, Torino, 2002)
47. M. Manassero, C. Deangeli, "Incapsulamento", Italian, in *Bonifica di siti contaminati. Caratterizzazione e tecnologie di risanamento*, L. Bonomo, Collana di istruzione scientifica (McGraw-Hill Education, 2005)
48. A. Mayer, S.M. Hassanzadeh, *Soil and Groundwater Contamination: Nonaqueous Phase Liquids-Principles and Observations, Water Resources Monograph 17* (American Geophysical Union, Washington, 2005)
49. X. Maymó-Gatell, Y.-T. Chien, J.M. Gossett, S.H. Zinder, Isolation of a bacterium that reductively dechlorinates tetrachloroethene to ethene, en. *Science* **276**, 1568–1571 (1997)
50. N. Moraci, P.S. Calabró, Heavy metals removal and hydraulic performance in zero-valent iron/pumice permeable reactive barriers. *J. Environ. Manag.* **91**(11), 2336–2341 (2010)
51. E.K. Nyer, *In Situ Treatment Technology*, 2nd edn. (CRC Press, USA, 2000)
52. D. Pedretti, M. Masetti, T. Marangoni, G.P. Beretta, Slurry wall containment performance: Monitoring and modeling of unsaturated and saturated flow. *Environ. Monit. Assess.* **184**(2), 607–624 (2012)
53. T. Phenrat, G.V. Lowry, *Nanoscale Zerovalent Iron Particles for Environmental Restoration. From Fundamental Science to Field Scale Engineering Applications* (2019)
54. M. Rolle, *Biorecupero di acquiferi contaminati da solventi clorurati*, Ph.D thesis (Politecnico di Torino, Torino (Italy), 2002)
55. D.S. Roote, *In situ flushing. Technology Overview Report* (Groundwater Remediation Technologies Analysis Center, 1997)
56. R.L. Satkin, P.B. Bedient, Effectiveness of various aquifer restoration schemes under variable hydrogeologic conditions, en. *Groundwater* **26**, 488–498 (1988)
57. H. Scholz-Muramatsu, A. Neumann, M. Meßmer, E. Moore, G. Diekert, Isolation and characterization of *Dehalospirillum multivorans* gen. nov., sp. nov., a tetrachloroethene-utilizing, strictly anaerobic bacterium, en, *Arch. Microbiol.* **163**, 48–56 (1995)

58. R. Sethi, Barriere reattive permeabili a ferro zerovalente: modellazione dei fenomeni di trasporto e degradazione multicomponente, Italian, Ph.D thesis (Politecnico di Torino, Torino (Italy), 2004)
59. R. Sethi, F.S. Freyria, S. Comba, A. Di Molfetta, Ferro nanoscopico per la bonifica di acquiferi contaminati. *Geam. Geoingegneria Ambientale E Mineraria* **3**, 39–46 (2007)
60. P.K. Sharma, P.L. McCarty, Isolation and characterization of a facultatively aerobic bacterium that reductively dehalogenates tetrachloroethene to cis-1,2-dichloroethene, *eng. Appl. Environ. Microbiol.* **62**, 761–765 (1996)
61. A. Tiraferri, K.L. Chen, R. Sethi, M. Elimelech, Reduced aggregation and sedimentation of zero-valent iron nanoparticles in the presence of guar gum. *J. Colloid Interface Sci.* **324**, 71–79 (2008)
62. T. Tosco, R. Sethi, Transport of non-newtonian suspensions of highly concentrated micro- and nanoscale iron particles in porous media: A modeling approach. *Environ. Sci. Technol.* **44**, 9062–9068 (2010)
63. T. Tosco, A. Tiraferri, R. Sethi, Ionic strength dependent transport of microparticles in saturated porous media: Modeling mobilization and immobilization phenomena under transient chemical conditions, *eng. Environ. Sci. Technol.* **43**, 4425–4431 (2009)
64. T. Tosco, J. Bosch, R.U. Meckenstock, R. Sethi, Transport of ferrihydrite nanoparticles in saturated porous media: role of ionic strength and flow rate. *Environ. Sci. Technol.* **46**, 4008–4015 (2012)
65. T. Tosco, M. Petrangeli Papini, C. Cruz Viggi, R. Sethi, Nanoscale zerovalent iron particles for groundwater remediation: a review. *J. Clean. Prod., Emerg. Ind. Process. Water Manag.* **77**, 10–21 (2014)
66. A. Tsionaki, B. Petri, M. Crimi, H. Mosbæk, R.L. Siegrist, P.L. Bjerg, In situ chemical oxidation of contaminated soil and groundwater using persulfate: A review. *Crit. Rev. Environ. Sci. Technol.* **40**, 55–91 (2010)
67. US EPA, How to effectively recover free product at leaking underground storage tank sites: a guide for state regulators, *en*, <https://www.epa.gov/ust/how-effectively-recover-free-product-leaking-underground-storage-tank-sites-guide-state>, Policies and Guidance, 1996
68. US EPA, How to evaluate alternative cleanup technologies for underground storage tank sites: a guide for corrective action plan reviewers, *en*, <https://www.epa.gov/ust/how-evaluate-alternative-cleanup-technologies-underground-storage-tank-sites-guide-corrective>, Policies and Guidance (1994)
69. US EPA, Hydraulic optimization demonstration for groundwater pump-and-treat systems, *en*, <https://www.epa.gov/remedytech/hydraulicoptimization-demonstration-groundwater-pump-and-treat-systems>, Reports and Assessments (1999)
70. US EPA, In situ treatment technologies for contaminated soil: engineering forum issue paper, *en*, <https://www.epa.gov/remedytech/situtreatment-technologies-contaminated-soil-engineering-forum-issue-paper>, Overviews and Factsheets (2006)
71. US EPA, Introduction to in situ bioremediation of groundwater, *en*, <https://www.epa.gov/remedytech/introduction-situ-bioremediationgroundwater>, Reports and Assessments (2013)
72. US EPA, Multi-phase extraction: state-of-the-practice, *en*, <https://www.epa.gov/remedytech/multi-phase-extraction-state-practice>, Reports and Assessments (1999)
73. N. VanStone, M. Elsner, G. Lacrampe-Couloume, S. Mabury, B. Sherwood Lollar, Potential for identifying abiotic chloroalkane degradation mechanisms using carbon isotopic fractionation. *Environ. Sci. Technol.* **42**, 126–132 (2008)
74. E.D. Vecchia, M. Luna, R. Sethi, Transport in porous media of highly concentrated iron micro- and nanoparticles in the presence of xanthan gum, *eng. Environ. Sci. Technol.* **43**, 8942–8947 (2009)
75. C.-B. Wang, W.-X. Zhang, Synthesizing nanoscale iron particles for rapid and complete dechlorination of TCE and PCBs. *Environ. Sci. Technol.* **31**, 2154–2156 (1997)
76. R.J. Watts, A.L. Teel, Treatment of contaminated soils and groundwater using ISCO. *Pract. Period. Hazard., Toxic, Radioact. Waste Manag.* **10**, 2–9 (2006)

77. A.D. Werner, M. Bakker, V.E.A. Post, A. Vandenbohede, C. Lu, B. Ataie-Ashtiani, C.T. Simmons, D.A. Barry, Seawater intrusion processes, investigation and management: recent advances and future challenges. *Adv. Water Resour.* **51**, 3–26 (2013)
78. T. Zhang et al., In situ remediation of subsurface contamination: opportunities and challenges for nanotechnology and advanced materials. *Environ Sci: Nano* **6**(5), 1283–1302 (2019)
79. V. Zolla, F.S. Freyria, R. Sethi, A. Di Molfetta, Hydrogeochemical and biological processes affecting the long-term performance of an ironbased permeable reactive barrier, *eng. J. Environ. Qual.* **38**, 897–908 (2009)

Appendix A

Exponential Integral or Well Function

See Table [A.1](#).

Table A.1 Exponential Integral or Well Function Values

N/u	$N \cdot 10^{-15}$	$N \cdot 10^{-14}$	$N \cdot 10^{-13}$	$N \cdot 10^{-12}$	$N \cdot 10^{-11}$	$N \cdot 10^{-10}$	$N \cdot 10^{-9}$	$N \cdot 10^{-8}$	$N \cdot 10^{-7}$	$N \cdot 10^{-6}$	$N \cdot 10^{-5}$	$N \cdot 10^{-4}$	$N \cdot 10^{-3}$	$N \cdot 10^{-2}$	$N \cdot 10^{-1}$	N
1.0	33.9616	31.6590	29.3564	27.0538	24.7512	22.4486	20.1461	17.8435	15.5409	13.2383	10.9357	8.6332	6.3315	4.0379	1.8229	$2.1938 \cdot 10^{-1}$
1.1	33.8663	31.5637	29.2611	26.9585	24.6559	22.3533	20.0507	17.7482	15.4456	13.1430	10.8404	8.5379	6.2363	3.9436	1.7371	$1.8599 \cdot 10^{-1}$
1.2	33.7792	31.4767	29.1741	26.8715	24.5689	22.2663	19.9637	17.6611	15.3586	13.0560	10.7534	8.4509	6.1494	3.8576	1.6595	$1.5841 \cdot 10^{-1}$
1.3	33.6992	31.3966	29.0940	26.7914	24.4889	22.1863	19.8837	17.5811	15.2785	12.9759	10.6734	8.3709	6.0695	3.7785	1.5889	$1.3545 \cdot 10^{-1}$
1.4	33.6251	31.3225	29.0199	26.7173	24.4147	22.1122	19.8096	17.5070	15.2044	12.9018	10.5993	8.2968	5.9955	3.7054	1.5241	$1.1622 \cdot 10^{-1}$
1.5	33.5561	31.2535	28.9509	26.6483	24.3458	22.0432	19.7406	17.4380	15.1354	12.8328	10.5303	8.2278	5.9266	3.6374	1.4645	$1.0002 \cdot 10^{-1}$
1.6	33.4916	31.1890	28.8864	26.5838	24.2812	21.9786	19.6760	17.3735	15.0709	12.7683	10.4657	8.1633	5.8621	3.5739	1.4092	$8.6308 \cdot 10^{-2}$
1.7	33.4309	31.1283	28.8258	26.5232	24.2206	21.9180	19.6154	17.3128	15.0103	12.7077	10.4051	8.1027	5.8016	3.5143	1.3578	$7.4655 \cdot 10^{-2}$
1.8	33.3738	31.0712	28.7686	26.4660	24.1634	21.8608	19.5583	17.2557	14.9531	12.6505	10.3479	8.0455	5.7446	3.4581	1.3098	$6.4713 \cdot 10^{-2}$
1.9	33.3197	31.0171	28.7145	26.4120	24.1094	21.8068	19.5042	17.2016	14.8990	12.5964	10.2939	7.9915	5.6906	3.4050	1.2649	$5.6204 \cdot 10^{-2}$
2.0	33.2684	30.9658	28.6632	26.3607	24.0581	21.7555	19.4529	17.1503	14.8477	12.5451	10.2426	7.9402	5.6394	3.3547	1.2227	$4.8901 \cdot 10^{-2}$
2.1	33.2196	30.9170	28.6145	26.3119	24.0093	21.7067	19.4041	17.1015	14.7989	12.4964	10.1938	7.8914	5.5907	3.3069	1.1829	$4.2614 \cdot 10^{-2}$
2.2	33.1731	30.8705	28.5679	26.2653	23.9628	21.6602	19.3576	17.0550	14.7524	12.4498	10.1473	7.8449	5.5443	3.2614	1.1454	$3.7191 \cdot 10^{-2}$
2.3	33.1287	30.8261	28.5235	26.2209	23.9183	21.6157	19.3131	17.0106	14.7080	12.4054	10.1028	7.8004	5.4999	3.2179	1.1099	$3.2502 \cdot 10^{-2}$
2.4	33.0861	30.7835	28.4809	26.1783	23.8758	21.5732	19.2706	16.9680	14.6654	12.3628	10.0603	7.7579	5.4575	3.1763	1.0762	$2.8440 \cdot 10^{-2}$
2.5	33.0453	30.7427	28.4401	26.1375	23.8349	21.5323	19.2298	16.9272	14.6246	12.3220	10.0194	7.7171	5.4167	3.1365	1.0443	$2.4915 \cdot 10^{-2}$
2.6	33.0060	30.7035	28.4009	26.0983	23.7957	21.4931	19.1905	16.8880	14.5854	12.2828	9.9802	7.6779	5.3776	3.0983	1.0139	$2.1850 \cdot 10^{-2}$
2.7	32.9683	30.6657	28.3631	26.0606	23.7580	21.4554	19.1528	16.8502	14.5476	12.2450	9.9425	7.6401	5.3400	3.0615	0.9849	$1.9182 \cdot 10^{-2}$
2.8	32.9319	30.6294	28.3268	26.0242	23.7216	21.4190	19.1164	16.8138	14.5113	12.2087	9.9061	7.6038	5.3037	3.0261	0.9573	$1.6855 \cdot 10^{-2}$
2.9	32.8968	30.5943	28.2917	25.9891	23.6865	21.3839	19.0813	16.7788	14.4762	12.1736	9.8710	7.5687	5.2687	2.9920	0.9309	$1.4824 \cdot 10^{-2}$
3.0	32.8629	30.5604	28.2578	25.9552	23.6526	21.3500	19.0474	16.7449	14.4423	12.1397	9.8371	7.5348	5.2349	2.9591	0.9057	$1.3048 \cdot 10^{-2}$
3.1	32.8302	30.5276	28.2250	25.9224	23.6198	21.3172	19.0146	16.7121	14.4095	12.1069	9.8043	7.5020	5.2022	2.9273	0.8815	$1.1494 \cdot 10^{-2}$
3.2	32.7984	30.4958	28.1932	25.8907	23.5881	21.2855	18.9829	16.6803	14.3777	12.0751	9.7726	7.4703	5.1706	2.8965	0.8583	$1.0133 \cdot 10^{-2}$

(continued)

Table A.1 (continued)

N/u	$N \cdot 10^{-15}$	$N \cdot 10^{-14}$	$N \cdot 10^{-13}$	$N \cdot 10^{-12}$	$N \cdot 10^{-11}$	$N \cdot 10^{-10}$	$N \cdot 10^{-9}$	$N \cdot 10^{-8}$	$N \cdot 10^{-7}$	$N \cdot 10^{-6}$	$N \cdot 10^{-5}$	$N \cdot 10^{-4}$	$N \cdot 10^{-3}$	$N \cdot 10^{-2}$	$N \cdot 10^{-1}$	N
3.3	32.7676	30.4651	28.1625	25.8599	23.5573	21.2547	18.9521	16.6495	14.3470	12.0444	9.7418	7.4395	5.1399	2.8668	0.8361	8.9390 · 10 ⁻³
3.4	32.7378	30.4352	28.1326	25.8300	23.5274	21.2249	18.9223	16.6197	14.3171	12.0145	9.7120	7.4097	5.1102	2.8379	0.8147	7.8910 · 10 ⁻³
3.5	32.7088	30.4062	28.1036	25.8010	23.4985	21.1959	18.8933	16.5907	14.2881	11.9855	9.6830	7.3807	5.0813	2.8099	0.7942	6.9701 · 10 ⁻³
3.6	32.6806	30.3780	28.0755	25.7729	23.4703	21.1677	18.8651	16.5625	14.2599	11.9574	9.6548	7.3526	5.0532	2.7827	0.7745	6.1604 · 10 ⁻³
3.7	32.6532	30.3506	28.0481	25.7455	23.4429	21.1403	18.8377	16.5351	14.2325	11.9300	9.6274	7.3252	5.0259	2.7563	0.7554	5.4478 · 10 ⁻³
3.8	32.6266	30.3240	28.0214	25.7188	23.4162	21.1136	18.8110	16.5085	14.2059	11.9033	9.6007	7.2985	4.9993	2.7306	0.7371	4.8202 · 10 ⁻³
3.9	32.6006	30.2980	27.9954	25.6928	23.3902	21.0877	18.7851	16.4825	14.1799	11.8773	9.5748	7.2725	4.9755	2.7056	0.7194	4.2671 · 10 ⁻³
4.0	32.5753	30.2727	27.9701	25.6675	23.3649	21.0623	18.7598	16.4572	14.1546	11.8520	9.5495	7.2472	4.9482	2.6813	0.7024	3.7794 · 10 ⁻³
4.1	32.5506	30.2480	27.9454	25.6428	23.3402	21.0376	18.7351	16.4325	14.1299	11.8273	9.5248	7.2225	4.9236	2.6576	0.6859	3.3489 · 10 ⁻³
4.2	32.5265	30.2239	27.9213	25.6187	23.3161	21.0136	18.7110	16.4084	14.1058	11.8032	9.5007	7.1985	4.8997	2.6344	0.6700	2.9688 · 10 ⁻³
4.3	32.5029	30.2004	27.8978	25.5952	23.2926	20.9900	18.6874	16.3819	14.0823	11.7797	9.4771	7.1749	4.8762	2.6119	0.6546	2.6329 · 10 ⁻³
4.4	32.4800	30.1774	27.8748	25.5722	23.2696	20.9670	18.6644	16.3619	14.0593	11.7567	9.4541	7.1520	4.8533	2.5899	0.6397	2.3360 · 10 ⁻³
4.5	32.4575	30.1549	27.8523	25.5497	23.2471	20.9446	18.6420	16.3394	14.0368	11.7342	9.4317	7.1295	4.8310	2.5684	0.6253	2.0734 · 10 ⁻³
4.6	32.4355	30.1329	27.8303	25.5277	23.2252	20.9226	18.6200	16.3174	14.0148	11.7122	9.4097	7.1075	4.8091	2.5474	0.6114	1.8410 · 10 ⁻³
4.7	32.4140	30.1114	27.8088	25.5062	23.2037	20.9011	18.5985	16.2959	13.9933	11.6907	9.3882	7.0860	4.7877	2.5268	0.5979	1.6352 · 10 ⁻³
4.8	32.3929	30.0904	27.7878	25.4852	23.1826	20.8800	18.5774	16.2748	13.9723	11.6697	9.3671	7.0650	4.7667	2.5068	0.5848	1.4530 · 10 ⁻³
4.9	32.3723	30.0697	27.7672	25.4646	23.1620	20.8594	18.5568	16.2542	13.9516	11.6491	9.3465	7.0444	4.7462	2.4871	0.5721	1.2915 · 10 ⁻³
5.0	32.3521	30.0495	27.7470	25.4444	23.1418	20.8392	18.5366	16.2340	13.9314	11.6289	9.3263	7.0242	4.7261	2.4679	0.5598	1.1483 · 10 ⁻³
5.1	32.3323	30.0297	27.7272	25.4246	23.1220	20.8194	18.5168	16.2142	13.9116	11.6091	9.3065	7.0044	4.7064	2.4491	0.5478	1.0213 · 10 ⁻³
5.2	32.3129	30.0103	27.7077	25.4051	23.1026	20.8000	18.4974	16.1948	13.8922	11.5896	9.2871	6.9850	4.6871	2.4306	0.5362	9.0862 · 10 ⁻⁴
5.3	32.2939	29.9913	27.6887	25.3861	23.0835	20.7809	18.4783	16.1758	13.8732	11.5706	9.2681	6.9659	4.6681	2.4126	0.5250	8.0861 · 10 ⁻⁴
5.4	32.2752	29.9726	27.6700	25.3674	23.0648	20.7622	18.4597	16.1571	13.8545	11.5519	9.2494	6.9473	4.6495	2.3948	0.5140	7.1980 · 10 ⁻⁴
5.5	32.2568	29.9542	27.6516	25.3491	23.0465	20.7439	18.4413	16.1387	13.8361	11.5336	9.2310	6.9289	4.6313	2.3775	0.5034	6.4093 · 10 ⁻⁴

(continued)

Table A.1 (continued)

N/u	$N \cdot 10^{-15}$	$N \cdot 10^{-14}$	$N \cdot 10^{-13}$	$N \cdot 10^{-12}$	$N \cdot 10^{-11}$	$N \cdot 10^{-10}$	$N \cdot 10^{-9}$	$N \cdot 10^{-8}$	$N \cdot 10^{-7}$	$N \cdot 10^{-6}$	$N \cdot 10^{-5}$	$N \cdot 10^{-4}$	$N \cdot 10^{-3}$	$N \cdot 10^{-2}$	$N \cdot 10^{-1}$	N
5.6	32.2388	29.9362	27.6336	25.3310	23.0285	20.7259	18.4233	16.1207	13.8181	11.5155	9.2130	6.9109	4.6134	2.3604	0.4930	$5.7084 \cdot 10^{-4}$
5.7	32.2211	29.9185	27.6159	25.3133	23.0108	20.7082	18.4056	16.1030	13.8004	11.4978	9.1953	6.8932	4.5958	2.3437	0.4830	$5.0855 \cdot 10^{-4}$
5.8	32.2037	29.9011	27.5985	25.2959	22.9934	20.6908	18.3882	16.0856	13.7830	11.4804	9.1779	6.8758	4.5785	2.3273	0.4732	$4.5316 \cdot 10^{-4}$
5.9	32.1866	29.8840	27.5814	25.2789	22.9763	20.6737	18.3711	16.0685	13.7659	11.4633	9.1608	6.8588	4.5615	2.3111	0.4636	$4.0390 \cdot 10^{-4}$
6.0	32.1698	29.8672	27.5646	25.2620	22.9595	20.6569	18.3543	16.0517	13.7491	11.4465	9.1440	6.8420	4.5448	2.2953	0.4544	$3.6008 \cdot 10^{-4}$
6.1	32.1533	29.8507	27.5481	25.2455	22.9429	20.6403	18.3378	16.0352	13.7326	11.4300	9.1275	6.8254	4.5283	2.2797	0.4454	$3.2109 \cdot 10^{-4}$
6.2	32.1370	29.8344	27.5318	25.2293	22.9267	20.6241	18.3215	16.0189	13.7163	11.4138	9.1112	6.8092	4.5122	2.2645	0.4366	$2.8638 \cdot 10^{-4}$
6.3	32.1210	29.8184	27.5158	25.2133	22.9107	20.6081	18.3055	16.0029	13.7003	11.3978	9.0952	6.7932	4.4963	2.2494	0.4280	$2.5547 \cdot 10^{-4}$
6.4	32.1053	29.8027	27.5001	25.1975	22.8949	20.5923	18.2898	15.9872	13.6846	11.3820	9.0795	6.7775	4.4806	2.2346	0.4197	$2.2795 \cdot 10^{-4}$
6.5	32.0898	29.7872	27.4846	25.1820	22.8794	20.5768	18.2742	15.9717	13.6691	11.3665	9.0640	6.7620	4.4652	2.2201	0.4115	$2.0343 \cdot 10^{-4}$
6.6	32.0745	29.7719	27.4693	25.1667	22.8642	20.5616	18.2590	15.9564	13.6538	11.3512	9.0487	6.7467	4.4501	2.2058	0.4036	$1.8158 \cdot 10^{-4}$
6.7	32.0595	29.7569	27.4543	25.1517	22.8491	20.5465	18.2439	15.9414	13.6388	11.3362	9.0337	6.7317	4.4351	2.1917	0.3959	$1.6211 \cdot 10^{-4}$
6.8	32.0446	29.7421	27.4395	25.1369	22.8343	20.5317	18.2291	15.9265	13.6240	11.3214	9.0189	6.7169	4.4204	2.1779	0.3883	$1.4476 \cdot 10^{-4}$
6.9	32.0300	29.7275	27.4249	25.1223	22.8197	20.5171	18.2145	15.9119	13.6094	11.3068	9.0043	6.7023	4.4059	2.1643	0.3810	$1.2928 \cdot 10^{-4}$
7.0	32.0157	29.7131	27.4105	25.1079	22.8053	20.5027	18.2001	15.8976	13.5950	11.2924	8.9899	6.6879	4.3916	2.1508	0.3738	$1.1548 \cdot 10^{-4}$
7.1	32.0015	29.6989	27.3963	25.0937	22.7911	20.4885	18.1860	15.8834	13.5808	11.2782	8.9757	6.6737	4.3775	2.1376	0.3668	$1.0317 \cdot 10^{-4}$
7.2	31.9875	29.6849	27.3823	25.0797	22.7771	20.4746	18.1720	15.8694	13.5668	11.2642	8.9617	6.6598	4.3636	2.1246	0.3599	$9.2188 \cdot 10^{-5}$
7.3	31.9737	29.6711	27.3685	25.0659	22.7633	20.4608	18.1582	15.8556	13.5530	11.2504	8.9479	6.6460	4.3500	2.1118	0.3532	$8.2387 \cdot 10^{-5}$
7.4	31.9601	29.6575	27.3549	25.0523	22.7497	20.4472	18.1446	15.8420	13.5394	11.2368	8.9343	6.6324	4.3364	2.0991	0.3467	$7.3640 \cdot 10^{-5}$
7.5	31.9467	29.6441	27.3415	25.0389	22.7363	20.4337	18.1311	15.8286	13.5260	11.2234	8.9209	6.6190	4.3231	2.0867	0.3403	$6.5851 \cdot 10^{-5}$
7.6	31.9334	29.6308	27.3282	25.0257	22.7231	20.4205	18.1179	15.8153	13.5127	11.2102	8.9076	6.6057	4.3100	2.0744	0.3341	$5.8859 \cdot 10^{-5}$
7.7	31.9203	29.6178	27.3152	25.0126	22.7100	20.4074	18.1048	15.8022	13.4997	11.1971	8.8946	6.5927	4.2970	2.0623	0.3280	$5.2633 \cdot 10^{-5}$
7.8	31.9074	29.6049	27.3023	24.9997	22.6971	20.3945	18.0919	15.7893	13.4868	11.1842	8.8817	6.5798	4.2842	2.0503	0.3221	$4.7072 \cdot 10^{-5}$

Appendix B

Hantush and Jacob Function

See Tables [B.1](#) and [B.2](#).

Table B.1 Values of the Hantush and Jacob Function

$u \setminus r/B$	$2 \cdot 10^{-3}$	$4 \cdot 10^{-3}$	$6 \cdot 10^{-3}$	$8 \cdot 10^{-3}$	$1 \cdot 10^{-2}$	$2 \cdot 10^{-2}$	$4 \cdot 10^{-2}$	$6 \cdot 10^{-2}$	$8 \cdot 10^{-2}$	$1 \cdot 10^{-1}$	$2 \cdot 10^{-1}$	$4 \cdot 10^{-1}$	$6 \cdot 10^{-1}$	$8 \cdot 10^{-1}$	1	2
0	12.661	11.275	10.464	9.889	9.442	8.057	6.673	5.866	5.295	4.854	3.505	2.229	1.555	1.131	0.842	0.228
$1 \cdot 10^{-6}$	12.442	11.271	10.464	9.889	9.442	8.057	6.673	5.866	5.295	4.854	3.505	2.229	1.555	1.131	0.842	0.228
$2 \cdot 10^{-6}$	12.101	11.226	10.462	9.889	9.442	8.057	6.673	5.866	5.295	4.854	3.505	2.229	1.555	1.131	0.842	0.228
$3 \cdot 10^{-6}$	11.832	11.146	10.451	9.888	9.442	8.057	6.673	5.866	5.295	4.854	3.505	2.229	1.555	1.131	0.842	0.228
$4 \cdot 10^{-6}$	11.617	11.055	10.429	9.885	9.442	8.057	6.673	5.866	5.295	4.854	3.505	2.229	1.555	1.131	0.842	0.228
$5 \cdot 10^{-6}$	11.438	10.964	10.399	9.879	9.441	8.057	6.673	5.866	5.295	4.854	3.505	2.229	1.555	1.131	0.842	0.228
$6 \cdot 10^{-6}$	11.287	10.876	10.364	9.869	9.439	8.057	6.673	5.866	5.295	4.854	3.505	2.229	1.555	1.131	0.842	0.228
$7 \cdot 10^{-6}$	11.154	10.793	10.325	9.856	9.436	8.057	6.673	5.866	5.295	4.854	3.505	2.229	1.555	1.131	0.842	0.228
$8 \cdot 10^{-6}$	11.038	10.715	10.285	9.840	9.431	8.057	6.673	5.866	5.295	4.854	3.505	2.229	1.555	1.131	0.842	0.228
$9 \cdot 10^{-6}$	10.933	10.642	10.245	9.822	9.425	8.057	6.673	5.866	5.295	4.854	3.505	2.229	1.555	1.131	0.842	0.228
$1 \cdot 10^{-5}$	10.838	10.572	10.204	9.802	9.418	8.057	6.673	5.866	5.295	4.854	3.505	2.229	1.555	1.131	0.842	0.228
$2 \cdot 10^{-5}$	10.193	10.052	9.839	9.578	9.296	8.056	6.673	5.866	5.295	4.854	3.505	2.229	1.555	1.131	0.842	0.228
$3 \cdot 10^{-5}$	9.804	9.708	9.558	9.367	9.150	8.048	6.673	5.866	5.295	4.854	3.505	2.229	1.555	1.131	0.842	0.228
$4 \cdot 10^{-5}$	9.525	9.452	9.337	9.186	9.010	8.032	6.673	5.866	5.295	4.854	3.505	2.229	1.555	1.131	0.842	0.228

(continued)

Table B.1 (continued)

$u \setminus r/B$	$2 \cdot 10^{-3}$	$4 \cdot 10^{-3}$	$6 \cdot 10^{-3}$	$8 \cdot 10^{-3}$	$1 \cdot 10^{-2}$	$2 \cdot 10^{-2}$	$4 \cdot 10^{-2}$	$6 \cdot 10^{-2}$	$8 \cdot 10^{-2}$	$1 \cdot 10^{-1}$	$2 \cdot 10^{-1}$	$4 \cdot 10^{-1}$	$6 \cdot 10^{-1}$	$8 \cdot 10^{-1}$	1	2
$5 \cdot 10^{-5}$	9.306	9.248	9.154	9.030	8.883	8.008	6.673	5.866	5.295	4.854	3.505	2.229	1.555	1.131	0.842	0.228
$6 \cdot 10^{-5}$	9.127	9.078	9.000	8.894	8.767	7.979	6.673	5.866	5.295	4.854	3.505	2.229	1.555	1.131	0.842	0.228
$7 \cdot 10^{-5}$	8.976	8.934	8.865	8.774	8.662	7.946	6.673	5.866	5.295	4.854	3.505	2.229	1.555	1.131	0.842	0.228
$8 \cdot 10^{-5}$	8.844	8.807	8.747	8.666	8.567	7.911	6.672	5.866	5.295	4.854	3.505	2.229	1.555	1.131	0.842	0.228
$9 \cdot 10^{-5}$	8.727	8.695	8.641	8.568	8.479	7.874	6.671	5.866	5.295	4.854	3.505	2.229	1.555	1.131	0.842	0.228
$1 \cdot 10^{-4}$	8.623	8.594	8.545	8.479	8.398	7.838	6.669	5.866	5.295	4.854	3.505	2.229	1.555	1.131	0.842	0.228
$2 \cdot 10^{-4}$	7.935	7.920	7.896	7.862	7.819	7.497	6.624	5.864	5.295	4.854	3.505	2.229	1.555	1.131	0.842	0.228
$3 \cdot 10^{-4}$	7.531	7.521	7.505	7.482	7.453	7.228	6.544	5.853	5.294	4.854	3.505	2.229	1.555	1.131	0.842	0.228
$4 \cdot 10^{-4}$	7.245	7.237	7.225	7.207	7.186	7.013	6.454	5.831	5.291	4.854	3.505	2.229	1.555	1.131	0.842	0.228
$5 \cdot 10^{-4}$	7.022	7.016	7.006	6.992	6.975	6.834	6.362	5.801	5.285	4.853	3.505	2.229	1.555	1.131	0.842	0.228
$6 \cdot 10^{-4}$	6.840	6.835	6.827	6.815	6.801	6.682	6.275	5.766	5.275	4.851	3.505	2.229	1.555	1.131	0.842	0.228
$7 \cdot 10^{-4}$	6.686	6.682	6.675	6.665	6.652	6.550	6.192	5.727	5.262	4.848	3.505	2.229	1.555	1.131	0.842	0.228
$8 \cdot 10^{-4}$	6.553	6.549	6.543	6.534	6.523	6.434	6.113	5.687	5.246	4.843	3.505	2.229	1.555	1.131	0.842	0.228
$9 \cdot 10^{-4}$	6.436	6.432	6.426	6.419	6.409	6.329	6.040	5.646	5.228	4.837	3.505	2.229	1.555	1.131	0.842	0.228
$1 \cdot 10^{-3}$	6.331	6.327	6.322	6.315	6.306	6.234	5.971	5.606	5.209	4.829	3.505	2.229	1.555	1.131	0.842	0.228

Table B.2 Values of the Hantush and Jacob Function

$u \setminus r/B$	$2 \cdot 10^{-3}$	$4 \cdot 10^{-3}$	$6 \cdot 10^{-3}$	$8 \cdot 10^{-3}$	$1 \cdot 10^{-2}$	$2 \cdot 10^{-2}$	$4 \cdot 10^{-2}$	$6 \cdot 10^{-2}$	$8 \cdot 10^{-2}$
$2 \cdot 10^{-3}$	5.639	5.637	5.635	5.631	5.626	5.590	5.451	5.241	4.984
$3 \cdot 10^{-3}$	5.235	5.234	5.232	5.229	5.226	5.201	5.107	4.960	4.774
$4 \cdot 10^{-3}$	4.948	4.948	4.946	4.944	4.942	4.922	4.851	4.739	4.593
$5 \cdot 10^{-3}$	4.726	4.726	4.725	4.723	4.721	4.705	4.648	4.557	4.437
$6 \cdot 10^{-3}$	4.545	4.544	4.544	4.543	4.541	4.527	4.479	4.403	4.301
$7 \cdot 10^{-3}$	4.392	4.391	4.391	4.390	4.389	4.377	4.335	4.269	4.181
$8 \cdot 10^{-3}$	4.259	4.259	4.259	4.258	4.257	4.246	4.209	4.151	4.074
$9 \cdot 10^{-3}$	4.142	4.142	4.142	4.141	4.140	4.131	4.098	4.046	3.977
$1 \cdot 10^{-2}$	4.038	4.038	4.038	4.037	4.036	4.028	3.998	3.951	3.888
$2 \cdot 10^{-2}$	3.355	3.355	3.355	3.354	3.354	3.352	3.337	3.311	3.279
$3 \cdot 10^{-2}$	2.959	2.959	2.959	2.959	2.959	2.958	2.950	2.933	2.910
$4 \cdot 10^{-2}$	2.681	2.681	2.681	2.681	2.681	2.680	2.676	2.664	2.647
$5 \cdot 10^{-2}$	2.468	2.468	2.468	2.468	2.468	2.467	2.464	2.456	2.444
$6 \cdot 10^{-2}$	2.295	2.295	2.295	2.295	2.295	2.295	2.293	2.287	2.278
$7 \cdot 10^{-2}$	2.151	2.151	2.151	2.151	2.151	2.151	2.149	2.145	2.137
$8 \cdot 10^{-2}$	2.027	2.027	2.027	2.027	2.027	2.027	2.025	2.022	2.016
$9 \cdot 10^{-2}$	1.919	1.919	1.919	1.919	1.919	1.919	1.918	1.915	1.910
$1 \cdot 10^{-1}$	1.823	1.823	1.823	1.823	1.823	1.823	1.822	1.820	1.816
$2 \cdot 10^{-1}$	1.223	1.223	1.223	1.223	1.223	1.223	1.222	1.222	1.221
$3 \cdot 10^{-1}$	0.906	0.906	0.906	0.906	0.906	0.906	0.906	0.905	0.905
$4 \cdot 10^{-1}$	0.702	0.702	0.702	0.702	0.702	0.702	0.702	0.702	0.702
$5 \cdot 10^{-1}$	0.560	0.560	0.560	0.560	0.560	0.560	0.560	0.560	0.560
$6 \cdot 10^{-1}$	0.454	0.454	0.454	0.454	0.454	0.454	0.454	0.454	0.454
$8 \cdot 10^{-1}$	0.311	0.311	0.311	0.311	0.311	0.311	0.311	0.311	0.311
1	0.219	0.219	0.219	0.219	0.219	0.219	0.219	0.219	0.219
2	$4.890 \cdot 10^{-2}$	$4.890 \cdot 10^{-2}$	$4.890 \cdot 10^{-2}$	$4.890 \cdot 10^{-2}$	$4.890 \cdot 10^{-2}$	$4.890 \cdot 10^{-2}$	$4.890 \cdot 10^{-2}$	$4.890 \cdot 10^{-2}$	$4.890 \cdot 10^{-2}$
4	$3.779 \cdot 10^{-3}$	$3.779 \cdot 10^{-3}$	$3.779 \cdot 10^{-3}$	$3.779 \cdot 10^{-3}$	$3.779 \cdot 10^{-3}$	$3.779 \cdot 10^{-3}$	$3.779 \cdot 10^{-3}$	$3.779 \cdot 10^{-3}$	$3.779 \cdot 10^{-3}$
6	$3.601 \cdot 10^{-4}$	$3.601 \cdot 10^{-4}$	$3.601 \cdot 10^{-4}$	$3.601 \cdot 10^{-4}$	$3.601 \cdot 10^{-4}$	$3.601 \cdot 10^{-4}$	$3.601 \cdot 10^{-4}$	$3.601 \cdot 10^{-4}$	$3.601 \cdot 10^{-4}$
8	$3.767 \cdot 10^{-5}$	$3.767 \cdot 10^{-5}$	$3.767 \cdot 10^{-5}$	$3.767 \cdot 10^{-5}$	$3.767 \cdot 10^{-5}$	$3.767 \cdot 10^{-5}$	$3.767 \cdot 10^{-5}$	$3.767 \cdot 10^{-5}$	$3.767 \cdot 10^{-5}$

(continued)

Table B.2 (continued)

$u \backslash r/B$	$1 \cdot 10^{-1}$	$2 \cdot 10^{-1}$	$4 \cdot 10^{-1}$	$6 \cdot 10^{-1}$	$8 \cdot 10^{-1}$	1	2
$2 \cdot 10^{-3}$	4.708	3.504	2.229	1.555	1.131	0.842	0.228
$3 \cdot 10^{-3}$	4.562	3.497	2.229	1.555	1.131	0.842	0.228
$4 \cdot 10^{-3}$	4.422	3.481	2.229	1.555	1.131	0.842	0.228
$5 \cdot 10^{-3}$	4.295	3.457	2.229	1.555	1.131	0.842	0.228
$6 \cdot 10^{-3}$	4.179	3.427	2.229	1.555	1.131	0.842	0.228
$7 \cdot 10^{-3}$	4.075	3.394	2.229	1.555	1.131	0.842	0.228
$8 \cdot 10^{-3}$	3.980	3.359	2.228	1.555	1.131	0.842	0.228
$9 \cdot 10^{-3}$	3.892	3.323	2.227	1.555	1.131	0.842	0.228
$1 \cdot 10^{-2}$	3.812	3.286	2.225	1.555	1.131	0.842	0.228
$2 \cdot 10^{-2}$	3.239	2.948	2.180	1.553	1.131	0.842	0.228
$3 \cdot 10^{-2}$	2.882	2.684	2.102	1.542	1.130	0.842	0.228
$4 \cdot 10^{-2}$	2.626	2.474	2.013	1.521	1.127	0.842	0.228
$5 \cdot 10^{-2}$	2.427	2.304	1.924	1.492	1.121	0.841	0.228
$6 \cdot 10^{-2}$	2.264	2.160	1.840	1.457	1.111	0.839	0.228
$7 \cdot 10^{-2}$	2.127	2.038	1.761	1.421	1.099	0.836	0.228
$8 \cdot 10^{-2}$	2.008	1.931	1.687	1.383	1.084	0.831	0.228
$9 \cdot 10^{-2}$	1.903	1.837	1.619	1.344	1.067	0.825	0.228
$1 \cdot 10^{-1}$	1.810	1.753	1.556	1.306	1.048	0.818	0.228
$2 \cdot 10^{-1}$	1.220	1.202	1.115	0.990	0.852	0.711	0.227
$3 \cdot 10^{-1}$	0.904	0.897	0.852	0.778	0.689	0.597	0.221
$4 \cdot 10^{-1}$	0.702	0.698	0.673	0.626	0.565	0.500	0.209
$5 \cdot 10^{-1}$	0.559	0.557	0.542	0.511	0.469	0.421	0.194
$6 \cdot 10^{-1}$	0.454	0.453	0.443	0.422	0.392	0.356	0.177
$8 \cdot 10^{-1}$	0.310	0.310	0.305	0.295	0.279	0.258	0.144
1	0.219	0.219	0.216	0.211	0.202	0.190	0.114
2	$4.890 \cdot 10^{-2}$	$4.886 \cdot 10^{-2}$	$4.862 \cdot 10^{-2}$	$4.806 \cdot 10^{-2}$	$4.712 \cdot 10^{-2}$	$4.575 \cdot 10^{-2}$	$3.406 \cdot 10^{-2}$
4	$3.779 \cdot 10^{-3}$	$3.778 \cdot 10^{-3}$	$3.770 \cdot 10^{-3}$	$3.751 \cdot 10^{-3}$	$3.717 \cdot 10^{-3}$	$3.667 \cdot 10^{-3}$	$3.171 \cdot 10^{-3}$
6	$3.601 \cdot 10^{-4}$	$3.600 \cdot 10^{-4}$	$3.595 \cdot 10^{-4}$	$3.583 \cdot 10^{-4}$	$3.563 \cdot 10^{-4}$	$3.532 \cdot 10^{-4}$	$3.214 \cdot 10^{-4}$
8	$3.766 \cdot 10^{-5}$	$3.766 \cdot 10^{-5}$	$3.762 \cdot 10^{-5}$	$3.753 \cdot 10^{-5}$	$3.738 \cdot 10^{-5}$	$3.714 \cdot 10^{-5}$	$3.464 \cdot 10^{-5}$

Appendix C

Function K_0

See Table C.1.

Table C.1 Values of the function $K_0(x)$

x	$K_0(x)$	x	$K_0(x)$
0.001	7.02	0.25	1.54
0.005	5.41	0.30	1.37
0.01	4.72	0.35	1.23
0.015	4.32	0.40	1.11
0.02	4.03	0.45	1.01
0.025	3.81	0.50	0.92
0.03	3.62	0.55	0.85
0.035	3.47	0.60	0.78
0.04	3.34	0.65	0.72
0.045	3.22	0.70	0.66
0.05	3.11	0.75	0.61
0.055	3.02	0.80	0.57
0.06	2.93	0.85	0.52
0.065	2.85	0.90	0.49
0.07	2.78	0.95	0.45
0.075	2.71	1.0	0.42
0.08	2.65	1.5	0.21
0.085	2.59	2.0	0.11
0.09	2.53	2.5	0.062
0.095	2.48	3.0	0.035
0.10	2.43	3.5	0.020
0.15	2.03	4.0	0.011
0.20	1.75	4.5	0.006
		5.0	0.004

Appendix D

Dimensionless Neuman's Function $s_D(t_s, \beta)$

Valid for Short Times

See Tables D.1 and D.2.

Table D.1 Dimensionless Neuman's Function $s_D(t_s, \beta)$ Valid for Short Times

t_s	$\beta = 0.001$	$\beta = 0.004$	$\beta = 0.01$	$\beta = 0.03$	$\beta = 0.06$	$\beta = 0.1$	$\beta = 0.2$	$\beta = 0.4$	$\beta = 0.6$
$1.0 \cdot 10^{-1}$	0.02336	0.02440	0.02403	0.02350	0.02297	0.02240	0.02140	0.01994	0.01880
$1.5 \cdot 10^{-1}$	0.07708	0.07647	0.07531	0.07326	0.07117	0.06908	0.06525	0.05977	0.05561
$2.0 \cdot 10^{-1}$	0.14411	0.14235	0.14013	0.13566	0.13127	0.12689	0.11885	0.10758	0.09884
$2.5 \cdot 10^{-1}$	0.21575	0.21279	0.20908	0.20178	0.19459	0.18744	0.17450	0.15589	0.14161
$3.0 \cdot 10^{-1}$	0.28790	0.28354	0.27825	0.26778	0.25749	0.24691	0.22809	0.20147	0.18105
$3.5 \cdot 10^{-1}$	0.35766	0.35187	0.34489	0.33108	0.31750	0.30400	0.27918	0.24374	0.21685
$4.0 \cdot 10^{-1}$	0.42407	0.41676	0.40807	0.39080	0.37383	0.35696	0.32648	0.28262	0.24906
$5.0 \cdot 10^{-1}$	0.54938	0.53813	0.52592	0.50160	0.47773	0.45399	0.41036	0.34870	0.30229
$6.0 \cdot 10^{-1}$	0.66174	0.64836	0.63261	0.60123	0.57042	0.53981	0.48266	0.40323	0.34335
$7.0 \cdot 10^{-1}$	0.76346	0.74710	0.72784	0.68951	0.65187	0.61447	0.54572	0.44803	0.37587
$8.0 \cdot 10^{-1}$	0.85606	0.83676	0.81408	0.76891	0.72459	0.68053	0.59956	0.48504	0.40145
$9.0 \cdot 10^{-1}$	0.93916	0.91697	0.89097	0.84081	0.78995	0.73940	0.64650	0.51580	0.42168
$1.0 \cdot 10^0$	1.01726	0.99227	0.96298	0.90467	0.84909	0.79219	0.68768	0.54237	0.43779
$2.0 \cdot 10^0$	1.57138	1.52166	1.46364	1.34798	1.23454	1.12187	0.91770	0.65874	0.49737
$3.0 \cdot 10^0$	1.92046	1.85021	1.76834	1.60524	1.44180	1.28367	1.00625	0.68571	0.50574
$4.0 \cdot 10^0$	2.17014	2.08217	1.97965	1.77538	1.57176	1.37588	1.04563	0.69300	0.50711
$5.0 \cdot 10^0$	2.36518	2.26122	2.14024	1.89908	1.66349	1.43260	1.06454	0.69513	0.50736
$6.0 \cdot 10^0$	2.52475	2.40628	2.26839	1.99358	1.72624	1.46917	1.07406	0.69579	0.50740
$7.0 \cdot 10^0$	2.65952	2.52762	2.37407	2.06814	1.77229	1.49348	1.07900	0.69599	0.50741
$8.0 \cdot 10^0$	2.77604	2.63154	2.46334	2.12836	1.80686	1.51001	1.08162	0.69606	0.50742
$9.0 \cdot 10^0$	2.87851	2.72210	2.54009	2.17784	1.83326	1.52144	1.08304	0.69608	0.50742
$1.0 \cdot 10^1$	2.96980	2.80216	2.60704	2.21906	1.85367	1.52946	1.08382	0.69609	0.50742
$2.0 \cdot 10^1$	3.55857	3.29914	2.99737	2.41285	1.92463	1.54914	1.08480	0.69610	0.50742
$3.0 \cdot 10^1$	3.88887	3.55845	3.17497	2.46644	1.93385	1.55007	1.08480	0.69610	0.50742
$4.0 \cdot 10^1$	4.11437	3.72399	3.27342	2.48450	1.93532	1.55013	1.08480	0.69610	0.50742

(continued)

Table D.1 (continued)

t_s	$\beta = 0.001$	$\beta = 0.004$	$\beta = 0.01$	$\beta = 0.03$	$\beta = 0.06$	$\beta = 0.1$	$\beta = 0.2$	$\beta = 0.4$	$\beta = 0.6$
$5.0 \cdot 10^1$	4.28328	3.83996	3.33309	2.49117	1.93558	1.55013	1.08480	0.69610	0.50742
$6.0 \cdot 10^1$	4.41682	3.92571	3.37120	2.49377	1.93563	1.55013	1.08480	0.69610	0.50742
$7.0 \cdot 10^1$	4.52621	3.99139	3.39638	2.49481	1.93564	1.55013	1.08480	0.69610	0.50742
$8.0 \cdot 10^1$	4.61820	4.04294	3.41342	2.49525	1.93564	1.55013	1.08480	0.69610	0.50742
$9.0 \cdot 10^1$	4.69702	4.08413	3.42516	2.49543	1.93564	1.55013	1.08480	0.69609	0.50742
$1.0 \cdot 10^2$	4.76556	4.11753	3.43335	2.49550	1.93564	1.55013	1.08480	0.69610	0.50742
$2.0 \cdot 10^2$	5.16256	4.25797	3.45340	2.49556	1.93564	1.55013	1.08480	0.69610	0.50742
$3.0 \cdot 10^2$	5.34090	4.28777	3.45434	2.49556	1.93564	1.55013	1.08480	0.69610	0.50742
$4.0 \cdot 10^2$	5.44001	4.29561	3.45439	2.49556	1.93564	1.55013	1.08480	0.69610	0.50742
$5.0 \cdot 10^2$	5.50104	4.29791	3.45440	2.49556	1.93564	1.55013	1.08480	0.69610	0.50742
$6.0 \cdot 10^2$	5.54054	4.29861	3.45440	2.49556	1.93564	1.55013	1.08480	0.69610	0.50742
$7.0 \cdot 10^2$	5.56673	4.29884	3.45440	2.49556	1.93564	1.55013	1.08480	0.69610	0.50742
$8.0 \cdot 10^2$	5.58431	4.29891	3.45440	2.49556	1.93564	1.55013	1.08480	0.69610	0.50742
$9.0 \cdot 10^2$	5.59622	4.29893	3.45440	2.49556	1.93564	1.55013	1.08480	0.69610	0.50742
$1.0 \cdot 10^3$	5.60436	4.29894	3.45440	2.49556	1.93564	1.55013	1.08480	0.69610	0.50742
$2.0 \cdot 10^3$	5.62263	4.29894	3.45440	2.49556	1.93564	1.55013	1.08480	0.69610	0.50742
$3.0 \cdot 10^3$	5.62340	4.29894	3.45440	2.49556	1.93564	1.55013	1.08480	0.69610	0.50742
$4.0 \cdot 10^3$	5.62346	4.29894	3.45440	2.49556	1.93564	1.55013	1.08480	0.69610	0.50742
$5.0 \cdot 10^3$	5.62346	4.29894	3.45440	2.49556	1.93564	1.55013	1.08480	0.69610	0.50742
$6.0 \cdot 10^3$	5.62346	4.29894	3.45440	2.49556	1.93564	1.55013	1.08481	0.69610	0.50742
$7.0 \cdot 10^3$	5.62346	4.29894	3.45440	2.49556	1.93564	1.55013	1.08481	0.69610	0.50742
$8.0 \cdot 10^3$	5.62346	4.29894	3.45440	2.49556	1.93564	1.55013	1.08481	0.69610	0.50742
$9.0 \cdot 10^3$	5.62346	4.29894	3.45440	2.49557	1.93564	1.55013	1.08481	0.69610	0.50742
$1.0 \cdot 10^4$	5.62346	4.29894	3.45440	2.49557	1.93564	1.55013	1.08481	0.69610	0.50742

Table D.2 Dimensionless Neuman's Function $s_D(t_s, \beta)$ Valid for Short Times

t_s	$\beta = 0.08$	$\beta = 1.0$	$\beta = 1.5$	$\beta = 2.0$	$\beta = 2.5$	$\beta = 3.0$	$\beta = 4.0$	$\beta = 5.0$	$\beta = 6.0$	$\beta = 7.0$
$1.0 \cdot 10^{-1}$	0.01786	0.01702	0.01526	0.01376	0.01247	0.01131	0.00933	0.00772	0.00639	0.00530
$1.5 \cdot 10^{-1}$	0.05210	0.04904	0.04248	0.03700	0.03238	0.02835	0.02184	0.01692	0.01318	0.01031
$2.0 \cdot 10^{-1}$	0.09148	0.08492	0.07131	0.06031	0.05111	0.04350	0.03172	0.02335	0.01737	0.01306
$2.5 \cdot 10^{-1}$	0.12944	0.11890	0.09713	0.07978	0.06596	0.05470	0.03817	0.02709	0.01954	0.01430
$3.0 \cdot 10^{-1}$	0.16411	0.14918	0.11850	0.09516	0.07682	0.06254	0.04217	0.02911	0.02057	0.01484
$3.5 \cdot 10^{-1}$	0.19435	0.17511	0.13588	0.10671	0.08464	0.06779	0.04454	0.03018	0.02105	0.01505
$4.0 \cdot 10^{-1}$	0.22084	0.19692	0.14990	0.11546	0.09023	0.07121	0.04592	0.03075	0.02127	0.01514
$5.0 \cdot 10^{-1}$	0.26382	0.23113	0.16961	0.12683	0.09681	0.07502	0.04720	0.03118	0.02142	0.01519
$6.0 \cdot 10^{-1}$	0.29552	0.25564	0.18174	0.13313	0.10002	0.07666	0.04760	0.03130	0.02145	0.01520
$7.0 \cdot 10^{-1}$	0.31914	0.27279	0.18946	0.13675	0.10160	0.07737	0.04774	0.03133	0.02145	0.01520
$8.0 \cdot 10^{-1}$	0.33682	0.28502	0.19433	0.13869	0.10237	0.07768	0.04779	0.03133	0.02145	0.01520
$9.0 \cdot 10^{-1}$	0.34965	0.29379	0.19741	0.13978	0.10275	0.07781	0.04781	0.03134	0.02145	0.01520
$1.0 \cdot 10^0$	0.35974	0.30011	0.19938	0.14039	0.10294	0.07787	0.04782	0.03134	0.02145	0.01520
$2.0 \cdot 10^0$	0.39076	0.31651	0.20291	0.14120	0.10314	0.07792	0.04782	0.03134	0.02145	0.01520
$3.0 \cdot 10^0$	0.39340	0.31736	0.20296	0.14120	0.10314	0.07792	0.04782	0.03134	0.02145	0.01520
$4.0 \cdot 10^0$	0.39367	0.31741	0.20296	0.14120	0.10314	0.07792	0.04782	0.03134	0.02145	0.01520
$5.0 \cdot 10^0$	0.39370	0.31741	0.20296	0.14120	0.10314	0.07792	0.04782	0.03134	0.02145	0.01520
$6.0 \cdot 10^0$	0.39370	0.31741	0.20296	0.14120	0.10314	0.07792	0.04782	0.03134	0.02145	0.01520
$7.0 \cdot 10^0$	0.39370	0.31741	0.20296	0.14120	0.10314	0.07792	0.04782	0.03134	0.02145	0.01520
$8.0 \cdot 10^0$	0.39370	0.31741	0.20296	0.14120	0.10314	0.07792	0.04782	0.03134	0.02145	0.01520
$9.0 \cdot 10^0$	0.39370	0.31741	0.20296	0.14120	0.10314	0.07792	0.04782	0.03134	0.02145	0.01520
$1.0 \cdot 10^1$	0.39370	0.31741	0.20296	0.14120	0.10314	0.07792	0.04782	0.03134	0.02145	0.01520
$2.0 \cdot 10^1$	0.39370	0.31741	0.20296	0.14120	0.10314	0.07792	0.04782	0.03134	0.02145	0.01520
$3.0 \cdot 10^1$	0.39370	0.31741	0.20296	0.14120	0.10314	0.07792	0.04782	0.03134	0.02145	0.01520
$4.0 \cdot 10^1$	0.39370	0.31741	0.20296	0.14120	0.10314	0.07792	0.04782	0.03134	0.02145	0.01520

(continued)

Table D.2 (continued)

t_s	$\beta = 0.08$	$\beta = 1.0$	$\beta = 1.5$	$\beta = 2.0$	$\beta = 2.5$	$\beta = 3.0$	$\beta = 4.0$	$\beta = 5.0$	$\beta = 6.0$	$\beta = 7.0$
$5.0 \cdot 10^1$	0.39370	0.31741	0.20296	0.14120	0.10314	0.07792	0.04782	0.03134	0.02145	0.01520
$6.0 \cdot 10^1$	0.39370	0.31741	0.20296	0.14120	0.10314	0.07792	0.04782	0.03134	0.02145	0.01520
$7.0 \cdot 10^1$	0.39370	0.31741	0.20296	0.14120	0.10314	0.07792	0.04782	0.03134	0.02145	0.01520
$8.0 \cdot 10^1$	0.39370	0.31741	0.20296	0.14120	0.10314	0.07792	0.04782	0.03134	0.02145	0.01520
$9.0 \cdot 10^1$	0.39370	0.31741	0.20296	0.14120	0.10314	0.07792	0.04782	0.03134	0.02145	0.01520
$1.0 \cdot 10^2$	0.39370	0.31741	0.20296	0.14120	0.10314	0.07792	0.04782	0.03134	0.02145	0.01520
$2.0 \cdot 10^2$	0.39370	0.31741	0.20296	0.14120	0.10314	0.07792	0.04782	0.03134	0.02145	0.01520
$3.0 \cdot 10^2$	0.39370	0.31741	0.20296	0.14120	0.10314	0.07792	0.04782	0.03134	0.02145	0.01520
$4.0 \cdot 10^2$	0.39370	0.31741	0.20296	0.14120	0.10314	0.07792	0.04782	0.03134	0.02145	0.01520
$5.0 \cdot 10^2$	0.39370	0.31741	0.20296	0.14120	0.10314	0.07792	0.04782	0.03134	0.02145	0.01520
$6.0 \cdot 10^2$	0.39370	0.31741	0.20296	0.14120	0.10314	0.07792	0.04782	0.03134	0.02145	0.01520
$7.0 \cdot 10^2$	0.39370	0.31741	0.20296	0.14120	0.10314	0.07792	0.04782	0.03134	0.02145	0.01520
$8.0 \cdot 10^2$	0.39370	0.31741	0.20296	0.14120	0.10314	0.07792	0.04782	0.03134	0.02145	0.01520
$9.0 \cdot 10^2$	0.39370	0.31741	0.20296	0.14120	0.10314	0.07792	0.04782	0.03134	0.02145	0.01520
$1.0 \cdot 10^3$	0.39370	0.31741	0.20296	0.14120	0.10314	0.07792	0.04782	0.03134	0.02145	0.01520
$2.0 \cdot 10^3$	0.39370	0.31741	0.20296	0.14120	0.10314	0.07792	0.04782	0.03134	0.02146	0.01520
$3.0 \cdot 10^3$	0.39370	0.31741	0.20296	0.14120	0.10314	0.07792	0.04782	0.03134	0.02146	0.01520
$4.0 \cdot 10^3$	0.39370	0.31742	0.20296	0.14120	0.10314	0.07793	0.04782	0.03134	0.02146	0.01520
$5.0 \cdot 10^3$	0.39370	0.31742	0.20296	0.14120	0.10314	0.07793	0.04782	0.03134	0.02146	0.01520
$6.0 \cdot 10^3$	0.39370	0.31742	0.20296	0.14121	0.10314	0.07793	0.04782	0.03134	0.02146	0.01520
$7.0 \cdot 10^3$	0.39371	0.31742	0.20297	0.14121	0.10314	0.07793	0.04783	0.03134	0.02146	0.01521
$8.0 \cdot 10^3$	0.39371	0.31742	0.20297	0.14121	0.10314	0.07793	0.04783	0.03134	0.02146	0.01521
$9.0 \cdot 10^3$	0.39371	0.31742	0.20297	0.14121	0.10315	0.07793	0.04783	0.03134	0.02146	0.01521
$1.0 \cdot 10^4$	0.39371	0.31742	0.20297	0.14121	0.10315	0.07793	0.04783	0.03135	0.02146	0.01521

Appendix E

Dimensionless Neuman's Function $s_D(t_s, \beta)$

Valid for Extended Periods of Times

See Tables [E.1](#) and [E.2](#).

Table E.1 Dimensionless Neuman's Function $s_D(t_s, \beta)$ Valid for Extended Periods of Times

t_y	$\beta = 0.001$	$\beta = 0.004$	$\beta = 0.01$	$\beta = 0.03$	$\beta = 0.06$	$\beta = 0.1$	$\beta = 0.2$	$\beta = 0.4$	$\beta = 0.6$
$1.0 \cdot 10^{-4}$	5.62346	4.29895	3.45440	2.49558	1.93566	1.55016	1.08485	0.69616	0.50750
$1.5 \cdot 10^{-4}$	5.62346	4.29895	3.45441	2.49558	1.93567	1.55018	1.08487	0.69620	0.50754
$2.0 \cdot 10^{-4}$	5.62346	4.29895	3.45441	2.49559	1.93568	1.55019	1.08490	0.69623	0.50578
$2.5 \cdot 10^{-4}$	5.62346	4.29895	3.45441	2.49559	1.93569	1.55021	1.08492	0.69626	0.50762
$3.0 \cdot 10^{-4}$	5.62346	4.29895	3.45442	2.49560	1.93570	1.55022	1.08494	0.69630	0.50766
$3.5 \cdot 10^{-4}$	5.62346	4.29895	3.45442	2.49561	1.93571	1.55024	1.08496	0.69633	0.50770
$4.0 \cdot 10^{-4}$	5.62346	4.29895	3.45442	2.49561	1.93572	1.55025	1.08499	0.69637	0.50774
$5.0 \cdot 10^{-4}$	5.62347	4.29896	3.45443	2.49562	1.93574	1.55028	1.08503	0.69643	0.50782
$6.0 \cdot 10^{-4}$	5.62347	4.29896	3.45443	2.49564	1.93576	1.55031	1.08508	0.69650	0.50790
$7.0 \cdot 10^{-4}$	5.62347	4.29896	3.45444	2.49565	1.93578	1.55034	1.08513	0.69657	0.50799
$8.0 \cdot 10^{-4}$	5.62347	4.29896	3.45444	2.49566	1.93580	1.55037	1.08517	0.69664	0.50807
$9.0 \cdot 10^{-4}$	5.62347	4.29897	3.45445	2.49567	1.93583	1.55040	1.08522	0.69670	0.50815
$1.0 \cdot 10^{-3}$	5.62347	4.29897	3.45445	2.49569	1.93585	1.55043	1.08527	0.69677	0.50823
$2.0 \cdot 10^{-3}$	5.62348	4.29899	3.45451	2.49581	1.93606	1.55074	1.08573	0.69745	0.50904
$3.0 \cdot 10^{-3}$	5.62348	4.29902	3.45456	2.49593	1.93627	1.55104	1.08619	0.69813	0.50986
$4.0 \cdot 10^{-3}$	5.62349	4.29905	3.45462	2.49605	1.93647	1.55134	1.08666	0.69880	0.51067
$5.0 \cdot 10^{-3}$	5.62350	4.29907	3.45467	2.49617	1.93668	1.55164	1.08712	0.69948	0.51149
$6.0 \cdot 10^{-3}$	5.62350	4.29910	3.45473	2.49630	1.93689	1.55195	1.08758	0.70015	0.51230
$7.0 \cdot 10^{-3}$	5.62351	4.29912	3.45478	2.49642	1.93710	1.55225	1.08804	0.70083	0.51311
$8.0 \cdot 10^{-3}$	5.62352	4.29915	3.45484	2.49654	1.93731	1.55255	1.08851	0.70151	0.51392
$9.0 \cdot 10^{-3}$	5.62353	4.29917	3.45489	2.49666	1.93752	1.55285	1.08897	0.70218	0.51474
$1.0 \cdot 10^{-2}$	5.62353	4.29920	3.45495	2.49678	1.93773	1.55316	1.08943	0.70286	0.51637
$2.0 \cdot 10^{-2}$	5.62360	4.29946	3.45550	2.49800	1.93982	1.55618	1.09405	0.70961	0.52448
$3.0 \cdot 10^{-2}$	5.62368	4.29971	3.45605	2.49922	1.94191	1.55919	1.09866	0.71635	0.53257
$4.0 \cdot 10^{-2}$	5.62375	4.29997	3.45660	2.50043	1.94399	1.56220	1.10327	0.72307	0.54064
$5.0 \cdot 10^{-2}$	5.62382	4.30023	3.45715	2.50164	1.94608	1.56520	1.10786	0.72978	0.54870
$6.0 \cdot 10^{-2}$	5.62389	4.30048	3.45769	2.50285	1.94816	1.56820	1.11245	0.73647	0.55673
$7.0 \cdot 10^{-2}$	5.62396	4.30074	3.45824	2.50407	1.95024	1.57472	1.11703	0.74315	0.56474

(continued)

Table E.1 (continued)

t_y	$\beta = 0.001$	$\beta = 0.004$	$\beta = 0.01$	$\beta = 0.03$	$\beta = 0.06$	$\beta = 0.1$	$\beta = 0.2$	$\beta = 0.4$	$\beta = 0.6$
$8.0 \cdot 10^{-2}$	5.62403	4.30100	3.45879	2.50528	1.95231	1.57771	1.12161	0.74982	0.57274
$9.0 \cdot 10^{-2}$	5.62410	4.30125	3.45934	2.50650	1.95439	1.58070	1.12617	0.75647	0.58071
$1.0 \cdot 10^{-1}$	5.62417	4.30151	3.45989	2.50771	1.95646	1.58369	1.13073	0.76311	0.58866
$2.0 \cdot 10^{-1}$	5.62488	4.30406	3.46535	2.51982	1.97705	1.61326	1.17584	0.82857	0.66698
$3.0 \cdot 10^{-1}$	5.62559	4.30661	3.47079	2.53187	1.99743	1.64235	1.22009	0.89086	0.74299
$4.0 \cdot 10^{-1}$	5.62630	4.30916	3.47620	2.54387	2.01760	1.67099	1.26346	0.95279	0.81653
$5.0 \cdot 10^{-1}$	5.62701	4.31170	3.48160	2.55580	2.03756	1.69918	1.30594	1.01291	0.88751
$6.0 \cdot 10^{-1}$	5.62772	4.31423	3.48696	2.56767	2.05731	1.72694	1.34752	1.07119	0.95419
$7.0 \cdot 10^{-1}$	5.62843	4.31675	3.49230	2.57948	2.07683	1.75426	1.38821	1.12766	1.02000
$8.0 \cdot 10^{-1}$	5.62913	4.31927	3.49762	2.59122	2.09616	1.78117	1.42801	1.18233	1.08327
$9.0 \cdot 10^{-1}$	5.62984	4.32178	3.50292	2.60290	2.11527	1.80767	1.46693	1.23522	1.14405
$1.0 \cdot 10^0$	5.63055	4.32428	3.50816	2.61448	2.13419	1.83377	1.50497	1.28639	1.20244
$2.0 \cdot 10^0$	5.63757	4.34899	3.55963	2.72657	2.31232	2.07401	1.84507	1.71954	1.68048
$3.0 \cdot 10^0$	5.64455	4.37309	3.60895	2.83133	2.47181	2.28050	2.11477	2.03791	2.01730
$4.0 \cdot 10^0$	5.65147	4.39661	3.65626	2.92900	2.61490	2.45931	2.33585	2.28584	2.27371
$5.0 \cdot 10^0$	5.65833	4.41959	3.70173	3.02006	2.74389	2.61578	2.52144	2.48720	2.47942
$6.0 \cdot 10^0$	5.66515	4.44205	3.74546	3.10519	2.86088	2.75423	2.68045	2.65605	2.65074
$7.0 \cdot 10^0$	5.67191	4.46401	3.78760	3.18493	2.96765	2.87800	2.81918	2.80117	2.79735
$8.0 \cdot 10^0$	5.67856	4.48549	3.82823	3.25984	3.06566	2.98964	2.94195	2.92826	2.92540
$9.0 \cdot 10^0$	5.68522	4.50652	3.86746	3.33041	3.15612	3.09115	3.05188	3.04123	3.03901
$1.0 \cdot 10^1$	5.69183	4.52710	3.90541	3.39705	3.24001	3.18411	3.15133	3.14287	3.14111
$2.0 \cdot 10^1$	5.75539	4.71277	4.22812	3.91226	3.84756	3.83144	3.82221	3.82059	3.82021
$3.0 \cdot 10^1$	5.81475	4.86999	4.47913	4.26437	4.23259	4.22655	4.22186	4.22138	4.22123
$4.0 \cdot 10^1$	5.87046	5.00682	4.68454	4.52975	4.51254	4.51013	4.50692	4.50681	4.50674
$5.0 \cdot 10^1$	5.92298	5.12830	4.85823	4.74177	4.73193	4.73114	4.72857	4.72863	4.72859
$6.0 \cdot 10^1$	5.97268	5.23766	5.00847	4.91782	4.91208	4.91216	4.90993	4.91007	4.91006
$8.0 \cdot 10^1$	6.06483	5.42851	5.25874	5.19918	5.19751	5.19834	5.19643	5.19665	5.19665
$1.0 \cdot 10^2$	6.14883	5.59154	5.46200	5.41939	5.41951	5.42069	5.41891	5.41916	5.41916

Table E.2 Dimensionless Neuman's Function $s_D(t_s, \beta)$ Valid for Extended

t_y	$\beta = 0.8$	$\beta = 1.0$	$\beta = 1.5$	$\beta = 2.0$	$\beta = 2.5$	$\beta = 3.0$	$\beta = 4.0$	$\beta = 5.0$	$\beta = 6.0$	$\beta = 7.0$
$1.0 \cdot 10^{-4}$	0.39379	0.31751	0.20306	0.14130	0.10324	0.07802	0.04791	0.03142	0.02152	0.01526
$1.5 \cdot 10^{-4}$	0.39383	0.31756	0.20311	0.14136	0.10329	0.07807	0.04795	0.03145	0.02156	0.01529
$2.0 \cdot 10^{-4}$	0.39388	0.31760	0.20316	0.14141	0.10334	0.07812	0.04800	0.03149	0.02159	0.01532
$2.5 \cdot 10^{-4}$	0.39392	0.31765	0.20322	0.14146	0.10339	0.07817	0.04804	0.03153	0.02163	0.01535
$3.0 \cdot 10^{-4}$	0.39397	0.31770	0.20327	0.14151	0.10344	0.07822	0.04808	0.03157	0.02166	0.01538
$3.5 \cdot 10^{-4}$	0.39401	0.31775	0.20332	0.14156	0.10349	0.07826	0.04813	0.03161	0.02169	0.01541
$4.0 \cdot 10^{-4}$	0.39406	0.31780	0.20337	0.14162	0.10354	0.07831	0.04817	0.03165	0.02173	0.01544
$5.0 \cdot 10^{-4}$	0.39415	0.31789	0.20347	0.14172	0.10365	0.07841	0.04826	0.03173	0.02180	0.01550
$6.0 \cdot 10^{-4}$	0.39424	0.31799	0.20358	0.14182	0.10375	0.07851	0.04835	0.03181	0.02187	0.01556
$7.0 \cdot 10^{-4}$	0.39433	0.31808	0.20368	0.14193	0.10385	0.07861	0.04844	0.03189	0.02193	0.01562
$8.0 \cdot 10^{-4}$	0.39442	0.31818	0.20378	0.14203	0.10395	0.07871	0.04853	0.03196	0.02200	0.01568
$9.0 \cdot 10^{-4}$	0.39451	0.31828	0.20389	0.14214	0.10405	0.07880	0.04861	0.03204	0.02207	0.01574
$1.0 \cdot 10^{-3}$	0.39460	0.31837	0.20399	0.14224	0.10415	0.07890	0.04870	0.03212	0.02214	0.01580
$2.0 \cdot 10^{-3}$	0.39550	0.31933	0.20502	0.14328	0.10507	0.07988	0.04959	0.03291	0.02284	0.01641
$3.0 \cdot 10^{-3}$	0.39640	0.32029	0.20605	0.14432	0.10609	0.08087	0.05048	0.03370	0.02353	0.01702
$4.0 \cdot 10^{-3}$	0.39731	0.32125	0.20708	0.14537	0.10711	0.08185	0.05138	0.03450	0.02425	0.01764
$5.0 \cdot 10^{-3}$	0.39821	0.32221	0.20812	0.14641	0.10814	0.08284	0.05227	0.03530	0.02496	0.01827
$6.0 \cdot 10^{-3}$	0.39911	0.32318	0.20915	0.14745	0.10916	0.08383	0.05317	0.03608	0.02568	0.01890
$7.0 \cdot 10^{-3}$	0.40001	0.32414	0.21018	0.14850	0.11019	0.08482	0.05408	0.03689	0.02640	0.01955
$8.0 \cdot 10^{-3}$	0.40091	0.32510	0.21121	0.14954	0.11122	0.08582	0.05498	0.03770	0.02712	0.02020
$9.0 \cdot 10^{-3}$	0.40181	0.32606	0.21225	0.15059	0.11225	0.08689	0.05589	0.03852	0.02784	0.02085
$1.0 \cdot 10^{-2}$	0.40271	0.32702	0.21328	0.15164	0.11328	0.08789	0.05680	0.03934	0.02857	0.02150
$2.0 \cdot 10^{-2}$	0.41170	0.33661	0.22362	0.16214	0.12364	0.09797	0.06614	0.04782	0.03624	0.02840
$3.0 \cdot 10^{-2}$	0.42067	0.34620	0.23398	0.17271	0.13413	0.10822	0.07566	0.05663	0.04438	0.03590
$4.0 \cdot 10^{-2}$	0.42963	0.35527	0.24436	0.18334	0.14487	0.11852	0.08551	0.06589	0.05293	0.04393
$5.0 \cdot 10^{-2}$	0.43857	0.36482	0.25508	0.19381	0.15556	0.12907	0.09569	0.07538	0.06201	0.05242
$6.0 \cdot 10^{-2}$	0.44749	0.37436	0.26549	0.20453	0.16634	0.13977	0.10602	0.08527	0.07144	0.06144
$7.0 \cdot 10^{-2}$	0.45639	0.38389	0.27590	0.21530	0.17721	0.15074	0.11645	0.09553	0.08118	0.07094

(continued)

Table E.2 (continued)

t_y	$\beta = 0.8$	$\beta = 1.0$	$\beta = 1.5$	$\beta = 2.0$	$\beta = 2.5$	$\beta = 3.0$	$\beta = 4.0$	$\beta = 5.0$	$\beta = 6.0$	$\beta = 7.0$
$8.0 \cdot 10^{-2}$	0.46527	0.39340	0.28632	0.22610	0.18814	0.16167	0.12719	0.10599	0.09134	0.08074
$9.0 \cdot 10^{-2}$	0.47413	0.40289	0.29673	0.23694	0.19892	0.17271	0.13811	0.11658	0.10190	0.09099
$1.0 \cdot 10^{-1}$	0.48297	0.41237	0.30715	0.24780	0.20998	0.18384	0.14935	0.12752	0.11266	0.10166
$2.0 \cdot 10^{-1}$	0.57103	0.50595	0.41026	0.35730	0.32277	0.29848	0.26628	0.24538	0.23100	0.22035
$3.0 \cdot 10^{-1}$	0.65558	0.59775	0.51163	0.46457	0.43449	0.41349	0.38596	0.36864	0.35725	0.34852
$4.0 \cdot 10^{-1}$	0.73721	0.68540	0.61030	0.56966	0.54318	0.52558	0.50293	0.48899	0.47956	0.47277
$5.0 \cdot 10^{-1}$	0.81572	0.76948	0.70370	0.66892	0.64744	0.63290	0.61451	0.60343	0.59605	0.59080
$6.0 \cdot 10^{-1}$	0.88931	0.84985	0.79240	0.76274	0.74476	0.73277	0.71786	0.70903	0.70321	0.69911
$7.0 \cdot 10^{-1}$	0.96140	0.92477	0.87634	0.85105	0.83598	0.82607	0.81390	0.80678	0.80214	0.79888
$8.0 \cdot 10^{-1}$	1.03033	0.99774	0.95394	0.93231	0.91963	0.91138	0.90135	0.89555	0.89178	0.88915
$9.0 \cdot 10^{-1}$	1.09621	1.06718	1.02883	1.01028	0.99954	0.99260	0.98427	0.97947	0.97637	0.97420
$1.0 \cdot 10^0$	1.15917	1.13326	1.09959	1.08358	1.07442	1.06856	1.06155	1.05753	1.05494	1.05313
$2.0 \cdot 10^0$	1.66297	1.65346	1.63855	1.63369	1.63103	1.62937	1.62739	1.62628	1.62556	1.62506
$3.0 \cdot 10^0$	2.00874	2.00429	1.99920	1.99702	1.99583	1.99508	1.99419	1.99369	1.99337	1.99314
$4.0 \cdot 10^0$	2.26887	2.26639	2.26356	2.26235	2.26168	2.26127	2.26077	2.26049	2.26031	2.26018
$5.0 \cdot 10^0$	2.47638	2.47482	2.47305	2.47228	2.47186	2.47160	2.47128	2.47111	2.47099	2.47091
$6.0 \cdot 10^0$	2.64868	2.64761	2.64640	2.64588	2.64559	2.64541	2.64520	2.64508	2.64500	2.64494
$7.0 \cdot 10^0$	2.79586	2.79510	2.79422	2.79385	2.79363	2.79351	2.79335	2.79326	2.79321	2.79316
$8.0 \cdot 10^0$	2.92427	2.92370	2.92304	2.92275	2.92260	2.92251	2.92239	2.92232	2.92228	2.92225
$9.0 \cdot 10^0$	3.03814	3.03770	3.03718	3.03696	3.03684	3.03676	3.03668	3.03663	3.03659	3.03657
$1.0 \cdot 10^1$	3.14041	3.14006	3.13965	3.13947	3.13937	3.13931	3.13925	3.13920	3.13918	3.13916
$2.0 \cdot 10^1$	3.82006	3.82000	3.81992	3.81988	3.81986	3.81984	3.81984	3.81983	3.81983	3.81983
$3.0 \cdot 10^1$	4.22118	4.22117	4.22114	4.22113	4.22112	4.22112	4.22113	4.22112	4.22113	4.22113
$4.0 \cdot 10^1$	4.50672	4.50673	4.50671	4.50670	4.50671	4.50671	4.50672	4.50672	4.50673	4.50673
$5.0 \cdot 10^1$	4.72859	4.72860	4.72860	4.72859	4.72860	4.72860	4.72861	4.72862	4.72863	4.72863
$6.0 \cdot 10^1$	4.91006	4.91007	4.91008	4.91007	4.91009	4.91009	4.91010	4.91011	4.91012	4.91012
$8.0 \cdot 10^1$	5.19665	5.19668	5.19669	5.19669	5.19670	5.19671	5.19672	5.19672	5.19673	5.19674
$1.0 \cdot 10^2$	5.41916	5.41918	5.41920	5.41920	5.41921	5.41921	5.41922	5.41923	5.41924	5.41924

Index

A

- Absorption, 210
- Acid-base
 - -dissociation, 206
 - -reactions, 205
- Active restoration, 331
- Adsorption, 210
- Advection, 193–195, 198, 199, 314
- Advection-dispersion equation, 220, 223
- Aerobic oxidation, 396, 398
 - cometabolic-, 399
 - direct-, 398
- Air sparging, 355
- Air stripping, 354
- Alkane, 173
- Alkene, 173, 175
- α -elimination, 400
- Anaerobic oxidation, 396, 398, 401
- Anaerobic reductive degradation, 396
- Anion exchange, 211
- Antoine equation, 185
- AQTESOLV software, 93, 96
- Aquiclude, 8, 38
- Aquifer, 1, 13
 - anisotropic-, 20, 23
 - artesian-, 9
 - confined-, 9, 16, 22, 30, 34, 58, 63, 65
 - heterogeneous-, 20, 124
 - homogeneous-, 20
 - isotropic-, 20, 23
 - leaky-, 9, 10, 22, 30, 38, 58, 63, 65, 81
 - phreatic-, 9
 - semi-confined -(see leaky -), 9
 - unconfined-, 9, 14, 22, 30, 42, 58, 63, 65, 72
 - water table-, 9
- Aquifer test, 56, 164

- Aquifuge, 8
- Aquitard, 8, 38
- Area of influence, 339, 360
- Arene, see Aromatic hydrocarbon, 174
- Arrival front, 166
- Arrival time, 108
- Autotrophic, 393
- Average daily intake, 322
- Average linear velocity, 18

B

- Baetsl's solution, 233, 246
- Bailer, 285, 286
- Barrier, 153, 337, 372, 376
 - hydraulic-, 154, 156
 - impermeable-, 344
 - permeable reactive-, 361
 - continuous trench, 361, 370
 - funnel and gate, 361
 - zero valent iron, 379
 - soil mixing-, 376
- Bear's solution, 232, 240, 245
- Benzene, 174, 183
 - -ring, 174
- Bessel function, 42, 46, 92, 232, 245
- β -elimination, 400
- Bioaugmentation, 391, 402
- Biodegradation, 194, 208, 311
 - -factor, 311
 - aerobic-, 356
- Bioremediation, 391
- Bioslurping, 336
- Biosparging, 356, 403
- Biostimulation, 391, 402
- Biotransformation, 208
- Blank, 297, 298

Bottom lining, 153
 Boundary, 77
 – barrier-, 77, 79, 80
 – recharging-, 77, 80
 Bouwer and Rice's method, 84, 88
 Branched chain, 174
 Breakthrough curve, 108
 BRGM method, 139
 BTEX, 174, 183, 256, 388

C

Capillary
 – force, 251
 – fringe, 7
 – pressure, 250, 251, 261
 – threshold-pressure, 254
 Capping, 337, 347
 Capture zone, 339
 Carcinogenic risk, 188
 Cation exchange, 211
 Chemisorption, 211
 Chezy's formula, 129
 Chlorinated solvents, 249, 363, 388
 Chlorobenzene, 176
 Chlorophenol, 176
 CNR-GNDCI method, 139, 140
 Cometabolism, 397, 400
 Complementary error function, 227, 228
 Complex, 207
 Complexation, 207
 Component of concern, 307
 Composite slurry walls, 337
 Compressibility, 4
 Cone of depression, 57, 78
 Constituent of Concern (COC), 303
 Contact angle, 250
 Container method, 59
 Containment, 156, 331, 336, 344
 – hydraulic-, 338
 – hydrodynamic-, 336
 – physical-, 336
 Contaminant, 170
 – emerging organic-, 179
 – inorganic-, 171
 – organic-, 171
 Cooper and Jacob solution, 37, 51, 65
 Cooper, Bredehoeft and Papadopoulos' method, 84, 90, 94
 Cosolvent effect, 387
 Critical micelle concentration, 386
 Cycloalkane, 173, 174
 Cycloparaffin, see Cycloalkane, 174

D

Darcy's law, 18, 20, 22, 251
 Darcy velocity, 18, 20
 De Glee solution, 42
 Dehalorespiration, 400
 Delayed gravity drainage, 44, 72
 Density, 4, 10, 19, 182
 Desorption, 211
 Diagnostic curve, 61
 Differential equation of mass transport, 219, 220, 223, 225
 Dilution attenuation factor, 313
 Direct push technique, 279
 Dispersion, 198, 199
 – hydrodynamic-, 199, 314
 – kinematic-, 193, 197
 – longitudinal mechanical-coefficient, 198
 – mechanical-, 193, 197
 – transverse mechanical- coefficient, 198
 Dispersivity, 201
 – longitudinal-, 198
 – transverse-, 198
 Displacement pressure, 254
 Dissolution, 208
 Domenico and Robbins' solution, 234
 Domenico's solution, 313
 Dose-response, 188
 Drainage, 250, 253
 – main-curve, 254
 – primary-curve, 255
 DRASTIC method, 141, 142
 Drawdown curve, 44, 60, 63, 66
 Drinking Water Directive (DWD), 190
 Drinking Water Protected Areas, 161

E

Effective porosity, 108
 Electron donor, 393
 Elutriate, 385
 Entry pressure, 254
 Equation, 27
 – of continuity, 27
 – groundwater flow-, 27, 34
 Equilibrium model, 203
 Equipotential line, 23, 31, 165
 Error function, 226, 228
 Exponential integral, 36
 Exposure
 – direct-, 308, 320
 – duration, 309, 321
 – frequency, 321
 – indirect-, 308, 320

- most likely-, 322
- -pathway, 303, 307
- point of-, 303, 307, 308, 319
- -rate, 305, 321
- reasonable maximum-, 322

F

- Fermentation, 393, 396
- Fick's law, 195, 197
- Filtration, 293
 - in-line-, 294
 - positive pressure-, 294
 - vacuum-, 294
- Flow line, 23, 165
- Flow net, 23, 105, 106
- Flumes, 59
- Force potential, 10

G

- Geomembrane, 153
- Geometric method, 162
- GOD method, 141
- Granulometry, 98, 110
- Groundwater, 2
 - -contamination, 170
- Groundwater flow equation, 61
- Grouting, 337
 - jet-, 337
- Guideline Value (GV), 190

H

- Half-life, 208
- Hantush and Jacob solution, 40, 69
- Hantush's method, 75
- Hantush's method for partially penetrating wells, 70
- Hazard, 151, 302
 - -hotspot, 140
 - -index, 325
 - -quotient, 325
- Hazardous, 151
- Hazen's formula, 98
- Head losses, 129
 - distributed-, 129
 - local-, 130
- Henry's constant, 185, 356
- Heterotrophic, 393
- Hvorslev's method, 84, 88
- Hydraulic conductivity, 17, 18, 20, 83, 97
- Hydraulic efficiency, 351
- Hydraulic gradient, 17, 25

- Hydraulic head, 10, 11, 22
- Hydrocarbon, 171
 - aliphatic-, 173
 - aromatic-, 173, 174
 - chlorinated aliphatic-, 175, 398
 - chlorinated aromatic-, 176
 - cyclic-, 173
 - halogenated aliphatic-, 175, 183
 - halogenated aromatic-, 183
 - polycyclic aromatic-, 175, 183, 388
 - saturate-, 173
 - unsaturated-, 173
- Hydrochemical efficiency, 351
- Hydrogenolysis, 364, 400
- Hydrolysis, 207
- Hydrophile-lipophile balance, 386
- Hydrophobic effect, 213

I

- Image well, 78
 - -system, 69, 77, 80
- Imbibition, 250, 253
 - main-curve, 254
 - primary-curve, 255
- Index method, 138, 141
- In line water meters, 59
- Input
 - continuous-, 226, 231, 234, 240, 246
 - pulse-, 229, 231, 233, 242, 244, 246
- Input
 - continuous-, 244
- In situ
 - -air stripping, 355
 - -bioremediation, 391
 - -flushing, 385
 - -oxidation, 388
 - -volatilization, 355
- Interfacial tension, 250, 251
- Interference test, 56
- Ion exchange, 211
- Ion pair, 207
- Isochrones, 162
- Isotherm, 211
 - Freundlich-, 212
 - Langmuir-, 211, 212
 - linear-, 211

J

- Jacob equation, 115
- Jet-stream method, 60

K

- KGS method, 84, 93
- Kinetic model, 203
- Kinetic reaction constant, 204
- Kutter's coefficient, 130

L

- Laplace–Plateau law, 251
- Law of mass action, 204
- Leachate, 308
 - attenuation factor, 312
 - dilution factor, 312
- Leakage, 22
 - coefficient, 22
 - factor, 22, 40
- Lefranc test, 99
 - constant head-, 99, 100
 - falling head-, 99, 100
 - injection-, 99
 - pumping-, 99
- Linearization, 65
- Lithology, 107, 108
- Local equilibrium hypothesis, 204
- Lowest-Observed-Adverse-Effect Level (LOAEL), 189
- Lysimeter, 274
 - pressure-vacuum-, 275, 276
 - suction-, 275

M

- Magnitude, 152
- Mass flux
 - advective-, 194
 - dispersive-, 197
 - hydrodynamic dispersion-, 199
- Match point, 66, 74
- Maximum Contaminant Level (MCL), 190
- Maximum Contaminant Level Goal (MCLG), 190
- Miscibility, 182
- Moench's method for partially penetrating wells, 70
- Molecular diffusion, 193, 195, 196, 199
 - coefficient, 196
- Monitoring network, 161, 166
- Monod's model, 209
- Mounding, 359
- Multilevel system, 279
- Multi-Phase Extraction (MPE), 336
- Multiple-well tracer tests, 108

N

- Nanoremediation, 378
- Naphthene, see Cycloalkane, 174
- NAPL, 182–186, 249, 255, 257, 259, 357
 - dense-, 183, 256, 261
 - light-, 183, 255, 332
- Natural attenuation, 331, 391
- Natural attenuation factor, 308, 318
- Neuman and Witherspoon, 41
- Neuman's method for partially penetrating wells, 70
- Neuman's solution, 46, 65, 69
 - simplified-, 47
- Nitroaromatic compound, 179
- Nitrophenol, 176
- Non Aqueous Phase Liquid, see NAPL, 182
- Non-threshold chemicals, 188, 189, 320
- No-Observed-Adverse-Effect Level (NOAEL), 189

O

- Ogata and Banks solution, 226, 236, 241
 - simplified-, 227
- Olefin, see Alkene, 175
- Organic carbon, 213
- Orifice buckets, 60
- Overlay method, 138, 139
- Oxygen releasing compound, 403

P

- Packer, 278
- Pankow's diagram, 285
- Paraffin, see Alkene
- Partition, 211
 - octanol-water-coefficient, 184, 213
 - organic carbon-water-coefficient, 213
 - soil-leachate-coefficient, 308
 - solid-liquid-coefficient, 211
 - water-air-coefficient, 185
 - water-solid, 184
- Peclet number, 200
- Permeability, 19
 - absolute-, 252
 - effective-, 250–252
 - intrinsic-, 19, 252
 - relative-, 250–252, 261
- Permeameter, 97
 - constant head-, 97
 - variable head-, 97
- Phenol, 175
- Phreatimeter, 59
- Physical state, 182

- Piezometer, 11
 - cluster, 278
 - nested-, 278
 - Piezometric level, 9
 - Pore Volume (PV), 348
 - Porosity, 12, 14, 16, 19, 28
 - effective-, 15, 19
 - fracture-, 13
 - intergranular-, 13
 - Potentiometric map, 164
 - Potentiometric surface, 22
 - Precipitation, 208
 - Primary hydration sphere, 207
 - Protection
 - area, 161, 166
 - dynamic-, 161, 166
 - static-, 161
 - Pseudo-skin factor, 121
 - Pump
 - bladder-, 286, 289
 - gas displacement-, 286
 - gear-drive-, 286
 - inertial-, 286
 - inertial lift-, 285, 291
 - multistage centrifugal-, 129
 - peristaltic-, 286, 290
 - piston-, 286
 - plunger-, 286
 - positive displacement-, 285, 286
 - progressing cavity-, 286
 - submersible-, 129
 - submersible centrifugal-, 285-287
 - suction lift-, 285, 286, 290
 - surface centrifugal-, 286
 - Pump and Treat (P&T), 338
 - Pumping test, 56, 61
 - Purging, 280
 - low-flow-, 281, 282, 289, 290
- Q**
- Quality assurance, 295
 - Quality control, 295
- R**
- Radial flow, 33
 - Radioactive decay, 208
 - Radius of influence, 38, 52, 379
 - Radius of investigation, 52
 - Reaction equilibrium constant, 204
 - Reactive zone, 378
 - Rebound, 353
 - Receptor, 302, 307
 - Recovery test, 56
 - Redox zone, 393
 - Reductive dechlorination, 396, 398
 - β -, 364
 - Reference dose, 189, 320
 - Remediation, 331, 344
 - ex situ-, 332
 - in situ-, 332
 - intrinsic-, 391
 - Representative Elementary Volume (REV), 28
 - Residual drawdown, 81
 - Residual NAPL content, 260
 - Residual water content, 260
 - Respiration, 393
 - Retardation factor, 214, 223, 350
 - Risk
 - assessment, 302, 303
 - backward-analysis, 306, 326
 - carcinogenic-, 322
 - contamination-, 302
 - direct-analysis, 326
 - element of-, 140
 - environmental-, 302
 - factor, 140
 - genotoxic-, 305
 - human health-, 302
 - human health-assessment, 320, 327
 - incremental lifetime cancer-, 322
 - management, 326
 - non-carcinogenic-, 325
 - of contamination, 152, 153
 - relative-assessment, 303
 - residual-, 152
 - scenario, 305
 - toxic-, 305
 - based screening level, 305
 - River dilution factor, 315
 - Rorabaugh's equation, 114, 129
- S**
- Safe Drinking Water Act, 190
 - Safeguard zones, 161
 - Sampler
 - filter tip-, 274, 276, 277
 - grab-, 285
 - syringe-, 285
 - Sampling, 283
 - active-, 272
 - adaptive cluster-, 266
 - composite-, 267

- design, 264
 - in-line, 284
 - judgemental-, 265
 - low-flow-, 284, 289, 290
 - passive, 273
 - ranked set-, 265
 - simple random-, 265
 - stratified-, 265
 - systematic and regular grid, 265
 - Saturation, 13, 252
 - funicular-, 252
 - insular-, 253
 - irreducible-, 252, 254
 - pendular-, 252
 - residual-, 252, 254, 261
 - Sauty's solution, 229
 - Scenario, 151
 - Scoring method
 - simple-, 141
 - weighted-, 141
 - Seepage velocity, 18, 108
 - Shape factor, 100
 - Sheet pile, 337, 376
 - Single-well point dilution tests, 102
 - SINTACS method, 141, 147, 149
 - Skimmer, 333
 - belt-, 333, 334
 - floating-, 333
 - Skin coefficient, 122
 - Skin effect, 68, 119
 - Slope factor, 189, 320, 322
 - Slug test, 56, 83, 123
 - injection-, 83
 - withdrawal-, 84
 - Slurry trench walls, 337
 - Smearing, 335
 - Soil Attenuation Model, 311
 - Soil Screening Level, 305
 - Soil vapor extraction, 355
 - Solubility, 182, 183
 - effective-, 184, 259
 - Solute, 182
 - conservative-, 220, 225
 - reactive-, 220, 222, 239
 - Solvent, 182
 - chlorinated-, 175
 - Sorbate, 210
 - Sorbent, 210
 - Sorption, 210, 222, 241, 314, 350
 - chemical-, 211
 - physical-, 211
 - Source
 - line-, 231, 232, 244
 - plane-, 234, 246
 - point-, 233, 246
 - Specific capacity, 113, 117, 123, 124
 - Specific discharge, 18
 - Specific retention, 15
 - Specific storage, 17, 107
 - Specific weight, 4
 - Specific yield, 14, 67, 107
 - Stagnation point, 339, 341
 - Stallman's method, 69, 78, 80
 - Statistical method, 138
 - Step-drawdown test, 114, 116
 - Storage, 15
 - Storativity, 14, 17, 44, 66, 106
 - Surface cap, 154, 156
 - Surface tension, 251
 - Surfactant, 385
 - anionic-, 386
 - cationic-, 386
 - non-ionic-, 386
 - Synthetic Organic Compound (SOC), 179
- T**
- Tailing, 353
 - Target, 140
 - of contamination, 140
 - Terminal electron acceptor, 393, 396
 - Theis' recovery method, 81
 - Theis solution, 35, 44, 65, 81
 - Thiem solution, 38, 52, 86
 - Threshold chemicals, 188, 189, 320
 - Time of travel, 162
 - method, 162, 163
 - Tolerable Daily Intake (TDI), 189
 - Tortuosity, 196, 197
 - Toxicity, 187
 - Transmissivity, 21, 66, 96, 98, 124
 - Type curve matching method, 65, 75, 80, 92
- V**
- Vacuum enhanced extraction, 336
 - Van der Gun correlation, 107
 - Van der Waals forces, 211
 - Vapor pressure, 4, 184, 356
 - Velocity
 - seepage-, 194, 198
 - Viscosity, 4
 - dynamic-, 4, 19
 - kinematic-, 4
 - Void ratio, 12
 - Volatile Organic Compound, 185

Volatility, 182

Volatilization factor

– indoor-, 318

– outdoor-, 316

Vulnerability, 137, 302

– assessment, 138

– maps, 151

intrinsic-, 137, 140, 152

– specific-, 138

W

Wall

– cement-bentonite slurry-, 374

– composite slurry-, 375

– soil-bentonite slurry-, 375

– thin slurry diaphragm-, 375

Walton's criterion, 119

Walton's method, 65

Walton's solution, 81

Walton's type curves, 40

Water, 2

– capillary-, 7, 8

– gravitational-, 5, 7, 8

– hygroscopic-, 6–8

– pellicular-, 6–8

– pendular-, 5, 8

Water Framework Directive, 190

Water level meter, 59

Water supply system, 128

– curve, 134

Weirs

– orifice-, 59

– sharp-crested-, 59

Weisbach's formula, 132

Well

– efficiency, 113, 118

– productivity, 117

– test, 113

Wellbore storage effect, 69

Well function, 36

– for leaky systems, 40

Wellhead protection areas, 161

Well-loss constant, 115, 119

Well loss equation, 98, 116

Well radius, 38

Well storage, 69

Wettability, 250

Wilson and Miller's solution, 231

Y

Young's modulus, 4

Z

Zero valent iron, 363

– microscale- (MZVI), 378

– nanoscale- (NZVI), 378